Investigation of Effects of Projected Climate Change on Eutrophication and Related Water Quality and Secondary Impacts on the Aquatic Ecosystem

Report to the
WATER RESEARCH COMMISSION

by

C Hughes, W Kamish, H Ally, T Coleman, C Allan, R Heath, P Dama-Fakir, M Mander and R Schulze

Golder Associates and the University of Stellenbosch

WRC Report No. 2028/1/14
ISBN 978-1-4312-0521-9

April 2014

Obtainable from

Water Research Commission
Private Bag X03
Gezina, 0031

orders@wrc.org.za or download from www.wrc.org.za

EXECUTIVE SUMMARY

This report has been compiled for the Water Research Commission project “Investigation of Effects of Climate Change on Eutrophication and Related Water Quality and Secondary Impacts on the Aquatic Ecosystem” (K5/2028), and constitutes Deliverable 7, the Draft Final Report. The project has been carried out over a three year period, from 2010 to 2013.

Developments such as urbanisation, mining, industry and agriculture give rise to large amounts of effluent discharge, a high degree of flow regulation by large impoundments and, in some instances, the releases needed to dilute polluted rivers. These effects have to be carefully managed to meet ecological flow requirements and sustain acceptable water quality. Management of eutrophication is of particular concern, since this presents severe problems for the treatment of water and presents a potential health threat when trihalomethanes (THMs) are formed after chlorination. Toxic algae also present a health threat for domestic use and livestock watering, and the clogging of drippers by algae hinders irrigation farming. Decaying algae and macrophytes can also cause oxygen depletion, to the detriment of fish and other aquatic life forms. Waterfowl are adversely affected by the closure of water surfaces with floating macrophytes. The presence of algae and water hyacinth is aesthetically unacceptable, impairing the use of watercraft, discolouring the water and causing taste and odour problems. The response of a river to nutrient enrichment is affected by many inter-related factors, including phosphate, nitrate and carbon cycling, decay, turbidity, sedimentation, sediment re-mobilization, temperature, seasonal and diurnal effects, effluent input, abstractions and the critically important hydraulic characteristics of the system. These complex interactions can only be assessed using computer models.

The Fourth Assessment Report of the Intergovernmental Panel on Climate Change (IPCC) recognizes global climate change as a reality. Changes in temperature are likely to severely affect freshwater systems and human populations which rely upon them. Projections of changes in climate (temperature, rainfall and runoff) are extremely difficult to model, and assessing projected climate impacts on freshwater ecosystems is even more challenging, particularly with regard to human influences and responses. It is important to note that algal blooms, and especially blue green algae, result in many human related impacts. The potential impacts of climate change are likely to increase the frequency of toxic algal blooms, increasing the likelihood of human-related impacts such as diarrhoea and potentially toxic algal related fatalities in communities that drink water directly from the river.

A variety of downscaled General Circulation Models (GCMs) were used to project changes in rainfall and temperature under climate scenarios across the country at Quinary catchment level (Schulze *et al*., 2010). This information was used as a basis for the identification of impacts on the selected case study systems. This report has been informed by an extensive literature study and various stakeholder meetings. The report documents the two separate modelling exercises (using two different modelling packages in two case study areas) to investigate the projected effects of climate change on water bodies, taking into account the following key aspects:

- Temperature;
- Dissolved oxygen; and
- Algae concentration.

The aim of the overall project is to investigate the impacts of climate change on eutrophication and to determine effects of resultant decreased dissolved oxygen on aquatic ecosystem. This report summarizes the modelling exercises carried out for this project, provides an investigation into the impacts of these changes, and provides recommendations for adaptation and mitigation options.

Climate change and eutrophication

Eutrophication is a process of nutrient enrichment of a water body, either natural or unnatural, resulting in a reduction in species diversity at all trophic levels (Codd, 2000). The process is described by the Organisation for Economic Cooperation and Development (OECD, quoted in Walmsley, 2000) as:

"the nutrient enrichment of waters which results in the stimulation of an array of symptomatic changes, amongst which increased production of algae and aquatic macrophytes, deterioration of water quality and other symptomatic changes are found to be undesirable and interfere with water uses."

Studies have found that the extent of eutrophication has increased in South African water bodies since its discovery in the 1970s (Rossouw, 2008), increasing the problems of high concentrations of algae and reduced water quality. Human activities are acknowledged as one of the main causes of eutrophication, as increased concentrations of phosphorous and nitrogen are discharged into water bodies. These water bodies respond directly to climatic

changes, and the variability in these responses is likely to affect water resources, water quality and aquatic ecosystems.

An increase in water temperatures with higher air temperatures could alter the hydrodynamics in water bodies, lengthening the thermal stratification period and deepening the thermocline, i.e. the interface between depths of different temperatures. These shifts may increase nutrient release from the sediments and lead to alterations in nutrient circulation. High concentrations of nutrients (phosphates and nitrogen in particular) and potential variability in climate can lead to an increased frequency of phytoplankton blooms and an alteration of the trophic balance. As a result, dissolved oxygen concentrations can fluctuate widely and algal productivity may reach problematic levels (Komatsu *et al*., 2007). Dissolved oxygen concentrations are determined by atmospheric inputs, photosynthesis, respiration and oxidation (Wetzel, 2001). A significant influence on oxygen concentrations is temperature – higher temperatures reduce the solubility of dissolved oxygen, thereby decreasing dissolved oxygen concentration. Higher temperatures also promote microbial action, and in turn the increased photosynthesis and respiration further reducing dissolved oxygen concentration. As the temperature increases due to projected climate change, the solubility of oxygen is likely to decrease when evaporation rates increase, further decreasing the oxygen solubility.

The consequences of climate change for some areas of South Africa could include increased air temperature, in turn increasing water temperature. This is likely to promote photosynthesis but may inhibit growth of some plants that are unable to cope with high light intensity (ultraviolet light levels), thereby imposing a selection criteria for certain species of plants and animals (Wotton, 1995). This may imply a shift in the dominance of algal classes from bacillariophyceae (a family of diatom) (<20°C) to chlorophyceae (green algae) (15-30°C) to cyanophyceae, a phylum of blue-green algae or cyanobacteria (>30°C), as the water body's temperature increases. At temperatures >30°C, biodiversity is reduced and cyanobacteria dominates (DeNicola, 1996). Cyanobacteria have a wide temperature tolerance, but when the water temperature exceeds 20^{o}C, a rapid increase in the biomass of cyanobacteria may occur if other factors support this (Owuor *et al.,* 2007). Higher temperatures also increase metabolic rates, oxygen demand and carbon dioxide production by aquatic organisms (Dallas and Day, 2004).

Cyanobacterial algal blooms may also extend beyond the conventional seasonal cycles (Paerl and Huisman, 2008). Studies have found that temperature changes could result in

peak cell concentrations of cyanobacterial blooms developing up to three months earlier in spring, depending on the surface water temperature, species diversity and environmental conditions of lakes.

A two year study conducted by Oberholster at the Hartbeespoort Dam (2005-2006) revealed a strong positive correlation ($p < 0.05$, $r^2 = 0.9201$) between the increase in surface water temperature during winter months and the increase in total cyanobacteria *Microcystis,* when other phytoplankton diatoms were found to have decreased. Such an increase in winter surface water temperature, which is generally projected in South Africa under climate change (Schulze *et al*., 2010), could favour cyanobacterial dominance, since several cyanobacterial taxa appear to perform well at higher temperatures compared to other phytoplankton taxa (De Senerpont Domis *et al*., 2007). Furthermore, cyanobacteria have generally higher temperature optima for growth, photosynthesis and respiration than green algae and diatoms (Robarts and Zohary, 1987).

Following team discussions based on experience of the country's river systems, previous modelling exercises and data availability, the following criteria were used to determine the case study systems for the project:

- Availability of existing water quality models;
- Data availability;
- Potential negative impact of climate change on nutrient status (i.e. is eutrophication likely to be an issue?);
- The importance of the system as a primary water supply (irrigation, ecological or human);
- The existence of an established forum for stakeholder engagement;
- Geographic spread (to ensure a spread of rainfall and climatic characteristics across the study); and
- The presence of a champion in the area.

Each potential case study system was considered according to each criterion, and the systems which met the most criteria were deemed the most suitable for the study. The two systems selected were:

- Berg River System (Voëlvlei Dam); and
- Middle Vaal River System.

The Climate Systems Analysis Group based at the University of Cape Town has statistically downscaled various General Circulation Models (GCMs) for use at a local level, and these have been quality controlled and processed by the School of Bioresource Engineering and Environmental Hydrology at the University of KwaZulu-Natal for use in hydrological models which project environmental climate and hydrological changes. The results of these analyses have been used in this project for present conditions (1971-90), and projected intermediate (2046-2065) and future (2081-2100) projections. The selected GCMs are listed below:

- Canadian Center for Climate Modelling and Analysis (CCCma), Canada (CGCM3.1(T47), first published 2005, abbreviated to CCC in this report);
- Meteo-France/Centre National de Recherches Meteorologiques (CNRM), France (CNRM-CM3, first published 2004, abbreviated to CRM in this report);
- Max Planck Institute for Meteorology (MPI-M), Germany (ECHAM5/MPI-OM, first published 2005, abbreviated to ECH in this report); and
- Institut Pierre Simon Laplace (IPSL), France (IPSL-CM4, first published 2005, abbreviated to IPS in this report).

Climate model outputs from simulations of the past, present and future climate were collected by the Program for Climate Model Diagnosis and Intercomparison (PCMDI) largely during the years 2005 and 2006, and this archived information constitutes phase 3 of the Coupled Model Intercomparison Project (CMIP3). The above models form part of this archive.

These four models were used to obtain the driving meteorological parameters for the Middle Vaal, Voëlvlei Dam and the Berg River Dam to establish a baseline study and the subsequent effect of climate change on eutrophication.

The water quality models chosen for this study were QUAL2K (Middle Vaal) and CE-QUAL-W2 (Voëlvlei Dam and the Berg River Dam).

Qual2K modelling exercise

The Vaal River was selected as a case study for this project due to several factors, including existing concerns over eutrophication (Heath *et al*., 2011). The study area for this part of the project is a 280 km reach of the Vaal River known as the Middle Vaal, extending from the Vaal Barrage (upstream), to below the confluence with the Vals River (downstream). A QUAL2K model was set up and verified for the Middle Vaal for the Department of Water Affairs (DWA) by Golder Associates in 2009 (Golder Associates, 2009). This model made use of existing water quality data made available by DWA, Rand Water, Sedibeng Water and Midvaal Water Company. For the current project, it was proposed that the climate change projections available from the UKZN database were used as input to this model to test the effects of climate change on water quality, as the hydraulics and base data had previously been set up. The time period originally modelled (15 August 2005) was therefore used as the recorded reference period for the climate change modelling exercise.

Once the effect of air temperature on water temperature had been modelled, it was noted that all future climate change projections indicate an increase in water temperature. There is a range of increase of approximately 1.5°C between the various models for the intermediate future. Into the distant future, for which the projections are less reliable due to uncertainty, there is a projected range in the increase of just over 3-3.5°C.

Breitburg *et al*. (1997) explain that concentration of dissolved oxygen in bottom waters of water bodies can be physiologically stressful or lethal to organisms dependent on aerobic respiration. The reduced dissolved oxygen in the modelled stretch of water indicates that there are higher air and water temperatures (a higher air temperature is likely to affect the rate at which oxygen is dissolved/absorbed into the water), and the amount of biological activity in the water has increased, as higher levels of aquatic life are likely to place higher demands on the oxygen contained in the water. The IPCC Working Group II (2007) explains: “Higher temperatures alone would lead to increases in concentrations of some chemical species but decreases in others. Dissolved oxygen concentrations are lower in warmer water, and higher temperatures also would encourage the growth of algal blooms, which consume oxygen on decomposition.” The application of this model indicated that dissolved oxygen in this stretch of river is likely to drop for the various climate change projections. This can be attributed to the higher temperatures and consequent reduced solubility of oxygen.

All modelled future projections projected a decrease in flow with changes in temperature and evaporation. In the most extreme intermediate future projection (2046-2065), the concentrations of phytoplankton show an increase of approximately 35 µg/L. For the most extreme projection into the distant future (2081-2100) an increase of over 70 µg/L was projected.

The concentration of phytoplankton in the Vaal Barrage is already particularly high due to the various industrial, agricultural and domestic discharges, leading to eutrophication problems. The average chlorophyll-a reading at the Midvaal Water Company monitoring point is 95 µg/l (January 2004-February 2012), with a maximum reading of 334 µg/l. The results are highly varied, and show a very slight increasing trend. The South African Water Quality Guidelines (Department of Water Affairs and Forestry, 1996) indicate that the Target Water Quality Range for algae (measured by chlorophyll-a) is 1 µg/l (for negligible taste and odours), with the limits for domestic use being 15 µg/l (acceptable) and 100 µg/l (tolerable). Measurements at the Midvaal Water Company indicate an exceedance of the acceptable algae concentration in approximately 40% of the readings. This therefore indicates that there is an overabundance of algae within this stretch of the Vaal River, exceeding the tolerable limits for domestic use, which has implications for the water treatment processes.

The original value for phosphate entering the study area (at the Vaal Barrage, or headwater) was set at 342 µg/l. It is evident that complete removal of inorganic phosphate from the system causes a decline in existing phytoplankton concentration. Complete removal of only organic phosphorous does not make a difference to phytoplankton concentration. Inorganic phosphorous therefore appears to be a limiting factor in the growth of algae. Hydrolysis of organic phosphorous also results in the generation of inorganic phosphate within the model (Chapra *et al*., 2011). With fairly large quantities of organic phosphorous entering the system at the Barrage and with point sources, this appears to compliment even a small amount of inorganic phosphorous.

These results indicate that a *significant* reduction in phosphate load in the Barrage and the various point sources would be required to reduce the quantity of phytoplankton in the Vaal River.

CE-QUAL-W2 modelling exercises

The objective of this part of the study was to find any potential links between various climate changes projections on eutrophication in waters of the Berg River Dam (BRD) and Voëlvlei

Dam. It has been postulated that with climate change from the present day (1971-1990) to intermediate future (2046-2065) and into the distant future (2081-2100) that the air temperature would increase by between 2 and 4.5^{o}C, and that this increase would heat the surface waters sufficiently to amplify the growth of algae within such waters. It was further postulated that the algae present would experience varying rates of increased growth because of the increased water temperature. Specifically the aims of the modelling exercise were to simulate the effect of climate change projections on:

- inlake water temperatures
- inlake concentrations of plant nutrients
- inlake concentrations of dissolved oxygen and
- inlake concentration of various algal species.

A variety of downscaled General Circulation Models (GCMs) have been used to project changes in rainfall, temperature and hydrological regimes under climate scenarios across the country at quinary catchment level (Schulze *et al*., 2010). This information was used as a basis for the identification of impacts on the selected case study systems. Downscaled meteorological information was provided by the Climate Systems Analysis Group (CSAG) based at the University of Cape Town and the following GCM were considered in this study:

- Canadian Center for Climate Modelling and Analysis (CCCma), Canada (CGCM3.1(T47), first published 2005, abbreviated to CCC in this report);
- Meteo-France/Centre National de Recherches Meteorologiques (CNRM), France (CNRM-CM3, first published 2004, abbreviated to CRM in this report);
- Max Planck Institute for Meteorology (MPI-M), Germany (ECHAM5/MPI-OM, first published 2005, abbreviated to ECH in this report); and
- Institut Pierre Simon Laplace (IPSL), France (IPSL-CM4, first published 2005, abbreviated to IPS in this report).

The hydrodynamic and water quality model used in this study was CE-QUAL-W2 CE-QUAL-W2 is a two-dimensional (2-D), laterally averaged, hydrodynamic water quality simulation model (Cole and Wells, 2008). The model is based on the assumption that the water body shows maximum variation in water quality along its length and depth. Therefore,

the model is suited to relatively long and narrow water bodies that show water quality gradients in the longitudinal and vertical directions. The two-dimensional model simulates the vertical and longitudinal distributions of thermal energy (water temperature) and selected biological and chemical constituents in a water body with time. The primary purpose of the model is to simulate time-varying concentrations of water quality constituents by coupling hydrodynamic and water quality components. The model has been applied to many rivers, lakes, reservoirs, and estuaries for nearly 20 years.

Three distinct algal groups were selected for this study – diatoms, green algae and blue-green algae (cyanobacteria). For each of the water quality scenarios considered the inflow volumes, water quality concentrations and temperature to the dam were kept constant, i.e. the same as was used in the present day scenario. In this way the effect of inflow characteristics on in-lake water quality could eliminated from the simulations.

Water quality simulations of the present day scenario (1971-1990) was performed and compared to intermediate future (2046-2065) and distant future (2081-2100) projections. The meteorological data driving these simulations included daily minimum and maximum temperature, rainfall, evaporation, solar radiation, minimum and maximum relative humidity, wind-speed and wind direction.

All of the future climate models showed varying ranges of annual percentage air temperature increase that in turn increased surface water temperatures. This increase in water temperature caused a decrease in the surface water elevation of the dams due to increased evaporation. It was concluded that air temperature was the major driver for surface water temperatures, but that solar radiation was important for capturing the diurnal effects.

Model simulation outputs also revealed that the effect of climate change on BRD could result in a seasonal shift in the diatom blooms by one month for the intermediate and distant future. Green algae and cyanobacteria did not establish themselves in the dam for the present and future climate projections. It is thus expected that the surface waters of BRD will not be negatively impacted by projected climate change.

Results from the Voëlvlei Dam simulations indicated that climate change could affect the surface waters of Voëlvlei Dam by heating the water and subsequently increased the evaporation rate of the water. This heated water evaporated more in the distant future than the intermediate future as a result of the increased water temperature. The surface phosphate concentration fluctuated marginally when progressing to intermediate future and

distant future climate scenarios. The maximum concentration occurred one month earlier in the future scenarios than in the present day, and the concentration was relatively unchanged. All GCM models showed changes in surface ammonium concentration, but overall a decreasing trend in progressing to future climate change scenarios was shown. The concentration of nitrite-nitrates for the future surface concentrations remained relatively unchanged when compared to present day surface concentrations, with spring having the lowest surface concentrations. The dissolved oxygen concentration was greatest during winter and spring, when the surface water was cooler and could hold more oxygen. The result of the climate change study was showed that the green algae was the dominant species in the dam and showed an increase and seasonal shift with climate change projections. Cyanobacteria, although it was present in small quantities, showed increases in concentration with the projected climate change, thus signally a worsening water quality scenario for Voëlvlei Dam.

A disadvantage of the statistical method of downscaling was that it relies on the availability of sufficient high resolution data over long periods so that statistical relationships may be established. It was not possible to be sure of the validity of the statistical relationships for a climate-changed situation (Houghton, 2007; Quintana-Seguí *et al.*, 2010). Wind-speed and direction was not supplied by CSAG (UCT) and was thus a limitation. CE-QUAL-W2 requires wind-speed and direction as part of its meteorological data input to predict water quality. In the absence of this wind-speed and direction was replicated from past data. No inflow and outflow data was available for the predicted future scenarios as it was assumed demand and allocation of the water resource would not change for the future simulation periods.

Monitoring data

Recorded water quality data for the modelling exercises was found to be limited and inconsistent, particularly with regard to parameters important for the assessment of eutrophication potential, such as temperature and chlorophyll-a. It appears that monitoring was consistent for a large number of points up until recent years, but the thoroughness and geographic range of monitoring has reduced. Both Midvaal Water Company and Sedibeng Water have good monitoring programs along the Vaal River, and in particular include the monitoring of water temperature and chlorophyll-a, which can be used for eutrophication modelling. These comprehensive monitoring programs can add significant value to water resource management going forward.

It is recommended that certain dams and sections of river should be selected as “case study” sites across South Africa. These should be selected based on various criteria, including:

- Varying climate regimes (summer and winter rainfall regions);
- Varying topographical characteristics;
- Varying land uses;
- Varying point/non-point sources of pollution.

Monitored parameters should include the following:

- Rainfall;
- Evaporation;
- Wind speed;
- Solar radiation;
- Sedimentation;
- Flow (in-stream for rivers and inflows/outflows for dams); and
- Water quality – a comprehensive suite of parameters including dissolved oxygen, algae (chlorophyll-a) and other biological indicators.

A parallel programme should be set up in terms of laboratory-based testing of algal growth parameters such that more reliable estimates may be established for South African conditions.

Secondary impacts of increased eutrophication under climate change

The modelling exercises outlined above have indicated that, with a projected increase in temperature under climate change, as well as the associated projected changes in evaporation and other physical variables, there are likely to be increases in suspended loads and nutrient release through deepened thermocline depths and increases in circulation.

The changes could include the following, amongst others:

- Increased microbial action due to warmer temperatures and associated reduction in DO;
- Increase in the rate of decomposition of organic material under higher temperatures;
- Decreased DO due to warmer water temperature which reduces its solubility and reduces the suitability of habitat for oxygen-breathing vertebrates and invertebrates;
- Increase in Biochemical Oxygen Demand resulting in anoxia and biomass reduction. The aquatic organisms would release their nutrients during decay compounding the situation (Meisner *et al.*, 1987);
- Reduced water volumes due to higher evaporation should this occur, and consequent concentration of nutrients in the water body, encouraging algal growth which is not likely to be nutrient limited;
- Potential longer retention times and decreased flushing resulting in increased eutrophication and salinity (Jørgensen, 2008);
- Altered hydrodynamics in the water body due to changes in water temperature, leading to deepening thermoclines, release of nutrients from sediments and increased circulation of these, increasing the movement of solutes and encouraging algal growth;
- Change in the trophic balance (food chain) of the water body;
- Alteration in terms of the species of algae, with increase in concentration of temperature-tolerant cyanobacteria, which can cause toxicity-associated health problems in cases of ingestion and treatment;
- Increases concentrations of algal growth, which reduces light penetration to lower strata of the water body, thus reducing the suitability of habitat for various plant and animal species;
- Seasonal shifts in algal blooms to potentially occur earlier in the year and to last for longer periods, leading to requirements for more lengthy, intensive and expensive treatment methods.

Specifically with regard to algal blooms, these can directly impact fish and other aquatic vertebrates through the toxins that certain algae release. This can indirectly impact aquatic life by changing fish community structures, the habitat of aquatic species, leading to changes in the behaviour of certain fish species and threats to their spawning grounds (Havens, 2008). In addition to the ecosystem and food web effects mentioned in preceding sections of this report, cyanobacterial toxins can impact on the tissue development of invertebrates and

lead to an accumulation of toxins within this tissue (Havens, 2008). The cyanobacterial toxins also affect aquatic snails by impacting their growth, their potential to reproduce and their general survival (Havens, 2008). Recreational activities, which are of great importance in areas such as the Vaal River can be severely affected by the increase of eutrophication under climate change, and in fact these are already under threat in certain parts of the Vaal area. Effects such as bad odour and discolouring of the water (aesthetics) lead to reduced appeal in terms of recreational activities in the river (Dennison and Lyne, 1997).

The social impacts of these changes are difficult to quantify, although there is likely to be a reduction in quality of life through the decrease in recreational activities, and the knock-on financial benefits that these activities bring into the local area (Brand *et al.*, 2009). Increased algal blooms lead to physical interference with recreational activities and the use of the river, as well as a general degrading of the beauty of the area (Dennison and Lyne, 1997). It is important to note that traditional communities have established practices based on existing ecosystems which are now affected by climate change and eutrophication threats. Algal blooms and cyanobacteria in particular, can result in many human health-related impacts. The potential impacts of climate change could increase the frequency of toxic algal blooms, and this could imply a greater incidence of human-related health impacts and potentially toxic algal-related fatalities for communities that drink water directly from the river.

Discussions with the Midvaal Water Company (Marina Kruger pers. Comm.) indicated that high levels of eutrophication are already problematic for their treatment process. The following points were raised:

- Specific types of algae cause severe filter blockage, with filamentous types forming “mats” on the surface of the sand, and slime builds up in the filter sand and reduces the filtration capacity;
- Algal build up leads to reduced filter operating cycles (e.g. reduce from the normal 24 hours between back wash cycles to as low as 6 hours between back wash cycles);
- More back washing results in extra operating costs, including labour, wash water requirements, electricity, the volume of waste water produced that has to be handled, maintenance, etc.;
- The method of back washing has to be changed to a more vigorous simultaneous air-and-water scenario, and had to increase the weir heights in the filters to prevent

excessive media/filter sand losses. This implies additional capital cost and future maintenance costs;

- The Company invested R 45 million in 2011 to increase filtration capacity; and
- At times of high algal concentrations in the raw water almost 30% more chemicals are required to improve the colour and/or taste and odour as a result of the algae.

Modelling results indicate that the Midvaal Water Company treatment plant has sufficient capacity to treat the algal concentrations projected for the intermediate and long-term time periods. The operational costs are likely to increase, as additional chemicals will be required and more frequent backwashes will be needed as the result of algal concentrations increasing. In the long-term, Granular Activated Carbon may be required to remove the odour and improve the taste of the water. This will result in capital expenditure, additional operational costs and annual carbon replacement costs. These costs are likely to be transferred to the consumer.

Mitigation and adaptation

Key concepts in the control of eutrophication, particularly in the face of climate change, include:

- Collaboration and integration (Government departments (DWA, provincial bodies), private companies, communities);
- Dam/river and upstream catchment management;
- Capacity building and education;
- Resourcing and compliance enforcement;
- The concept of treating the cause and not the symptom; and
- Job creation and community involvement (sustainability).

It is evident from both of the modelling exercises that stringent control over nutrient release to South Africa's water courses and impoundments is vital for the management of eutrophication. Furthermore, investigation of climate change projections indicates that with higher temperatures and varying evaporation, climate change is likely to exacerbate the effects of eutrophication. The environmental impacts of climate change on eutrophication are

extensive and are difficult to thoroughly capture due to their complexities and knock-on effects. However it should also be noted that many of these impacts already exist, and climate change is only likely to accelerate and or exacerbate the current problems in South Africa’s water courses.

ACKNOWLEDGEMENTS

The project team would like to thank the Water Research Commission for the opportunity to be involved in this project. We would also like to thank our Reference Group for their invaluable time, expertise and advice throughout the project:

Name	Surname	Organisation
Lisa	Coop	University of Cape Town
Chris	Moseki	Water Research Commission
Kevin	Murray	Water Research Commission
Jan	Roos	Water Quality Consultants
Nico	Rossouw	Aurecon
Roland	Schulze	University of KwaZulu-Natal
Nadine	Slabbert	Department of Water Affairs

The project team would furthermore like to thank Marica Erasmus and Mike Silberbauer at the Department of Water Affairs, as well as Jan Pietersen, Marina Kruger and Shalene Janse van Rensburg at the Midvaal Water Company for their kind assistance with data collection. The team would also like to thank Professor Steven Chapra at Tufts University for assisting with the alteration of the QUAL2K model to simulate evaporation.

We would particularly like to thank Chris Moseki and Kevin Murray of the WRC for their guidance throughout the project.

TABLE OF CONTENTS

LIST OF FIGURES

LIST OF TABLES

LIST OF ABBREVIATIONS

ACRU	A multipurpose model that integrates water budgeting and runoff components of the terrestrial hydrological system with risk analysis, and can be applied in crop yield modelling, design hydrology, reservoir yield simulation and irrigation water demand/supply, regional water resources assessment, planning optimum water resource allocation and utilization, climate change, land use and management impacts, and resolving conflicting demands on water resources (after Agricultural Catchments Research Unit).
AR4	IPCC Fourth Assessment Report
BDCM	Bromodichloromethane
BOD	Biochemical Oxygen Demand
BRD	Berg River Dam
BWP	Berg Water Project
CFUs	Colony Forming Units
CMIP3	Phase 3 of the Coupled Model Intercomparison Project
CO_2	Carbon Dioxide
CSAG	Climate Systems Analysis Group
CTP	Cyanobacteria Toxin Poisoning
DAF	Dissolved Air Flotation
DBCM	Dibromochloromethane
DBPs	Disinfection by-products
DO	Dissolved Oxygen
DOM	Dissolved Organic Matter
DWA(F)	Department of Water Affairs (and Forestry)
GAC	Granular Activated Carbon
GCM	General Circulation Model (Global atmospheric model of projected climate change)
IFR	Instream Flow Requirements
IPCC	Intergovernmental Panel on Climate Change
ISS	Inorganic Suspended Solids
LPOM	Labile Particulate Organic Matter
MASL	Metres above sea level
MCL	Maximum Contaminant Level
PCMDI	Program for Climate Model Diagnosis and Intercomparison

POM	Particulate Organic Matter
PWV	Pretoria-Witwatersrand-Vereeniging
RDOM	Refractory Dissolved Organic Matter
RPOM	Refractory Particulate Organic Matter
SAWS	South African Weather Service
SOD	Sediment oxygen demand
SRES	Special Report on Emissions Scenarios
TAR	IPCC Third Assessment Report
TDS	Total Dissolved Solids
THMs	Trihalomethanes
TOR	Terms of Reference
TRIX	Trophic Index
TSS	Total Suspended Solids
UCT	University of Cape Town
UKZN	University of KwaZulu-Natal
WMA	Water Management Area
WRC	Water Research Commission
WTW	Water Treatment Works
WWTW	Wastewater Treatment Works

1 INTRODUCTION

This report has been compiled for the project “Investigation of Effects of Projected Climate Change on Eutrophication and Related Water Quality and Secondary Impacts on the Aquatic Ecosystem” (K5/2028), and constitutes Deliverable 8, the Final Report. The aims of this report are indicated in Section 2.

2 AIMS AND OBJECTIVES

The aim of this report is to provide a synthesis of the entire project, including modelling, stakeholder interaction and impact assessment carried out to investigate the effects of climate change on water quality, with a focus on eutrophication.

The aim of the overall project is to investigate the impacts of climate change on eutrophication and to determine effects of resultant decreased dissolved oxygen on aquatic ecosystem. The project team selected two sites to be the focus and case studies for this project. These case studies assisted the team in addressing the following aims as specified in the Terms of Reference as specified by the Water Research Commission:

- Investigation into the nature and type of suspended load, nutrients or solutes that characterize return flows, inflows into rivers or in-situ conditions within dams and how these contribute to increased algal blooms and the extent of its toxicity to fish and human health within the context of climate change;
- Investigation of likely impacts of climate change on temperature and irradiation (heat content) of water in reservoirs, rivers and canals. Other studies that were previously undertaken or that are ongoing as well as case studies on related work done in hypertrophic studies and elsewhere should also be considered in this project;
- Determine the nature and extent of impacts of changes in dissolved oxygen on aquatic life; and
- Establish the direct or indirect associations between climate change and harmful algal blooms, water chemistry and potential human health impacts.

A variety of downscaled General Circulation Models (GCMs) have been used to project changes in rainfall, temperature and hydrological regimes under climate projections across the country at quinary catchment level (Schulze *et al*., 2010). This information was used as a basis for the identification of impacts on the selected case study systems.
This report has been informed by an extensive literature study and various stakeholder meetings, and documents the two separate modelling exercises (using two different modelling packages in two case study areas) to investigate the projected effects of climate change on water bodies, taking into account the following aspects:

- Temperature;
- Dissolved oxygen; and

- Algae and salt concentration.

This report summarizes the modelling exercises carried out for this project, provides an investigation into the impacts of these changes, and provides recommendations for adaptation and mitigation options.

3 BACKGROUND AND HYPOTHESIS

3.1 Factors influencing algal growth

Eutrophication is a process of nutrient enrichment of a water body, either natural or unnatural, resulting in a reduction in species diversity at all trophic levels (Codd, 2000). The process is described by the Organisation for Economic Cooperation and Development (OECD) as:

"the nutrient enrichment of waters which results in the stimulation of an array of symptomatic changes, amongst which increased production of algae and aquatic macrophytes, deterioration of water quality and other symptomatic changes are found to be undesirable and interfere with water uses" (Walmsley, 2000)

Studies have found that the extent of eutrophication has increased in South African water bodies since it was first noticed in the 1970s (Rossouw, 2008), increasing the problems of high concentrations of algae and reduced water quality. Human activities are acknowledged as one of the main causes of eutrophication, as increased concentrations of phosphorous and nitrogen are discharged into water bodies. Dams, reservoirs and other water bodies respond directly to climatic changes and the variability in these responses are likely to affect water resources, water quality and aquatic ecosystems.

An increase in water temperatures with higher air temperatures could alter the hydrodynamics in water bodies, lengthening the thermal stratification period and deepening the thermocline, i.e. the interface between depths of different temperatures. These shifts may increase nutrient release from the sediments and lead to alterations in nutrient circulation. High concentrations of nutrients (phosphates and nitrogen in particular) and potential variability in climate can lead to an increased frequency of phytoplankton blooms and an alteration of the trophic balance. As a result, dissolved oxygen concentrations can fluctuate widely and algal productivity may reach problematic concentrations (Komatsu *et al*., 2007).

Algal growth is dependent on several variables for its lifecycle, such as suitable environmental conditions and nutrients, including temperature and solar radiation, the amount of dissolved oxygen, light penetration, turbidity and suspended solids, dissolved solids, salinity and conductivity, pH, availability of nitrogen and phosphorous and micronutrients within the water body. More detailed discussion on some of these elements in the context of algal growth is provided below.

The effect of temperature and solar radiation

The natural thermal or background thermal characteristic of a water body is dependent on the hydrological, climatological and structural features of its region and catchment area. Temperature primarily affects algal photosynthetic metabolism by controlling the enzyme reaction rate of the algae and an optimum temperature for each species is observed (DeNicola, 1996). Water temperature is primarily determined by direct solar radiation as well as other factors such as latitude, elevation, shading vegetation and morphology (Wetzel, 2001, DeNicola, 1996).

Dissolved oxygen

Dissolved oxygen concentration is determined by atmospheric inputs, photosynthesis, respiration and oxidation (Wetzel, 2001). A significant influence in terms of oxygen concentration is temperature – higher temperatures reduce the solubility of dissolved oxygen, thereby decreasing dissolved oxygen concentration. Higher temperatures also promote microbial action, and in turn the increased photosynthesis and respiration further reducing dissolved oxygen concentration. As the temperature increases due to projected climate change, the solubility of oxygen is likely to decrease when evaporation rates increase, further decreasing the oxygen solubility. Reduced inflow caused by a reduction in rainfall (in certain areas) could also decrease the re-aeration potential. Increased frequencies of oxygen depletion may occur at the hypolimnion (dense bottom layer) of eutrophied water bodies, where anaerobic decomposition of material occurs (Wotton, 1995 and Wetzel, 2001).

Light Penetration

Light penetration in a water body influences species composition and biomass of phytoplankton. A reduction in the availability of light limits phytoplankton production and the rate of photosynthesis of organisms, although availability of light in the lower strata of a water body could be caused by phytoplankton itself (self-shading). In fact, when cyanobacterial blooms occur, irradiance is reduced in the water column, reducing the growth of producers that cannot maintain a position near the surface of the water (see below), including epiphyton, benthic algae and rooted vascular plants. Thus, lakes with very dense algal blooms, especially if they are frequent or long-lasting, may not support large populations of other producers. In shallow eutrophic lakes, research has shown that the transition from plant to phytoplankton dominance can occur rapidly (Scheffer *et al*. 1993).

Total Dissolved Solids (TDS)

The total amount of organic matter, inorganic matter and ions dissolved in water contributes to the total dissolved solids. Natural TDS is determined by geographical location (soil type, etc.), as well as atmospheric conditions. Sources of anthropogenic TDS include industrial effluent, mining, aquaculture and irrigation. In addition, accelerated evaporation caused by climate change can increase the concentration of matter in water, effectively increasing TDS.

3.2 Climate change and eutrophication

The consequences of climate change for some areas could include increased air temperature, in turn increasing water temperature. This is likely to promote photosynthesis but may inhibit growth of some plants that are unable to cope with high light intensity (ultraviolet light levels), thereby imposing a selection criteria for certain species of plants and animals (Wotton, 1995). This may imply a shift in the dominance of algal classes from bacillariophyceae (a type of diatom) (<20°C) to chlorophyceae (green algae) (15-30°C) to cyanophyceae, a phylum of blue-green algae or cyanobacteria (>30°C), as the water body's temperature increases. At temperatures >30°C, biodiversity is reduced and cyanobacteria dominates (DeNicola, 1996). Cyanobacteria have a wide temperature tolerance, but when the water temperature exceeds 20°C, a rapid increase in the biomass of cyanobacteria may occur if other factors support this (Owuor *et al.,* 2007). Higher temperatures also increase metabolic rates, oxygen demand and carbon dioxide production by aquatic organisms (Dallas and Day, 2004).

Increased variability in climatic conditions is likely to create favourable conditions for cyanobacterial bloom formation extending beyond the conventional seasonal cycles (Paerl and Huisman, 2008). Studies have found that temperature changes could result in peak cell concentrations of cyanobacterial blooms developing up to three months earlier in spring, depending on the surface water temperature, species diversity and environmental conditions of lakes.

A two year study conducted by Oberholster at the Hartbeespoort Dam (2005-2006) revealed a strong positive correlation ($p < 0.05$, $r^2 = 0.9201$) between the increase in surface water temperature during winter months and the increase in total cyanobacteria *Microcystis,* when other phytoplankton diatoms were found to have decreased. Such an increase in winter surface water temperature, which is generally projected in South Africa under climate change (Schulze *et al*., 2010), could favour cyanobacterial dominance, since several cyanobacterial taxa appear to perform well at higher temperatures compared to other

phytoplankton taxa (De Senerpont Domis *et al*., 2007). Furthermore, cyanobacteria have generally higher temperature optima for growth, photosynthesis and respiration than green algae and diatoms (Robarts and Zohary, 1987).

Eutrophication is therefore likely to be exacerbated by projected changes in climate in South Africa. The effect of these changes has therefore been modelled in this part of the project. The results of this analysis should estimate the potential effects of climate change (temperature changes in particular). These results could allow managers to explore whether mitigating factors may be employed to prevent projected poor water quality into the future.

3.3 **Modelling hypothesis**

It is likely that, with rising air temperatures, water temperature is likely to rise in association. This is likely to make conditions more conducive to growth for algal organisms. The following hypotheses are made with regard to the modelling of water quality using climate change projection data:

- Into the future, water temperatures are projected to **increase** (Solomon *et al*., 2007). This temperature increase is likely to be higher towards the end of the century ("distant future", 2081-2100) than towards mid-century ("intermediate future", 2045-2065);
- Into the future, algal growth is likely to **increase** with the higher temperatures, particularly in certain species such as cyanobacteria (represented by phytoplankton and chlorophyll-a concentration);
- Associated changes in water quality are projected with an increase in algal growth, including changes in diurnal temperature range**,** decreased concentrations of dissolved oxygen and light penetration and increase in BOD, with subsequent effect on ecosystem and fish survival and health.
- The following sections describe the process followed during the modelling exercises to illustrate the potential effects of climate change on eutrophication in two South African systems.

4 CLIMATE CHANGE PROJECTIONS

The Climate Systems Analysis Group based at the University of Cape Town has downscaled various General Circulation Models (GCMs) for use at a local level, and these have been quality controlled and processed by the School of Bioresource Engineering and Environmental Hydrology at the University of Natal for use in hydrological models which project environmental climate and hydrological changes. A full discussion on the selection of climate change projections for use in this project is provided in Hughes *et al*. (2011).

The results of these analyses have been used in this project for present conditions (1971-1990) and projected intermediate (2046-2065) and future (2081-2100) projections. The results from these analyses have been processed using the ACRU Model (Schulze and Smithers, 2004).

4.1 Collection of climate projections[1]

GCMs use projections of future emissions of greenhouse gases under different population and economic development settings to project potential future climatic conditions. Climate change impacts however occur at finer scales. Therefore, outputs from global GCMs have to be downscaled to an appropriate spatial resolution to obtain relevant future projections (Figure 1) for local-level impact assessment.

GCMs are numerical models which are designed to replicate the physical processes of the atmosphere, oceans, troposphere (snow and ice) and land surfaces. GCMs are considered to be the most advanced tools currently available for simulating the response of the global climate system to increasing greenhouse gas concentrations (Carter *et al*., 2007). Climate is represented in the models as a global grid. The grid cells range in size from 250 to 600 km. The vertical component, which further enables the third dimension within the model, is modelled through the use of 10 to 20 vertical pressure levels in the atmosphere, up to 30 layers in the ocean. Due to the fact that the earth's various processes occur at finer scales than those simulated by these models, they cannot be specifically modelled, and their resultant impact is parameterized. The common differences between the various available GCMs are due to these parameterizations being carried out using different methods (particularly cloud radiative effects and precipitation processes). Successes of GCMs also vary greatly from continent to continent, and although certain models may be judged to accurately represent current climate, there is no guarantee that greenhouse gas forcing will

1 Chapter condensed, but contributed largely by Professor Roland Schulze, School of Bioresources Engineering and Environmental Hydrology, University of KwaZulu-Natal (Schulze *et al*., 2010)

be well represented by the same models. For this reason, it is better to use an “ensemble” or envelope approach, with several models which can be used to assess trends.

Each GCM is likely to have its own bias, particularly with regard to precipitation, which varies between regions and parameters. When assessing future projections, it is recommended that anomalies between the GCM historic period simulation and the future simulation are assessed, rather than raw outputs from the models. Anomalies are calculated for each GCM and represent the GCM response or change, given the greenhouse gas forcing, and therefore are likely to remove the inherent bias (L. Coop *pers. Comm*.).

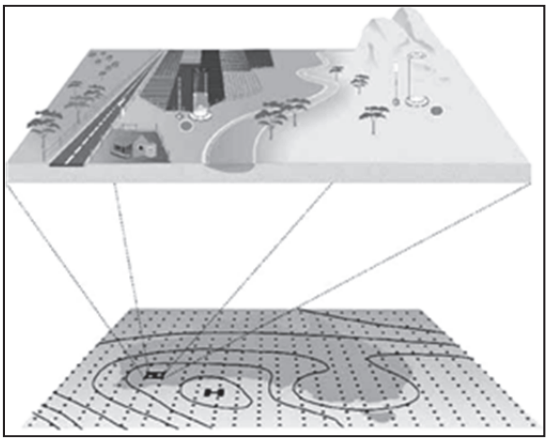

Figure 1: A schematic diagram of downscaling. GCMs provide the large-scale atmospheric patterns (top). The local features (top) influence the climate beyond the resolution of GCMs (Australian Bureau of Meteorology, 2003)

For the climate projections used in this project, the downscaling process was undertaken by the Climate Systems Analysis Group (CSAG) of the University of Cape Town by empirical downscaling to climate station level. All of the future global climate projections were simulated based on the A2 emissions scenario defined by the IPCC Special Report on Emission Scenarios (SRES) (Nakićenović and Swart, 2000, Figure 2). The A2 storyline represents the least optimistic scenario in terms of human development, where emissions are at their highest. It must be noted that global emissions have already surpassed the emissions levels projected in this scenario (Global Carbon Project, 2010). This scenario of greenhouse gas emissions suggests that efforts to reduce global emissions this century are relatively ineffective. Regardless of the emissions scenario selected, a further increase of at least 0.6°C in global mean temperature is likely, owing to past greenhouse gas emissions (Hewitson *et al*., 2005).

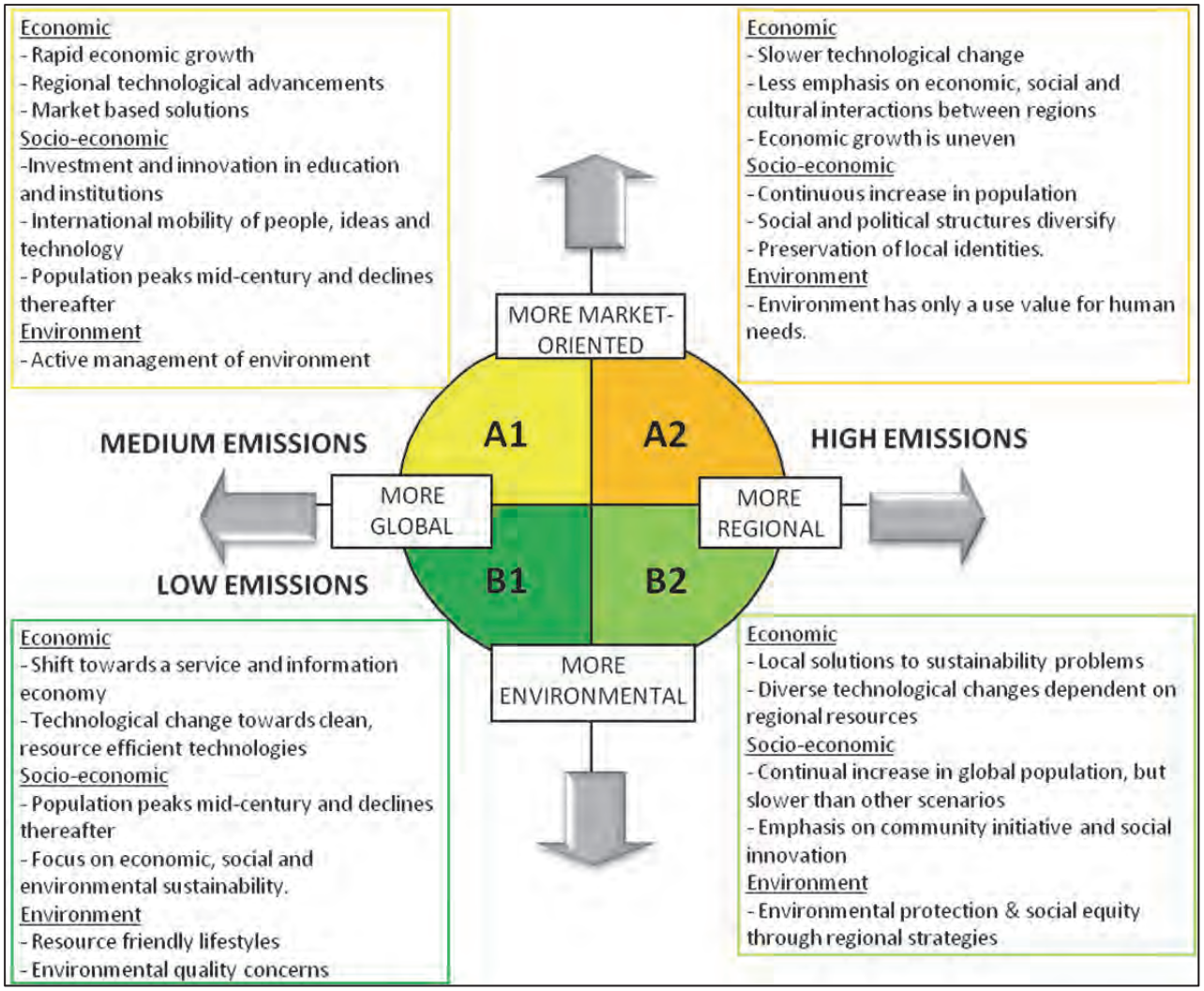

Figure 2: SRES scenarios (after the Special Report on Emissions Scenarios, Nakićenović *et al.*, 2000)

The GCMs used in this project were derived from an earlier Coupled Model Inter-comparisons Project Phase 3 (CMIP3) archive. This archive contains simulations of the historic and future climate from multiple different GCMs run by the world's leading climate modelling institutes. The simulations were run for the historic period using the observed greenhouse gas concentrations and then continued into the future using greenhouse gas concentrations based on the A2 emissions scenario.

Daily climate values from future climate change projections were obtained from CSAG in both grid and point formats. In order to apply these values from the climate projections in hydrological impacts assessment, techniques had to be developed to represent the projections at the scale of catchments, rather than at grid or point scales. Point scale climate change projections were used in this project.

4.2 Description of point scale climate change projections

The point scale climate change projections developed by CSAG and used in this project were derived from global scenarios produced by four GCMs, all of which were applied in the IPCC's (2007) Fourth Assessment Report (AR4). In Table 4, the names of the GCMs, the institutes which developed them, the year of the first publication of results from each model and links to further information are given.

The point scale climate change projections were generated by empirically downscaling the GCM simulation output. The points at which projections were produced were the locations of the climate stations used in the empirical downscaling process. Projections of daily rainfall were produced at 2,642 southern African stations (Figure 4), while daily maximum and minimum temperature projections were produced at 440 and 427 stations, respectively (Figure 5).

The number of years considered in the present climate when comparing this period to the other climate projections was a consistent 20 years for all climates. The period 1971-1990 was selected for the present climate. The periods considered in comparative analyses in this report were therefore:

- present climate: 1971-1990
- intermediate future climate: 2046-2065
- distant future climate: 2081-2100.

4.3 Methodology to Represent Point Scale Projections of Rainfall at the Scale of Quinary Catchments

The representation of the point scale projections of rainfall at the scale of Quinary catchments was achieved using the same "driver" station approach adopted for baseline historical conditions. The number of driver stations previously selected for baseline conditions and for which values for future rainfall projections were also available, was determined to be 1,023 (from the set of 2,642 possible stations). These driver stations were assumed to represent future climatic conditions in their associated Quinary Catchments, which numbered 4,863. For the remaining 975 Quinary Catchments (out of the total of 5,838 covering southern Africa) alternative driver stations for which future rainfall projections were available needed to be selected. The criteria used to re-select these driver stations were:

- Distance from the Quinary Catchment's centroid;
- Mean annual precipitation compared with that of observed data;
- Altitude difference between the station and the mean Quinary altitude;
- Length of the observed record; and
- Reliability of the observed record.

Table 1: Information on GCMs used in this project

Institute	GCM	Abbreviation in this report
Canadian Center for Climate Modelling and Analysis (CCCma), Canada	**Name:** CGCM3.1(T47) **First published:** 2005 **Website:** http://www.cccma.bc.ec.gc.ca/models/cgcm3.shtml	**CCC**
Meteo-France/Centre National de Recherches Meteorologiques (CNRM), France	**Name:** CNRM-CM3 **First published:** 2004 **Website:** http://www.cnrm.meteo.fr/scenario2004/indexenglish.html	**CRM**
Max Planck Institute for Meteorology (MPI-M), Germany	**Name:** ECHAM5/MPI-OM **First published:** 2005 **Website:** http://www.mpimet.mpg.de/en/wissenschaft/modelle.html	**ECH**
Institut Pierre Simon Laplace (IPSL), France	**Name:** IPSL-CM4 **First published:** 2005 **Website:** http://mc2.ipsl.jussieu.fr/simules.html	**IPS**

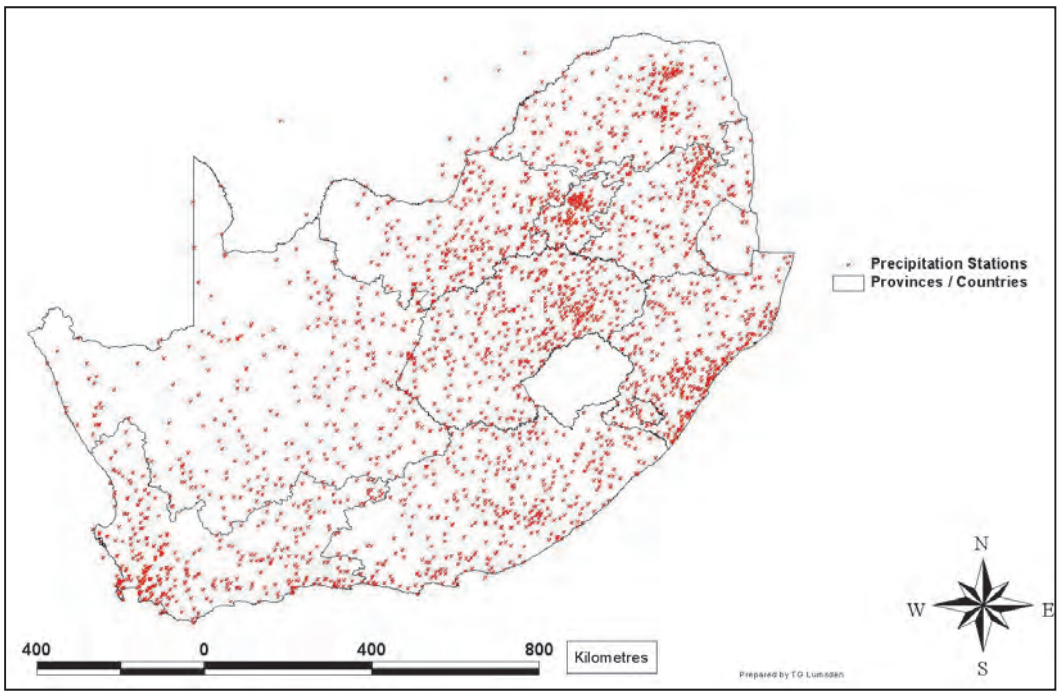

Figure 3: Climate stations for which point scale climate change projections for daily rainfall were developed

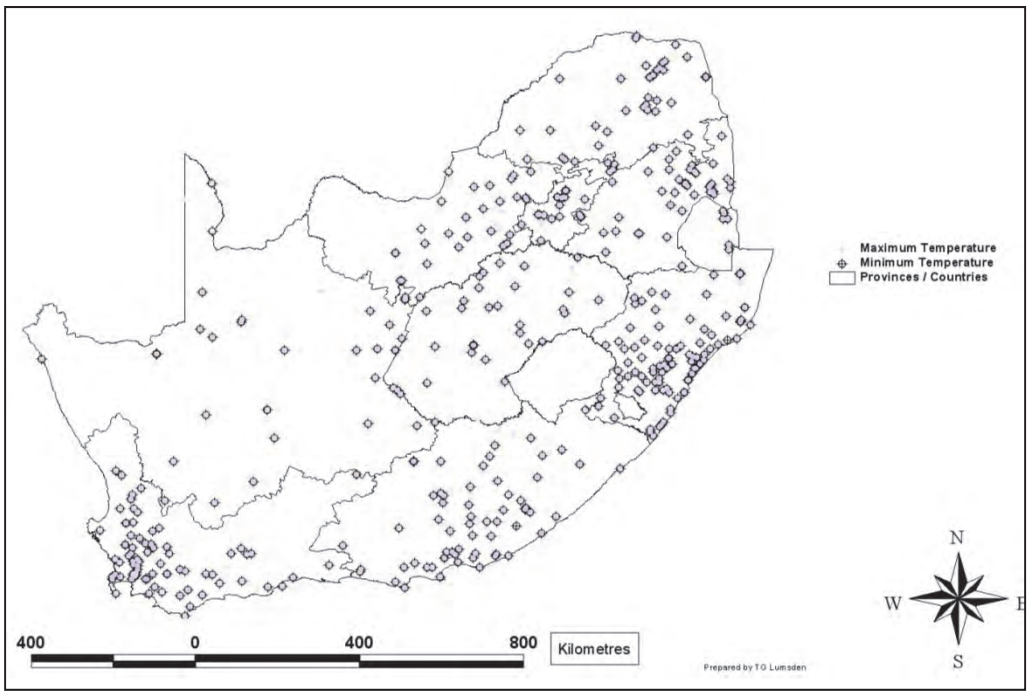

Figure 4: Climate stations for which point scale climate change projections for daily temperature were developed

Of the above 975 Quinaries, 687 were assigned to stations that already acted as driver stations for other catchments. The number of driver stations concerned numbered 134. The remaining 288 Quinaries were assigned to stations that had not previously been used as driver stations. This resulted in 38 new driver stations being selected. The total number of all rainfall driver stations used in assessing future rainfall impacts therefore numbered 1,061 (i.e. 1,023 + 38).

As was the case for the baseline historical climate, the daily rainfall values for the above 1,061 driver stations were adjusted to better represent the rainfall of each Quinary Catchment, resulting in the development of a unique representative rainfall record for each Quinary. This was done on the assumption that the monthly adjustment factors calculated for the baseline historical climate would also be applicable under the GCM derived climates considered (present, intermediate future and distant future). This assumption was made in the absence of fine resolution (e.g. one arc minute) national grids of median monthly rainfall for these new climate periods which would ideally have been required if adjustment factors specific to the periods were to have been calculated. In the calculation of the adjustment factors for the baseline historical climate, limits were placed on the magnitude of the adjustment factors to prevent unrealistic adjustments being made to the driver station data. These limits ensured that adjustment factors fell between 0.5 and 2.0. These limits were relaxed relative to previous studies (e.g. Schulze *et al.*, 2005; Schulze, 2007) where the factors were constrained to be between 0.7 and 1.3. The relaxed adjustments were deemed necessary because of the finer scale of modelling performed in this study (Quinary Catchments) relative to previous studies (Quaternary Catchments). Quaternary Catchment driver stations are now assumed to drive their component Quinary Catchments, which are often distinctly different from one another in their topographic characteristics.

4.4 Methodology to Represent Point Scale Projections of Temperature at the Scale of Quinary Catchments

An examination of the climate stations for which projections of temperature change were obtained from CSAG revealed that there were 425 stations which both had maximum and minimum temperature data sets. Of these 425 stations, 21 had immediately adjacent ‘twin’ stations with identical geographical coordinates (i.e. the same station, but reporting to two different data agencies). Since only one station at a particular location could be considered for application in hydrological modelling, the quality of the historical (observed) records of the 42 (21 x 2) implicated stations were analysed to identify the ‘better’ station at each location. This therefore resulted in 404 unique stations being identified for representation of maximum

and minimum temperatures in the 5,838 Quinary Catchments across South Africa, Lesotho and Swaziland.

The methodology adopted to represent maximum and minimum temperatures at Quinary Catchment scale involved selecting the two most representative stations for each Quinary Catchment, and obtaining a daily weighted average of their data. Adjustments were simultaneously applied to each of the two stations' data to account for differences between the stations' altitudes and that of the respective Quinary. This was done using the adiabatic temperature lapse rates (i.e. the rate of change of temperature with altitude) which had been determined for each month of the year, and separately for maximum and minimum temperatures, by Schulze and Maharaj (2004) for 12 defined lapse rate regions in southern Africa (Schulze, 1997). Only temperature stations falling within the specific lapse rate region relevant to a particular Quinary Catchment were considered for representation of temperature in that catchment. In certain lapse rate regions some stations were excluded from consideration based on altitude related criteria.

The algorithm to select the two most representative stations for a Quinary Catchment represented a modification of the algorithm developed in Schulze and Maharaj (2004) for selecting target stations for infilling of missing data at representative control stations (control stations were used in the generation of the 1 arc minute resolution daily maximum and minimum temperature grid for South Africa, Lesotho and Swaziland). The modified algorithm involved performing a preliminary suitability ranking of all stations considered in order to determine the five most suitable stations. This suitability ranking was sensitive to the distance of a station from the centroid of a catchment, together with the difference in altitude of the station relative to the catchment's mean altitude. A final suitability ranking of the five stations identified above was then performed to determine the 'best' two stations in terms of both distance and altitude. Having identified the two 'best' temperature stations to represent a Quinary Catchment, the data from these stations were then averaged in order to obtain the final temperature record for the catchment.

5 LIMITATIONS IN THE APPROACH AND MODELS

This section briefly describes the limitations in terms of climate data and the two modelling packages used.

Limitations in terms of climate data

As described in the section below, there are various uncertainties and limitations in terms of projected climate change values. The models used vary due to their differing approaches to parameterization of finer-scale processes than allowed for in the model. The availability of climate data is also a limitation, as the large-scale model results take a significant amount of time to be processed to an appropriate scale, and the processing through the ACRU model further takes time. The most updated results that were available at the start of the project were therefore used in the project.

GCMs are considered to be skilful at reproducing large-scale weather patterns, but not climate change at the finer scales required for identification of impacts and adaptation actions. The two different types of GCM downscaling (dynamical and empirical/statistical), inherently have their own limitations. The process of downscaling assumes that the local-scale climate is largely a function of the large-scale climate modified by some local forcing such as topography, distance to water bodies, etc. This project made use of statistical downscaling, which utilises a statistical technique. The technique used is called Self-Organizing Map based Downscaling (SOMD), and was developed at the CSAG. This is a leading downscaling technique for Africa and provides meteorological station level (or gridded) response to global climate change forcing (See Hewitson and Crane (2006) for methodological details and Wilby *et al.* (2004) for a review of this and other statistical downscaling methodologies).

The following explanation is provided by CSAG:
"downscaling of a GCM is accomplished by deriving the normative local response from the atmospheric state on a given day, as defined from historical observed data. The method recognises that the regional response is both stochastic as well as a function of the large scale synoptics. As such, it generates a statistical distribution of observed responses to past large-scale observed synoptic states. These distributions are then sampled based on the GCM generated synoptics in order to produce a time series of GCM downscaled daily values for the variable in question (in this case temperature and rainfall). An advantage of this method is that the relatively unskilled grid scale GCM precipitation and surface temperature

are not used by the downscaling but rather the relatively highly skilled large scale circulation (pressure, wind and humidity) fields are employed."

Uncertainty in climate change implies uncertainty in understanding of the underlying climate system, and does not imply uncertainty in terms of science with regard to the fundamental physics and dynamics of climate change. The understanding of human-induced greenhouse gas emissions resulting in increasing surface temperatures is robust. The uncertainty is introduced around the reflection of this understanding at a particular location, and is a function of various factors and hence as spatial scales become progressively finer, the range of possible responses increases. Sources of uncertainty in downscaled climate projections include:

- Natural variability;
- Future emissions;
- Uncertainty in the science (e.g. thresholds);
- Structural uncertainty; and
- Data uncertainties.

Despite advances in the development of improved methodologies, some proportion of uncertainty will always remain. It is therefore best to understand the possible range of projected change as a probability using the ensemble/envelope approach as mentioned above.

Limitations in terms of the QUAL2K model

The QUAL2K model inherently exhibits some limitations to its application as a management tool. Due to non-steady state conditions in the catchment, the specific use and physical characteristics of the river and the difficulty in determining flow, the usefulness of a steady-state stream water quality model as a management tool is limited.

A good river water quality model management tool should have the following requirements (Golder Associates, 2009):

Non-steady-state

It is necessary to use a truly dynamic model capable of accepting variations in temporal inputs of the inflow water quality, which are used to compute associated output responses downstream. This is essential to:

- Effectively employ the time series of flow and water quality data to achieve reliable calibration; and
- Represent the full range of dynamically changing conditions when evaluating options, including algal and macrophyte growth as water is transported down the river system.

User-friendly

The model should be as simple as possible to use, while retaining the ability to adequately characterize the important aspects of the system behaviour. It should provide more guidelines for the numerous various rates to facilitate use by non-expert users. To a large extent QUAL2K fulfils this requirement, although for a complex problem like eutrophication skilled expertise will always be required for model calibration and to interpret the results.

Non-Deterministic model

A deterministic model produces a single prediction, rather than a range of possible predictions. A model to be used as a management tool need not be deterministic, if the modelling effort includes an analysis of prediction uncertainty. Therefore it should account for both the uncertainty associated with sampling and laboratory analysis and for the uncertainty associated with imprecise knowledge of the different rates. Moreover, the use of percentiles is more and more required during the decision making process.

QUAL2K effectively fulfils all of the above requirements, with the exception that it cannot yet model dynamic conditions.

Limitations in terms of the CE-QUAL-W2 model

Several limitations exist in the CE-QUAL-W2 modelling component of the study and the major ones are listed below:

- The CE-QUAL-W2 model is laterally averaged and therefore does not account for any variation in the lateral direction
- Although literature quoted values are used for maximum algal growth rates, temperature rate multipliers and half saturation constants, there is still inherent uncertainty present in the selected values.
- The windspeed and wind direction was not readily available from the provided downscaled data and a representative year's data was repeated for the 20 year simulations
- Simulated inflow information to the dams, under climate change conditions, were not readily available and present day inflows were used instead.

6 STAKEHOLDER CONSULTATION PROCESS

Two stakeholder workshops were held in each of the case study areas. The first stakeholder workshop for the Vaal River area was held at the Midvaal Water Company in the Klerksdorp District, North West Province, on 24 August 2011, and the second at the same venue on 29 March 2012. Both meetings in the Western Cape were held at DWA Western Cape regional office on 27 September 2011 and 5 April 2012.

A full list of stakeholders is provided in Appendix A. Full proceedings were compiled following each meeting, with the key findings listed below.

6.1 Vaal River System Stakeholder Meeting 24 August 2011

- The Vaal River System is a highly impacted system, and it is difficult to assess the impacts attributable to climate change as opposed to the other numerous factors affecting the system;
- It was recommended that the modelling process take a scenario-based approach that can simulate not only climate change projections, but various management interventions as well;
- It is important that the “chain of impacts” are addressed during this project, i.e. that the consequences of climate change impacts in terms of eutrophication on ecology, human health and water quality are assessed and that feasible management interventions may be recommended;
- Strong collaboration with experts in the field is necessary.

6.2 Berg River Stakeholder Meeting 27 September 2011

- A scenario-based approach for the modelling of water quality under climate change conditions in Voëlvlei Dam was recommended. This approach would allow for the assessment of the effect of future management options as well climate change on water quality;
- The assessment of potential water quality changes in Theewaterskloof Dam and the Berg River Dam (BRD) under climate change conditions may be required for the development of effective management strategies in the future;
- The BRD was also included as a case study for the current project, as it was expected to remain unimpacted, and would therefore serve as a reference case. However, the

potential impact of nutrient-enriched inflows from the supplement scheme under climate change conditions could be evaluated and included as an additional scenario.

6.3 Vaal River System Stakeholder Meeting 29 March 2012

- The preliminary results were received positively, and useful discussion was held regarding the various parameters and their effects on eutrophication, as well as how these could be further investigated, including focus on:
  - Dissolved oxygen;
  - Flow;
  - Sensitivity analysis; and
  - Uncertainty.
- The next stage of the project was discussed, including the impacts of climate change-related increases in eutrophication on fish, other animal species and humans, which mainly related to Yellowfish as an indicator species, domestic users (public perception), recreation, farming and water treatment works.

6.4 Berg River Stakeholder Meeting 5 April 2012

- The second meeting with the stakeholder stressed the importance of finding a strategy to successfully reduce the nutrient loads from the Kleinberg River without negatively impacting on the yield of the Dam;
- Quantification of uncertainty of results is considered important for water resources managers and an attempt to provide first order quantification should be considered for the project; and
- It is important to maintain unimpacted inflows to the Berg River Dam as far as possible, as this should ensure that problems with nuisance algal growth will not be experienced in future.

Interactions with stakeholders attending the Vaal River stakeholder workshop were positive. Although not all stakeholders felt that the impacts of climate change on eutrophication would be significant when compared to other impacts, the stakeholders appreciated the value of the project and were willing to participate in the development of project concepts and the provision of data.

The stakeholder meeting with the DWA WC regional office reinforced the fact that nutrient reduction at wastewater treatment plants and other discharging sources were important in

the control of eutrophication in South African dams. Failure to address the aforementioned could exacerbate eutrophication-related problems under climate change conditions. The outputs from the current project could be used to support requests to upgrade poorly functioning wastewater treatment works, and for stringent policing of discharge water quality.

7 VAAL RIVER CASE STUDY – QUAL2K MODEL

The Vaal River was selected as a case study for this project for several reasons, including existing concerns over eutrophication (Heath *et al*., 2011). The study area for this part of the project is a 280 km reach of the Vaal River extending from the Vaal Barrage (upstream), to below the confluence with the Vals River (downstream). The stretch of river is shown in Figure 6.

In this section of the river, water is released from the Vaal Barrage to provide for downstream users such as municipalities, mining industries and agriculture. The river receives heavy discharges of domestic and industrial wastewater resulting in winter blooms of algae in several sections of the river. During the 1970s there were no nutrient controls in place with resultant high effluent phosphate concentrations. The then prevalent system operating policy, which was based on quantitative water conservation only, called for the minimisation of water release from Vaal Dam. Consequently, the September winter release from the Vaal Barrage was only approximately 3 to 4 m^3/s. This resulted in effluent inputs periodically comprising a very high proportion of the low flow into and released from Vaal Barrage. The lack of dilution exacerbated downstream nutrient concentrations.

During 1978, a point source effluent 1 mg/l Special Standard for phosphate was introduced. This costly measure took some time to implement, but it has reportedly failed to reduce nutrient concentrations sufficiently to curb eutrophication. In the meantime effluent flows, and hence nutrient loads, continued to increase with development growth. In response to high salinity, the Pretoria-Witwatersrand-Vereeniging (PWV) blending option was introduced around 1988. This operating rule again called for minimising releases from the Vaal Dam, but with the proviso that if this resulted in the peak Total Dissolved Solids (TDS) concentration in the Rand Water supply exceeding the blending target (set at 300 mg/l), then less water was abstracted from the polluted Vaal Barrage intakes. The difference was then drawn directly from the fresh water stored in Vaal Dam via the Vaal Dam-Zuikerbosch canal and the Vaal Dam pipeline. This resulted in a small increase in outflows from Vaal Barrage during low flow periods.

In the early 1990s, the Vaal Barrage dilution option was implemented. This operating rule calls for larger releases of fresh water from Vaal Dam to dilute the TDS concentration in the Vaal Barrage (<600 mg/l). This option was intended to result in a supply to the Rand Water utility which was capped at 300 mg/l TDS. However, in practice, Rand Water consumers have experienced a far better water quality with a TDS virtually the same as that of Vaal

Dam. This is due to the fact that the water released from Vaal Dam must pass all of Rand Water's Vaal Barrage raw water intakes before it can dilute the Barrage. This has also resulted in a large increase in the quantity of water regularly released from Vaal Barrage, with the September Barrage flow at approximately 18 m^3/s because about a third of Rand Water's supply is returned to Vaal Barrage as effluent. The effect of this on eutrophication in the Middle Vaal is mostly beneficial. On the negative side, virtually the entire nutrient load now passes down the Vaal River, since Rand Water and other users are no longer abstracting. This has little effect on nutrient concentrations; however, it must imply an increase in the phosphate load deposited in sediments, particularly impoundments, which could have the long-term effect of prolonging the recovery time should the point source nutrient load be reduced. Phosphate leaching from the bottom sediments is expected to drive eutrophication for many years, even decades, after the upstream nutrient input has been curbed. In the short-term, this potential negative consequence is outweighed by dilution and increased flow rate, which could inhibit the growth of algae.

The Middle Vaal Water Management Area (WMA) has two points for major water suppliers. Sedibeng Water extracts water from the Vaal River downstream of the Vaal-Vals confluence at Balkfontein. The Midvaal Water Company, the main supplier to urban areas in the North West Goldfields, extracts water from the Vaal River upstream of Orkney (River Health Programme, 2003).

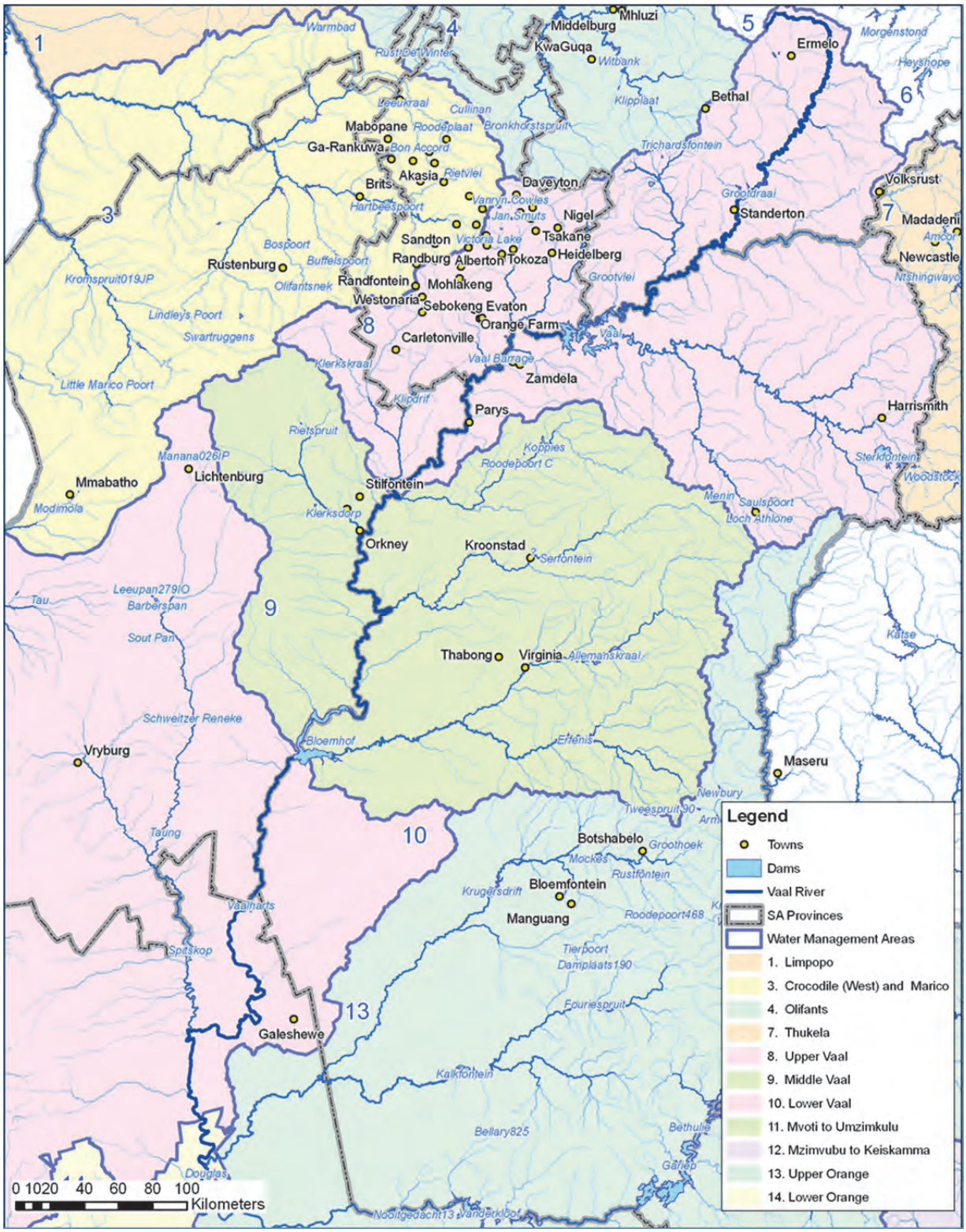

Figure 5: Location of the Vaal River

Management of eutrophication in the Middle Vaal River is of importance as eutrophication can present severe problems for the treatment of water by Rand Water, Midvaal Water and Sedibeng Water and presents a potential health threat when trihalomethanes (THMs) are

formed after chlorination. Toxic algae also present a health threat for domestic use and livestock watering. The clogging of drippers by algae hinders irrigation farming. Decaying algae and macrophytes can also cause oxygen depletion, to the detriment of fish and other aquatic life forms. Waterfowl are adversely affected by the closure of water surfaces with floating macrophytes. The presence of algae and water hyacinth is aesthetically unacceptable, impairing the use of watercraft, discolouring the water and causing taste and odour problems. The impacts of eutrophication are therefore ecological, social and economic. Infestations of alien vegetation are also found along the Vaal River (DWAF, 2009).

Erfenis, Koppies and Allemanskraal dams are classified as oligotrophic, however, toxic cyanobacterial incidents have been recorded. Bloemhof Dam is eutrophic and experiences cyanobacterial blooms usually dominated by *Microcystis* spp. and *Oscillatoria* spp. (Van Ginkel, 2004).

According to the River Health Programme (2003), the overall health of the Middle and Lower Vaal River is fair to poor. The Vaal River downstream of the Vaal Barrage is impacted upon and dominated by activities and effluent discharges from southern Gauteng. The Klip River and Blesbokspruit systems drain large areas of southern Gauteng, and are affected by urban development, mining, industrialization and farming (River Health Programme, 2003).

Factors affecting the water quality of the Upper, Middle and Lower Vaal WMAs have been identified as:

- **Urban and informal developments** – runoff and point source discharges such as sewage discharges;
- **Diamond mining operations** – sedimentation and habitat modification of the Skoonspruit and Vaal River banks;
- **Gold mining operations** – mine seepage in the Vaal River and several tributaries such as the Bamboes and Makwassie spruits; and
- **Agriculture** – abstraction from the Skoonspruit and nutrient-rich irrigation return flows at the Vaalharts scheme.

There have been recent renewed concerns over eutrophication in the Vaal Barrage and further downstream, including reported health warnings over the algal blooms in the Vaal Barrage due to toxic cyanobacterial blooms (Tempelhoff, 2012). Correspondence from concerned citizens, as well as the information centre for the Upper Vaal WMA and Rand Water (2012) indicates the following:

- An *Escherichia coli* count just below Suikerbosrant, at Klip River, at Dickenson Park and Loch Vaal Hotel area of over 1,000 Colony Forming Units (CFUs) (per 100 ml) at 29 February 2012. This implies a high risk of gastrointestinal disorders;
- A cyanobacterial count at moderate risk (45,079 cells/ml) downstream of the Rietpruit tributary and at high risk (468,198 cells/ml) at the Loch Vaal area of skin irritations, infections and intestinal disorders if ingested; and
- Chlorophyll-a concentrations greater than 30 µg/l (high risk), i.e. nuisance conditions at Dickenson Park, Baddrift Bridge, downstream of the Rietspruit and Loch Vaal.

Conditions are reportedly severely impacted in terms of suitability for recreational activities. Recommendations for the alleviation of the algal bloom are receiving political attention, and include the flushing of the Barrage through releases from the Vaal Dam. However, the potential success of such measures is uncertain.

7.1 The QUAL2K Model

A QUAL2K model was set up and verified for the Middle Vaal for the Department of Water Affairs (DWA) by Golder Associates in 2009 (Golder Associates, 2009; Figure 6). This model made use of existing water quality data made available by DWA, Rand Water, Sedibeng and Midvaal water companies. For the current project, it was proposed that the climate change projections available from the UKZN database be used as input to this model to test the effects of climate change on water quality, as the hydraulics and base data were already set up. The time period originally modelled (15 August 2005) was therefore used as the reference period for the climate change modelling exercise.

The outputs from the climate change projections were anticipated to be changes in algae (phytoplankton), water temperature and dissolved oxygen. The outputs from these projections could then be related to the response of organisms such as fish, algae and humans.

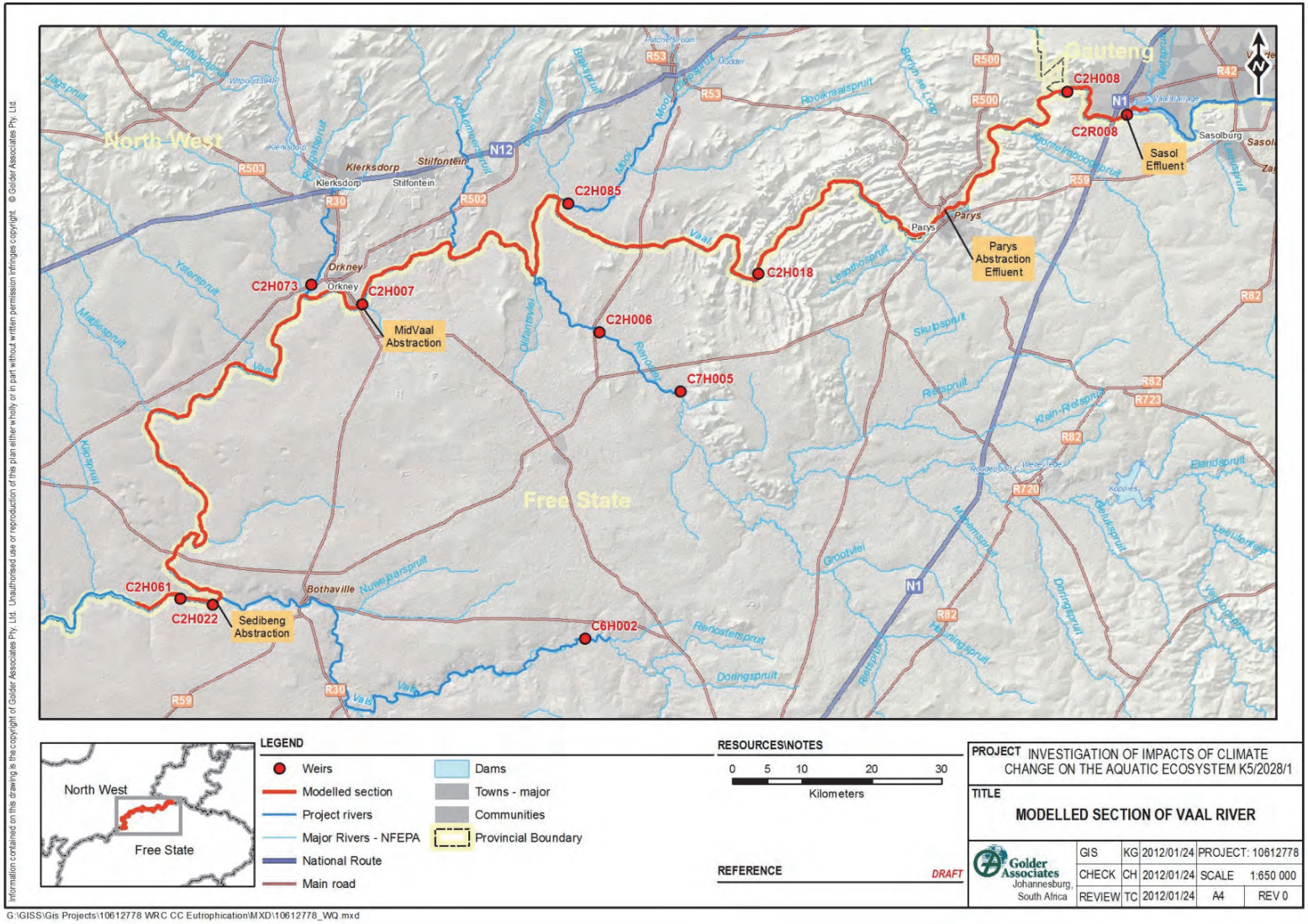

Figure 6: Section of the Vaal River studied

QUAL2K is a river and stream water quality model. The model was developed by the Department of Civil Engineering of Tufts University and the Laboratory of Environmental Research of the US-EPA, with the documentation and user manual for the model provided in Chapra *et al*. (2011). The model has gained wide acceptance due to its application and calibration to various rivers-basins in many countries around the world, which has enhanced its application potential. The model is essentially an upgrade of the QUAL2E model (Brown and Barnwell, 1987), and has the following characteristics:

- The model operates in a single dimension, with the channel being well-mixed vertically and laterally;
- Ability to accommodate branching of the river, including a main stem river with branched tributaries;
- Modelling of non-uniform, steady flow (steady state hydraulics);
- Heat budget and temperature simulated as a function of meteorological parameters on a diel time scale (daily fluctuations);
- Water quality variables simulated on a diel time scale; and
- Heat and mass inputs from point and non-point loads and withdrawals.

All interface operations of QUAL2K are programmed in Microsoft Office macro language, i.e. Visual Basic for Applications (VBA), with numerical calculations implemented in Fortran 90 for speed of execution. Microsoft Excel is used as the graphical user interface. New features of QUAL2K (as opposed to QUAL2E) include the following aspects which are pertinent to this project:

- Two types of carbonaceous BOD speciation (slow and fast oxidising) to represent organic carbon;
- Anoxia;
- Sediment-water interactions of dissolved oxygen and nutrients;
- Bottom algae; and
- Light extinction.

Segmentation and hydraulics

QUAL2K represents the river as a series of reaches which have constant hydraulic characteristics (slope, bottom width, etc.). As shown in

Figure 7, the reaches are numbered in ascending order from the headwater of the main stem. Both point and non-point source and withdrawals can be positioned anywhere along the channel's length. For systems with tributaries, reaches are numbers in ascending order continuing at the various tributary's headwater (Figure 8).

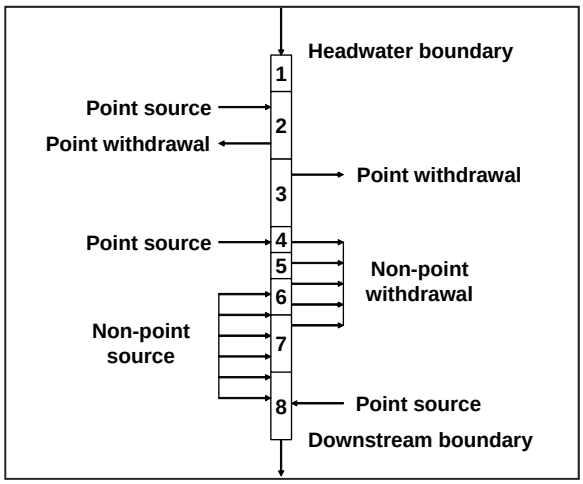

Figure 7: QUAL2K segmentation scheme for a river with no tributaries (Chapra *et al*., 2011)

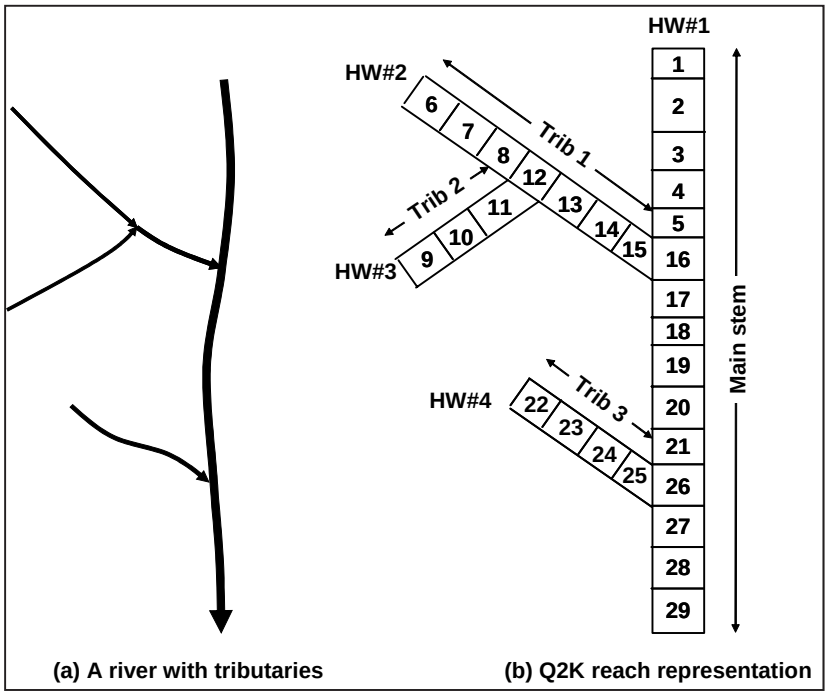

Figure 8: QUAL2K segmentation scheme for (a) a river with tributaries. The QUAL2K reach representation in (b) illustrates the reach, headwater and tributary numbering schemes (Chapra *et al*., 2011)

Each reach is subdivided equally into a number of segments or computational **elements** of equal length.

Flow balance

A steady-state flow balance (

Figure 9) is implemented for each model element, as:

$$Q_i = Q_{i-1} + Q_{in,i} - Q_{out,\,i} - Q_{evap,i}$$

Where:

- Q_i = outflow from element *i* into downstream element *i* + 1 [m^3/d];
- Q_{i-1} = inflow from the upstream element *i* – 1 [m^3/d];
- $Q_{in,i}$ = total inflow into the element from point and non-point sources [m^3/d];
- $Q_{out,\,i}$ = total outflow from the element due to point and non-point withdrawals [m^3/d]; and
- $Q_{evap,i}$ = outflow due to evaporation [m^3/d].

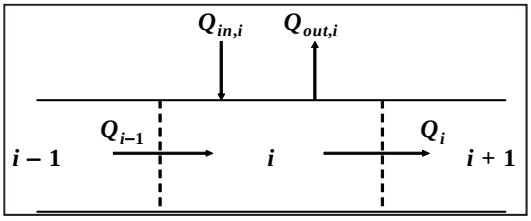

Figure 9: Element flow balance (Chapra *et al*., 2011)

The original QUAL2K model used for the 2009 modelling exercise did not include evaporation due to the fact that the model was developed in North America where evaporative losses are less of a concern. Professor Steven Chapra, the developer of the model, was asked by the project team to add this functionality to the model, which was done. Although the flow balance includes evaporative water losses, it should be noted that these are not computed, but must be specified as an optional input by the user in the reach worksheet.

Once the outflow for each element is computed, the depth and velocity are calculated in one of three ways:

- Weirs;
- Rating curves; or
- Manning equations (default).

When using the Manning equation, each element in a reach can be idealised as a trapezoidal channel. Under steady conditions, the Manning equation can be used to express the relationship between flow and depth as:

$$Q = \frac{S_0^{1/2}}{n} \frac{A_c^{5/3}}{P^{2/3}}$$

Where:

- Q = flow [m^3/s];
- S_0 = bottom slope [m/m];
- n = the Manning roughness coefficient;
- A_c = the cross-sectional area [m^2]; and
- P = the wetted perimeter [m].

Temperature Model

The heat balance takes into account heat transfers from adjacent elements, loads, withdrawals, the atmosphere and sediments, as illustrated in Figure 10.

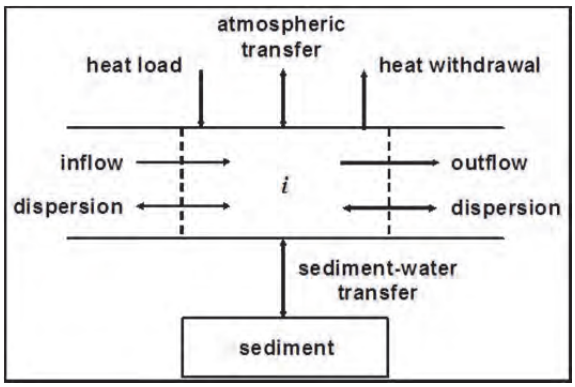

Figure 10: Heat balance in a reach segment "i" (Chapra *et al*., 2011)

Surface heat exchange is modelled as depicted in Figure 11.

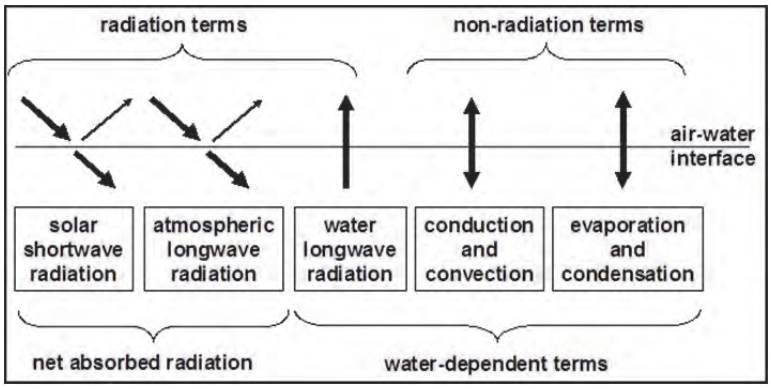

Figure 11: The components of surface heat exchange (Chapra *et al*., 2011)

QUAL2K computes the amount of solar radiation entering the water at a particular latitude (Lat) and longitude (Llm) on the earth's surface. This quantity is a function of the radiation at the top of the earth's atmosphere which is attenuated by atmospheric transmission, cloud cover, reflection, and shade.

Constituent Model

The constituent and general mass balance takes into account the sources and sinks of the constituent due to reactions and mass transfer mechanisms. The model constituents are listed in Table 2 below.

Table 2: Model state variables (Chapra *et al*., 2011)

Variable	Symbol	Units*
Conductivity	s	µmhos
Inorganic suspended solids	m_i	mgD/L
Dissolved oxygen	o	mgO_2/L
Slowly reacting CBOD	c_s	mgO_2/L
Fast reacting CBOD	c_f	mgO_2/L
Organic nitrogen	n_o	µgN/L
Ammonia nitrogen	n_a	µgN/L
Nitrate nitrogen	n_n	µgN/L
Organic phosphorous	p_o	µgP/L
Inorganic phosphorous	p_i	µgP/L
Phytoplankton	a_p	µgA/L
Phytoplankton nitrogen	IN_p	µgN/L
Phytoplankton phosphorous	IP_p	µgP/L
Detritus	m_o	mgD/L
Pathogen	X	cfu/100 mL

Variable	Symbol	Units*
Alkalinity	*Alk*	$mgCaCO_3/L$
Total inorganic carbon	c_T	mole/L
Bottom algae biomass	a_b	mgA/m^2
Bottom algae nitrogen	IN_b	mgN/m^2
Bottom algae phosphorous	IP_b	mgP/m^2

* mg/L ≡ g/m^3; In addition, the terms D, C, N, P, and A refer to dry weight, carbon, nitrogen, phosphorous, and chlorophyll *a*, respectively. The term cfu stands for colony forming unit which is a measure of viable bacterial numbers.

The mass balance is graphically illustrated in Figure 12.

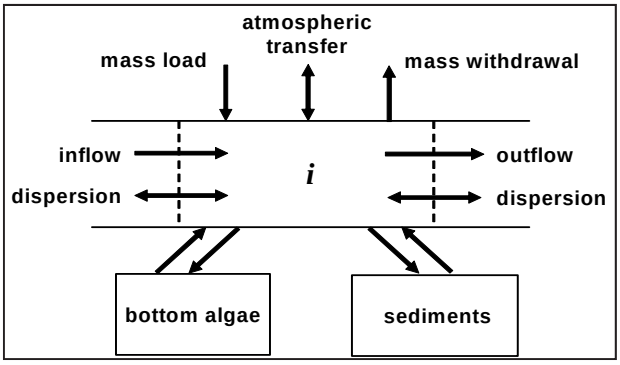

Figure 12: Mass balance for constituents in a reach segment "i" (Chapra *et al*., 2011)

Kinetic processes included in the model include dissolution, hydrolysis, oxidation, nitrification, denitrification, photosynthesis, respiration, excretion, death, and respiration/excretion. Mass transfer processes include reaeration, settling, sediment oxygen demand, sediment exchange and sediment inorganic carbon flux.

7.2 Time period studied

The modelled time period in QUAL2K is critical due to the limitation to steady-state flow and the availability of data. The main criteria involved in the selection process for the original modelling set up were:

- Relatively uniform flow for as many months as possible, therefore restricted to winter months and avoidance of years when winter flows vary considerably;
- Periods when algal blooms appear, which tend to occur towards the end of winter;
- Availability and quality of flow and quality data for the various tributaries and point discharges; and

- Availability and quality of flow and quality data along the Vaal River necessary to calibrate the model.

The availability of chlorophyll-a data (point 4) proved to be the most severe limitation, which confined the choice to the most recent years. This type of data was also measured sporadically for earlier studies, but the condition of steady state flow did not pertain. The time period 1 August 2005-31 August 2005 was selected as representative of the winter flow period.

Data was drawn from numerous sources, and data from several years had to be examined before a period complying with the criteria could be found. This serves to demonstrate how difficult the acquisition of input data is, and highlights the need to consistently monitor the required water quality variables.

7.3 **Model setup**

The first step in modelling the system for the initial exercise (based on 2005 data) was to divide the river into reaches, which are stretches of the river having uniform hydraulic characteristics. Therefore, the following factors were taken into account:

- channel width;
- elevation; and
- presence of a weir.

The weir positions were obtained from the DWA website. Due to lack of information, elevations and widths were extracted from Google Earth. Figure 13 shows the channel elevation, width and weir location in longitudinal section. This plot was used to define the various reaches. For the purpose of this study, this section of the Vaal River was divided into a total of 19 river reaches

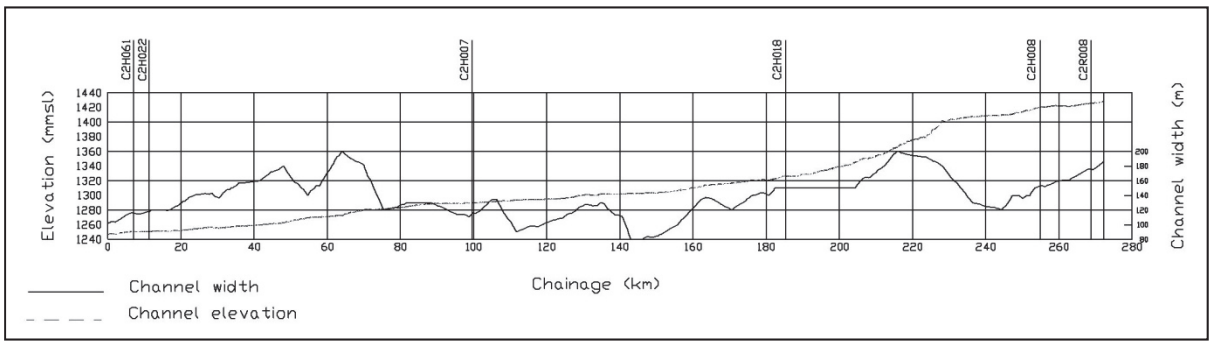

Figure 13: Channel elevation, width and weir location for the studied area

Once the segmentation was completed, the hydraulic information was entered into QUAL2K. The headwater, tributary, incremental flows and wastewater discharge concentrations were then entered to simulate mass loads of the various constituents. A schematic of the modelled river is presented in Figure 14, showing the reaches and various discharge and abstraction points. For each arrow indicated, information on flows and water quality was entered.

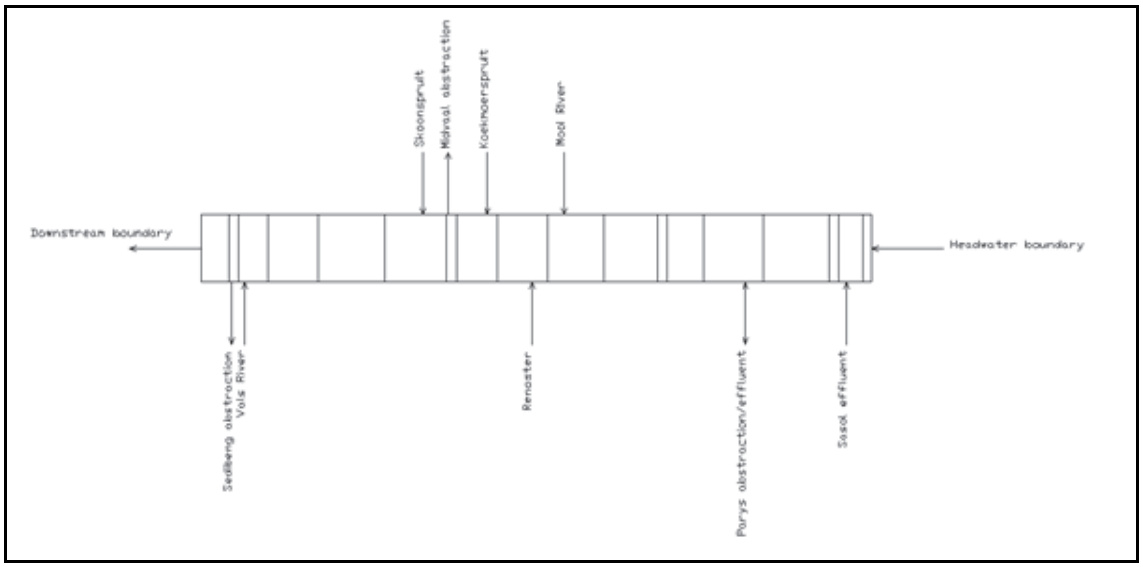

Figure 14: Schematic representation of the modelled river and its reaches

7.4 Model calibration

Application of the QUAL2K model should be carried out in conjunction with a field sampling and laboratory measurement program. Such a program is essential for the identification of the model parameter values and for initial prediction to ensure the forecasting accuracy of the model. In the absence of such a program, the various model rates were taken within the ranges given by a number of literature sources including an EPA guidance document (Bowie *et al*., 1985), the QUAL2K manual (Chapra *et al*., 2007) and Park and Lee (2002). Values used during calibration are given in Table 3. These were adjusted during calibration.

Table 3: Calibrated system parameters for stoichiometry and rates for inorganic suspended solids and oxygen, assuming a fixed stoichiometry of plant and detrital matter

Parameter	*Value*	*Units*	*Symbol*
Stoichiometry:			
Carbon	**40**	**gC**	**gC**
Nitrogen	**7.2**	**gN**	**gN**
Phosphorus	**1**	**gP**	**gP**
Dry weight	**100**	**gD**	**gD**
Chlorophyll	**1**	**gA**	**gA**
Inorganic suspended solids:			
Settling velocity	**0**	**m/d**	v_i
Oxygen:			
Reaeration model	**Internal**		
User reaeration coefficient α	**0**		α
User reaeration coefficient β	**0**		β

Parameter	*Value*	*Units*	*Symbol*
User reaeration coefficient γ	**0**		γ
Temp correction	**1.024**		θ_a
Reaeration wind effect	**None**		
O2 for carbon oxidation	**2.67**	**gO_2/gC**	r_{oc}
O2 for NH4 nitrification	**4.57**	**gO_2/gN**	r_{on}
Oxygen inhib model CBOD oxidation	**Exponential**		
Oxygen inhib parameter CBOD oxidation	**0.60**	**L/mgO2**	K_{socf}
Oxygen inhib model nitrification	**Exponential**		
Oxygen inhib parameter nitrification	**0.60**	**L/mgO2**	K_{sona}
Oxygen enhance model denitrification	**Exponential**		
Oxygen enhance parameter denitrification	**0.60**	**L/mgO2**	K_{sodn}
Oxygen inhib model phyto resp	**Exponential**		
Oxygen inhib parameter phyto resp	**0.60**	**L/mgO2**	K_{sop}
Oxygen enhance model bot alg resp	**Exponential**		
Oxygen enhance parameter bot alg resp	**0.60**	**L/mgO2**	K_{sob}
Slow CBOD:			
Hydrolysis rate	**0**	**/d**	k_{hc}
Temp correction	**1.05**		θ_{hc}
Oxidation rate	**0**	**/d**	k_{dcs}
Temp correction	**1.05**		θ_{dcs}
Fast CBOD:			
Oxidation rate	**0.25**	**/d**	k_{dc}
Temp correction	**1.05**		θ_{dc}
Organic N:			
Hydrolysis	**0**	**/d**	k_{hn}
Temp correction	**1.05**		θ_{hn}
Settling velocity	**0.1**	**m/d**	v_{on}
Ammonium:			
Nitrification	**0**	**/d**	k_{na}
Temp correction	**1.05**		θ_{na}
Nitrate:			
Denitrification	**0.1**	**/d**	k_{dn}
Temp correction	**1.05**		θ_{dn}
Sed denitrification transfer coeff	**0.2**	**m/d**	v_{di}
Temp correction	**1.05**		θ_{di}
Organic P:			
Hydrolysis	**0**	**/d**	k_{hp}
Temp correction	**1.05**		θ_{hp}
Settling velocity	**0.5**	**m/d**	v_{op}
Inorganic P:			
Settling velocity	**0.07**	**m/d**	v_{ip}
Inorganic P sorption coefficient	**0**	**L/mgD**	K_{dpi}
Sed P oxygen attenuation half sat constant	**0**	**mgO_2/L**	k_{spi}
Phytoplankton:			
Max Growth rate	**0.2**	**/d**	k_{qp}
Temp correction	**1.066**		θ_{qp}
Respiration rate	**0**	**/d**	k_{rp}
Temp correction	**1.05**		θ_{rp}
Excretion rate	**0**	**/d**	k_{ep}
Temp correction	**1.05**		θ_{dp}
Death rate	**0**	**/d**	k_{dp}
Temp correction	**1.05**		θ_{dp}
External Nitrogen half sat constant	**0**	**ugN/L**	k_{sPp}
External Phosphorus half sat constant	**0**	**ugP/L**	k_{sNp}
Inorganic carbon half sat constant	**0.00E+00**	**moles/L**	k_{sCp}
Light model	**Half saturation**		
Light constant	**0**	**langleys/d**	K_{Lp}
Ammonia preference	**15**	**ugN/L**	k_{hnxp}
Subsistence quota for nitrogen	**0**	**mgN/mgA**	q_{0Np}
Subsistence quota for phosphorus	**0**	**mgP/mgA**	q_{0Pp}
Maximum uptake rate for nitrogen	**0.2**	**mgN/mgA/d**	ρ_{mNp}
Maximum uptake rate for phosphorus	**0.2**	**mgP/mgA/d**	ρ_{mPp}
Internal nitrogen half sat constant	**0**	**mgN/mgA**	K_{qNp}
Internal phosphorus half sat constant	**0**	**mgP/mgA**	K_{qPp}
Settling velocity	**0**	**m/d**	v_a
Bottom Algae:			
Growth model	**Zero-order**		
Max Growth rate	**0**	**mgA/m^2/d or /d**	C_{qb}
Temp correction	**1.066**		θ_{qb}

Parameter	*Value*	*Units*	*Symbol*
First-order model carrying capacity	**0**	**mgA/m^2**	$a_{b,max}$
Respiration rate	**0**	**/d**	k_{rb}
Temp correction	**1.05**		θ_{rb}
Excretion rate	**0**	**/d**	k_{eb}
Temp correction	**1.05**		θ_{db}
Death rate	**0**	**/d**	k_{db}
Temp correction	**1.05**		θ_{db}
External nitrogen half sat constant	**0**	**ugN/L**	k_{sPb}
External phosphorus half sat constant	**0**	**ugP/L**	k_{sNb}
Inorganic carbon half sat constant	**0.00E+00**	**moles/L**	k_{sCb}
Light model	**Half saturation**		
Light constant	**0**	**langleys/d**	K_{Lb}
Ammonia preference	**15**	**ugN/L**	k_{hnxb}
Subsistence quota for nitrogen	**0**	**mgN/mgA**	q_{0N}
Subsistence quota for phosphorus	**0**	**mgP/mgA**	q_{0P}
Maximum uptake rate for nitrogen	**1**	**mgN/mgA/d**	ρ_{mN}
Maximum uptake rate for phosphorus	**0**	**mgP/mgA/d**	ρ_{mP}
Internal nitrogen half sat constant	**0**	**mgN/mgA**	K_{qN}
Internal phosphorus half sat constant	**0**	**mgP/mgA**	K_{qP}
Detritus (POM):			
Dissolution rate	**0**	**/d**	k_{dt}
Temp correction	**1.05**		θ_{dt}
Fraction of dissolution to fast CBOD	**0.00**		F_f
Settling velocity	**0**	**m/d**	v_{dt}
Pathogens:			
Decay rate	**0**	**/d**	k_{dx}
Temp correction	**1.07**		θ_{dx}
Settling velocity	**0**	**m/d**	v_x
Light efficiency factor	**0.00**		α_{path}
pH:			
Partial pressure of carbon dioxide	**0**	**ppm**	p_{CO2}

7.5 **Input data**

For the initial modelling exercise (Golder Associates, 2009), several data sets were collected to set up and run the model including:

- Hourly temperature, wind velocity and relative humidity from Vereeniging and Klerksdorp provided by the South African Weather Service for the studied period;
- Water quantity and quality from the DWA website;
- River flow supplemented with data gathered and patched during other studies (Vaal River System Analysis Update, Vaal IWQMP, WR2005);
- Effluent discharges to Vaal and abstractions (VRSAU, Vaal IWQMP, WR2005); and
- Data on anthropogenic point sources (civil and industrial) were taken from available information supplied in current DWA reports on the Upper and Middle Vaal (DWAF 2006).

7.6 Climate change modelling exercise

The original reaches, hydraulics and parameters (Table 3) were used for the running of the 2012 climate change modelling exercise. However, due to data availability, the weather data for Vereeniging was used (as opposed to Klerksdorp as originally used) as data was available for Vereeniging for relative humidity from the South African Weather Service for the month of August 2005 (which is required for the calculation of dew point temperature). Average values for the month of August 2005 for the various hours in the day were therefore used to represent a steady state.

In terms of climate change projection values, the Vereeniging Quinary catchment (C22F3, sub_cat 1317 in ACRU database) was used as representative for the stretch of river to ensure consistency with the weather station data (see Hughes *et al*., 2011 for a full documentation on the derivation and selection of climate change projection values). The values are in the format of a text file as output from the ACRU hydrological model. The information was extracted and manipulated for input to QUAL2K, including air temperature (maximum and minimum daily), relative humidity (maximum and minimum daily) and evaporation.

Figure 15 shows a graphical representation of the air temperature at the relevant catchment under the various climate change models (refer to Section 4).

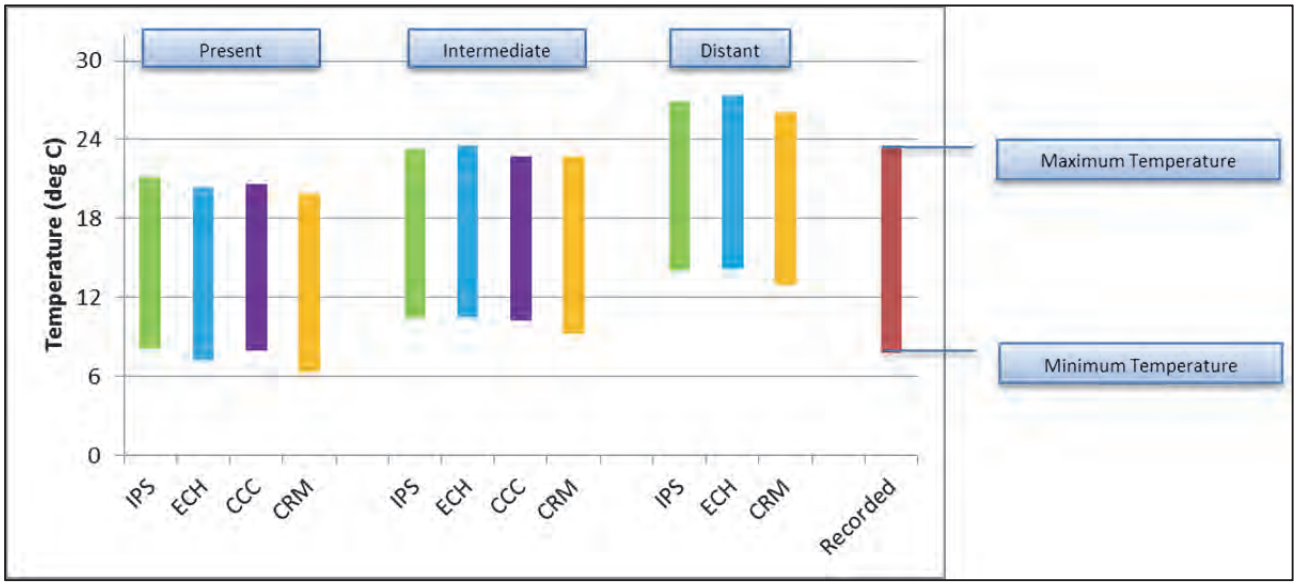

Figure 15: Recorded air temperature data in the study area, and air temperature projected for the intermediate and distant future under various climate change projections

7.7 Assumptions

A number of assumptions were made regarding data and the modelling process for the climate change modelling exercise.

- If several values were available for one site corresponding to the studied period, an average of the value was used;
- Climate change projection values from the Vereeniging quinary catchment were used for the climate change modelling exercise. Although the Vaal River study area spanned a number of quinaries, this was assumed to be appropriate for the entire stretch of river for simplicity;
- It is assumed that the abstractions and effluents used in the 2005 modelling exercise were to continue unchanged into the future. These include Sasol Effluent, Parys Effluent, Vanderbijlpark Effluent, Midvaal abstraction, Sedibeng Abstraction, Parys Abstraction, Mine Effluent, Vaal Reefs abstraction and Vierfontein abstraction. Although these are likely to change, it is uncertain how they will change into the future under climate change. It was therefore simpler to keep these values constant for the modelling exercise.

7.8 Calculation of hourly values

Hourly temperature (air and dew point) values are required for the QUAL2K model. Although recorded hourly data is available, it is necessary to calculate hourly readings for the future projections, from which only daily minimum and maximum values are available.

Hourly values were calculated using adjusted methodology described in Reicosky *et al*. (1989). A comparison between the real data (average of hourly temperatures for the month of August 2005) and those modelled using the manually adjusted formula is shown in Figure 16.

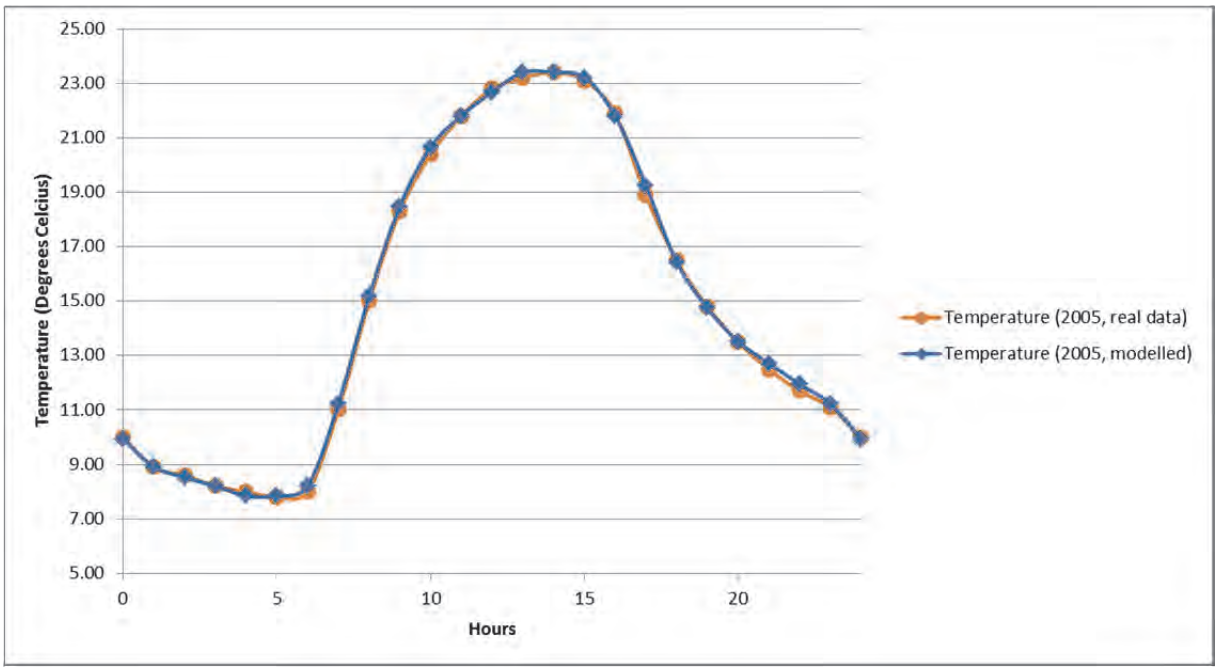

Figure 16: Comparison between recorded hourly air temperature data for August (average hourly temperatures) and modelled values

Similarly, in order to calculate dew point temperatures (which were not available from recorded data), real hourly relative humidity data was used. A comparison between the real and modelled values is shown in Figure 17. A description of the methodology used for calculation of dew point temperature is provided in Section 7.10.

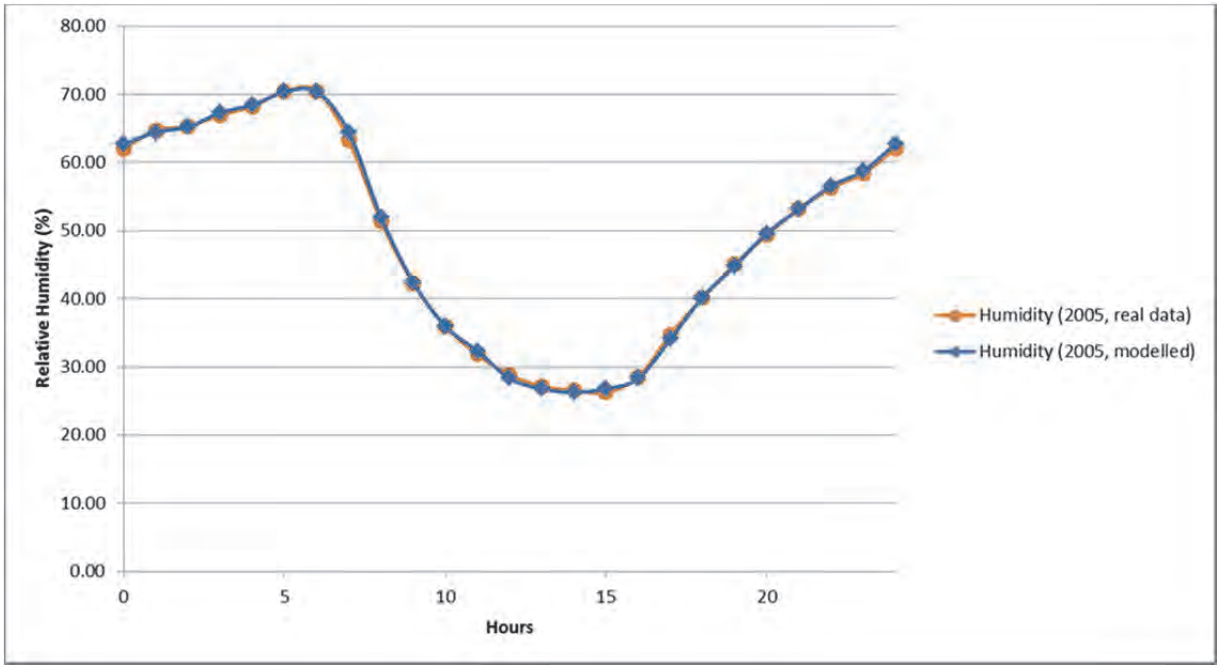

Figure 17: Comparison between recorded hourly relative humidity data for August (average hourly temperatures) and modelled values

7.9 Climate change model comparison – Temperature

For the climate change projections, modelling was carried out for the dry season (as per the original exercise), with the average of all of the months of August selected for the "intermediate future" time period (2046-2065) and the average of all of the months of August for the "distant future" time period (2081-2100).

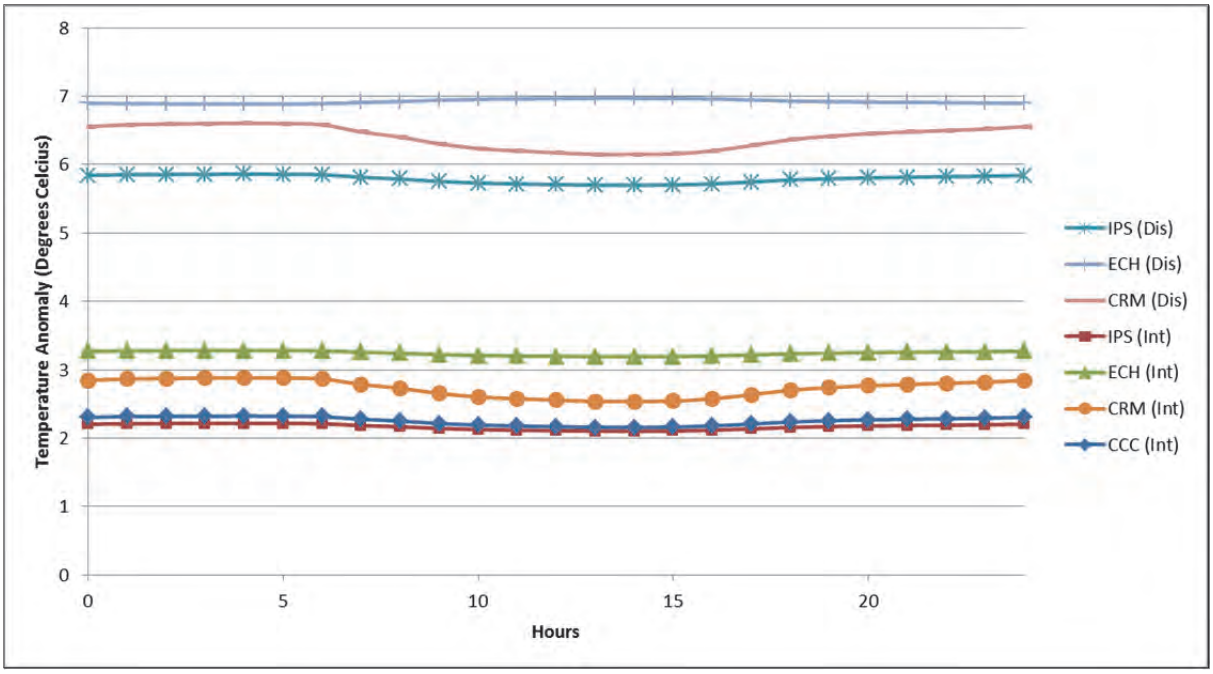

Figure 18: Anomaly between modelled present and projected intermediate future (2045-2065) and modelled present and distant future (2081-2100) hourly air temperatures for August

As shown in Figure 18, for the intermediate future, the anomaly between present modelled and intermediate modelled temperatures is between 2 and 3.5°C. For the distant future the anomaly is between 5.5 and 7°C, with the ECH model showing the largest anomaly in both cases.

7.10 Climate change model comparison – Relative Humidity

Projected relative humidity values were calculated from maximum and minimum daily values (average of August for the entire intermediate and distant future periods) to hourly values.

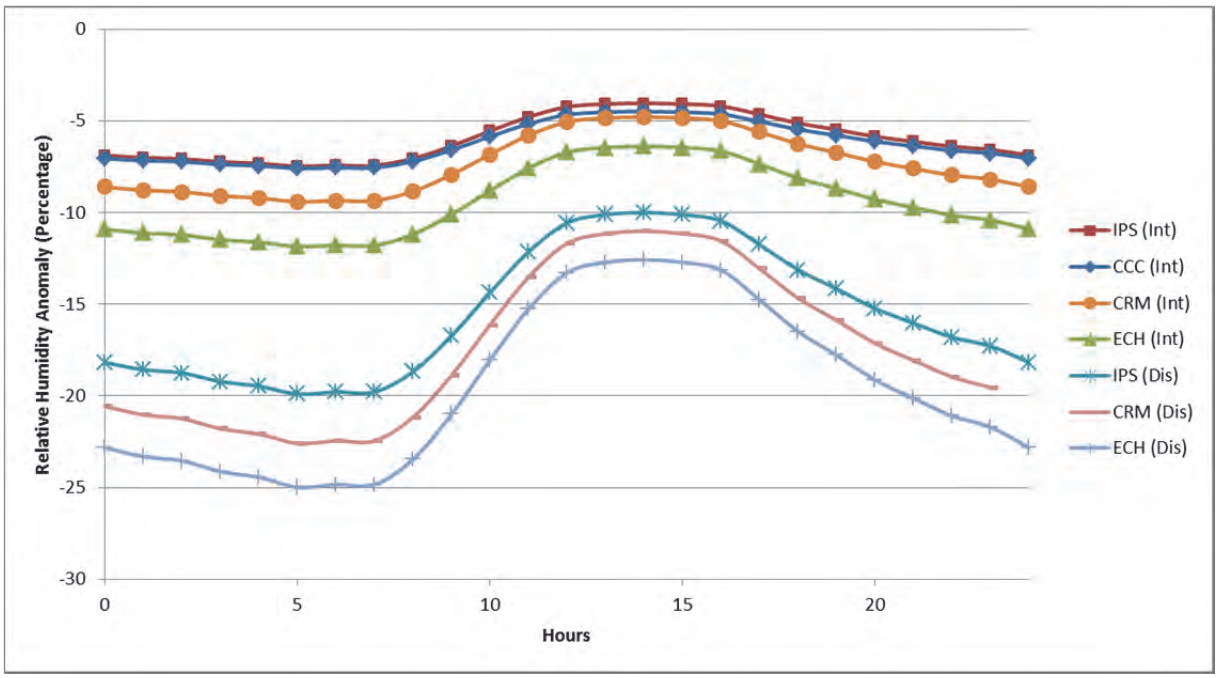

Figure 19: Anomaly between historical and projected intermediate and distant future hourly relative humidity for August

Relative humidity is projected to be lower into the future (Figure 19), with a decrease of 4 to 12 percent into the intermediate future, and between 10 and 25 percent into the distant future. The changes in relative humidity are particularly apparent during the night (i.e. non-daylight hours).

7.11 Climate change model comparison – Dew Point Temperature

Hourly dew point temperature values are also required for input to QUAL2K. Measured dew point temperature data was not available from the SAWS, and was therefore calculated based on the following formula:

$$Td = b*V/(a-V)$$

where

$$V = a*T/(b+T) + \ln(RH/100)$$

where the temperatures are in degrees Celsius. The constants are:

$$a = 17.271$$
$$b = 237.7\ °C$$

This expression is based on the Magnus-Tetens formula for the saturation vapour pressure of water in air as a function of temperature (Barenbrug, 1974). It is considered valid for

$$0°C < T < 60°C$$
$$1\% < RH < 100\%$$
$$0°C < Td < 50°C$$

The calculated dew point temperatures are illustrated in the graphs which follow.

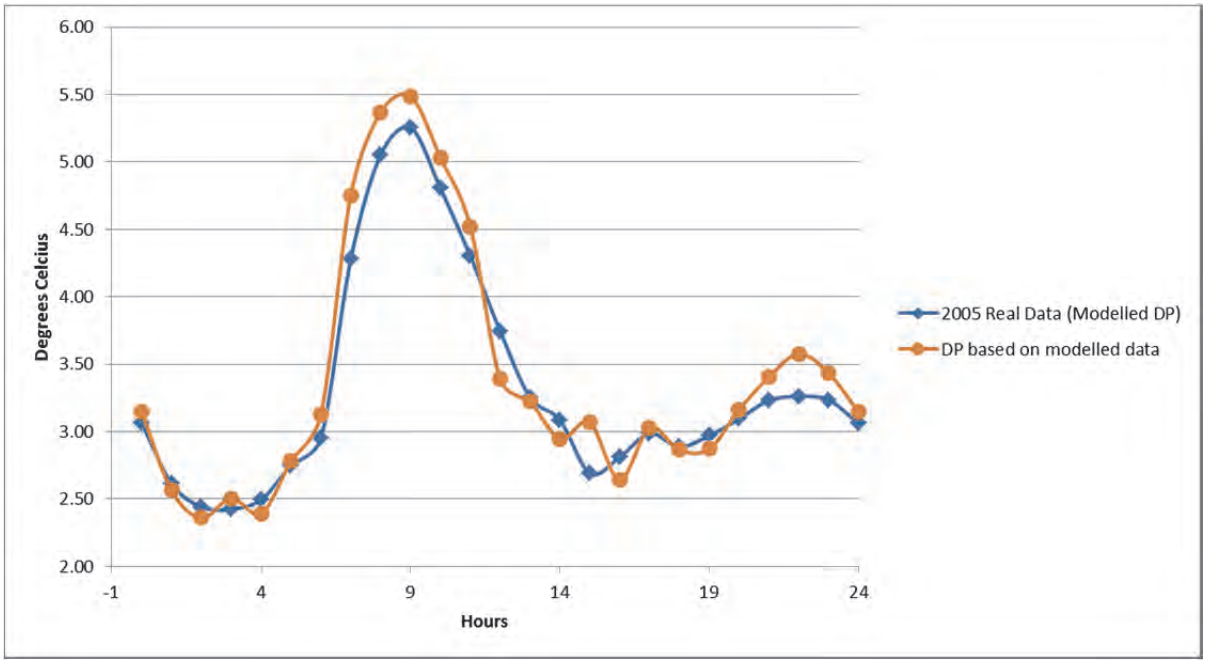

Figure 20: Comparison between calculated hourly dew point temperatures for August (average hourly temperatures) based on recorded (relative humidity and air temperature) and modelled values

Into the intermediate future (Figure 21), calculated dew point temperatures appear to be higher than those currently experienced in the Vereeniging area. The anomaly varies from 0.1°C for the intermediate future (around midday for the ECH model) and 1.7°C for the distant future (around 06h00 for the CRM model). The highest anomalies are evident around midnight.

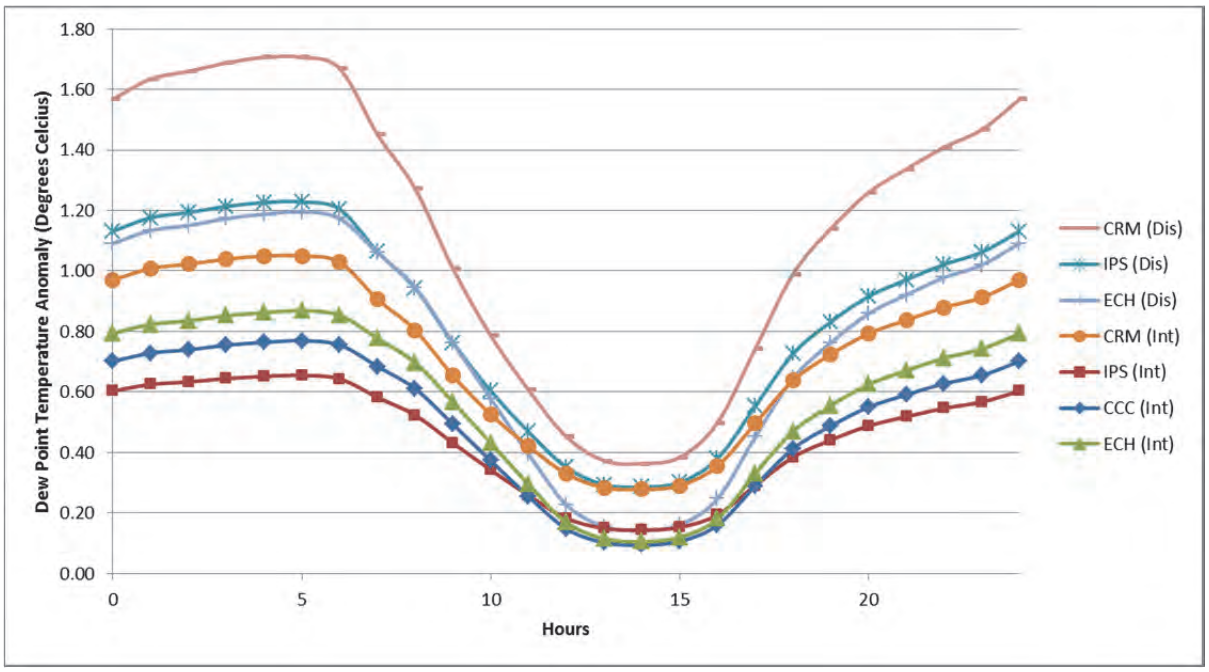

Figure 21: Comparison between calculated historical and projected future hourly dew point temperatures for August

7.12 Note on water temperature

Due to the poor availability of water temperature data, a starting water temperature for the month of August of 14°C was applied both to the Barrage and to the entry tributaries. This value was selected based on data available from Midvaal Water Company for the period under study (August 2005), and was assumed not to vary significantly along the stretch of the Vaal River (including entry points). This was a difference from the original modelling exercise. The difference between the two scenarios (starting temperature at 23°C as opposed to the revised temperature of 14°C) is illustrated in Figure 22, which shows the modelled difference in the two scenarios with a focus on phytoplankton. As anticipated, the higher starting temperature (and temperatures of point sources) leads to higher concentrations of phytoplankton, as warmer temperatures are more conducive to the growth of these organisms. This illustrates the sensitivity of phytoplankton growth to water temperatures in the model.

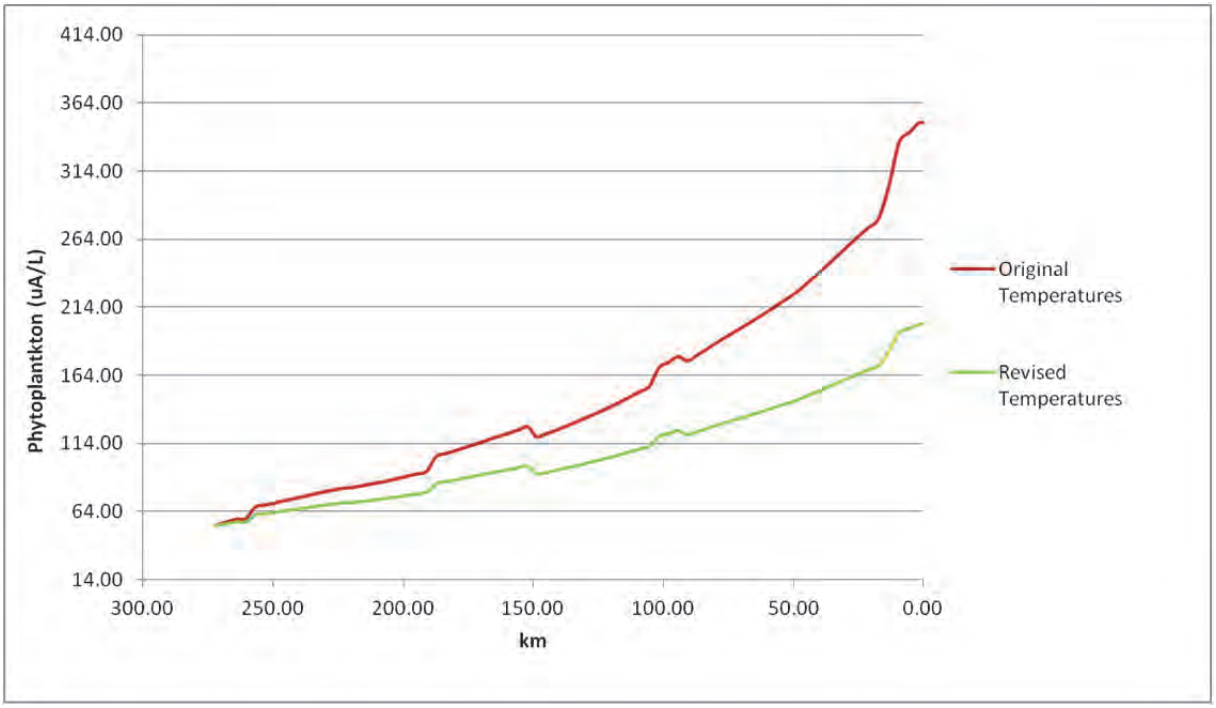

Figure 22: Comparison between modelled concentrations of phytoplankton under original (warmer) and revised temperatures

7.13 Comparison between the original model (without evaporation) and the revised model including evaporative losses

Using the original data used in the 2005 modelling exercise, the following graphs illustrate the sensitivity of the model to evaporation. As mentioned above, upon request from the project team, Professor Chapra's research group added evaporation functionality to apply to the South African situation.

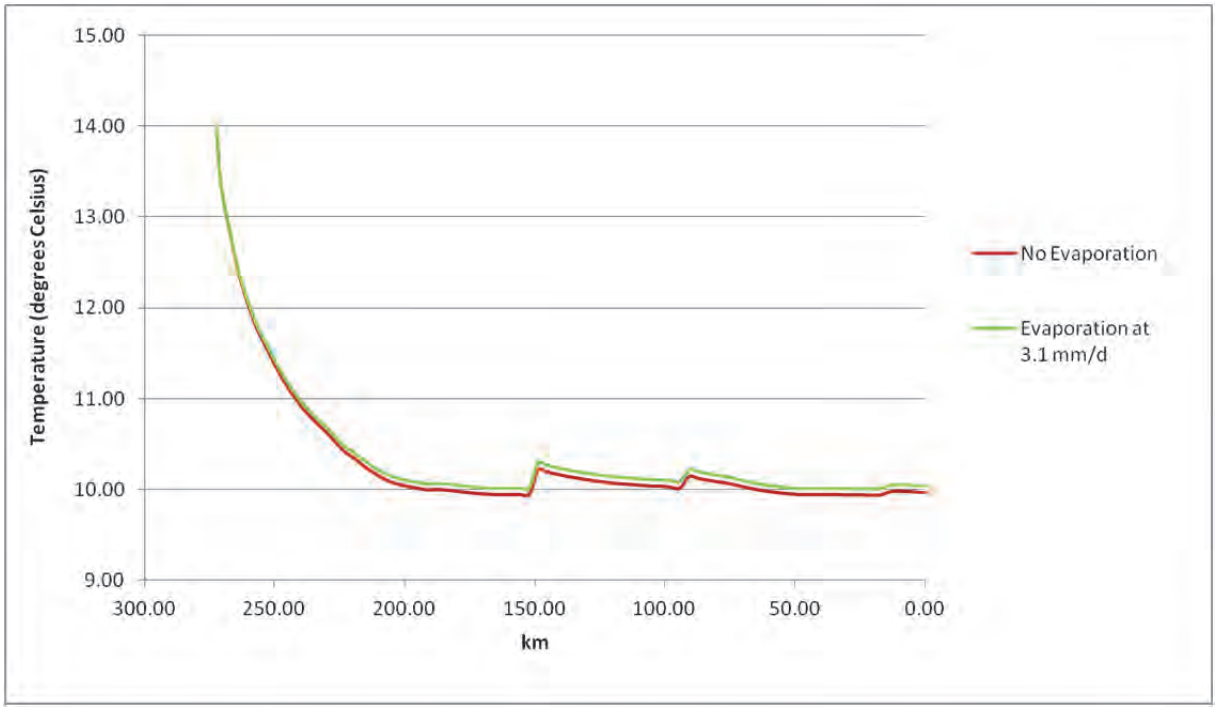

Figure 23: Comparison between evaporation values of zero, and 3.1 mm/day – water temperature

As anticipated, water temperature is calculated to be higher with evaporation, most likely due to lower flow (Figure 23).

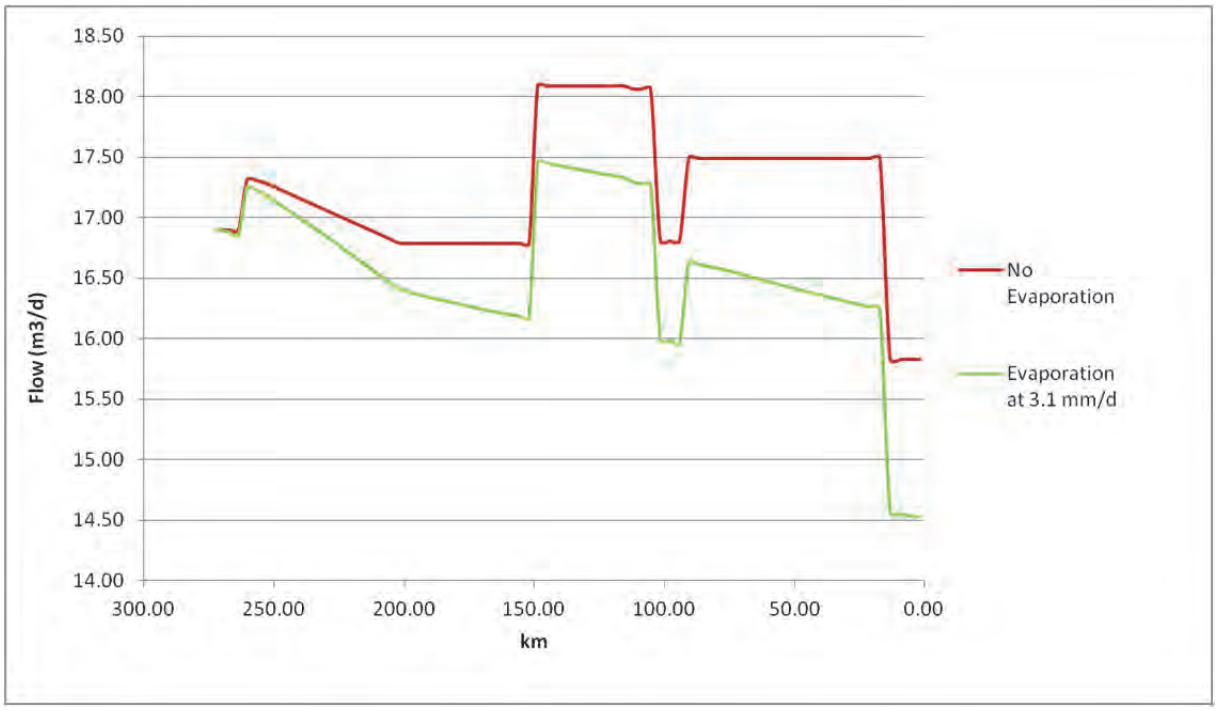

Figure 24: Flow comparison between evaporation values of zero and 3.1 mm/day

As anticipated, modelled flow is found to be lower under the evaporation scenario due to moisture losses (Figure 24).

7.14 Results and Discussion – Vaal River Case Study

As mentioned previously, the QUAL2K model was run using the hydraulics and flow set up in the 2009 exercise. To illustrate the changes in algae-related parameters under climate change, for each modelling run, the following was changed for each modelling scenario:

- Air temperature;
- Dew Point Temperature; and
- Evaporation.

This section presents the results of the various modelled climate change projections.

Water temperature

Anomalies between *present modelled* and *future* projections (intermediate and distant) of water temperature for the modelled stretch of river are presented in Figure 25 below. As mentioned previously, for these scenarios, starting temperature at the headwater (due to lack of data availability with regard to water temperature) and all point sources are modelled at 14°C. It should be noted that anomalies are presented as the difference between the future and present modelled projection (as opposed to future and historical values) in order to remove any biases in the GCMs.

All future projections indicate an increase in water temperature, with the CRM model being the most extreme model in terms of heat increase. There is a range of increase of approximately 1.5°C between the various models for the intermediate future. Into the distant future, for which the projections are less reliable due to various uncertainties, there is a projected range of just over 3-3.5°C.

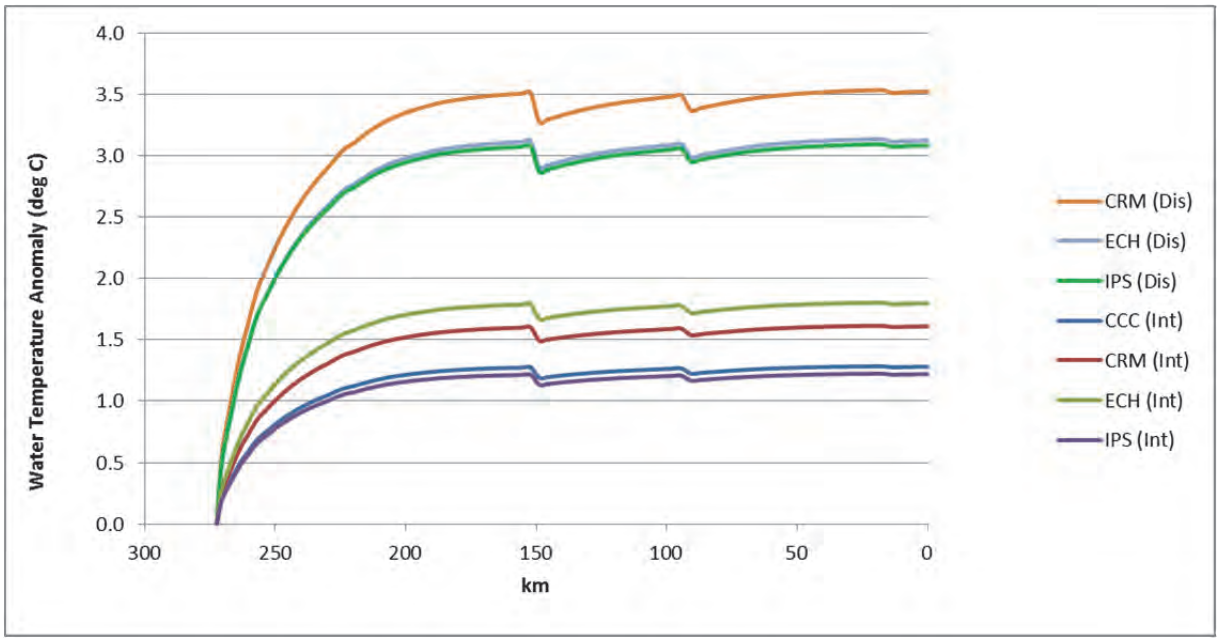

Figure 25: Comparison between historical and projected future water temperature

Dissolved oxygen

Breitburg *et al*. (1997) explain that concentration of dissolved oxygen in bottom waters of water bodies can be physiologically stressful or lethal to organisms dependent on aerobic respiration. Figure 26 illustrates the amount of dissolved oxygen in the modelled stretch of water, the concentration of which is indicative of:

- Air and water temperature (a higher air temperature will affect the rate at which oxygen is dissolved/absorbed into the water); and
- The amount of biological activity in the water, as higher levels of aquatic life are likely to place higher demands on the oxygen contained in the water.

The amount of dissolved oxygen in this stretch of river appears to drop with various climate change projections. This can be attributed to the higher temperatures and consequent reduced solubility of oxygen. The peaks in the plot below correspond to the locations of the various weirs along this stretch of the Vaal River (at approximately 260, 190, 104, 15 and 11 km). The project team explained the peaks in dissolved oxygen as being caused by the effect of weirs within QUAL2K, as this is determined through the depth of the weir and the temperature of the water. Therefore, the higher temperatures under the more extreme climate change projections and the larger difference in depth with the lower flow were deemed to explain the high peaks in dissolved oxygen.

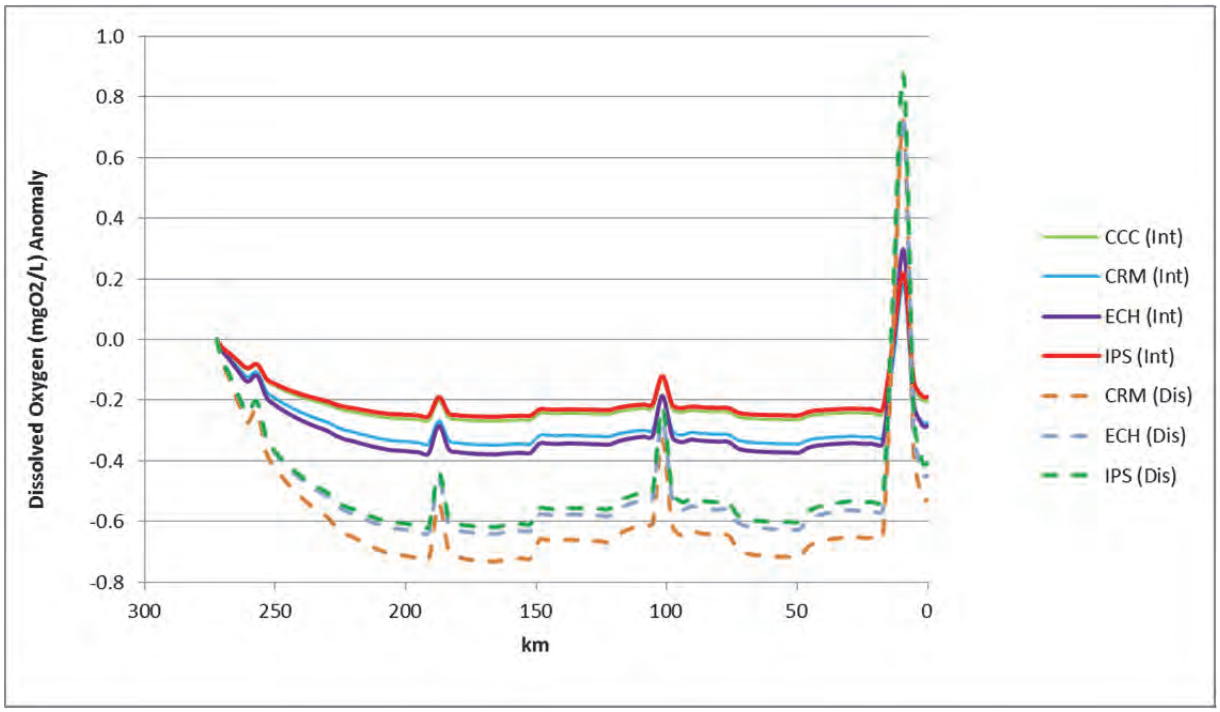

Figure 26: Comparison between present modelled and projected future dissolved oxygen concentrations

Flow

The anomaly between present modelled and future projections (intermediate and distant) of flow for the modelled stretch of river is presented in Figure 27 below. All future projections project a decrease in flow with changes in temperature and evaporation, with the ECH model being the most extreme.

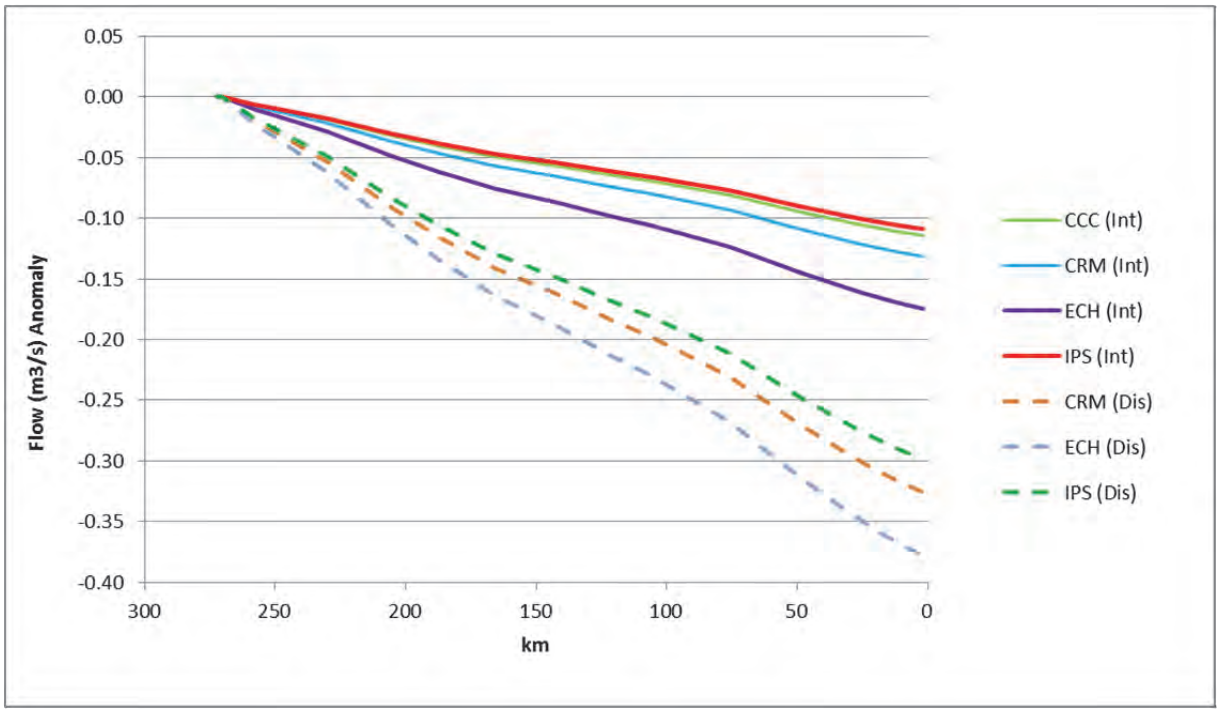

Figure 27: Comparison between present modelled and projected future flow

Phytoplankton (algae)

The term *phytoplankton* refers to representatives of several types of algae and bacteria, amongst other freshwater organisms such as the infective stages of fungi (Reynolds, 1984). With climate change (taking air temperature, dew point temperature and evaporation into account), it is apparent that the concentration of phytoplankton in this stretch of river increases (Figure 28).

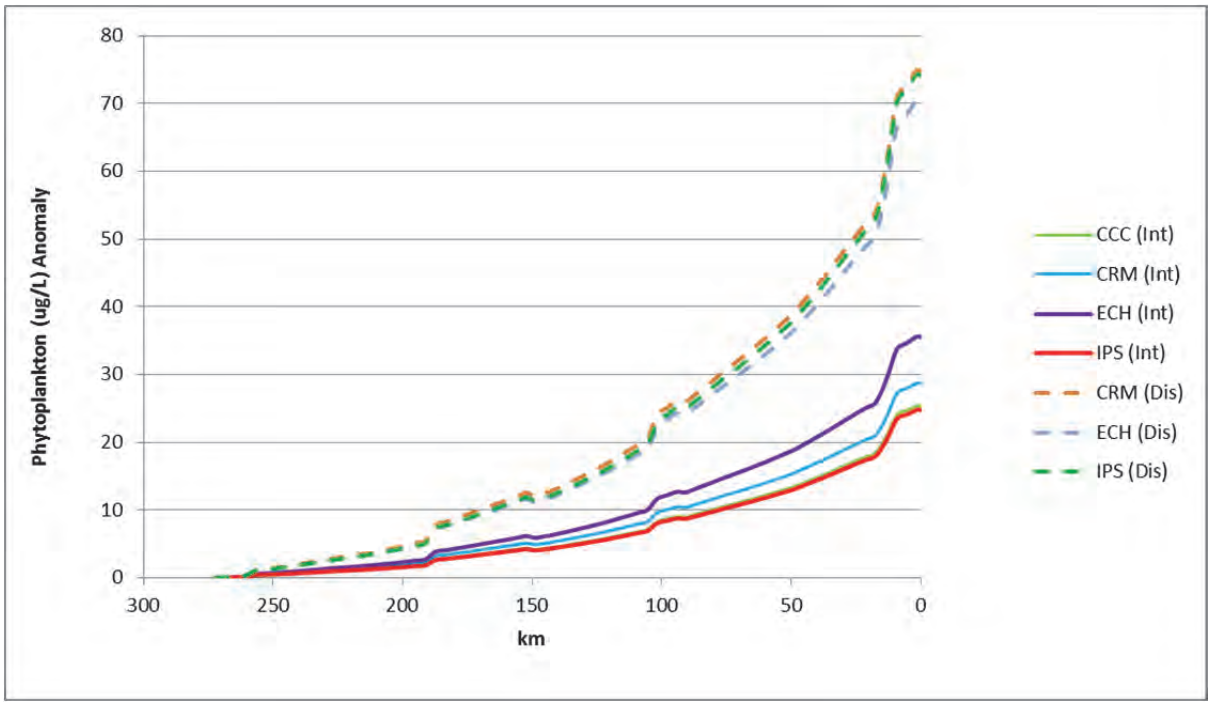

Figure 28: Comparison between historical and projected future phytoplankton concentrations

In the most extreme intermediate future projection (2046-2065), the concentration of phytoplankton shows an increase of approximately 35 µg/L. For the most extreme projection into the distant future (2081-2100), an increase of over 70 µg/L is indicated.

The series of figures below spatially indicates the modelled changes in phytoplankton under present, projected intermediate and distant future conditions. The increase in the lower reaches of the stretch of river modelled is apparent, particularly in the distant future projection.

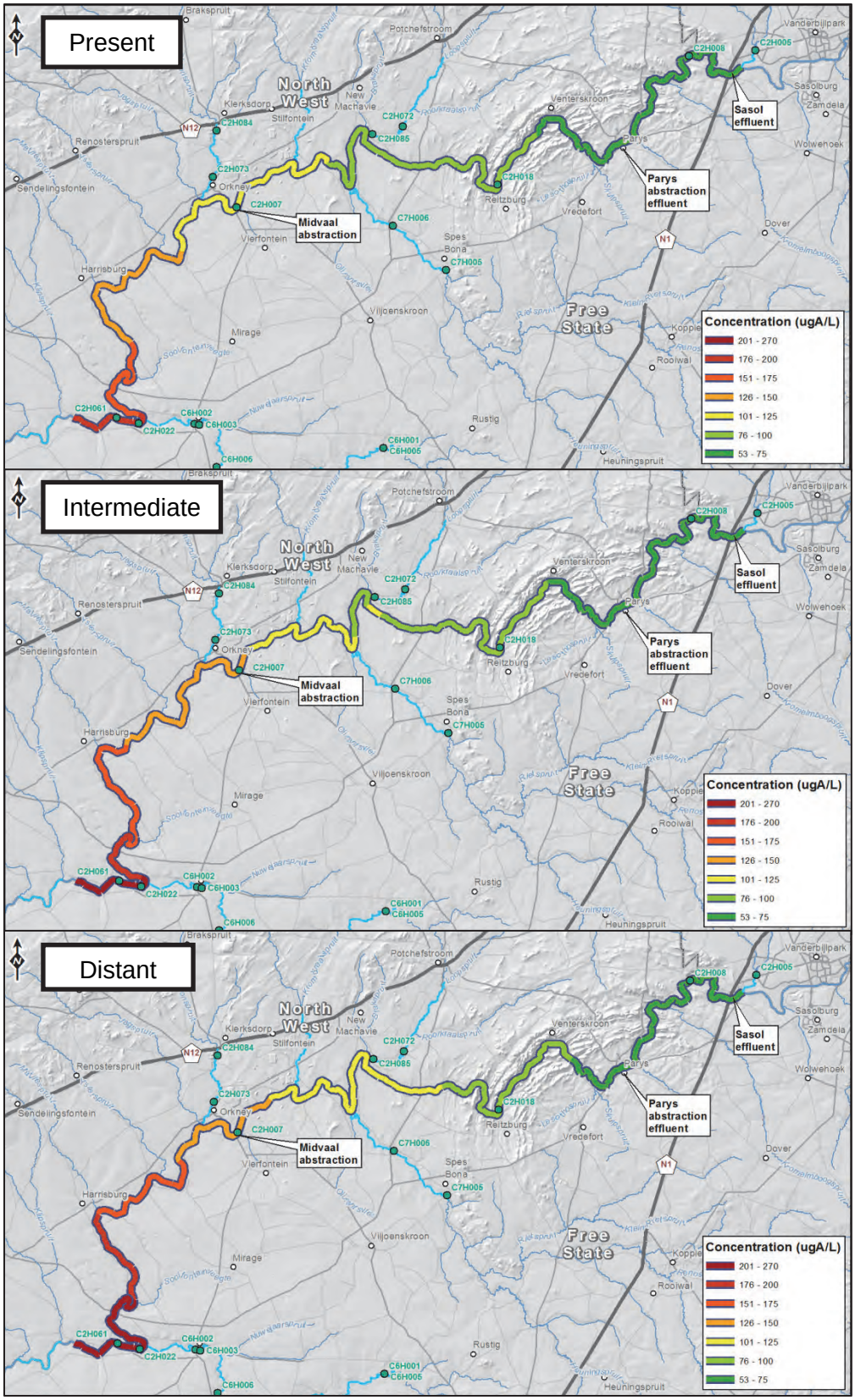

Figure 29: Modelled changes in phytoplankton concentration (µg/l) under projected climate change

Increase in algal growth is therefore likely to increase with the following modelled changes:

- Increase in air temperature;
- Associated change in dew point temperature; and
- Increased evaporation, should this occur.

Concentrations of phytoplankton in the Vaal Barrage are already particularly high due to the various industrial, agricultural and domestic discharges, leading to the common eutrophication problems.

The reading of phytoplankton (chlorophyll-a) in the Vaal River at the Midvaal Water Company was **139 µg/l** for August 2005. Total chlorophyll at Vermaasdrift (Midvaal effluent) is 45 µg/l.

Data available from the Department of Water Affairs for Chlorophyll-a concentration is limited in terms of monitoring duration. As shown below, data is only available from August 1992 until June 1993 for these stations (Figure 29). Monitoring data was provided to the project team however by the Midvaal Water Company (situated near Orkney) for more recent years, and this data is provided in Figure 31.

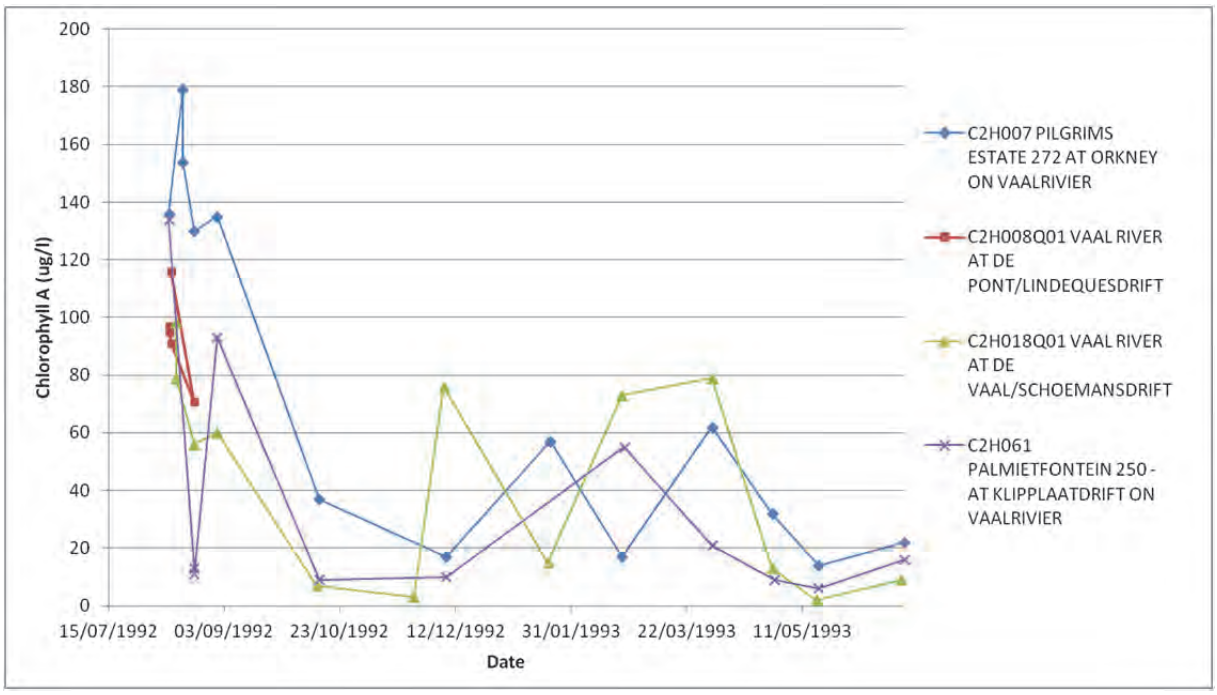

Figure 30: Available DWA monitoring data for Chlorophyll-a (for 1992-1993)

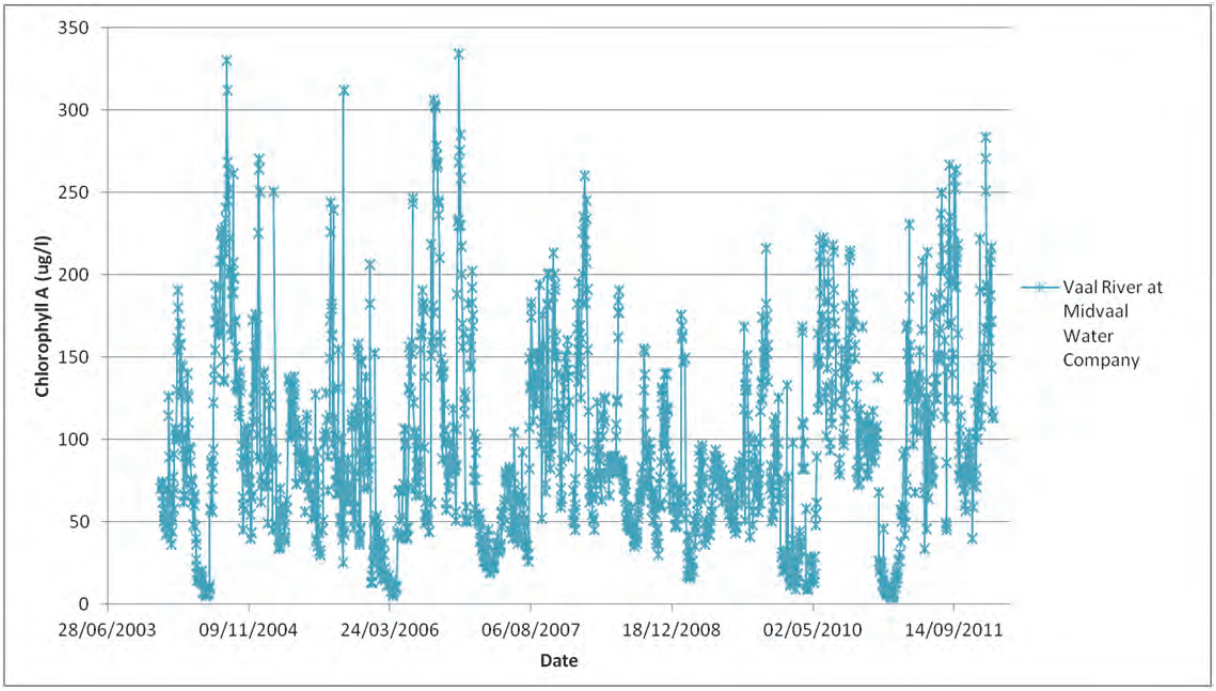

Figure 31: Midvaal Water Company monitoring data for Chlorophyll-a (01/2004-01/2012)

The average chlorophyll-a reading is 95 µg/l (January 2004-February 2012), with a maximum reading of 334 µg/l. The results are highly varied, and show a very slight increasing trend. The South African Water Quality Guidelines (Department of Water Affairs and Forestry, 1996) indicate that the Target Water Quality Range for algae (measured by chlorophyll-a) is 1 µg/l, with the limits for domestic use being 1 µg/l (acceptable) and 100 µg/l (tolerable). At the Midvaal measurement, an exceedance of this criterion appears to occur in approximately 40% of the readings. This therefore indicates that there is an overabundance of algae within this stretch of the Vaal River, exceeding the tolerable limits for domestic use, which has implications for water treatment processes.

Phosphate load

As phosphorous is deemed to be a major contributor to the eutrophication problem, this constituent was investigated further. The following water quality guidelines apply to phosphate in South Africa (Table 4):

Table 4: Guidelines for phosphate concentration

Guideline or RWQO	Limits		
South African National Water Quality Guidelines (DWA, 2011) for phosphorous (inorganic) for the aquatic ecosystem	*Target Water Quality Range*	*Acute Effect Value*	*Chronic Effect Value*
	<5 µg/l	25 µg/l	>25 µg/l
Generic Resource Water Quality Objectives at a National Level (Resource Water Quality Objectives (RWQOs) Model (Version 4.0, DWAF, 2006)	*Ideal (Ecological)*	*Acceptable (Ecological)*	*Tolerable (Ecological)*
	< 5 µg/l	15 µg/l	25 µg/l
Vaal River (proposed RWQOs for phosphate for identified reaches in the Vaal River main stem, Directorate National Water Resource Planning, DWA 2009) (Eutrophic levels considered to be: 50-150 µg/l)	*Upper reaches of the study area, south of the Barrage (Vaal River downstream of the Mooi Confluence to Sandspruit confluence) – irrigation, domestic, recreation, industry, aquatic ecosystem*		*Lower reaches of the study area, Vaal River downstream of the Lethabo weir to upstream of the Mooi confluence – irrigation, domestic, recreation, industry, aquatic ecosystem*
	RWQO: 100 µg/l		RWQO: 150 µg/l

The original value for phosphate entering the study area (at the Vaal Barrage, or headwater) was set at 342 µg/l. The effect of the removal of inorganic and organic phosphate from the base scenario (2005) is illustrated in the graph which follows. It is evident that complete removal of inorganic phosphate from the system causes a decline in existing phytoplankton concentration. Complete removal of only organic phosphorous does not make a difference to phytoplankton concentration. Inorganic phosphorous therefore appears to be a limiting factor in the growth of algae. Hydrolysis of organic phosphorous also results in the generation of inorganic phosphate within the model (Chapra *et al*., 2011). With fairly large quantities of organic phosphorous entering the system at the Barrage and with point sources, this appears to compliment even a small amount of inorganic phosphorous.

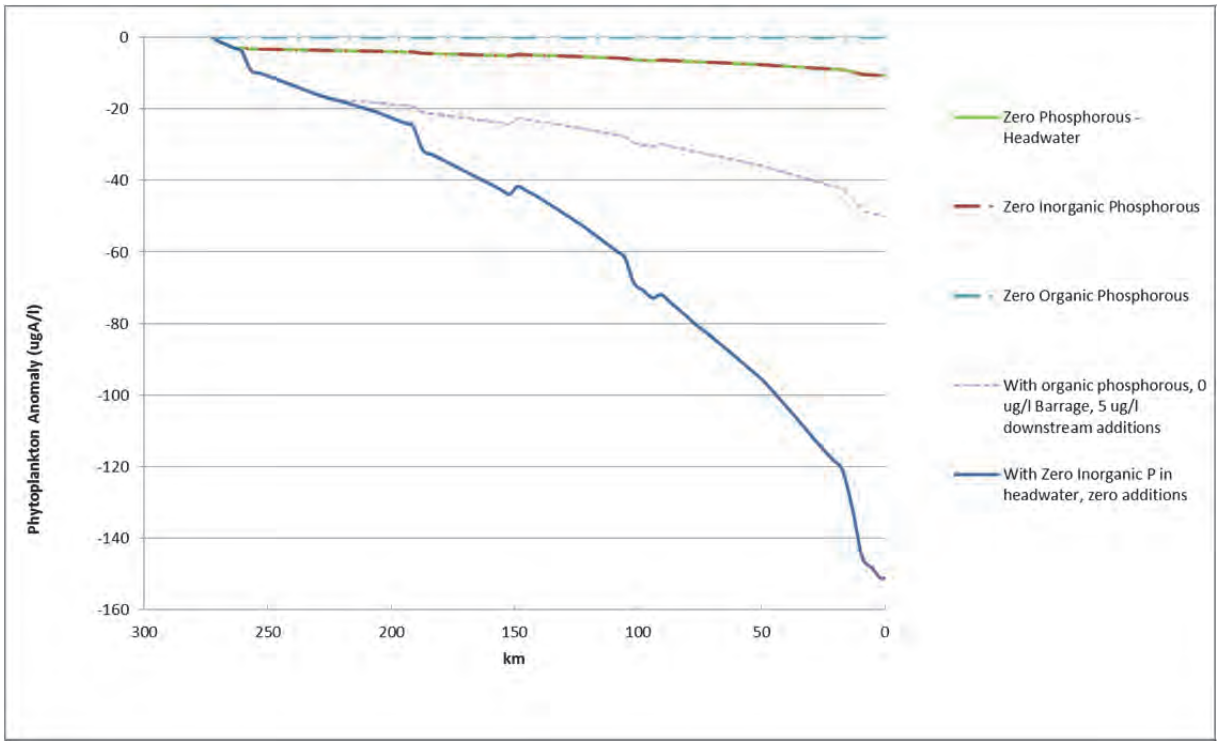

Figure 32: Modelled anomaly (compared to Base Case scenario, real data 2005) in phytoplankton concentration with changes in phosphate load

These results require further investigation, but appear to indicate that a *significant* reduction in phosphate load in the Barrage and the various point sources would be required to reduce the quantity of phytoplankton in the Vaal River.

8 BERG RIVER DAM CASE STUDY – CE-QUAL-W2 MODEL

8.1 Introduction

Hydrodynamic and water quality modelling of the Berg River Dam (BRD) was not specifically included in the original proposal of the current project, but since a pre-configured model existed it was considered an ideal opportunity to benchmark the behaviour of a dam which is not expected to exhibit algae-related problems in the foreseeable future. The ability of algal species to naturally seed waterbodies may, however, lead to a completely different scenario when water temperatures start increasing under climate change conditions.

Based on the findings of the literature review submitted as Deliverable 1 of this study, it can be inferred that cyanobacteria would out-compete diatoms and greens at higher water temperatures if they are present in a waterbody.

The ensuing sections of this report will document the configuration and application of the hydrodynamic and water quality model, CE-QUAL-W2 (Cole and Wells, 2008), to the BRD and Voëlvlei Dam under various climate change scenarios.

8.2 Background to Berg River Dam

The BRD is situated is situated on the Berg River in the Western Cape Province, some 6.5 km south west of the town Franschhoek (see Figure 33).

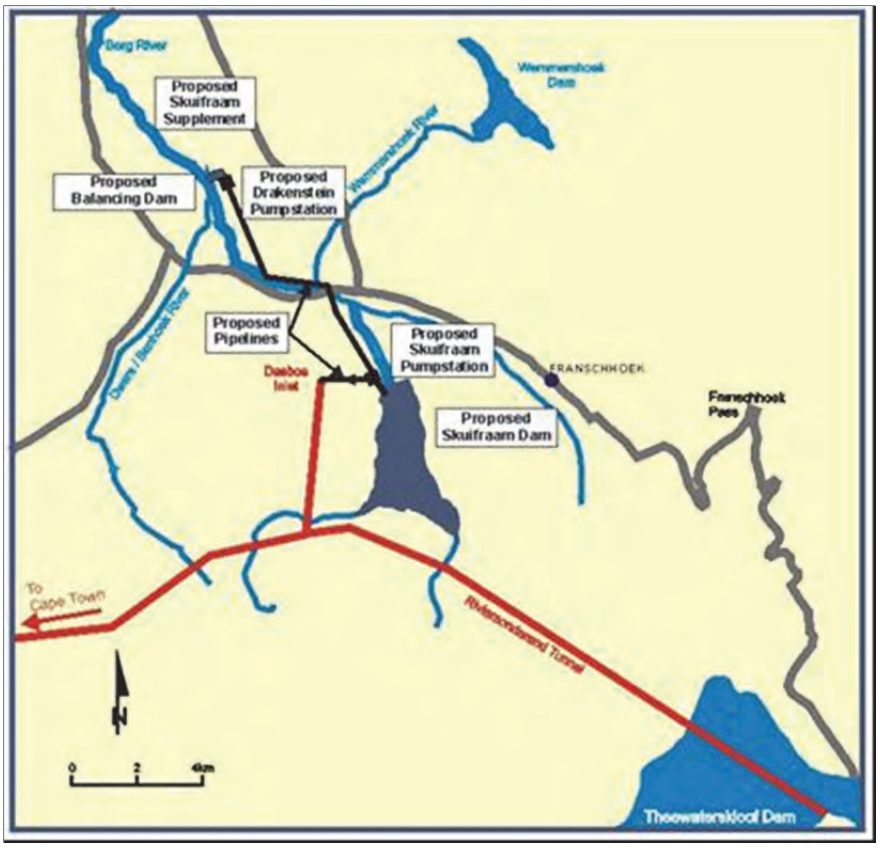

Figure 33: Locality of Berg River Dam

The BRD is filled with winter flows from the upper Berg River and a strong flowing tributary, the Wolwekloof. The dam has a gross capacity of 127 Mm^3 and a system yield of 56 Mm^3/a. The yield is increased to 81 Mm^3/a because of the supplement scheme which returns water from downstream of the BRD.

Findings from the preliminary Ecological Reserve Determination, undertaken during the initial phase of the Berg Water Project (BWP), indicated that the reach of the Berg River immediately downstream of the BRD was ecologically important and sensitive, and proposed that the temperatures of the ecological BRD releases should aim to mimic the temperature regime that would have occurred under non-impacted conditions (i.e. temperature of BRD inflow in this case). Environmental releases from the BRD can thus either be made through large sleeve valves situated near the base of the dam or through multi-level outlet gates located higher up the wall in an attempt to meet the downstream water requirements. The BRD is also the first in South Africa to incorporate structures that permit both low and high flow environmental releases, the latter up to 200 m^3/s.

Since the BRD is newly constructed and situated in a virtually unimpacted catchment, it is not expected to have any water quality-related problems. However, it is possible that the

water quality from the supplement scheme could deteriorate substantially in the future, possibly causing eutrophication.

8.3 Background to Voëlvlei Dam

Voëlvlei Dam is an off-channel storage dam located off the Berg River about 5 km south of Gouda as shown in Figure 34. The catchment of the Dam is relatively small (± 39 km^2) and the dam receives water in two canals which divert water from the Klein Berg, Twenty-Four, and Leeu Rivers (see Figure 35). Historically, water quality in Voëlvlei Dam was regarded as good, and an assessment of the trophic status (i.e. degree of nutrient enrichment) by the Institute for Water Quality Studies found that Voëlvlei Dam could be classified as turbid and mesotrophic (i.e. moderately enriched with nutrients) (eWISA website).

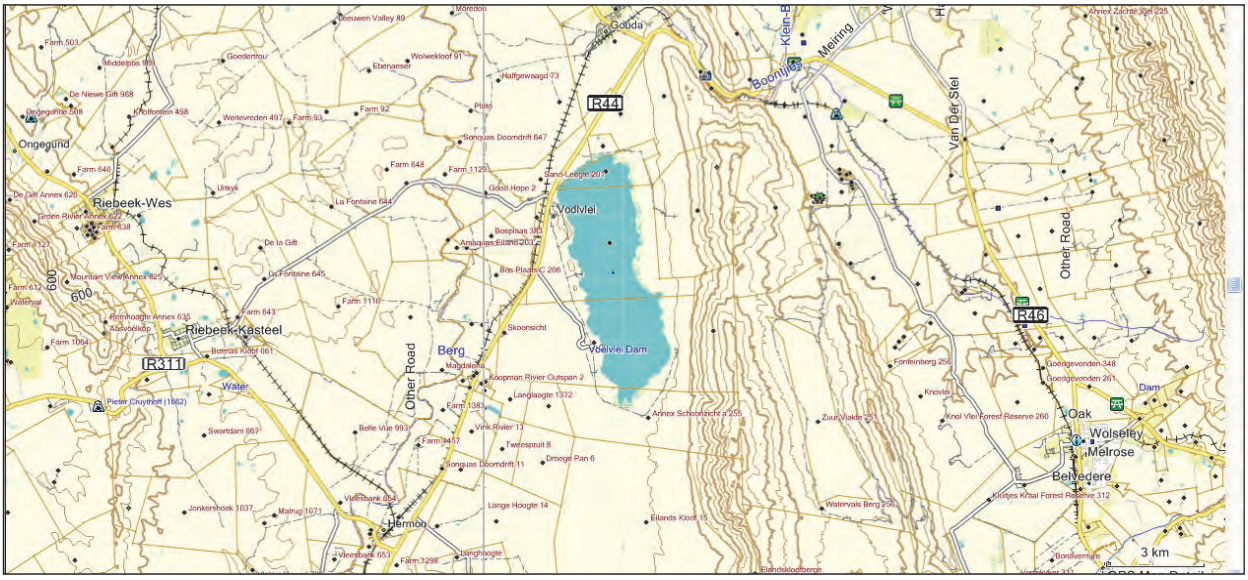

Figure 34: Topographic map of Voëlvlei dam and surrounds

The Voëlvlei Dam was the first large water supply scheme developed in the Berg River. The first Voëlvlei scheme was completed in 1953 when the natural Vogelvlei Lake was impounded by building a small wall structure. The natural vlei had a catchment of only 40 km², and additional water was diverted from the Klein Berg River into a canal to the dam. In 1971, the dam was raised to its present full supply capacity of 172 Mm³. The Dam is currently supplied by diverted runoff from the Klein Berg River; Twenty-four Rivers and Leeu River catchments via canals (see Figure 35). The Dam supplies water to Cape Town, the Swartland water treatment works (WTW) and irrigation water for downstream users. The water for the Swartland Scheme supplies Riebeekkasteel, Riebeek Wes and Malmesbury, while the Voëlvlei WTW supplies Cape Town. The irrigation water is released into the Berg

River along with water for the Withoogte Scheme, which is then abstracted from Misverstand weir further downstream. The Dam has no spillway infrastructure (eWISA website).

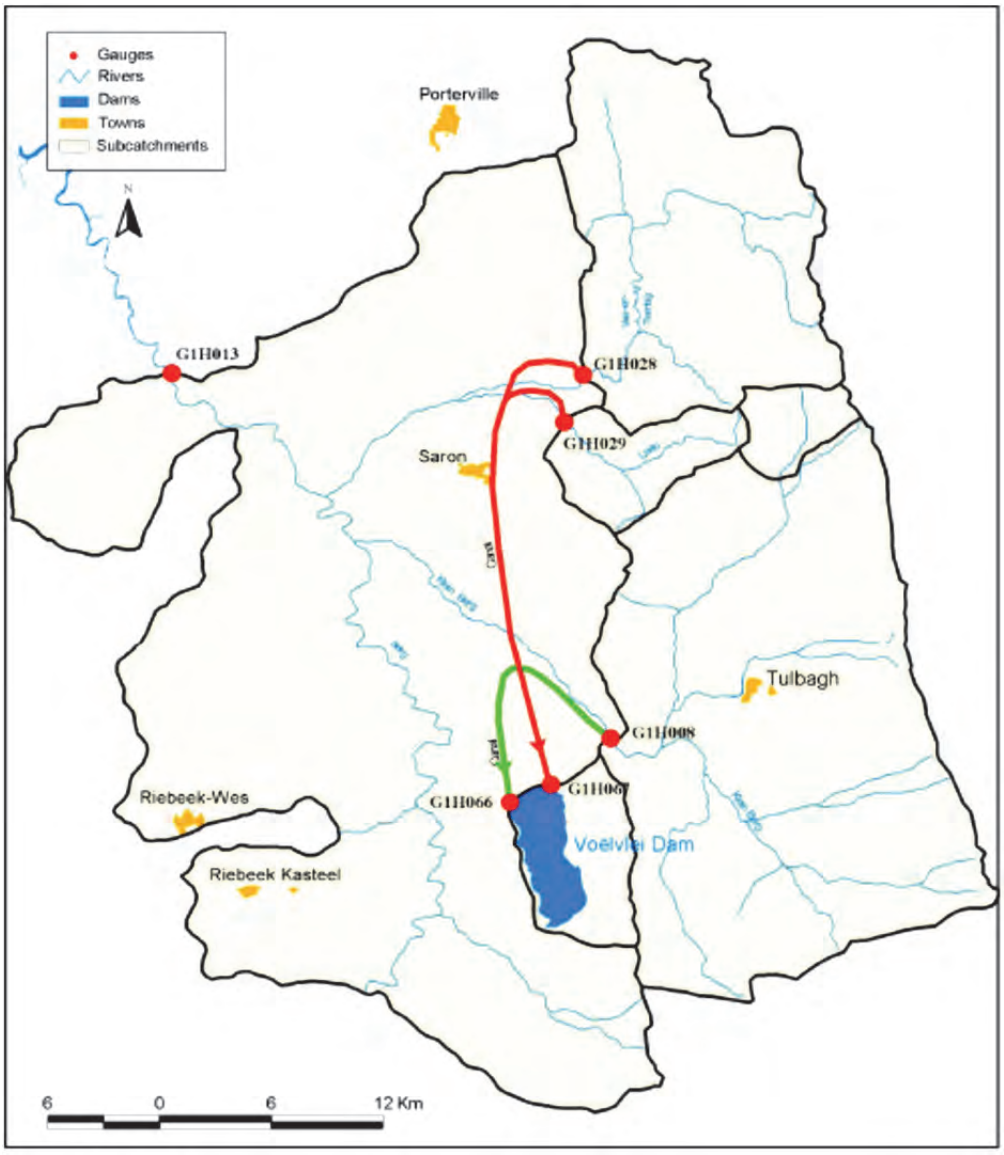

Figure 35: Voëlvlei dam locality and its inlet canal system

8.4 Background to the CE-QUAL-W2 Hydrodynamic and Water Quality Model

CE-QUAL-W2 is a two-dimensional (2-D), laterally averaged, hydrodynamic water quality simulation model (Cole and Wells, 2008). The model is based on the assumption that the water body shows maximum variation in water quality along its length and depth. Therefore, the model is suited to relatively long and narrow water bodies that show water quality gradients in the longitudinal and vertical directions. The two-dimensional model simulates the vertical and longitudinal distributions of thermal energy (water temperature) and selected biological and chemical constituents in a water body with time. The primary purpose of the model is to simulate time-varying concentrations of water quality constituents by coupling

hydrodynamic and water quality components. The model has been applied to many rivers, lakes, reservoirs, and estuaries for nearly 20 years. The model will simulate water temperature, salinity, DO, carbon balance, N, P, Si, phytoplankton, bacteria as well as first-order decay. Geometry data is required to define the finite difference representation of the water body. Initial and boundary conditions have to be specified and the required hydraulic parameters include horizontal and vertical dispersion coefficients for momentum and temperature/constituents as well as the Chezy coefficient, used to calculate boundary friction. Simulation of water quality kinetics requires the specification of approximately 60 coefficients. Data is required to provide boundary conditions and assess model performance during calibration. Because the model assumes lateral homogeneity, it is best suited for relatively strong longitudinal and vertical water quality gradients; it may be inappropriate for large waterbodies. The model has extensive data requirements. It allows for user-defined numbers of algal, zooplankton and macrophytes groups (Cole and Wells, 2008).

Amongst the limitations of CE-QUAL-W2 are:

- **Hydrodynamics and transport**: The governing equations are laterally (x-z axis) and layer averaged (bank to bank for rives). Lateral averaging assumes lateral variations in velocities, temperatures, and constituents are negligible. This assumption may be inappropriate for large waterbodies exhibiting significant lateral variations in water quality. Whether this assumption is met is often a judgment call on the user and depends in large part on the questions being addressed. Eddy coefficients are used to model turbulence. Currently, the user must decide among several vertical turbulence schemes the one that is most appropriate for the type of waterbody being simulated. The equations are written in the conservative form using the Boussinesq and hydrostatic approximations. Since vertical momentum is not included, the model may give inaccurate results where there is significant vertical acceleration (Cole and Wells, 2008).

- **Water quality**: Water quality interactions are, by necessity, simplified descriptions of an aquatic ecosystem that is extremely complex. Improvements will be made in the future as better means of describing the aquatic ecosystem in mathematical terms and time for incorporating the changes into the model become available in this one area (Cole and Wells, 2008).

- **Sediment oxygen demand (SOD)**: The model includes a user-specified sediment oxygen demand that is not coupled to the water column. SOD only varies according to temperature. The first order model is tied to the water column settling of organic matter. The model does not have a sediment compartment that models kinetics in the sediment and at

the sediment-water interface. This places a limitation on long-term predictive capabilities of the water quality portion of the model (Cole and Wells, 2008).

- **Solution scheme:** The model provides three different numerical transport schemes for temperature and constituents – upwind differencing, the higher-order QUICKEST and Leonard's ULTIMATE algorithm. Upwind differencing introduces numerical diffusion often greater than physical diffusion. The QUICKEST scheme reduces numerical diffusion, but in areas of high gradients generates overshoots and undershoots which may produce small negative concentrations. In addition, discretisation errors are introduced as the finite difference cell dimensions or the time-step increase. This is an important point to keep in mind when evaluating model predictions that are spatially and temporally averaged versus observed data collected at discrete points in time and space.

- **Computer limits:** A considerable effort has been invested in increasing model efficiency including a vertically implicit solution for vertical turbulence in the horizontal momentum equation. However, the model still places computational and storage burdens on a computer when making long-term simulations. Year-long water quality simulations for a single water body can take from a few minutes to days for multiple waterbodies in a large river basin. Applications to dynamic river systems can take considerably longer than water bodies because of much smaller time-steps needed for river numerical stability (Limno-Tech, 2002 and Cole and Wells 2008).

Inputs to the model include the following:

- ***Bathymetric Data*** – data representing the layout and volumetric dimensions of the water body.

- ***Initial Conditions*** – data representing the starting conditions within the reservoir in terms of temperature and reactant distribution.

- ***Meteorological Data*** – this data includes the site specific values for air temperature, wind speed, wind direction, dew point temperature and cloud cover.

- ***Upstream Boundary Conditions*** – this data includes the flow rates of the incoming streams as well as the time varying concentrations of the reactants being modelled.

- ***Flow Rates of Releases*** – this includes the data describing the predicted (or measured) release pattern from the reservoir and is essential for volume balance calculations.

8.5 Water Quality Interactions considered for the Berg River and Voëlvlei Dam models

The interactions between water quality constituents in CE-QUAL-W2 and which were used for both the BRD and Voëlvlei Dams are shown in the sections which follow.

Algae

The internal fluxes between algae and other water quality variables are reflected in Figure 36.

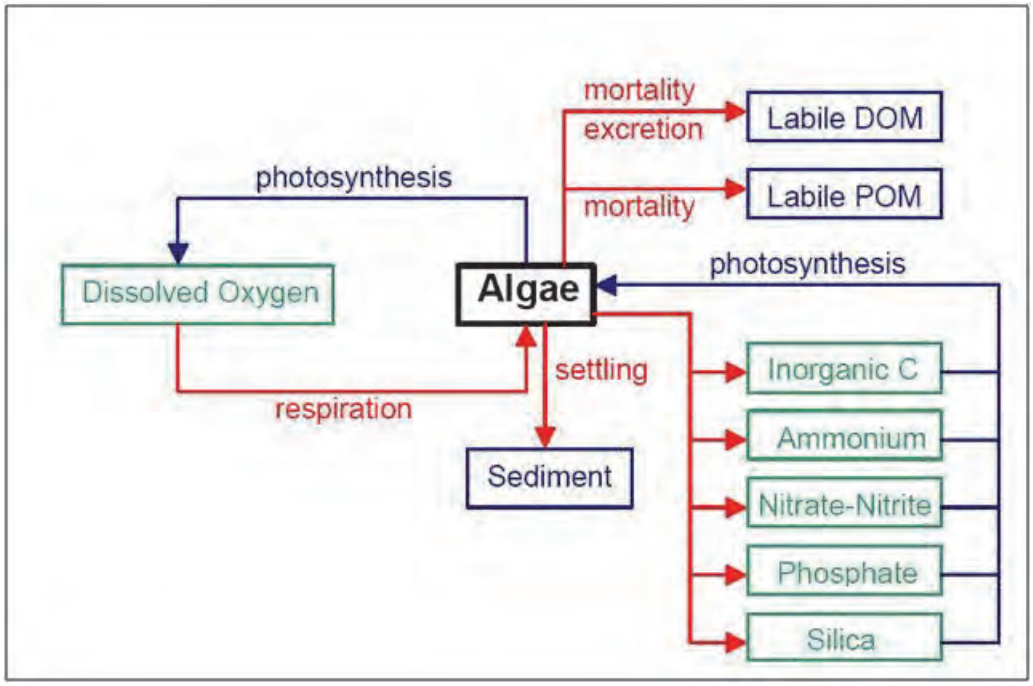

Figure 36: Internal flux between algae and other components

It is immediately evident that the modelling of algae would demand the inclusion of all related water quality variables. The rate equation for the interaction of algae is:

$$S_{a\lg ae} = K_{ag}\Phi_a - K_{ar}\Phi_a - K_{ae}\Phi_a - K_{am}\Phi_a - \frac{\omega_a}{\Delta Z}\Phi_a$$

Where,

Δz = cell thickness (m)

K_{ag} = algal growth rate (per second)

K_{ar} = algal dark respiration rate (per second)

K_{ae} = algal excretion rate (per second)

K_{am} = algal mortality rate (per second)

ω_a = algal settling rate (m/s)

Φ_a = algal concentration (g/m^3)

The rate equation for algae production was used unchanged, but the units of the rate constant were changed to per day. The algal concentration can be obtained by multiplying the chlorophyll-*a* concentration with a user-defined algae/chlorophyll ratio.

Phosphates

The internal fluxes between phosphate and other water quality variables are shown in Figure 37

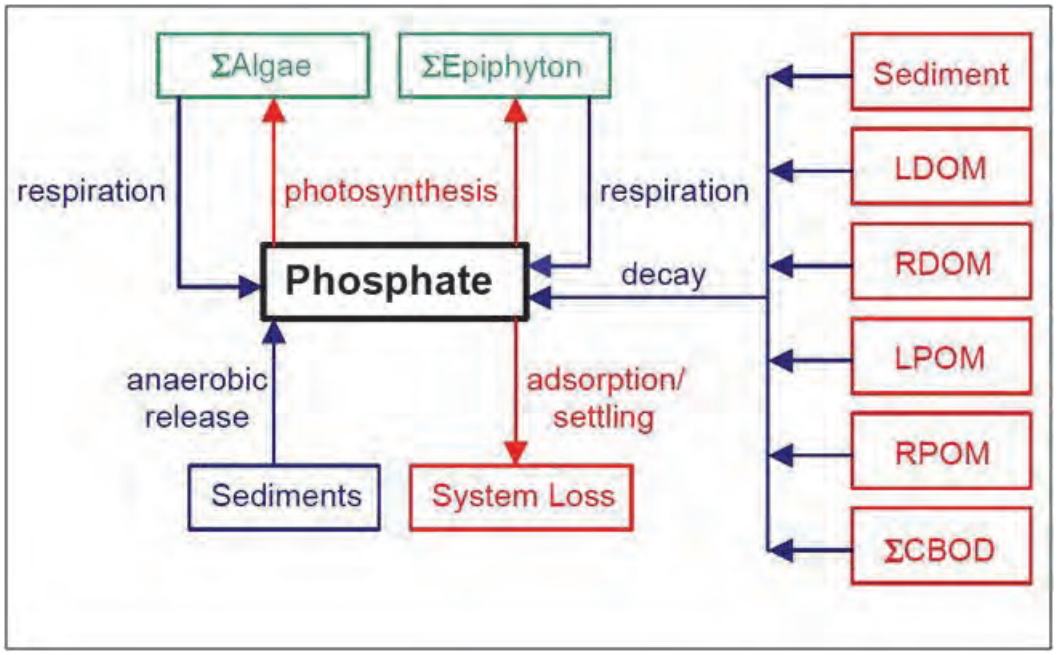

Figure 37: Internal flux between phosphorous and other components

The rate equation describing the phosphate reaction is:

$$S_p = \sum\left(K_{ar} - K_{ag}\right)\delta_p\Phi_a + K_{ldom}\delta_p\gamma_{om}\Phi_{ldom} + K_{poml}\delta_p\gamma_{om}\Phi_{poml} + K_{pomr}\delta_p\gamma_{om}\Phi_{pomr}$$
$$K_{rdom}\delta_p\gamma_{om}\Phi_{rdom} + K_s\delta_p\gamma_{om}\Phi_s + SOD\,\gamma_{om}\,A_s/V_{cell}$$
$$-\frac{P_p\left(\sum\omega_{ss}\Phi_{ss} + \omega_{pom}\Phi_{poml} + \omega_{pom}\Phi_{pomr} + \omega_{FE}\Phi_{FE}\right)}{\Delta Z}\Phi_p$$

Where,

ΔZ = model cell thickness (m)

As = sediment area (m^2)

V_{cell} = volume of cell (m^3)

P_p = adsorption coefficient (m^3/g)

δ_P = stoichiometric coefficient for phosphorous

γ_{om} = temperature rate multiplier for organic matter decay

ω_i = settling velocities (m/s)

K_{ar} = algal dark respiration rate (per second)

K_{ag} = algal growth rate (per second)

K_{ldom} = labile DOM decay rate (per second)

K_{POML} = POML decay rate (per second)

K_{POMR} = POMR decay rate (per second)

K_S = sediment decay rate (per second)

SOD = anaerobic sediment release rate ($g/(m^2/s)$)

K_{rdom} = refractory DOM decay rate (per second)

Φ_{rdom} = refractory DOM concentration (g/m^3)

Φ_a = algal concentration (g/m^3)

Φ_{ldom} = labile Dom concentration (g/m^3)

Φ_{POML} = POML concentration (g/m^3)

Φ_{POMR} = POMR concentration (g/m^3)

Φ_S = organic sediment concentration (mass divided by cell volume) (g/m^3)

Φ_{SS} = inorganic suspended solids (ISS) concentration (g/m^3)

Φ_P = phosphorous concentration (g/m^3)

Φ_{Fe} = total iron (Fe) concentration (g/m^3)

The contribution of algae to the phosphate rate shown in the first term of the equation above, K_{ar} is much smaller that K_{ag} and the net effect is the disappearance of phosphates. The contribution of Particulate Organic Matter (POM) and Dissolved Organic Matter (DOM) to phosphates is reflected in Terms 2 to 5. Organic sediments are accumulated when algae die and settle to the bottom. Phosphates from these sediments can be released from either first order decay of from zero order decay. These contributions are indicated by Terms 6 and 7, respectively. Phosphates that are adsorbed onto Inorganic Suspended Solids (ISS) and on to Iron (Fe) settle out at the same rate as the particles to which they are attached and are removed from the water column. Phosphates can also be temporarily removed from the water column by adsorbing onto POM – when decay of this material occurs, the phosphates

are released back into the water column. ***In this particular exercise no ISS or Fe were modelled, implying that phosphates could not be removed from the water column***.

Refractory Dissolved Organic Matter (RDOM)

The interactions between RDOM and other water quality constituent are depicted in Figure 38.

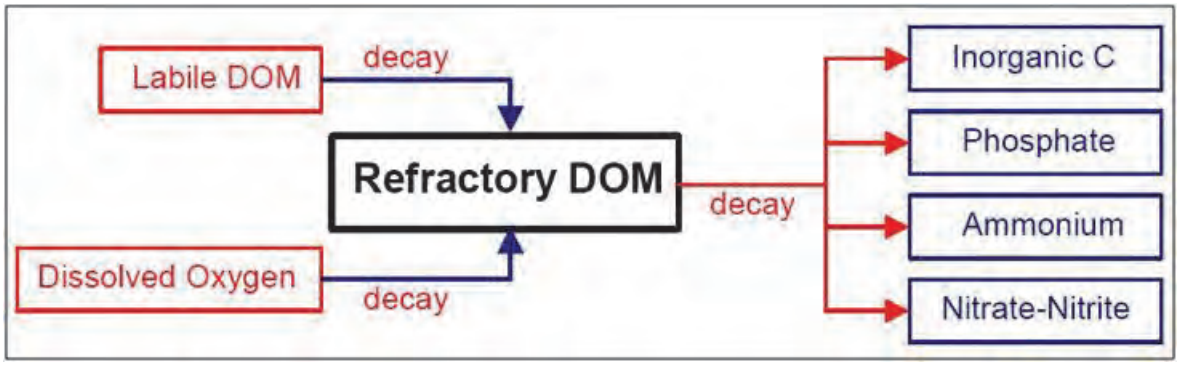

Figure 38: Internal flux between refractory DOM and other components

The rate equation describing the refractory DOM concentration is shown below:

$$S_{rdom} = K_{l->r}\Phi_{ldom} - K_{rdom}\gamma_{om}\Phi_{rdom}$$

Where,

K_{l_r} = rate constant for conversion from labile DOM (per second)

Φ_{ldom} = labile DOM concentration (g/m^3)

γ_{om} = temperature rate multiplier for organic matter decay

K_{rdom} = RDOM decay rate (per second)

Φ_{rdom} = RDOM concentration (g/m^3)

It should be noted that since RDOM is not measured or included in the inflows, it could only be produced by the decay of LDOM, which is in turn obtained from algal mortality.

Labile Particulate Organic Matter (LPOM)

The interactions between LPOM and other water quality constituents are shown in Figure 39.

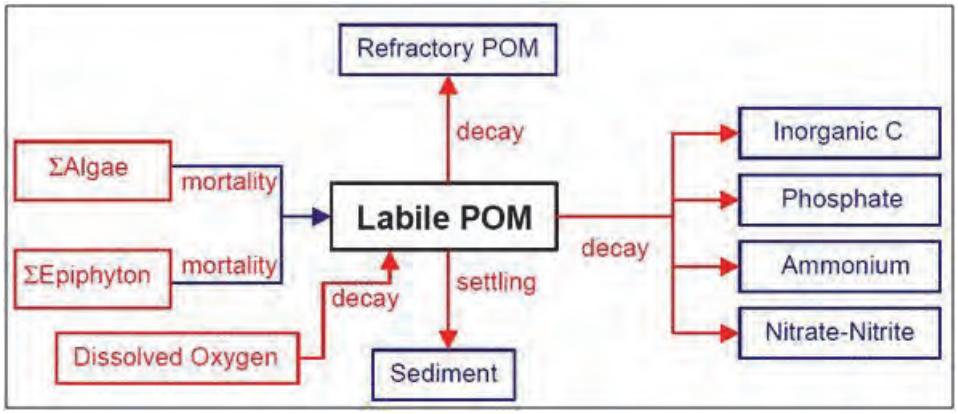

Figure 39: Internal flux between detritus and other components

The rate equation describing the Labile POM concentration is depicted below:

$$S_{POML} = \sum P_{am} K_{am} \Phi a - K_{POML} \gamma_{om} \Phi_{POML} - K_{ar} \Phi a - K_{l->r} \Phi_{POML} - \omega_{POM} \frac{\partial \Phi_{POML}}{\partial Z}$$

Where,

P_{am} = partition coefficient for algal mortality

K_{am} = algal mortality rate (per second)

Φ_a = algal concentration (g/m^3)

K_{POML} = POML decay rate (per second)

ω_i = settling velocities (m/s)

Φ_{POML} = POML/Detritus concentration (g/m^3)

γ_{om} = temperature rate multiplier for organic matter decay

K_{l_r} = rate constant for conversion from labile DOM (per second)

Refractory Particulate Organic Matter (RPOM)

The interactions between RPOM and other water quality constituents are depicted in Figure 40.

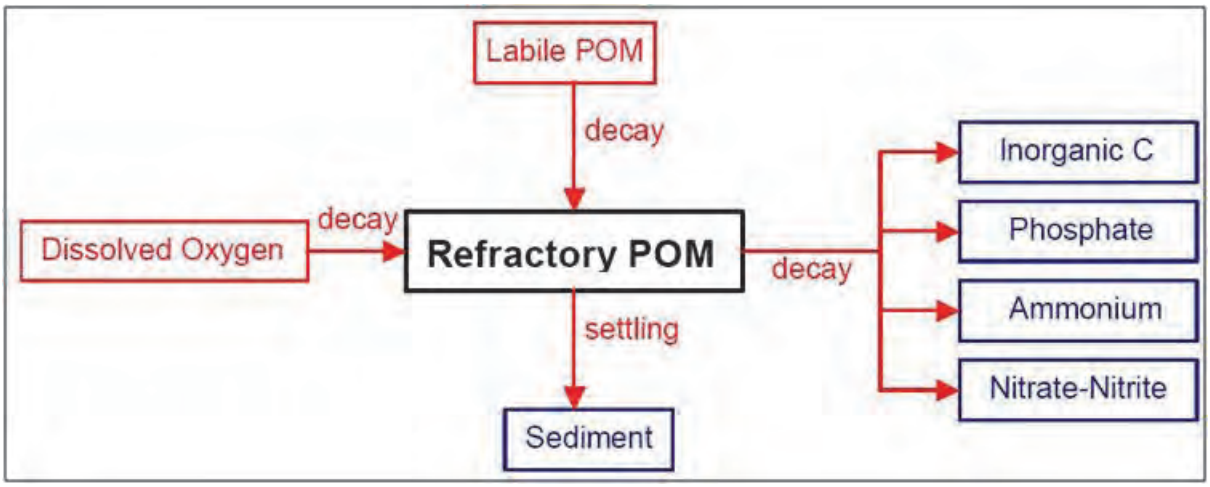

Figure 40: Refractory particulate organic matter pathways

The rate equation describing the concentration of refractory POM is shown in the equation below:

$$S_{rdom} = K_{l->r}\Phi_{POML} - K_{POMR}\gamma_{om}\Phi_{POMR} - \omega_{POM}\frac{\partial\Phi_{POMR}}{\partial Z}$$

Where,

K_{l_r} = rate constant for conversion from labile DOM (per second)

Φ_{POML} = POML/Detritus concentration (g/m^3)

γ_{om} = temperature rate multiplier for organic matter decay

ω_i = settling velocities (m/s)

K_{POMR} = POMR decay rate (per second)

Φ_{POMR} = POMR concentration (g/m^3)

Ammonium

The interaction between ammonium and other water quality constituents is depicted in Figure 41.

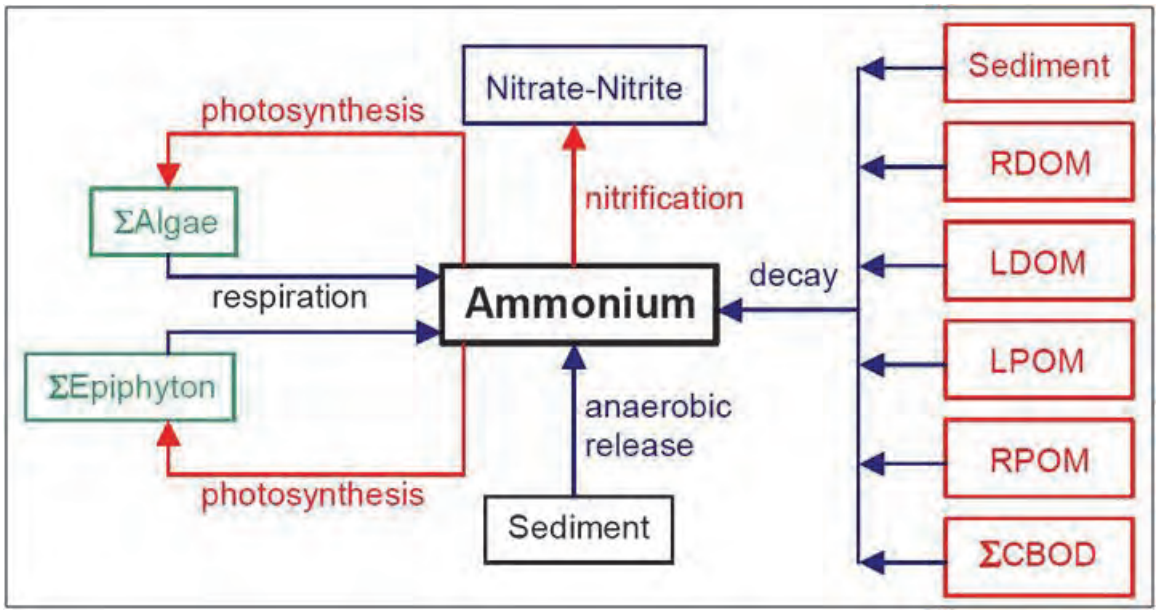

Figure 41: Internal flux between ammonia-nitrogen and other components

The rate equation describing the ammonium concentration is shown below:

$$s_p = \sum(K_{ar})\delta_N \Phi_a - \sum K_{ag}\delta_N \Phi_a \frac{\Phi_{NH4}}{\Phi_{NH4}+\Phi_{NO3}} + K_{ldom}\delta_N \gamma_{om}\Phi_{ldom}$$
$$+ K_{poml}\delta_N \gamma_{om}\Phi_{poml} + K_{pomr}\delta_N \gamma_{om}\Phi_{pomr} + K_{rdom}\delta_N \gamma_{om}\Phi_{rdom} + K_s\delta_N \gamma_{om}\Phi_s$$
$$+ SOD_{NH4}\gamma_{om}\frac{A_s}{V_{cell}} + K_{NO3}\gamma_{NO3}\Phi_{NO3} - K_{NH4}\gamma_{NH4}\Phi_{NH4}$$

Where,

A_s = sediment area (m^2)

V_{cell} = volume of cell (m^3)

ΔZ = model cell thickness (m)

δ_N = stoichiometric coefficient for nitrogen

γ_{om} = temperature rate multiplier for organic matter decay

γ_{NH4} = temperature rate multiplier for nitrification

γ_{NO3} = temperature rate multiplier for denitrification

K_{ar} = algal dark respiration rate (per second)

K_{ag} = algal growth rate (per second)

K_{ldom} = labile DOM decay rate (per second)

K_{rdom} = refractory DOM decay rate (per second)

K_{POML} = POML decay rate (per second)

K_{POMR} = POMR decay rate (per second)

K_S = sediment decay rate (per second)

SOD_{NH4} = sediment ammonia release rate ($g/m^{-2}/s$)

K_{NO3} = nitrate-nitrogen decay rate (per second)

K_{NH4} = ammonia-nitrogen decay rate (per second)

Φ_{SS} = inorganic suspended solids concentration (g/m^3)

Φ_{ldom} = labile Dom concentration (g/m^3)

Φ_{rdom} = refractory DOM concentration (g/m^3)

Φ_{a} = algal concentration (g/m^3)

Φ_{POML} = POML/Detritus concentration (g/m^3)

Φ_{POMR} = POMR concentration (g/m^3)

Φ_{NH4} = ammonia-nitrogen concentration (g/m^3)

Φ_{NO3} = nitrate-nitrogen concentration (g/m^3)

Φ_{S} = organic sediment concentration (mass divided by cell volume) (g/m^3)

All the terms in the rate equation were used in calculating the in-lake ammonium concentration. The zero order decay and release only occurs when the dissolved oxygen is below the minimum value of 0.1 mg/l.

Nitrate (NO_2) / Nitrite (NO_3)

The interactions between NO_2+NO_3 and other water quality constituents are reflected in Figure 42.

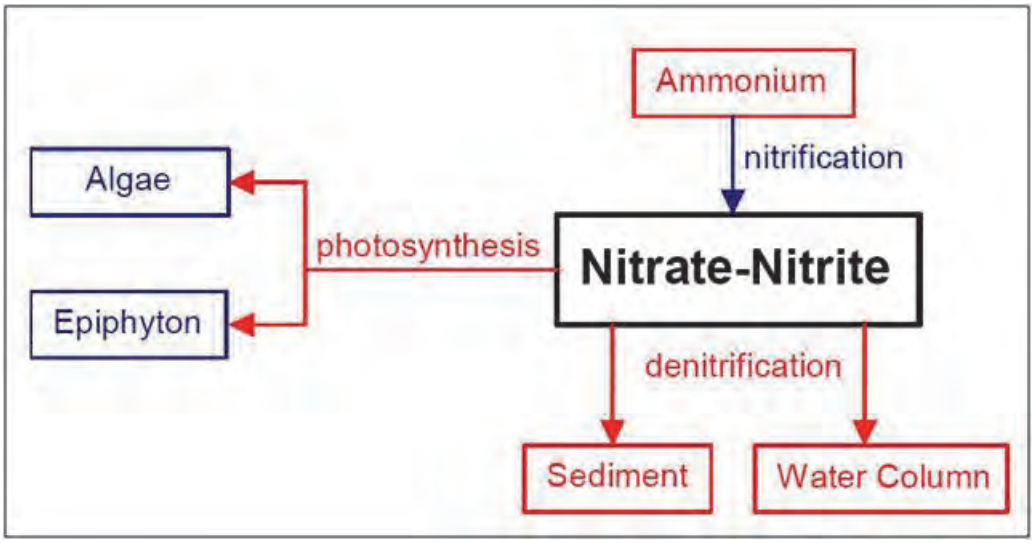

Figure 42: Internal flux between nitrate/nitrite-nitrogen and other components

The rate equation describing the NO_2+NO_3 concentration is reflected in the equation below. Nitrification was only allowed to occur if oxygen was present and denitrification was only allowed to occur when the oxygen concentration was below the specified minimum of 0.1 mg/l.

$$S_{NO3} = K_{NH4}\gamma_{NH4}\Phi_{NH4} - K_{NO3}\gamma_{NO3}\Phi_{NO3} - \sum K_{ag}\delta_N\Phi_a\left(1 - \frac{\Phi_{NH4}}{\Phi_{NH4}+\Phi_{NO3}}\right) - \omega_{NO3}\frac{\partial\Phi_{NO3}}{\partial Z}$$

Where,

γ_{NH4}	=	temperature rate multiplier for nitrification
γ_{NO3}	=	temperature rate multiplier for denitrification
δ_N	=	stoichiometric coefficient for nitrogen
K_{NH4}	=	ammonia-nitrogen decay rate (per second)
ω_i	=	settling velocities (m/s)
K_{NO3}	=	nitrate-nitrogen decay rate (per second)
K_{ag}	=	algal growth rate (per second)
Φ_a	=	algal concentration (g/m^3)
Φ_{NH4}	=	ammonia-nitrogen concentration (g/m^3)
Φ_{NO3}	=	nitrate-nitrogen concentration (g/m^3)
K_{POML}	=	POML decay rate (per second)

Dissolved Oxygen

The interactions between dissolved oxygen and other water quality constituents are depicted in Figure 43.

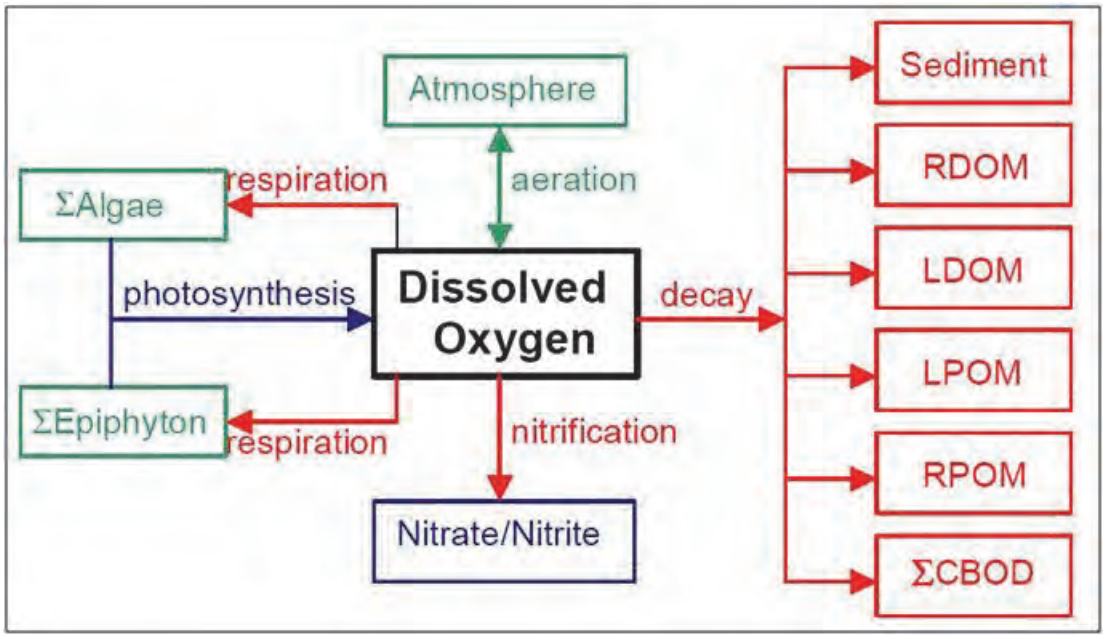

Figure 43: Internal flux between dissolved oxygen and other constituents

The rate equation describing the oxygen concentration is shown in the equation below:

$$S_{DO} = \sum K_{ag}\delta_{om}\Phi_a - \sum K_{ar}\delta_{om}\Phi_a - K_{NH4}\delta_{NH4}\gamma_{NH4}\Phi_{NH4} - K_{POMR}\delta_{om}\gamma_{om}\Phi_{POMR} -$$
$$K_{POML}\delta_{om}\gamma_{om}\Phi_{POML} - K_s\delta_{om}\gamma_{om}\Phi_s - SOD\,\gamma_{om}\,A_s/V_{cell} - K_{ldom}\gamma_{om}\delta_{om}\Phi_{ldom}$$
$$- K_{rdom}\delta_{om}\gamma_{om}\Phi_{rdom} + A_{kt}K_L(\Phi_{DO} - \Phi_{DO}) - \sum K_{BOD}R_{BOD}\Theta^{T-20}\Phi_{BOD}$$

Where,

K_{ag}	=	algal growth rate (per second)
δ_{OM}	=	stoichiometric coefficient for organic matter
Φ_a	=	algal concentration (g/m^3)
K_{ar}	=	algal dark respiration rate (per second)
K_{NH4}	=	ammonia-nitrogen decay rate (per second)
δ_{NH4}	=	oxygen stoichiometric coefficient for nitrification
γ_{NH4}	=	temperature rate multiplier for nitrification
Φ_{NH4}	=	ammonia-nitrogen concentration (g/m^3)
K_{POMR}	=	POMR decay rate (per second)
γ_{OM}	=	temperature rate multiplier for organic matter decay
Φ_{POMR}	=	POMR concentration (g/m^3)

Φ_{POML} = POML/Detritus concentration (g/m^3)

K_S = sediment decay rate (per second)

Φ_S = organic sediment concentration (mass divided by cell volume) (g/m^3)

SOD = sediment oxygen demand (g/m^2/s)

A_s = sediment surface area (m^2)

V_{cell} = volume of cell (m^3)

K_{ldom} = labile DOM decay rate (per second)

Φ_{ldom} = labile DOM concentration (g/m^3)

K_{rdom} = refractory DOM decay rate (per second

Φ_{rdom} = refractory DOM concentration (g/m^3)

A_{kt} = water surface area (m^2)

K_L = interfacial exchange rate for oxygen (m/s)

$\Phi_{'DO}$ = saturation DO concentration (g/m^3)

Φ_{DO} = dissolved oxygen concentration (g/m^3)

$\mathbf{K}_{BOD}$ = CBOD decay rate (per second)

$\mathbf{R}_{BOD}$ = conversion from CBOD in the model to CBOD ultimate

Θ = BOD temperature rate multiplier

Φ_{BOD} = CBOD concentration (g/m^3)

No information was available on the carbonaceous biological oxygen demand (CBOD) concentration and it was subsequently omitted from the oxygen concentration equation.

Sediment (Organic)

The interactions between sediment and other water quality variables are depicted in Figure 44 below:

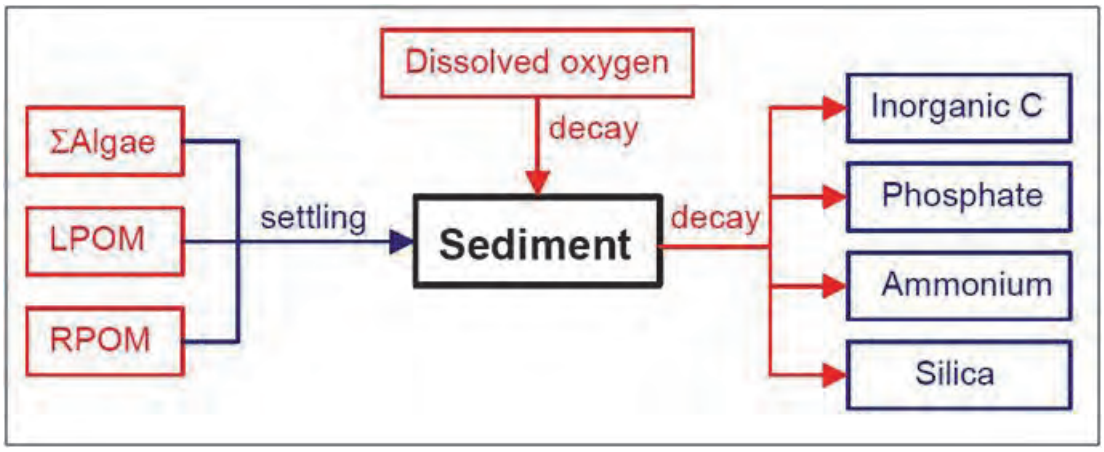

Figure 44: Internal flux between organic sediments and other components

The rate equation describing the sediment concentration is depicted below:

$$S_s = \frac{\omega_{POM}}{\Delta Z}\Phi_{POMR} + \frac{\omega_{POM}}{\Delta Z}\Phi_{POML} + \sum\frac{\omega_a}{\Delta Z}\Phi_a - \gamma_{om}K_s\Phi_s$$

Where,

ΔZ = model thickness (m)

ω_{POM} = POM settling velocities (m/s)

ω_a = algal settling velocities (m/s)

γ_{OM} = temperature rate multiplier for organic matter decay

K_S = sediment decay rate (per second)

Φ_a = algal concentration (g/m^3)

Φ_{POML} = POML/Detritus concentration (g/m^3)

Φ_{POMR} = POMR concentration (g/m^3)

Φ_s = organic sediment concentration (sediment mass divided by cell volume) (g/m^3)

Dissolved Silica

The interaction between dissolved silica and other water quality constituents is depicted in Figure 45.

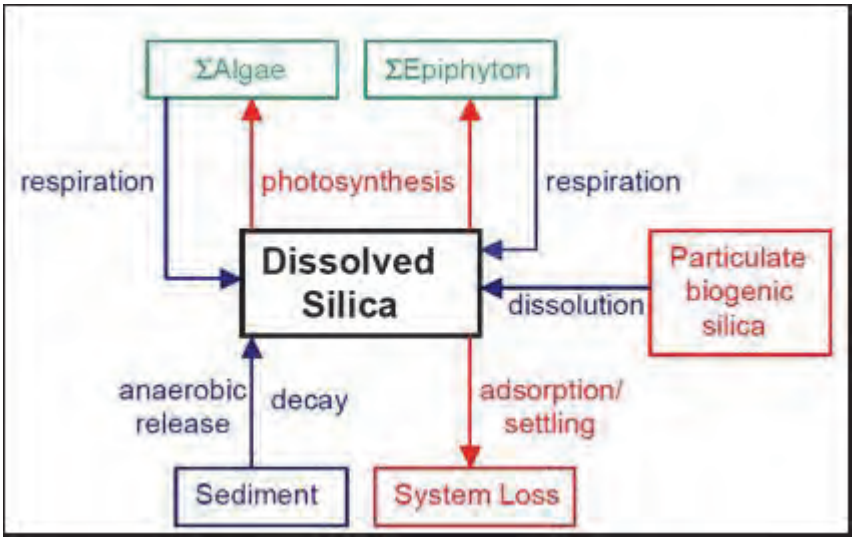

Figure 45: Source/Sinks terms for dissolved biogenic silica

The rate equation describing the dissolved silica concentration is shown below:

$$S_{DSi} = -\sum(K_{ag})\delta_{Si}\Phi_{a} + K_{ldom}\delta_{Si}\gamma_{om}\Phi_{ldom} + K_{POML}\delta_{si}\gamma_{om}\Phi_{POML} + K_{POMR}\delta_{Si}\gamma_{om}\Phi_{POMR}$$
$$+ K_{rdom}\delta_{Si}\gamma_{om}\Phi_{rdom} + K_{s}\delta_{Si}\gamma_{om}\Phi_{s} + SOD\,\gamma_{om}\,A_s/V_{cell}$$
$$- \frac{P_{Si}\left(\sum\omega_{ss}\Phi_{ss} + \omega_{POM}\Phi_{POML} + \omega_{POM}\Phi_{POMR} + \omega_{Fe}\Phi_{Fe}\right)}{\Delta Z}\Phi_{DSi}$$

Where,

ΔZ = model thickness (m)

A_s = sediment surface area (m^2)

V_{cell} = volume of cell (m^3)

P_{Si} = adsorption coefficient (m^3/g)

δ_{Si} = stoichiometric coefficient for Si

γ_{OM} = temperature rate multiplier for organic matter decay

ω_i = settling velocities (m/s)

K_{ag} = algal growth rate (per second)

K_{ldom} = labile DOM decay rate (per second)

K_{POML} = POML decay rate (per second)

K_{POMR} = POMR decay rate (per second)

K_S = sediment decay rate (per second)

SOD = sediment oxygen demand ($g/m^2/s$)

K_{rdom} = refractory DOM decay rate (per second)

Φ_{rdom} = refractory DOM concentration (g/m^3)

Φ_{a} = algal concentration (g/m^3)

Φ_{ldom} = labile DOM concentration (g/m^3)

Φ_{POML} = POML/Detritus concentration (g/m^3)

Φ_{POMR} = POMR concentration (g/m^3)

Φ_{s} = organic sediment concentration (sediment mass divided by cell volume) (g/m^3)

Φ_{ss} = inorganic suspended solids concentration (g/m^3)

Φ_{Dsi} = dissolved Silica concentration (g/m^3)

Φ_{Fe} = total Iron concentration (g/m^3)

No inorganic suspended solids or Fe was modelled in the simulations and silica could not be consumed via this mechanism.

Particulate Silica

The interaction between particulate silica and other water quality constituents is shown in Figure 46.

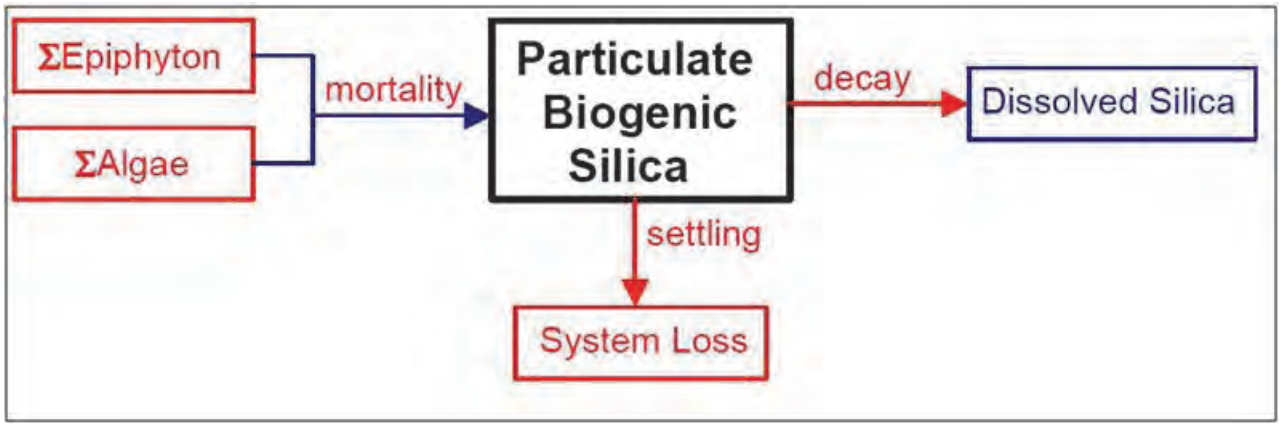

Figure 46: Source/Sink terms for biogenic particulate silica

The rate equation describing the particulate silica concentration is reflected in the equation below:

$$S_{SiP} = P_{am} K_{am} \Phi_a - K_{SiP} \gamma_{om} \Phi_{SiP} - \frac{\omega_{SiP} \partial \Phi_{SiP}}{\partial Z}$$

Where,

P_{am}	=	partition coefficient for algal mortality
K_{am}	=	algal mortality rate (per second)
Φ_a	=	algal concentration (g/m^3)
K_{SiP}	=	Si particulate decay rate (per second)
ω_{SiP}	=	Si particulate settling rate (m/s)
Φ_{SiP}	=	Si particulate concentration (g/m^3)
γ_{OM}	=	temperature rate multiplier for organic matter decay

8.6 Effect of Temperature on Algal Growth and Algal Succession

The effect of water temperature on phytoplankton growth rates can be accounted for in several ways – the simplest being a linear model with a prescribed minimum temperature below which no growth will occur. According to Chapra (2008), this formulation can be represented as:

$$k_{g,T} = 0 \qquad \text{for } T \leq T_{min} \text{ and}$$

$$k_{g,T} = k_{g,ref} \frac{T - T_{min}}{T_{ref} - T_{min}} \text{ for } T > T_{min}$$

where $k_{g,T}$ = growth rate (d^{-1}) at temperature T (in °C)

$k_{g,ref}$ = The growth rate (d^{-1}) at a reference temperature, T_{ref} (°C)

T_{min} = The minimum temperature below which plant growth does not occur

The aforementioned formulation for variation of phytoplankton growth rate with temperature indicates that growth rate would increase with temperature, but sets maximum limit for phytoplankton growth rate – a serious flaw if inhibition due to temperature is to be simulated realistically.

A more realistic model for representing the dependence of phytoplankton growth rate on temperature is one in which the growth rate is zero at a minimum temperature and then increases to an optimum growth rate followed by a decrease in growth as the temperature extends beyond the optimum range, commonly referred to as the optimal temperature model (Chapra, 2008). The CE-QUAL-W2 (Cole and Wells, 2008) simulation tool used in this

research employs the optimal temperature model in which temperature rate multipliers are used. Temperature rate multipliers are the multiplicative factors which are used to vary the phytoplankton growth rate according to the prevailing temperature. The general format of the graph from which the temperature rate multipliers are obtained is depicted in Figure 47 which shows that the lowest temperature for growth (AT1) is 5°C and that the corresponding fraction of the maximum growth rate (AK1) at this temperature would be 0.1. Similarly, the optimum temperature range would be between 25°C (AT2) and 35°C (AT3) and the highest temperature would be 40°C (AT4).

The advantages of using the optimum temperature range formulation for the simulation of phytoplankton growth are that:

1. Growth inhibition due to temperature can be taken into account, and
2. Algal succession due to varying water temperature can be simulated.

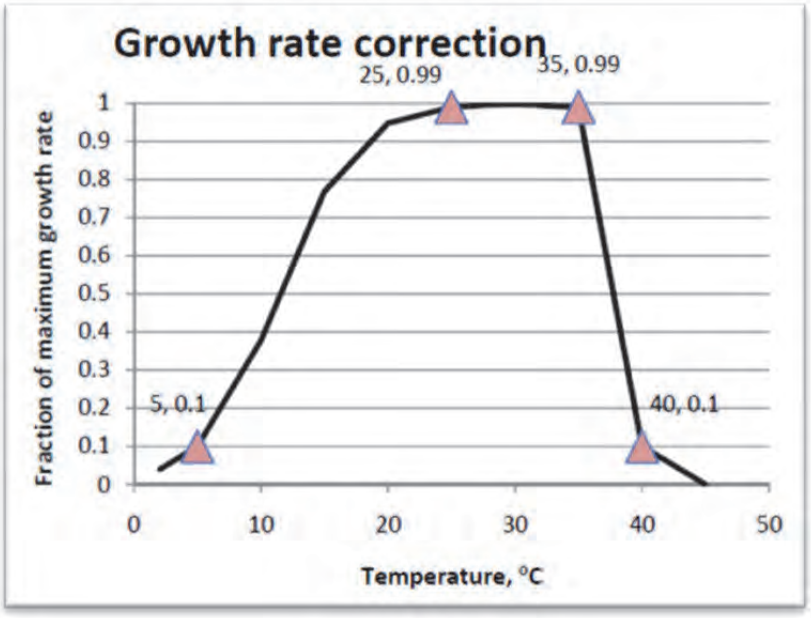

Figure 47: A typical temperature rate multiplier curve for phytoplankton growth rates (after Cole & Wells, 2008)

In light of what has been mentioned in the previous paragraph about temperature rate multipliers, it is evident that these rate multipliers are one of the most important parameters for determining algal succession when more than one algal assemblage is being simulated (Cole & Wells, 2008). The temperature ranges defining the growth behaviour of the algal assemblages considered in this study are shown in Table 5 and shows that diatoms would dominate at lower temperatures, greens at slightly higher temperatures and blue-green at

the highest temperatures. The values of other parameters also affecting algal growth is shown in Table 6.

Table 5: Temperature rate multiplier for algal species for Berg River dam

Variable	Diatoms	Greens	Cyanobacteria
Lower temperature AT1 (^oC)	4	5	5
Lower temperature for maximum algal growth AT2 (^oC)	20	20	24
Upper temperature for maximum algal growth AT3 (^oC)	25	25	31
Upper temperature for algal growth AT4 (^oC)	28	32	38

Adopted from Nielsen, 2005, Cole, 2008, Bowie, 1985, Tsujimura, 2003, Tamiya, 1965 and Talling, 1955.

Table 6: Parameters used in the Berg River dam study

Symbol	Model Parameters	Diatoms	Greens	Cyanobacteria
Parameters affecting algal growth				
K_{ag}	Maximum algal growth rate	5 $day^{-1}(T_{opt})$ Bowie *et al*., 1985:291	4.1day^{-1} (T_{opt}) Bowie *et al*., 1985:292	0.7 day^{-1} Bowie *et al*., 1985:292
K_{am}	Maximum algal mortality rate	0.1 day^{-1}	0.1 day^{-1}	0.1 day^{-1}
K_{ae}	Maximum algal excretion rate	0.04 day^{-1}	0.04 day^{-1}	0.04 day^{-1}
K_{ar}	Maximum algal respiration rate	0.04 day^{-1}	0.04 day^{-1}	0.04 day^{-1}
h_n	Michaelis-Menten algal half-saturation constant for nitrogen limited growth	0.01 mg/l Eppley et al., 1969	0.14 mg/l Bowie *et al*., 1985:328	0 mg/l Baldia *et al*., 2007:607
h_p	Michaelis-Menten algal half-saturation for phosphorous limited growth	0.002 mg/l Holm & Armstrong, 1981	0.38 mg/l Rhee, 1973	0.011 mg/l Holm & Armstrong, 1981
His	*Michaelis-Menten algal half-saturation for silica limited growth*	*0.08 mg/l* Bowie *et al*., 1985:327	*not required*	*not required*
ASAT	Light saturation intensity at maximum photosynthetic rate	61.2 W/m^2 Bowie *et al*., 1985:320	81.6 W/m^2 Bowie *et al*., 1985:320	21.42 W/m^2 Bowie *et al*., 1985:320
EXH20	Extinction of pure water	0.45 m^{-1} Cole & Wells,	0.45 m^{-1} Cole & Wells,	0.45 m^{-1} Cole & Wells,

Symbol	Model Parameters	Diatoms	Greens	Cyanobacteria
		2008:C-134	2008:C-134	2008:C-134
EXSS	Extinction due to inorganic suspended solids	Not modelled	Not modelled	Not modelled
EXOM	Extinction due to organic suspended solids	$0.3m^{-1}$ Cole & Wells, 2008:C-134	$0.3m^{-1}$ Cole & Wells, 2008:C-134	$0.3m^{-1}$ Cole & Wells, 2008:C-134
BETA	Fraction of incident solar radiation absorbed at water surface	0.45 Cole & Wells, 2008:C-134	0.45 Cole & Wells, 2008:C-134	0.45 Cole & Wells, 2008:C-134
AS	Algal settling velocity	0.5 m day^{-1} Smayda & Boleyn, 1965	0.18 m day^{-1} Burns & Rosa, 1980	0.1 m day^{-1} Burns & Rosa, 1980
ALGP	Stoichiometric equivalent between algal biomass and phosphorous	0.01 Bowie *et al*., 1985:286	0.012 Reynolds, 1984	0.007 Reynolds, 1984
ALGN	Stoichiometric equivalent between algal biomass and nitrogen	0.072 Bowie *et al*., 1985:286	0.066 Reynolds, 1984	0.08 Reynolds, 1984
ALGC	Stoichiometric equivalent between algal biomass and carbon	0.4 Bowie *et al*., 1985:286	0.49 Reynolds, 1984	0.46 Reynolds, 1984
ALSI	Stoichiometric equivalent between algal biomass and silica	0.2 Bowie *et al*., 1985:286	0 Bowie *et al*., 1985:286	0 Bowie *et al*., 1985:286
ACHLA	Ratio between algal biomass and chlorophyll-a in terms of mg algae/µg chlorophyll-a	0.02 Bowie *et al*., 1985:286	0.02 Bowie *et al*., 1985:286	0.02 Bowie *et al*., 1985:286

8.7 Climate change scenarios considered

As mentioned earlier in this report, the Climate Systems Analysis Group based at the University of Cape Town has downscaled five GCMs for use at local level, and these have been quality controlled and processed by the School of Bioresource Engineering and Environmental Hydrology at the University of Natal for use in hydrological models which project environmental climate and hydrological changes. The results of these analyses will be used in this project for present conditions (1971-90) and projected intermediate (2046-

2065) and future (2081-2100) scenarios. The GCMs used for the water quality modelling study are listed below:

- Canadian Center for Climate Modelling and Analysis (CCCma), Canada (CGCM3.1(T47), first published 2005, abbreviated to CCC in this report);
- Meteo-France/Centre National de Recherches Meteorologiques (CNRM), France (CNRM-CM3, first published 2004, abbreviated to CRM in this report);
- Max Planck Institute for Meteorology (MPI-M), Germany (ECHAM5/MPI-OM, first published 2005, abbreviated to ECH in this report); and
- Institut Pierre Simon Laplace (IPSL), France (IPSL-CM4, first published 2005, abbreviated to IPS in this report).

This data includes daily minimum and maximum temperature, rainfall, evaporation, solar radiation, minimum and maximum relative humidity and a surrogate wind speed and wind direction. The data was further manipulated (See section on data manipulation) to produce hourly values for dry bulb and dew point temperature, cloud cover as well as solar radiation for weather stations in the Berg river catchment.

Windspeed and direction was not supplied by CSAG (UCT). CE-QUAL-W2 requires windspeed and direction as part of its meteorological data input. Thus windspeed and direction was simulated from past data. For 1996 the recorded windspeed and direction from 1 January 1996 to 31 December 1996 is repeated for the 20 years of all the simulation periods including the intermediate and future events, in the absence of downscaled data. This should not be a problem as the exercise is to examine trends as to how eutrophication is affected under varying climate conditions. This modelling exercise will thus reflect trends by the various climate change models.

The CE-QUAL-W2 model was run with meteorological input data (air temperature, dew point temperature, wind-speed and direction, cloud cover and solar radiation) from the four climate models (CCC, CRM, ECH and IPS) and trends were noted from each of the runs and compared. For this study, 1/1/1971-31/12/1990 represented the present time, 1/1/2046-31/12/2065 was the intermediate future and 1/1/2081-31/12/2100 was the distant future as seen in Figure 48.

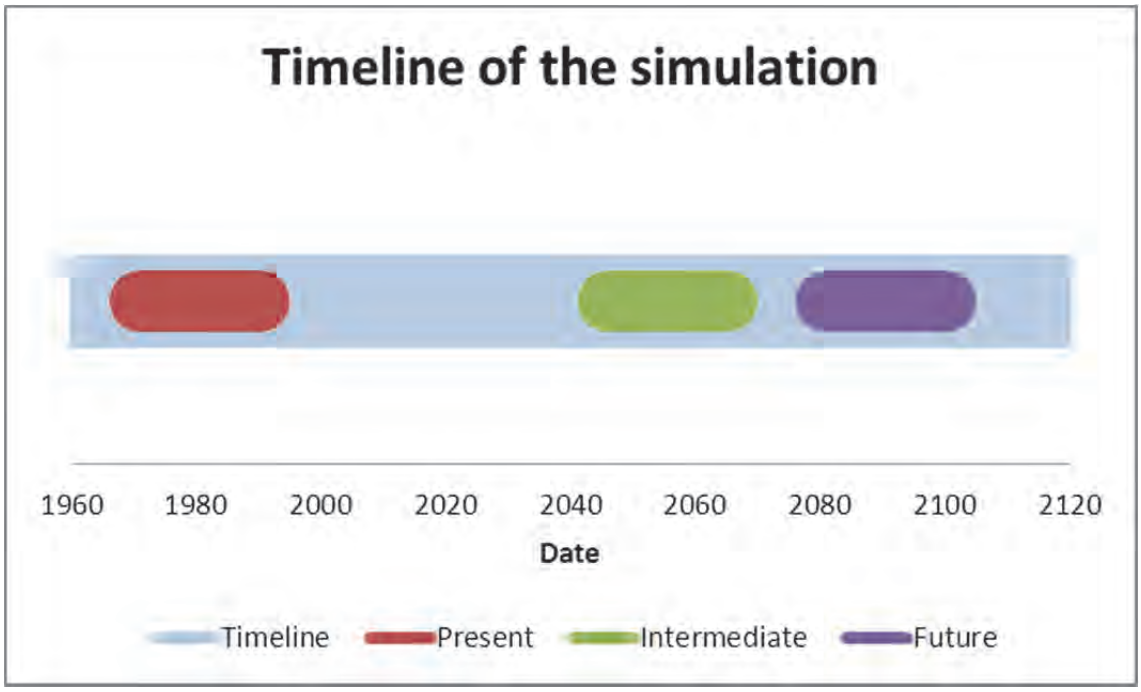

Figure 48: The timeline for the climate change study

This figure shows that the period between the present day and the intermediate future was substantially longer than from the intermediate future to the distant future. This was a result of the climate change studies, which predicted an acceleration of climate change effects for the later part of the century due to the increased anthropogenic loadings. Any change from present day to intermediate future would happen at a slower pace than that from intermediate future to distant future.

This study presents an attempt to determine the long-term effect of climate change on surface water quality and the subsequent effect on eutrophication of surface water of BRD and the resultant algal growth and possible algal succession. The present day simulations were used as the basis for comparison to the intermediate future and distant future scenarios, effectively highlighting and changes caused by climate change. This procedure was considered accurate as it was validated that the present day quantification simulations for one year compared favourably to the actual measured data for the BRD. Climate model inter-variation would also be discussed, as it was clear that different climate models projected varying climate change.

The most important site on the dam was considered to be the spillway site, and hence all outputs and discussions were concentrated on this area.

High algal concentrations are indicative of poor water quality, and that algal growth was affected by temperature, light and nutrients. In the event of climate change, the air temperature was expected to increase as well as anthropogenic loadings. Thus, the process towards identification of the variable that managers and operators of large dams could control to limit poor water quality with respect to algal growth consisted of:

- Identification of factors affecting algal growth;
- Quantification of how much it affects algal growth; and
- Identification of possible means of reduction of these variables.

Thus, temperature and light are two of the variables that are to impractical to try to manipulate to control algal growth. It was only nutrients, which may be removed before they enter the catchment and receiving waters.

8.8 Meteorological data manipulation

Meteorological data required as a boundary condition include:

- Air temperature in °C;
- Dew point temperature in °C;
- Wind speed in m/s;
- Wind direction in radians; and
- Short wave solar radiation in W/m^2.

To quantify primary production it was useful to specify meteorological parameters on an hourly basis (Brock, 1981) such that the short term response of algal concentrations, for example, are more accurately captured. For the modelling of BRD and Voëlvlei Dam, daily data for minimum and maximum air temperature as well as solar radiation were disaggregated to hourly values over a twenty year period using the methods described by Brock (1981) and Wang *et al*. (2002) for solar radiation and those described by Linvill (1990) for temperature. The aforementioned disaggregated values for temperature and solar radiation were then further used to deduce hourly values of dew point temperature using the methods of Waichler and Wigmosta (2002) for dew point temperature and those of Luo *et al*. (2010) for cloud cover. Hourly wind speed and wind direction data was not available and

data for single year (1996) was repeated for the twenty year period so that the seasonality of the parameters is at least preserved.

The change in the average daytime air temperature is shown in Table 7, which shows an increase for all months and the highest relative increase being predicted by the CRM climate change model in the case of the intermediate future scenario, and by the IPS climate change model for the distant future scenario.

Table 7: Absolute Change in Monthly Average Daytime Air Temperatures for the Berg River Catchment

Climate Change model	**Jan**	**Feb**	**Mar**	**Apr**	**May**	**Jun**	**Jul**	**Aug**	**Sep**	**Oct**	**Nov**	**Dec**
	Absolute change in daily average daytime* temperatures predicted for *intermediate future scenario* relative to daily average daytime* temperatures predicted for *present day scenario* (in °C)											
IPS	2.5	2.6	2.8	2.8	3.7	2.4	2.7	2.3	2.4	2.4	2.8	2.9
ECHAM	1.6	1.8	2.0	1.6	2.1	1.4	1.8	1.6	1.9	2.1	1.5	1.9
CRM	4.9	4.9	4.8	5.6	4.8	3.8	3.9	4.1	4.3	4.3	4.8	5.1
CCC	3.4	2.8	2.6	3.4	3.1	1.8	1.7	1.7	2.3	2.9	2.9	3.1
	Absolute change in daily average daytime* temperatures predicted for *distant future scenario* relative to daily average daytime* temperatures predicted for *present day scenario* (in °C)											
IPS	7.2	7.3	6.9	8.2	8.2	5.5	5.0	4.6	5.2	6.2	6.9	8.0
ECHAM	5.4	5.3	5.5	5.5	3.6	3.3	4.0	3.6	3.9	4.2	4.8	5.4
CRM	6.1	6.4	6.2	6.9	6.5	4.8	4.2	4.5	4.4	5.0	5.4	5.7
CCC	Data not available for this climate change model											

**Refers to actual hours between sunrise and sunset*

The change in shortwave solar radiation data is shown in Table 8 which indicates a general decrease in the monthly average solar radiation values obtained from the intermediate future climate change scenario compared with values obtained from the present day climate change scenario for most of the climate change models, excepts for the CRM model which exhibited an increase in monthly averaged solar radiation values. The absolute change in monthly-averaged shortwave solar radiation values obtained from the comparison of values from the distant future climate change scenario and present day climate change scenario exhibit inter monthly variability with some months showing an increase while others show a decrease in shortwave solar radiation.

Table 8: Absolute Change in Monthly Average Daytime Shortwave Solar Radiation for the Berg River

Climate Change Model	Jan	Feb	Mar	Apr	May	Jun	Jul	Aug	Sep	Oct	Nov	Dec
	Absolute change in daily average daytime* shortwave solar radiation predicted for *intermediate future scenario* relative to daily average daytime* shortwave solar radiation predicted for *present day scenario* (W/m^2)											
IPS	-13.2	-14.9	-11.9	-4.0	2.8	-2.9	-1.1	0.2	-3.1	-9.0	-4.5	-10.7
ECHAM	-5.1	0.0	3.5	-2.5	1.0	-7.2	-3.3	-2.0	9.8	9.9	0.3	7.1
CRM	7.5	14.5	12.8	10.7	8.6	13.7	11.1	19.0	17.9	15.4	15.8	11.2
CCC	6.8	-6.4	-1.6	-0.2	-0.4	-1.8	0.3	-5.3	5.7	8.7	7.0	7.4
	Absolute change in daily average daytime* shortwave solar radiation predicted for distant *future scenario* relative to daily average daytime* shortwave solar radiation predicted for *present day scenario* (W/m^2)											
IPS	-2.2	3.1	-5.6	15.1	-3.8	-0.7	-1.0	-3.1	10.3	40.0	-9.1	-5.0
ECHAM	3.2	2.4	21.5	-6.0	-10.7	9.0	1.8	-1.6	16.6	1.9	10.3	3.1
CRM	-5.4	-2.2	-6.0	-6.5	-0.9	2.6	-9.4	13.3	9.5	6.1	-2.4	11.0
CCC												

**Refers to actual hours between sunrise and sunset*

8.9 Application of the CE-QUAL-W2 model to the BRD under various climate change scenarios

To provide a realistic simulation of the BRD it was necessary to represent the physical constraints as accurately as possible. As mentioned previously, these include bathymetric data, initial conditions, meteorological data and upstream/downstream boundary conditions. These will be discussed in more detail in the ensuing chapters.

Bathymetric Data

The bathymetric description of the BRD is probably the most fundamental data required to construct a numerical grid which is used in the model. The numerical grid is a simplified mathematical description of the volume and shape of the BRD. It is absolutely essential to construct an accurate description of the BRD, as this will determine how well the water level in the BRD is modelled. The water level in the BRD is closely linked to water quality modelling and if the initial hydraulic calibration is not achieved, then water quality calibration will be difficult, if not impossible.

Data for construction of the numerical grid was obtained from the DWAF and was available as contours through the BRD basin. The original data was imported into the Civil Designer programme where break-lines (joining high and low points) were generated. This surface

was used to calculate the volume in the BRD at 1m intervals. The orientation of a segment was obtained by connecting the midpoint of the cross-section (between banks) to the midpoint of the following cross-section with the angle being measured relative to north, in a clockwise direction. The procedure used is outlined below:

1. Discretise the reservoir into segments.
2. Draw a line from the midpoint of the downstream segment boundary to the midpoint of the upstream segment boundary.
3. At the outlet of the segment draw in a North-South line.
4. The angle between the two lines (defined in 2 and 3 above) in a clockwise direction from north was then measured and taken to be the segment orientation.

Each segment was then divided into a number of layers, 1 m in thickness, extending from the full supply level (FSL) to the bottom of the BRD. The width of each cell was calculated by using the formula below:

$$\frac{Volume\ in\ cell}{length\ of\ segment\ x\ height\ of\ segment}$$

Using this method, the calculated volume of each cell in the grid was preserved. The entire grid for BRD and the downstream river reach was made up of 22 segments and 58 layers with segments 1 and 22 representing boundary segments while layers 1 and 58 represented boundary layers that have zero width. These cells, however, need to be specified to enable the model to function. A visual representation of the grid is depicted in Figure 49. It should be noted that the main branch has 20 active segments.

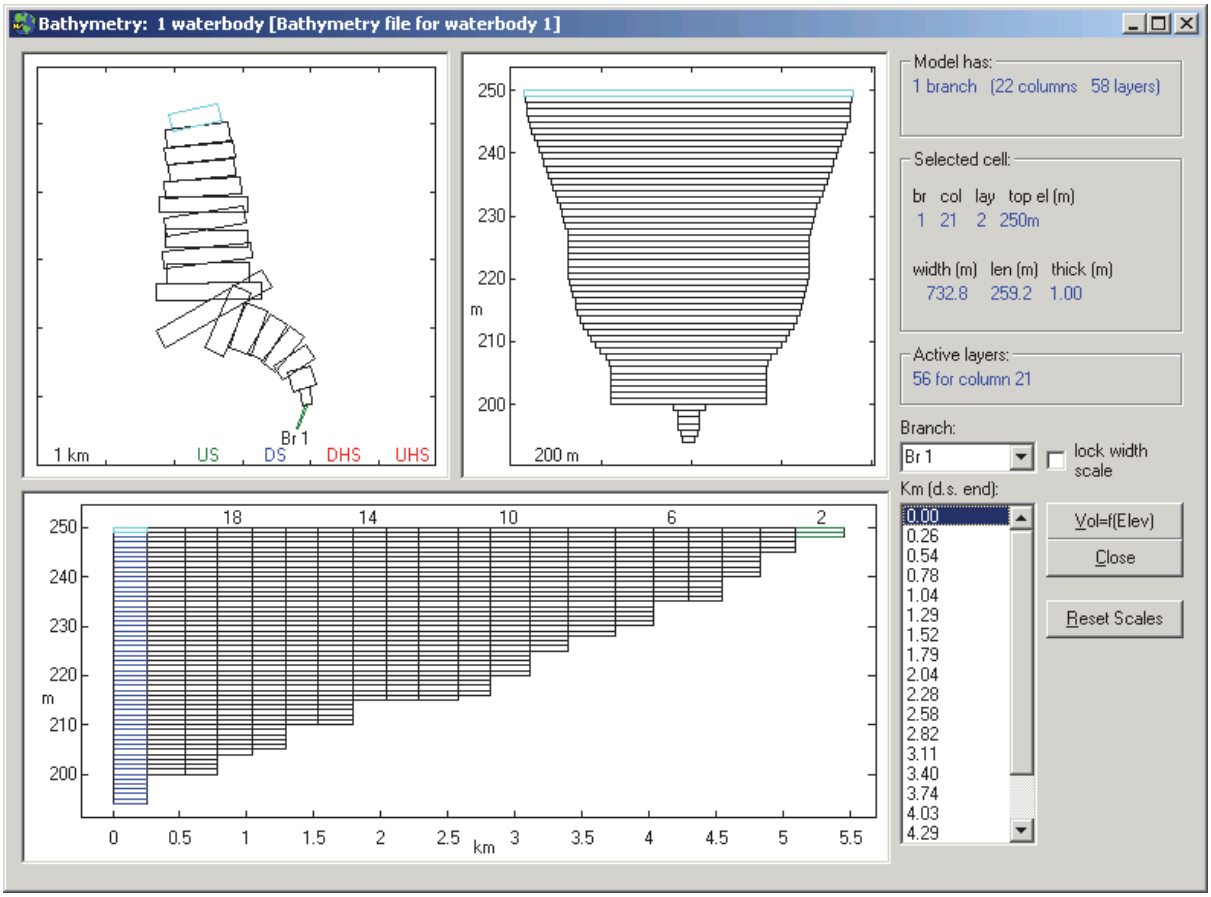

Figure 49: Berg River Dam bathymetry

The mathematical grid is only a representation of reality and should be compared with measured data to ensure that the grid is realistic. Since the calculated volume-height relationship was determined from contour surveys it was expected (based on previous experiences) to under-estimate the official volume-height relationship reported by the DWAF and that a scaling factor would be required to match the official volume-height relationship.

The comparison of the calculated and official (obtained from the contour survey) volume-height relationships is shown in Figure 50 and it shows that the calculated volume-height relationship is representative of the official relationship.

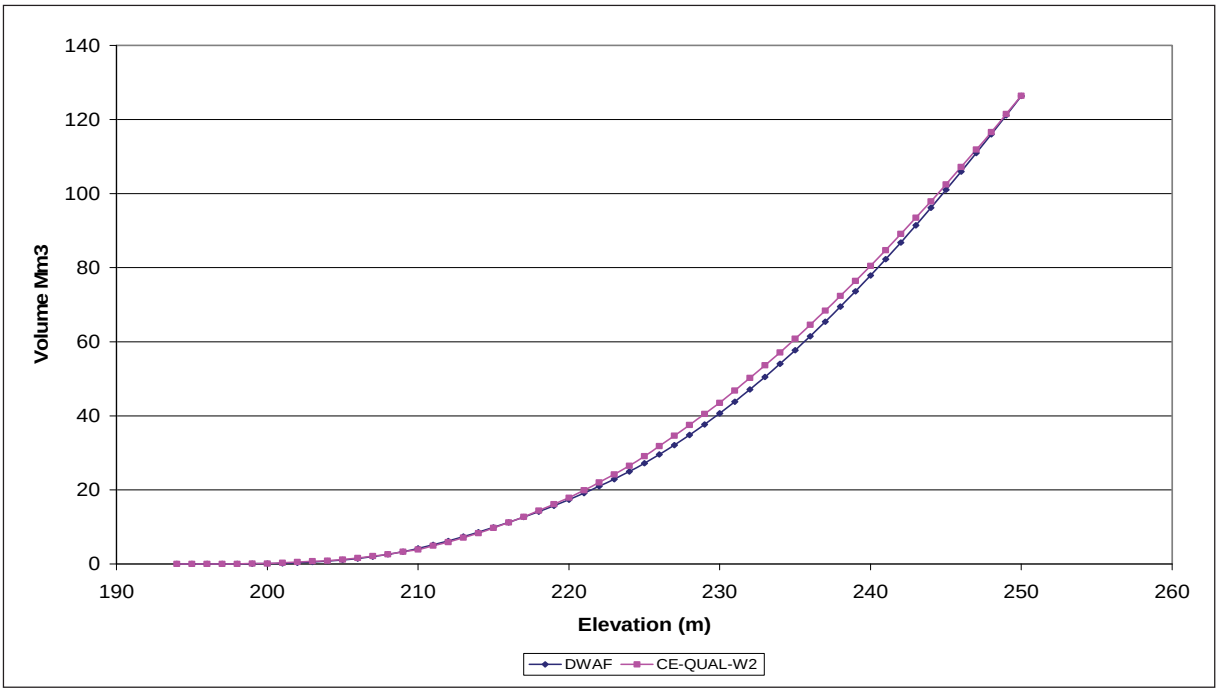

Figure 50: Comparison of volume-height relationships of the BRD

Boundary Condition Data

The latest instream flow requirements (IFR) for the downstream river and the operating rules of the BRD were used to create a spreadsheet to calculate the time series outflows from the reservoir. The observed flow record at G1H004 was used as the raw data, from which other flows were calculated. These calculated flows were then extracted from the spreadsheet to create input files for the CE-QUAL-W2 model. Table 9 represents the calculated flows and the inputs files that are associated with Branch 1.

Table 9: Summary Boundary Conditions, Inflows and Outflows for the Reservoir

Extracted Flow Data	CE-QUAL-W2 Input file
Upstream Boundary Condition: Berg River Inflow	Qin_Br1
Wolwekloof Tributary Inflow	Qin_Tr1
Supplement Inflow	Qin_Tr2
Downstream Boundary Condition: Environmental base flow and flood releases into downstream river	Qot_Br1
Urban Abstractions	QWD

Berg River and Wolwekloof Tributary Inflow

The combined inflow of the Berg River and the Wolwekloof tributary was recorded at G1H004. Included in this record were the summer irrigation releases from the Theewaterskloof Dam, which in future will be released downstream of the BRD. In order to account for the omission of the Theewaterskloof releases, the monthly mean inflows from the G10A quaternary catchment (as stated in the document, *Preliminary Determination of the Reserve and Resource Class in Terms of Section 14(1)(b) and 17 (1)(b) of the National Water Act*, 1998 (Act No. 36 of 1998)) (see Table 10: Natural Duration Curve), were taken as the combined Berg River and Wolwekloof inflow from 1 November to 24 May. For the rest of the year, the recorded flow at G1H004 was used for the inflow data, thus allowing all winter floods to enter the dam. The Theewaterskloof Dam releases were then quantified as the difference between the recorded data and the monthly summer Mean Base Inflows.

The contribution of the flow of the spills bypassing the Wolwekloof inlet as a proportion of the total flow at G1H004 is $\frac{6.3}{115.9}$. This fraction was obtained by extracting flows from the Water Resource Yield Model (WRYM) developed for the Western Cape System Analysis. Therefore, the inflow was distributed between the Berg River and Wolwekloof Tributary in the proportions of $\frac{109.6}{115.9}$ and $\frac{6.3}{115.9}$, respectively.

Supplement (Drakenstein) Inflow

The Supplement Inflow was calculated as the difference between the accruals downstream of the BRD and the environmental flow requirements downstream of the Supplement site. The accruals were estimated to be 88% of the flow at G1H004 during winter and 88% of the median base inflow in summer (i.e. once the irrigation releases have been subtracted). The quantity of water delivered by the Supplement Scheme to the BRD was limited by the maximum diversion capacity of 4 m^3/s.

Environmental Base flow Releases

The environmental base flow releases were calculated from the exceedance values in Table 10, which were extracted from the document, *Preliminary Determination of the Reserve and Resource Class in Terms of Section 14(1)(b) and 17 (1)(b) of the National Water Act*, 1998 (Act No. 36 of 1998).

Table 10: Summary IFR Curves for IFR Environmental Base Flow Releases

Summary of IFR rule curves for G10A at IFR Site 1 Regional Type : W. Cape (wet) **Ecological Category = C** Data are given in m^3/s mean monthly flow										
Month	**% Points**									
	10%	20%	30%	40%	50%	60%	70%	80%	90%	99%
Oct	0.957	0.957	0.952	0.939	0.909	0.845	0.733	0.587	0.503	0.503
Nov	0.826	0.826	0.821	0.806	0.773	0.702	0.579	0.417	0.324	0.324
Dec	0.700	0.700	0.693	0.671	0.621	0.523	0.379	0.240	0.184	0.175
Jan	0.359	0.359	0.356	0.348	0.329	0.291	0.236	0.183	0.149	0.082
Feb	0.359	0.359	0.356	0.348	0.328	0.248	0.198	0.141	0.083	0.058
Mar	0.359	0.359	0.357	0.351	0.338	0.302	0.262	0.161	0.116	0.049
Apr	0.926	0.926	0.920	0.903	0.863	0.780	0.635	0.443	0.313	0.158
May	1.195	1.195	1.188	1.168	1.121	1.025	0.855	0.632	0.504	0.504
Jun	3.882	3.882	3.858	3.804	3.682	3.420	2.882	1.908	0.998	0.829
Jul	8.629	7.926	7.292	6.712	6.125	4.951	4.119	2.612	1.206	1.206
Aug	1.914	1.914	1.907	1.889	1.851	1.768	1.599	1.292	1.006	1.006
Sep	1.795	1.795	1.786	1.763	1.710	1.600	1.406	1.151	1.005	1.005
Natural Duration curves										
Oct	6.623	4.730	4.114	3.289	2.811	2.401	2.005	1.542	1.247	0.743
Nov	3.403	2.944	2.292	1.836	1.609	1.246	0.957	0.760	0.590	0.440
Dec	2.378	1.579	1.206	0.993	0.706	0.653	0.485	0.366	0.310	0.175
Jan	1.930	0.937	0.665	0.541	0.403	0.329	0.258	0.198	0.149	0.082
Feb	2.298	1.343	0.806	0.537	0.422	0.248	0.198	0.141	0.083	0.058
Mar	2.117	1.602	0.866	0.586	0.429	0.302	0.265	0.161	0.116	0.049
Apr	6.975	4.252	3.268	2.768	2.303	1.763	1.269	0.610	0.313	0.158
May	14.531	11.156	8.654	7.027	6.299	5.320	4.077	2.912	1.744	0.769
Jun	20.089	16.647	12.720	9.877	7.793	6.543	4.811	4.178	3.580	0.829
Jul	17.884	15.438	12.578	11.130	9.476	7.038	6.250	5.496	3.580	1.956
Aug	13.008	11.156	9.431	8.957	7.799	6.840	6.313	5.444	4.958	2.595
Sep	11.034	7.820	6.721	6.084	5.150	4.240	3.893	3.140	2.631	1.921

The lower half of the table represents the possible monthly inflow and the upper half of the table represents the environmental base release that was associated with the inflow in the month that it occurred. For example, if the inflow during November was 1.609 m^3/s, then the base flow release would have a flow of 0.773 m^3/s.

The table was not used 'as is'. The exceedance curves for April, June and July included flood releases. Therefore, the March exceedance curve was used for April and the August exceedance curve was used for June and July.

Environmental Flood Releases

Table 11 summarises the IFR environmental flood releases of the BRD. The data was extracted from the report: Western Cape Water System Operating Rules (Annexure H of DWAF 2002, Memorandum of Agreement).

Table 11: IFR Environmental Flood Releases

MONTH	Maximum Peak Intensity m^3/s		Duration of Flood Releases (Days)	Total Volume of Flood (Mm^3)
	Daily Average	Instantaneous Peak		
April	5		5	0.8
June	30	65	7	4.5
July	65	160	7	9.8
November	1		1	0.5
December	1		1	0.5

For practical reasons, the winter flood releases will not necessarily be made in the months that are prescribed in Table 11. Each flood will only be made once, between 25 May and 31 October, and the timing of the release will depend on whether the magnitude of the inflow to the BRD meets the thresholds that are required for the flood releases.

The threshold for the most intense flood release was assumed to be that the daily average inflow (at G1H004) exceeds 65 m^3/s or alternatively, that the instantaneous flow approaches 160 m^3/s. The threshold for the moderate flood release in winter was that the daily average flow exceeds 30m^3/s or the instantaneous flow approaches 65 m^3/s.

In addition, Table 11 shows that the flood releases had specified durations and volumes. The flood releases were distributed across the duration period such that the total volume added up to the volume specified in Table 11. The flood release hydrographs were shaped to the pattern of the incoming flood flows, as shown in Figure 51.

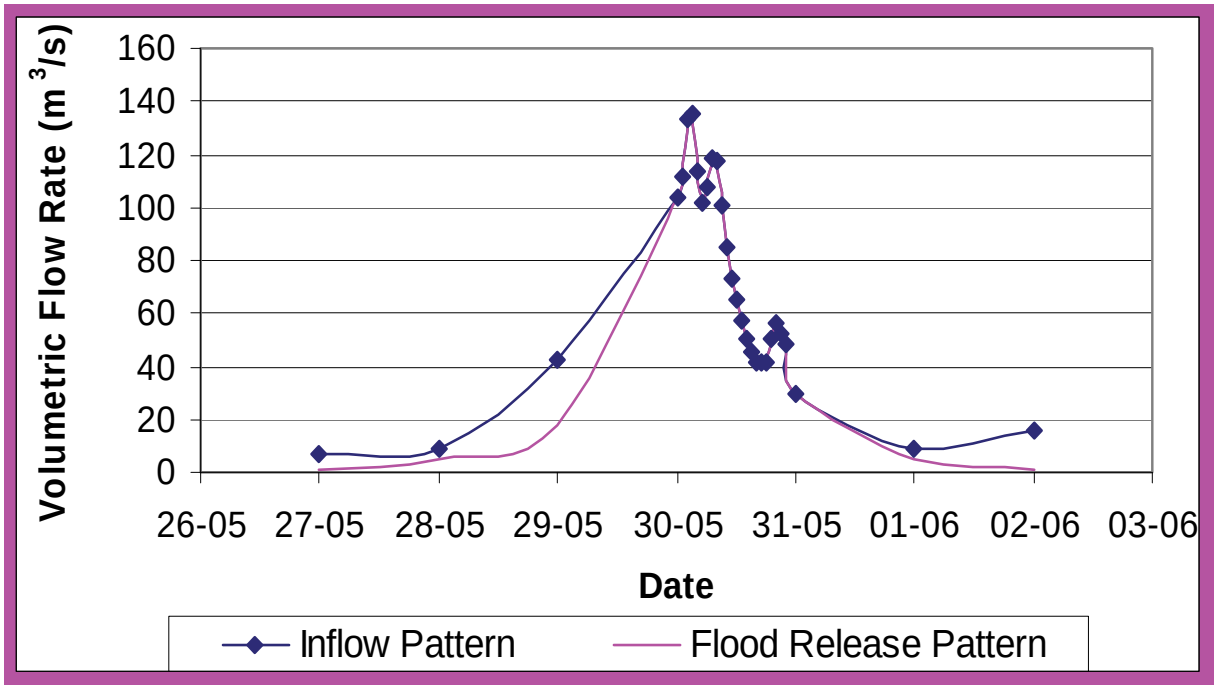

Figure 51: Environmental flood release pattern

Urban Abstractions

Data for urban abstractions by the City of Cape Town from the Berg River Dam were extracted from the document, *Western Cape Water System Operating R*ules (Annexure H of DWAF 2002, Memorandum of Agreement). The data followed a monthly pattern, and is represented in Table 12.

Table 12: Monthly Withdrawal Rates for Urban Demands

Month	Urban Demand (m^3/s)
1	2.80
2	3.18
3	2.46
4	2.35
5	2.13
6	2.20
7	2.17
8	2.20
9	2.59
10	2.73
11	3.09
12	2.95

Water Quality data

Data Acquisition

Raw water quality data were obtained from DWAF's grab sample data collected on a two-weekly basis. Table 13 summarises the tributaries and rivers of the modelled system and its associated station (or source of measurement) as well as the CE-QUAL-W2 input files.

Table 13: Water Quality Boundary Conditions

River or Tributary	Monitoring Station	CE-QUAL-W2 Input File
Berg River	G1H004	Cin_Br1
Wolwekloof Tributary	G1H004	Cin_Tr1
Supplement Inflow	G1h020 and B3 (Note 1)	Cin_Tr2
Franschhoek River	G1H003	Cin_Tr3
Wemmershoek River	G1R002 *(Note 2)	Cin_Tr4
Banghoek River	G1H019	Cin_Tr5

Note 1 : The water quality of the supplement supply was estimated by the water quality that was measured at G1H020 and the Drakenstein Municipal Station B3**.**

Note 2 : There is no water quality data for the gauge G1H071 for 2000-2001, and the data was only available from 1988 to 1992. Therefore, it was decided that the best estimate for water quality of the Wemmershoek Tributary was to apply the monthly average values from 1996 to 1999 that were averaged from measurements at G1R002, from 1996 and 1999 at the Wemmershoek Dam.

The water quality constituents that were infilled include total dissolved salts, ammonia, nitrate-nitrites, phosphates and dissolved silica. For dissolved oxygen, it was assumed that the concentration was 14 mg/l, the saturated concentration of oxygen in water at 25°C.

Temperature Data

The only available raw data for G1H004 with respect to temperature was the data that was supplied by L de Wet for 2003 to 2005 (DWAF, Worcester Office). It was assumed that this temperature data represented the raw temperature data for the Berg River inflow and the Wolwekloof tributary inflow.

Initial Condition

Initial conditions for the reservoir were supplied as vertical profiles, in the form of a VPR.npt file for use by CE-Qual, due to the stratifying nature of deep dams. Since there was no

measured data available, the initial conditions had to be 'calculated' using the following procedure:

i. Initialise the concentration of each constituent with a constant value that was weighted from the loads from G1H004 and temperature.

ii. Simulate the reservoir model for a one year period.

iii. Extract the vertical profile concentration for each component on the last day of the simulation using the AGPM post-processor of CE-QUAL.

iv. Prepare the vertical profile file with the vertical profiles of concentrations for each constituent and temperature.

Scenarios considered for simulation

Several scenarios were considered for the modelling exercise, each scenario adding to the degree of complexity of the final model. The “base scenario” assumes that only one algal group, the diatoms, is present in the dam the while scenario 2 assumes a mixture of diatoms and greens and scenario 3 a mixture of diatoms, greens and cyanobacteria.

The model requires a set of input parameters to solve each of the equations presented in this report. As is evident from the list, many parameters need to be defined and it was not practical to assume that all or even most of the parameters could be calibrated. Where possible, parameter values were obtained from literature, where a prescribed range was suggested.

Earlier reports on Voëlvlei Dam (Southern Waters, 1999) reported that prior to 1995 the algae problems were limited to seasonal blooms of filamentous diatoms, Aulacoseira and was also related to low impoundment levels and wind-mixing in autumn. In more recent years, however, blooms of Anabaena solitaria and Microcystis aeruginosa have been detected and have been associated with taste and odour (geosmin-A.solitaria) and hepatotoxins. Based on the aforementioned information it was decided that the initial setup of the BRD model should initially consist of only one algae compartment modelling the behaviour of a culture consisting mostly of diatoms. Parameter values were obtained from a comprehensive list of rate constants prepared by Bowie et al (1985) and the user’s manual for CE-QUAL-W2 v3.6. The simulations will include 3 algal compartments and will rely on the optimum temperature ranges for growth to calculate the specific abundance of a specific algal species under the various climate change conditions.

Berg River dam Present day scenario

The model was run for 20 years with the flow inputs and withdrawals using the four climate models present day meteorological data and a baseline is established to which the future scenarios will be compared.

The factors that limit algal growth are water temperature and solar radiation, if all other factors such as light, nutrients and dissolved oxygen are in adequate (Wetzel, 2001). Solar radiation emitted by the sun is relatively constant and the incident solar radiation over Berg River Dam is affected largely only by cloud cover. Thus, the only factors that directly affect surface water temperature are air temperature (by conduction) and short-wave solar radiation and their relative contributions are to be assessed.

Air temperature

Carbon dioxide (CO_2), methane (CH_4), chlorofluorocarbons (CFCs), nitrous oxides (NO_x) and water vapour (H_2O) in the atmosphere allow the passage of shortwave solar radiation from the sun onto the earth surface, whilst absorbing the re-radiated radiation from the earth allowing the heating of the earth and the air. This heating is dubbed the *Greenhouse Effect* (Carter, 1994).

Four GCMs' were downscaled statistically to RCMs' over Berg River Dam and these climate models predict amongst others, air temperature. The mechanism of the greenhouse effect will in effect heat the air from the present day temperatures to a higher future temperature. It was postulated that this increase would alter the state of dams and contribute to worsening water quality by increasing algal biomass concentrations due to warmer surface waters.

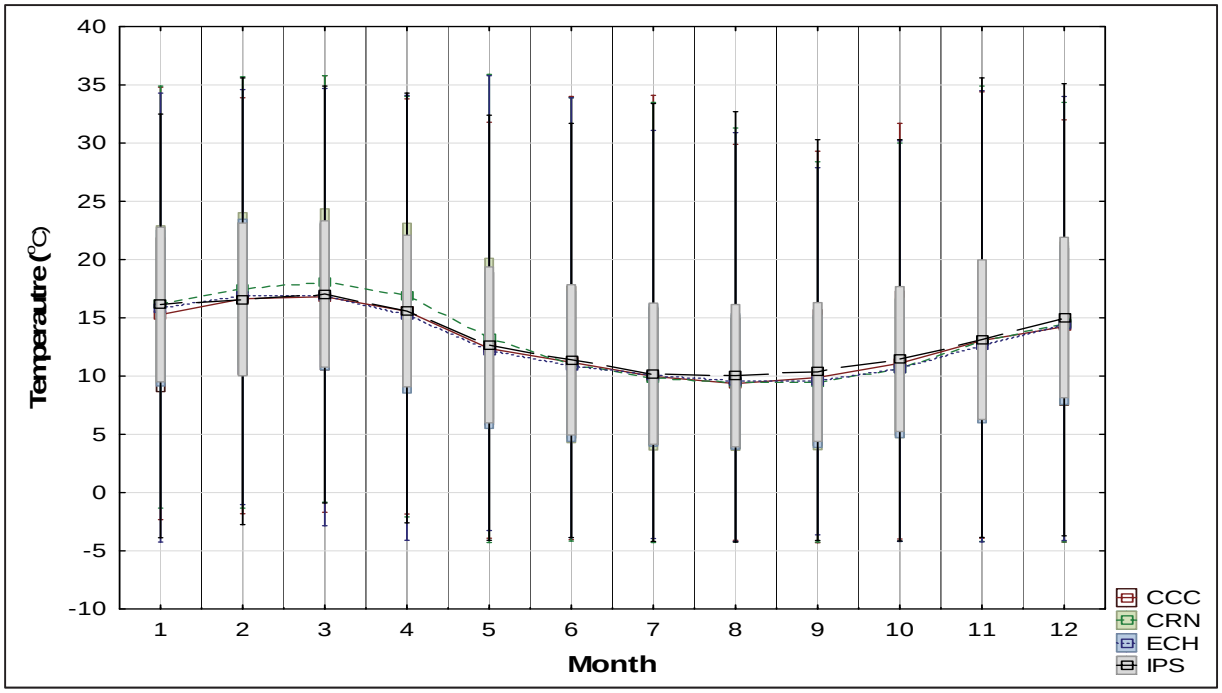

Figure 52: The present day air temperature for Berg River Dam

It is shown in Figure 52 and Table 14 that all four climate models predict similar mean monthly air temperatures for the 20 year present day simulation period. This mean temperature includes day and night-time temperatures and it was seen that the mean air temperature does drop below 0^{o}C at times. The inter-variation between climate models was minimal.

Table 14: The present day monthly mean air temperatures for Berg River Dam

	Jan	Feb	Mar	Apr	May	Jun	Jul	Aug	Sep	Oct	Nov	Dec
CCC	16.56	17.53	17.12	14.34	10.40	9.16	9.03	9.11	10.23	12.27	14.33	15.82
CRM	17.92	18.74	18.47	15.95	10.74	8.61	8.60	8.87	9.87	11.80	14.57	16.17
ECH	17.50	18.01	17.15	13.80	10.13	9.08	8.81	9.13	10.00	11.44	14.11	16.03
IPS	17.59	17.64	17.38	14.81	10.51	9.34	8.93	9.44	10.69	12.32	14.75	16.78

The mean monthly air temperatures of the four climate models are similar in magnitude and cycle. The colour represents the magnitude with red being greater than green. Winter was May to July and summer was December to March. The annual mean temperature of all the models is 13.6^{o}C that was expected to increase with climate change into the future because of the greenhouse effect. There was almost a 7^{o}C difference between mean winter and mean summer temperatures.

8.10 **Solar radiation**

Each of the present day climate models predicts similar levels of solar radiation as shown in Figure 53 for the 20 year modelling period. It was discussed by Wetzel, 2001 and DeNicola, 1996 that solar radiation was the major driver for diurnal surface water temperature and hence algal growth with all the other factors that may affect algal growth being equal. Thus, water temperature may limit algal growth even in the presence of abundant nutrients and light which favouring growth.

All organisms have a temperature range at which optimal growth occurs thus their life cycles are directly linked to temperature. Temperature primarily affects algal photosynthetic metabolism by controlling the enzyme reaction rate of the algae and an optimum temperature for each species was observed (DeNicola *et al.*, 1996). Thus, diurnal algal growth was directly influenced by solar radiation intensity.

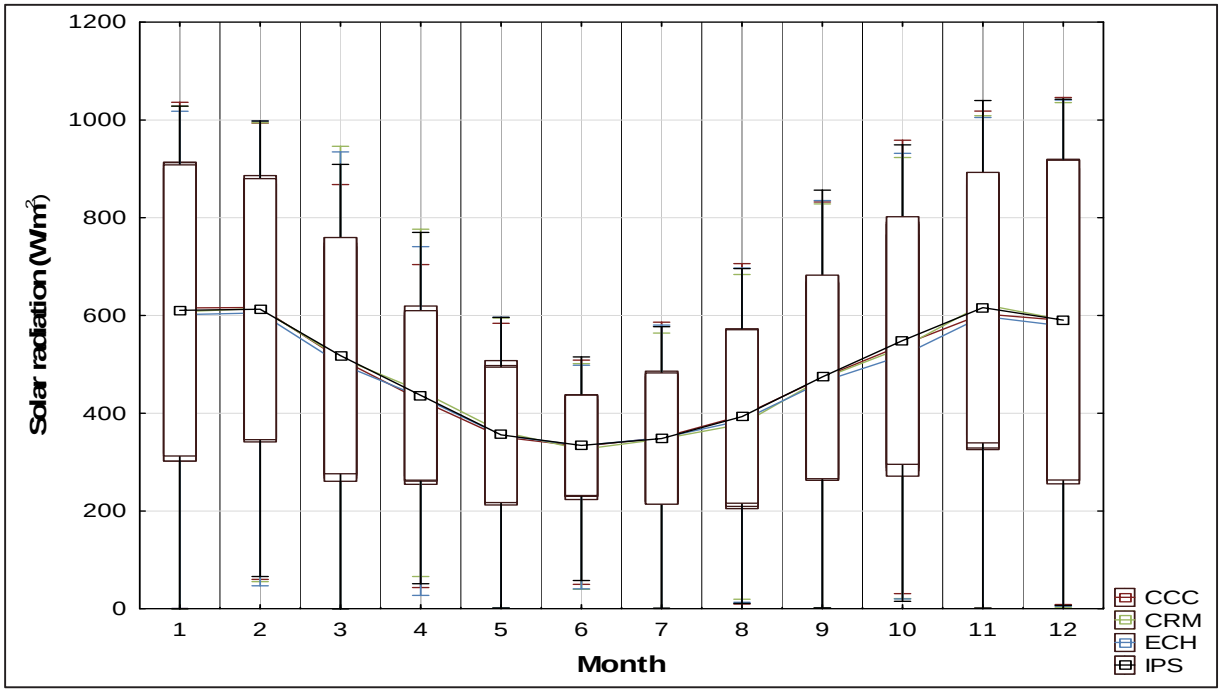

Figure 53: The present day mean monthly solar radiation for Berg River Dam

This figure shows higher solar radiation rates during the summer months as opposed to winter. Wetzel, 2001, DeNicola, 1996 and other argue that solar radiation was the major driver for diurnal surface water temperature.

Table 15: The present day mean monthly solar radiation for Berg River Dam (W/m^2)

	Jan	Feb	Mar	Apr	May	Jun	Jul	Aug	Sep	Oct	Nov	Dec
CCC	615.6	616.6	510.6	426.7	351.6	332.2	350.3	395.2	472.6	539.7	603.5	590.0
CRM	607.4	614.4	513.3	445.5	362.4	325.9	347.3	377.8	471.1	534.5	622.4	590.8
ECH	601.8	605.4	500.9	433.4	355.0	333.9	349.4	385.1	464.6	518.3	598.5	578.2
IPS	610.4	613.0	517.8	436.6	355.8	334.1	348.2	393.3	474.4	548.8	616.0	590.5

From the table and figure, it was seen that the climate models agreed well with each other. Summer was December, January and February, whilst winter was June, July and August for the Western Cape Province, the location of Berg River Dam. The solar radiation was on average almost double in summer to that of winter, which was attributed to the longer daylight hours during summer. The phenomena of higher solar radiation in summer should have a marked effect on the diurnal temperature of the dam (Wetzel, 2001 and others) and its influence along with air temperature was investigated in the following sections.

8.11 Wind speed and direction

Wind-speed and direction was not supplied by CSAG (UCT). CE-QUAL-W2 requires wind-speed and direction as part of its meteorological data input to predict water quality. In the absence of this wind-speed and direction was replicated from past data. This should not be a problem as the study was to examine changes in eutrophication due to varying climate conditions.

Figure 54: The N-S orientation of Berg River dam

Figure 54 Shows that the reach of Berg River Dam is just west of the N-S directions and the subsequent effect of the prevalent wind over the dam was investigated.

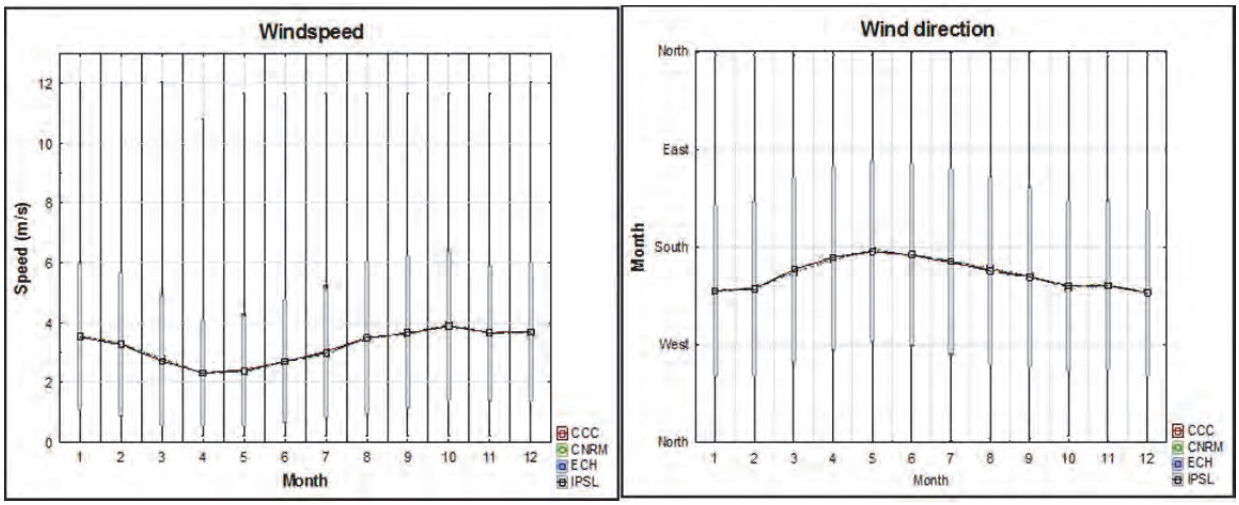

Figure 55: The present day wind speed and direction for Berg River Dam

The predominant wind is south to south-west for most of the year over the dam with maximum wind speeds during summer. The wind speed was seen to increase from the winter to summer. The wind speed is much less than that over Berg River dam.

8.12 Surface water temperature

Wetzel (2001), DeNicola (1996) and other argued that solar radiation was the major driver for surface water temperature, thus the following figure shows the surface water temperature of segment 21 for the present day 20 year climate models. It was expected that months that have higher mean daily solar radiation rates should have warmer surface waters.

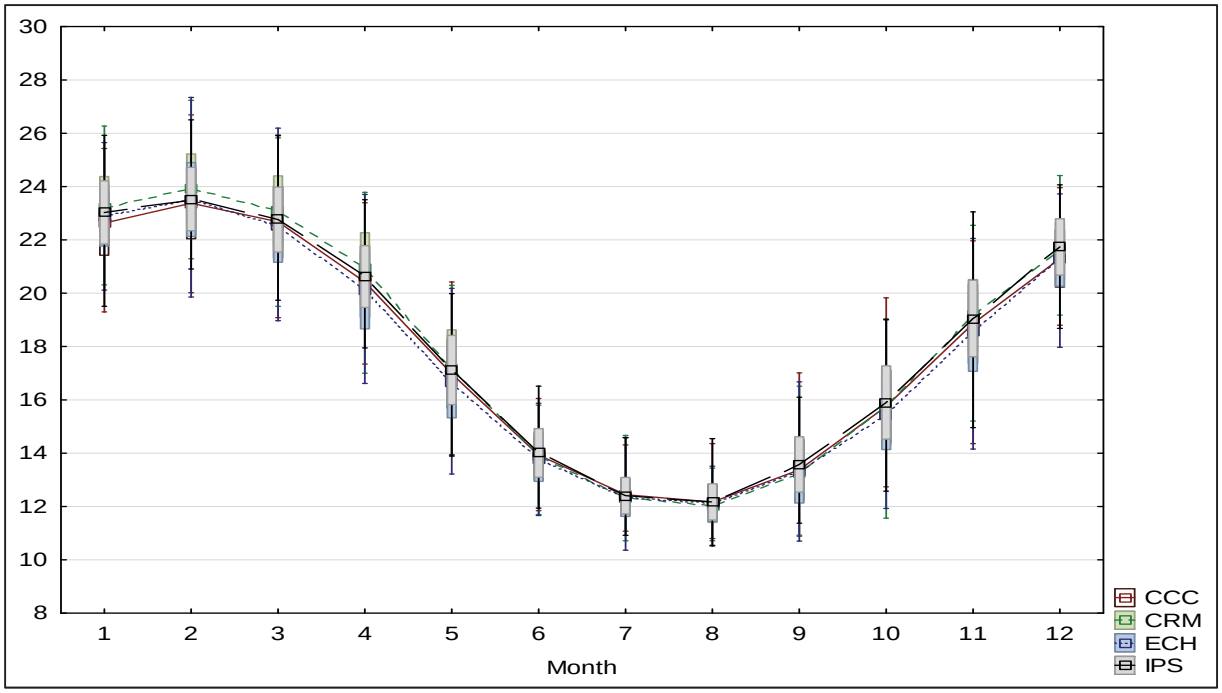

Figure 56: The present day mean monthly surface water temperature for Berg River Dam

When comparing this to figure to that of solar radiation (Figure 53) it is clear that solar radiation does not drive the surface water temperature but rather air temperature (Figure 52) albeit it being lower. It was clear that the surface water temperature follows the same pattern as that of the air temperature but was warmer. This was mainly due to the high specific heat capacity of water. Once the incident solar radiation has heated the water it retains this heat efficiently even though the air temperature was less and had a cooling effect on the water. Coupled with this was the relatively low wind speed over the dam which also limits evaporation thereby limiting heat loss.

Table 16: The present day mean surface water temperature for Berg River Dam (°C)

	Jan	Feb	Mar	Apr	May	Jun	Jul	Aug	Sep	Oct	Nov	Dec	Annual me
CCC	22.6	23.4	22.7	20.4	17.0	13.9	12.4	12.2	13.4	15.8	18.9	21.3	17.8
CRM	23.2	23.9	23.1	20.9	17.2	13.9	12.3	12.0	13.3	15.7	19.2	21.6	18.0
ECH	22.9	23.5	22.5	20.1	16.6	13.8	12.3	12.1	13.3	15.4	18.6	21.3	17.7
IPS	23.0	23.5	22.8	20.6	17.1	14.0	12.4	12.2	13.6	15.9	19.1	21.7	18.0

Table 16 shows that the surface water temperature of Berg River Dam was on average 10.8°C warmer in summer than winter with an annual surface water temperature of 17.9°C. All four climate models showed similar trends and values. Thus, it was expected that if all conditions are favourable, then an increase in the concentration of algae was expected in the summer period due to the average summer surface water temperature coinciding within the temperature rate multipliers for the diatoms, greens and cyanobacteria modelled in Berg River Dam (Table 5). The inter-climate change temperature values are very similar and they agree well.

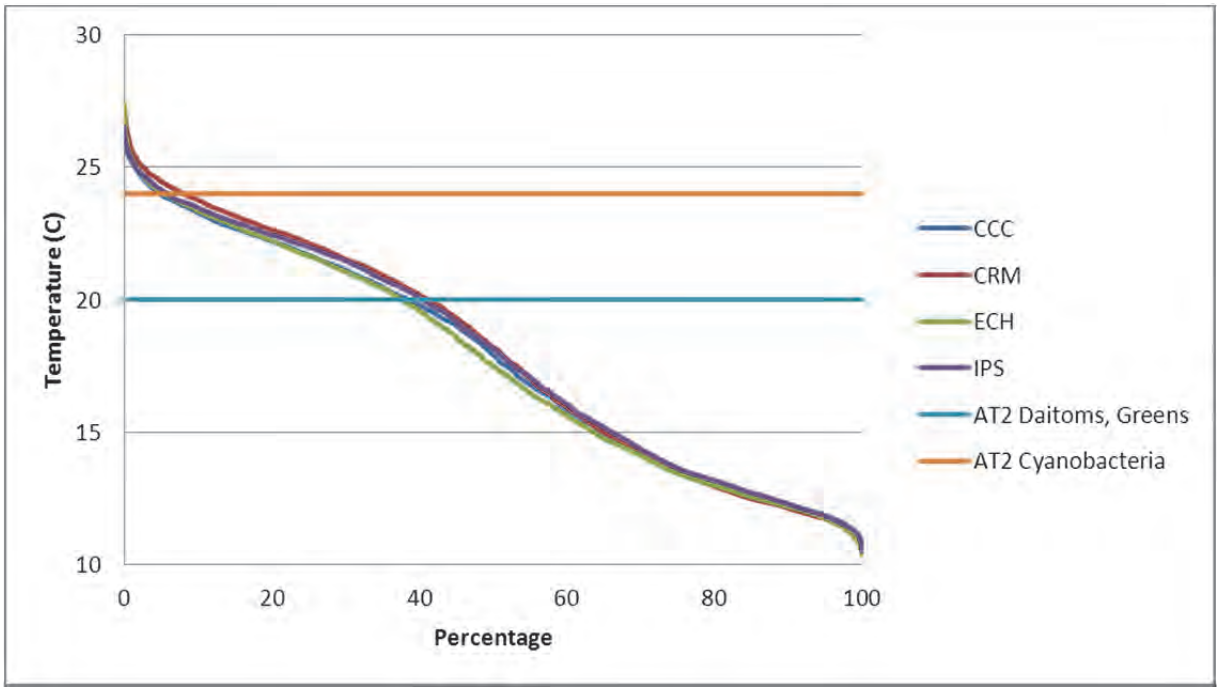

Figure 57: The present day surface water temperature exceedance plot of algae for Berg River Dam

To establish the probability of the type's algal blooms, an exceedance plot (Figure 57) is generated showing the algal temperature growth multipliers. The temperature rate multiplier for diatoms and greens that set the lower temperature limits (20°C) for maximum growth is exceeded between 40% of the simulation time. Cyanobacteria have a higher maximum temperature growth rate (24°C) and this temperature is exceeded between 5 and 8% of the

time of the 20 year simulation. It was hereby supposed that diatoms and green algae could be present in Berg River dam for up to 40% of the time and cyanobacteria up to 8% of the time, due to the temperature being favourable for their growth.

To investigate the premise that Berg River Dam was monomictic a temperature profile plot was required.

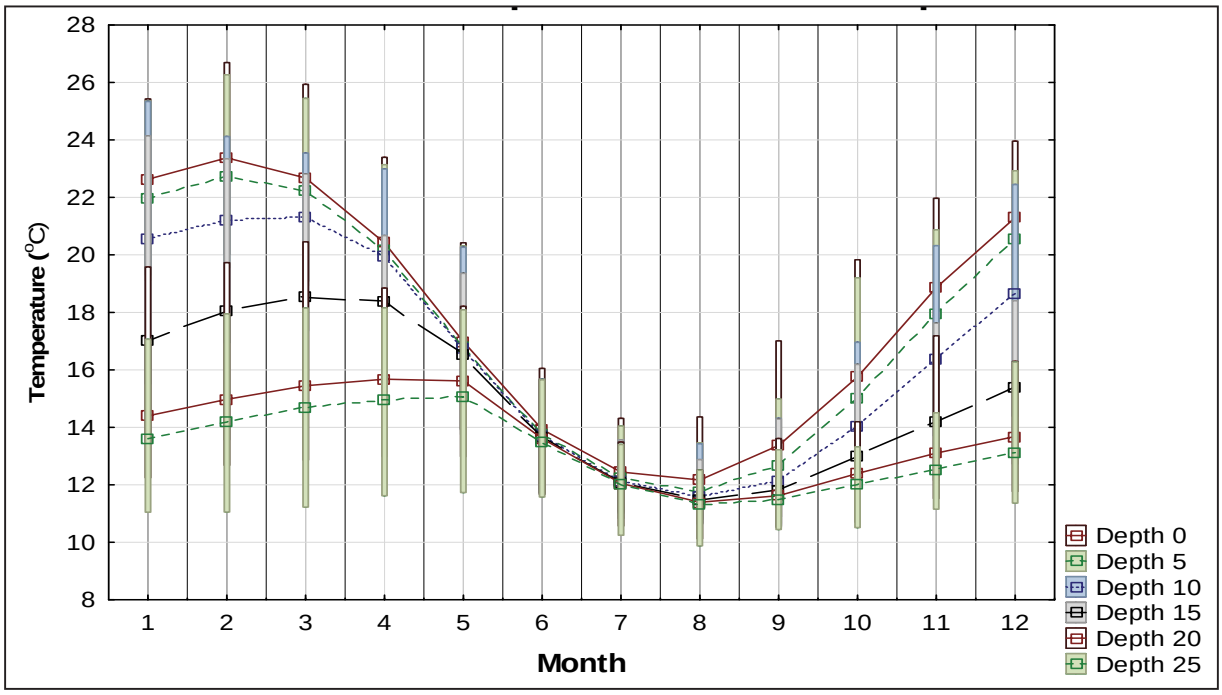

Figure 58: The present day mean water-depth temperature relationship for Berg River Dam as projected by the CCC climate model

From this figure, it is seen that the difference between surface water temperature and that at depth is greatest during the warmer months, confirming the existence of the thermocline during the warmer months. This thermocline occurs somewhere between 10 and 15m depth and was negligible during winter. During winter, the dam was virtually uniform in temperature and fully mixed, which allowed for re-suspension of nutrients throughout the dam. Thus at the onset of spring, the warmer water would facilitate the growth of algae even though no additional nutrients was added to the dam.

8.13 Surface water elevation

The factors affecting surface water elevations are:

- Inflow
- Withdrawals
- Evaporation

The inflows and withdrawals are kept the same for each year as well as for each model, thereby implying that the only evaporation has a changing effect on water levels due to climate change. The surface water elevation for the 20 year present day period is shown in the following figure as well as its monthly values. The various undulations are a product of the inflow and withdrawals and the inter-variation between climate models was a result of the evaporative differences between models.

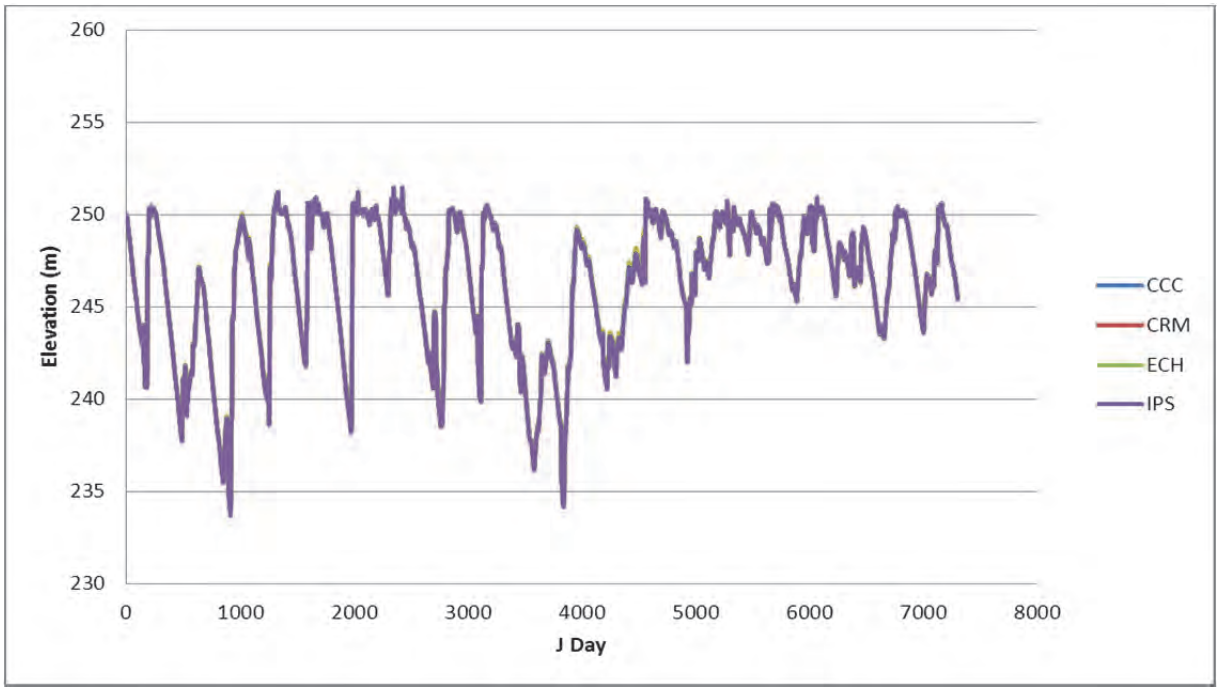

Figure 59: The present day surface water elevations for Berg River Dam (m)

Figure 59 and Figure 60 shows very close agreement within all the climate models for the 20 year present day simulation period. The surface water level discrepancies between the four climate models were negligible.

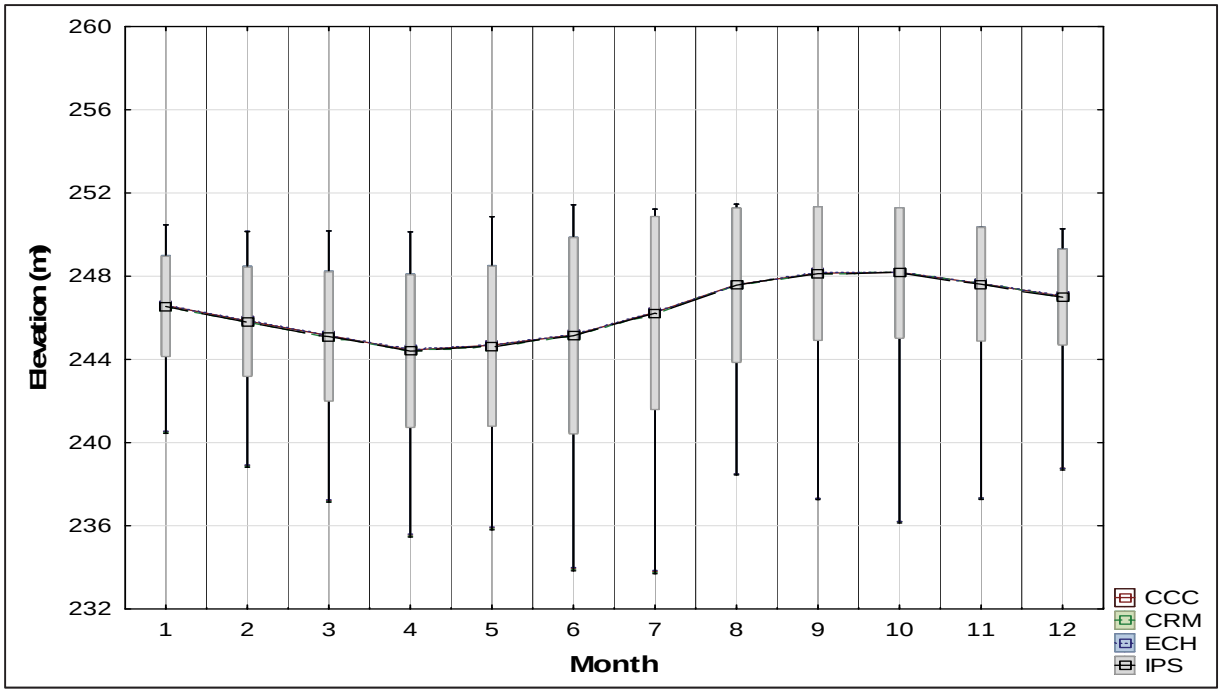

Figure 60: The present day mean monthly surface water elevation for Berg river Dam (m)

Figure 60 and Table 17 show the monthly surface elevations as well as the inter-variation between climate models for the current set of inflow and withdrawals into Berg River Dam during the period of the simulation. It was clear that the air temperature difference between climate models was similar and that the subsequent surface water elevations were relatively small.

Table 17: The present day mean surface water elevation for Berg River Dam (m)

	Jan	Feb	Mar	Apr	May	Jun	Jul	Aug	Sep	Oct	Nov	Dec
CCC	246.6	245.9	245.1	244.5	244.7	245.2	246.3	247.6	248.2	248.2	247.6	247.0
CRM	246.6	245.8	245.1	244.4	244.6	245.1	246.2	247.6	248.1	248.2	247.6	247.0
ECH	246.6	245.9	245.2	244.5	244.7	245.2	246.3	247.6	248.2	248.2	247.7	247.0
IPS	246.5	245.8	245.1	244.4	244.6	245.1	246.2	247.6	248.1	248.2	247.6	247.0

8.14 Algal nutrient inflow concentrations

Since Berg River Dam is newly constructed and is situated in a virtually unimpacted catchment it is not expected to have any water quality related problems. It is expected that because Berg River dam is relatively deep it will be monomictic i.e. thermally stratified throughout much of the year.

The Dam is filled with winter flows from the upper Berg River and a strong flowing tributary, the Wolwekloof so most of its inflow algal nutrients are to be found in the environment and the dam is subjected to natural eutrophication.

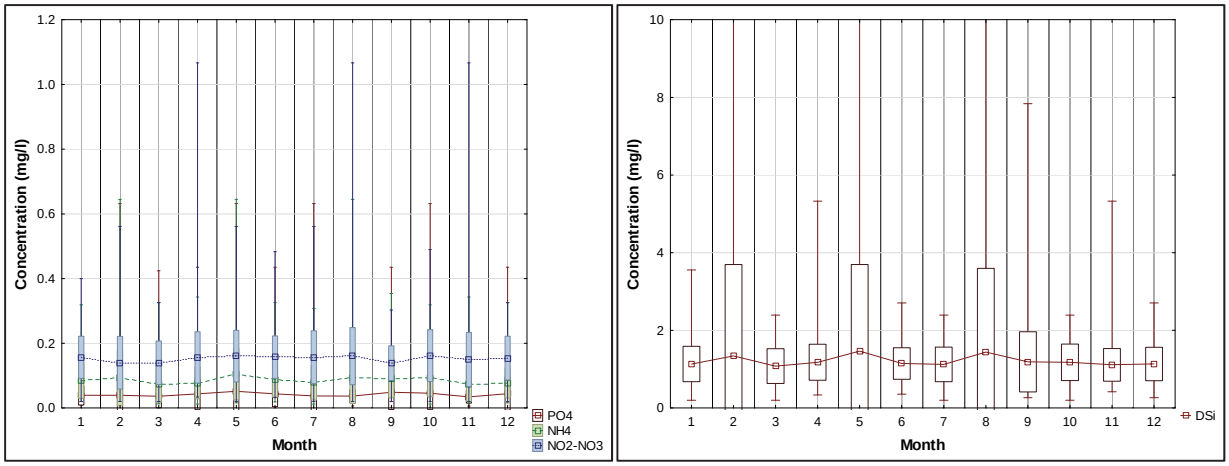

Figure 61: The present day mean monthly constituent inflows into Berg River Dam

From Figure 61 it is seen that mean monthly inflow of phosphorous is below the DWA effluent limit of 1mg/l and relatively constant. It is expected that the dam may be phosphorous limited for algal growth as nitrogen is abundant in the system and the cyanobacteria was capable of fixing nitrogen from the atmosphere.

The dissolved silicon inflow concentration shown fluctuates monthly but the overall concentration is not low enough to be limiting for diatom growth in the dam.

These inflow concentrations and volumes will not change for the intermediate future and distant future simulations thus allowing for a direct comparison with the only effect on the surface water being that of climate change. This allows for a direct comparison of climate change influence on Berg River dam, as it assumes that the current set of operating parameters would be valid.

8.15 Ortho-Phosphorous concentration

The phosphorous concentration within the dam was influenced by various factors such as inflow and withdrawal quantities as well as assimilation by the various algae as it was the limiting nutrient for algal growth. The fluxes affecting in-dam phosphorous concentrations are shown in (Figure 37) as used by the CE-QUAL-W2 model. The present day ortho-phosphorous concentration for Berg River dam of the four climate models is shown in the following figures.

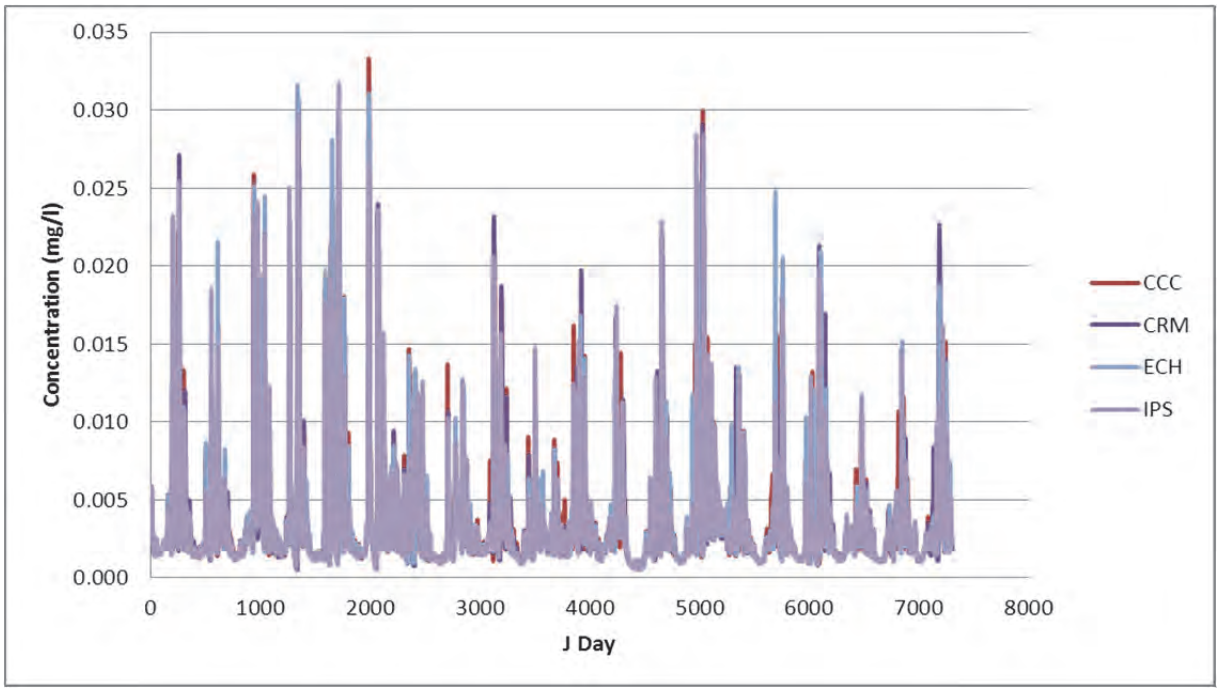

Figure 62: The present day surface ortho-phosphate concentration for Berg River Dam (mg/l)

The phosphorous concentrations agree well using the recorded set of inflow and withdrawals from Berg River Dam. This shows that the inter-climate sink of phosphorous is the same as all the climate models agree well with each other. The average concentration is shown in Figure 63 and is well below the level of 0.025 mg/l set by the then DWAF in 1985. It is noted that this value is still critiqued and suggestions are that a value of 0.1mg/l of phosphorus in effluent could limit eutrophication.

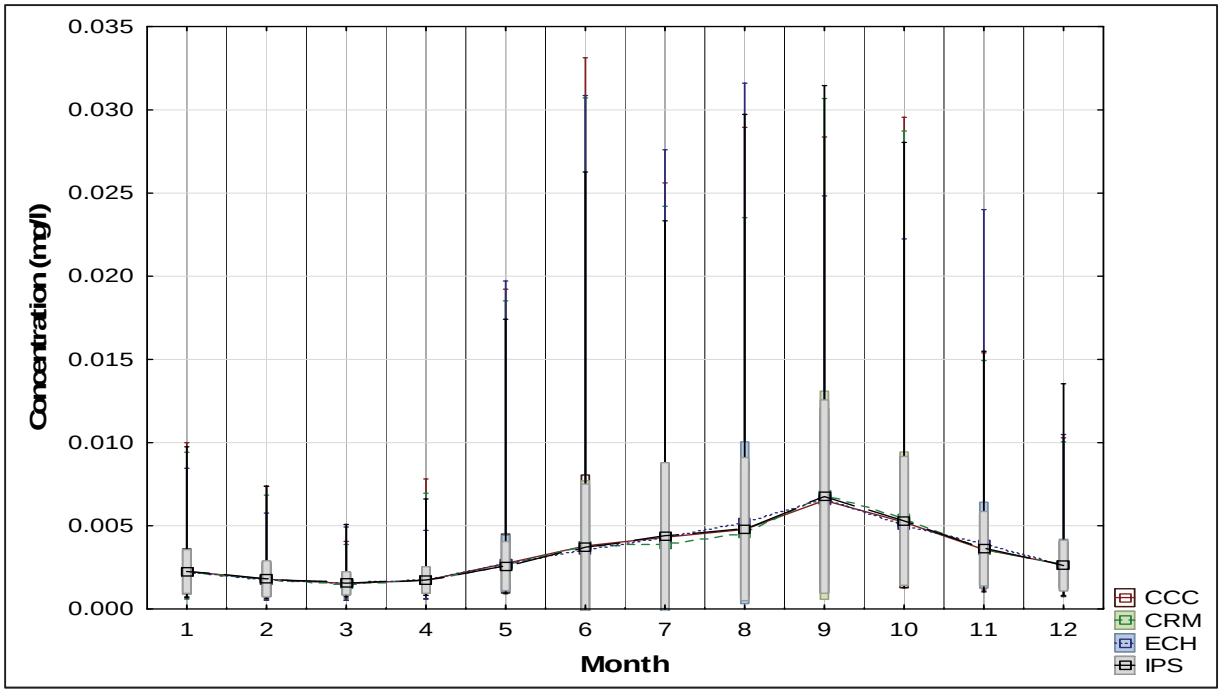

Figure 63: The present day mean monthly surface ortho-phosphate concentration for Berg River Dam (mg/l)

Table 18: The present day surface ortho-phosphate concentration for Berg River Dam (mg/l)

	Jan	Feb	Mar	Apr	May	Jun	Jul	Aug	Sep	Oct	Nov	Dec
CCC	0.0023	0.0018	0.0015	0.0017	0.0027	0.0038	0.0043	0.0048	0.0065	0.0052	0.0036	0.0027
CRM	0.0022	0.0017	0.0015	0.0017	0.0026	0.0038	0.0039	0.0045	0.0068	0.0054	0.0036	0.0026
ECH	0.0022	0.0017	0.0015	0.0017	0.0027	0.0036	0.0043	0.0052	0.0066	0.0050	0.0038	0.0027
IPS	0.0023	0.0018	0.0016	0.0017	0.0026	0.0037	0.0044	0.0048	0.0068	0.0053	0.0036	0.0026

It was clear that phosphorous has an annual cycle with maximum surface concentrations reached during spring due to the collapse of the thermocline and re-suspension of nutrients, and the concentration is sufficiently high enough so as not to limit algal. The half saturation is defined as the concentration at which the uptake of phosphorous is half the maximum rate, thereby limiting algal growth. The phosphorous half saturation constants for diatoms are 0.002 mg/l, greens 0.38 mg/l and cyanobacteria 0.011 mg/l. From Table 18 it is seen that the cyanobacteria half saturation of phosphorous was always exceeded allowing for maximum growth rates of cyanobacteria if other factors such as ideal water temperature, favoured it. The concentration of surface ortho-phosphates would limit diatoms and green for certain months. This would imply that should the inflow concentration of phosphorous increase Berg River dam would change its trophic status and worse water quality would result.

If algal blooms were to be controlled, it would be imperative to abate the inflow of phosphorous into the dam. The mean level of 1mg/l of phosphorous (DWA limit) in the dam is never exceeded for the duration of the present day simulation. Only green algae may become limited as its phosphorous half saturation constant is seldom exceeded

8.16 Nitrogen concentration

Nitrogen is an abundant element in nature and is an essential building block of proteins and a constituent of chlorophyll. The sources of N with respect to water quality tests are ammonia (NH_3), ammonium (NH_4^+), nitrites (NO_2^-) and nitrates (NO_3^-) as well as atmospheric N which is fixed by certain algae. From the aspect of eutrophication, it is very seldom that nitrogen is the limiting nutrient within a waterbody as it is so abundant.

Ammonia is produced by the decomposition of organic matter that contains ammonia as well as being a constituent of sewage and industrial effluents. Nitrite occurs naturally as an anion in fresh and sea waters, whereas anthropogenically it is introduced to receiving waters as wastes from aquaculture, sewage effluents and industrial effluents. Nitrates are scarce in natural water sources as they are constantly being depleted by the process of photosynthesis, converting nitrates to organic nitrogen. For the purpose of this modelling exercise, both ammonium and nitrites are included in the inflow into Berg River dam.

8.17 Ammonium concentration

Ammonia exists in two forms in nature (ammonium and ammonia) and the equilibrium concentrations are governed largely by pH (Chapra, 2008). The following figures show the surface ammonia concentration at segment 21 of Berg River dam for the 20 year present day simulation.

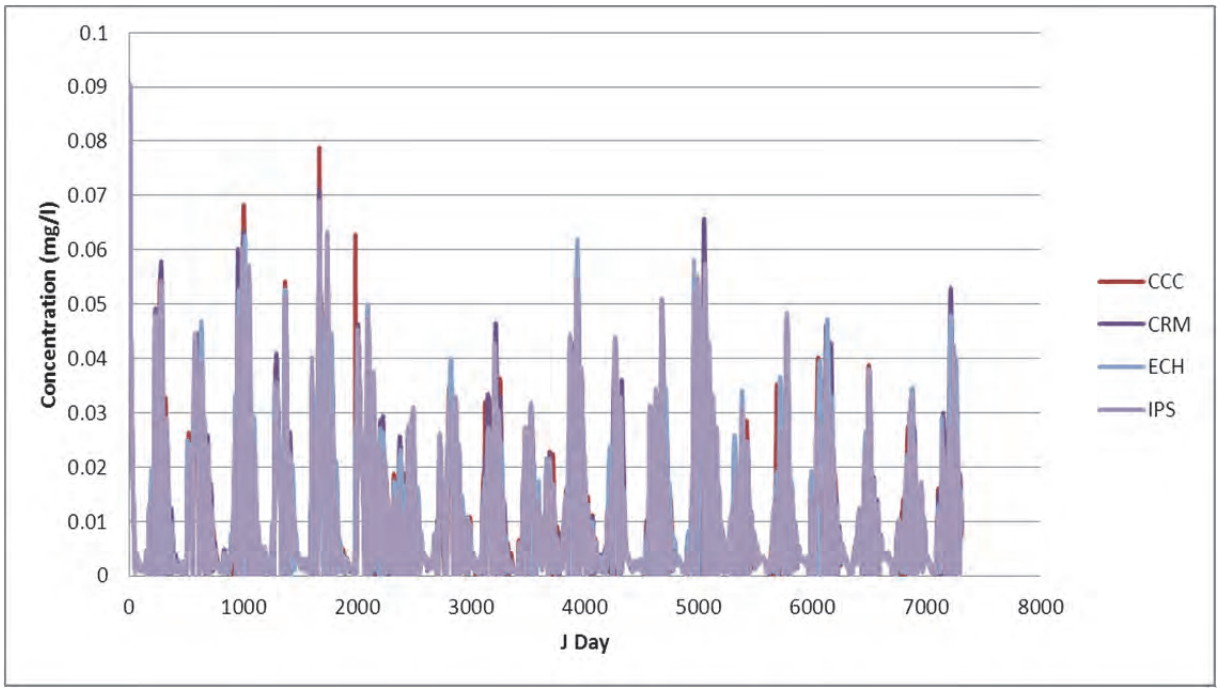

Figure 64: The present day surface ammonium concentration for Berg River Dam (mg/l)

Cyanobacteria such as *Anabaena* sp. and others can utilise the nitrogen present in the atmosphere for growth and hence it is not seen as limiting for their growth (Dallas, 2004). From an eutrophication management aspect, it is easier to manage and police the anthropogenic loading of a water system so that the subsequent abatement of eutrophication may take place but the case for nitrogen management is not easy or practical as it is abundant in the system. Nitrogen is essential for growth but rarely a limiting growth element for algae.

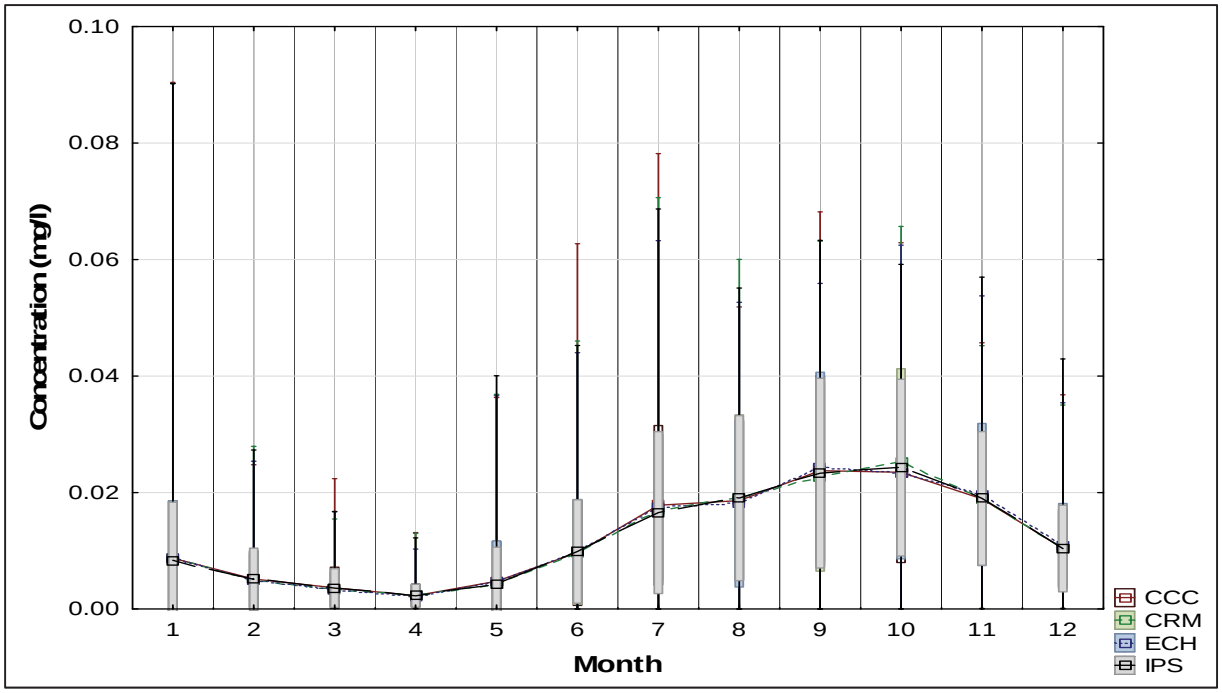

Figure 65: The present day mean monthly surface ammonium concentration for Berg River Dam (mg/l)

From Table 19 and Figure 64 it was seen that the surface ammonium concentration was a maximum during spring and was in sufficient concentration so as not to limit algal growth. The climate models also show little inter-variability and the results compare well with each other.

Table 19: The present day mean monthly surface ammonium concentration for Berg River Dam (mg/l)

	Jan	Feb	Mar	Apr	May	Jun	Jul	Aug	Sep	Oct	Nov	Dec
CCC	0.009	0.005	0.004	0.002	0.005	0.010	0.018	0.019	0.024	0.023	0.019	0.010
CRM	0.009	0.005	0.003	0.002	0.004	0.010	0.017	0.019	0.023	0.025	0.019	0.010
ECH	0.009	0.005	0.003	0.002	0.005	0.010	0.017	0.018	0.024	0.023	0.020	0.011
IPS	0.008	0.005	0.004	0.002	0.004	0.010	0.017	0.019	0.023	0.024	0.019	0.010

It is seen that the concentration of surface ammonium is cyclic and follows that of phosphorous with peaks in late spring and minimum during autumn. Ammonium is generated by the respiration of algae, zooplankton as well as decay of organic material and anaerobic release from the sediments. Ammonium is depleted via the mechanism of nitrification to nitrate-nitrites and photosynthesis.

The statutory limit for ammonium is surface water is set at 1mg/l by DWA and for Berg River dam this limit is never exceeded on the surface.

8.18 Nitrate-nitrite concentrations

Figure 66, Figure 67 and Table 20 show the surface Nitrate-nitrite concentrations for segment 21 of the present day 20 year simulation. It is assumed that a low concentration of nitrate-nitrites is due to assimilation by algae as well as redistribution in the water column (Figure 42).

The figures show an increase in concentrations at the surface during summer and autumn months as well as close agreement for the four climate models.

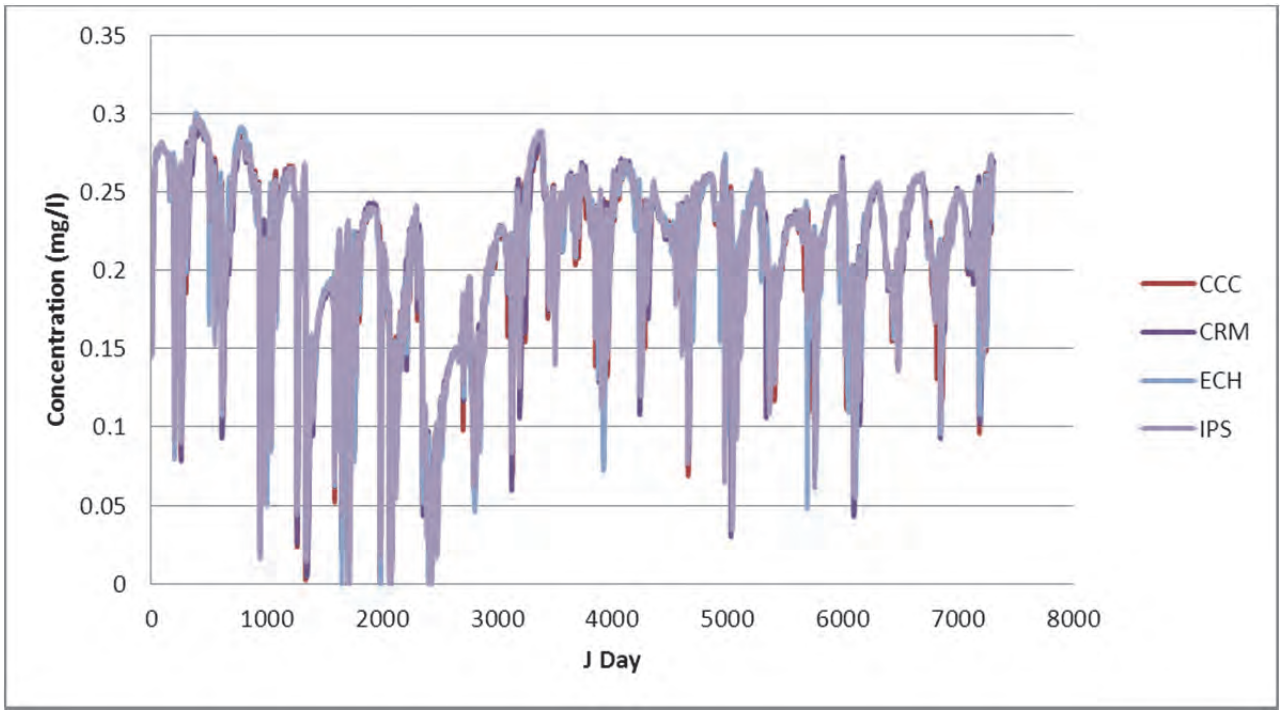

Figure 66: The present day surface nitrate-nitrite concentration for Berg River Dam (mg/l)

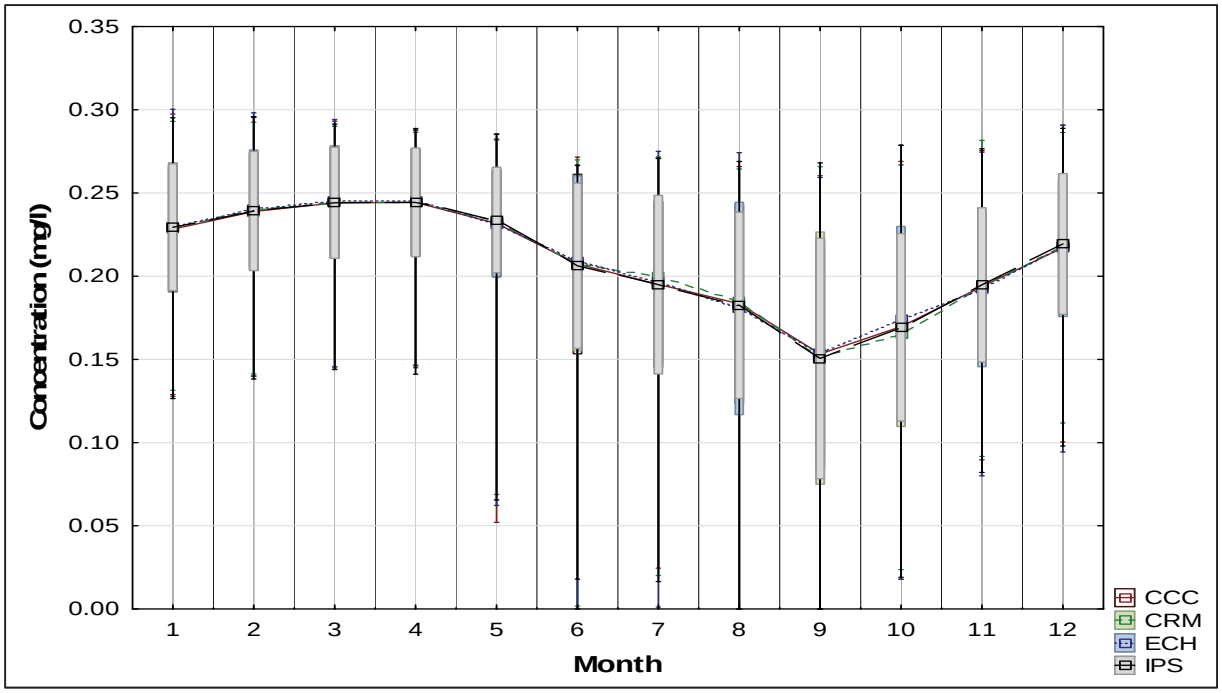

Figure 67: The present day mean monthly surface nitrate-nitrite concentration for Berg River Dam (mg/l)

As the inflow of nitrate-nitrite is relatively constant into the dam Figure 61) the dip in concentration during winter and continues until spring, may be attributed to de-nitrification and photosynthesis. Since this decrease occurs during spring, it is expected that this is due to an increase in the growth of surface algae.

Table 20: Present day mean monthly surface nitrate-nitrite concentration for Berg River Dam (mg/l)

	Jan	Feb	Mar	Apr	May	Jun	Jul	Aug	Sep	Oct	Nov	Dec
CCC	0.228	0.239	0.244	0.244	0.232	0.207	0.195	0.183	0.153	0.170	0.194	0.217
CRM	0.229	0.240	0.244	0.244	0.233	0.207	0.200	0.185	0.151	0.165	0.194	0.218
ECH	0.230	0.241	0.245	0.245	0.231	0.209	0.197	0.181	0.153	0.174	0.192	0.218
IPS	0.229	0.239	0.244	0.244	0.234	0.206	0.195	0.183	0.151	0.169	0.195	0.219

The statutory limit of 6mg/l of nitrate-nitrite as set by DWA is never exceeded for the present day simulation runs for all four climate models.

8.19 Total nitrogen concentration and the half-saturation constant

The algal half-saturation constant for nitrogen and is defined as the nitrogen concentration (ammonium + nitrate/nitrite) at which the uptake rate is one-half the maximum rate. This represents the upper concentration at which algal growth is proportional to nitrogen and algal growth is nitrogen limited below this value. The nitrogen half-saturation constant is 0.01, 0.14

and 0 for diatoms, green algae and cyanobacteria respectively. From this, it is seen that only green algae could become growth limited by surface nitrogen.

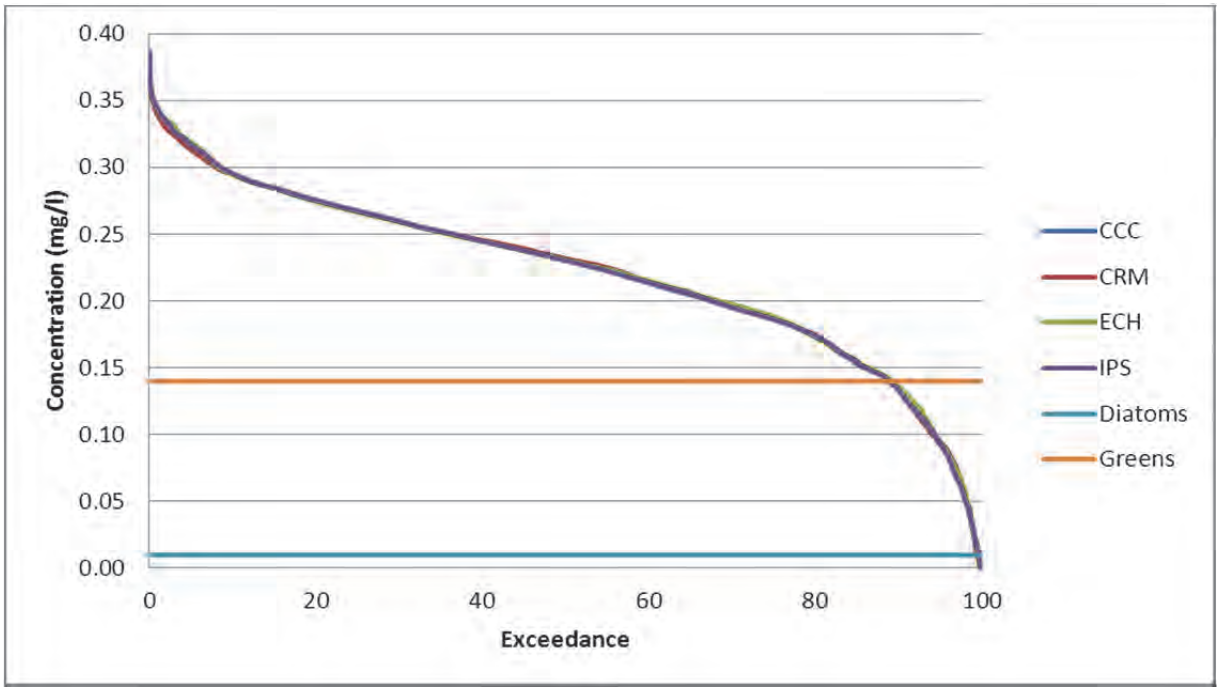

Figure 68: The present day total nitrogen half-saturation exceedance plot for Berg River Dam

From the exceedance plot in Figure 68, for about 10% of the simulation the green algae was growth limited to half its maximum rate at the surface in the present day scenario. This would imply that if the total nitrogen concentration into the dam were to increase for the same conditions, the growth of green algae would be greater than currently presented but not markedly as it was close to its maximum already.

8.20 Identifying the limiting nutrient

It has been established that the green algal species in Berg River dam was limited for both phosphorous and nitrogen concentration at the surface. DWA uses the standard that if N:P > 25:1 then there is no problem with water quality. If N:P < 10 then eutrophic conditions exist. If N/P > 10 then P limits algal growth and if N/P < 10 the N limits algal growth.

The concentration of surface total nitrogen is always high enough so as to not limit algal growth.

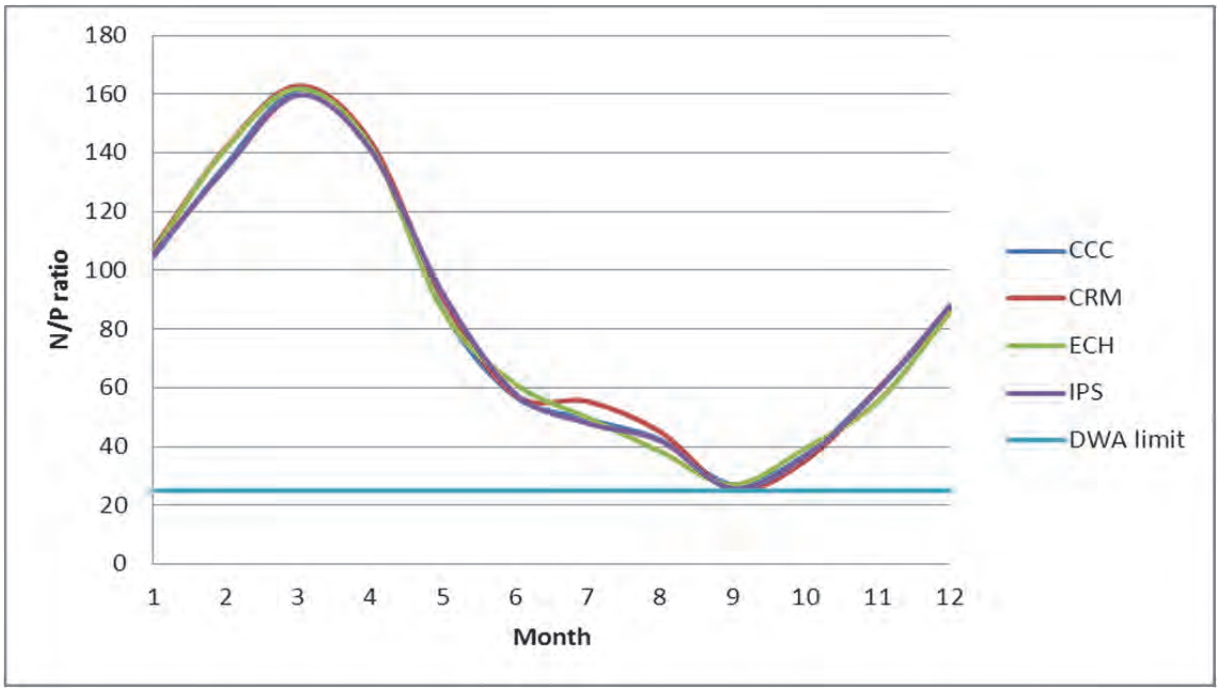

Figure 69: The ratio of N/P for the present day to identify the limiting nutrient with respect to DWA standards

From Figure 69 it is seen that N:P is always greater than 25 implying that there is no problem with water quality at the surface of Berg River Dam. The dam was phosphorous limited for the entire year and changes in the inflow concentration of phosphorous will adversely affect this ratio and the DWA limit could be exceeded. It is thus deduced that to control the ingress of nitrogen into the dam would be unfeasible due to its natural abundance and the only realistic methods to limit algal growth would be to limit the inflow of phosphorous into the dam.

8.21 Dissolved silicon concentration

The dissolved silicon concentration of the surface water for segment 21 is show in Figure 70, Figure 71 and Table 21. From the growth aspect of algae of this modelling exercise it was only diatoms that were silicon growth limited, green algae and cyanobacteria were capable fixing nitrogen directly from the atmosphere. The inflow concentration of dissolved silicon into Berg river dam is shown in Figure 61.

The inter-variability between the climate models is negligible. It is seen that the mean monthly surface concentration of dissolved silicon is greater in winter than the rest of the year, implying that diatom growth is not limited during winter but severely limited during summer.

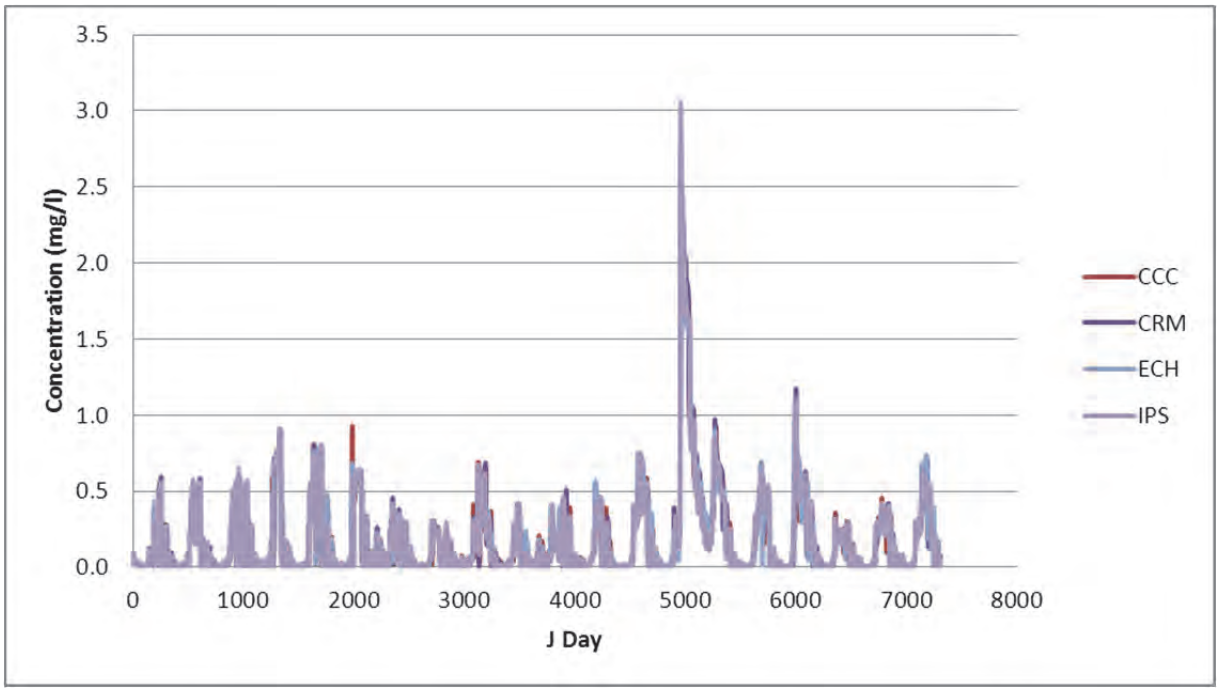

Figure 70: The present day surface dissolved silicon concentration for Berg River Dam (mg/l)

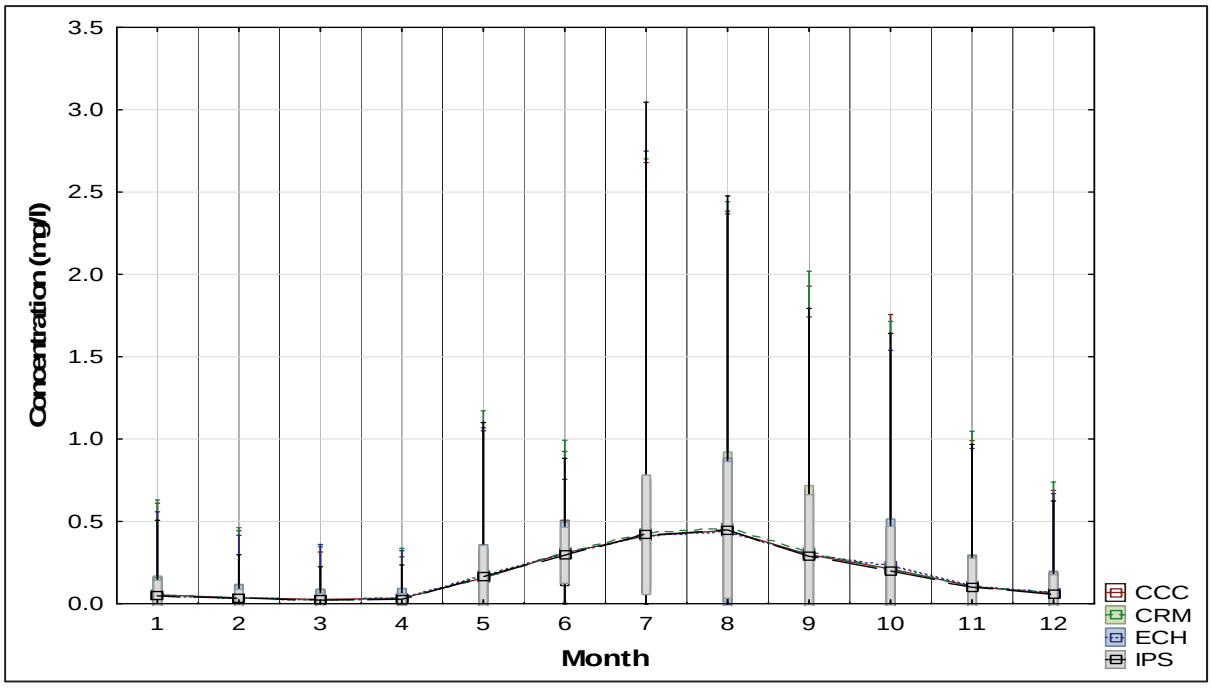

Figure 71: The present day mean surface dissolved silicon concentration for Berg River Dam (mg/l)

Table 21: Present day mean surface dissolved silicon concentration for Berg River Dam (mg/l)

	Jan	Feb	Mar	Apr	May	Jun	Jul	Aug	Sep	Oct	Nov	Dec
CCC	0.054	0.037	0.027	0.034	0.157	0.308	0.413	0.446	0.298	0.212	0.106	0.062
CRM	0.054	0.036	0.027	0.033	0.159	0.315	0.428	0.460	0.311	0.203	0.106	0.064
ECH	0.052	0.036	0.028	0.036	0.176	0.309	0.414	0.434	0.297	0.229	0.108	0.065
IPS	0.048	0.030	0.022	0.028	0.166	0.295	0.419	0.449	0.288	0.202	0.101	0.058

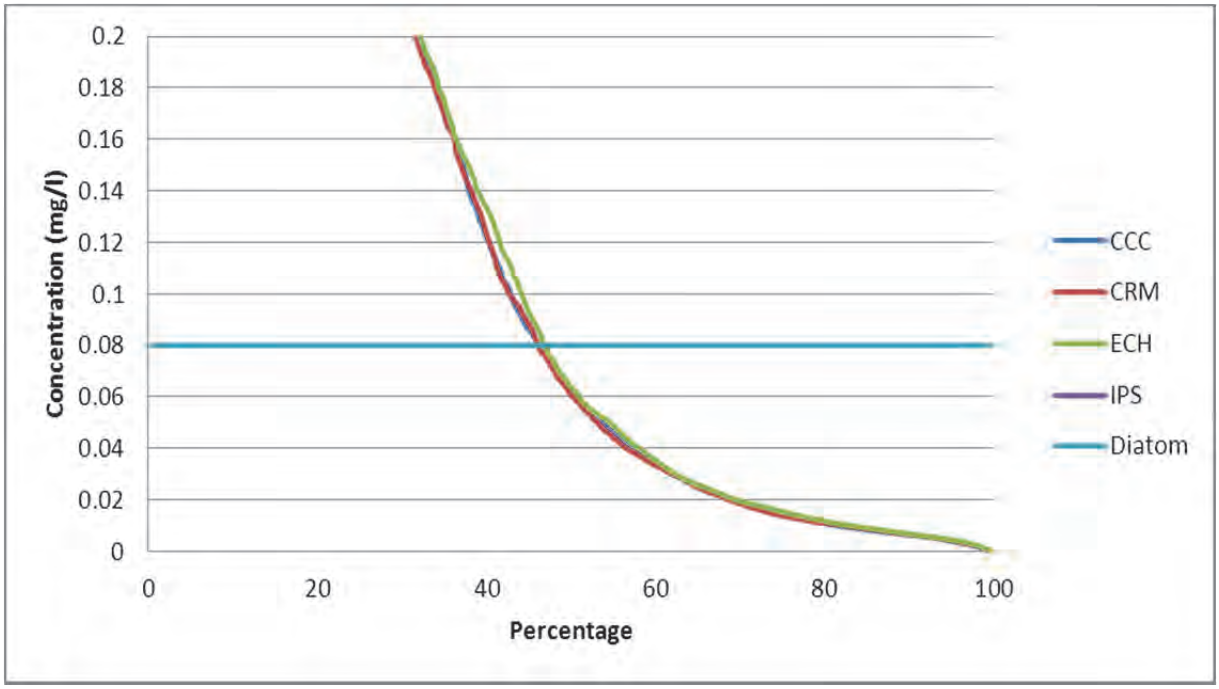

Figure 72: The present day dissolved silicon half-saturation exceedance plot for Berg River Dam (mg/l)

From the exceedance plot of half saturation constant for diatoms, it is seen that the concentration of surface dissolved silicon is lower than the half-saturation of 0.08 mg/l for approximately 45% of the 20 years. Thus, for this diatom, its growth was hampered by low levels of dissolved silicon and any increase in the inflow of dissolved silicon would allow for a greater growth rate of diatoms at the surface. The in-situ sources of dissolved silicon are algal respiration, anaerobic decay from the sediments and particulate silicon. Since none of these sources can be managed for a reduction in dissolved silicon, the source reduction of silicon before it enters the dam seems a viable method to limit diatom growth.

8.22 Dissolved oxygen concentration

Similarly, the dissolved oxygen concentrations for the 20 year period, monthly and statistics are shown below. The inflow concentration of dissolved oxygen is 14 mg/l for the inflow for the duration of the simulation.

Upon examination of Figure 73, Figure 74 and Table 22 it is seen that the dissolved oxygen concentration is cyclic and greater concentration of dissolved oxygen was detected in winter. This is due to less dissociation of oxygen from the water because of the lower water temperature. The DWA TWQR level for dissolved oxygen is that it should not be less than 80% or greater than 120% of saturation levels.

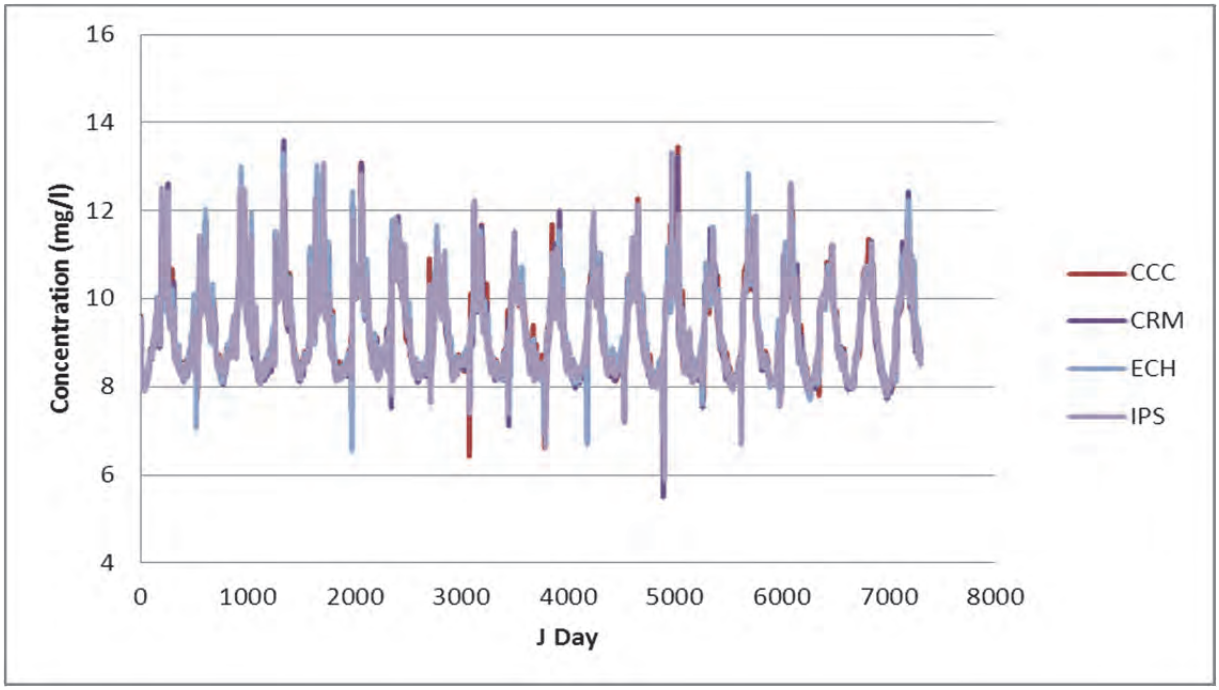

Figure 73: The present day surface dissolved oxygen concentration for Berg River Dam (mg/l)

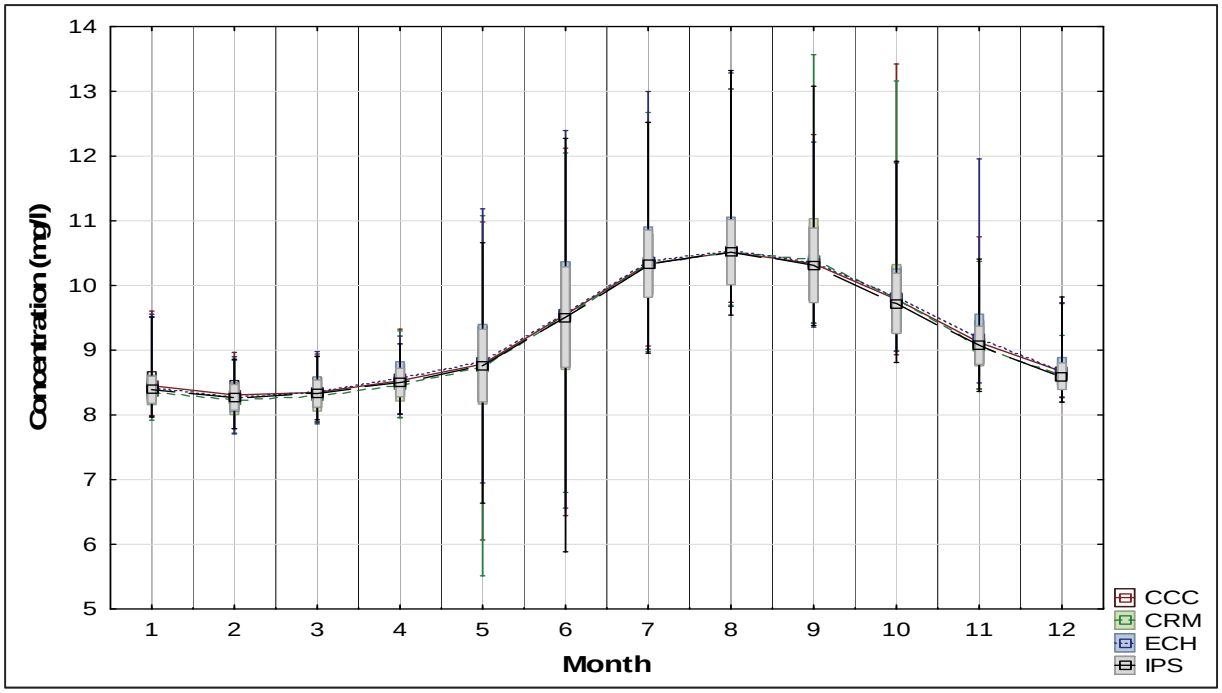

Figure 74: The present day mean surface dissolved oxygen concentration for Berg River Dam (mg/l)

Table 22: The present day mean surface dissolved oxygen concentration for Berg River Dam (mg/l)

	Jan	Feb	Mar	Apr	May	Jun	Jul	Aug	Sep	Oct	Nov	Dec
CCC	8.45	8.31	8.35	8.53	8.79	9.55	10.33	10.51	10.34	9.79	9.12	8.67
CRM	8.36	8.22	8.28	8.46	8.75	9.51	10.33	10.52	10.40	9.79	9.06	8.62
ECH	8.41	8.27	8.36	8.57	8.83	9.58	10.37	10.54	10.34	9.83	9.18	8.67
IPS	8.39	8.27	8.33	8.50	8.76	9.51	10.34	10.51	10.31	9.72	9.08	8.60

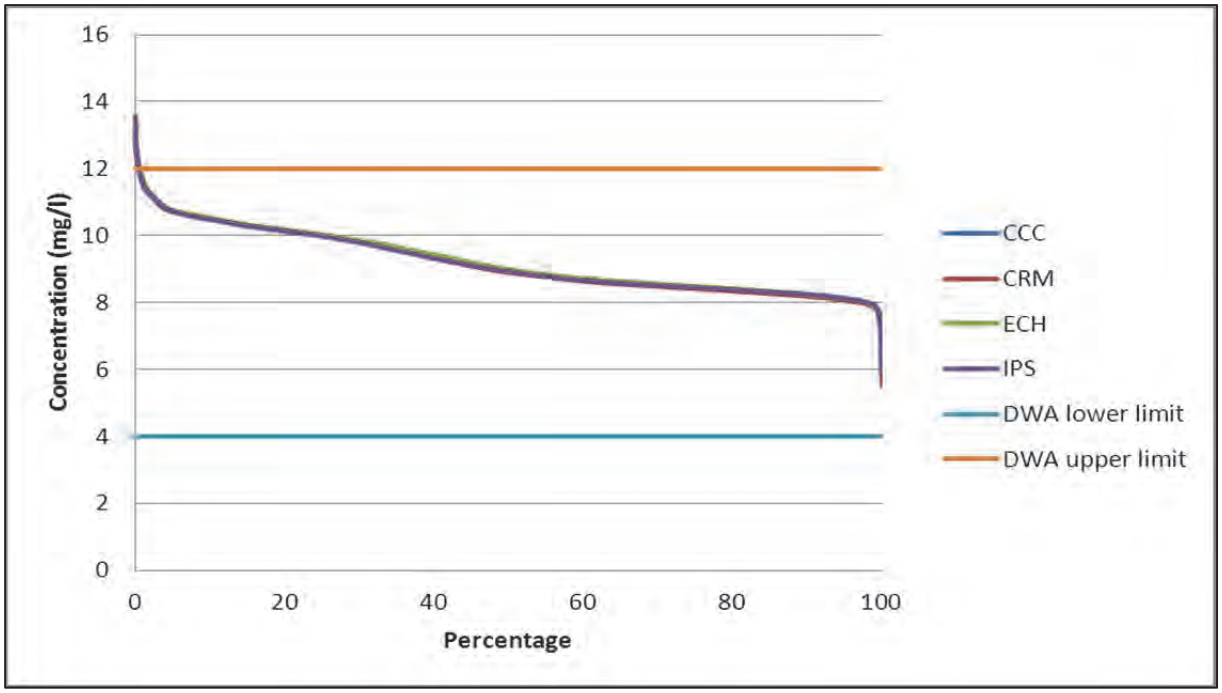

Figure 75: The present day surface dissolved oxygen exceedance plot for Berg River Dam (mg/l)

From Figure 75 it is seen that no surface dissolved oxygen problems exist at segment 21 in Berg River dam as shown by the exceedance plot.

8.23 Total algal concentration

Algal growth is a function of temperature, light, and nutrients (Cole, 2008) and thus maximum algal growth occurs at or near the surface. The total algal concentration incorporating diatoms, greens and cyanobacteria are shown in the following figures for the present day simulation.

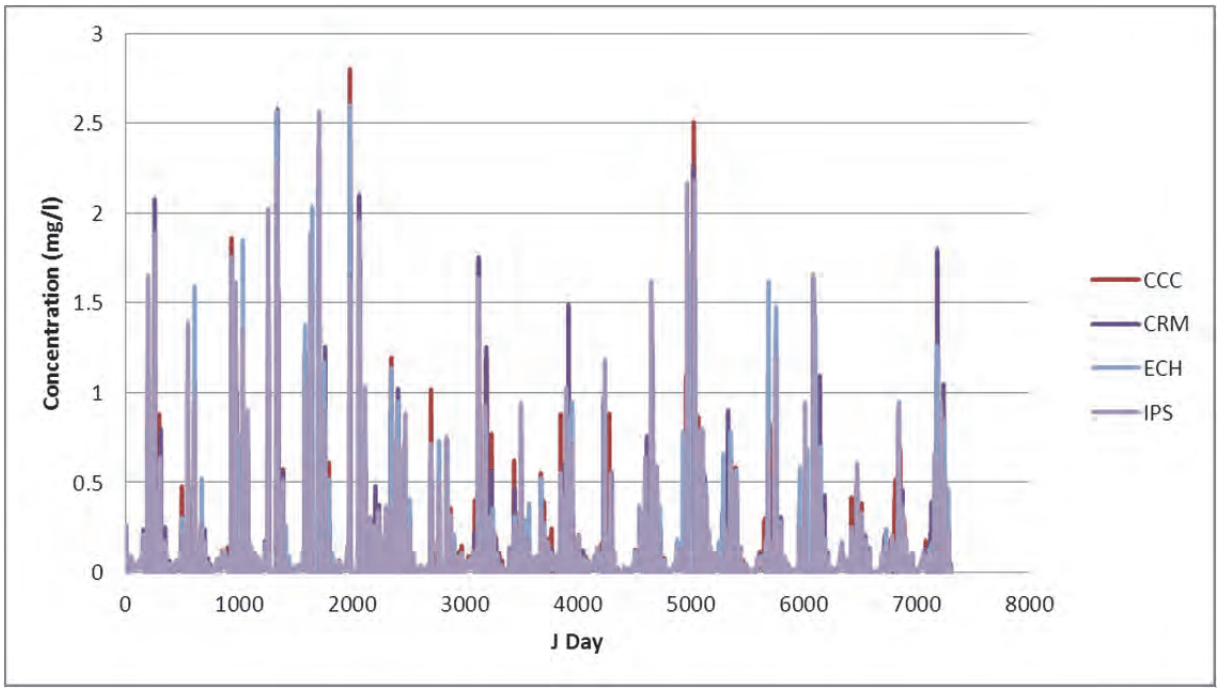

Figure 76: The present day surface total algal concentration for Berg River Dam (mg/l)

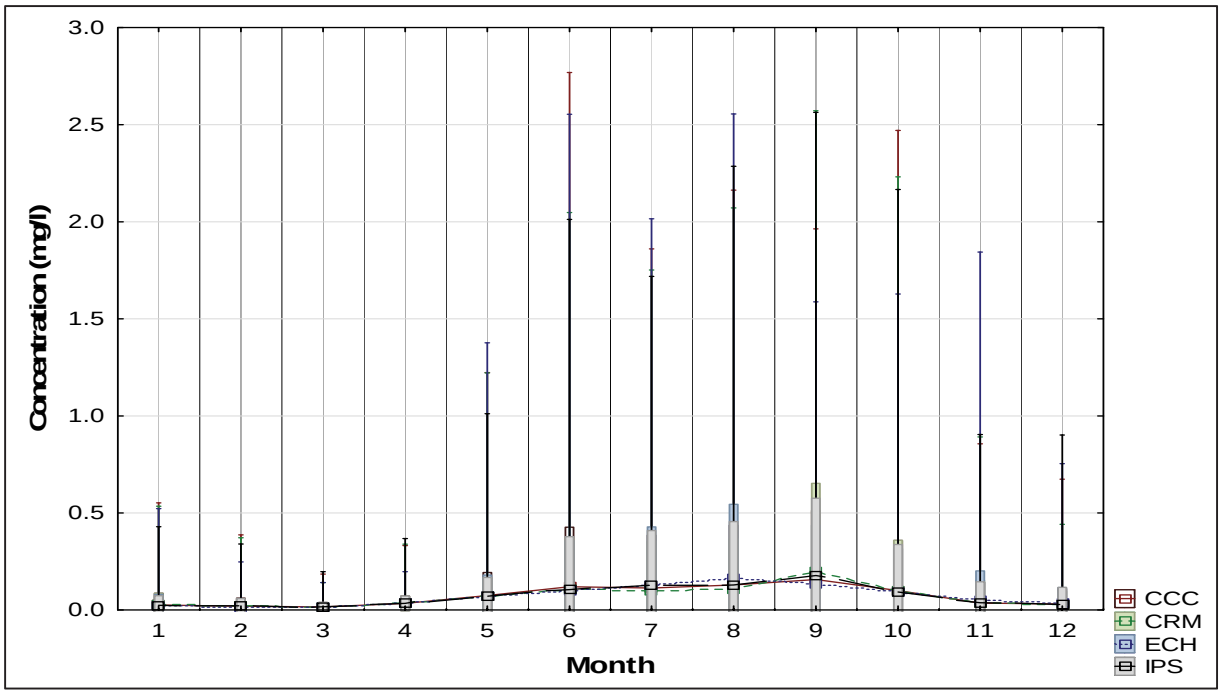

Figure 77: The present day surface monthly total algal concentration for Berg River Dam (mg/l)

Table 23: The present day surface monthly total algal concentration for Berg River Dam (mg/l)

	Jan	Feb	Mar	Apr	May	Jun	Jul	Aug	Sep	Oct	Nov	Dec
CCC	0.026	0.020	0.016	0.034	0.074	0.120	0.113	0.129	0.157	0.100	0.036	0.031
CRM	0.025	0.018	0.016	0.034	0.070	0.109	0.100	0.110	0.199	0.098	0.039	0.030
ECH	0.024	0.017	0.017	0.034	0.072	0.099	0.125	0.164	0.138	0.091	0.048	0.033
IPS	0.024	0.020	0.017	0.034	0.070	0.105	0.129	0.129	0.177	0.094	0.038	0.031

Figure 76 shows the total algal concentrations at the surface of segment 21 as well as the close agreement between the climate models. From Figure 77 it was seen that the mean total algal growth was greater for winter and spring than for summer. It is know that diatoms blooms occur more often in winter (Cole, 2008) than summer and to establish which type of algae (diatom, green or cyanobacteria) constitutes the greater portion would have to be investigated further.

From the model parameterisation diatoms and cyanobacteria share lower light saturation values than greens, implying that they should grow better in winter than summer and conversely greens would grow better the entire year as it had a higher light saturation value and thereby could utilise the greater solar radiation of summer for photosynthesis.

In comparing the winter total algal concentration of the present day to that of summer, it is seen that winter has a greater concentration of algae. This confirms that the algae are light sensitive and total algal growth is more in winter than summer.

It was clear that the surface total algae never exceed the DWA limit of 15mg/l for the entire simulation period.

8.24 Diatoms concentration

It is known that diatoms have low light saturation values and tend to grow better in winter, as the winter water temperature is within its maximum growth rates. The following graph shows the diatom concentration for the 20 year period and it was noted that each of the peaks seen corresponds to a winter season.

Figure 78 shows the cyclic peaks of diatoms concentrations as well as the good agreement between models for the present day.

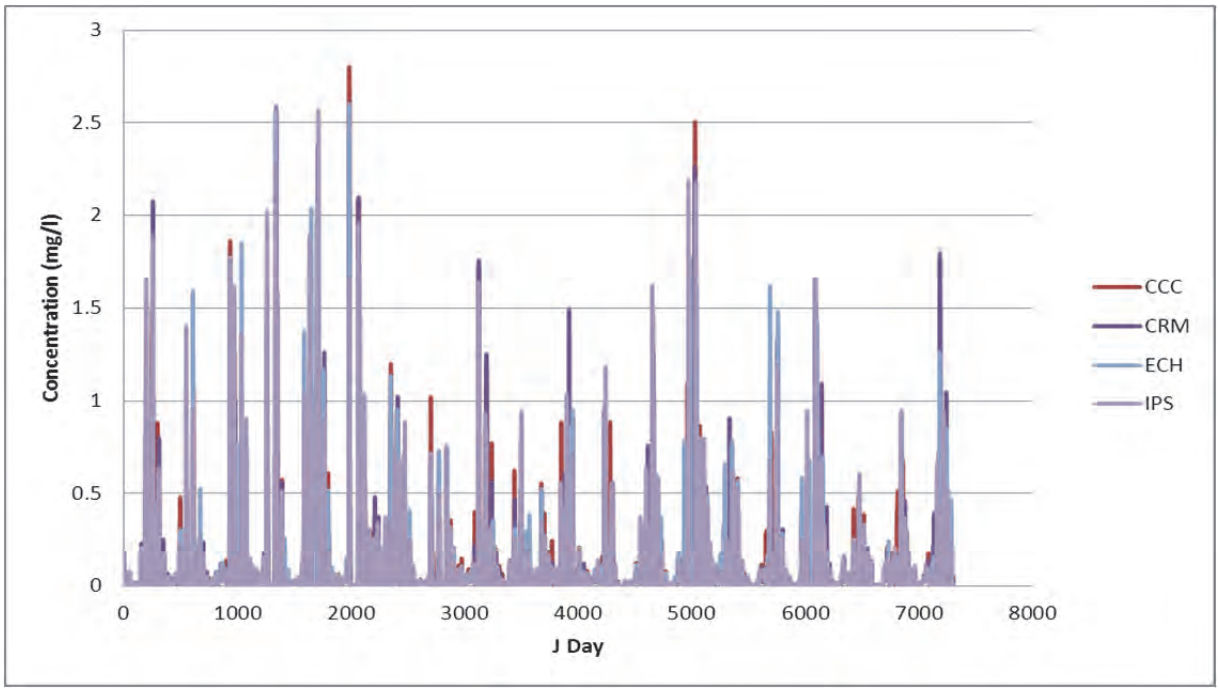

Figure 78: The present day surface diatom concentration for Berg River Dam (mg/l)

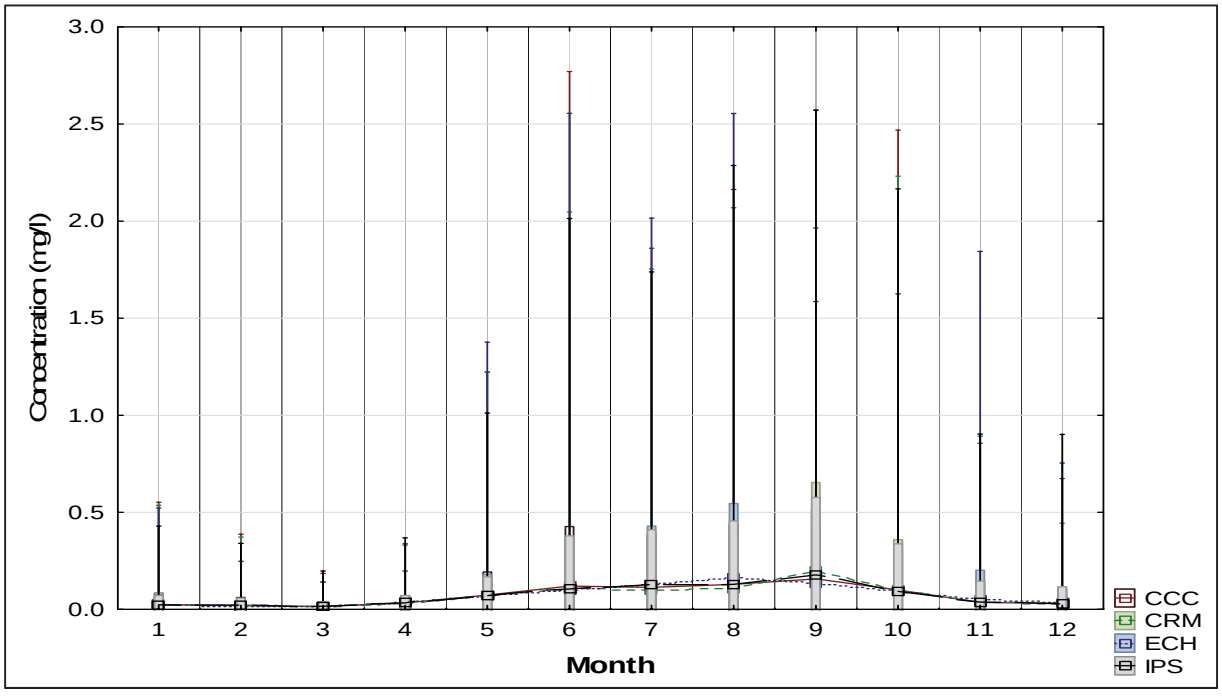

Figure 79: The present day mean surface diatom concentration for Berg River Dam (mg/l)

Table 24: The present day mean surface diatom concentration for Berg River Dam

	Jan	Feb	Mar	Apr	May	Jun	Jul	Aug	Sep	Oct	Nov	Dec
CCC	0.025	0.019	0.016	0.033	0.074	0.120	0.114	0.129	0.157	0.100	0.036	0.031
CRM	0.024	0.018	0.016	0.032	0.069	0.109	0.100	0.110	0.199	0.098	0.039	0.030
ECH	0.024	0.017	0.016	0.033	0.071	0.099	0.125	0.164	0.138	0.091	0.048	0.033
IPS	0.023	0.019	0.016	0.033	0.069	0.105	0.129	0.129	0.177	0.094	0.038	0.031

From Figure 79 and Table 24 is seen that there is a much greater mean concentration of diatoms during the winter and spring as opposed to summer. This would seem counterintuitive as only during summer was the water temperature high enough to promote maximum growth. This difference could solely be attributed to the diatoms lower light saturation inhibiting plant growth in the high solar radiation summer months. The temperature growth multipliers for diatoms predict that their growth should be limited in winter as the water temperature is below the levels for maximum algal growth. It was noted that there is good agreement within climate models

8.25 Green algae concentration

The type of green algae chosen for this modelling exercise has a higher light saturation than the diatoms. Thus, it is expected to grow throughout the entire year. Figure 80 shows the growth of green algae for the simulation period in Berg River Dam.

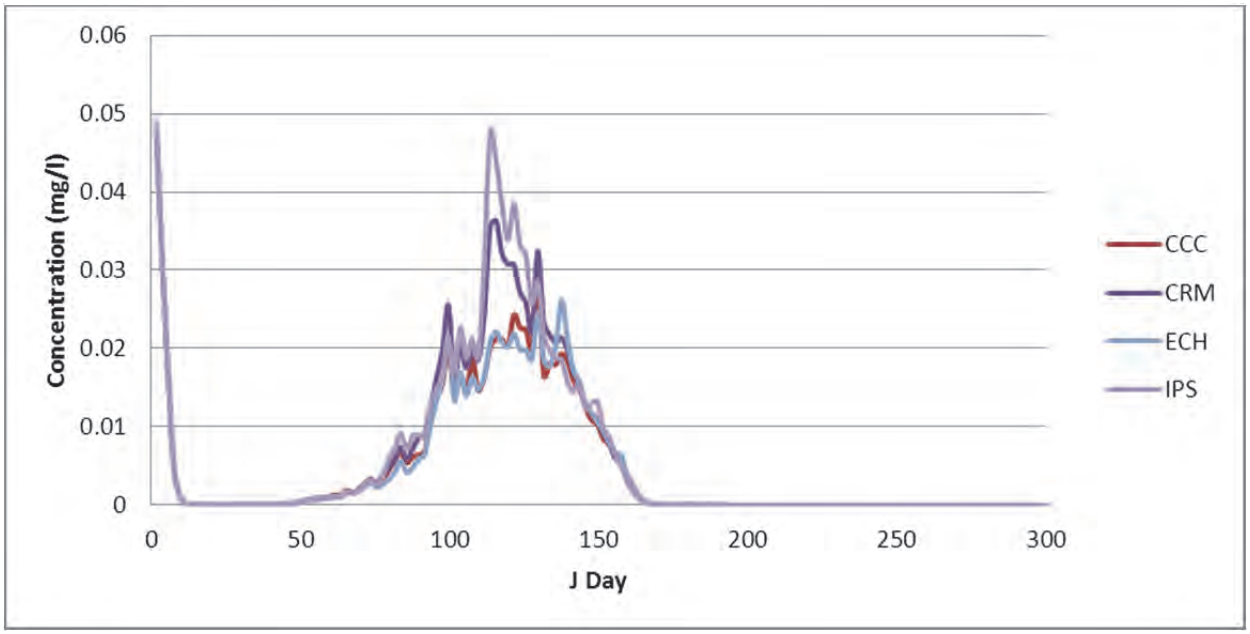

Figure 80: The present day surface green concentration for Berg River Dam (mg/l)

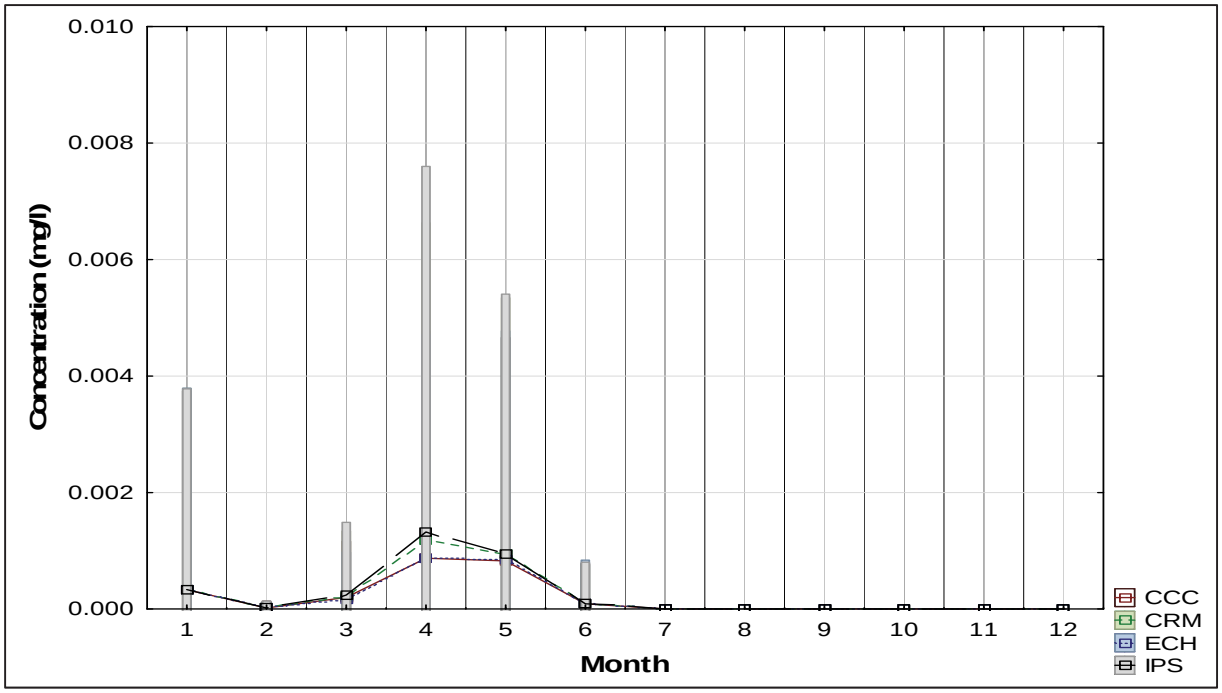

Figure 81: The present day mean monthly surface green concentration for Berg River Dam (mg/l)

From the Figure 80 and Figure 81 it is seen that the green algae do not persist in the dam for the simulation, as conditions were not conducive for them. It was evident that the green algae that were seeded to the dam die within the first year and never re-populate the dam thereby confirming that this species of green algae will not pose a water quality problem.

8.26 Cyanobacteria concentration

The cyanobacteria modelled have the lowest light saturation intensities relative to the diatoms and greens. It was expected that maximum cyanobacteria concentrations should occur mainly in summer due to the additional light and warmer water. Figure 82 shows the cyanobacteria concentration for the 20 year simulation period.

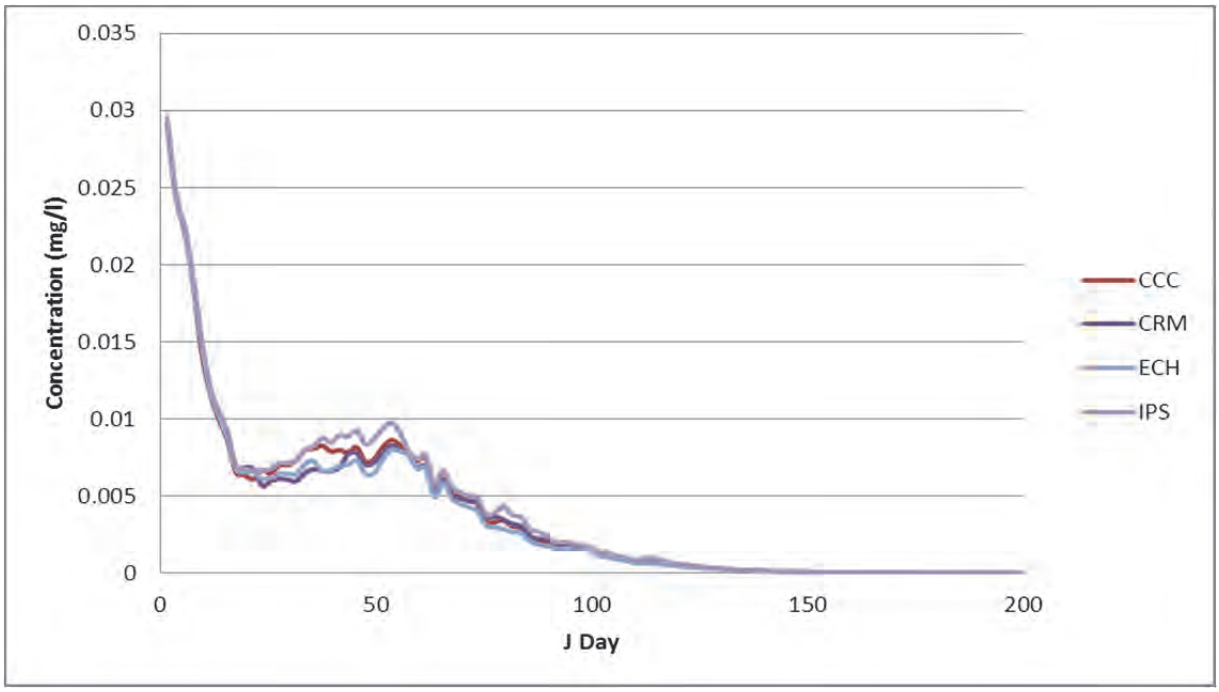

Figure 82: The present day surface cyanobacteria concentration for Berg River Dam (mg/l)

Similarly as with the green algae the cyanobacteria that was seeded to the dam, die completely within the first year of the simulation and never populates the dam.

It may thus be concluded that only diatoms will dominate in Berg River dam and their maximum growth was expected during winter until spring.

8.27 Zooplankton growth

To investigate the effect of predation on diatoms and green algae, zooplankton was also modelled to prefer diatoms and green algae over cyanobacteria and the resulting concentrations are shown in Figure 83, Figure 84 and Table 25. This figure resembles Figure 78 in shape and this is because diatoms are present throughout the entire year and that zooplankton feed on them.

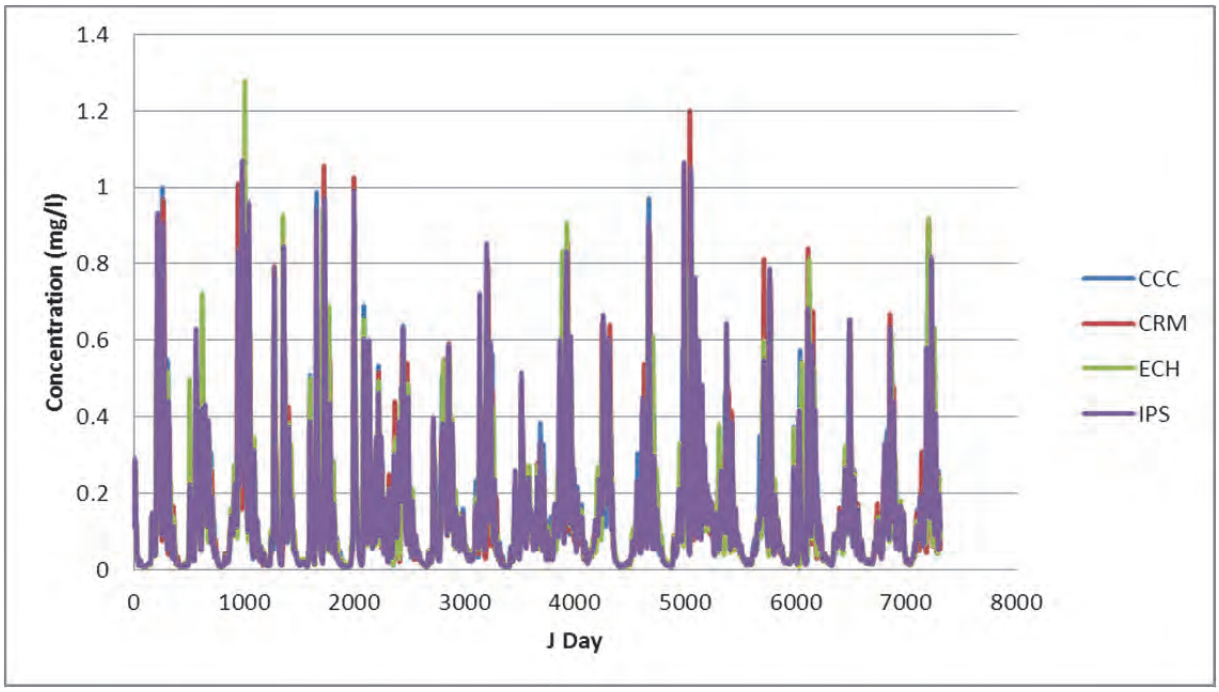

Figure 83: The present day surface zooplankton concentration for Berg River Dam (mg/l)

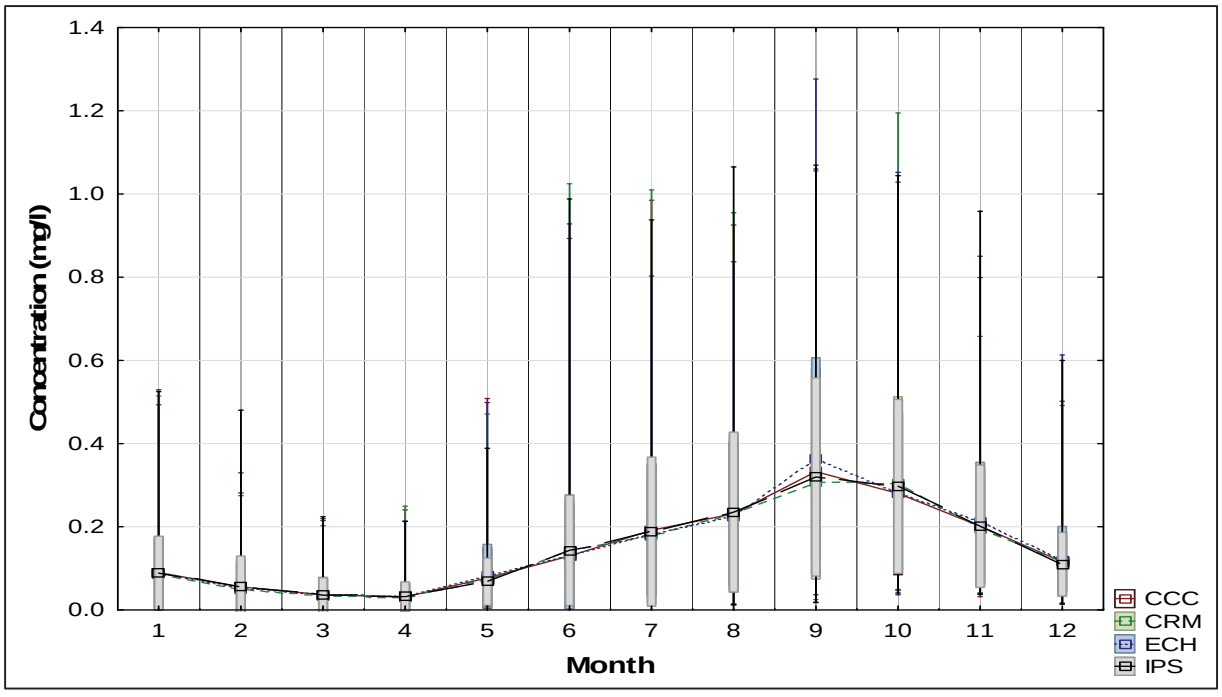

Figure 84: The present day mean surface zooplankton concentration for Berg River Dam (mg/l)

Table 25: The present day mean surface zooplankton concentration for Berg River Dam (mg/l)

	Jan	Feb	Mar	Apr	May	Jun	Jul	Aug	Sep	Oct	Nov	Dec
CCC	0.090	0.056	0.037	0.031	0.077	0.130	0.192	0.231	0.333	0.280	0.201	0.116
CRM	0.085	0.051	0.035	0.031	0.072	0.142	0.177	0.232	0.307	0.305	0.196	0.115
ECH	0.089	0.054	0.037	0.033	0.082	0.133	0.182	0.225	0.363	0.281	0.213	0.117
IPS	0.089	0.056	0.036	0.032	0.068	0.144	0.188	0.235	0.320	0.297	0.202	0.110

8.28 Eutrophication level

The trophic level indicator chosen for this study was the trophic index (TRIX level), but its shortcoming was that it did not include secchi depth, which was not measured as part of this modelling process. This index characterised the trophic levels in coastal marine areas and was adopted by the Italian national legislation and was applied here as way of representing the trophic level. It was the linearization of chlorophyll-*a* concentration (ChA in µg/ℓ), the dissolved oxygen concentration in percent (DO %), the total nitrogen (N_{min} = $N_{nitrate}$ + $N_{nitrite}$ + $N_{ammonia}$ in µg/ℓ) and the total phosphorous (TP µg/ℓ). This was represented mathematically as:

$$TRIX = \frac{(\log(ChA + aDO\% + N\min + TP) + 1.5)}{1.2}$$

From this the following states of water was classified (Table 26).

Table 26: The categories of TRIX values

TRIX value	Trophic category
< 4	Low trophic level
4-5	Middle trophic level
5-6	High trophic level
6-8	Very high trophic level

From Pavluk et al., 2008:3602

The output of the study for mean monthly surface trophic level was shown in Figure 85 for the present day. It was clear that Berg River dam was at the low trophic level for the entire year.

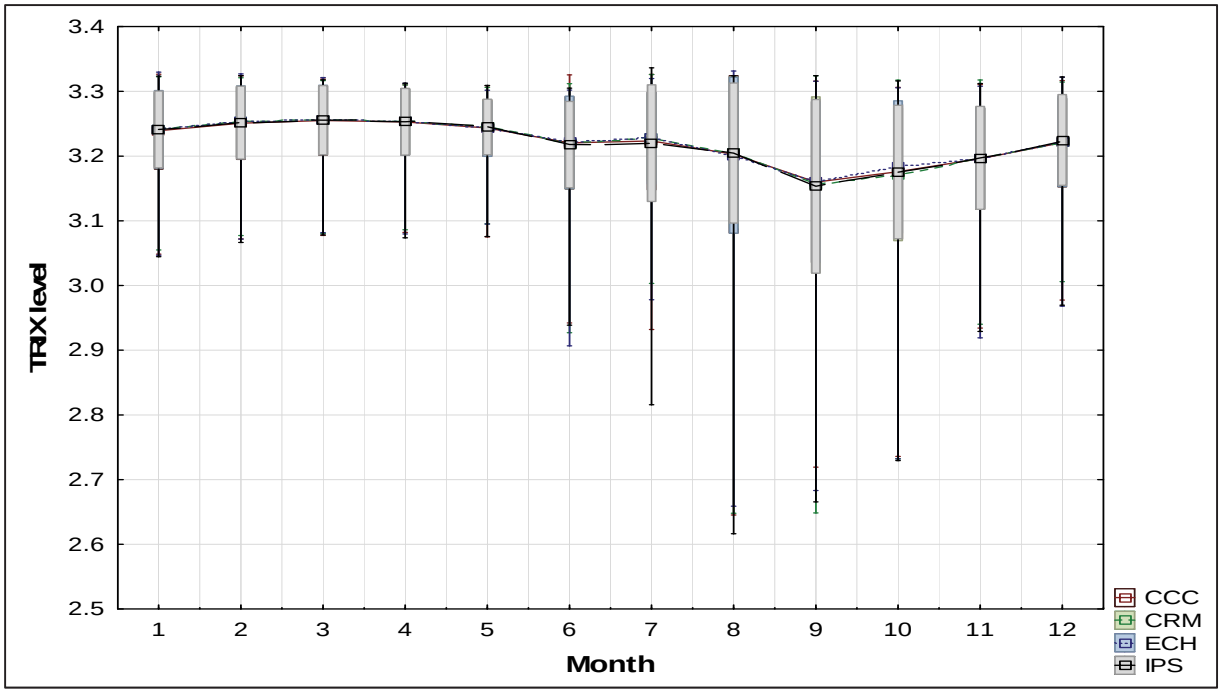

Figure 85: The present day TRIX level for Berg River Dam

Table 27 shows that the TRIX level of Berg River Dam peaks during late summer and autumn for all four present day climate models with minimum reached during winter and early spring. Although the total algae was increasing during this period the TRIX level decreases because the concentrations of NO_3-NO_2 was decreasing, the concentration of dissolved oxygen increased signalling better water quality. During this period the concentration of phosphates increased but it remained low it did not influence the TRIX levels much. It was expected that with climate change that this levels should increase due to changes in total algal concentration.

Table 27: The present day monthly mean surface TRIX level for Berg River Dam

	Jan	Feb	Mar	Apr	May	Jun	Jul	Aug	Sep	Oct	Nov	Dec
CCC	3.24	3.25	3.26	3.25	3.24	3.22	3.22	3.20	3.16	3.18	3.20	3.22
CRM	3.24	3.25	3.26	3.25	3.24	3.22	3.23	3.21	3.16	3.17	3.20	3.22
ECH	3.24	3.25	3.26	3.25	3.24	3.22	3.23	3.20	3.16	3.18	3.20	3.22
IPS	3.24	3.25	3.26	3.25	3.25	3.22	3.22	3.20	3.15	3.18	3.20	3.22
Monthly mean	3.24	3.25	3.26	3.25	3.24	3.22	3.22	3.20	3.16	3.18	3.20	3.22

BRD climate change scenarios

Now, once the preliminary present day climate had been established as the baseline, the effect of future climate change on the eutrophication of Berg River dam was investigated. This effect was determined by rerunning the water quality model, CE-QUAL-W2 but with the climate changed meteorological input data (air temperature, dew point temperature, wind-speed and direction, cloud cover and solar radiation) from the four climate change models (CCC, CRM, ECH and IPS). Trends were noted from each of the runs and compared with the present day runs. For this study, 1/1/2046-31/12/2065 represented the intermediate future and 1/1/2081-31/12/2100 was the distant future. The CCC model only had present day and intermediate future data.

The inflow streams were not adjusted for increased temperature for the future runs but since the inflow was at segment 1 and the segment under study was segment 21, this was considered not a problem.

Air temperature

Once the mean monthly air temperature for the present day had been established, the effect of climate change on Berg River dam was quantified. The water quality model (CE-QUAL-W2) was rerun with the same initial conditions and parameters but with the intermediate future and distant future meteorological inputs. The intermediate future and distant future for each of the four climate change models was shown in the following figure.

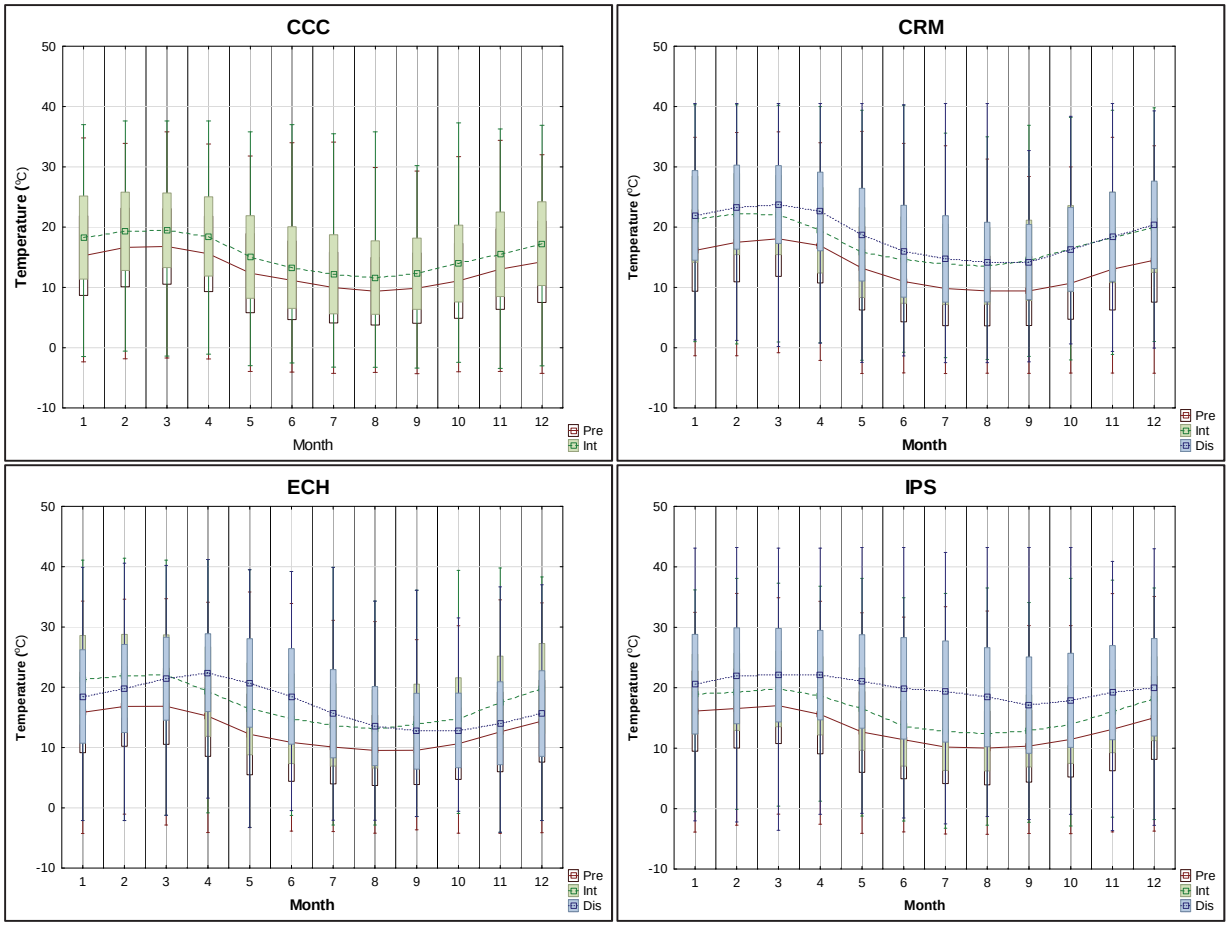

Figure 86: The projected climate change air temperature for Berg River Dam (^{o}C)

Figure 86 shows that the mean air temperature increased into the intermediate future and rose even higher into the distant future for all four climate models. The greatest inter-variability between climate model projections is for the distant future, thus the future algal growth should show the greatest variability. This higher air temperature was expected to have a marked effect on the surface water temperature in the form of energy transfer at the surface interface, thereby increasing water temperature. The extent of this increase was investigated in conjunction with solar radiation, the other source of energy that influences water temperature.

Table 28: The mean monthly air temperature for Berg River Dam (^{o}C) under projected climate change

	Jan	Feb	Mar	Apr	May	Jun	Jul	Aug	Sep	Oct	Nov	Dec
CCC pre	15.3	16.6	16.8	15.6	12.4	11.2	10.0	9.4	9.9	11.1	13.0	14.2
Difference	3.0	2.7	2.7	2.9	2.7	2.1	2.2	2.3	2.4	2.9	2.5	3.0
CCC int	18.3	19.3	19.5	18.5	15.1	13.3	12.2	11.6	12.3	14.0	15.5	17.3
CRM pre	16.1	17.5	18.1	16.9	13.2	11.0	9.8	9.4	9.4	10.7	13.0	14.5
Difference	5.2	4.7	3.9	2.5	2.6	3.6	4.0	4.1	5.1	5.7	5.3	5.4
CRM int	21.3	22.2	22.0	19.5	15.8	14.5	13.8	13.6	14.5	16.4	18.3	19.9
CRM int	21.3	22.2	22.0	19.5	15.8	14.5	13.8	13.6	14.5	16.4	18.3	19.9
Difference	0.6	1.1	1.7	3.1	3.0	1.5	0.9	0.6	-0.3	-0.1	0.1	0.5
CRM fut	21.9	23.3	23.8	22.6	18.7	16.0	14.7	14.2	14.2	16.3	18.4	20.4
ECH pre	15.8	16.8	16.9	15.2	12.2	10.8	10.1	9.5	9.5	10.7	12.6	14.4
Difference	5.4	5.1	5.2	4.1	4.2	3.9	3.7	3.6	4.3	4.1	4.9	5.4
ECH int	21.2	21.9	22.1	19.3	16.4	14.8	13.8	13.1	13.9	14.8	17.5	19.8
ECH int	21.2	21.9	22.1	19.3	16.4	14.8	13.8	13.1	13.9	14.8	17.5	19.8
Difference	-2.7	-2.1	-0.7	3.1	4.3	3.7	1.9	0.5	-1.2	-1.9	-3.5	-4.1
ECH fut	18.5	19.8	21.4	22.4	20.7	18.5	15.6	13.6	12.7	12.9	14.0	15.7
IPS pre	16.1	16.6	17.0	15.6	12.7	11.4	10.2	10.0	10.4	11.5	13.1	15.0
Difference	2.8	2.7	2.7	3.1	3.8	2.2	2.6	2.5	2.5	2.5	3.0	3.2
IPS int	18.9	19.3	19.8	18.7	16.5	13.6	12.8	12.5	12.8	13.9	16.1	18.2
IPS int	18.9	19.3	19.8	18.7	16.5	13.6	12.8	12.5	12.8	13.9	16.1	18.2
Difference	1.6	2.7	2.3	3.4	4.6	6.3	6.6	5.9	4.3	4.0	3.1	1.9
IPS fut	20.6	22.0	22.1	22.1	21.0	19.9	19.4	18.4	17.1	17.9	19.2	20.1

From the table and the figure, it was seen that the mean monthly temperature increases when going from present day to intermediate day and was maximum for the distant future scenario. The warmest months are shown are the orange to red colours and the cooler months are greener. It was clear from this that May to September was the cooler months and November to April was the warmer months.

It was interesting to note that the change in mean air temperature in progressing from the present day to the intermediate future was similar of that from intermediate future to distant future. This was a consequence of the accelerated anthropogenic loading as the time span

from present day to intermediate future was much greater than that of intermediate future to distant future.

The inter-variability between the climate models was now more evident and some discrepancies are noticed. The inter-variability was produced from the climate models themselves in assigning different assumptions of greenhouse gas loadings to the atmosphere.

Solar radiation

Wetzel in 2001 and others had established the diurnal link between solar radiation and surface water temperature from the aspect of an energy balance. Increased water temperature was the direct result of the diurnal shortwave solar radiation on a water-body. Figure 53 shows the present day solar radiation over Berg River dam and it was seen that May, June, July and August has the lowest radiation values. Figure 87 shows the incident solar radiation over Berg River dam for climate change for the four climate change models.

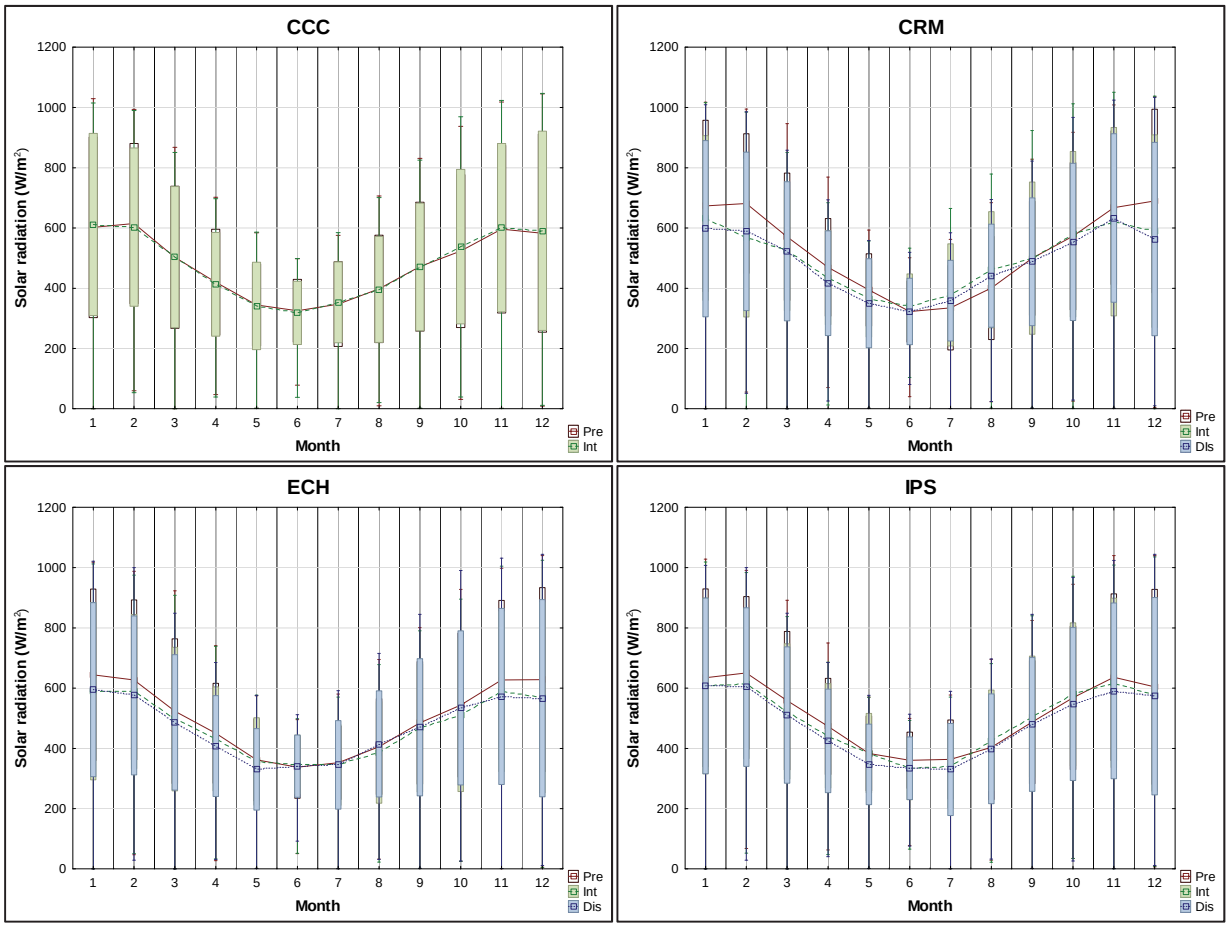

Figure 87: The projected climate change solar radiation for Berg River Dam (W/m^2)

This figure shows that for the intermediate future and distant future climates the change in incident solar radiation was negligible over that of the present day for all four climate change models although it showed also that during summer the incident solar radiation was relatively lower. This would imply that the effect of solar radiation of the present time and the future was comparably the same and does not have a substantial change on the growth of algae in the future. The months with the greatest incident solar radiation was that of January and February for all climate models as well as into the distant future.

When comparing the driving effect of air temperatures and solar radiation on surface water temperatures for future events, air temperatures had the greatest effect, as solar radiation remained unchanged for future climate change events.

Surface water temperature change

Long-term surface water temperature change had now been linked to air temperature increase due to climate change and the perceived changes due to diurnal fluxes are seen to be negligible within the four climate models used. Solar radiation influenced water temperature on a daily basis, but there was no nett climate change effect on solar radiation and thus it did not contribute to a long-term increase in water temperature. Essentially the long-term increase in surface water temperature was a result of increased air temperature, due to the greenhouse effect.

Figure 88 and Table 29 show the mean surface water temperature increase due to climate change into the intermediate future and distant future. They show that surface water temperature increases progressive for each month of the simulation period for all the future scenarios of climate change. If all other factors that support algal growth were favourable during this time then this increase in water temperature would have a marked increase in total algal growth in Berg River dam throughout the entire year. This premise was investigated further in the ensuing sections.

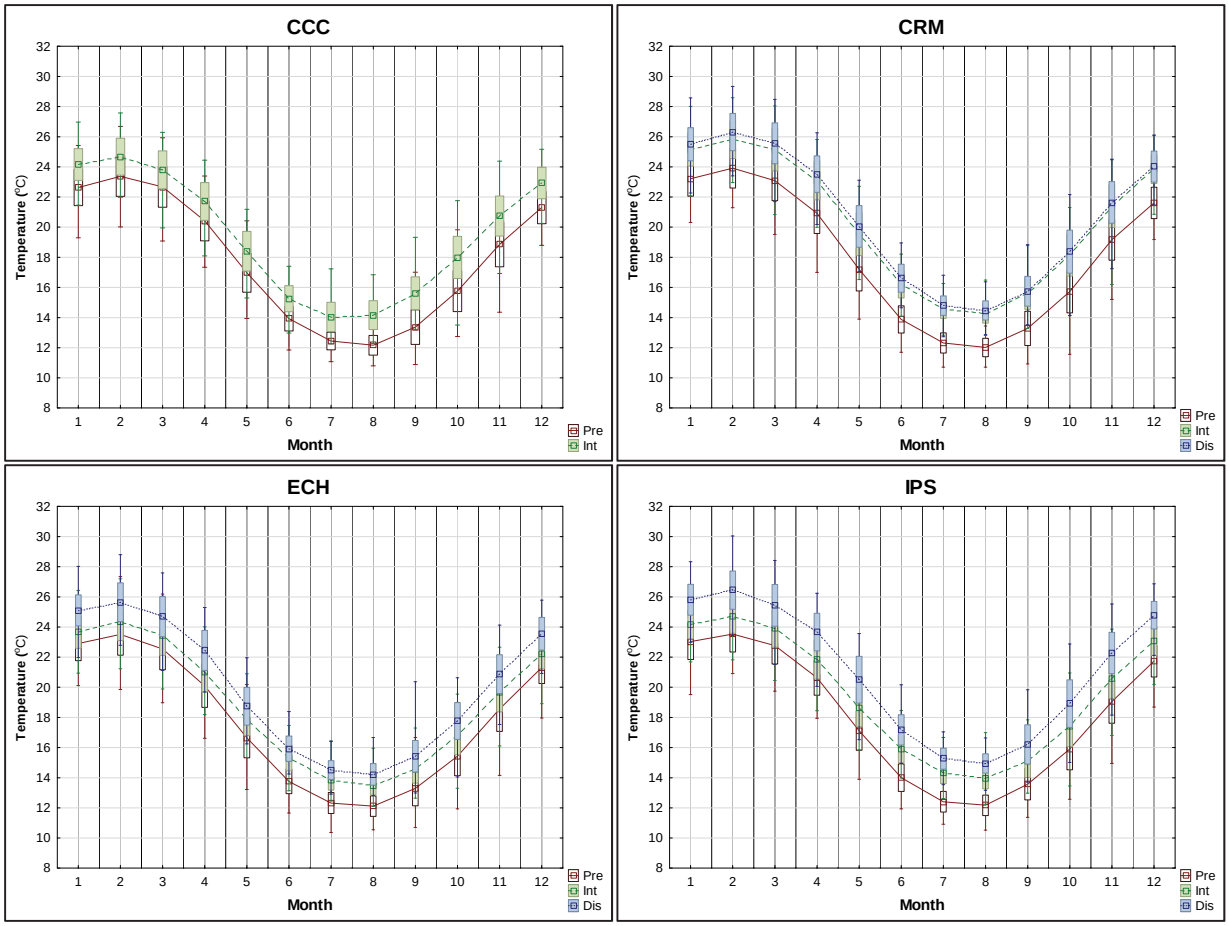

Figure 88: The projected climate change surface water temperature for Berg River Dam (^{o}C)

It was noted that for the CRM model that the intermediate future and distant future predicted similar surface water temperatures. For all models the mean surface water temperature increased from present day to distant future, with the intermediate future mean water temperatures between them.

Table 29: The mean monthly surface water temperature for Berg River Dam (^{o}C) under projected climate change

	Jan	Feb	Mar	Apr	May	Jun	Jul	Aug	Sep	Oct	Nov	Dec
CCC pre	22.6	23.4	22.7	20.4	17.0	13.9	12.4	12.2	13.4	15.8	18.9	21.3
Difference	1.5	1.3	1.1	1.3	1.4	1.3	1.6	2.0	2.2	2.2	1.9	1.6
CCC int	24.2	24.7	23.8	21.7	18.4	15.3	14.0	14.2	15.6	18.0	20.7	22.9
CRM pre	23.2	23.9	23.1	20.9	17.2	13.9	12.3	12.0	13.3	15.7	19.2	21.6
Difference	1.9	1.9	2.0	2.2	2.3	2.3	2.2	2.2	2.3	2.4	2.2	2.2
CRM int	25.2	25.8	25.1	23.1	19.5	16.2	14.5	14.3	15.6	18.1	21.4	23.8
CRM int	25.2	25.8	25.1	23.1	19.5	16.2	14.5	14.3	15.6	18.1	21.4	23.8
Difference	0.3	0.5	0.4	0.4	0.5	0.4	0.3	0.2	0.2	0.2	0.2	0.2
CRM fut	25.5	26.3	25.6	23.5	20.0	16.6	14.8	14.5	15.7	18.4	21.6	24.0
ECH pre	22.9	23.5	22.5	20.1	16.6	13.8	12.3	12.1	13.3	15.4	18.6	21.3
Difference	0.8	0.9	0.9	0.9	1.2	1.6	1.5	1.4	1.3	1.4	1.1	0.9
ECH int	23.7	24.4	23.4	21.0	17.9	15.3	13.8	13.5	14.6	16.8	19.7	22.2
ECH int	23.7	24.4	23.4	21.0	17.9	15.3	13.8	13.5	14.6	16.8	19.7	22.2
Difference	1.4	1.3	1.3	1.5	0.9	0.6	0.7	0.7	0.8	1.0	1.2	1.3
ECH fut	25.1	25.6	24.7	22.4	18.7	15.9	14.5	14.2	15.4	17.8	20.9	23.6
IPS pre	23.0	23.5	22.8	20.6	17.1	14.0	12.4	12.2	13.6	15.9	19.1	21.7
Difference	1.1	1.2	1.1	1.2	1.5	1.9	1.9	1.8	1.5	1.5	1.5	1.3
IPS int	24.2	24.7	23.9	21.9	18.7	15.9	14.3	14.0	15.1	17.4	20.6	23.1
IPS int	24.2	24.7	23.9	21.9	18.7	15.9	14.3	14.0	15.1	17.4	20.6	23.1
Difference	1.6	1.7	1.5	1.8	1.8	1.3	0.9	1.0	1.1	1.5	1.7	1.7
IPS fut	25.8	26.4	25.4	23.7	20.5	17.2	15.3	14.9	16.2	18.9	22.3	24.8

The accelerated trend of surface water heating due to climate change from intermediate future to distant future was also evident. From the table it was seen that the pattern for mean surface water temperatures follows that of mean air temperatures for monthly trends and climate change events, thereby consolidating the premise that air temperature was the driver for surface water temperature.

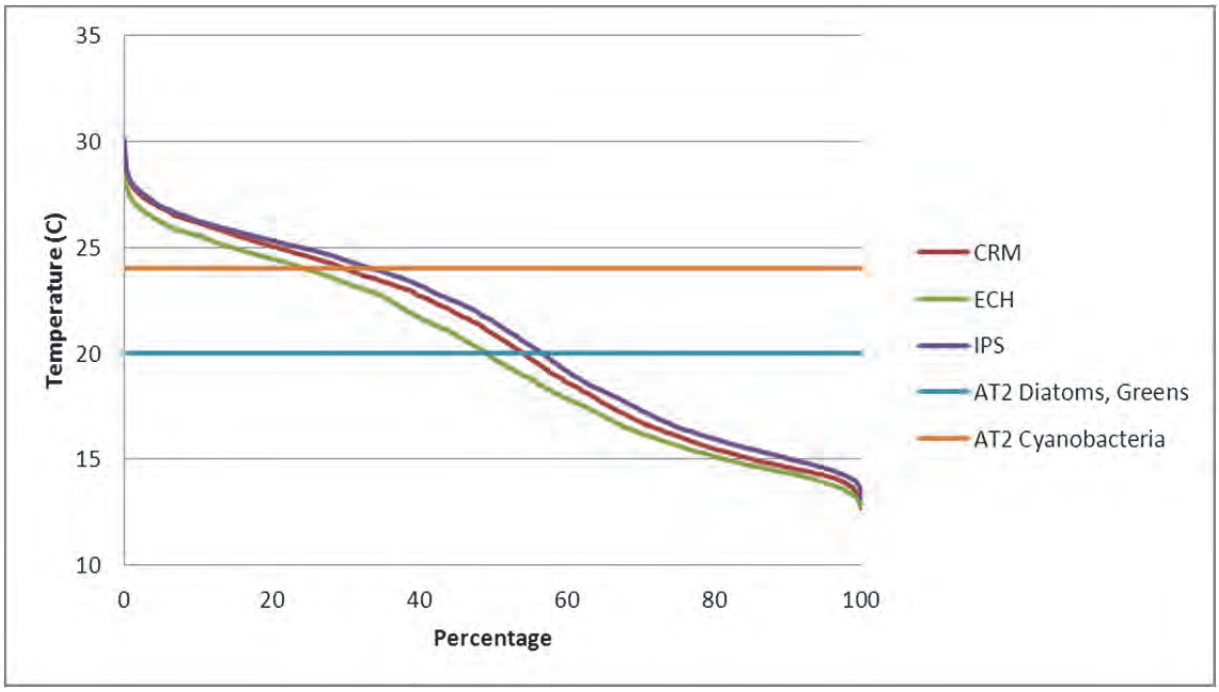

Figure 89: The distant future surface water temperature exceedance for Berg River Dam with respect to algal temperature growth multipliers

To investigate the effect of a raised water temperature on the algae an exceedance plot was performed related to the algal growth rate multipliers. In comparing Figure 89 to Figure 57 and using Table 29 as a guide, it was seen that the mean surface water temperature increased in progressing from present day to distant future. This had a direct effect on the perceived favourable growth rates of all algae in Berg River dam. For diatoms and greens, the favourable temperature was exceeded between 50-58% of the time, which was an increase of at least 10% over that of the present day, thereby implying twice as much blooms or greater concentrations for a future scenario than the present day. Similarly, for cyanobacteria the exceedance was 25-34% compared to 5% in the present day.

It was noted that for the three distant future climate models, their surface water temperatures was more spread than for the present day and it was possible to rate their individual effect on the surface water temperature with ECH being the coolest and IPS the hottest with CRM the intermediate climate model.

Surface water elevations

It was expected that since the air temperature and surface water temperature increased, that the rate of evaporation from Berg River would be greater than for the present day period. The result of fixing the inflow and withdrawals the same for the future simulations would be a decreased water level for the dam.

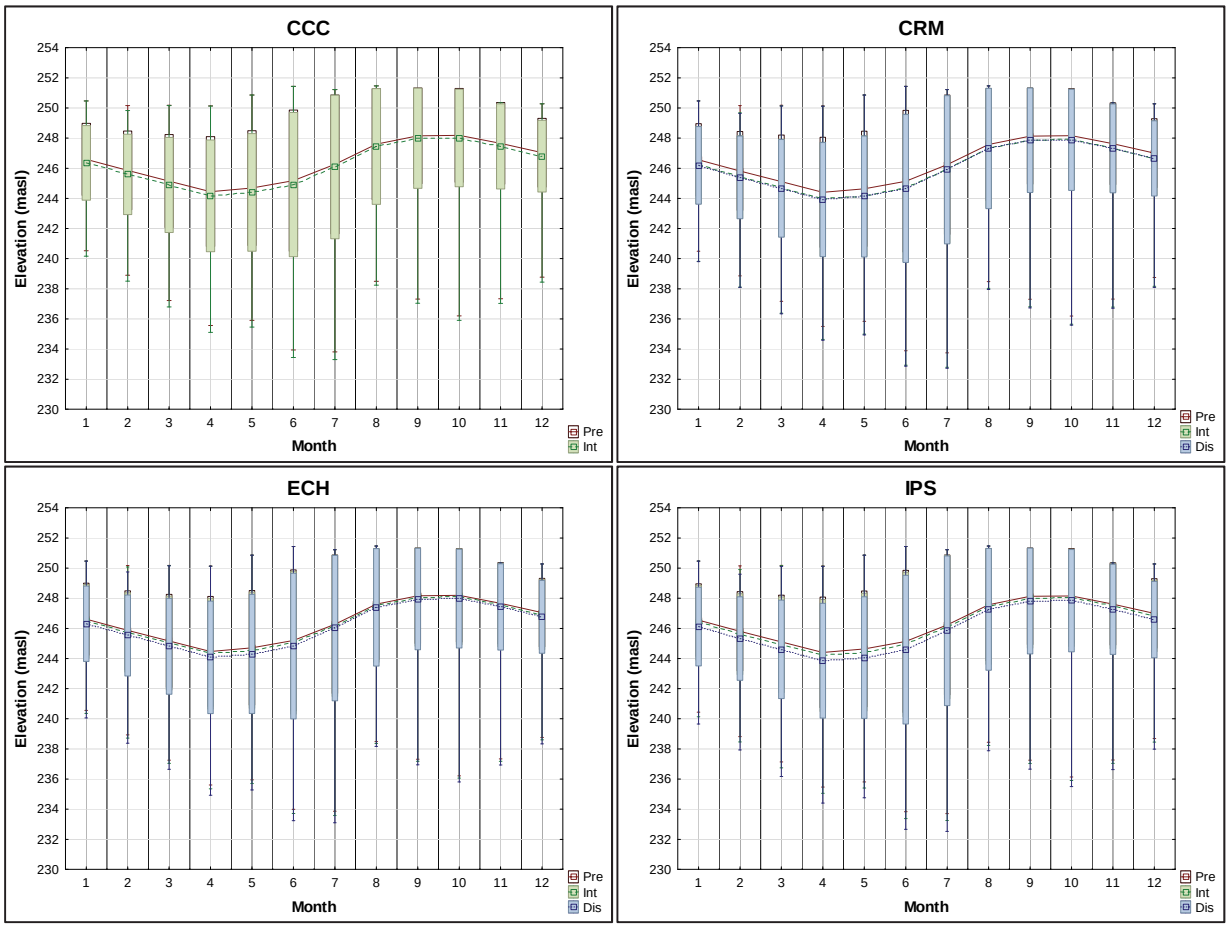

Figure 90: The projected climate change surface water elevations for Berg River Dam (masl)

This phenomenon was shown in Figure 90 and Table 30 where green represents a minimum and red a maximum. The mean monthly surface water levels was decreasing in going from present day to intermediate future and finally distant future scenarios at the accelerated rate explained before.

It was clear that the mean monthly surface water levels decreased for future climate change scenarios due to increased air temperatures causing greater rates of evaporation. If the inflow concentration of constituents remained the same for climate change scenarios, which it did for this study, this phenomenon would concentrate all constituents in the dam as concentration was directly related to the volume of the dam, which was decreasing.

Table 30: Surface water elevations for Berg River Dam (masl) under projected climate change

	Jan	Feb	Mar	Apr	May	Jun	Jul	Aug	Sep	Oct	Nov	Dec
CCC pre	246.6	245.9	245.1	244.5	244.7	245.2	246.3	247.6	248.2	248.2	247.6	247.0
Difference	-0.24	-0.26	-0.26	-0.28	-0.29	-0.26	-0.18	-0.15	-0.16	-0.17	-0.20	-0.23
CCC int	246.4	245.6	244.9	244.2	244.4	244.9	246.1	247.4	248.0	248.0	247.4	246.8
CRM pre	246.6	245.8	245.1	244.4	244.6	245.1	246.2	247.6	248.1	248.2	247.6	247.0
Difference	-0.35	-0.40	-0.41	-0.45	-0.47	-0.44	-0.31	-0.25	-0.25	-0.26	-0.29	-0.33
CRM int	246.2	245.4	244.7	244.0	244.2	244.7	245.9	247.3	247.9	247.9	247.3	246.7
CRM int	246.2	245.4	244.7	244.0	244.2	244.7	245.9	247.3	247.9	247.9	247.3	246.7
Difference	-0.02	-0.02	-0.03	-0.04	-0.04	-0.04	-0.03	-0.02	-0.02	-0.02	-0.02	-0.02
CRM fut	246.2	245.4	244.7	243.9	244.1	244.7	245.9	247.3	247.9	247.9	247.3	246.7
ECH pre	246.6	245.9	245.2	244.5	244.7	245.2	246.3	247.6	248.2	248.2	247.7	247.0
Difference	-0.13	-0.14	-0.14	-0.16	-0.16	-0.16	-0.11	-0.09	-0.09	-0.10	-0.11	-0.12
ECH int	246.5	245.7	245.0	244.3	244.5	245.0	246.2	247.5	248.1	248.1	247.6	246.9
ECH int	246.5	245.7	245.0	244.3	244.5	245.0	246.2	247.5	248.1	248.1	247.6	246.9
Difference	-0.17	-0.20	-0.21	-0.24	-0.24	-0.22	-0.15	-0.12	-0.12	-0.12	-0.13	-0.16
ECH fut	246.3	245.5	244.8	244.1	244.3	244.8	246.0	247.4	247.9	248.0	247.4	246.8
IPS pre	246.5	245.8	245.1	244.4	244.6	245.1	246.2	247.6	248.1	248.2	247.6	247.0
Difference	-0.17	-0.18	-0.18	-0.20	-0.21	-0.21	-0.14	-0.12	-0.12	-0.13	-0.14	-0.16
IPS int	246.4	245.6	244.9	244.2	244.4	244.9	246.1	247.5	248.0	248.0	247.5	246.8
IPS int	246.4	245.6	244.9	244.2	244.4	244.9	246.1	247.5	248.0	248.0	247.5	246.8
Difference	-0.26	-0.30	-0.31	-0.34	-0.36	-0.34	-0.25	-0.19	-0.19	-0.19	-0.21	-0.24
IPS fut	246.1	245.3	244.6	243.9	244.1	244.6	245.8	247.3	247.8	247.8	247.3	246.6

In conclusion, if the dam were to be operated at the current inflows and withdrawal rates for the future, it was see that the surface water levels decreased due to increased evaporation from the dam. This effective decrease was discussed in the following sections.

Ortho-Phosphorous concentration

The phosphorous concentration within the dam was influenced by various factors such as inflow and withdrawal as well as assimilation by the various algae as it was the limiting nutrient for algal growth. The future inflow concentration of phosphorous was kept the same as was for the present day scenario. The future in-dam surface concentration of phosphorous was shown for the four climate models in Figure 91.

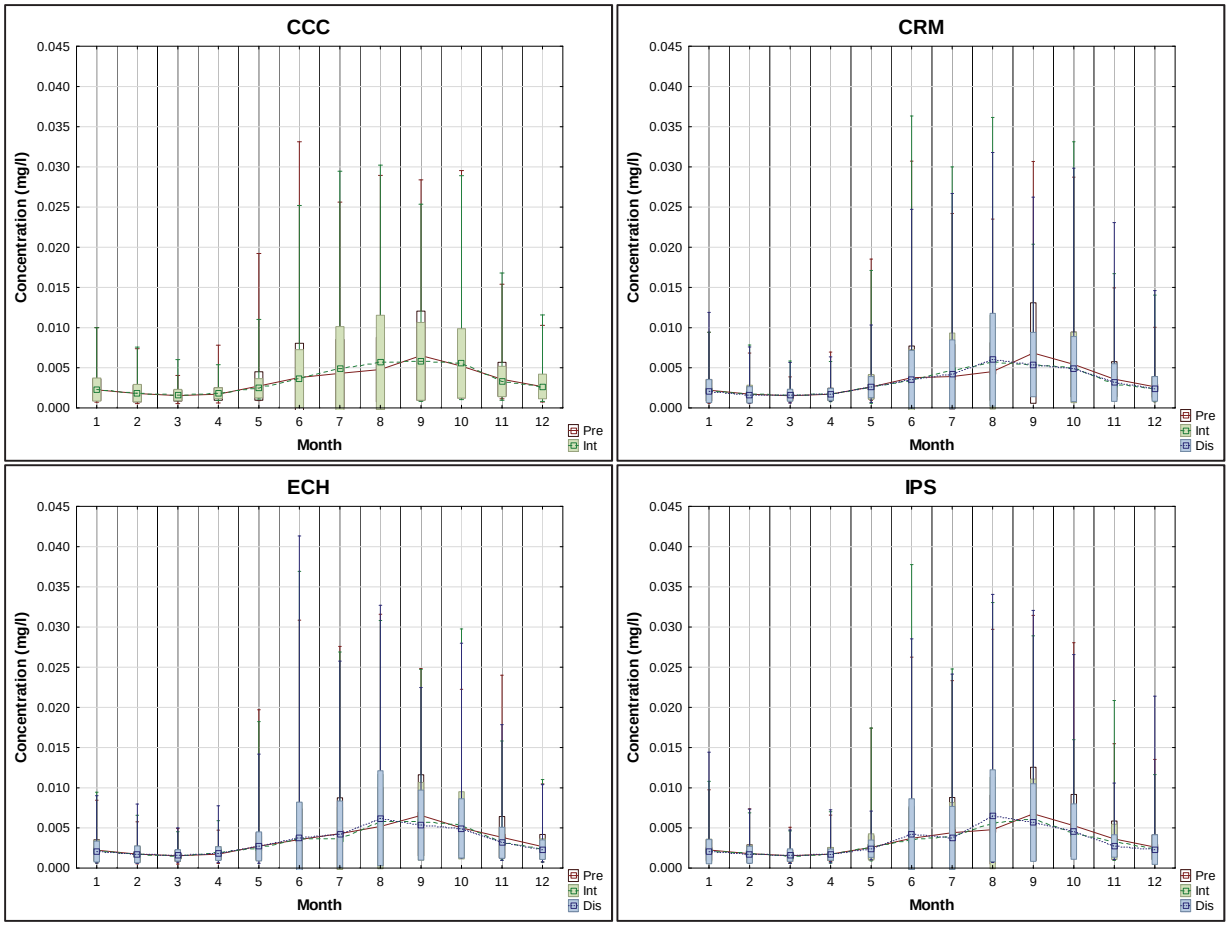

Figure 91: The projected climate change surface phosphate concentration for Berg River Dam (mg/l)

From Figure 91 it was seen that the surface phosphate concentration fluctuated marginally when progressing to intermediate future and distant future. The maximum concentration occurs one month earlier in the future scenarios than in the present day and the concentration is relatively unchanged.

Table 31: The mean monthly surface phosphate concentration for Berg River Dam (mg/l) under projected climate change

	Jan	Feb	Mar	Apr	May	Jun	Jul	Aug	Sep	Oct	Nov	Dec
CCC pre	0.00227	0.00180	0.00153	0.00173	0.00273	0.00380	0.00431	0.00478	0.00652	0.00522	0.00358	0.00266
Difference	0.00003	0.00006	0.00008	0.00012	-0.00027	-0.00014	0.00059	0.00089	-0.00072	0.00034	-0.00028	0.00002
CCC int	0.00229	0.00186	0.00161	0.00184	0.00246	0.00366	0.00490	0.00567	0.00581	0.00556	0.00330	0.00268
CRM pre	0.00222	0.00173	0.00152	0.00171	0.00262	0.00377	0.00391	0.00454	0.00684	0.00542	0.00359	0.00264
Difference	-0.00005	0.00002	0.00009	-0.00001	0.00002	-0.00038	0.00076	0.00118	-0.00150	-0.00038	-0.00068	-0.00027
CRM int	0.00217	0.00175	0.00161	0.00170	0.00263	0.00339	0.00467	0.00572	0.00534	0.00504	0.00292	0.00237
CRM int	0.00217	0.00175	0.00161	0.00170	0.00263	0.00339	0.00467	0.00572	0.00534	0.00504	0.00292	0.00237
Difference	-0.00006	-0.00011	-0.00001	0.00001	-0.00004	0.00015	-0.00048	0.00029	0.00007	-0.00019	0.00025	0.00002
CRM fut	0.00210	0.00164	0.00159	0.00171	0.00259	0.00354	0.00419	0.00601	0.00541	0.00485	0.00317	0.00239
ECH pre	0.00224	0.00174	0.00154	0.00174	0.00274	0.00356	0.00430	0.00518	0.00657	0.00502	0.00384	0.00268
Difference	-0.00007	0.00000	-0.00001	0.00017	-0.00027	0.00011	-0.00059	0.00061	-0.00074	0.00031	-0.00063	-0.00024
ECH int	0.00216	0.00173	0.00153	0.00190	0.00247	0.00368	0.00371	0.00579	0.00583	0.00533	0.00321	0.00244
ECH int	0.00216	0.00173	0.00153	0.00190	0.00247	0.00368	0.00371	0.00579	0.00583	0.00533	0.00321	0.00244
Difference	-0.00010	-0.00003	0.00007	-0.00010	0.00024	0.00010	0.00052	0.00041	-0.00047	-0.00038	-0.00006	-0.00014
ECH fut	0.00206	0.00171	0.00159	0.00181	0.00270	0.00378	0.00423	0.00621	0.00536	0.00495	0.00315	0.00231
IPS pre	0.00226	0.00181	0.00155	0.00175	0.00258	0.00372	0.00441	0.00480	0.00676	0.00530	0.00363	0.00261
Difference	-0.00008	-0.00004	-0.00002	0.00001	0.00006	-0.00019	-0.00041	0.00082	-0.00065	-0.00096	-0.00035	-0.00025
IPS int	0.00218	0.00178	0.00153	0.00176	0.00265	0.00354	0.00400	0.00562	0.00611	0.00434	0.00328	0.00236
IPS int	0.00218	0.00178	0.00153	0.00176	0.00265	0.00354	0.00400	0.00562	0.00611	0.00434	0.00328	0.00236
Difference	-0.00012	-0.00012	0.00009	-0.00008	-0.00023	0.00070	-0.00024	0.00091	-0.00043	0.00021	-0.00052	-0.00004
IPS fut	0.00206	0.00166	0.00162	0.00168	0.00242	0.00423	0.00376	0.00653	0.00568	0.00455	0.00276	0.00232

From Table 31 it was seen that the mean monthly phosphorous concentration remained unchanged for future events. The only variable between these models was the air temperature difference that causes the lower surface water levels. Thus, the lower surface water levels have a concentrating effect on the surface phosphorous concentration. The increase in phosphorous was seen during summer as well as having the greatest increases during autumn.

It was concluded that Berg River dam was phosphorous limited for algal growth and that the concentration of phosphorous in Berg River was sufficiently great that it never posed a limitation for algal growth from the present day to distant future climate events. For this dam,

a point source reduction of phosphorous for the catchment could greatly reduce algal blooms in all climate change scenarios, based on the premise that phosphorous was the limiting nutrient for algal growth. This would imply that upstream of the dam no additional sources of phosphorous be introduced into the catchment in the form of a WWTP or industrial effluent discharge.

The sources of phosphorous that could contribute to an increase are increased algal respiration, increased anaerobic release from sediments as well as decay. Decreases are due to photosynthesis and system losses to withdrawal and adsorption/settling.

Ammonium concentration

For the future climate change events it was seen in Figure 92 and Table 32 that the surface concentration of ammonium was increased for all the climate models and that the mean monthly concentration was below the DWA limit of 1mg/l, although peaks greater than this this did occur.

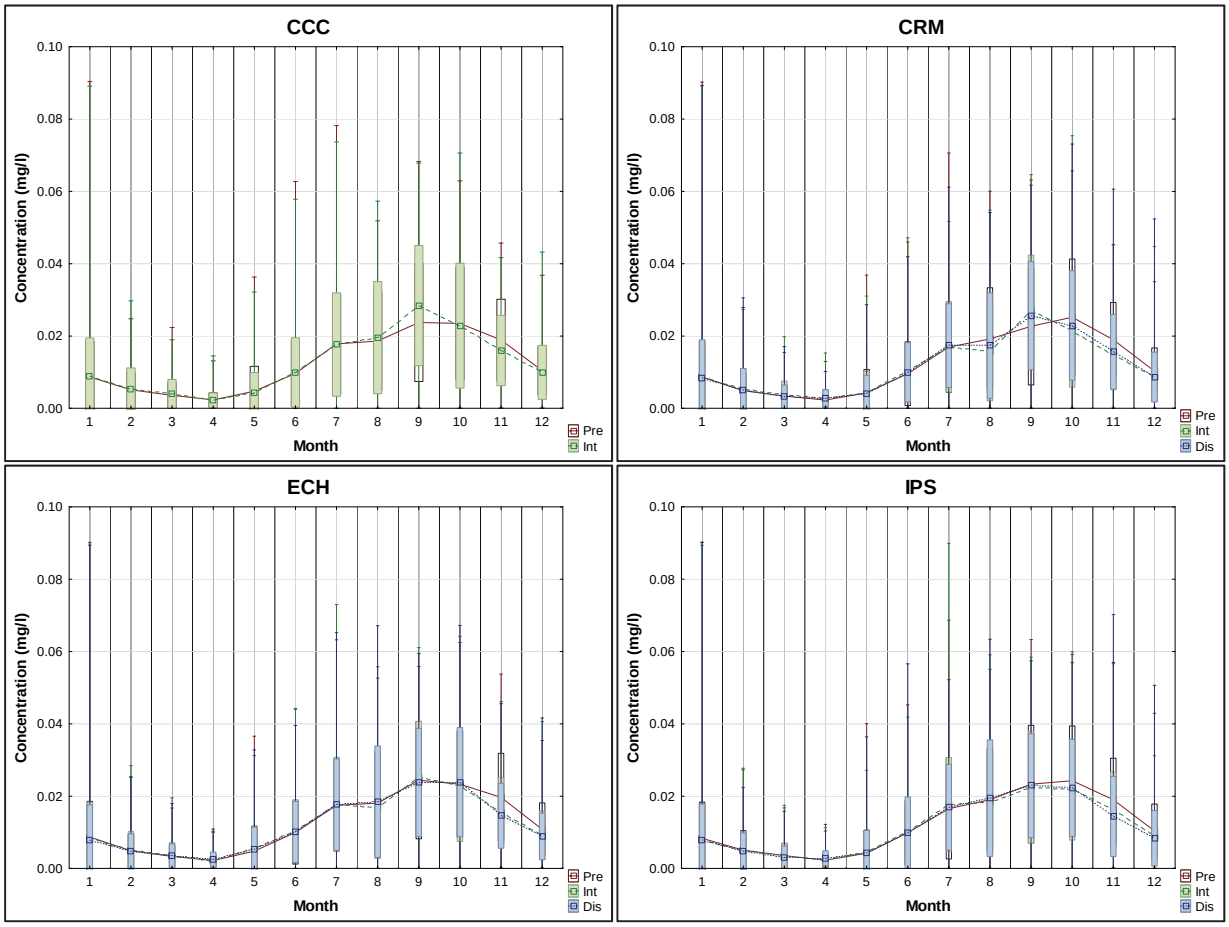

Figure 92: The projected climate change surface ammonium concentration for Berg River Dam (mg/l)

Table 32: The mean monthly surface ammonium concentration for Berg River Dam (mg/l) under projected climate change

	Jan	Feb	Mar	Apr	May	Jun	Jul	Aug	Sep	Oct	Nov	Dec
CCC pre	0.0087	0.0051	0.0036	0.0023	0.0048	0.0097	0.0178	0.0186	0.0238	0.0235	0.0189	0.0104
Difference	0.0002	0.0003	0.0003	-0.0001	-0.0006	0.0002	-0.0002	0.0009	0.0047	-0.0006	-0.0029	-0.0005
CCC int	0.0089	0.0054	0.0040	0.0022	0.0042	0.0099	0.0177	0.0196	0.0284	0.0229	0.0160	0.0100
CRM pre	0.0087	0.0049	0.0034	0.0023	0.0043	0.0096	0.0169	0.0192	0.0227	0.0252	0.0190	0.0103
Difference	-0.0002	0.0004	0.0004	0.0004	0.0001	0.0007	0.0001	-0.0034	0.0044	-0.0039	-0.0042	-0.0017
CRM int	0.0085	0.0053	0.0038	0.0027	0.0044	0.0103	0.0170	0.0158	0.0271	0.0213	0.0147	0.0086
CRM int	0.0085	0.0053	0.0038	0.0027	0.0044	0.0103	0.0170	0.0158	0.0271	0.0213	0.0147	0.0086
Difference	0.0000	-0.0002	-0.0006	0.0001	-0.0003	-0.0003	0.0003	0.0016	-0.0015	0.0016	0.0009	0.0001
CRM fut	0.0085	0.0051	0.0032	0.0028	0.0041	0.0100	0.0174	0.0174	0.0256	0.0229	0.0156	0.0087
ECH pre	0.0087	0.0049	0.0034	0.0022	0.0048	0.0100	0.0175	0.0181	0.0244	0.0233	0.0197	0.0108
Difference	-0.0005	0.0002	0.0002	-0.0001	0.0007	0.0004	0.0002	-0.0014	0.0008	-0.0005	-0.0041	-0.0017
ECH int	0.0082	0.0051	0.0036	0.0021	0.0056	0.0104	0.0177	0.0167	0.0253	0.0228	0.0155	0.0092
ECH int	0.0082	0.0051	0.0036	0.0021	0.0056	0.0104	0.0177	0.0167	0.0253	0.0228	0.0155	0.0092
Difference	-0.0005	-0.0004	0.0000	0.0003	-0.0003	-0.0003	-0.0001	0.0018	-0.0014	0.0011	-0.0010	-0.0003
ECH fut	0.0077	0.0047	0.0036	0.0024	0.0052	0.0101	0.0176	0.0185	0.0238	0.0239	0.0146	0.0089
IPS pre	0.0084	0.0051	0.0036	0.0023	0.0042	0.0099	0.0166	0.0190	0.0233	0.0243	0.0190	0.0104
Difference	-0.0004	-0.0001	0.0000	-0.0001	0.0004	0.0002	0.0012	-0.0009	-0.0008	-0.0025	-0.0027	-0.0015
IPS int	0.0079	0.0050	0.0036	0.0022	0.0046	0.0101	0.0177	0.0182	0.0225	0.0217	0.0163	0.0089
IPS int	0.0079	0.0050	0.0036	0.0022	0.0046	0.0101	0.0177	0.0182	0.0225	0.0217	0.0163	0.0089
Difference	0.0000	-0.0003	-0.0005	0.0006	-0.0004	-0.0002	-0.0008	0.0013	0.0004	0.0005	-0.0018	-0.0005
IPS fut	0.0079	0.0048	0.0032	0.0028	0.0042	0.0099	0.0170	0.0195	0.0229	0.0223	0.0144	0.0084

All models showed changes in surface ammonium concentration but overall it is a decreasing trend in progressing to future climate change scenarios.

An increase in ammonium was attributed to increased algal respiration, decay of dissolved organic material and anaerobic release from the sediments. System losses of ammonium were due to photosynthesis and nitrification to form the nitrate-nitrite complex ion.

Nitrate-nitrite concentration

The surface nitrate-nitrite concentration was shown in Figure 93 and Table 33. The nitrate-nitrite complex was an intermediately and its losses are due to photosynthesis and de-nitrification to the water column. From this, it was seen that the future surface concentrations remain relatively unchanged when compared to present day surface concentrations, with spring having the minimum surface concentrations.

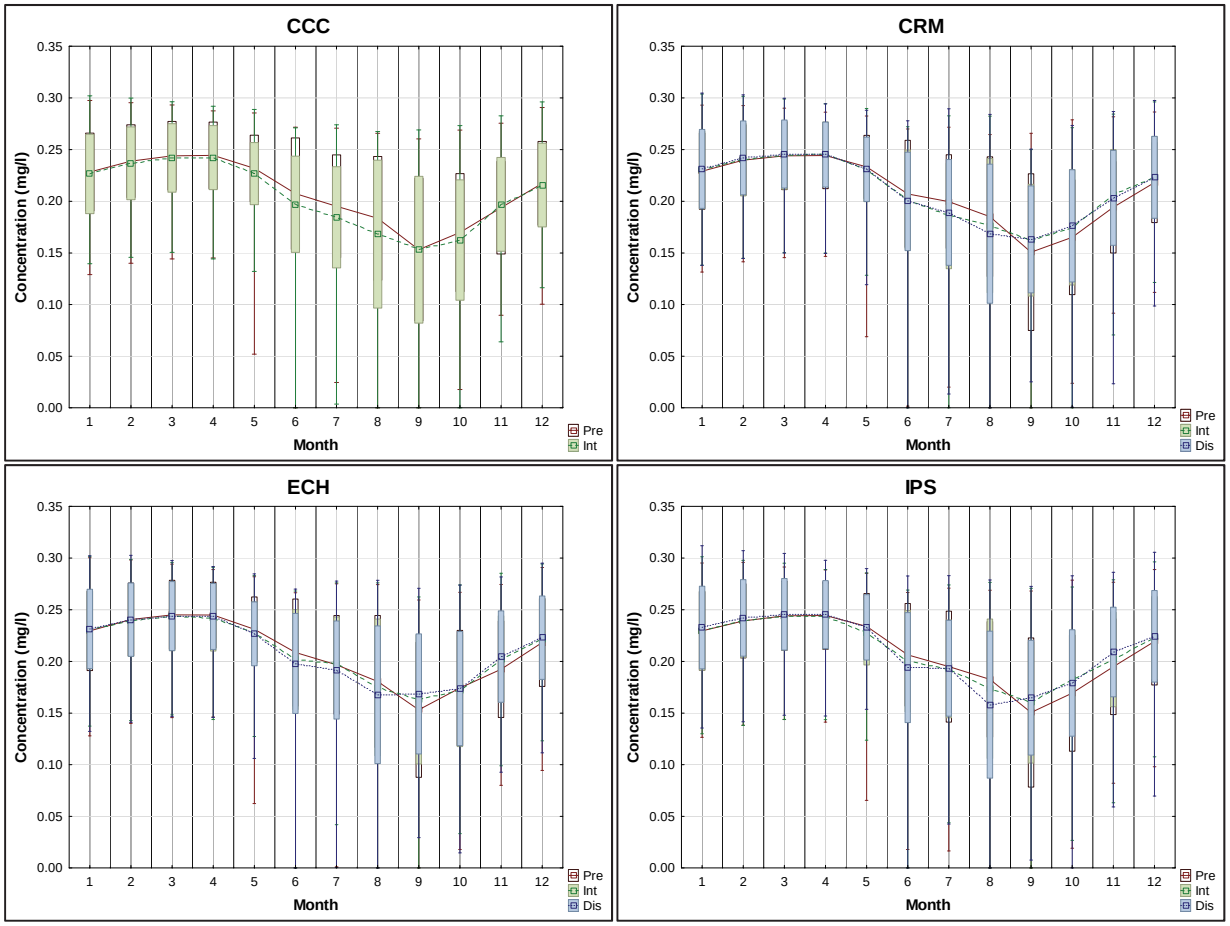

Figure 93: The projected climate change surface nitrate-nitrite concentration for Berg River Dam (mg/l)

Table 33: The mean monthly surface nitrate-nitrite concentration for Berg River Dam (mg/l) under projected climate change

	Jan	Feb	Mar	Apr	May	Jun	Jul	Aug	Sep	Oct	Nov	Dec
CCC pre	0.228	0.239	0.244	0.244	0.232	0.207	0.195	0.183	0.153	0.170	0.194	0.217
Difference	-0.002	-0.002	-0.002	-0.002	-0.005	-0.010	-0.011	-0.015	0.000	-0.007	0.003	-0.002
CCC int	0.226	0.237	0.242	0.242	0.227	0.197	0.184	0.168	0.153	0.162	0.197	0.216
CRM pre	0.229	0.240	0.244	0.244	0.233	0.207	0.200	0.185	0.151	0.165	0.194	0.218

	Jan	Feb	Mar	Apr	May	Jun	Jul	Aug	Sep	Oct	Nov	Dec
Difference	0.001	0.001	0.001	0.001	-0.003	-0.006	-0.014	-0.009	0.012	0.010	0.012	0.005
CRM int	0.230	0.240	0.245	0.246	0.231	0.202	0.186	0.176	0.162	0.175	0.206	0.223
CRM int	0.230	0.240	0.245	0.246	0.231	0.202	0.186	0.176	0.162	0.175	0.206	0.223
Difference	0.001	0.002	0.001	0.000	0.000	-0.002	0.003	-0.008	0.001	0.001	-0.003	0.000
CRM fut	0.231	0.242	0.246	0.245	0.231	0.200	0.189	0.169	0.163	0.176	0.203	0.223
ECH pre	0.230	0.241	0.245	0.245	0.231	0.209	0.197	0.181	0.153	0.174	0.192	0.218
Difference	0.001	-0.001	-0.001	-0.002	-0.003	-0.007	0.001	-0.006	0.010	-0.003	0.010	0.004
ECH int	0.230	0.240	0.244	0.242	0.228	0.202	0.198	0.175	0.163	0.172	0.202	0.222
ECH int	0.230	0.240	0.244	0.242	0.228	0.202	0.198	0.175	0.163	0.172	0.202	0.222
Difference	0.001	0.001	0.000	0.001	-0.001	-0.004	-0.006	-0.007	0.005	0.002	0.002	0.001
ECH fut	0.231	0.240	0.244	0.243	0.227	0.198	0.192	0.168	0.168	0.174	0.205	0.223
IPS pre	0.229	0.239	0.244	0.244	0.234	0.206	0.195	0.183	0.151	0.169	0.195	0.219
Difference	0.000	0.000	0.000	-0.001	-0.006	-0.006	-0.002	-0.009	0.010	0.013	0.007	0.004
IPS int	0.230	0.239	0.244	0.244	0.228	0.200	0.193	0.174	0.160	0.182	0.202	0.223
IPS int	0.230	0.239	0.244	0.244	0.228	0.200	0.193	0.174	0.160	0.182	0.202	0.223
Difference	0.003	0.003	0.002	0.002	0.005	-0.006	0.001	-0.015	0.005	-0.003	0.007	0.001
IPS fut	0.233	0.242	0.246	0.245	0.233	0.194	0.193	0.158	0.165	0.179	0.209	0.224

When examining Figure 94 it was seen that the exceedance of total surface N does not vary significantly with respect half-saturation constant for green algae and is very similar to the present day exceedance. This would imply that total surface N concentration did not affect the growth of green algae from an increased limiting aspect, in the event of climate change.

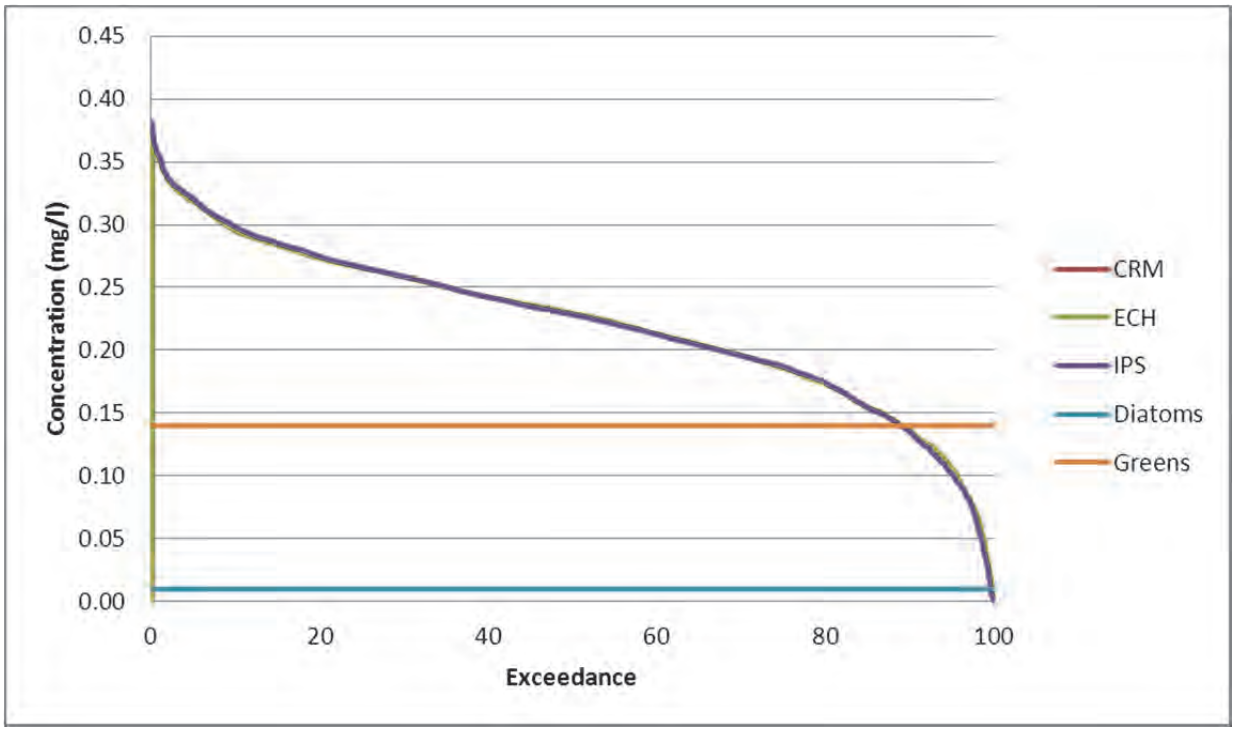

Figure 94: The projected distant future total surface N exceedance with respect to algal growth for Berg River Dam

Dissolved silicon

It had been established that only diatoms are silicon limited for growth and when comparing Figure 95 and Table 33 to their present day counterparts, it was seen that the mean monthly surface dissolved silicon concentration showed a decrease in progressing into the future. It was noted that the surface dissolved silicon concentration did not exceed the DWA limit of 150mg/l.

The inter-variability of the climate models was shown but was insignificant from an algal growth point of view and the greatest changes are seen when progressing from the present day to the intermediate future.

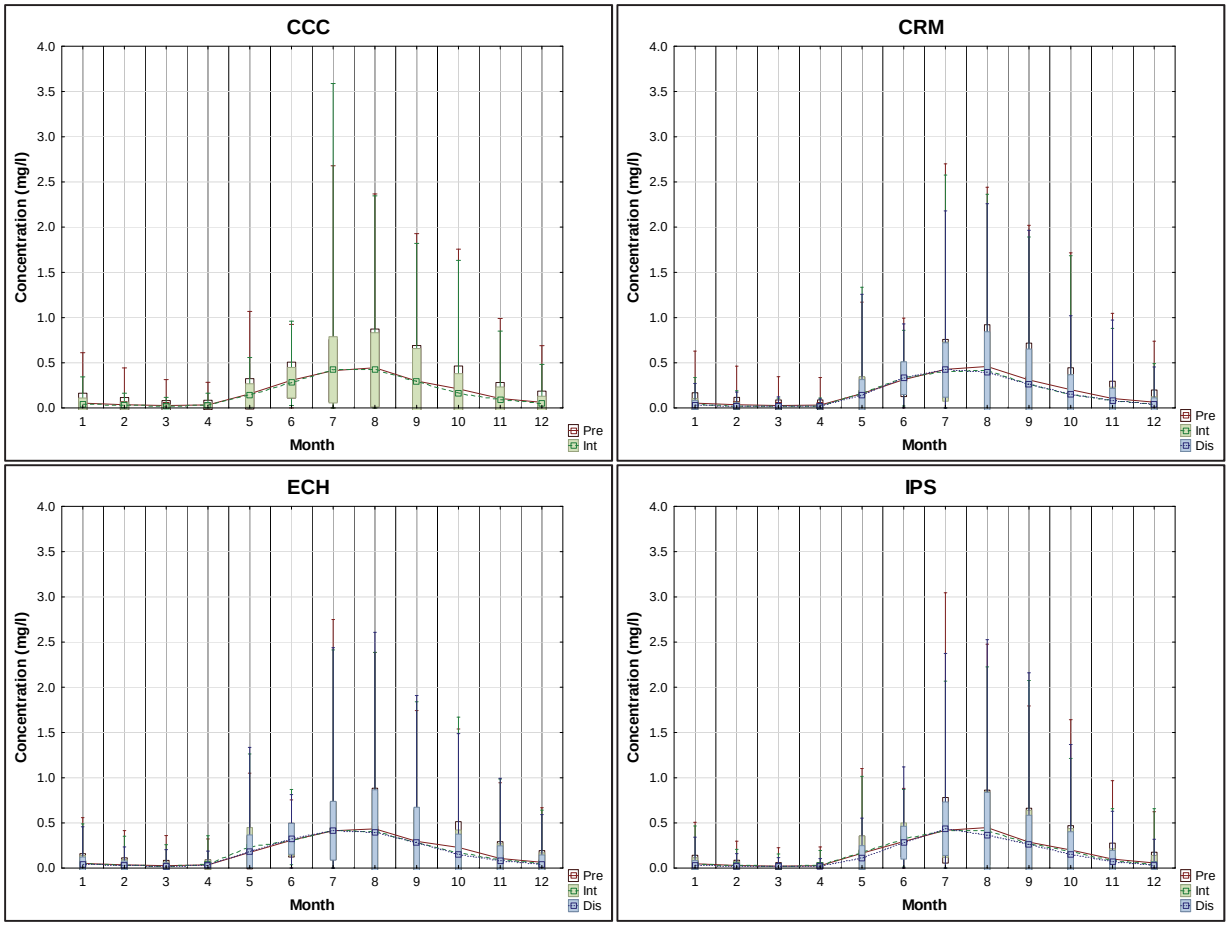

Figure 95: The projected climate change surface dissolved silicon concentration for Berg River Dam (mg/l)

The inter-variability and effect of climate change is shown in the Table 34 for surface dissolved silicon.

Table 34: The mean monthly surface dissolved silicon concentration for Berg River Dam (mg/l) under projected climate change

	Jan	Feb	Mar	Apr	May	Jun	Jul	Aug	Sep	Oct	Nov	Dec
CCC pre	0.054	0.037	0.027	0.034	0.157	0.308	0.413	0.446	0.298	0.212	0.106	0.062
Difference	-0.011	-0.010	-0.008	-0.006	-0.019	-0.029	0.010	-0.024	0.000	-0.045	-0.017	-0.015
CCC int	0.043	0.026	0.019	0.028	0.138	0.280	0.423	0.422	0.298	0.167	0.088	0.047
CRM pre	0.054	0.036	0.027	0.033	0.159	0.315	0.428	0.460	0.311	0.203	0.106	0.064
Difference	-0.014	-0.011	-0.011	-0.010	0.003	0.020	-0.025	-0.042	-0.052	-0.055	-0.026	-0.021
CRM int	0.041	0.026	0.017	0.022	0.162	0.335	0.403	0.418	0.259	0.148	0.080	0.043
CRM int	0.041	0.026	0.017	0.022	0.162	0.335	0.403	0.418	0.259	0.148	0.080	0.043
Difference	-0.006	-0.001	0.004	0.000	-0.017	-0.004	0.018	-0.019	0.005	0.008	-0.003	-0.004
CRM fut	0.034	0.025	0.021	0.022	0.145	0.331	0.421	0.399	0.264	0.156	0.077	0.039

	Jan	Feb	Mar	Apr	May	Jun	Jul	Aug	Sep	Oct	Nov	Dec
ECH pre	0.052	0.036	0.028	0.036	0.176	0.309	0.414	0.434	0.297	0.229	0.108	0.065
Difference	-0.005	-0.004	-0.004	0.002	0.055	-0.001	0.002	-0.028	-0.008	-0.060	-0.013	-0.012
ECH int	0.047	0.031	0.024	0.038	0.231	0.309	0.416	0.406	0.289	0.170	0.094	0.053
ECH int	0.047	0.031	0.024	0.038	0.231	0.309	0.416	0.406	0.289	0.170	0.094	0.053
Difference	-0.005	-0.002	-0.002	-0.010	-0.044	0.015	-0.001	-0.014	-0.001	-0.014	-0.011	-0.008
ECH fut	0.042	0.030	0.022	0.028	0.186	0.324	0.415	0.392	0.288	0.155	0.084	0.045
IPS pre	0.048	0.030	0.022	0.028	0.166	0.295	0.419	0.449	0.288	0.202	0.101	0.058
Difference	-0.007	-0.002	-0.003	0.000	0.006	0.027	-0.006	-0.035	-0.010	-0.018	-0.022	-0.012
IPS int	0.041	0.027	0.019	0.028	0.172	0.322	0.413	0.414	0.278	0.184	0.078	0.046
IPS int	0.041	0.027	0.019	0.028	0.172	0.322	0.413	0.414	0.278	0.184	0.078	0.046
Difference	-0.008	-0.003	0.002	-0.007	-0.055	-0.040	0.024	-0.051	-0.014	-0.032	-0.008	-0.017
IPS fut	0.033	0.024	0.022	0.020	0.116	0.282	0.437	0.363	0.264	0.151	0.070	0.029

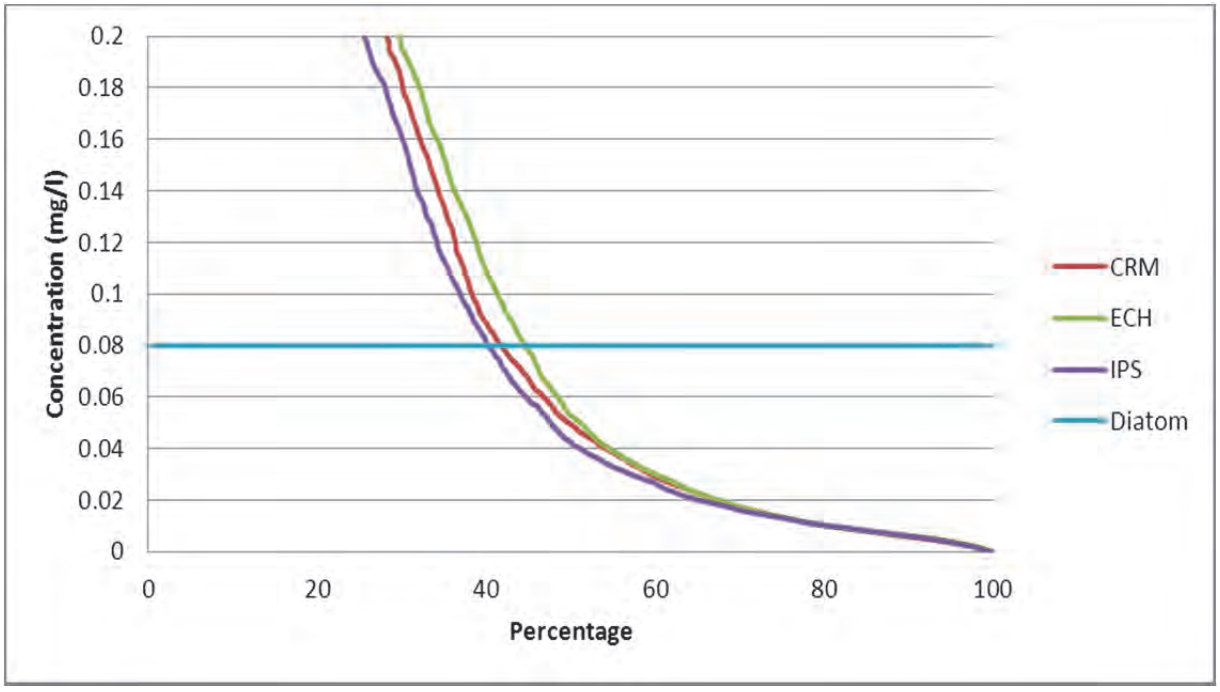

Figure 96: The distant future surface dissolved silicon concentration exceedance with respect to diatom growth for Berg River Dam

From the exceedance plot for surface dissolved silicon with regards the half-saturation constant (0.08 mg/l) for diatoms it was seen that this had decreased to between 40 and 45% depending on the climate model. This would imply that the concentration of surface dissolved silicon would decrease for future climate events and possible reduction in diatom

growth, but was great enough to allow the maximum growth of diatoms for at least 40% of the simulation period.

Dissolved oxygen

It was expected from the dissolved oxygen concentration that for the surface water it would decrease due to the increased temperature causing greater dissociation of oxygen to the atmosphere. This phenomenon was shown in Figure 97 with climate change events the concentration of dissolved oxygen in the surface water levels decreased. The figure also shows that the dissolved oxygen concentration was greatest during winter and spring, when the surface water was cooler and could hold more oxygen as showed by the mean surface dissolved oxygen concentrations in Table 35.

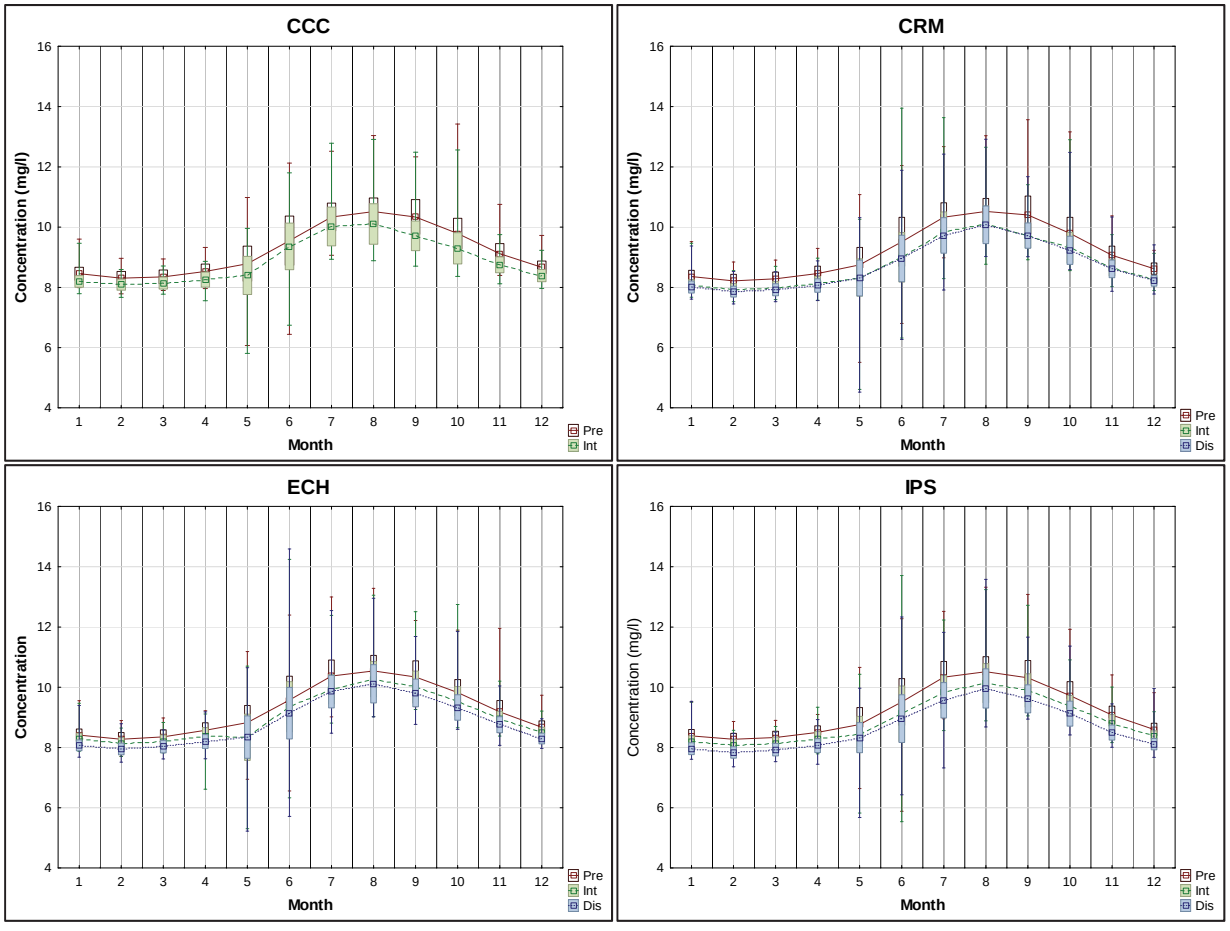

Figure 97: The climate change surface dissolved oxygen concentration for Berg River Dam (mg/l)

Table 35: The mean monthly surface dissolved oxygen concentration for Berg River Dam (mg/l) under projected climate change

	Jan	Feb	Mar	Apr	May	Jun	Jul	Aug	Sep	Oct	Nov	Dec
CCC pre	8.45	8.31	8.35	8.53	8.79	9.55	10.33	10.51	10.34	9.79	9.12	8.67
Difference	-0.25	-0.22	-0.20	-0.27	-0.39	-0.19	-0.31	-0.41	-0.63	-0.49	-0.37	-0.28
CCC int	8.20	8.09	8.15	8.26	8.40	9.36	10.02	10.10	9.71	9.30	8.75	8.39
CRM pre	8.36	8.22	8.28	8.46	8.75	9.51	10.33	10.52	10.40	9.79	9.06	8.62
Difference	-0.30	-0.28	-0.30	-0.33	-0.42	-0.51	-0.49	-0.42	-0.69	-0.47	-0.40	-0.37
CRM int	8.06	7.93	7.98	8.13	8.33	9.00	9.84	10.10	9.72	9.32	8.66	8.24
CRM int	8.06	7.93	7.98	8.13	8.33	9.00	9.84	10.10	9.72	9.32	8.66	8.24
Difference	-0.05	-0.08	-0.06	-0.06	-0.02	-0.04	-0.12	-0.02	0.00	-0.09	-0.05	-0.02
CRM fut	8.01	7.86	7.92	8.06	8.31	8.96	9.72	10.08	9.72	9.23	8.61	8.22
ECH pre	8.41	8.27	8.36	8.57	8.83	9.58	10.37	10.54	10.34	9.83	9.18	8.67
Difference	-0.13	-0.14	-0.15	-0.19	-0.49	-0.22	-0.44	-0.27	-0.34	-0.29	-0.24	-0.17
ECH int	8.29	8.14	8.21	8.38	8.34	9.35	9.93	10.27	10.00	9.54	8.94	8.50
ECH int	8.29	8.14	8.21	8.38	8.34	9.35	9.93	10.27	10.00	9.54	8.94	8.50
Difference	-0.21	-0.18	-0.18	-0.18	0.00	-0.21	-0.08	-0.16	-0.19	-0.21	-0.19	-0.21
ECH fut	8.07	7.95	8.03	8.20	8.34	9.14	9.86	10.11	9.81	9.33	8.76	8.30
IPS pre	8.39	8.27	8.33	8.50	8.76	9.51	10.34	10.51	10.31	9.72	9.08	8.60
Difference	-0.18	-0.19	-0.18	-0.21	-0.32	-0.39	-0.49	-0.38	-0.42	-0.34	-0.29	-0.22
IPS int	8.21	8.09	8.15	8.29	8.44	9.12	9.85	10.14	9.89	9.38	8.79	8.38
IPS int	8.21	8.09	8.15	8.29	8.44	9.12	9.85	10.14	9.89	9.38	8.79	8.38
Difference	-0.25	-0.25	-0.22	-0.23	-0.12	-0.16	-0.28	-0.17	-0.28	-0.25	-0.29	-0.27
IPS fut	7.96	7.84	7.93	8.06	8.33	8.96	9.57	9.96	9.62	9.12	8.50	8.11

From Table 35 it was seen that dissolve oxygen concentrations for the surface decreased with all climate models for future events. The distant future showed the greatest changes due to climate. The inter-variability between the models was not much and all showed a decrease with increased water temperature. The difference between present day and intermediate future is greater than between intermediate future and distant future showing the accelerated decreasing water quality for the distant future.

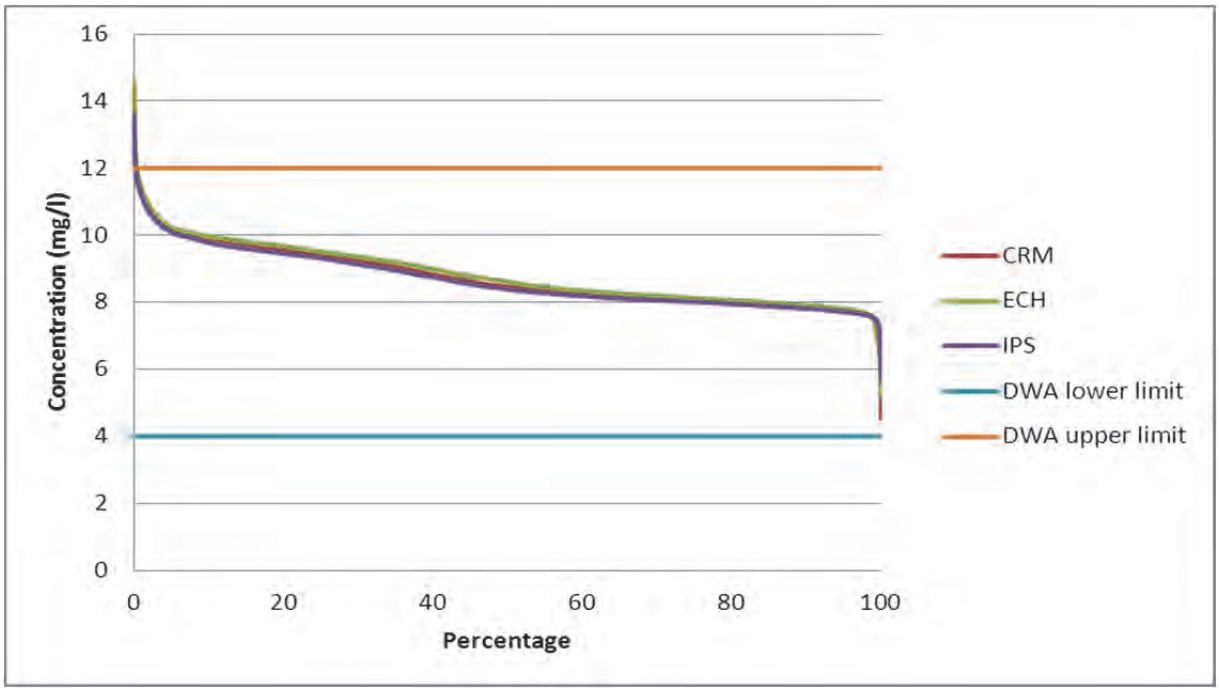

Figure 98: The projected distant future surface dissolved oxygen exceedance plot for Berg River Dam

From the plot in Figure 98 it was seen that the surface dissolved oxygen exceedance had not changed significantly from the present day and that the surface dissolved oxygen within TWQR limits set by DWA.

Total algae concentration

It was seen that with climate change the increased air temperatures would lead to increased surface water temperatures. To establish a link to this increased water temperature and algal blooms the total algae was plotted in Figure 99 for Berg River dam.

From Figure 99 it was seen that with climate change the mean monthly total algal concentration was relatively unchanged for the present day. What was noted is that the months of peak concentrations shifted one month earlier in the year, but this was not for all the climate models. This phenomenon could be seen as a season shift in surface total algal concentrations. This was attributed directly to the increased air temperature driving the growth of the algae.

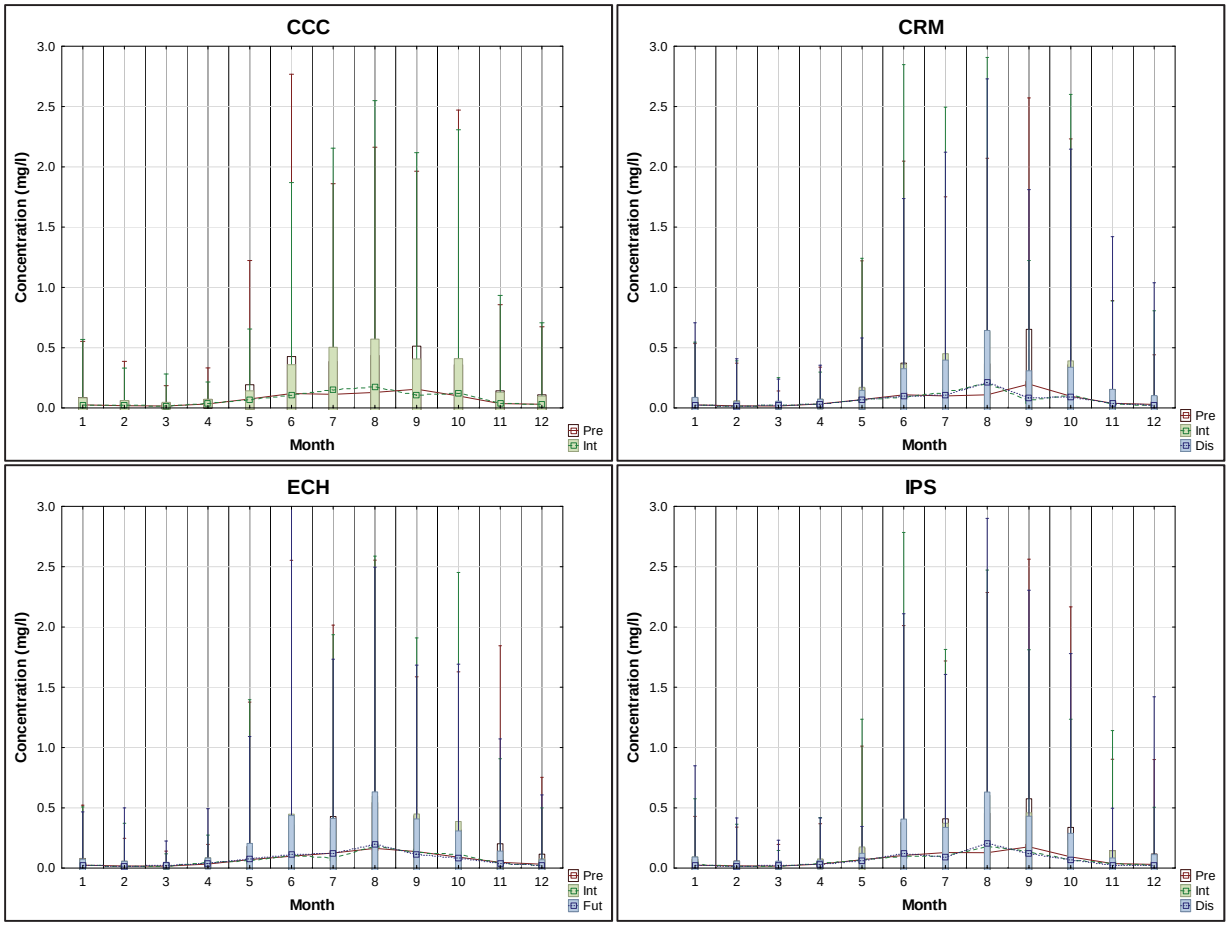

Figure 99: The projected climate change surface total algae concentration for Berg River Dam (mg/l)

It was seen that the mean monthly surface total algae concentration was greatest for winter and that for a climate change scenario the concentration was relatively unchanged in going from present day to intermediate future to distant future.

Table 36: The mean monthly surface total algae concentration for Berg River Dam (mg/l) under projected climate change

	Jan	Feb	Mar	Apr	May	Jun	Jul	Aug	Sep	Oct	Nov	Dec
CCC pre	0.026	0.020	0.016	0.034	0.074	0.120	0.113	0.129	0.157	0.100	0.036	0.031
Difference	-0.001	0.001	0.002	0.004	-0.010	-0.016	0.035	0.048	-0.050	0.019	0.001	-0.002
CCC int	0.025	0.020	0.019	0.039	0.065	0.104	0.149	0.177	0.107	0.120	0.037	0.029
CRM pre	0.025	0.018	0.016	0.034	0.070	0.109	0.100	0.110	0.199	0.098	0.039	0.030
Difference	-0.003	0.000	0.005	0.000	0.001	-0.018	0.028	0.099	-0.136	0.006	-0.005	-0.006
CRM int	0.023	0.018	0.021	0.033	0.071	0.091	0.128	0.209	0.063	0.104	0.034	0.024
CRM int	0.023	0.018	0.021	0.033	0.071	0.091	0.128	0.209	0.063	0.104	0.034	0.024
Difference	0.001	-0.003	0.002	-0.001	-0.004	0.007	-0.021	0.001	0.020	-0.014	0.002	0.002

	Jan	Feb	Mar	Apr	May	Jun	Jul	Aug	Sep	Oct	Nov	Dec
CRM fut	0.023	0.015	0.023	0.032	0.067	0.098	0.108	0.210	0.083	0.090	0.036	0.026
ECH pre	0.024	0.017	0.017	0.034	0.072	0.099	0.125	0.164	0.138	0.091	0.048	0.033
Difference	0.000	0.001	-0.001	0.009	-0.014	0.009	-0.039	0.018	-0.009	0.019	-0.011	-0.009
ECH int	0.024	0.018	0.016	0.044	0.057	0.108	0.086	0.182	0.129	0.110	0.036	0.023
ECH int	0.024	0.018	0.016	0.044	0.057	0.108	0.086	0.182	0.129	0.110	0.036	0.023
Difference	-0.001	-0.001	0.004	-0.006	0.016	0.003	0.038	0.018	-0.012	-0.027	0.001	-0.004
ECH fut	0.023	0.017	0.020	0.038	0.073	0.111	0.124	0.201	0.117	0.083	0.038	0.020
IPS pre	0.024	0.020	0.017	0.034	0.070	0.105	0.129	0.129	0.177	0.094	0.038	0.031
Difference	0.003	-0.001	0.000	0.001	0.000	-0.008	-0.027	0.056	-0.038	-0.029	-0.002	-0.005
IPS int	0.028	0.019	0.017	0.036	0.070	0.097	0.102	0.185	0.139	0.065	0.035	0.026
IPS int	0.028	0.019	0.017	0.036	0.070	0.097	0.102	0.185	0.139	0.065	0.035	0.026
Difference	-0.004	-0.002	0.007	-0.006	-0.010	0.028	-0.009	0.022	-0.018	0.006	-0.012	-0.002
IPS fut	0.024	0.017	0.024	0.030	0.060	0.125	0.093	0.207	0.121	0.071	0.024	0.023

The above table shows the percentage mean monthly increase in total algae concentration in going from the present day to the distant future. It was clear that all the climate models predicted dissimilar scenarios. The total surface algal concentration had changes from peaks in September to August signalling a seasonal shift. The maximum concentrations remained relatively unchanged.

Diatom concentration

Since only diatoms thrived in Berg River dam, it was assumed that diatom concentration represented the total algal concentration. The mean annual increase in algal growth in going from the present day to the distant future was to remain relatively unchanged but what was required was to investigate if any species thrived at the expense of another. It was clear from Figure 100 that the surface concentration of diatoms that it does shift its peak concentration one month earlier for two climate models in the distant future.

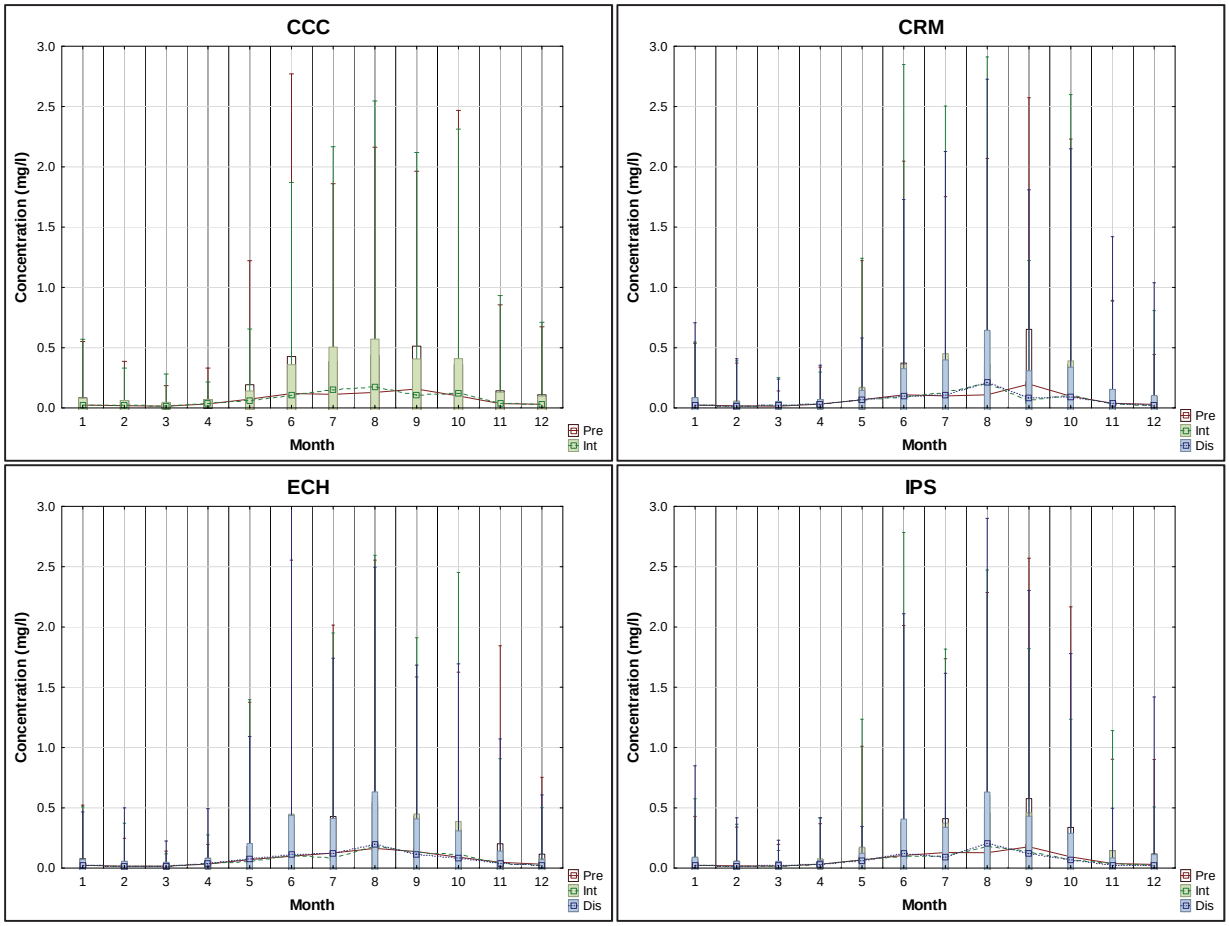

Figure 100: The projected climate change surface diatom concentration for Berg River Dam (mg/l)

From Table 37 it was seen that the monthly mean surface diatom concentration was a decreasing trend for most months except where the perceived season shift was observed.

Table 37: The mean monthly surface diatom concentration for Berg River Dam (mg/l) under projected climate change

	Jan	Feb	Mar	Apr	May	Jun	Jul	Aug	Sep	Oct	Nov	Dec
CCC pre	0.025	0.019	0.016	0.033	0.074	0.120	0.114	0.129	0.157	0.100	0.036	0.031
Difference	-0.001	0.001	0.002	0.003	-0.010	-0.016	0.035	0.048	-0.050	0.019	0.001	-0.002
CCC int	0.024	0.020	0.018	0.037	0.064	0.105	0.149	0.177	0.107	0.120	0.037	0.029
CRM pre	0.024	0.018	0.016	0.032	0.069	0.109	0.100	0.110	0.199	0.098	0.039	0.030
Difference	-0.003	-0.001	0.004	-0.002	0.002	-0.018	0.028	0.100	-0.136	0.006	-0.005	-0.006
CRM int	0.022	0.018	0.020	0.031	0.071	0.091	0.129	0.209	0.063	0.104	0.034	0.024
CRM int	0.022	0.018	0.020	0.031	0.071	0.091	0.129	0.209	0.063	0.104	0.034	0.024
Difference	0.001	-0.003	0.002	-0.001	-0.004	0.007	-0.021	0.001	0.020	-0.013	0.002	0.002
CRM fut	0.022	0.014	0.021	0.030	0.066	0.098	0.108	0.210	0.083	0.090	0.036	0.026
ECH pre	0.024	0.017	0.016	0.033	0.071	0.099	0.125	0.164	0.138	0.091	0.048	0.033
Difference	0.000	0.001	-0.001	0.009	-0.015	0.009	-0.039	0.018	-0.009	0.019	-0.011	-0.009
ECH int	0.023	0.018	0.016	0.042	0.056	0.108	0.086	0.183	0.129	0.110	0.036	0.023
ECH int	0.023	0.018	0.016	0.042	0.056	0.108	0.086	0.183	0.129	0.110	0.036	0.023
Difference	-0.001	-0.001	0.004	-0.007	0.017	0.003	0.038	0.018	-0.012	-0.027	0.001	-0.004
ECH fut	0.022	0.017	0.019	0.035	0.073	0.111	0.124	0.201	0.117	0.083	0.038	0.020
IPS pre	0.023	0.019	0.016	0.033	0.069	0.105	0.129	0.129	0.177	0.094	0.038	0.031
Difference	0.003	-0.001	0.000	0.001	0.000	-0.008	-0.027	0.056	-0.038	-0.029	-0.002	-0.005
IPS int	0.027	0.018	0.016	0.034	0.069	0.097	0.102	0.185	0.139	0.065	0.035	0.026
IPS int	0.027	0.018	0.016	0.034	0.069	0.097	0.102	0.185	0.139	0.065	0.035	0.026
Difference	-0.004	-0.002	0.006	-0.007	-0.010	0.028	-0.009	0.022	-0.018	0.006	-0.012	-0.002
IPS fut	0.023	0.016	0.022	0.028	0.059	0.125	0.093	0.207	0.121	0.071	0.024	0.023

The surface growth of diatoms was significant as for Berg River dam green algae and cyanobacteria did not thrive. Diatoms were light limited and have low light saturation (61.2 W/m^2 for maximum photosynthetic rate) thus thereby limited to mainly surface growth.

Green algae concentration

As with the present day, the green algal species present in Berg River dam died in the first year and never established itself in the dam. This would be decisive proof that green algae does not pose a threat to the dam if the inflow of nutrients remain the same for future climate change events.

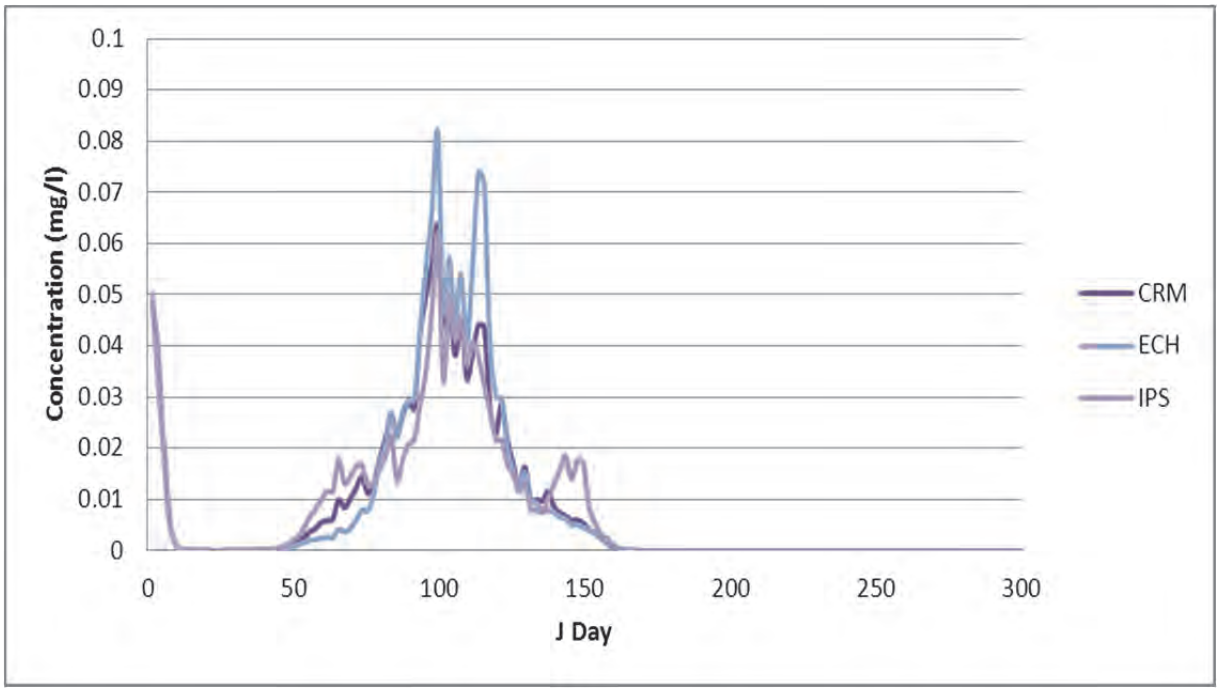

Figure 101: The projected distant future surface green algae concentration for Berg River Dam (mg/l)

Cyanobacteria concentration

The final group of algae examined for the effect of climate change on surface concentrations was cyanobacteria. The surface concentrations are shown in Figure 102 and it was similar to that of the present day scenario in that the cyanobacteria did not establish itself in the dam and died out like the green algae. It was clear that cyanobacteria posed no threat to Berg River dam in the distant future for a climate change scenario.

Thus, the dominant algal group in Berg River Dam was diatoms.

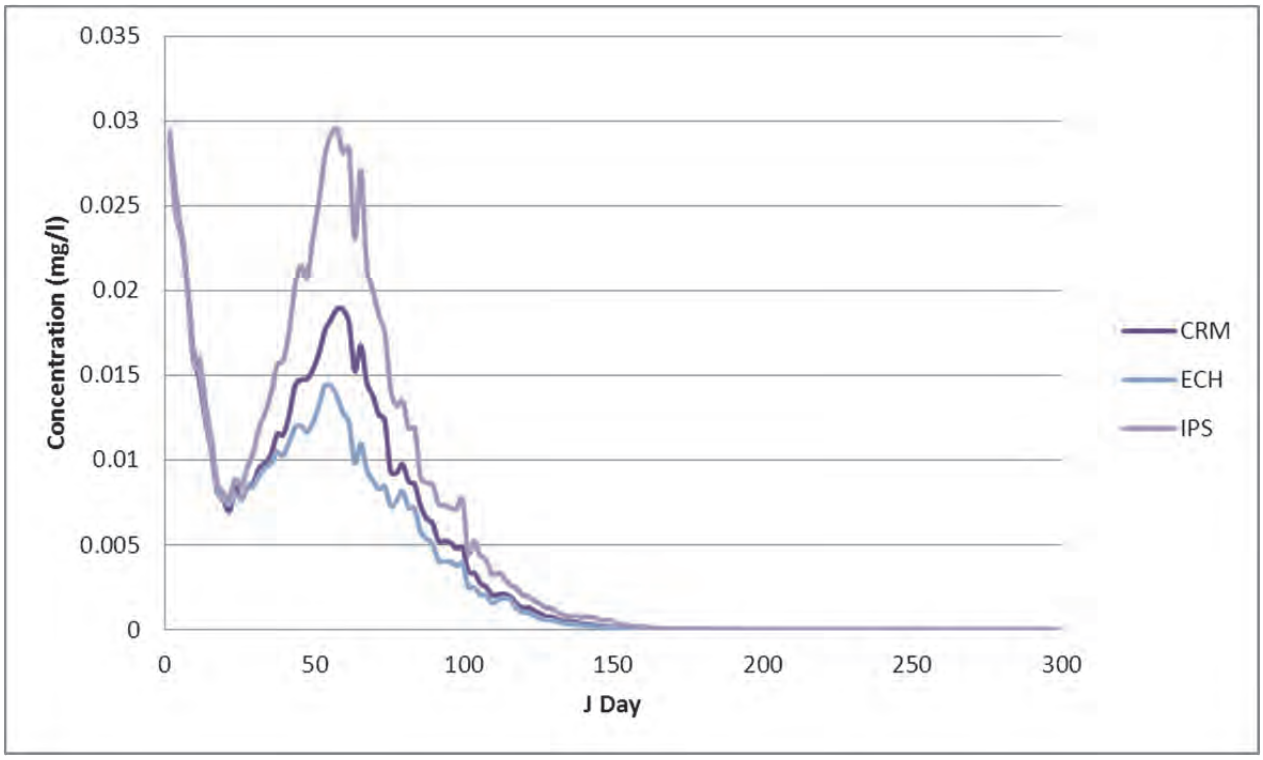

Figure 102: The distant future projected surface cyanobacteria concentration for Berg River Dam (mg/l)

Zooplankton concentration

The zooplankton modelled in Berg River dam would only on diatoms, green algae and other zooplankton present and if their surface concentration increased, it was expected that the surface concentrations of zooplankton should increase. For the purpose of this study, the predation of cyanobacteria by zooplankton was set to zero, i.e. zooplankton did not feed on cyanobacteria. The surface zooplankton concentration is shown in Figure 103 where all future climate models predicted a slight decrease in concentration of surface zooplankton with maximum concentrations in spring, mimicking diatom growth.

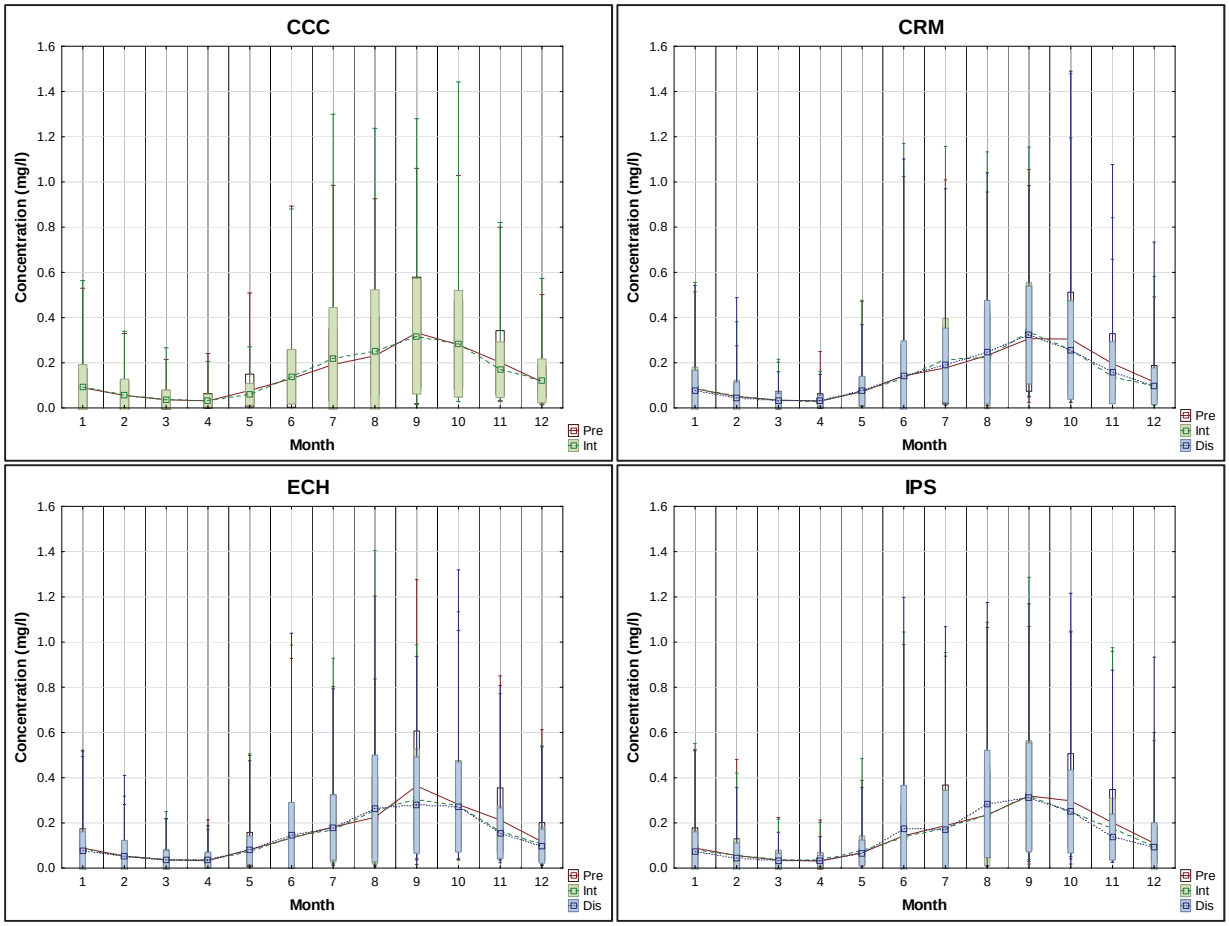

Figure 103: The projected climate change surface zooplankton concentration for Berg River Dam (mg/l)

This emulation of diatoms by the zooplankton is shown numerically in Table 38.

Table 38: The mean monthly surface zooplankton concentration for Berg River Dam (mg/l) under projected climate change

	Jan	Feb	Mar	Apr	May	Jun	Jul	Aug	Sep	Oct	Nov	Dec
CCC pre	0.090	0.056	0.037	0.031	0.077	0.130	0.192	0.231	0.333	0.280	0.201	0.116
Difference	0.002	0.003	0.001	0.001	-0.017	0.008	0.027	0.019	-0.015	0.004	-0.031	0.004
CCC int	0.092	0.058	0.037	0.033	0.061	0.139	0.219	0.250	0.317	0.284	0.170	0.120
CRM pre	0.085	0.051	0.035	0.031	0.072	0.142	0.177	0.232	0.307	0.305	0.196	0.115
Difference	0.001	0.003	-0.001	-0.001	0.001	-0.007	0.038	-0.008	0.030	-0.045	-0.058	-0.016
CRM int	0.086	0.053	0.034	0.030	0.074	0.135	0.215	0.225	0.337	0.260	0.138	0.099
CRM int	0.086	0.053	0.034	0.030	0.074	0.135	0.215	0.225	0.337	0.260	0.138	0.099
Difference	-0.009	-0.007	-0.003	0.002	0.002	0.006	-0.026	0.022	-0.014	-0.003	0.018	-0.003
CRM fut	0.077	0.046	0.031	0.032	0.075	0.141	0.189	0.247	0.323	0.256	0.156	0.096

	Jan	Feb	Mar	Apr	May	Jun	Jul	Aug	Sep	Oct	Nov	Dec
ECH pre	0.089	0.054	0.037	0.033	0.082	0.133	0.182	0.225	0.363	0.281	0.213	0.117
Difference	-0.005	-0.001	0.000	0.005	-0.007	0.004	-0.012	0.030	-0.059	-0.006	-0.049	-0.011
ECH int	0.084	0.053	0.037	0.037	0.075	0.138	0.170	0.255	0.304	0.276	0.164	0.107
ECH int	0.084	0.053	0.037	0.037	0.075	0.138	0.170	0.255	0.304	0.276	0.164	0.107
Difference	-0.008	0.000	-0.001	-0.002	0.005	0.007	0.010	0.009	-0.026	-0.006	-0.009	-0.009
ECH fut	0.076	0.052	0.036	0.035	0.079	0.145	0.180	0.264	0.279	0.270	0.154	0.098
IPS pre	0.089	0.056	0.036	0.032	0.068	0.144	0.188	0.235	0.320	0.297	0.202	0.110
Difference	-0.008	0.000	0.001	0.003	0.010	-0.005	-0.011	-0.002	0.000	-0.051	-0.029	-0.014
IPS int	0.080	0.056	0.037	0.035	0.078	0.138	0.178	0.233	0.320	0.246	0.173	0.097
IPS int	0.080	0.056	0.037	0.035	0.078	0.138	0.178	0.233	0.320	0.246	0.173	0.097
Difference	-0.007	-0.010	-0.005	-0.003	-0.011	0.037	-0.006	0.051	-0.007	0.005	-0.035	-0.001
IPS fut	0.073	0.046	0.032	0.032	0.067	0.176	0.172	0.284	0.313	0.251	0.138	0.095

Eutrophication level

The influence of climate change was seen to have implications for Berg River dam in the form of a seasonal shift in diatom concentration and this had a direct effect on the surface TRIX levels. From Figure 104 and it was seen that for climate change, the mean monthly TRIX levels remained relatively unchanged with slight decreases in certain seasons following a pattern similar to that of surface nitrate-nitrite.

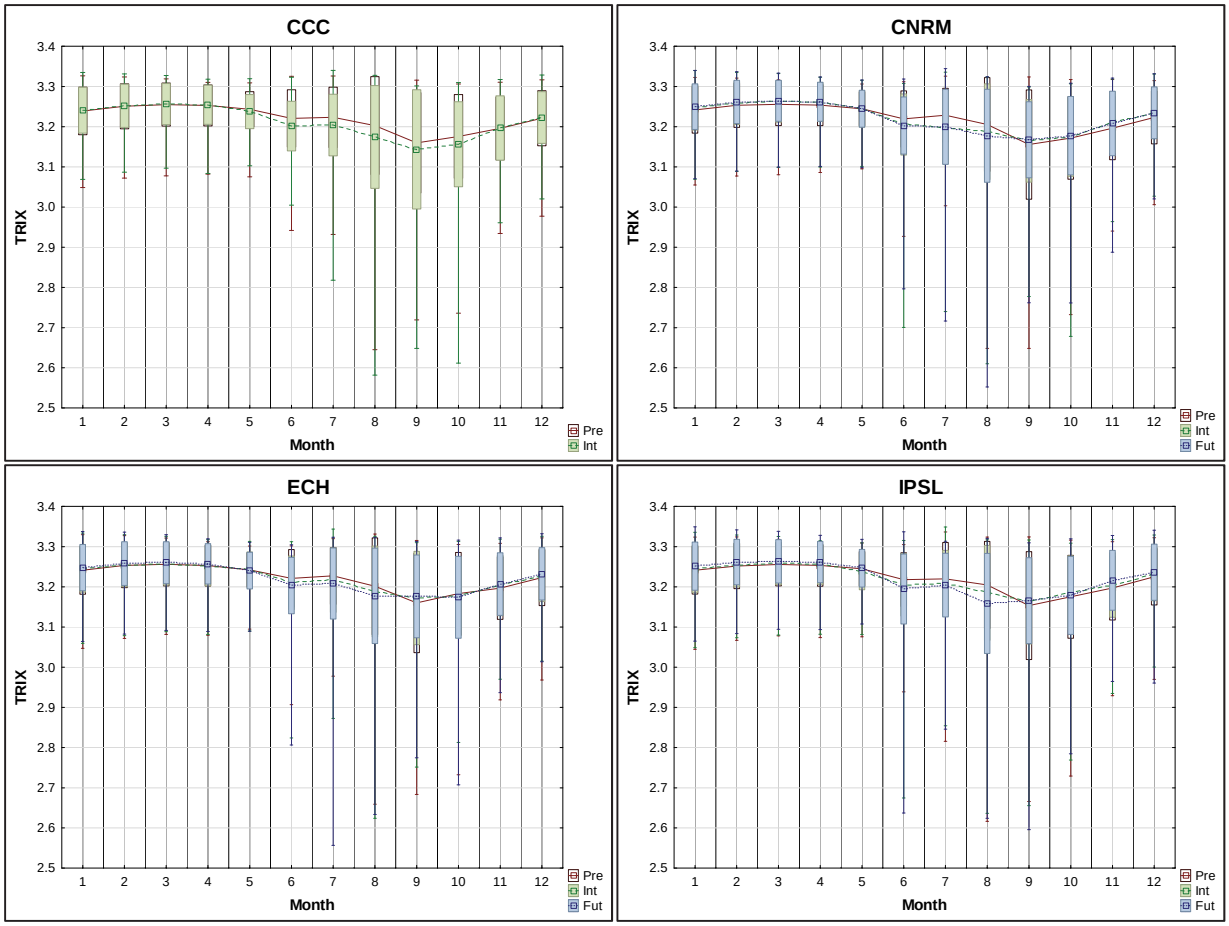

Figure 104: The projected climate change effect on the TRIX level for Berg River dam

The inter-variability between climate models was similar from these findings. The TRIX levels showed decreases in winter and spring with increases in summer and autumn for all climate models.

Table 39: The mean monthly surface TRIX level for Berg River Dam under projected climate change

	Jan	Feb	Mar	Apr	May	Jun	Jul	Aug	Sep	Oct	Nov	Dec
CCC pre	3.24	3.25	3.26	3.25	3.24	3.22	3.22	3.20	3.16	3.18	3.20	3.22
Difference	0.00	0.00	0.00	0.00	-0.01	-0.02	-0.02	-0.03	-0.02	-0.02	0.00	0.00
CCC int	3.24	3.25	3.26	3.25	3.24	3.20	3.20	3.17	3.14	3.16	3.20	3.22
CRM pre	3.24	3.25	3.26	3.25	3.24	3.22	3.23	3.21	3.16	3.17	3.20	3.22
Difference	0.01	0.01	0.01	0.01	0.00	-0.01	-0.03	-0.02	0.01	0.00	0.01	0.01
CRM int	3.25	3.26	3.26	3.26	3.24	3.21	3.20	3.19	3.16	3.17	3.21	3.23
CRM int	3.25	3.26	3.26	3.26	3.24	3.21	3.20	3.19	3.16	3.17	3.21	3.23
Difference	0.00	0.00	0.00	0.00	0.00	0.00	0.00	-0.01	0.00	0.00	0.00	0.00
CRM fut	3.25	3.26	3.26	3.26	3.24	3.20	3.20	3.18	3.17	3.18	3.21	3.23

	Jan	Feb	Mar	Apr	May	Jun	Jul	Aug	Sep	Oct	Nov	Dec
ECH pre	3.24	3.25	3.26	3.25	3.24	3.22	3.23	3.20	3.16	3.18	3.20	3.22
Difference	0.00	0.00	0.00	0.00	0.00	-0.01	-0.01	-0.01	0.01	-0.01	0.01	0.01
ECH int	3.24	3.25	3.26	3.25	3.24	3.21	3.22	3.19	3.17	3.18	3.20	3.23
ECH int	3.24	3.25	3.26	3.25	3.24	3.21	3.22	3.19	3.17	3.18	3.20	3.23
Difference	0.00	0.00	0.00	0.00	0.00	-0.01	-0.01	-0.01	0.00	0.00	0.00	0.00
ECH fut	3.25	3.26	3.26	3.26	3.24	3.20	3.21	3.18	3.18	3.17	3.21	3.23
IPS pre	3.24	3.25	3.26	3.25	3.25	3.22	3.22	3.20	3.15	3.18	3.20	3.22
Difference	0.00	0.00	0.00	0.00	-0.01	-0.01	-0.01	-0.02	0.01	0.01	0.01	0.01
IPS int	3.24	3.25	3.26	3.26	3.24	3.21	3.21	3.18	3.16	3.19	3.20	3.23
IPS int	3.24	3.25	3.26	3.26	3.24	3.21	3.21	3.18	3.16	3.19	3.20	3.23
Difference	0.01	0.01	0.01	0.01	0.01	-0.01	0.00	-0.03	0.00	-0.01	0.01	0.00
IPS fut	3.25	3.26	3.26	3.26	3.25	3.19	3.20	3.16	3.17	3.18	3.22	3.24

Thus, water quality of BRD is not adversely affected with future climate change scenarios when utilising the TRIX formula.

Limitations of this Study

All water quality studies have inherent limitations especially where algal growth was to be simulated as algae adapts and modifies its growth to its environment and conditions. Some species are known to be motile which was virtually impossible to model accurately. This studies limitation was subdivided into:

- Model and data limitations
- Data limitations

CE-QUAL-W2 model limitations

The model had successfully been applied to Berg River in the past and the limitations were specifically on the model and not its application to Berg River. From the aspect of hydrodynamics and transport, the models governing equations are laterally and layer averaged. Lateral averaging assumes lateral variations in velocities, temperatures, and constituents are negligible. This assumption may be inappropriate for large water-bodies exhibiting significant lateral variations in water quality. Eddy coefficients are used to model

turbulence. Currently, the user must decide among several vertical turbulence schemes the one that was most appropriate for the type of water-body being simulated. The equations are written in the conservative form using the Boussinesq and hydrostatic approximations. Since vertical momentum was not included, the model may give inaccurate results where there was significant vertical acceleration (Cole, 2008)

Water quality interactions are, by necessity, simplified descriptions of an aquatic ecosystem that was extremely complex. This was especially so for modelling algae as they adapt to varying environmental conditions such as low light and nutrient sparse zones. Some species are capable of independent movement throughout the water column, something not modelled by CE-QUAL-W2. This could explain difference between measured and modelled values.

The model includes a user-specified sediment oxygen demand that was not coupled to the water column. SOD only varies according to temperature. The first order model was tied to the water column settling of organic matter. The model does not have a sediment compartment that models kinetics in the sediment and at the sediment-water interface, i.e., a complete sediment diagenesis model. This places a limitation on long-term predictive capabilities of the water quality portion of the model (Cole, 2008). It was hope that this limitation if carried forward by each of the modelling periods studies and that what was presented was still the different in state of water quality in proceeding from the present day to the distant future. Future releases of CE-QUAL-W2 will include additional capabilities that will remedy this limitation (Cole, 2008) and version 3.7 has just been released (2012).

Climate change data limitations

The availability of input data was not a limitation of the model itself. However, it was most often the limiting factor in the application or misapplication of the model. The GCMs employed in this study was of such coarse resolution (about 300km) that they cannot be used directly for the meteorological data. The GCMs are firstly downscaled statistically to regional level (RCMs). The advantage of this technique was that it was easily applied. One disadvantage of the statistical method of downscaling was that it relies on the availability of sufficient high-resolution data over long periods so that statistical relationships may be established. It was not possible to be sure how valid the statistical relations are for a climate-changed situation (Houghton, 2007; Quintana-Seguí *et al.*, 2010).

In the absence of another type of downscaling such as dynamic downscaling, it was not possible to determine the accuracy of the downscaled data or compare it.

Wind-speed and direction as supplied by CSAG (UCT) was an average value for the entire country and was thus a limitation. CE-QUAL-W2 requires wind-speed and direction as part of its meteorological data input to predict water quality. In the absence of this, wind-speed and direction was replicated from past data. For 1971 the recorded wind-speed and direction from 1 January 1971 to 31 December 1971 was repeated for the 20 years of all the simulation periods including the intermediate and future events, in the absence of any downscaled data.

Inflow and withdrawal limitations

The limitations of the inflow and withdrawals were highlighted previously and it had been assumed that with climate change scenarios that the inflows, releases and withdrawals would remain unchanged, thereby simulating the same operating conditions in the future.

Algal growth rates

For the study it was imperative that the growth of the three groups of algae namely diatoms, greens and cyanobacteria be modelled as accurately as possible to show the changes with climate change. The more important parameters were discussed in the parameterisation section and summarised in Table 5. To predict the growth of algae these parameters have to be as accurate as possible for the species of algae present in the water-body under study. Finding some of these parameters proved difficult and futile in some instances and default values were used.

General

For each run, the initial conditions were the same as the present day initial conditions. This allowed for a direct comparison of present day to intermediate future and distant future. In essence, for each simulation period it was the same original dam being subjected to climate change. What was absent was climate date from 1971 to 2100 so that the dam may be modelled for the entire period. This mean that when the time of simulation approaches 2045 the model has already run for over 50 years and the in-situ conditions are that of 2045. Currently the intermediate future and distant future initial conditions are that of the present day.

Discussion of results for Berg River dam

The object of this study was to find any links between predicted climate changes on eutrophication of surface waters. It was postulated that with climate change from the present day to intermediate future and into the distant future that the air temperature would increase by between 2 and 4.5^{o}C for southern Africa and this increase would heat the surface waters sufficiently to amplify the growth of algae within such waters. It was also postulated that the three groups of algae (namely diatoms, green and cyanobacteria) that are present, would experience varying rates of growth because of the increased water temperature with a preference for warmer conditions. This would be due to the temperature growth multipliers, which stipulate algal growth for different water temperatures. It was possible that seasonal shifts of the bloom season would become apparent with climate change. It was postulated that cyanobacteria would be the algal group that benefits the most from the increased water temperature and all other factors remaining constant, thereby allowing for the unabated growth of cyanobacteria and a greater frequency of harmful algal blooms.

Water temperature, pH, available light, turbidity, suspended solids (TSS), dissolved solids (TDS), nitrogen, phosphorous, salinity and trace elements influence water quality and algal growth. Water quality and algal growth was dependent on several variables for its lifecycle, such as conducive environmental conditions and nutrients, which for the purpose of this study may be categorised as:

- Water temperature and solar radiation;
- The quantity of dissolved oxygen in the water-body;
- Availability of nitrogen within the water-body;
- Availability of phosphorous within the water-body; and

The present day study was conducted by utilising the water quality model CE-QUAL-W2 and establishing baseline water quality conditions for all the relevant factors that affect algal growth in the dam. The air temperature over the dam site was the classical southern hemisphere climate with summer being roughly December to March and winter June to August. The inflow and withdrawal quantity and quality as well as wind-speed and direction was constrained to be the same for the duration of each the simulation periods, namely present day, intermediate future and distant future thereby allowing for more controlled comparison as only the effect of increased temperature on the dam was investigated.

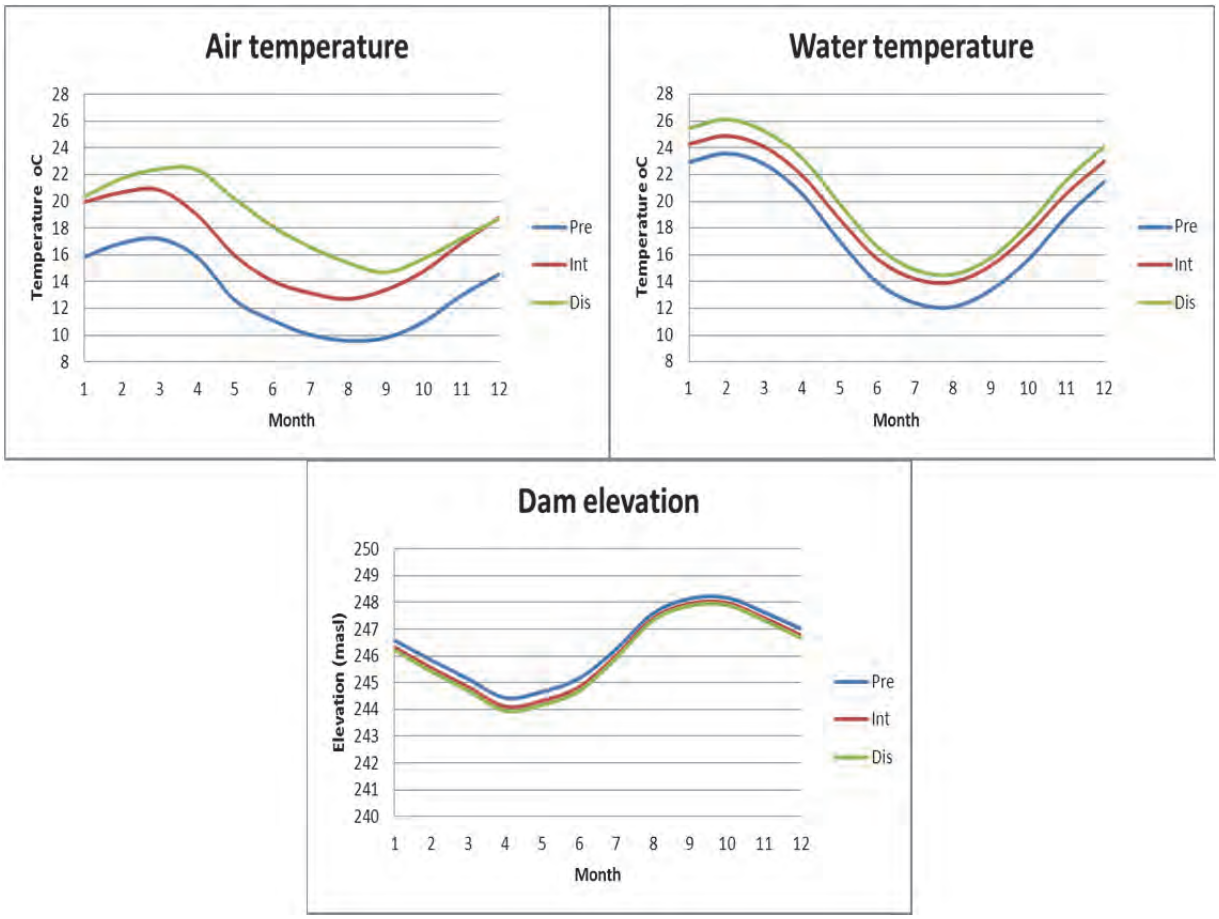

Figure 105: The projected mean monthly air temperature and subsequent effect on Berg River Dam

From Figure 105 all of the future climate models showed varying ranges of monthly air temperature increases, which drive an increase in surface water temperatures, which then affected the algal growth. The change in air temperature occurred as a seasonal shift producing a later summer, an earlier winter season and increasing the winter air temperature such that the difference between and summer air temperatures was less It was thought that this would enhance algal growth especially the diatom growth in winter as well as start a shift towards earlier annual algal blooms. The variability between scenarios is most prominent for the intermediate future climate models and in progressing to the distant future, the changes were not so pronounced. This was a consequence of the anthropogenic assumptions used to generate the GCM. It was concluded that air temperature was the major driver for surface water temperatures and solar radiation was the diurnal driver.

The intermediate future surface water temperature changes from present day were the greatest and the distant future scenario showed less difference from the intermediate future temperatures. The mean surface water temperature of Berg River dam was notably higher than the mean air temperature. This was attributed to the high specific heat capacity of water

that allowed it to store heat and not lose it as fast. From Figure 56 shows that the maximum air temperatures and the statistical standard deviation from the mean were higher than the mean surface water temperatures for the dam. Thus, it was plausible that the mean surface water temperatures were more than the mean air temperatures for Berg River dam.

Climate change thus affected the surface waters by heating the water and subsequently increased the evaporation rate of the water. This heating should have the effect of enhancing algal growth as well as lowering the surface water level if the dam was to be operated at the present day levels. Figure 105 shows that the surface water elevations drop for the intermediate future and the subsequent distant future changes are less pronounced. Thus, the capacity Berg River dam was not adversely affected by future climate change scenarios.

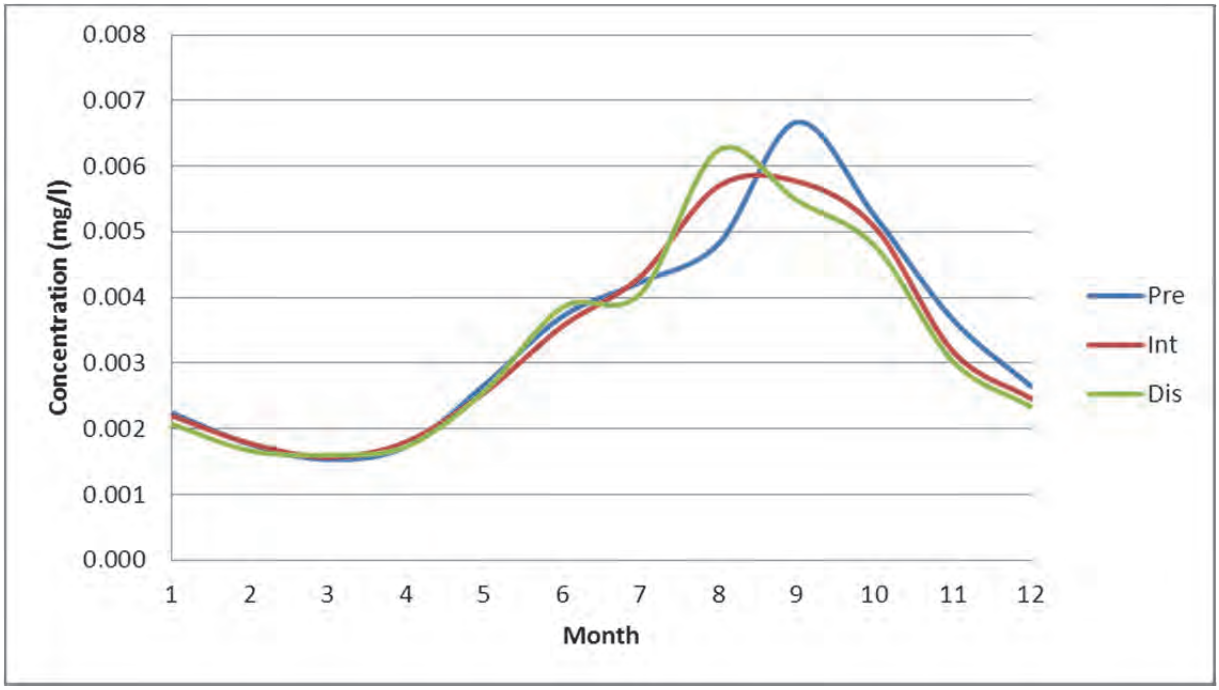

Figure 106: The projected mean monthly surface phosphorous concentration for Berg River Dam (mg/l)

Once climate change has heated the surface waters of the dam and lowered its surface level a concentration increase for the constituents in the dam was expected. This did not occur, as the surface water elevation did not decrease as much as was expected. Figure 106 shows the peak surface phosphates decreased for future events and an earlier season shift resulted. With no changes in inflow nutrient concentration, the explanation for this was an increase in algal growth that used phosphates as nutrients. Together with the warmer water and a greater supply of nutrients the total algal growth was expected to increased annually

but especially during autumn, signalling a seasonal shift toward an earlier annual increased concentration of total algae as well as compounding the annual load in the dam.

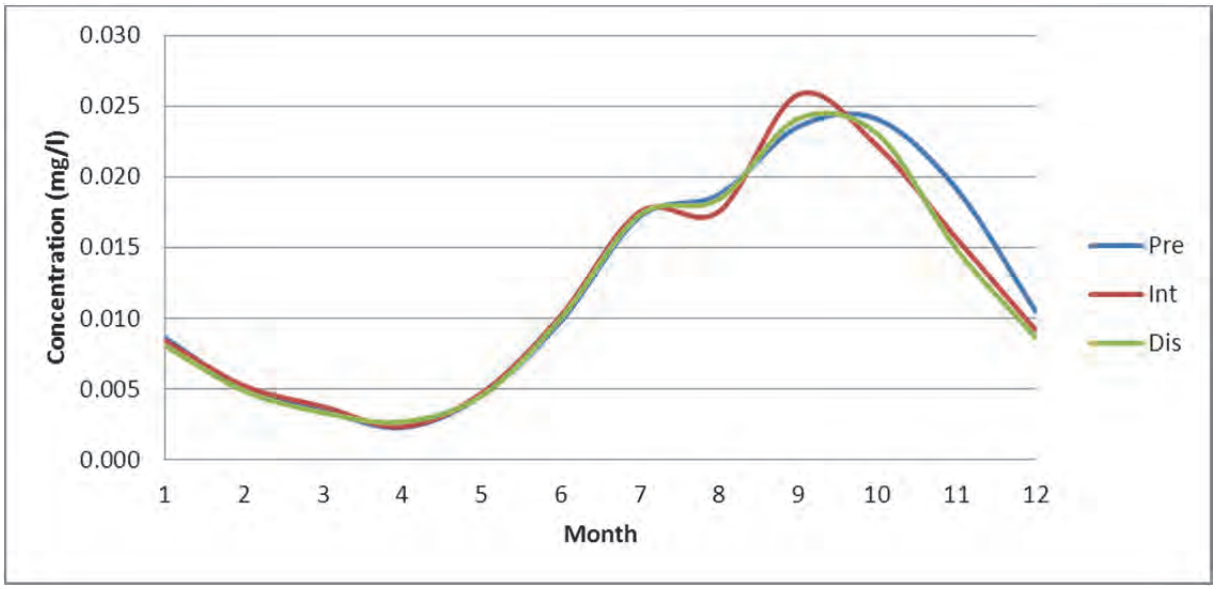

Figure 107: The projected mean monthly surface ammonium concentration for Berg River Dam (mg/l)

The surface ammonium was used by the algae during photosynthesis so it was expected that for an increase in algal concentrations that the ammonium concentrations would decrease. Figure 107 shows that this marginally happened for the intermediate and distant futures. This decrease along with the increase in phosphorous should not limit algal growth, as the algae were not nitrogen limited.

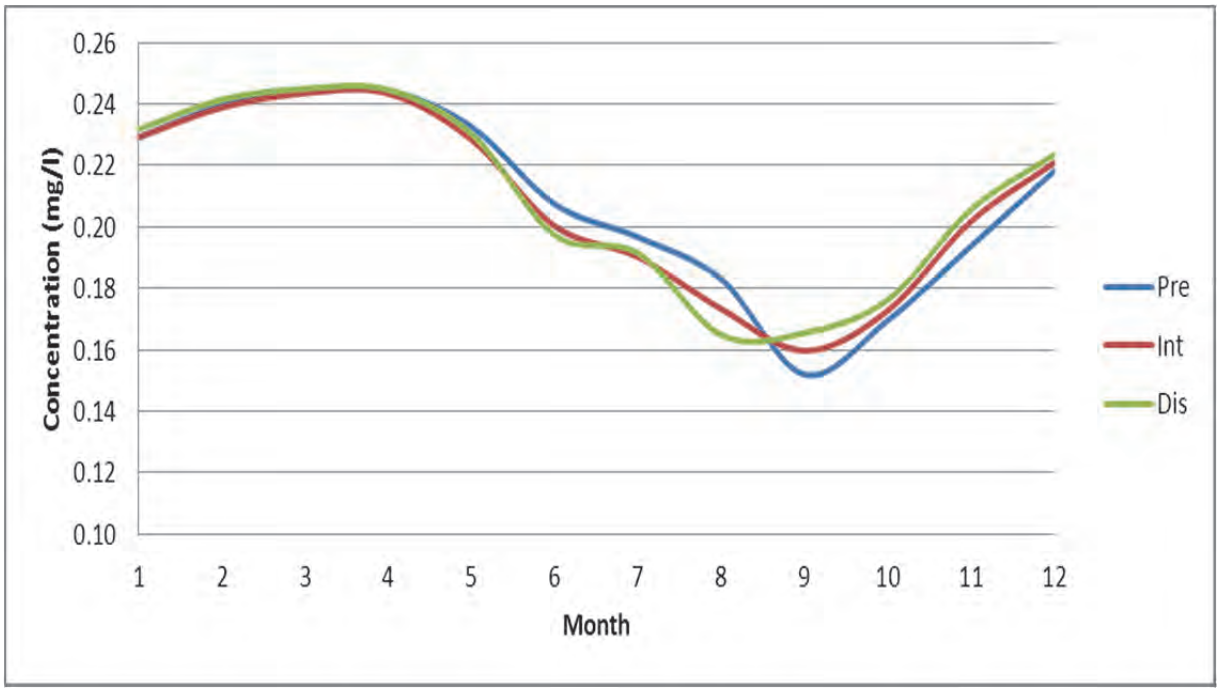

Figure 108: The projected mean monthly surface Nitrate-nitrite concentration for Berg River Dam (mg/l)

Nitrate-nitrites are an intermediate product as well as a source of nitrogen during photosynthesis. From Figure 108 the effect of climate change on nitrate-nitrites resulted in a slight decrease in the months that surface ammonium decreased as its main source was from the nitrification of ammonium. It was expected that for an increase in temperature and ammonium that the nitrification reaction would respond in an Arrhenius manner and produce more nitrate-nitrite but this was not so.

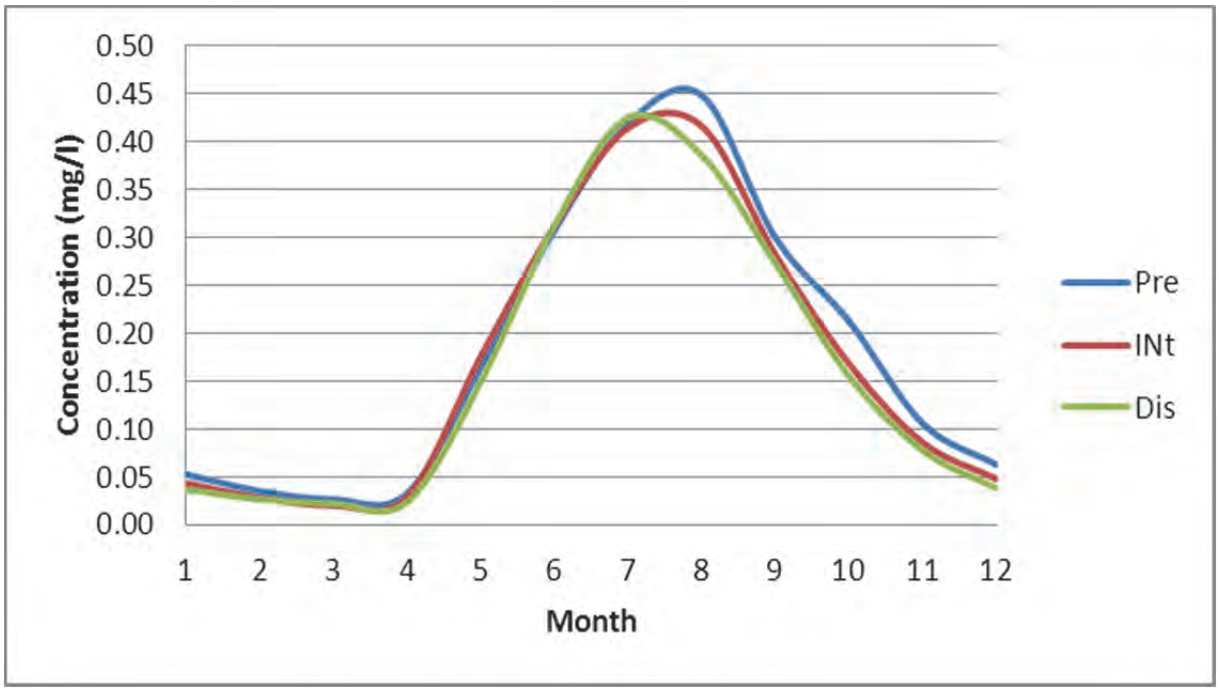

Figure 109: The projected mean monthly surface dissolved silicon concentration for Berg River Dam (mg/l)

Dissolved silicon was exclusively used by diatoms during photosynthesis for the Berg River dam system. From Figure 109 the concentration of dissolved silicon showed slight decreases during winter until summer annually, for future climate change events. The concentration of dissolved silicon was high enough that it never limited diatom growth. This would allow for diatom growth throughout the year.

Thus, the effect of warmer water due to climate change, favours the growth of diatoms throughout the year in the distant future, with the possibility of a seasonal shift.

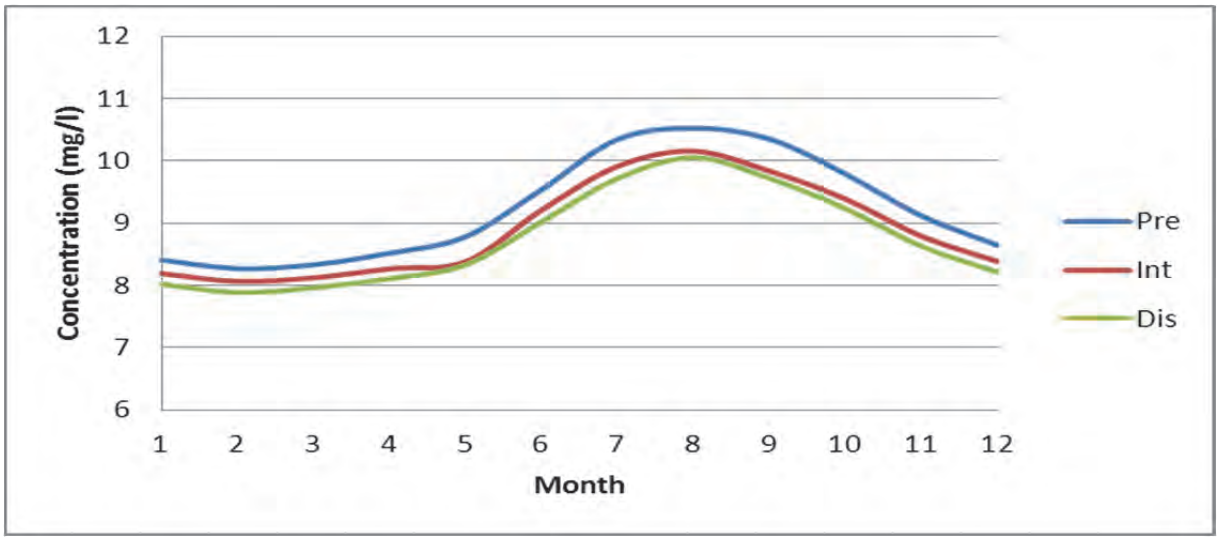

Figure 110: The projected mean monthly surface dissolved oxygen concentration for Berg River Dam (mg/l)

Figure 110 shows that the surface dissolved oxygen concentration decrease for the climate change scenarios. The greatest decreases were in progressing from present day to intermediate future and alluded to an accelerated worsening water quality condition. This was attributed to the warmer surface waters dissociating oxygen easier to the atmosphere. It was noted that the DWA TWQR levels for dissolved oxygen was not exceeded in any of the climate scenarios.

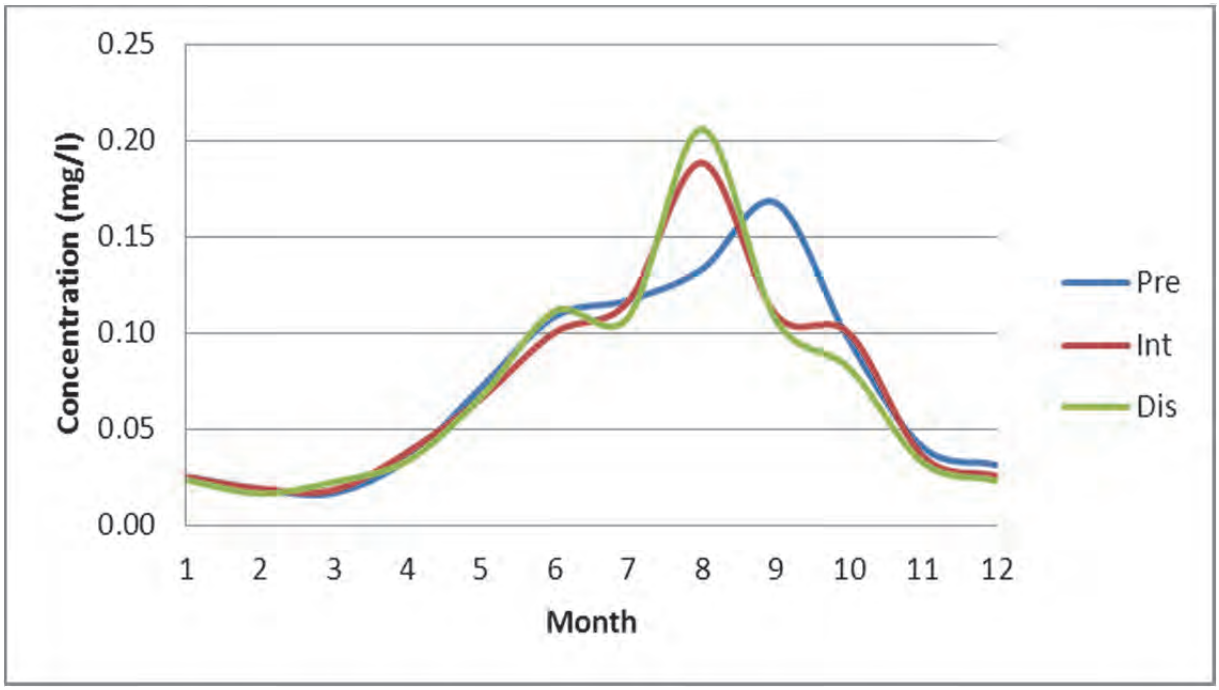

Figure 111: The projected mean monthly surface total algae concentration for Berg River Dam (mg/l)

Upon examining, the total surface algal growth it was seen that for climate change the concentration of total algae increased at the surface with a prominent shift earlier in the year for both intermediate and distant future. Since no green algae or cyanobacteria thrived in Berg River dam for any climate scenario, diatoms were representative of the total algal concentration. Diatoms were thus the dominant group in the system.

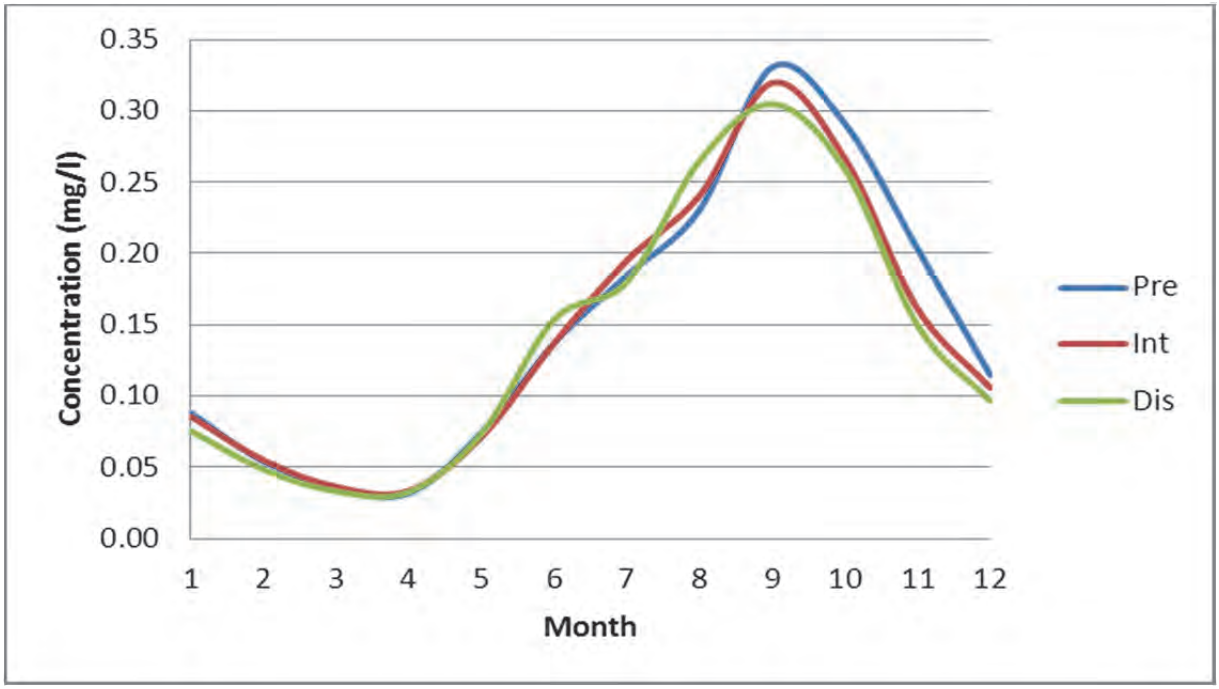

Figure 112: The projected mean monthly surface zooplankton concentration for Berg River Dam (mg/l)

Zooplankton concentrations remained relatively unchanged except during summer when slight decrease was observed. The growth of the zooplankton mimicked the growth of diatoms but did not show the seasonal shift that was seen with diatoms. The zooplankton grazed exclusively on diatoms and themselves.

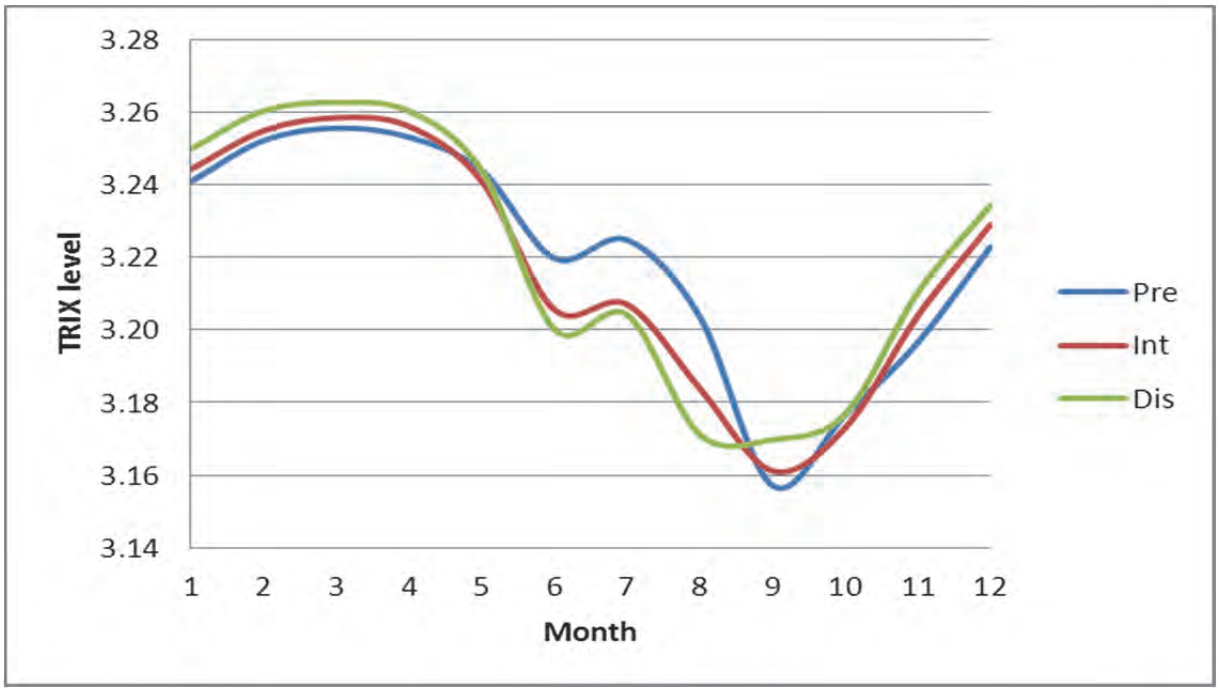

Figure 113: The projected mean monthly surface TRIX level for Berg River Dam

The influence of climate change was seen to have limited implications for Berg River dam in the form of a seasonal shift for diatoms and this had a direct effect on the surface eutrophication level especially for the distant future. For the intermediate and distant future, the water quality improved during winter and worsened during summer. The concentration of diatoms in the dam was low enough that they did not influence the water quality significantly, as a seasonal shift in water quality was not noted. On average, the water quality improved annually for climate change scenarios for berg river dam.

The following table (Table 40) summarise the water quality of Berg River dam for the climate change events.

Table 40: Summary of water quality for Berg River Dam under projected climate change

	Jan	Feb	Mar	Apr	May	Jun	Jul	Aug	Sep	Oct	Nov	Dec
Air temperature (°C)												
Present day	15.8	16.9	17.2	15.8	12.6	11.1	10.0	9.6	9.8	11.0	13.0	14.5
Difference	4.1	3.8	3.6	3.1	3.3	2.9	3.1	3.1	3.6	3.8	3.9	4.2
Intermediate	19.9	20.7	20.8	19.0	15.9	14.1	13.1	12.7	13.4	14.8	16.9	18.8
Difference	0.4	1.0	1.6	3.4	4.2	4.1	3.4	2.7	1.3	0.9	0.3	-0.1
Future	20.3	21.7	22.4	22.4	20.2	18.1	16.6	15.4	14.7	15.7	17.2	18.7
Overall change	4.5	4.8	5.2	6.5	7.6	7.0	6.6	5.8	4.9	4.7	4.3	4.2
Water temperature (°C)												
Present day	22.9	23.6	22.8	20.5	17.0	13.9	12.4	12.1	13.4	15.7	18.9	21.5
Difference	1.3	1.3	1.3	1.4	1.6	1.8	1.8	1.9	1.8	1.9	1.7	1.5
Intermediate	24.3	24.9	24.1	21.9	18.6	15.7	14.2	14.0	15.2	17.6	20.6	23.0
Difference	1.2	1.2	1.2	1.3	1.1	0.9	0.7	0.6	0.6	0.8	1.0	1.1
Future	25.5	26.1	25.2	23.2	19.8	16.6	14.9	14.5	15.8	18.4	21.6	24.1
Overall change	2.5	2.6	2.5	2.7	2.8	2.7	2.5	2.4	2.4	2.7	2.7	2.6
Total algae (mg/l)												
Present day	0.03	0.02	0.02	0.03	0.07	0.11	0.12	0.13	0.17	0.10	0.04	0.03
Difference	0.00	0.00	0.00	0.00	-0.01	-0.01	0.00	0.06	-0.06	0.00	0.00	-0.01
Intermediate	0.02	0.02	0.02	0.04	0.07	0.10	0.12	0.19	0.11	0.10	0.04	0.03
Difference	0.00	0.00	0.00	0.00	0.00	0.01	-0.01	0.02	0.00	-0.02	0.00	0.00
Future	0.02	0.02	0.02	0.03	0.07	0.11	0.11	0.21	0.11	0.08	0.03	0.02
Overall change	0.08	0.08	0.08	0.08	0.08	0.08	0.08	0.08	0.08	0.08	0.08	0.08
TRIX												
Present day	3.24	3.25	3.26	3.25	3.24	3.22	3.22	3.20	3.16	3.18	3.20	3.22
Difference	0.00	0.00	0.00	0.00	0.00	-0.01	-0.02	-0.02	0.00	0.00	0.01	0.01
Intermediate	3.24	3.25	3.26	3.26	3.24	3.21	3.21	3.18	3.16	3.17	3.20	3.23
Difference	0.01	0.01	0.00	0.00	0.00	-0.01	0.00	-0.01	0.01	0.00	0.01	0.01
Future	3.25	3.26	3.26	3.26	3.24	3.20	3.20	3.17	3.17	3.18	3.21	3.23
Overall change	0.08	0.08	0.08	0.08	0.08	0.08	0.08	0.08	0.08	0.08	0.08	0.08

Conclusions

Study limitations

The GCMs employed in this study were of such coarse resolution (about 300 km) that they cannot be used directly for the meteorological data. The GCMs were firstly downscaled statistically to regional level. The disadvantage of the statistical method of downscaling is that it relies on the availability of sufficient high resolution data over long periods so that statistical relationships may be established. It is unfortunately not possible to be certain how valid the statistical relations are for a climate-changed situation, however the data is

validated against historical records where possible (Houghton, 2007; Quintana-Seguí *et al.*, 2010).

Wind speed and direction was not supplied by CSAG (UCT) and was thus a limitation. CE-QUAL-W2 requires wind-speed and direction as part of its meteorological data input to predict water quality.

Inflow water quality data was not as readily available as flow data, and was at best measured only on a weekly basis. No inflow and outflow data was available for the projected future scenarios; it was proposed to use the current DWA HIS database flow-data of the present scenario for each of the subsequent intermediate and future simulations. This would assume that demand and allocation of the water resource did not change for the simulation periods.

In order to predict the growth of algae, parameters should be as accurate as possible. Sourcing some of these parameters proved difficult, and futile in some instances, and default values were used.

For each run, initial conditions were specified to be the same as the present day initial conditions. This allowed for a direct comparison of present day to intermediate future and distant future. For each simulation period, the original dam was consistently subjected to climate change. Climate data was unfortunately not available from 1971 to 2100, which would have allowed the dam to be modelled for the entire climatic period. This implied that when the time of simulation approached 2045 the model has already run for over 50 years and the in-situ conditions are that of 2045. Currently the intermediate future and distant future initial conditions are that of the present day.

Water quality modelling

The variability between the four climate models was noted, and they all projected an increase in air temperatures for each of the time scenarios studied. It was concluded that air temperature was the major driver for surface water temperatures and solar radiation was the diurnal driver.

The BRD was monomictic, and had a thermocline between depths of 10 and 15 m, which was negligible during winter. During winter, the dam was virtually uniform in temperature and fully mixed, which allowed for re-suspension of nutrients throughout the dam. Thus, at the

onset of spring, the warmer water would facilitate the growth of algae even though no additional nutrients were added to the dam.

Climate change affected the surface waters by heating the water and subsequently increased the evaporation rate of the water. This heated water evaporated more in the distant future than the intermediate future a result of the increased water temperature.
Once climate change has heated the surface waters of the dam, the water level dropped due to increased evaporation.

It was seen that the surface phosphate concentration fluctuated marginally when progressing to intermediate future and distant future climate scenarios. The maximum concentration occurred one month earlier in the future scenarios than in the present day and the concentration was relatively unchanged.

All models showed changes in surface ammonium concentration but overall it is a decreasing trend in progressing to future climate change scenarios.

The effect of climate change on nitrate-nitrites for the future surface concentrations remain relatively unchanged when compared to present day surface concentrations, with spring having the least surface concentrations.

The dissolved oxygen concentration was greatest during winter and spring, when the surface water was cooler and could hold more oxygen. The limits set by DWA were never exceeded.

The total surface algal growth was only diatoms. Months of peak concentrations shifted one month earlier in the year, but this was not for all the climate models. This phenomenon could be seen as a season shift in surface total algal concentrations. This was attributed directly to the increased air temperature driving the growth of the algae. Thus, the effect of warmer water due to climate change, favours the growth of diatoms throughout the year in the distant future, with the possibility of a seasonal shift.

It was expected to see larger growths of all algae and/or algal succession but this was not the findings of the study.

The surface zooplankton concentration for all future climate models predicted a slight decrease in concentration of surface zooplankton with maximum concentrations in spring, mimicking diatom growth.

The influence of climate change was seen to have implications for Berg River dam in the form of a seasonal shift in diatom concentration and this had a direct effect on the surface TRIX levels. The TRIX levels showed decreases in winter and spring with increases in summer and autumn implying improved water quality.

It was thus concluded that if the inflows and withdrawal remain the same for future climate scenarios, the impact of climate change on Berg River dam would be minimal and a slight improvement in water quality at segment 21.

Recommendations

This study concentrated on the water quality of the surface waters of BRD. The study produces vast amounts of data, and the limitation of presenting the only the surface waters only was vindicated for this dam, as it was almost entirely mixed for the simulation time. The model used was CE-QUAL-W2, which is a two dimensional laterally averaged model which returns an adequate solution. A more representative model would produce a true 3 dimensional solution but this would only be possible with using a three dimensional model and greater accuracy for inflow and withdrawals.

The most cost effective management of the problem of future eutrophication is judged by the team to be the reduction in inflow of nutrients into the dam, particularly that of phosphorous. Source reduction at the facilities that discharge phosphorous into the catchment is required, to limit its concentration in the dam.
Monitoring and measuring of all the channels into and out of BRD should be implemented so that models that are more accurate could be built. This would include flow and water quality constituents. Profile sampling of the variables of concern would be required so that a profile of the dam may be compared, thereby increasing the understanding of the hydrodynamics and the accuracy.

The parameters that govern algal growth should be measured in a laboratory or *in situ* for the BRD. These new values should then be used and the simulations rerun to ascertain whether the result differ markedly. This would also provide a quantitative analysis on the sensitivity of certain parameters as well as their effect on dissolved oxygen concentrations.

A universal mathematical method of presenting the trophic level of a body of water should be adopted. The TRIX level provided a starting point but has its limitations, as it does not account for transparency. This would allow for direct comparisons of different water bodies.

The complete meteorological dataset from 1971 to 2100 should be used for modelling. The model should be rerun with a complete set of meteorological data from 1971 to 2100 and all initial conditions should be pegged at 1971.

No data on sedimentation was available. Sedimentation data should be measured and incorporated and the simulation rerun to investigate this effect on the eutrophication rate and subsequent water quality.

9 VOËLVLEI DAM CASE STUDY – CE-QUAL-W2 MODEL

9.1 Bathymetric data

The bathymetric description of the dam is probably the most fundamental data required to construct a numerical grid which is used by the model. The numerical grid is thus a simplified mathematical description of the volume and shape of the dam. It is essential to construct an accurate description of the dam as this will determine how well the water level in the Dam is modelled. The water level in the dam is linked to water quality modelling and if the initial hydraulic calibration (i.e. volumetric) is not achieved, then water quality calibration will be difficult, if not impossible. In this particular case, the occurrence of algal blooms is of importance, making it vital to correctly simulate the water levels.

Data for construction of the numerical grid was obtained from the DWAF – Geomatics Directorate, in the form of a sedimentation survey. Each cross-section had data consisting of X and Y co-ordinates for the banks of the Dam as well as distances and height above sea-level of other points relative to the banks. Sixteen cross-sections, approximately 500 m apart were surveyed in 1998 (See Figure 114).

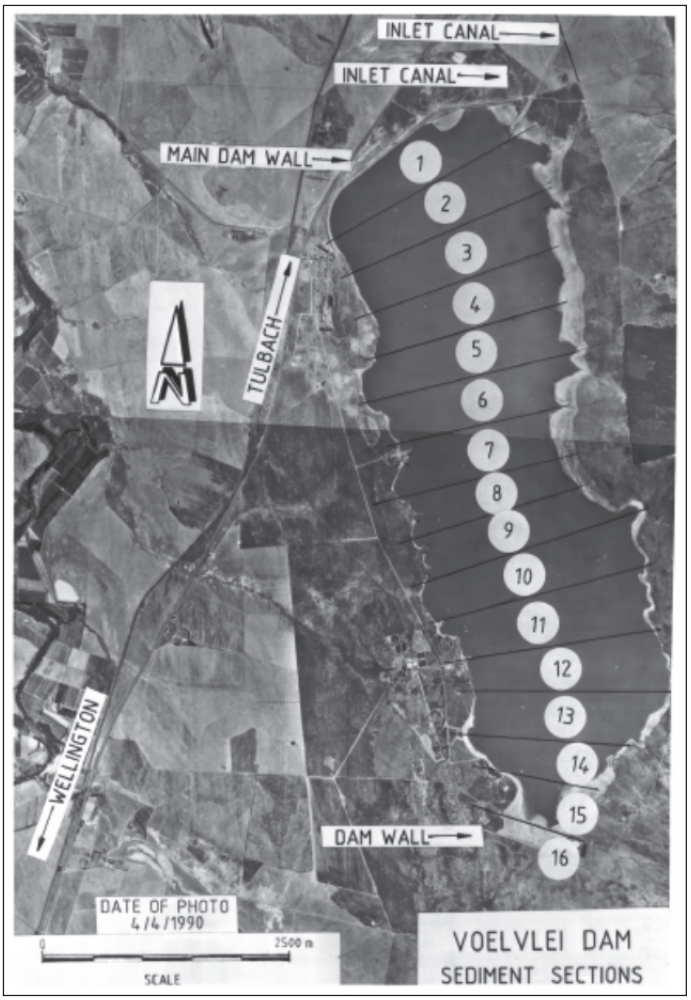

Figure 114: The sediment survey of Voëlvlei dam (1998)

This original data was transformed into X,Y,Z format and provided for this case study and subsequently imported into the Surfer programme where contours of the Dam were generated (See

Figure 115). From this contours the dam was divided into 20 vertical sections of approximately 400m wide. Each of these sections was further divided into volumes 0.5m thick.

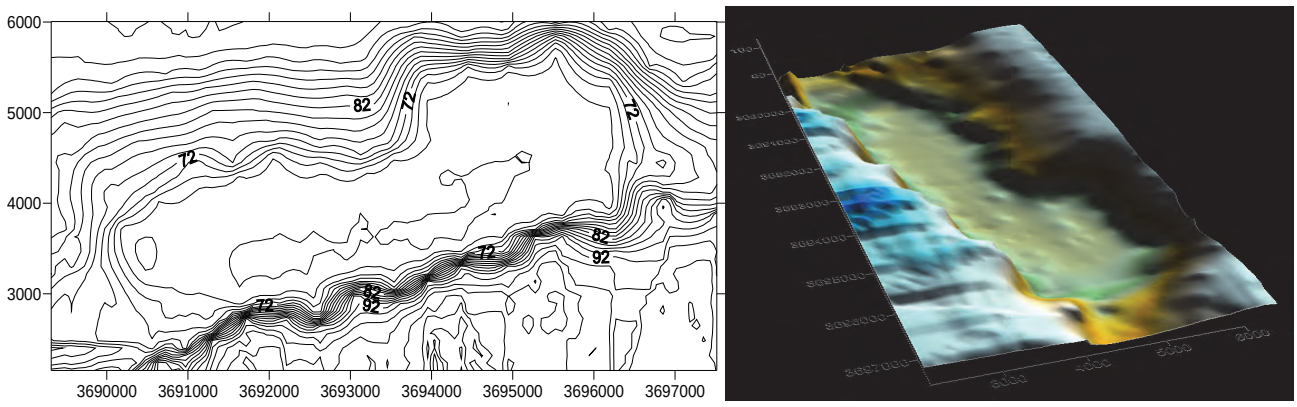

Figure 115: The contour map and 3D shape of Voëlvlei as produced by Surfer

The orientation of a segment was obtained by connecting the mid-point of the cross-section at the maximum supply level of 80m to the mid-point of the following cross-section with the angle being measured, relative to north in a clockwise direction. Figure 116 depicts a top view of the segments in a N-S direction (21 to 2) as used by the model CE-QUAL-W2.

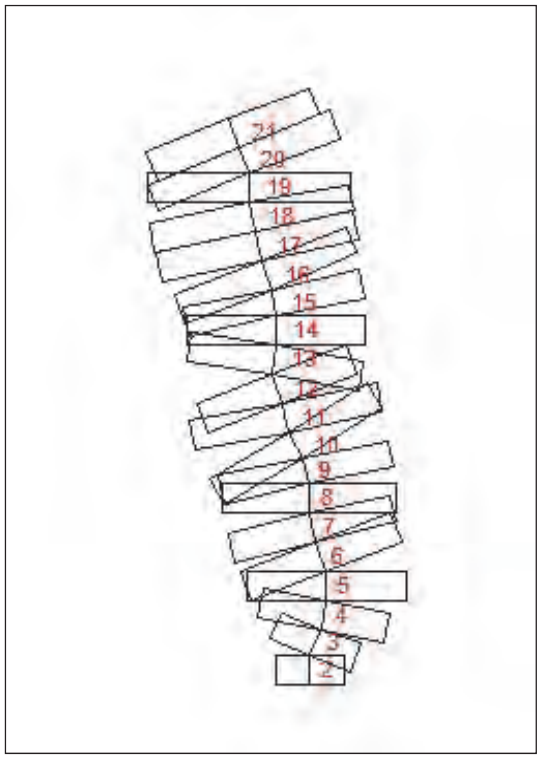

Figure 116: The segments for Voëlvlei dam as used by CE-QUAL-W2 (NS direction)

The bank to bank width of each cell was then calculated from the following deductive formula:

$$\text{Width} = \frac{\text{Volume in cell}}{\text{length of segment x height of segment}}$$

Thereby allocating a width for every segment at 0.5 m vertical intervals as shown in Figure 117.

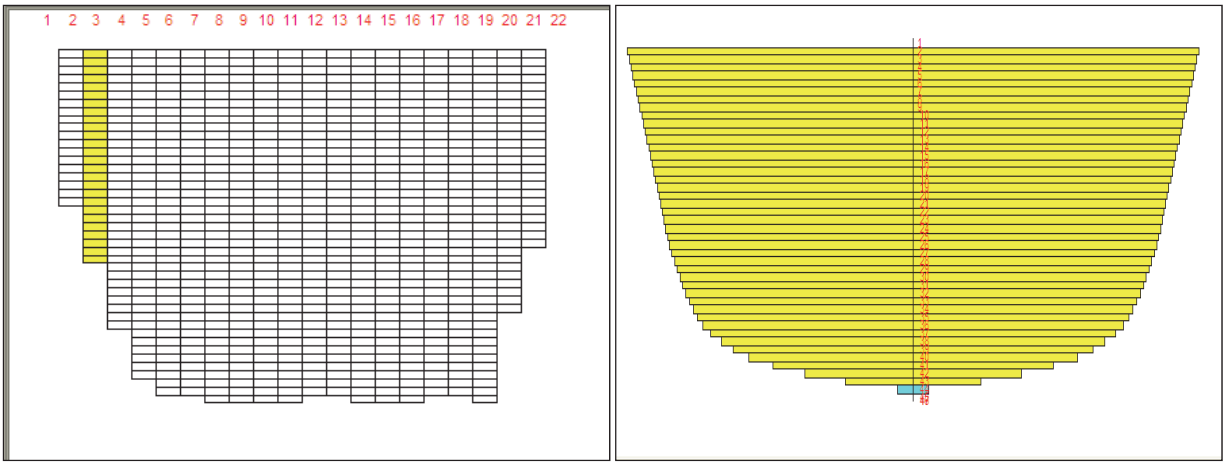

Figure 117: The sectional and end view of Voëlvlei as used by CE-QUAL-W2

Using this method, the volume of each cell in the grid was preserved. The entire grid for Voëlvlei dam is made up of 46 layers and 22 segments, with segments 1 and 22 as well as layers 1 and 46 representing the boundary cells that have zero width. These cells are required to enable the model to function.

It was noted for segments having widths (bank to bank) of less than 30m the segment is added to the level above it as this helps increase timesteps, freeing computer time with minimal impact on the volume-area-elevation curves. However increasing the bottom layers can affect water quality since sediment oxygen demand and nutrient fluxes are dependent on bottom surface areas (Cole and Wells, 2008). It was assumed that this would not be the case as the model had a vertical interval of 0.5m which is considered relatively small.

The mathematical grid is only a representation of reality and should be compared with measured data to ensure that the generated grid is realistic. This was done by comparing the volume-height relationship obtained by the process described above with measured data reported in the Western Cape System Analysis Report (Reference).

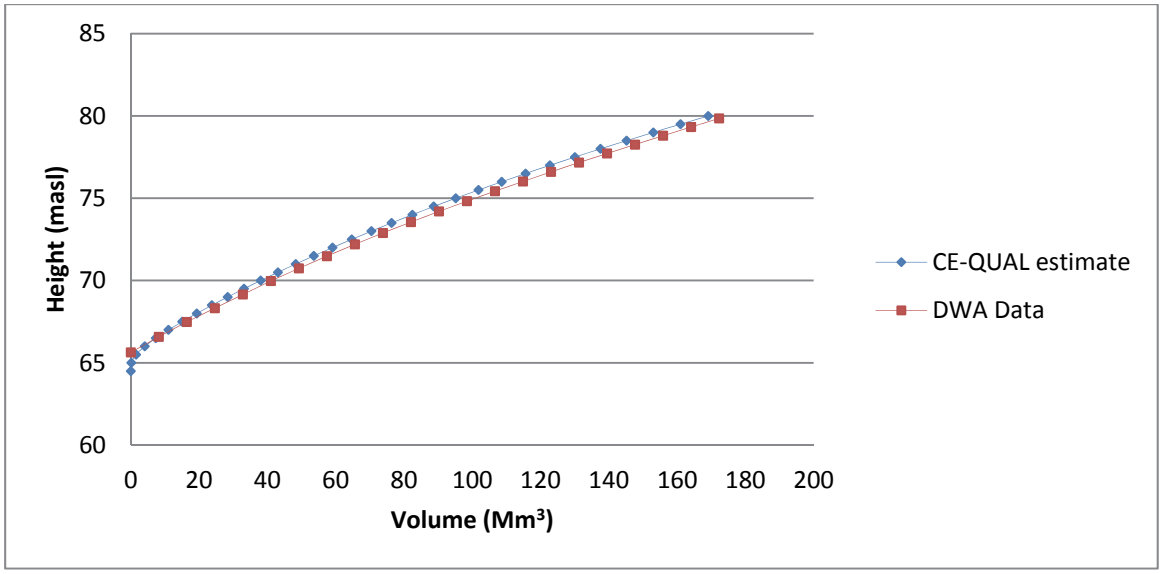

Figure 118: The comparison of modelled and measured Voëlvlei dam volumes

This figure shows that the model grid agrees well with the actual measured values except for low water levels approximately between 65 and 66 masl were the model underestimates the volume. This is not considered a problem as it is nearly below minimum operating level.

9.2 Boundary condition data

The major driving forces of CE-QUAL-W2 are the inflows, inflow concentrations, outflows and meteorological data. In addition, the model also requires calibration data and kinetic data for algal growth and settling. Once algae are modelled in a system, almost all the water quality variables become important because of the various interactions between the constituents.

9.3 Inflow water quantity and quality data

Inflow to Voëlvlei Dam is diverted from the Twenty-four Rivers, the Leeu River and the Klein Berg River. The daily averaged inflow to the Dam was obtained from the DWAF's Hydrological Information System (HIS) database. Details of the flow gauges measuring the inflow are listed in Table 41.

Table 41: Flow gauging stations recording inflow to Voëlvlei Dam

Gauge Number	River	Latitude	Longitude	Period of record
G1H066A01	Klein Berg inlet canal at Voëlvlei Dam	33°21'05"	19°01'12"	1-10-1951 to 14-2-2002
G1H067A01	Twenty- Four Rivers inlet canal at Voëlvlei Dam	33°21'05"	19°01'12"	1-10-1972 to 14-2-2002

Outflows from Voëlvlei Dam consist of abstractions of raw water to supply the Voëlvlei (G1H070M01) and Swartland (G1H068M01) WTW. Water is also released via an outlet canal (G1H065A01) to the Berg River for run-of-river irrigation (DWAF, 1999).

The minimum level of operation for the Voëlvlei WTW is 68.33 metres above sea level (masl). No information was available for the minimum draw down level at the Swartland WTW but it was assumed to be equal to that at Voëlvlei WTW. The minimum draw down level for the Berg River release is 65.62 masl (CCT, 2002). An additional outflow to the ICS pipeline was also operational but flow data for this gauging station (G1H069M01) was only available up to 1982. This pipeline was excluded from the simulation as it was deemed to have too little effect on the water quality. This would be borne out in the volumetric estimation of the dam.

Inflow water quality data is not as readily available as flow data, and is at best measured only on a weekly basis. For a graphical layout of where pertinent water quality monitoring stations are located for the Voëlvlei Dam system, refer to Figure 35. Although a reasonably good water quality record exists at gauging station G1H029Q01, it was not used. This is because the volume of water diverted from the Twenty-Four Rivers River is substantially greater than that diverted from the Leeu River and it was therefore assumed that the water quality of the Twenty-Four Rivers River would more representative of the water quality entering the Dam at G1H067Q01. Similarly, gauging station G1H008Q01 is representative of the water quality at G1H066Q01.

Since no inflow and outflow data is available for the predicted future scenarios it is proposed to use the current DWA HIS databases' flow data from 1 January 1971 until 31 December 1990 (present scenario) for each of the subsequent intermediate and future simulations. This would assume that demand and allocation of the water resource does not change for the simulation periods.

Water quality of all the inflowing canals is not measured and it was assumed that water quality at upstream monitoring points could be used to describe the boundary conditions at these inflows. These inflows were modelled as tributaries that were evenly distributed into Segment 21.

The modelled outflows from the Dam consisted of the Berg River irrigation release (segment 6) and two lateral withdrawals for the water treatment works and evaporation which was calculated based on the air temperature, dew point temperature and wind speed. Table 42 summarises the flow boundary conditions.

Table 42: Summary of the boundary conditions

Inflow/outflow	Segment	Layer
Tributary 1 inflow	21	Evenly distributed
Tributary 2 inflow	21	Evenly distributed
Withdrawal 1 (Voëlvlei WTW)	11	68.33 masl
Withdrawal 2 (Swartland WTW)	18	68.33 masl
Release (Berg river irrigation modelled as a withdrawal)	6	65.62 masl
Evaporation	All active surface segments	Top surface

9.4 The initial conditions

The dates of the modelling exercise for the four climate change scenarios are:

- Present day (1/1/1971-31/12/1990);
- Intermediate future (1/1/2046-31/12/2065); and
- Distant future (1/1/2081-31/12/2100).

In each of the modelling exercises Julian day 1 is 1 January for each of the respective climate change scenario dates. An initial condition of temperature and concentration profiles, the number of inflows and outflows and the type of water modelled (saltwater or freshwater) is determined by the user. These conditions are typically measured values from the previous day or any day closest to the start of the simulation. These conditions were initialised in the ‘control’ file and the 'vertical profile' input files of the model. Meteorological and flow data was available for the years 1996 to 1997, it was decided that initial runs would be used to quantify the outputs and determine if further more rigorous calibration would be required.

It was assumed that reservoir is completely mixed (as it is relatively shallow with winds along it axis) and that a single value initial condition for concentration would be a good initial guess. The in-lake conditions were obtained from the DWAF (HIS) database on the date closest to the start date of the simulation period. The constituents that were modelled are listed in Table 43.

Table 43: Constituents modelled and initial values

Constituent	Initial Value
Total dissolved solids (TDS)	50 mg/l
Generic tracer	5 mg/l
Age	0.0 /day
Phosphates	0.022 mg P/l
Ammonium	0.073 mg N/l
Nitrates and nitrites	0.119 mg N/l
Dissolved Silica (DSI)	0.4 mg/l
Particulate Silica (PSI)	0.0 mg/l
Labile dissolved organic matter (LDOM)	0.0 mg/l
Refractory dissolved organic matter (RDOM)	0.0 mg/l
Labile particulate organic matter (LPOM)	0.0 mg/l
Refractory particulate organic matter (RPOM)	0.0 mg/l
Algae	0.1 mg/l
Zooplankton	0.1 mg/l
Dissolved oxygen (DO)	10 mg/l
Total inorganic carbon (TIC)	0 mg/l
Alkalinity ($CaCO_3$)	16 (mg/l)
Temperature	14.3 °C

9.5 Model parameterisation

The model requires a set of input parameters to run, which are measured or taken from literature. All the model parameters used in this study are listed in Table 44 Many parameters need to be defined and parameter values were chosen from literature but in most cases it was a range of possible parameter values. Without being able to measure these values parameters were chosen and the model was allowed to run thereby presenting a possible solution. In many instances inflow concentrations for inorganic suspended solids, labile organic matter, refractory organic matter, particulate silica and inorganic carbon was not found and these were taken from literature.

Table 44: Parameters used in the Voëlvlei dam model

Symbol	Model Parameters	Value
Parameters affecting diatom growth		
K_{ag}	Maximum algal growth rate	5 day^{-1}
K_{am}	Maximum algal mortality rate	0.1 day^{-1}
K_{ae}	Maximum algal excretion rate	0.04 day^{-1}
K_{ar}	Maximum algal respiration rate	0.05 day^{-1}
h_n	Algal half-saturation constant for nitrogen limited growth	0.01 mg/l
h_p	Algal half-saturation for phosphorous limited growth	0.002 mg/l
h_p	Algal half-saturation for silicon limited growth	0.08 mg/l
AS	Algal settling velocity	0.5 m day-1
ALGP	Stoichiometric equivalent between algal biomass and phosphorous	0.01
ALGN	Stoichiometric equivalent between algal biomass and nitrogen	0.072
ALGC	Stoichiometric equivalent between algal biomass and carbon	0.4
ALSI	Stoichiometric equivalent between algal biomass and silica	0.2
ACHLA	Ratio between algal biomass and chlorophyll-a	0.8
ASAT	Light saturation intensity at maximum photosynthetic rate	61.2 Wm^{-2}
Parameters affecting green algae growth		
K_{ag}	Maximum algal growth rate	4.1 day^{-1}
K_{am}	Maximum algal mortality rate	0.1 day^{-1}
Kae	Maximum algal excretion rate	0.04 day-1
Kar	Maximum algal respiration rate	0.05 day-1
hn	Algal half-saturation constant for nitrogen limited growth	0.14 mg/l
hp	Algal half-saturation for phosphorous limited growth	0.38 mg/l
h_p	Algal half-saturation for silicon limited growth	0 mg/l
AS	Algal settling velocity	0.18 m day-1
ALGP	Stoichiometric equivalent between algal biomass and phosphorous	0.012
ALGN	Stoichiometric equivalent between algal biomass and nitrogen	0.066
ALGC	Stoichiometric equivalent between algal biomass and carbon	0.49
ALSI	Stoichiometric equivalent between algal biomass and silica	0

Symbol	Model Parameters	Value
ACHLA	Ratio between algal biomass and chlorophyll-a	0.8
ASAT	Light saturation intensity at maximum photosynthetic rate	81.6 Wm-2
Parameters affecting cyanobacteria growth		
K_{ag}	Maximum algal growth rate	1 day^{-1}
K_{am}	Maximum algal mortality rate	0.1 day^{-1}
Kae	Maximum algal excretion rate	0.04 day-1
Kar	Maximum algal respiration rate	0.05 day-1
hn	Algal half-saturation constant for nitrogen limited growth	0 mg/l
hp	Algal half-saturation for phosphorous limited growth	0.011mg/l
h_p	Algal half-saturation for silicon limited growth	0 mg/l
AS	Algal settling velocity	0.1 m day-1
ALGP	Stoichiometric equivalent between algal biomass and phosphorous	0.007
ALGN	Stoichiometric equivalent between algal biomass and nitrogen	0.08
ALGC	Stoichiometric equivalent between algal biomass and carbon	0.45
ALSI	Stoichiometric equivalent between algal biomass and silica	0
ACHLA	Ratio between algal biomass and chlorophyll-a	0.8
ASAT	Light saturation intensity at maximum photosynthetic rate	60 Wm-2
Other parameters affecting all algal growth		
EXH20	Extinction of pure water	0.45 m^{-1}
EXOM	Extinction due to organic suspended solids	0.1 m^{-1}
BETA	Fraction of incident solar radiation absorbed at water surface	0.45
Parameters affecting ammonia nitrification and sedimentary phosphorous		
NH4DK	Maximum ammonia nitrification rate	0.12 day^{-1}
NH4R	Sediment release rate under anaerobic conditions (as a fraction of the sediment oxygen demand (SOD))	0.001
PARTP	Phosphorous partitioning coefficient for suspended solids	0.5
PO4R	Sediment release rate of phosphorous under anaerobic conditions (as a fraction of the sediment oxygen demand (SOD))	0.001
SEDDK	First order sediment decay rate	0.1 day^{-1}
Parameters affecting dissolved and particulate organic matter		

Symbol	Model Parameters	Value
LDOMDK	Labile Dissolved Organic Matter (DOM) decay rate	0.1 day^{-1}
RDOMDK	Refractory DOM decay rate	0.001 day^{-1}
LRDDK	Labile DOM to refractory DOM decay rate	0.001 day^{-1}
LPOMDK	Labile particulate organic matter (POM) decay rate	0.08 day^{-1}
RPOMDK	Refractory POM decay rate	0.001 day^{-1}
LRPDK	Labile to refractory POM decay rate	0.01 day^{-1}
POMS	POM settling rate	0.1 m day^{-1}
Stoichiometric coefficients		
O2NH4	Oxygen stoichiometry for nitrification	4.57
O2OM	Oxygen stoichiometry for organic matter decay	1.4
O2AR	Oxygen stoichiometry for algal respiration	1.1
O2AG	Oxygen stoichiometry for algal primary production	1.4

9.6 Voëlvlei dam model performance and validation

Modelled Dam hydraulics

Although the bathymetry of the dam was well captured by the model as shown by the volume-height relationship in Figure 119 it was still necessary to check the hydraulic performance of the dam. Data from the DWAF HIS database was composite surface measurements and no profile data was available. The water volumetric balance for the dam was the inflows and outflows that are measured daily. An outflow from the Dam (ICS pipeline) was not monitored but was small in relation to the Berg River outflow and the abstractions for the Voëlvlei and Swartland WTW. The meteorological and inflow data for this simulation period was obtained from the DWA HIS database. The daily water levels in Voëlvlei Dam were obtained from the DWAF HIS database for the annual period of 1 September 1996 to 30 August 1997 and used to compare the measured levels to the modelled output from CE-QUAL-W2 for the same period. The results are shown graphically below.

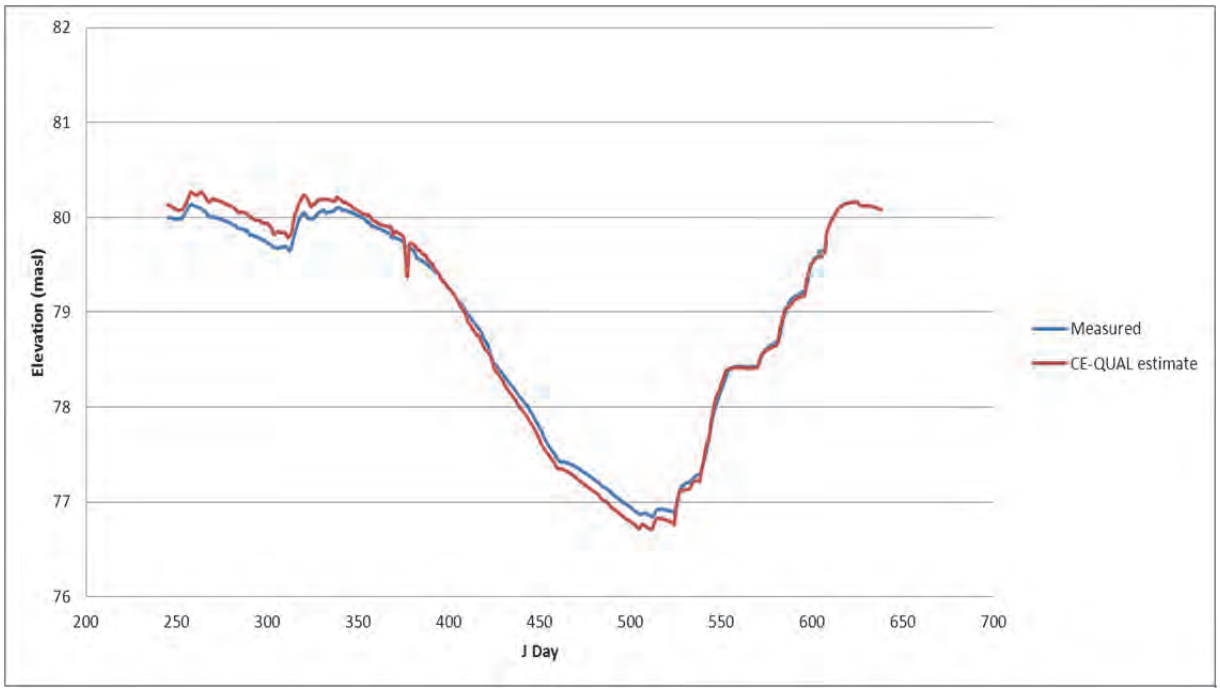

Figure 119: The comparison of modelled surface water level and measured data for hydraulic calibration of Voëlvlei Dam (masl)

It was seen that the model agrees relatively well with the surface water elevations measurement and that the overall trend was followed closely. The additional outflow to the ICS pipeline that was excluded from the simulation could explain the discrepancy in surface water levels. The trend between the measured data and the simulated output was good enough to accept that the bathymetry that had been constructed for the dam was hydraulically calibrated for the model. The climate change scenario modelling study would attempt to show differences in algal growth thus any discrepancies will not be compounded rather carried through each modelling scenario.

Model temperature predictions

Water temperature data on the dam surface, close to the dam wall (Segment 21) was measured by the DWAF on an irregular basis and the model output temperature was compared to this. This comparison would provide an indication of the hydrodynamics of the dam. This could only be done for surface water temperature, as no profile data was available.

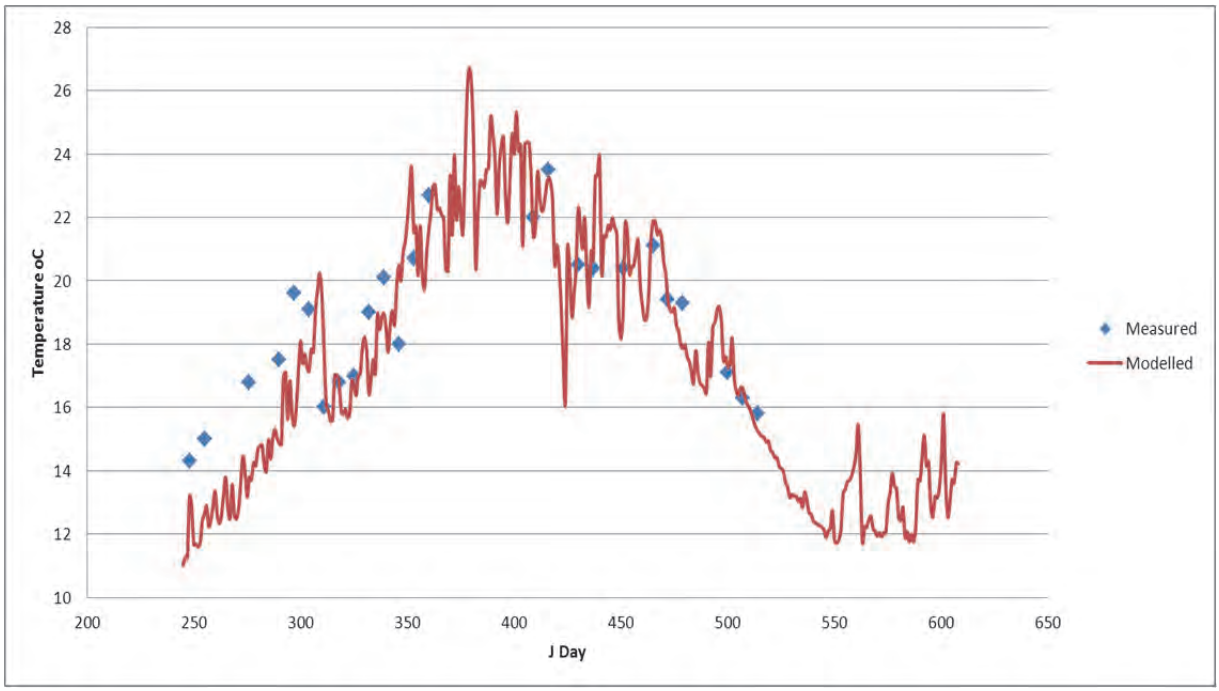

Figure 120: The comparison of modelled and measured surface water temperatures for Voëlvlei Dam (^{o}C)

The modelled output agreed well with the measured data (2 September 1996 to 1 September 1997. Overall, the trends between the modelled and actual measurements agreed thus confirming that the hydrodynamics of the dam was mimicked by the model and that it was sufficiently accurate to proceed. For the purpose of this study, it was deemed unnecessary to calibrate further as this study shows the relative changes under climate change scenarios. It was noted that since no profile temperature measurements are made there was no way of knowing the accuracy of the model for incremental depths.

The seven measured water quality variables of concern were available from the DWAF HIS database. These included chl-a, chlorine as tracer data, NH_4, PO_4, Si, Total P and NO_2+NO_3. These constituents are grab samples and are collected near the dam wall on an irregular basis.

Ortho phosphorous comparison

When modelling algae, the phosphate concentration (PO_4) was probably the most affected water quality constituent because it was constantly being recycled from one form to another as shown previously in Figure 37. Total phosphorous, although not a conservative, was less dynamic than phosphate and was often treated as a pseudo-conservative substance. In this model setup, the sinks for phosphate included the outflows and photosynthetic process while

the sources included the inflows, respiration and the decay of organic material including dead algae (organic sediments).

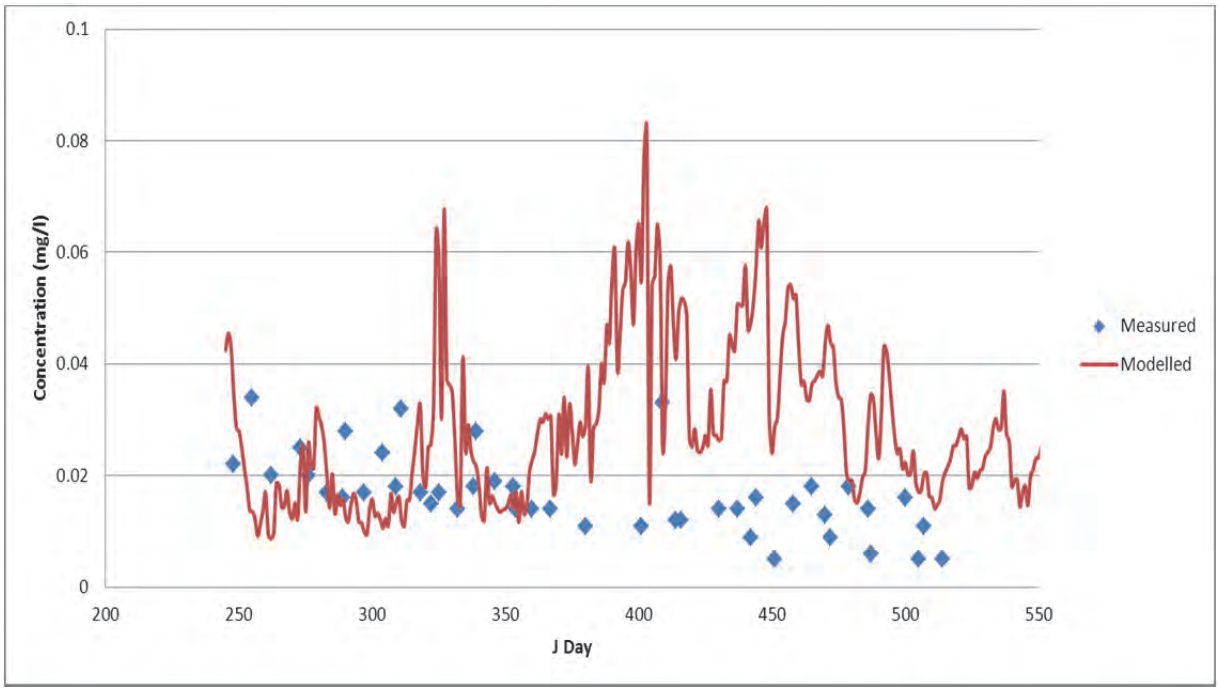

Figure 121: The comparison of modelled and measures surface phosphate concentration for Voëlvlei Dam (mg/l)

From Figure 118 it was seen that the model predicted the concentration of P in the dam well in spite of not having the additional withdrawal pipeline. The model however seemed to exaggerate the peaks. It thought the difference could be attributed to the measured value being a composite and the modelled concentration was for the entire segment. In spite of the difference, the concentrations are well represented by the modelled values.

Ammonium and nitrate-nitrite comparison

It was expected that algal growth would be dependent on the amount of nitrogen available, either in the form of ammonium or nitrate-nitrites. The modelled results compared to measured samples are shown in Figure 119 and Figure 120. When comparing these figures to Figure 121 it was seen that the algal growth was greatest for larger concentrations of ammonium and nitrites-nitrates. Overall, the modelled data simulates the measured data satisfactorily. The discrepancies could be attributed to the measured value being a composite and the modelled concentration was for the entire segment.

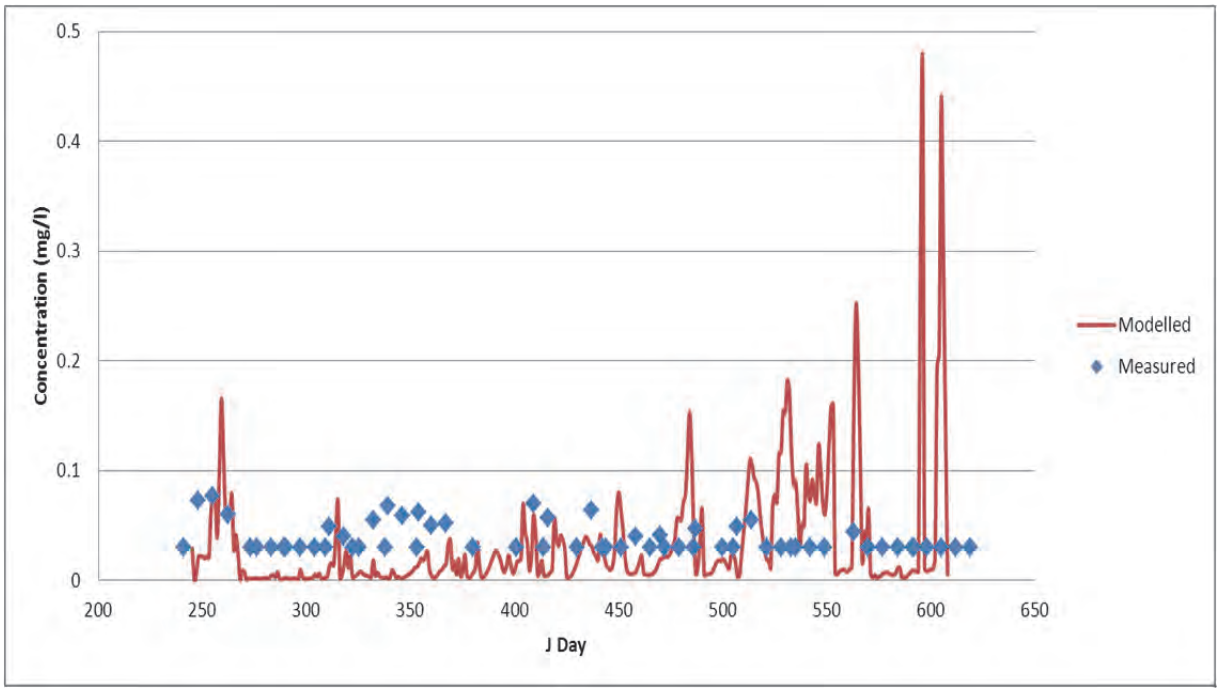

Figure 122: The comparison of modelled and measured surface ammonium for Voëlvlei Dam (mg/l)

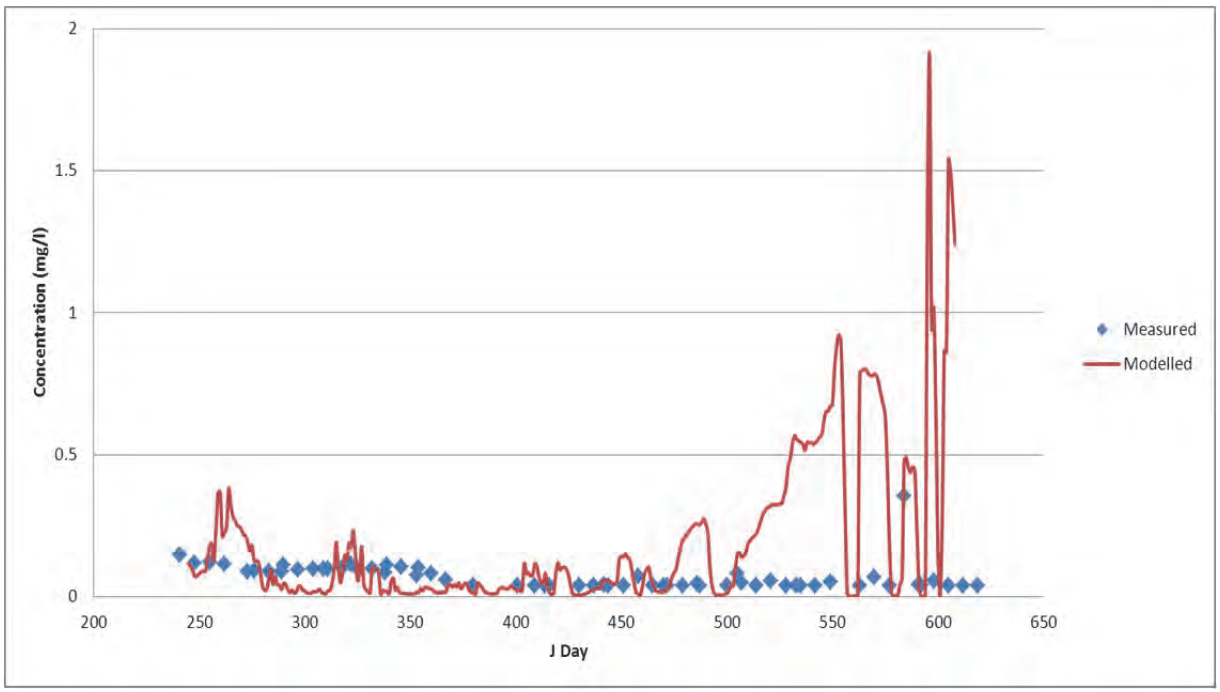

Figure 123: The comparison of modelled and measured surface Nitrate-nitrite concentration for Voëlvlei Dam (mg/l)

Chlorophyll-a comparison

From the DWA HIS database it was seen that only total chlorophyll-a was measured and Figure 121 shows the results. It was clear that the algal growth was similar to that being measured as the concentration was sufficiently low but the model produced chlorophyll-a concentrations similar to the measured values.

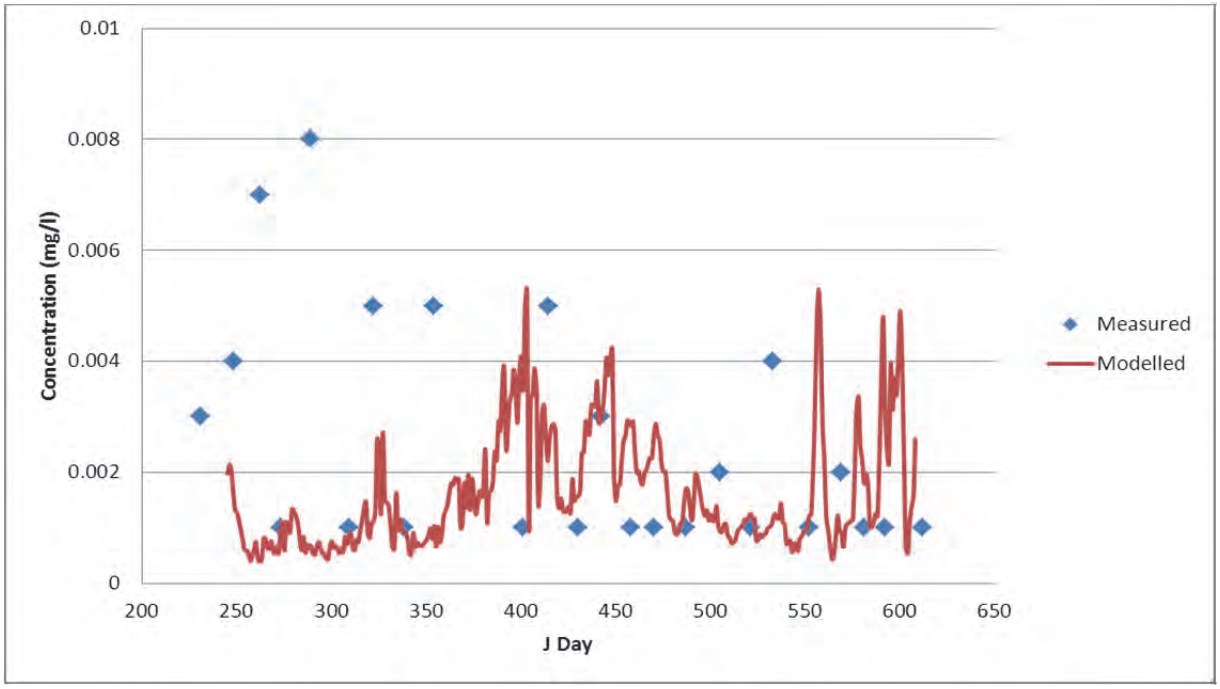

Figure 124: The comparison of modelled and measured surface chlorophyll-a concentrations for Voëlvlei Dam (mg/l)

The discrepancies could be explained by the fact that the measured concentrations are a composite value of various samples at the surface and depth, at the dam wall. The modelled results are only for the surface layer and the entire dam wall was treated as one area as the model was laterally averaged. In spite of this, the algal growth was well represented by the model in the context of low concentrations being modelled.

Conservative tracer tracking

The addition of a conservative tracer was to ascertain whether a sizeable source or sink of water had been omitted from the dam in form of inflows, outflows, sources or sinks. From Figure 125 it was seen that the concentration of the modelled tracer mimics that of the measured values adequately. It may be concluded that the transport processes were realistically modelled.

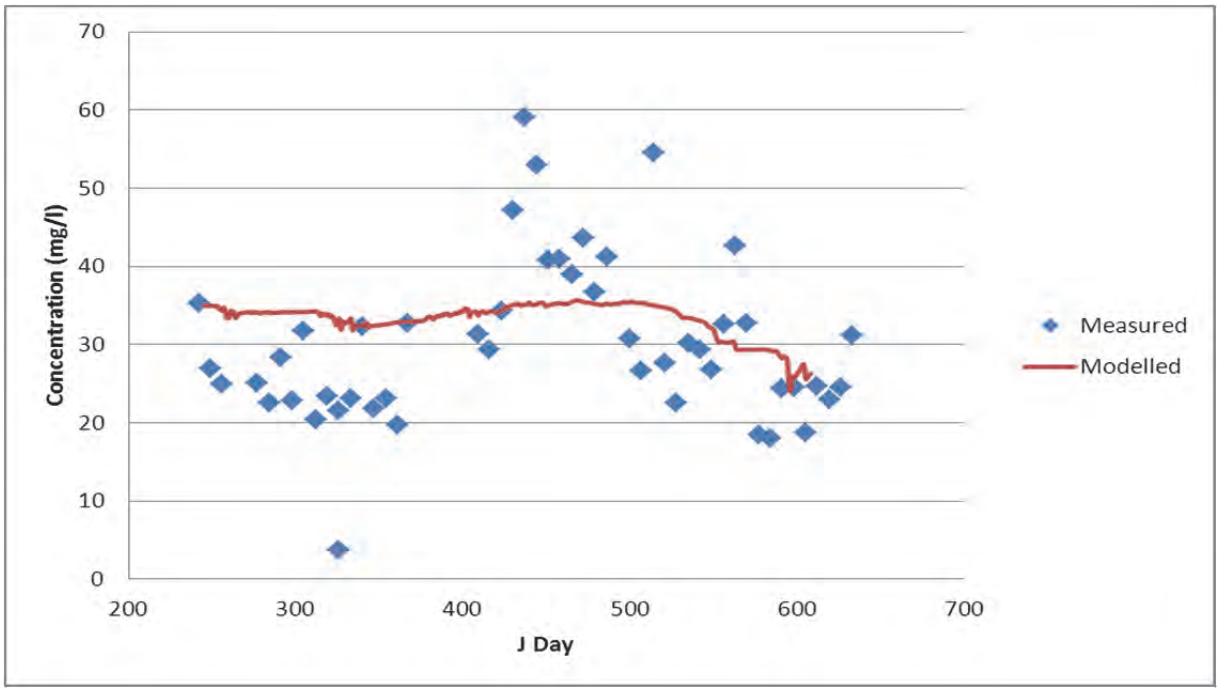

Figure 125: The comparison of modelled and measured surface conservative tracer for Voëlvlei Dam (mg/l)

Validation of the assumption of complete mixing of Voëlvlei dam

For this study, it was assumed that Voëlvlei was holomictic i.e. it was completely mixed and the dam was not stratified for extended periods during summer or winter. To validate this, a tracer profile was plotted of the dam at segment 11 (the MWTP extraction point) for a series of depths as shown in Figure 123.

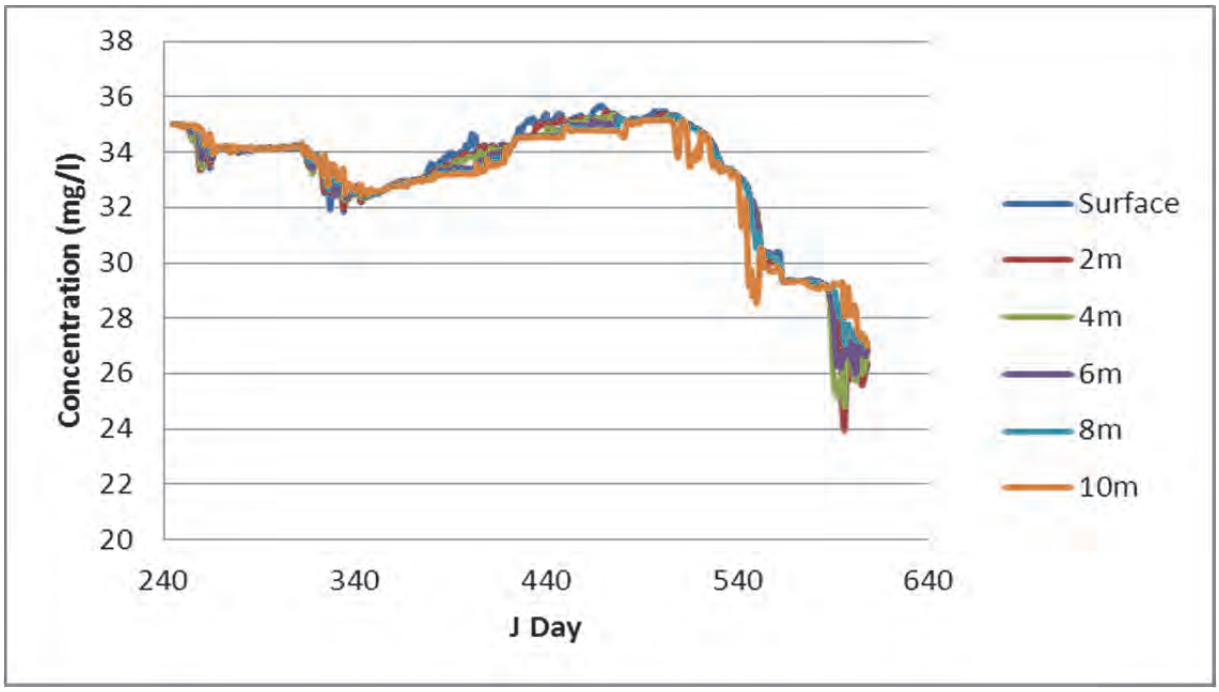

Figure 126: A tracer profile at segment 11 for various depths using calibration data for Voëlvlei dam to confirm a fully mixed Voëlvlei Dam

Thus, the assumption of complete mixing was vindicated as the tracer has equal concentration for a vertical profile in Voëlvlei dam for the entire run period of 1 year. The applicability of this assumption was vindicated by the profile tracer concentration plot for a 20-year run as shown in Figure 127.

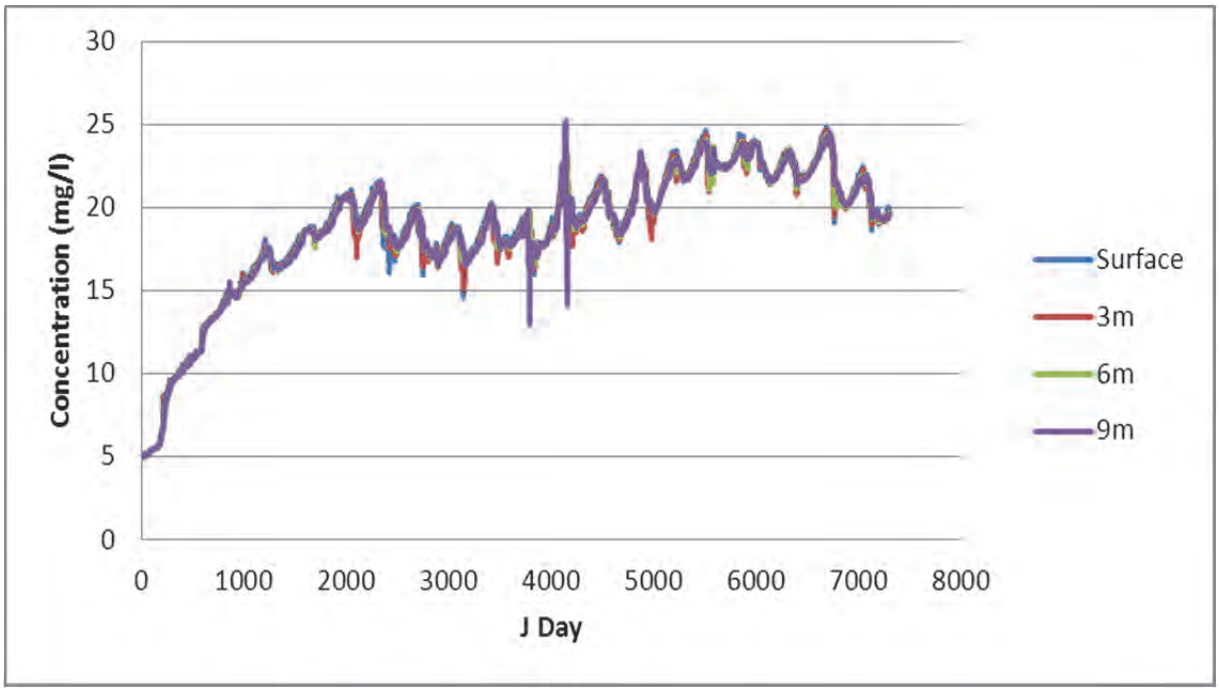

Figure 127: Vindication of the fully mixed assumption for the 20 year climate projections for Voëlvlei Dam

For the entire 20-year simulation, a tracer concentration was plotted at various depths as shown in Figure 124 using the present day CCC climate change data. From this figure, it was seen that tracer concentration was relatively uniform for the various depth for the entire period, thereby justifying the assumption that Voëlvlei was fully mixed.

To investigate whether the dam was stratified for any significant period in winter or summer, the present day CCC air temperature and water temperature at various depths for a 20 year period was plotted. The result is shown in Figure 128.

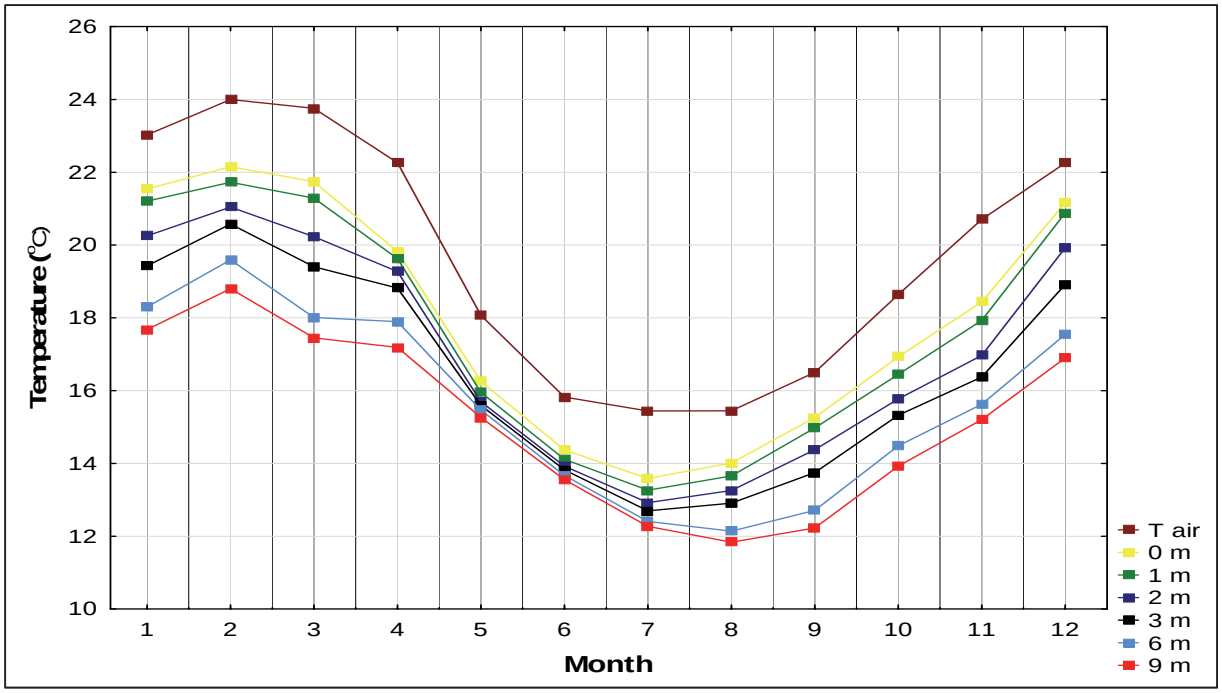

Figure 128: The 20 year present day air temperature and water temperature at various depths for Voëlvlei dam (°C)

This figure shows that mean air temperature was warmer than mean surface water temperature. Upon examining the water temperatures it was seen that for the deeper water was cooler than the surface could be attributed to less penetration of solar radiation due scattering as well as to increased mass of algae on the surface and at the surface interface the greatest heat transfer occurs, ensuring that the surface was warmer than water below. The temperature decrease with depth was linear for each month and hence it was assumed that if stratification does occur it was not for a statistically significant period, as it does not show in the figure. The vertical temperature variation was greater in summer than that of winter, implying that during winter the entire segment has nearly the same temperature.

It was thus safe to assume that Voëlvlei dam was fully mixed and not stratified for any significant length of time.

DWA Target Water Quality Ranges

The South African Water Quality Guidelines Field Guide, Volume 8 of the South African Water Quality Guidelines series, is a compilation of all the different Target Water Quality Ranges (TWQR) for all the different water use sectors dealt with in volumes one to seven. These include Domestic Water Use (Volume 1), Recreational Water Use (Volume 2),

Industrial Water Use (Volume 3), Irrigation Water Use (Volume 4), Livestock Watering (Volume 5), Aquacultural Water Use (Volume 6) and Aquatic Ecosystems (Volume 7).

The Target Water Quality Range (TWQR) for a particular constituent and water use was defined as the range of concentrations or levels at which the presence of the constituent would have no known adverse or anticipated effects on the fitness of the water assuming long-term continuous use, and for safeguarding the health of aquatic ecosystems. For the aquatic ecosystems guidelines the TWQR was not a water quality criterion as it was for other water uses, but rather a management objective that has been derived from quantitative and qualitative criteria.

The following tables are a summary of the TWQR field guide with specific emphasis on the constituents modelled for water quality.

Table 45: TWQR for the modelled water quality constituents

Constituent	TWQR			
	Aquatic ecosystem	**Full contact recreational use**	**Human consumption**	**Other**
Phosphate	0.025 mg/l	N/A		<0.1 mg/l for aquaculture
Ammonium	0-1 mg/l N has no health or aesthetic effects	N/A	0-1 mg/l	0-0.025 mg/l for cold water aquaculture 2-0.3 mg/l for warm water aquaculture
Nitrate-nitrite	0-6 mg/l N has no adverse health effects	N/A	0-6 mg/l for both species	0-100 mg/l for nitrite 0-10 mg/l nitrate for livestock watering
Dissolved oxygen	80-120% saturation	N/A	N/A	6-9 mg/l for cold water species and 5-8 mg/l warm water species for aquaculture
Dissolved silicon	N/A	N/A	N/A	0-150 mg/l for selected industries
Algae	See Table 45	0-15 mg/l	0-1 µg/l chl-a 0-50 algal cells/l 0-0.8 µg/l Microsystis	<6 µg/l Microsystis for livestock watering

Table 46: TWQR for all algae

Algal range (µg/l chl-a)	**Effects**
TWQR 0-1	Negligible risk of taste and odour
1-15	Slight green colouration of water at concentrations above 7 µg/l. Taste and odour problems can occur
Blue-green algae (cells/ml)	
TWQR 0-50	No health effects are experienced
50-14000	Possible chronic effects associated with long term ingestion
14000-42000	Possible acute hepatotoxic effects
>42000	Significant risk of acute and chronic effects
Microcystis range (µg/l)	
TWQR 0-0.8	No health effects expected
0.8-1	Possible chronic effects associated with long term ingestion
>1	Possible acute hepatotoxic effects

These limits were used to quantify the effect of the water quality variables for the climate study and their relative changes as influenced by climate change.

9.7 Voëlvlei dam present day scenario

The model had been calibrated previously and was now run for 20 years using the provided climate model data as meteorological input. The inflows, withdrawals and wind-speed are kept the same for each year of the simulation.

The factors that limit algal growth are water temperature and solar radiation, if all other factors such as light, nutrients and dissolved oxygen are in abundance (Wetzel, 2001). Solar radiation emitted by the sun was relatively constant and the incident solar radiation over Voëlvlei dam was affected largely only by cloud cover. Thus, the only factors that directly affect surface water temperature were air temperature (by conduction) and short-wave solar radiation and their relative contributions were to be assessed.

9.8 Air temperature

Carbon dioxide (CO_2), methane (CH_4), chlorofluorocarbons (CFCs), nitrous oxides (NO_x) and water vapour (H_2O) in the atmosphere allow the passage of shortwave solar radiation from the sun onto the earth surface, whilst absorbing the re-radiated radiation from the earth allowing the heating of the earth and the air. This heating was dubbed the *Greenhouse Effect* (Carter, 1994).

Four GCMs' were downscaled statistically to RCMs' over Voëlvlei dam and these climate models predict amongst others, air temperature. The mechanism of the greenhouse effect would in effect heat the air from the present day temperatures to a higher future temperature. It was postulated that this increase would alter the state of dams and contribute to worsening water quality by increasing algal biomass concentrations at the current cultural eutrophication rate.

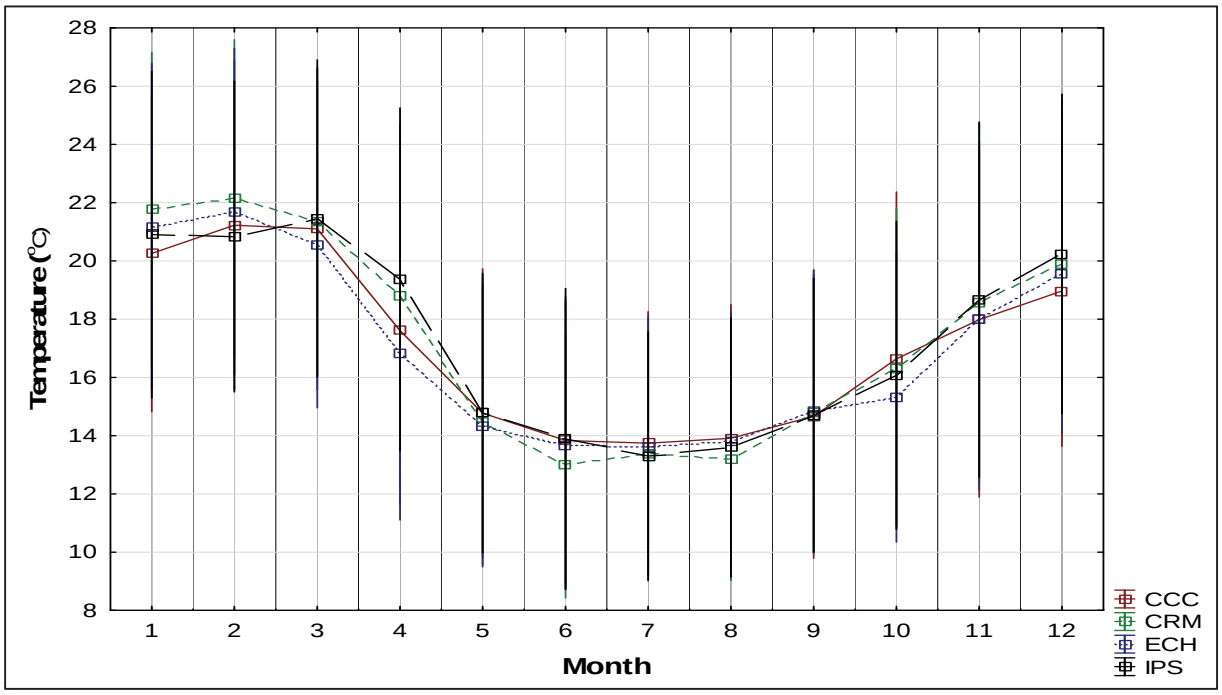

Figure 129: The present day mean monthly air temperature for Voëlvlei Dam (°C)

Figure 129 and Table 47 show that all four climate models predicted similar mean monthly air temperatures for the 20 year present day simulation period. This mean temperature included day and night time temperatures. The inter-variation between climate models was minimal but they could be ranked in order of increasing present day temperatures as ECH, CCC then CRM and IPS models.

Table 47: The present day mean monthly air temperature for Voëlvlei Dam (°C)

	Jan	Feb	Mar	Apr	May	Jun	Jul	Aug	Sep	Oct	Nov	Dec
CCC	20.3	21.2	21.1	17.6	14.8	13.8	13.7	13.9	14.7	16.6	18.0	19.0
CRM	21.8	22.1	21.3	18.8	14.5	13.0	13.4	13.2	14.8	16.3	18.6	19.9
ECH	21.2	21.7	20.6	16.8	14.3	13.7	13.6	13.8	14.9	15.3	18.0	19.6
IPS	20.9	20.8	21.5	19.4	14.8	13.9	13.3	13.6	14.7	16.1	18.7	20.2

The mean monthly air temperatures of the four climate models were similar in magnitude and cycle. The colour represents the magnitude with red being greater than green. Winter was May to July and summer was December to March. The annual mean temperature of all the models was 17.2^{o}C, which was expected to increase with climate change into the future because of the greenhouse effect. There was almost a 7^{o}C difference between winter and summer.

9.9 Solar radiation

Each of the present day climate models predicted similar levels of solar radiation as shown in Figure 130 for the 20-year modelling period. It was discussed by Wetzel (2001) and DeNicola (1996) that solar radiation was the major driver for diurnal surface water temperature and hence algal growth with all the other factors that may affect algal growth being equal. Thus, water temperature may limit algal growth even in the presence of abundant nutrients and light, which favoured growth.

All organisms have a temperature range at which optimal growth occurred, thus their life cycles are directly linked to temperature. Temperature primarily affects algal photosynthetic metabolism by controlling the enzyme reaction rate of the algae and an optimum temperature for each species was observed (DeNicola *et al.*, 1996). Thus, diurnal algal growth was directly influenced by solar radiation intensity.

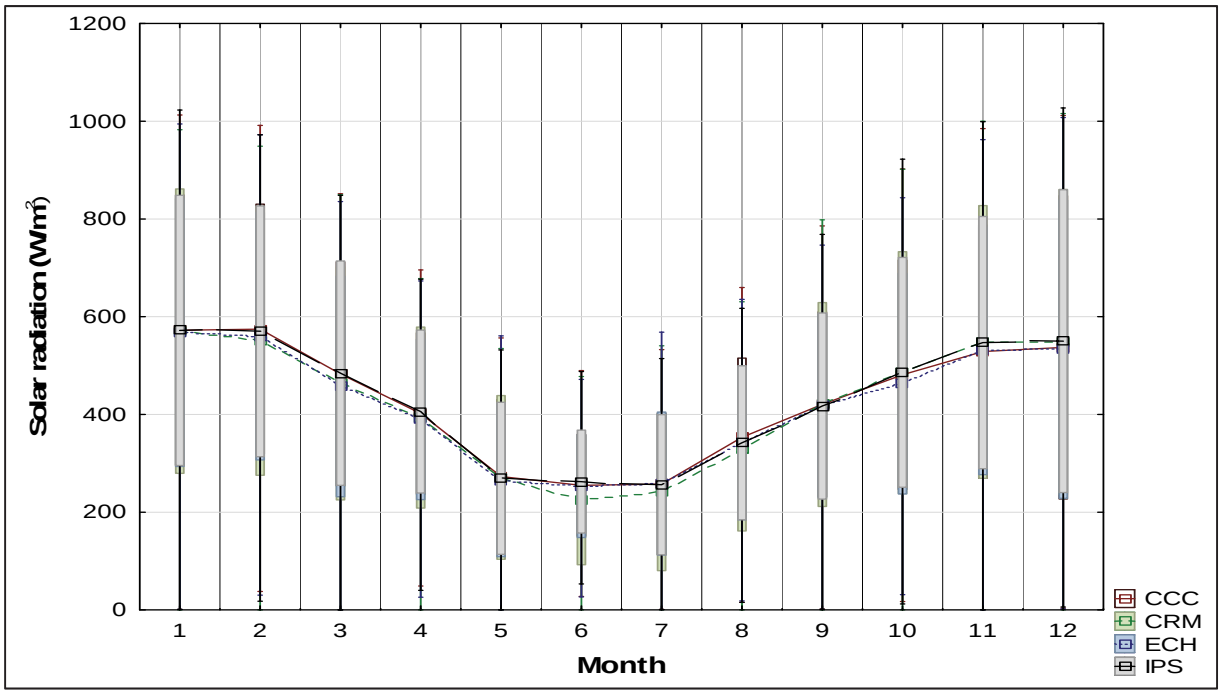

Figure 130: The present day mean monthly solar radiation for Voëlvlei Dam (W/m^2)

Figure 130 and Table 48 show the mean monthly daily solar radiation for the 20 year present day simulation period for each of the four climate change models over Voëlvlei dam. This figure followed a similar shape as that for air temperature.

Table 48: The present day mean monthly solar radiation for Voëlvlei Dam (W/m^2)

	Jan	Feb	Mar	Apr	May	June	July	Aug	Sep	Oct	Nov	Dec
CCC	572.41	574.81	482.98	401.93	272.96	255.17	257.74	353.15	420.71	481.32	528.79	537.51
CRM	570.46	550.86	463.63	393.87	271.20	224.97	241.44	329.92	420.39	485.71	548.43	548.74
ECH	567.62	560.20	457.54	390.07	265.55	253.29	258.58	341.92	417.73	463.23	530.32	533.86
IPS	572.12	570.31	484.59	406.02	269.51	262.68	256.26	342.25	417.40	486.36	547.11	550.12

From the table and figure, it was seen that the climate models agreed well with each other. Summer was December, January and February, whilst winter was June, July and August for the Western Cape Province, the location of Voëlvlei dam. The solar radiation was on average almost double in summer to that of winter, which was attributed to the longer daylight hours during summer. The phenomena of higher solar radiation in summer should have a marked effect on the diurnal temperature of the dam (Wetzel, 2001 and others) and its influence along with air temperature was investigated in the following sections.

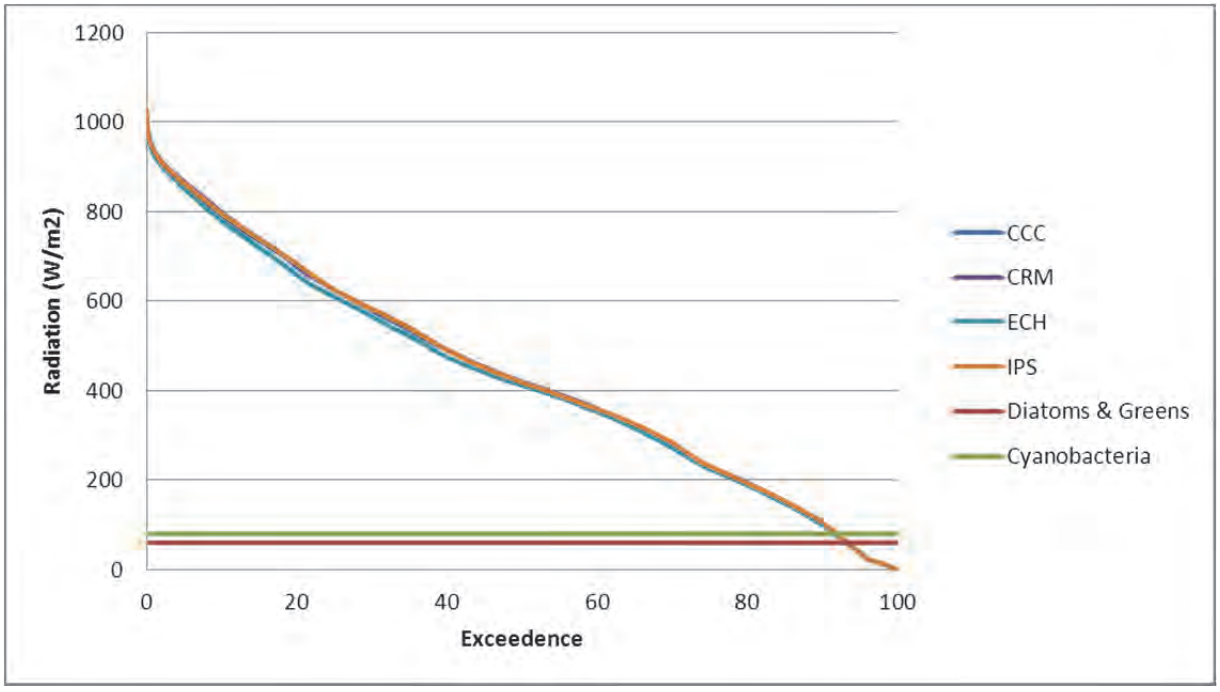

Figure 131: The present day solar radiation exceedance for light saturation with respect to algal growth for Voëlvlei dam

To investigate the effect of solar radiation on the light saturation of algal groups modelled, Figure 131 shows that approximately for 93% of the simulation period that the solar radiation

exceeded that of the maximum algal light intensity for maximum photosynthetic rate for all the algal groups. This would implied that only for 7% of the time the light intensity was such that the surface algal groups were at maximum growth and for the rest of the time it was less than this. This was a consequence of the choice of algal constants but these values were supported by literature. This would imply that these particular algal groups prefer less sunny conditions i.e. they prefer shade.

The four climate models agreed in solar radiation magnitude and its peaks were greater in summer than winter.

9.10 Wind-speed and direction

Wind-speed and direction was not supplied by CSAG (UCT) and was a limitation. CE-QUAL-W2 requires wind-speed and direction as part of its meteorological data input to predict water quality. In the absence of this wind-speed and direction was replicated from past data. For 1971 the recorded wind-speed and direction from 1 January 1971 to 31 December 1971 was repeated for the 20 years of all the simulation periods including the intermediate and future events, in the absence of any downscaled data. This should not be a problem as the study was to examine changes in eutrophication due to varying climate conditions.

Figure 132: The N-S orientation of Voëlvlei dam

Figure 132 shows that the reach of Voëlvlei dam was almost exactly oriented in a NS direction and the subsequent effect of the prevalent wind over the dam was investigated.

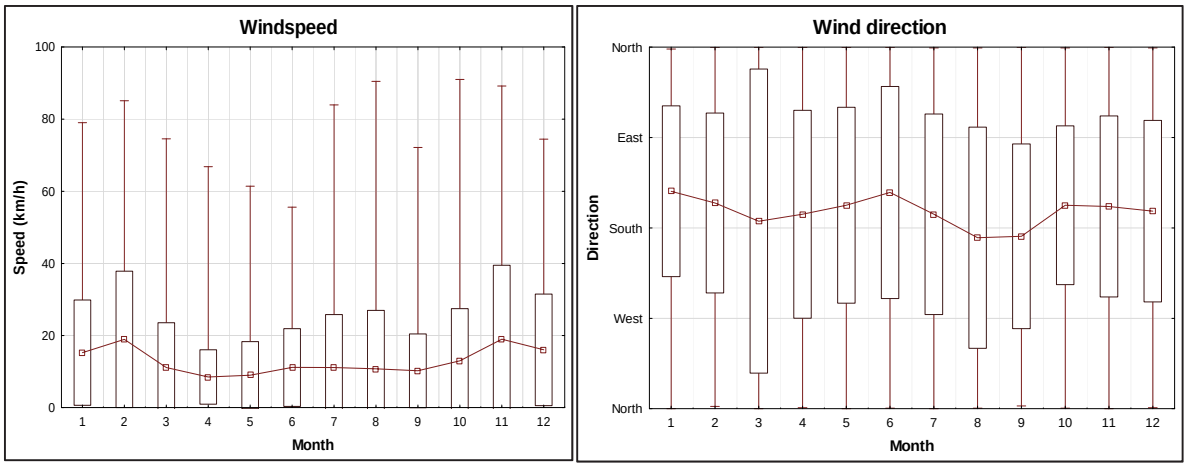

Figure 133: The present day wind-speed and direction for Voëlvlei dam

From Figure 133 it was seen that the predominant annual wind was between south and south-west and thus somewhat along the S-N axis and was strongest during summer. Since the dam was relatively shallow (10-15m) this wind and the hydraulics of the dam caused complete mixing as confirmed by the tracer concentrations as seen in Figure 126.

9.11 Surface water temperature

Wetzel (2001), DeNicola (1996) and other argue that solar radiation was the major driver for surface water temperature, thus the following two figures shows the surface water temperature of segment 11 for the present day 20 year climate models.

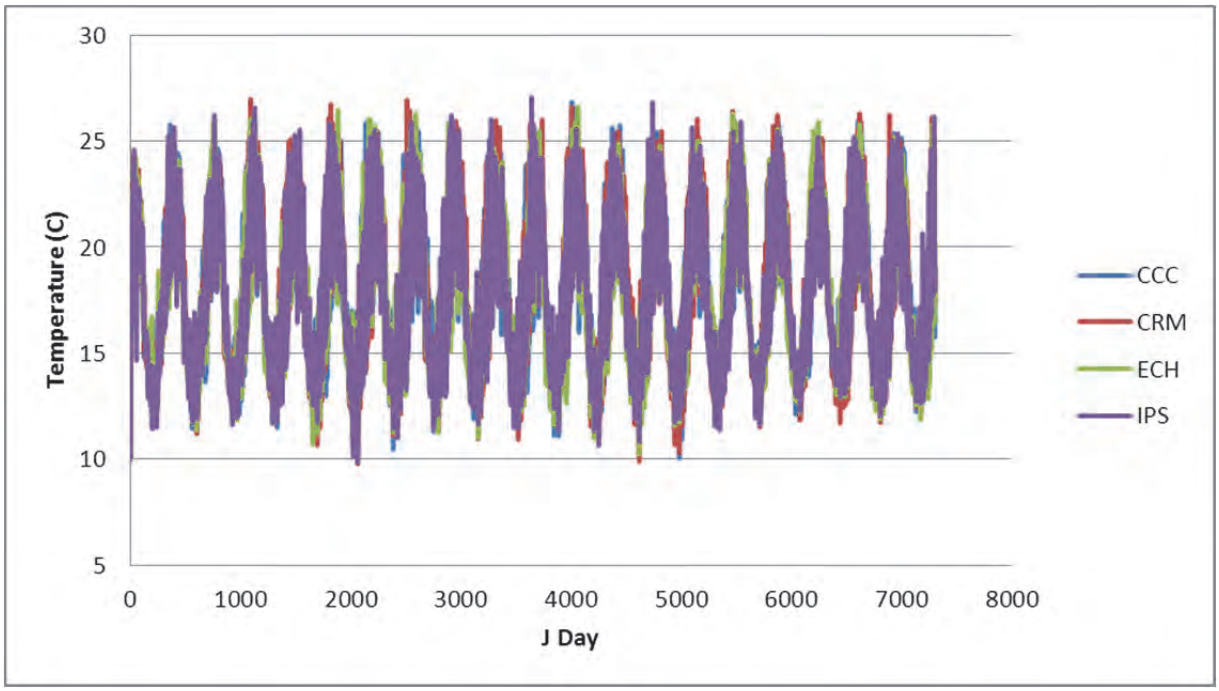

Figure 134: The present day surface water temperature at segment 11 of Voëlvlei Dam (°C)

This figure shows the seasonal temperature fluctuations coinciding with the peaks and troughs of Figure 134 as well as the agreement between the various climate models producing similar surface water temperatures at segment 11. If the 20 year present day simulation period was further subdivided into monthly segments the following figure results.

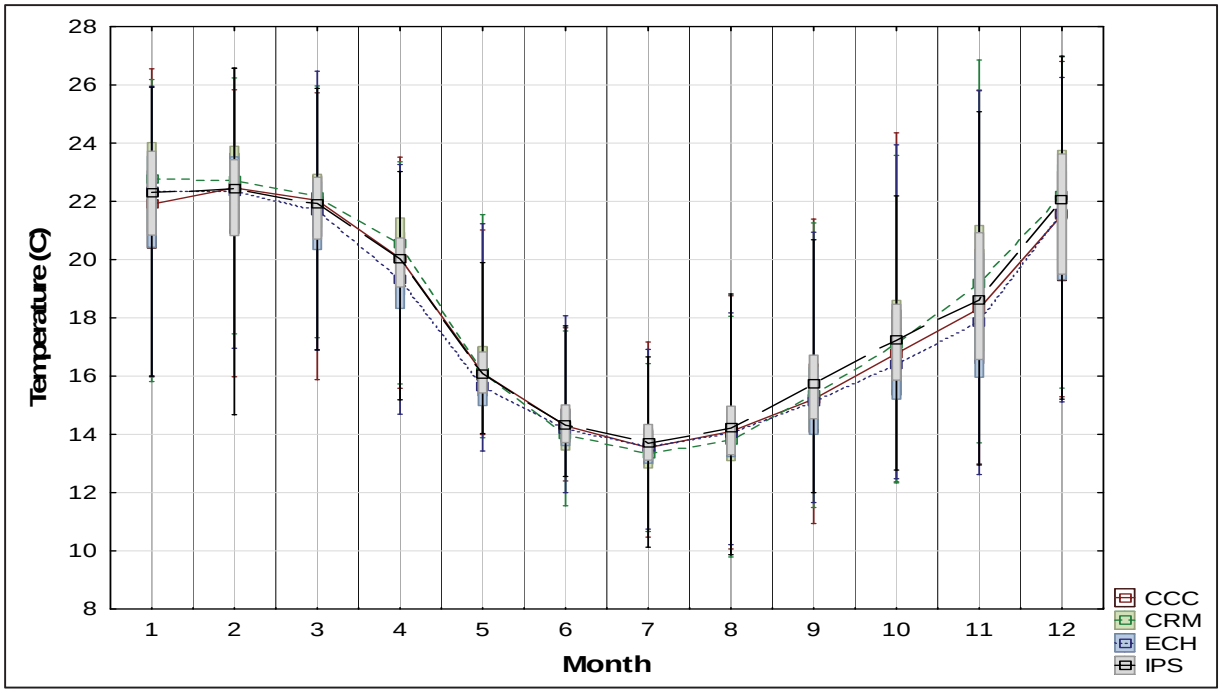

Figure 135: The present day mean monthly surface water temperature for segment 11 of Voëlvlei Dam (°C)

When comparing Figure 130 and Figure 135 a confirming relationship was observed in that months with high solar radiation resulted in high surface water temperatures. There was a notable temperature drop between April and May and this was considered the onset of winter just as there was a notable temperature increase from November to December signalling the onset of summer. These trends are verified by the four climate change models. From this, it was deduced that an increase in solar radiation would increase the surface water temperatures and consequently may cause an increase in the number of algal blooms if all other conditions (nutrients, turbidity etc.) are favourable. This cycle would predict the annual seasonal blooms in the dam.

Table 49: The present day mean monthly surface water temperature of Voëlvlei Dam (^{o}C)

	Jan	Feb	Mar	Apr	May	June	July	Aug	Sep	Oct	Nov	Dec
CCC	21.6	22.2	21.7	19.8	16.3	14.4	13.6	14	15.3	16.9	18.4	21.2
CRM	22.4	22.5	22.0	20.3	16.3	14.1	13.4	13.7	15.3	17.2	19.1	21.7
ECH	22.0	22.2	21.4	19.3	15.8	14.3	13.6	14.0	15.2	16.5	18.1	21.3
IPS	22.1	22.1	21.7	19.8	16.2	14.4	13.7	14.1	15.7	17.2	18.8	21.6

Table 49 shows that the surface water temperature of Voëlvlei dam was on average 5.3^{o}C warmer in summer than winter with an annual surface water temperature of 18^{o}C. All four climate models showed similar trends and values. Thus, it was expected that if all conditions are favourable, then an increase in the concentration of algae was expected in the summer period due to the average summer surface water temperature coinciding within the temperature rate multipliers for the diatoms, greens and cyanobacteria modelled in Voëlvlei dam (Table 44).

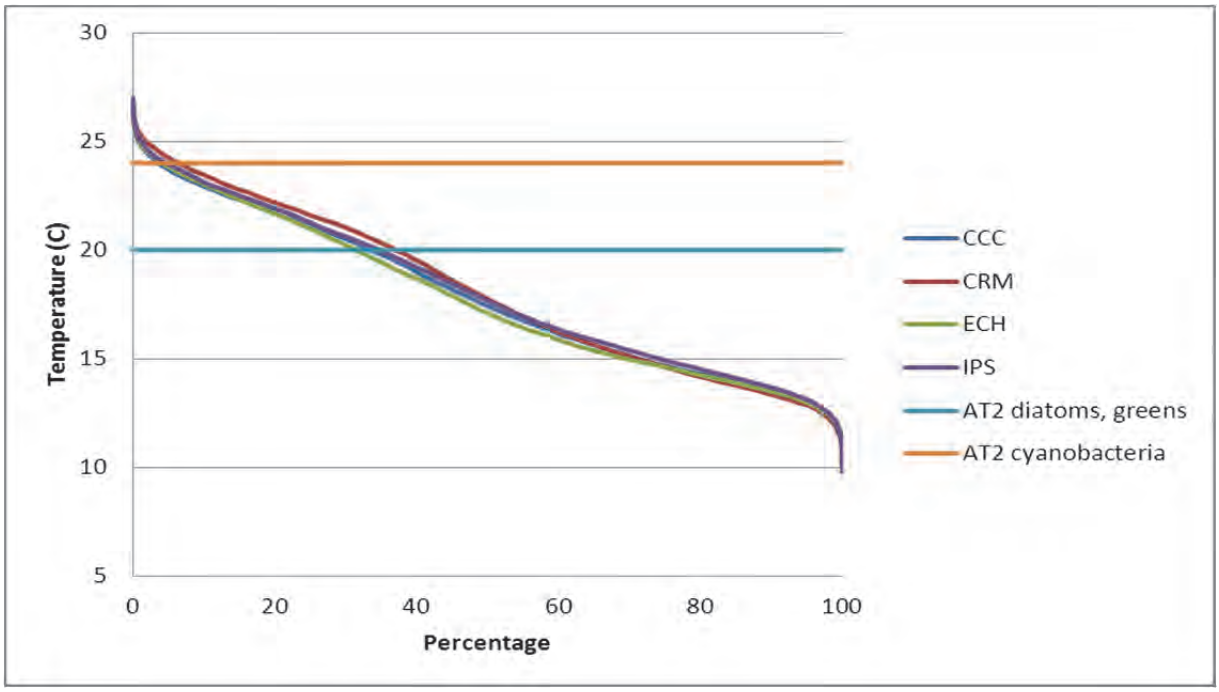

Figure 136: The present day surface water temperature exceedance plot with respect to algal growth for Voëlvlei Dam

To establish the probability of the types algal blooms, an exceedance plot (Figure 136) was generated showing the algal temperature growth multipliers. The temperature rate multiplier for diatoms and greens that set the lower temperature limit for maximum growth was exceeded between 33 and 38% of the simulation time. Cyanobacteria have a higher maximum temperature growth rate and this temperature was exceeded between 5 and 8% of the time of the 20-year simulation at segment 11. It was hereby supposed that diatoms and green algae could be present in Voëlvlei dam for up to 38% of the time and cyanobacteria up to 8% of the time, due to the temperature being favourable for their growth.

The higher solar radiation of summer caused higher surface water temperatures in summer than winter.

9.12 Surface water elevation

The factors affecting surface water elevations were:

- Inflow
- Withdrawals
- Evaporation

The inflows and withdrawals were kept the same for each year as well as for each model, thereby implying that the only evaporation could change water levels due to climate change. The surface water elevation for the 20-year present day period was shown in the following figure as well as its monthly values. The various undulations are a product of the inflow and withdrawals and the inter-variation between climate models was a result of the evaporative differences between models.

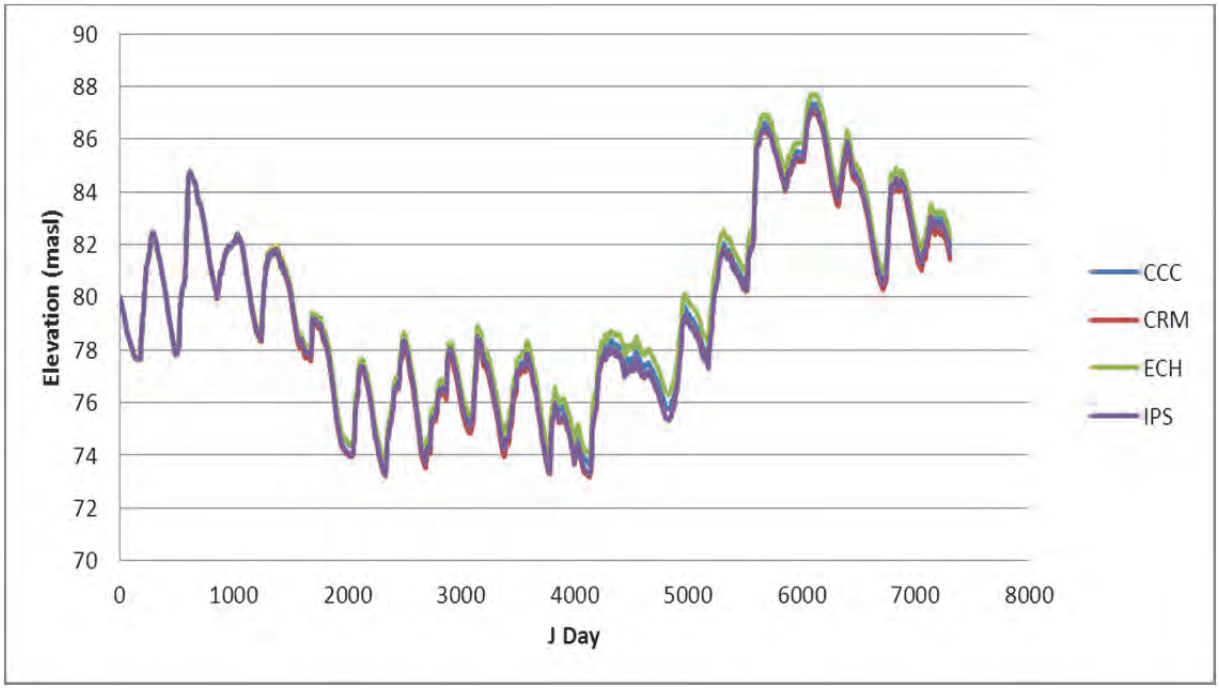

Figure 137: The present day surface water elevation of Voëlvlei Dam (masl)

Figure 137 shows close agreement within all the climate models for the 20 year present day simulation period. The surface water level discrepancies are attributed to the inter-climate model air temperature and solar radiation causing varying rates of evaporation and subsequent different surface elevations.

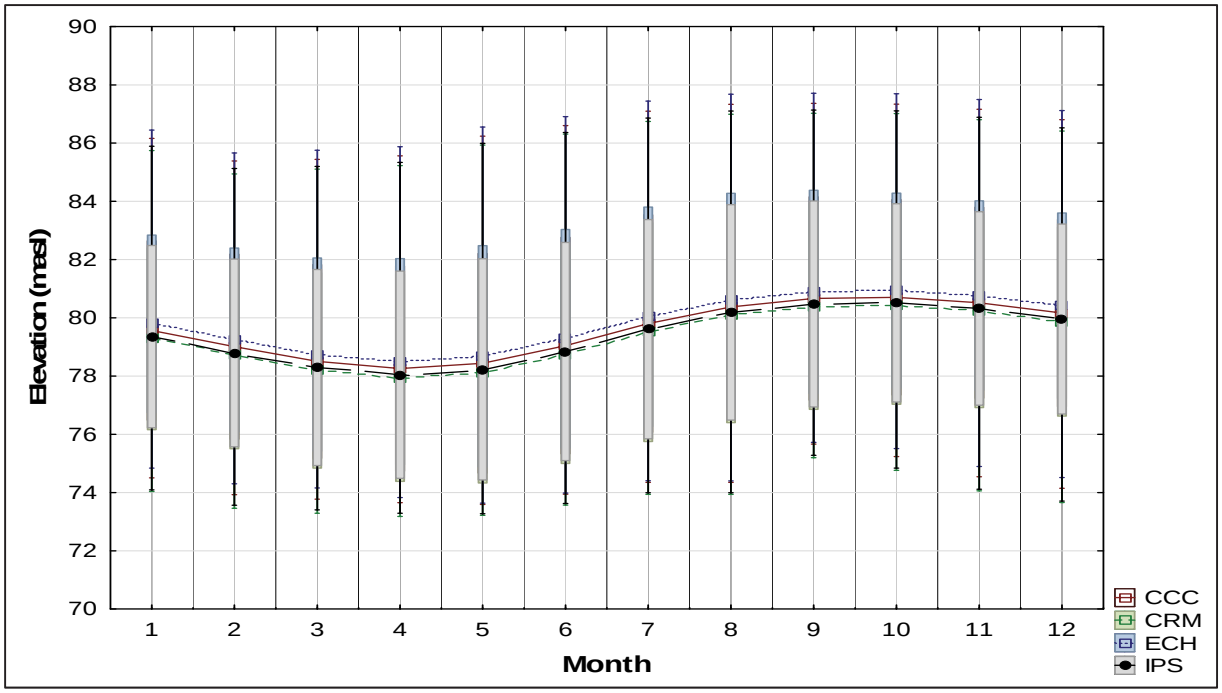

Figure 138: The present day monthly surface water elevations of Voëlvlei Dam (masl)

Figure 138 and Table 50 show the monthly surface elevations as well as the inter-variation between climate models for the current set of inflow and withdrawals into Voëlvlei dam during the period of the simulation. It was clear that the air temperature difference between climate models was similar and that the subsequent surface water elevations were relatively small.

Table 50: The present day mean monthly surface water elevations of Voëlvlei Dam (masl)

	Jan	Feb	Mar	Apr	May	June	July	Aug	Sep	Oct	Nov	Dec
CCC	79.6	79.0	78.5	78.3	78.4	79.0	79.8	80.4	80.7	80.7	80.5	80.2
CRM	79.3	78.7	78.2	77.9	78.1	78.7	79.5	80.1	80.4	80.4	80.2	79.9
ECH	79.8	79.2	78.7	78.5	78.7	79.3	80.0	80.6	80.9	80.9	80.8	80.4
IPS	79.4	78.8	78.3	78.0	78.2	78.8	79.6	80.2	80.5	80.5	80.3	80.0

The dam showed the lowest level at the end of summer and onset of autumn, corresponding to March and April and this continued until the rains of late autumn and early winter inflow whereby the capacity was augmented.

It was seen that the dam has a stable monthly surface elevation that oscillates by about 2 masl on a monthly basis and that all the climate models agreed well with each other.

9.13 **Algal nutrient inflow concentrations**

Voëlvlei dam is an off-channel dam and water is pumped to it from the Klein Berg and Twenty Fours Rivers. The only water quality constituents pertinent to this study were measured on an irregular basis was the surface concentrations of PO_4, ammonium, nitrate-nitrites and dissolved silicon at the dam wall.

The total inflow of PO_4, NH_4 and NO_3 is shown in Figure 139 and it shows that the concentration of phosphates and ammonium entering the dam was stable but that the nitrate-nitrite concentration fluctuates on a monthly basis, probably due to it being downstream of a MWWTP. The inflow concentration of phosphates and nitrogen was of adequate concentration so that it was not considered to be limiting for algal growth.

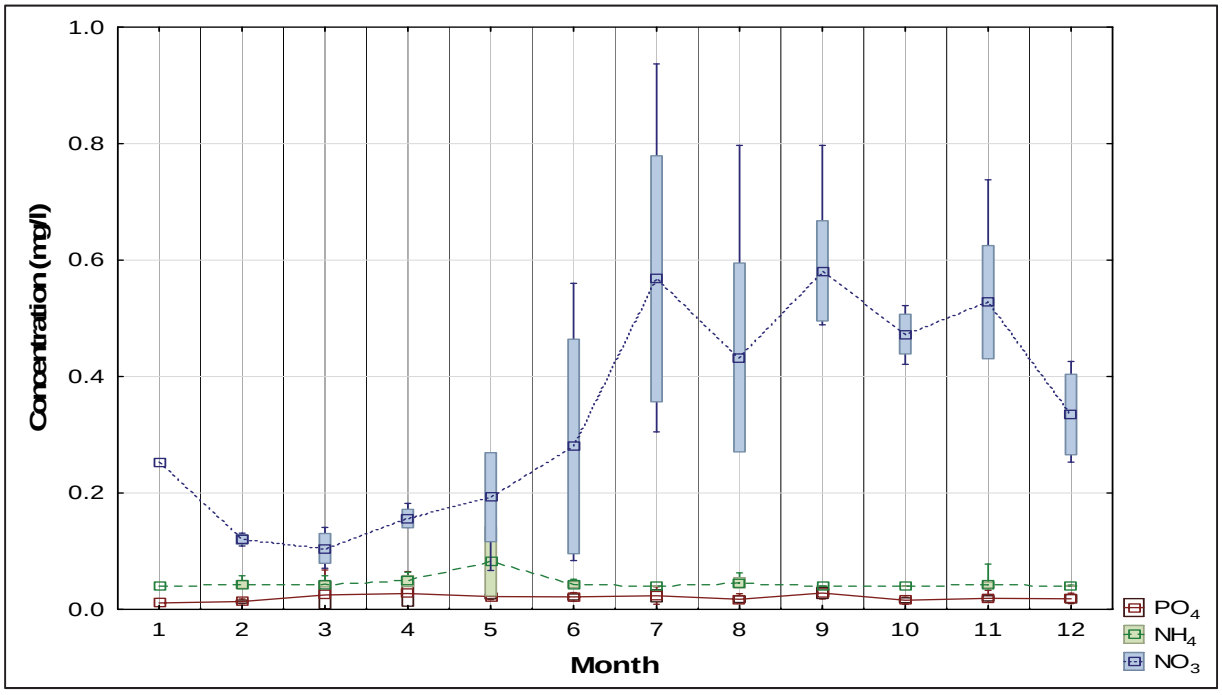

Figure 139: The present day algal nutrient inflow concentration of Voëlvlei dam (mg/l)

The dissolved silicon inflow concentration for the two inflow canals shown in Figure 140 fluctuates monthly but the overall concentration was not low enough to be limiting for diatom growth.

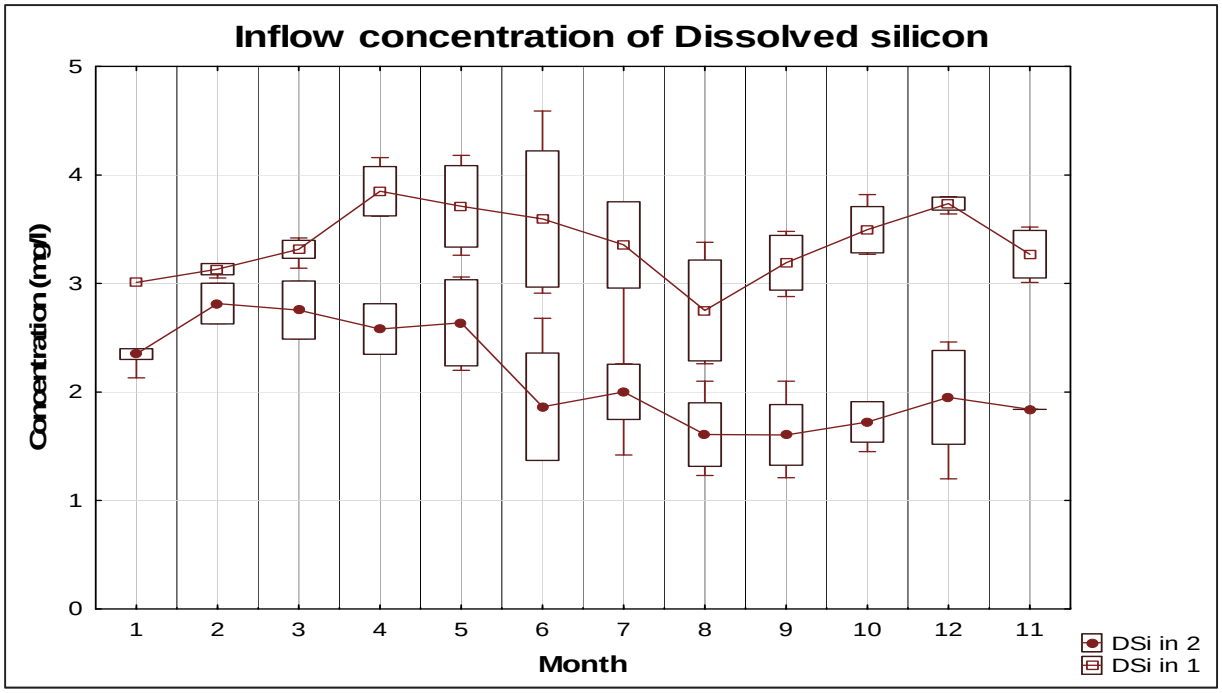

Figure 140: The present day dissolved silicon inflow concentration of Voëlvlei Dam (mg/l)

These inflow concentrations and volumes would not change for the intermediate future and distant future simulations thus allowing for a direct comparison with the only effect on the surface water being that of climate change. This allowed for a direct comparison of climate change influence on Voëlvlei dam, as it assumed that the current set of operating parameters would be valid.

9.14 Ortho-Phosphorous concentration

The phosphorous concentration within the dam was influenced by various factors such as inflow and withdrawal quantities as well as assimilation by the various algae as it was the limiting nutrient for algal growth. The fluxes affecting in-dam phosphorous concentrations are shown in Figure 37 as used by the CE-QUAL-W2 model. The present day ortho-phosphorous concentration for Voëlvlei dam of the four climate models was shown in Figure 141, Figure 142 and Table 51.

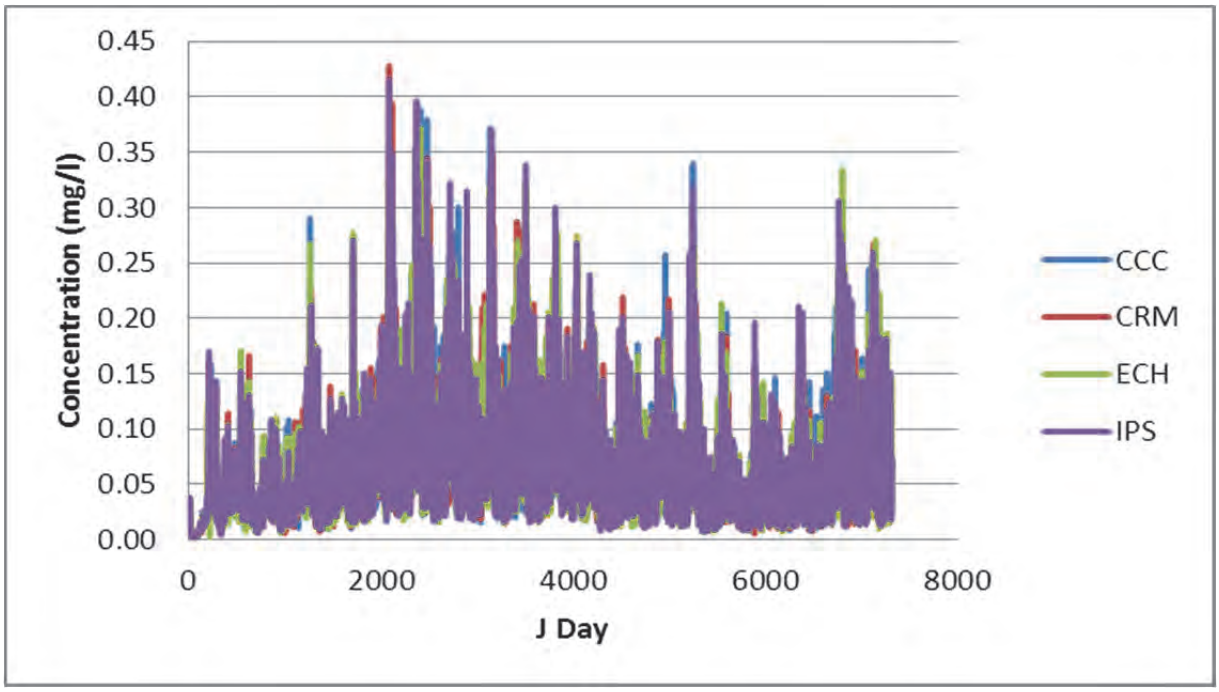

Figure 141: The present day surface ortho-phosphorous concentration of Voëlvlei Dam (mg/l)

The phosphorous concentrations agree well using the recorded set of inflow and withdrawals from Voëlvlei dam. This shows that the inter-climate sink of phosphorous was the same as all the climate models agree well with each other. The average concentration was shown in Figure 142 and was above the level of 0.025 mg/l set by the then DWAF in 1985 (DWA, 2011). It noted that Harding still critiques this value and suggests a value of 0.35 µg/l could limit eutrophication.

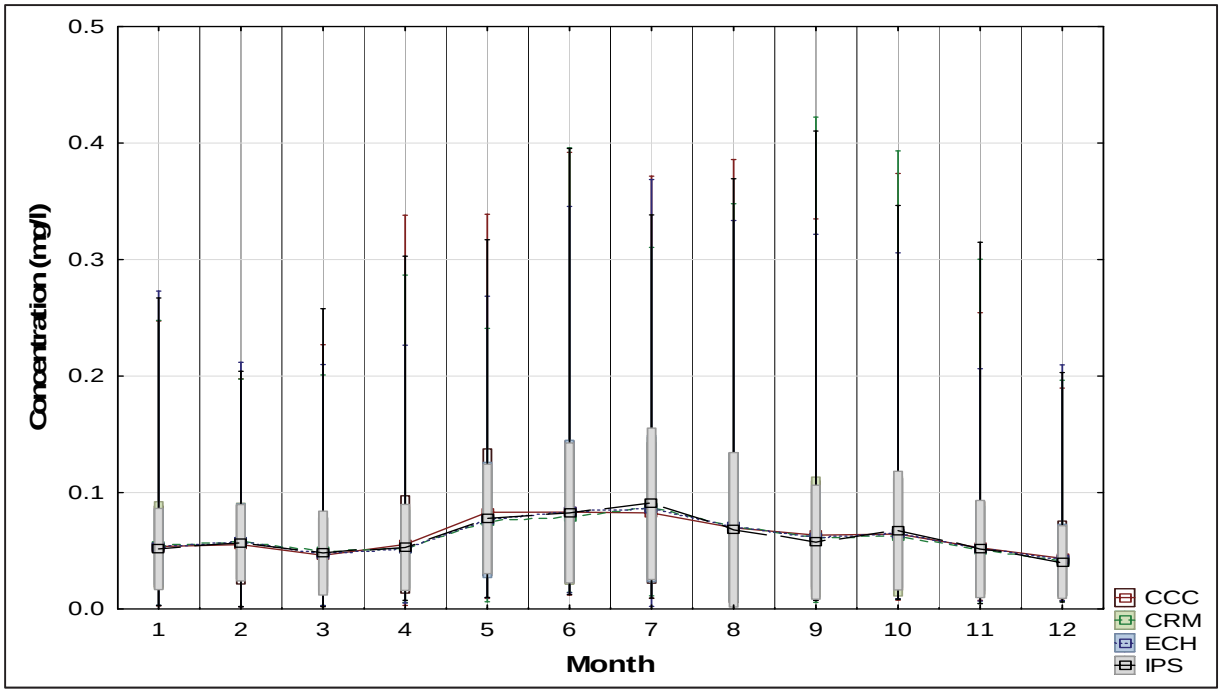

Figure 142: The present day monthly surface ortho-phosphorous concentration of Voëlvlei Dam (mg/l)

Table 51: The present day mean monthly surface ortho-phosphorous concentration of Voëlvlei Dam (mg/l)

	Jan	Feb	Mar	Apr	May	Jun	Jul	Aug	Sep	Oct	Nov	Dec
CCC	0.054	0.055	0.046	0.055	0.083	0.083	0.083	0.070	0.063	0.064	0.053	0.044
CRM	0.055	0.058	0.049	0.052	0.076	0.079	0.087	0.070	0.062	0.063	0.051	0.041
ECH	0.053	0.058	0.047	0.052	0.076	0.084	0.086	0.071	0.061	0.065	0.052	0.042
IPS	0.052	0.057	0.048	0.053	0.077	0.083	0.090	0.068	0.057	0.067	0.051	0.040
Monthly mean	0.053	0.057	0.048	0.053	0.078	0.082	0.087	0.070	0.061	0.065	0.052	0.042

It was clear that phosphorous has an annual cycle with maximum concentrations reached during winter and the concentration was sufficiently high enough so as not to limit algal. From Table 44 it was seen that the phosphorous half saturation constants for diatoms are 0.002 mg/l, greens 0.38 mg/l and cyanobacteria 0.011 mg/l. The half saturation was defined as the concentration at which the uptake of phosphorous was half the maximum rate, thereby limiting algal growth. From Table 51 it was seen that these values are always exceeded except for that of the greens. This would imply that on average green algae was phosphorous limited for segment 11 at the surface. The corollary was that should the phosphorous loading increase, the growth of green algae could become unabated, as presently there are already peak concentrations beyond 0.38 mg/l.

If algal blooms were to be controlled, it would be imperative to abate the inflow of phosphorous into Voëlvlei dam. This would be achieved by lowering the inflow concentrations via legislation and applying new technologies or some form of cleaner production to the WWTP upstream to the dam of phosphates as well as eliminating non-point source.

The mean level of 0.025mg/l of phosphorous (DWA limit) in the dam was exceeded for most the duration of the present day simulation, thus ensuring an oversupply of phosphorus as nutrient for algal growth. Only green algae may become limited as its phosphorous half saturation constant was seldom exceeded.

9.15 Nitrogen concentration

Nitrogen was an abundant element in nature and was an essential building block of proteins and a constituent of chlorophyll. The sources of N with respect to water quality tests are ammonia (NH_3), ammonium (NH_4^+), nitrites (NO_2^-) and nitrates (NO_3^-) as well as atmospheric N which was fixed by certain algae. From the aspect of eutrophication, it was very seldom that nitrogen was the limiting nutrient within a water-body as it was so abundant.

Ammonia was produced by the decomposition of organic matter that contains ammonia as well as being a constituent of sewage and industrial effluents. Nitrite occurs naturally as an anion in fresh and sea waters, whereas anthropogenically it was introduced to receiving waters as wastes from aquaculture, sewage effluents and industrial effluents. Nitrates are scarce in natural water sources as they are constantly being depleted by the process of photosynthesis, converting nitrates to organic nitrogen. For the purpose of this study both ammonium and nitrites were included in the inflow into Voëlvlei dam.

9.16 Ammonium concentration

Ammonia exists in two forms in nature (ammonium and ammonia) and the equilibrium concentrations are governed largely by pH (Chapra, 2008). Figure 143, Figure 144 and Table 52 shows the surface ammonia concentration at segment 11 of Voëlvlei dam for the 20-year present day simulation.

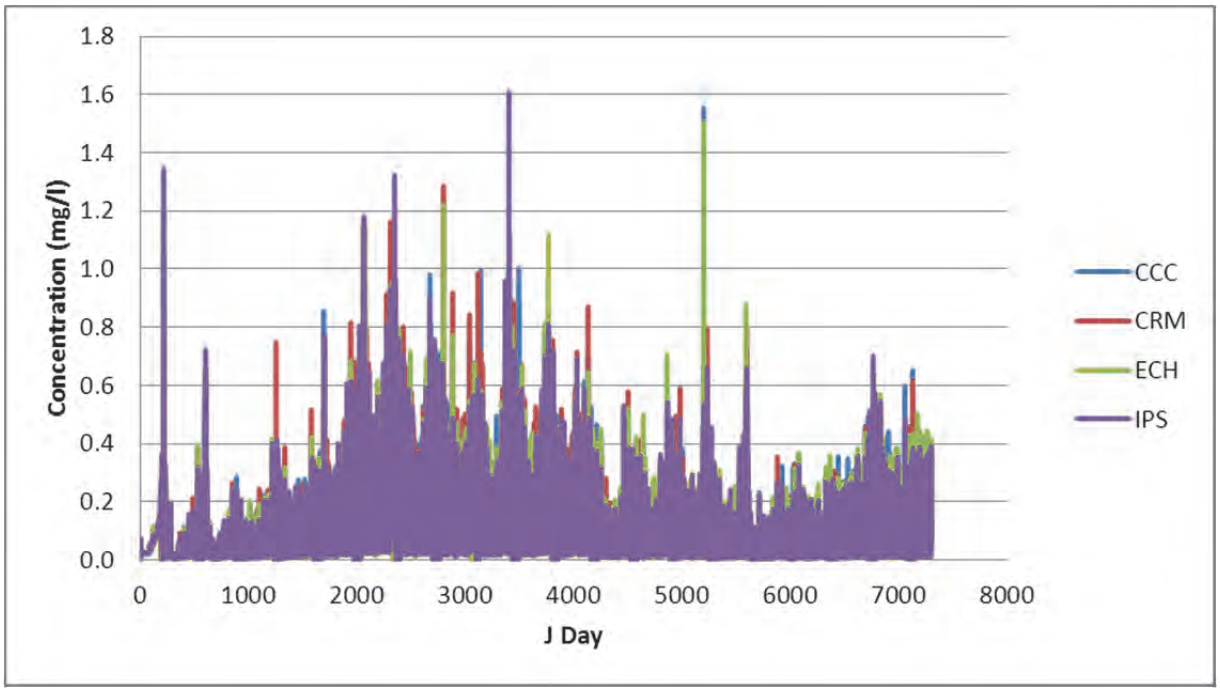

Figure 143: The present day surface ammonium concentration of Voëlvlei dam (mg/l)

Cyanobacteria such as *Anabaena* sp. and others can utilise the nitrogen present in the atmosphere for growth and hence it was not seen as limiting for their growth (Dallas, 2004) and for this study they were modelled as nitrogen fixing. From an eutrophication management aspect, it was easier to manage and police the anthropogenic loading of a water system so that the subsequent abatement of eutrophication may take place but the case for nitrogen management was not easy or practical as it was abundant in the system. Nitrogen was essential for growth but rarely a limiting growth element for algae.

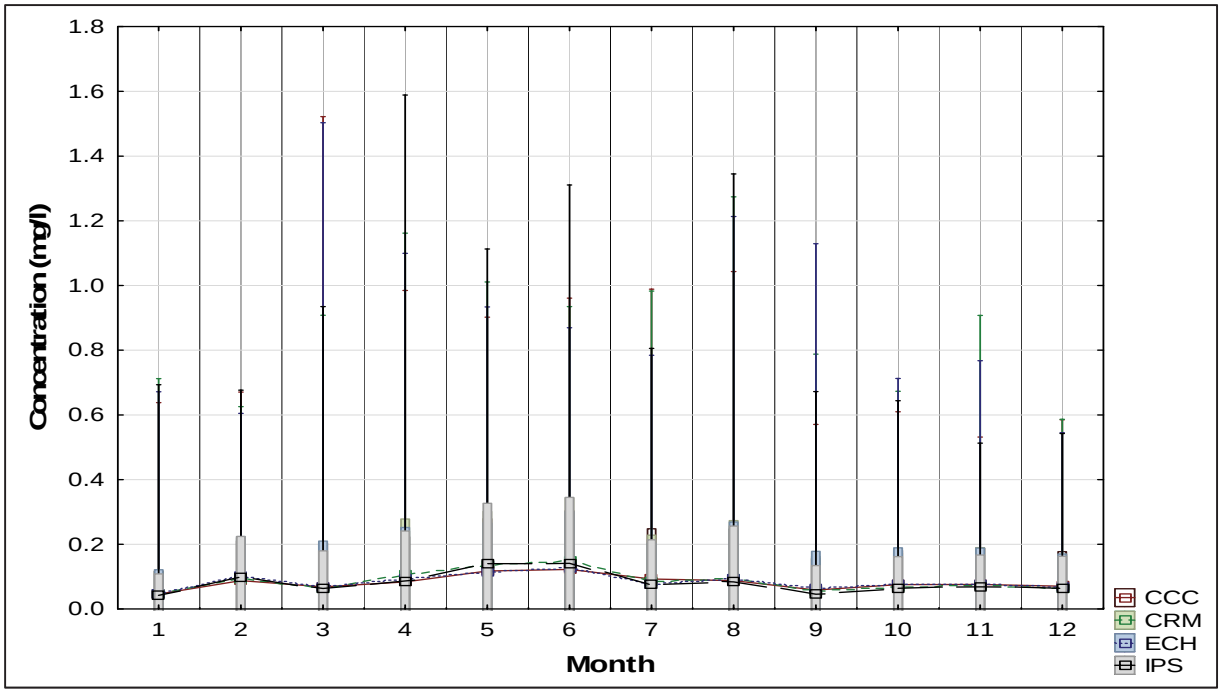

Figure 144: The monthly present day surface ammonium concentration of Voëlvlei Dam (mg/l)

From Figure 144 and Table 52 it was seen that the surface ammonium concentration was a maximum during May and June and was in sufficient concentration so as not to limit algal growth. The climate models also show little inter-variability and the results compare well with each other.

Table 52: The present day mean monthly surface ammonium concentration of Voëlvlei Dam (mg/l)

	Jan	Feb	Mar	Apr	May	June	July	Aug	Sep	Oct	Nov	Dec
CCC	0.046	0.088	0.069	0.084	0.118	0.123	0.093	0.088	0.058	0.076	0.076	0.071
CRM	0.046	0.096	0.063	0.105	0.136	0.149	0.086	0.093	0.056	0.068	0.073	0.065
ECH	0.049	0.101	0.068	0.095	0.115	0.125	0.076	0.094	0.064	0.078	0.077	0.067
IPS	0.042	0.098	0.064	0.087	0.142	0.141	0.078	0.084	0.046	0.064	0.069	0.065

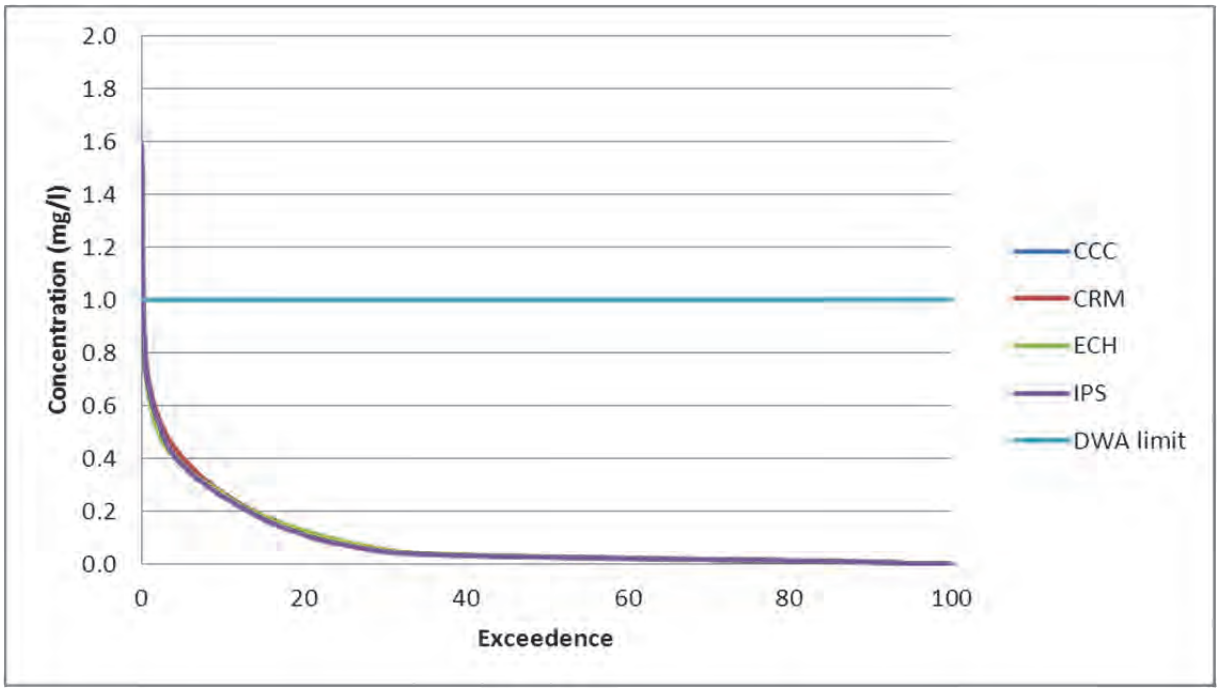

Figure 145: The present day surface ammonium exceedance plot of Voëlvlei dam

The statutory limit for ammonium in surface water was set at 1mg/l by DWA and Figure 145 shows the exceedance plot for this limit. The figure shows that the surface ammonium concentration never exceeded the DWA limit of 1mg/l for any relevant time.

9.17 Nitrate-nitrite concentrations

Figure 146, Figure 147 and Table 53 show the surface Nitrate-nitrite concentrations for segment 11 of the present day 20-year simulation. It was assumed that low concentrations of nitrate-nitrites are due to assimilation by algae as well as redistribution in the water column (Figure 42).

The figures show an increase in concentrations at the surface during the winter months as well as close agreement for the climate models.

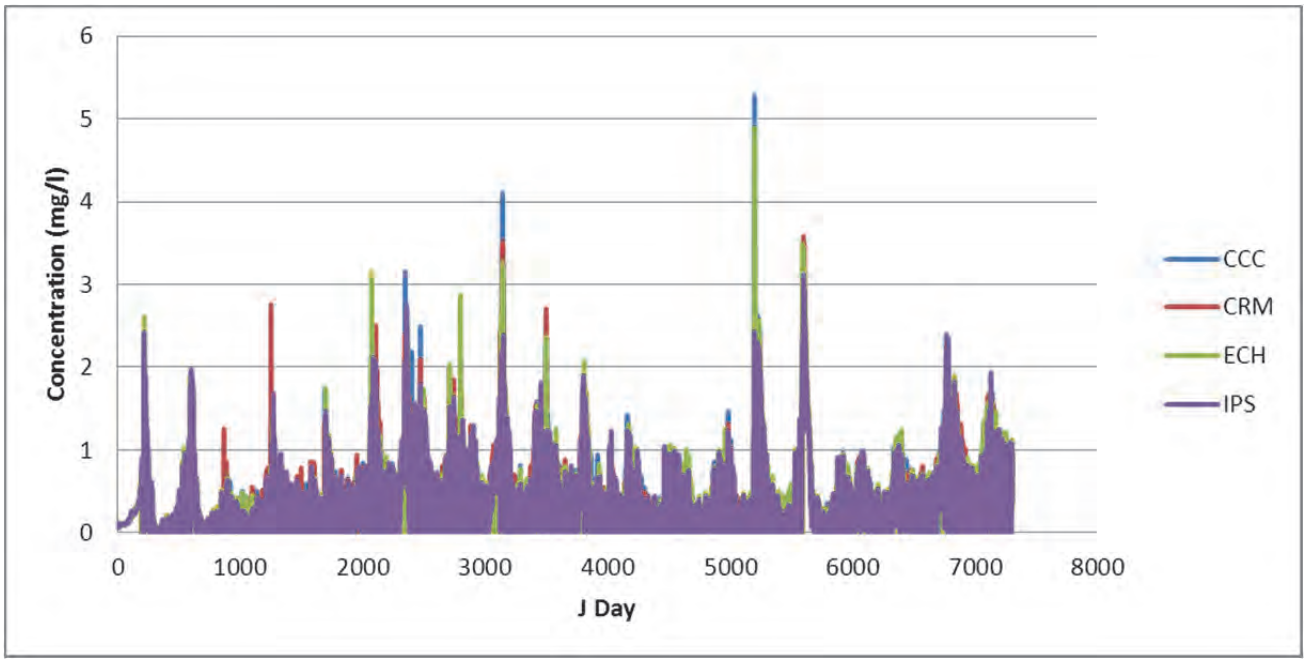

Figure 146: The present day surface nitrate-nitrite concentration of Voëlvlei Dam (mg/l)

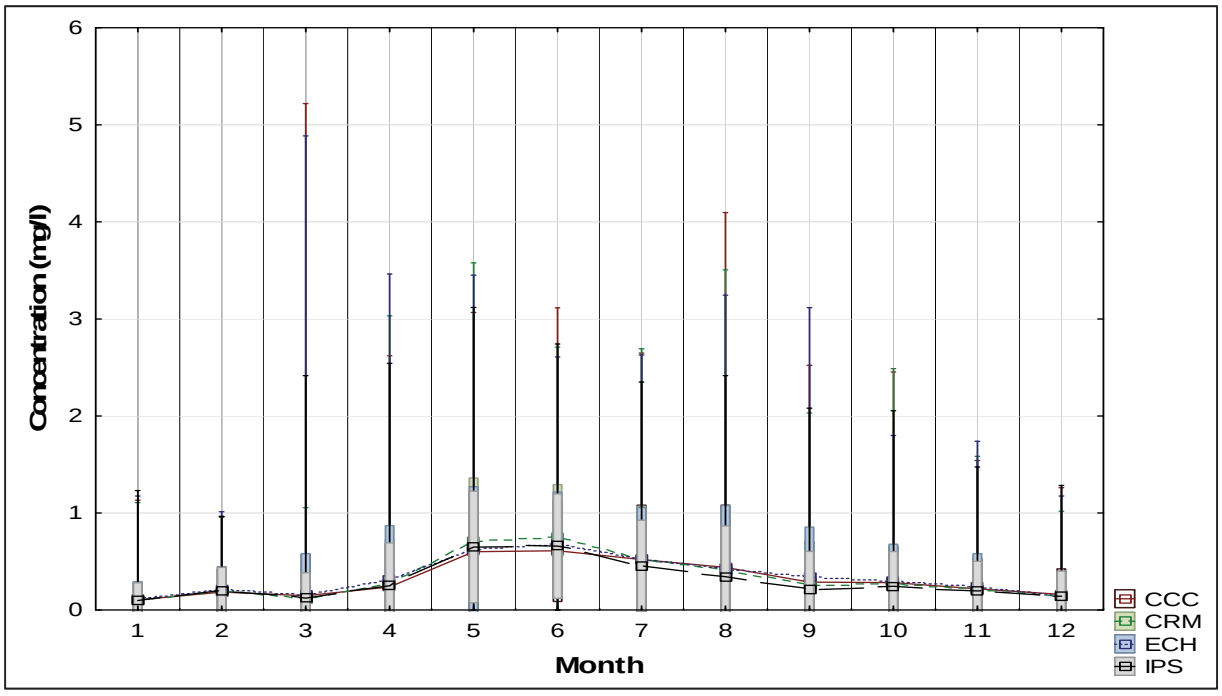

Figure 147: The present day monthly surface nitrate-nitrite concentration of Voëlvlei Dam (mg/l)

Table 53: The present day mean surface nitrate-nitrite concentration of Voëlvlei Dam (mg/l)

	Jan	Feb	Mar	Apr	May	June	July	Aug	Sep	Oct	Nov	Dec
CCC	0.105	0.185	0.147	0.239	0.603	0.611	0.522	0.441	0.288	0.284	0.218	0.161
CRM	0.105	0.204	0.116	0.264	0.715	0.746	0.522	0.409	0.260	0.263	0.208	0.136
ECH	0.112	0.214	0.152	0.314	0.622	0.676	0.524	0.432	0.345	0.297	0.241	0.148
IPS	0.099	0.205	0.123	0.25	0.65	0.659	0.454	0.345	0.211	0.246	0.198	0.142

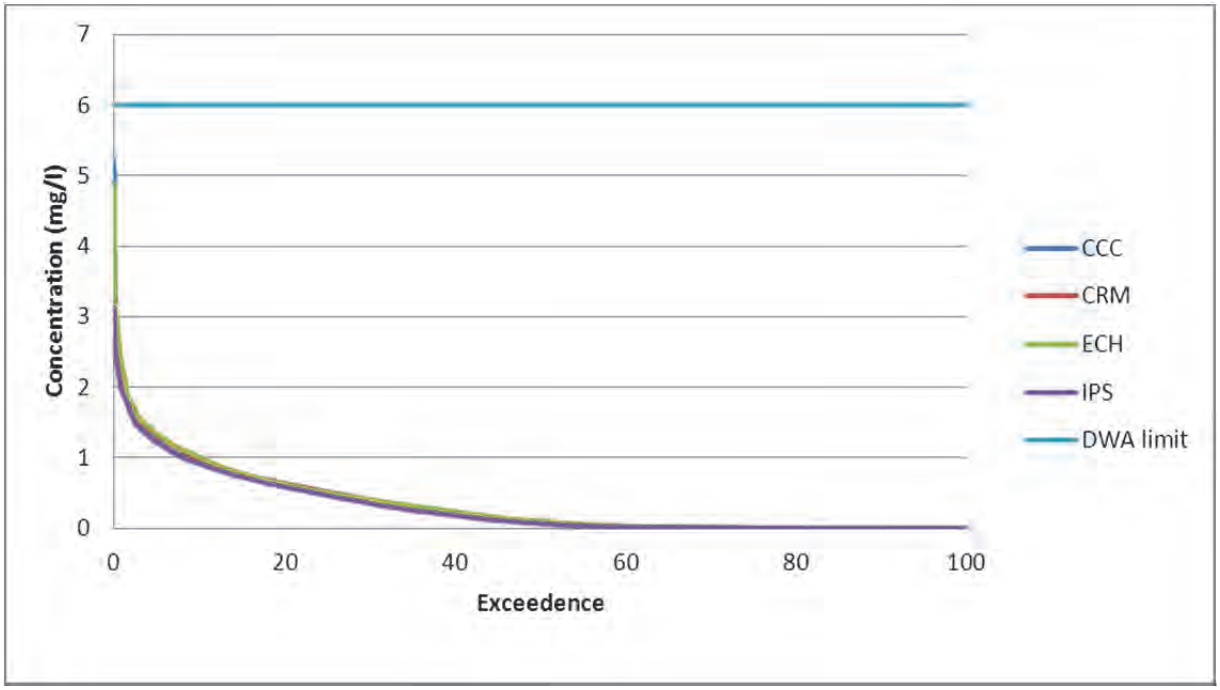

Figure 148: The present day surface nitrate-nitrite exceedance plot of Voëlvlei Dam

The statutory limit of 6mg/l of nitrate-nitrite as set by DWA was never exceeded for the present day simulation runs. This plot was shown in Figure 148.

9.18 Total nitrogen concentration and the half-saturation constant

The algal half-saturation constant for nitrogen and was defined as the nitrogen concentration (ammonium + nitrate/nitrite) at which the uptake rate was one-half the maximum rate. This represents the upper concentration at which algal growth was proportional to nitrogen and algal growth was nitrogen limited below this value. Table 54 gives the mean monthly surface nitrogen concentration. The nitrogen half-saturation constant was 0.01, 0.14 and 0 for diatoms, green algae and cyanobacteria respectively. From this, it was seen that only green algae could become growth limited by surface nitrogen.

Table 54: The present day mean monthly surface total nitrogen concentration of Voëlvlei Dam (mg/l)

	Jan	Feb	Mar	Apr	May	June	July	Aug	Sep	Oct	Nov	Dec
CCC	0.151	0.273	0.216	0.323	0.721	0.734	0.615	0.529	0.346	0.360	0.294	0.232
CRM	0.151	0.300	0.179	0.369	0.851	0.895	0.608	0.502	0.316	0.331	0.281	0.201
ECH	0.161	0.315	0.220	0.409	0.737	0.801	0.600	0.526	0.409	0.375	0.318	0.215
IPS	0.141	0.303	0.187	0.337	0.792	0.800	0.532	0.429	0.257	0.310	0.267	0.207

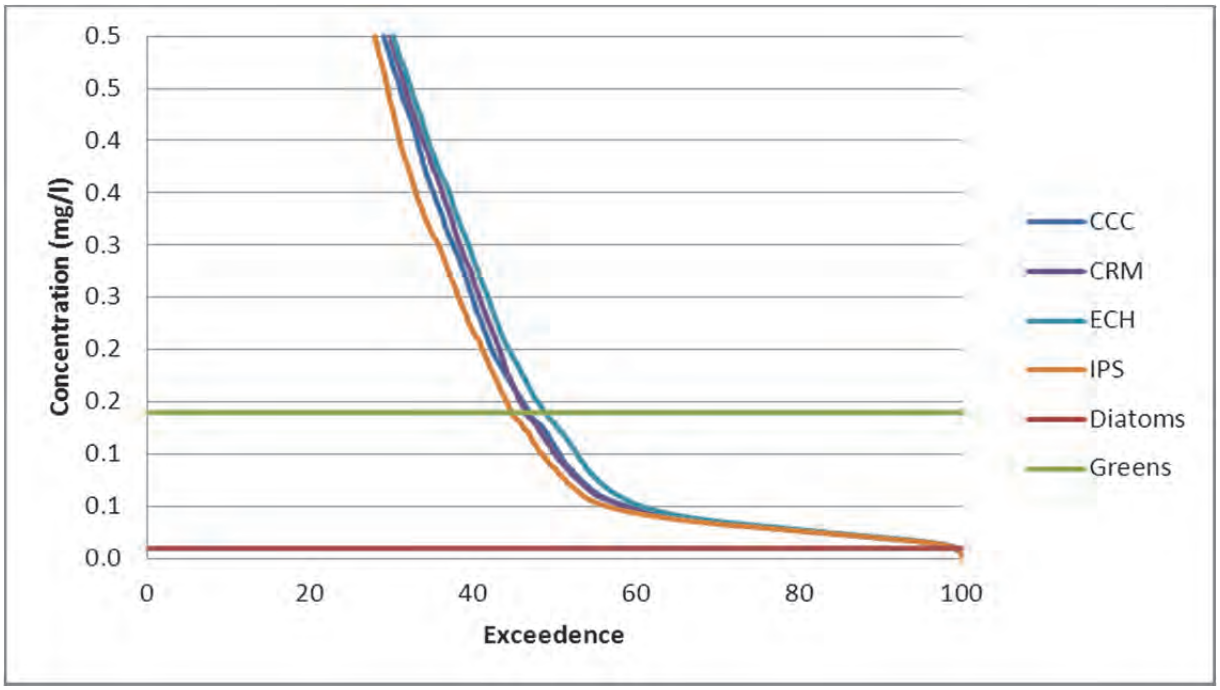

Figure 149: The present day surface total nitrogen half-saturation exceedance plot with respect to algae of Voëlvlei Dam

From the exceedance plot in Figure 149 green algae growth was limited as its half-saturation was not exceeded at the surface. Thus between 50 and 45% of the time this species of green algae was growth limited to half its maximum rate at the surface in the present day scenario. This would imply that if the total nitrogen concentration into the dam were to increase for the same conditions, the growth of green algae would be greater than currently presented.

9.19 Identifying the limiting nutrient

It had been established that the green algal species in Voëlvlei dam was limited for both phosphorous and nitrogen concentration at the surface. DWA uses the standard that if N:P > 25:1 then there was no problem with water quality. If N:P < 10 then eutrophic conditions exist. If N/P > 10 then P limits algal growth and if N/P < 10 the N limits algal growth.

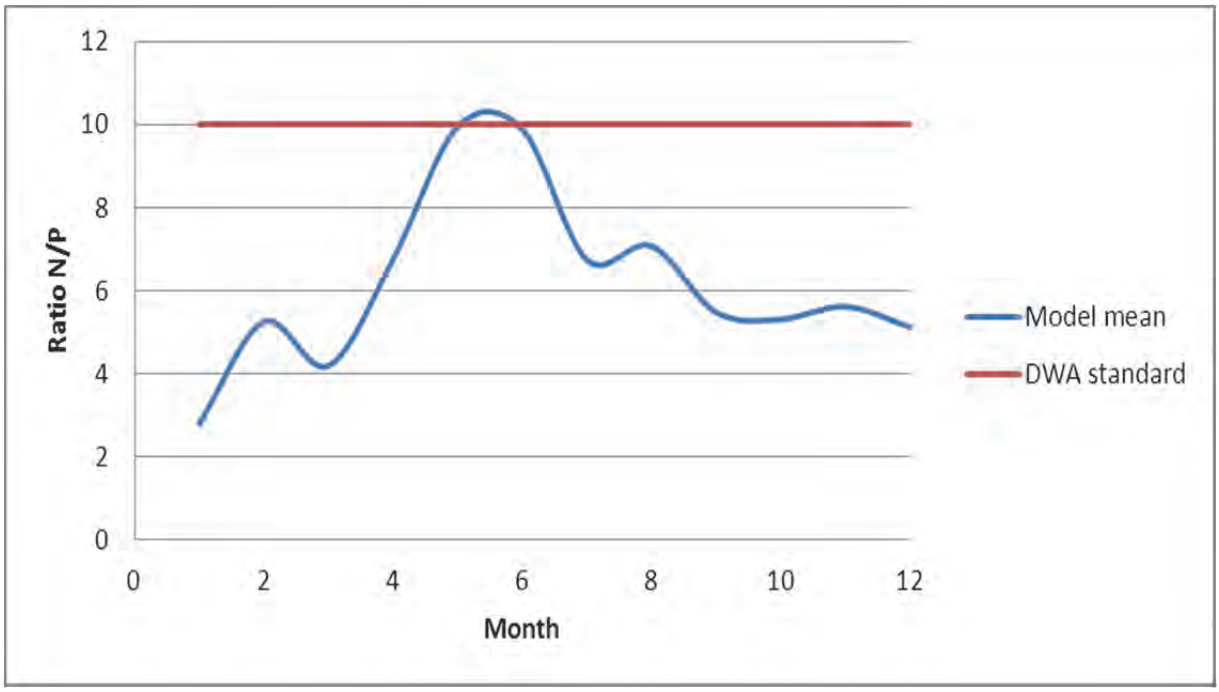

Figure 150: The present day limiting nutrient and trophic status as estimated from DWA standards of Voëlvlei Dam

From Figure 150 it was seen that the dam was eutrophic and nitrogen limits algal growth for the entire year except during winter when it switches to phosphorous limited algal growth at the surface. Thus, the limiting nutrient was seasonal.

It was thus deduced that to control the ingress of nitrogen into the dam would be unfeasible due to its natural abundance and the only realistic method to limit algal growth would be to limit the inflow of phosphorous into the dam.

9.20 Dissolved silicon concentration

The dissolved silicon concentration of the surface water for segment 11 was show in Figure 151. From the growth aspect of algae of this study it was only diatoms that are silicon growth limited as both the green algae and cyanobacteria are capable fixing nitrogen directly from the atmosphere and phosphorous was in abundance. The inflow concentration of dissolved silicon into Voëlvlei dam was shown in
Table 55 and graphically in Figure 140.

Table 55: Inflow concentration of dissolved silicon into Voëlvlei

Inflow	Mean (mg/l)	Minimum (mg/l)	Maximum (mg/l)	Std.Dev (mg/l).
1	3.385	2.26	4.59	0.453
2	2.050	1.20	3.06	0.535

The following figure shows that the dissolved silicon concentration was seasonal for the duration of the 20-year simulation period. It followed seasonal cycles with peaks and troughs, with the peaks occurring in winter.

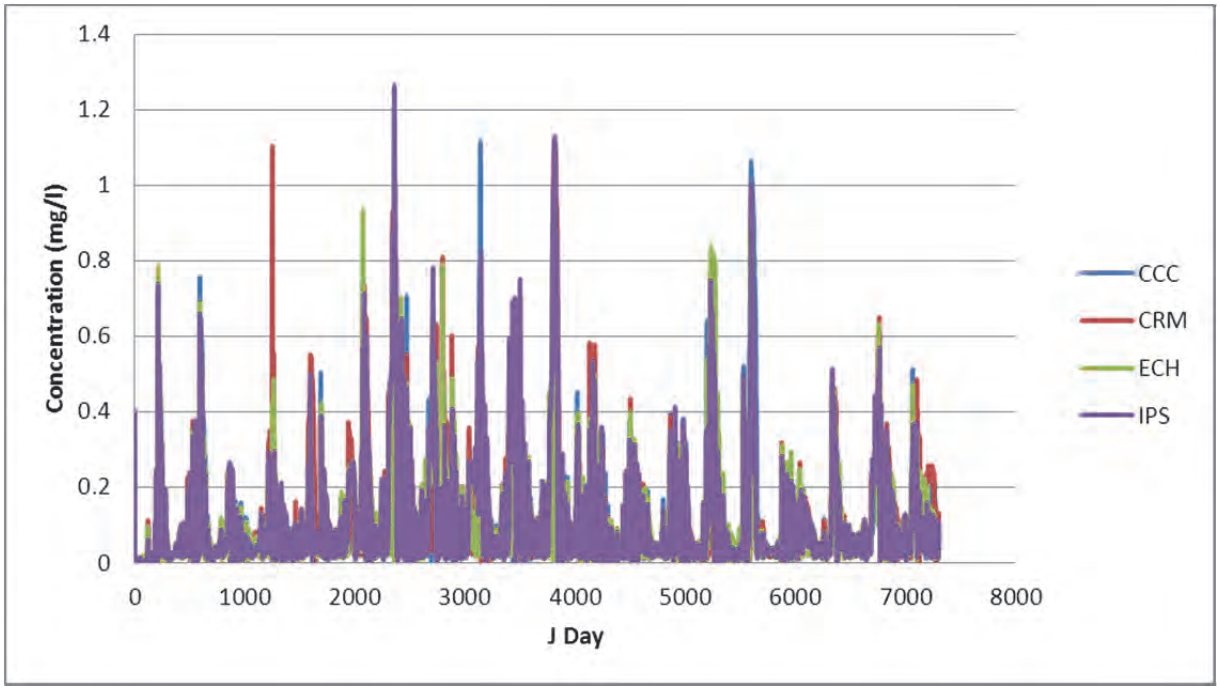

Figure 151: The present day surface dissolved silicon concentration of Voëlvlei Dam (mg/l)

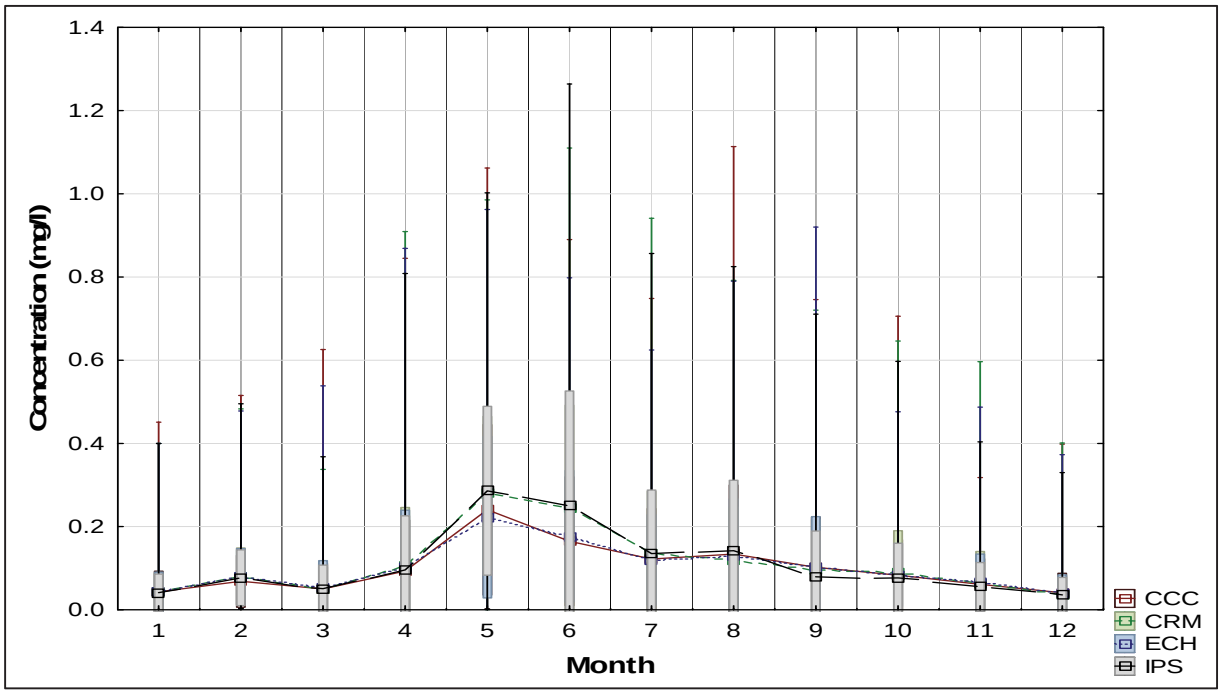

Figure 152: The present day monthly surface dissolved silicon concentration of Voëlvlei Dam (mg/l)

Figure 152 shows that the winter concentration of dissolved silicon was greater than that of summer which means that diatom growth should be silicon limited during summer and more growth during winter if conditions like temperature and solar radiation support viable diatom growth.

Table 56: The present day mean monthly surface dissolved silicon concentration of Voëlvlei Dam (mg/l)

	Jan	Feb	Mar	Apr	May	June	July	Aug	Sep	Oct	Nov	Dec
CCC	0.043	0.069	0.050	0.093	0.241	0.165	0.122	0.134	0.102	0.084	0.062	0.041
CRM	0.043	0.080	0.050	0.105	0.280	0.244	0.134	0.120	0.097	0.088	0.062	0.037
ECH	0.043	0.080	0.055	0.102	0.223	0.177	0.120	0.128	0.103	0.084	0.066	0.039
IPS	0.041	0.077	0.051	0.096	0.286	0.250	0.135	0.142	0.079	0.077	0.055	0.036

Diatoms are known to bloom in winter and from Figure 152 it was seen that the maximum silicon concentrations occur during winter months (May to August) in effect not inhibiting diatom growth during the winter months.

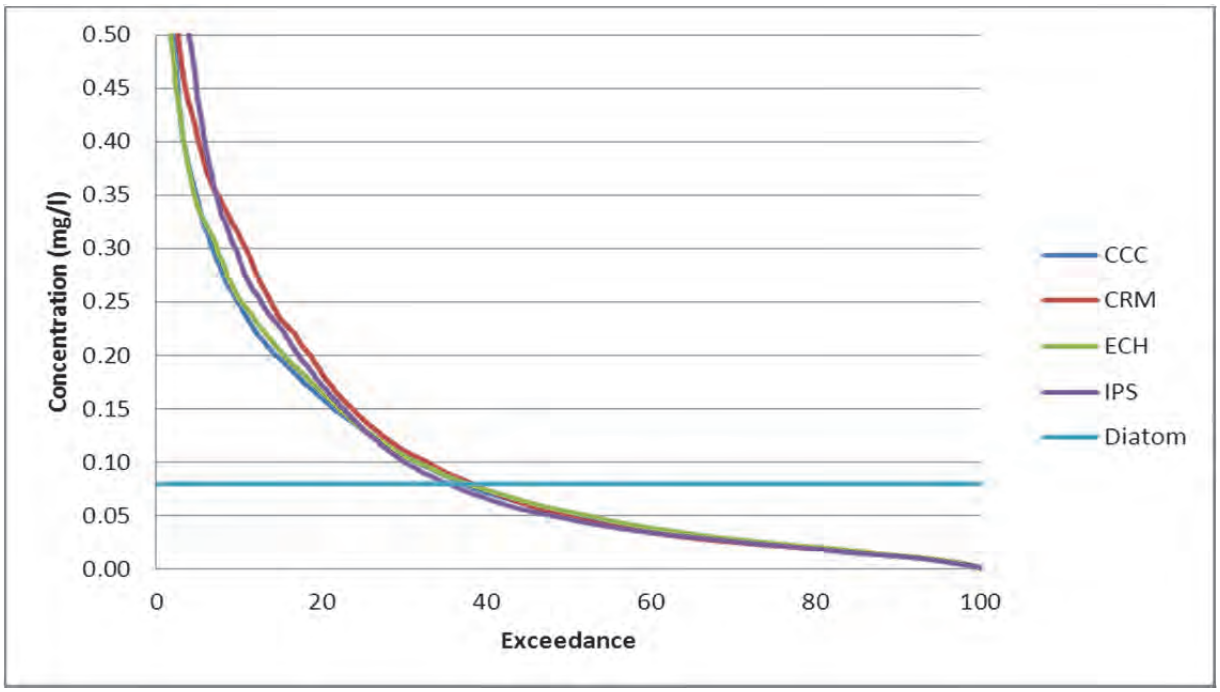

Figure 153: The present day surface dissolved silicon half-saturation exceedance plot with respect to diatoms for Voëlvlei Dam

From the exceedance plot for half saturation constant for diatoms, it was seen that the concentration of surface dissolved silicon was lower than the half-saturation of 0.08 mg/l for approximately 63% of the 20 year. Thus, for this diatom, its growth was hampered by low levels of dissolved silicon and any increase in the inflow of dissolved silicon would allow for a

greater growth rate of diatoms at the surface. The in-situ sources of dissolved silicon are algal respiration, anaerobic decay from the sediments and particulate silicon. Since none of these sources can be managed for a reduction in dissolved silicon the source reduction of silicon before it enters the dam seems a viable method to limit diatom growth.

9.21 Dissolved oxygen concentration

Similarly, the dissolved oxygen concentrations for the 20-year period, monthly and statistics are shown below. The inflow concentration of dissolved oxygen was 12.5 mg/l for both inflow canals for the duration of the simulation.

Upon examination of Figure 154 it was seen that the dissolved oxygen concentration was cyclic and greater concentration of dissolved oxygen was detected in winter. This was due to less dissociation of oxygen from the water because the water temperature was lower. The DWA TWQR level for dissolved oxygen was that it should not be less than 80% or greater than 120% of saturation levels. It was clear that the TWQR for dissolved oxygen was not met during the period, especially for the water below the surface.

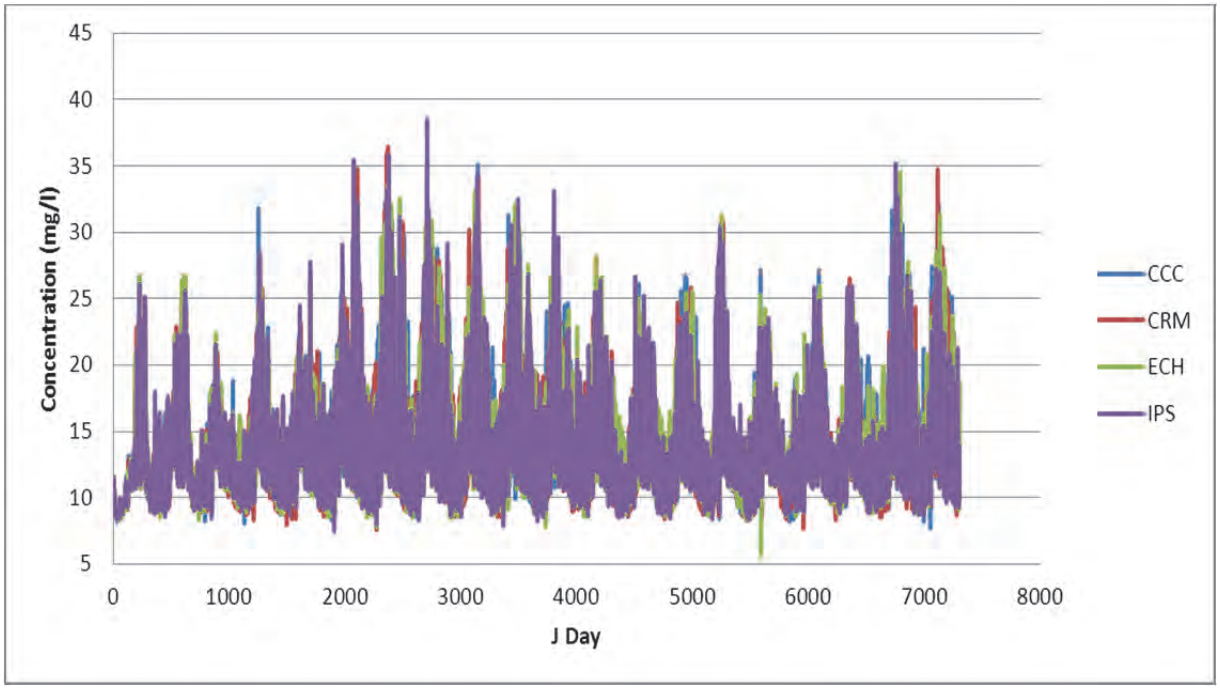

Figure 154: The present day surface dissolved oxygen concentration of Voëlvlei Dam (mg/l)

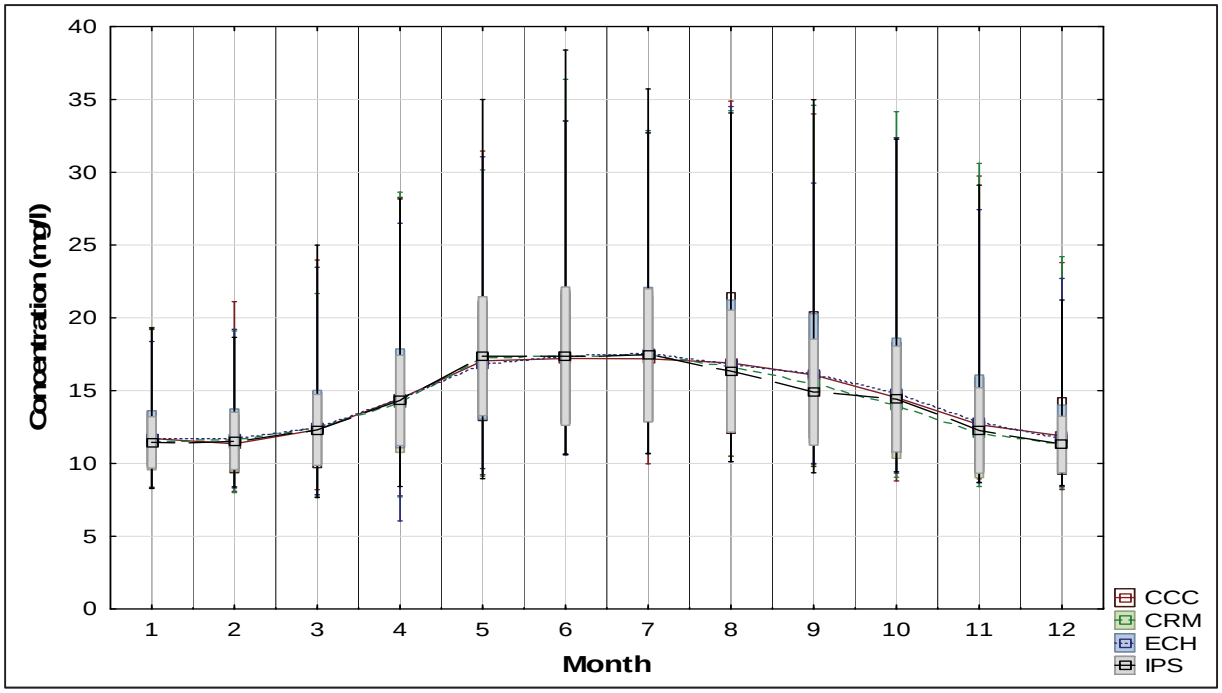

Figure 155: The present day monthly surface dissolved oxygen concentration of Voëlvlei Dam (mg/l)

Table 57: The present day mean monthly surface dissolved oxygen concentration of Voëlvlei Dam (mg/l)

	Jan	Feb	Mar	Apr	May	June	July	Aug	Sep	Oct	Nov	Dec
CCC	11.71	11.34	12.32	14.45	17.05	17.21	17.18	16.90	16.08	14.53	12.66	11.89
CRM	11.49	11.61	12.41	14.13	17.26	17.36	17.47	16.60	15.51	14.01	12.06	11.28
ECH	11.70	11.68	12.50	14.47	16.80	17.37	17.50	16.83	16.18	14.78	12.86	11.74
IPS	11.44	11.55	12.30	14.33	17.37	17.37	17.43	16.34	14.90	14.42	12.26	11.30

It was clear that the dam was supersaturated with dissolved oxygen for a greater part of the year, which needed further investigation as Figure 156 shows that for 30% of the simulation that the DO concentration was greater than 15mg/l, an unrealistically high concentration and a maximum of 38 mg/l.

It was noted that the calibration of DO was not possible as there were no measured values to compare to. Calibration would involve assessing the aeration rate at the surface as well as the effect of the algal growth rates on the observed DO concentrations. A sensitivity analysis should show which parameters affected the DO concentrations and changes for calibration may be implemented.

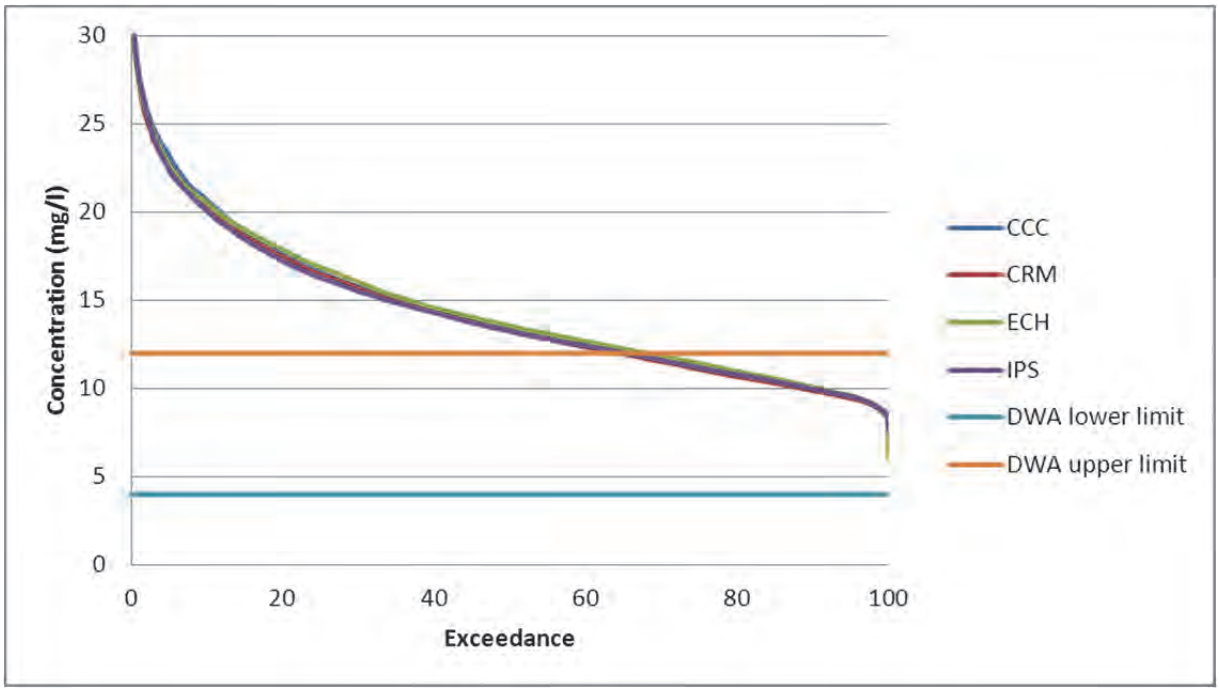

Figure 156: The present day surface dissolved oxygen exceedance plot of Voëlvlei Dam

From the exceedance plot for surface dissolved oxygen it was seen that the DWA lower limit was never exceeded for the simulation period and that the upper limit of 120% saturation was exceeded 65% of the time. This happened in winter when the water temperature was cooler and less dissociation of oxygen from the water took place.

In order to explain the high levels of super-saturation, the module of CE-QUAL-W2 that calculated DO was closer examined for viable sources of oxygen at the surface. Within the model, dissolved oxygen saturation was calculated as a function of water temperature and altitude of the dam. Figure 43 shows the fluxes for DO within the model and the only sources are photosynthesis and atmospheric transfer. The possible variable for the user to affect DO concentrations would be the algal growth constants, thereby directly affecting DO levels by varying the photosynthetic rate. As an exercise, the algal growth rates (AG) for the three groups were set as equal to 1 and the model rerun for the CCC present day. It was assumed that the one model (CCC) was representative of all four models as model inter-variance was negligible as seen in Figure 155.

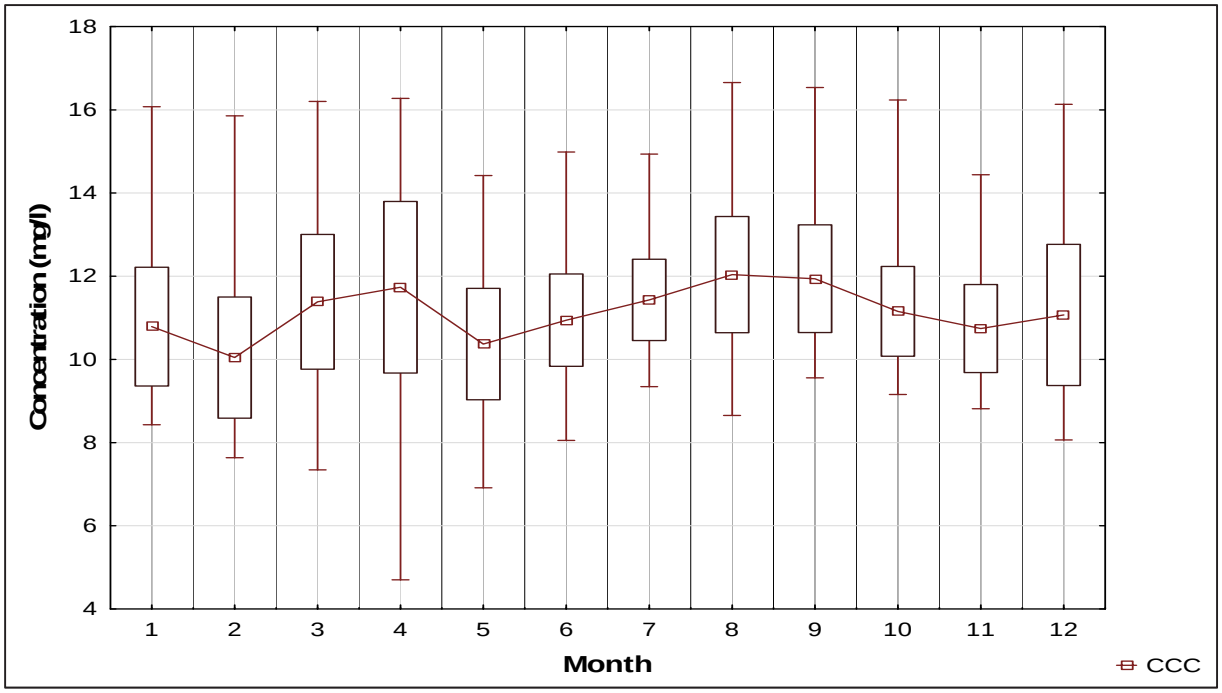

Figure 157: The effect of varied algal growth rates on surface dissolved oxygen for the CCC climate model of Voëlvlei Dam (mg/l)

In comparing Figure 157 and Figure 155 it was seen that changing the algal growth rates the DO concentration levels are more representative of actual in-dam conditions. The problem with this approach in proceeding further was that the algal growth was now affected and not representative of in-dam conditions. The choice of algal growth rates and various parameters are critical for an accurate representation of in-dam conditions as previously mentioned.

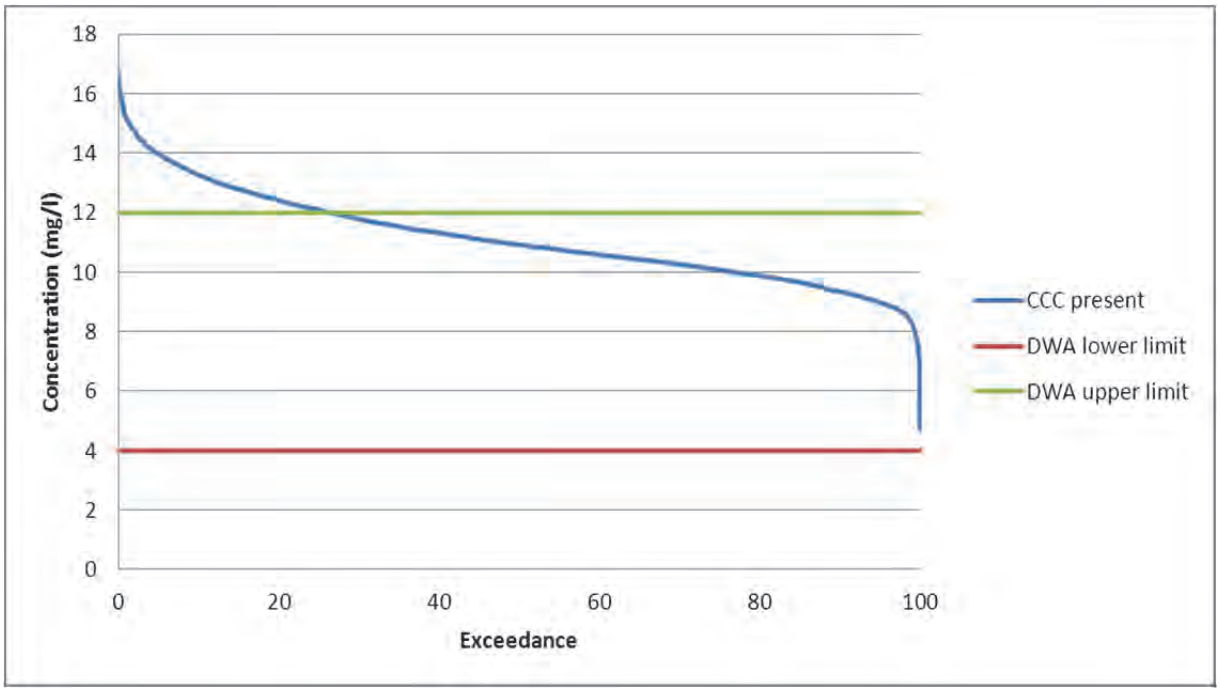

Figure 158: The CCC climate model present day surface dissolved oxygen exceedance of Voëlvlei Dam

In comparing Figure 156 with Figure 158 it was seen that the DWA minimum level was not exceeded but that the upper limit was exceeded for at least 28% of the simulation. It was noted that although this was similar to the previous run but the maximum concentration was only 16.5mg/l of DO. This was considered a more realistic value for surface DO.

It was thus concluded that for the chosen algal parameters CE-QUAL-W2 predicted an unrealistic supersaturated surface DO concentration for the simulation and that by changing the algal parameters more realistic surface DO concentrations were obtained. Since this study was an investigation into the effects of climate change and comparative values were presented, it was considered that the initially presented present day DO concentrations are still valid in this context although noted to be an overestimation. The future DO concentrations would be shown as a change due to climate and thus were considered valid.

9.22 Total algal concentration

Algal growth was a function of temperature, light, and nutrients (Cole, 2008) and thus maximum algal growth occurs at or near the surface if the water-body was well mixed. The total algal concentration incorporating diatoms, greens and cyanobacteria are shown in the following figures for the present day simulation.

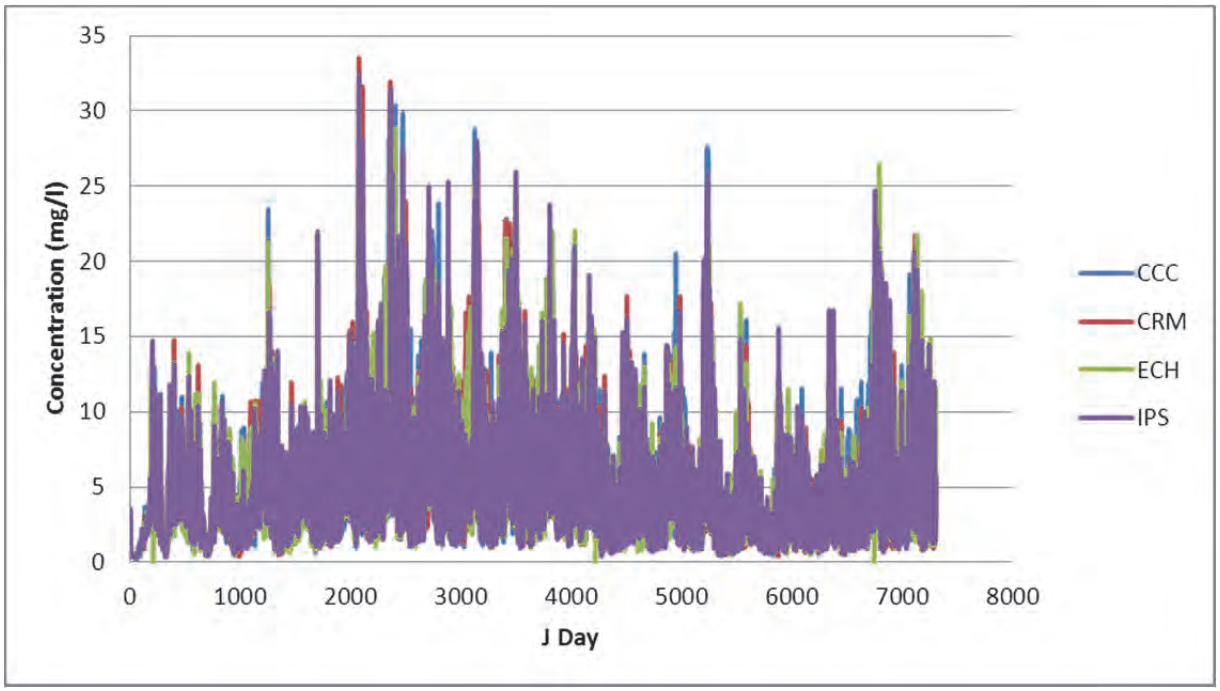

Figure 159: The present day surface total algal concentration of Voëlvlei Dam (mg/l)

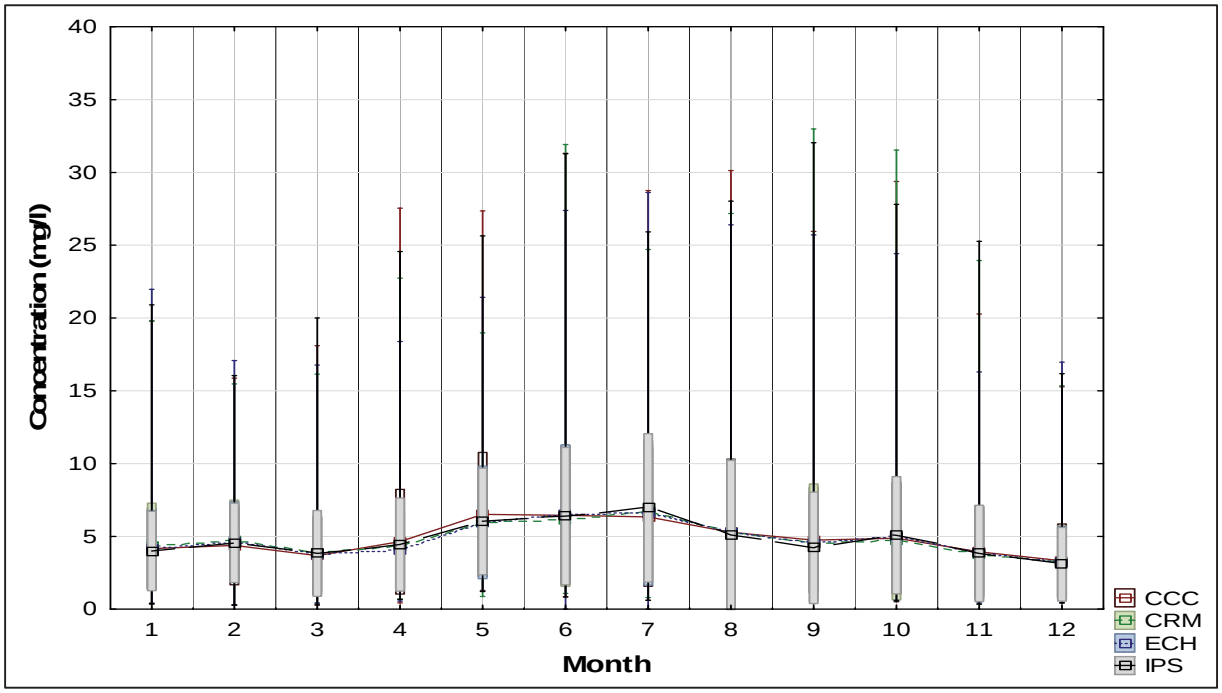

Figure 160: The present day monthly surface total algal concentration of Voëlvlei Dam (mg/l)

Table 58: The present day mean monthly surface total algae concentration of Voëlvlei Dam (mg/l)

	Jan	Feb	Mar	Apr	May	June	July	Aug	Sep	Oct	Nov	Dec
CCC	4.161	4.381	3.680	4.637	6.507	6.449	6.340	5.283	4.742	4.874	3.941	3.325
CRM	4.309	4.712	3.915	4.370	5.939	6.136	6.714	5.297	4.572	4.700	3.805	3.225
ECH	4.166	4.637	3.738	4.109	5.964	6.546	6.621	5.314	4.564	4.962	3.905	3.228
IPS	3.995	4.556	3.832	4.445	6.036	6.395	6.955	5.097	4.220	5.076	3.834	3.084

Figure 159 shows the total algal concentrations at the surface of segment 11 as well as the agreement between the climate models. From Figure 160 it was seen that the mean total algal growth was greater for the winter months than for summer. It was known that diatoms blooms occur more often in winter (Cole, 2008) than summer and to establish which type of algae (diatom, green or cyanobacteria) constitutes the greater portion was investigated further.

From the model parameterisation diatoms and cyanobacteria shared lower light saturation values than greens, implying that they should grow better in winter than summer and conversely greens would grow better the entire year as it had a higher light saturation value and thereby could utilise the greater solar radiation of summer for photosynthesis.

In comparing the winter total algal concentration of the present day to that of summer, it was seen that winter has a greater concentration of algae with the drop in August attributed to an increase in the average solar radiation. This confirmed that the algae are light sensitive and total algal growth was more in winter than summer.

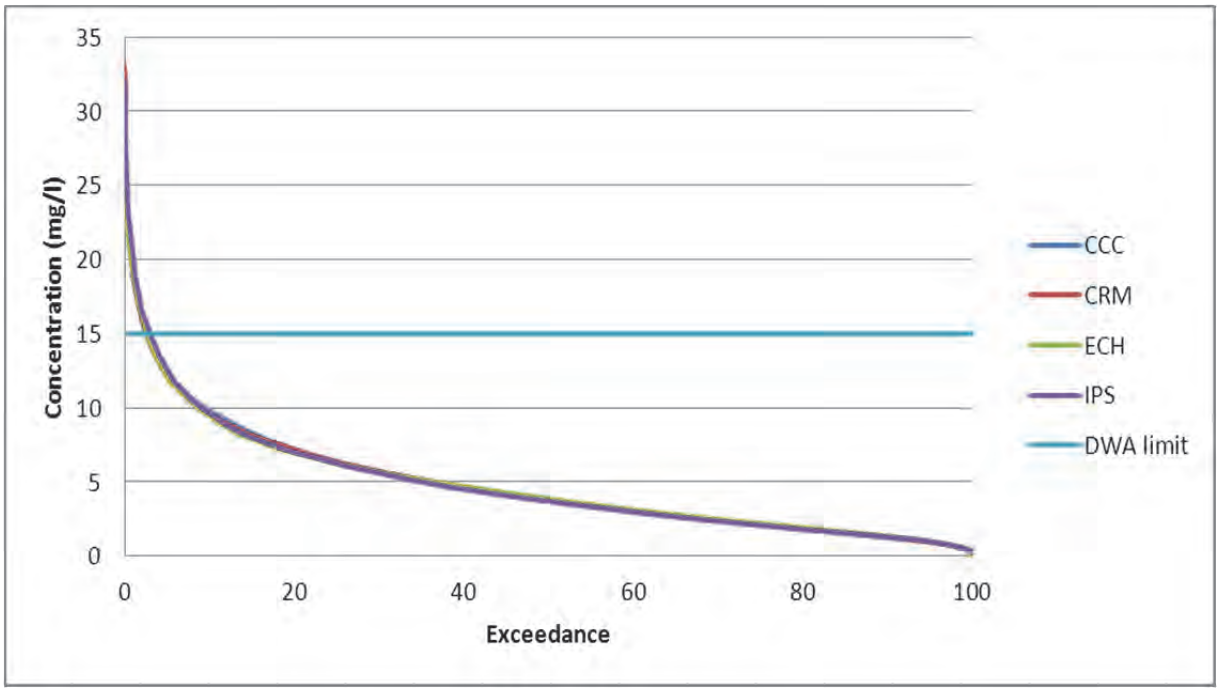

Figure 161: The present day surface total algae exceedance plot of Voëlvlei Dam

From the exceedance plot, it was seen that the total surface algae concentration was greater than 15mg/l (DWA limit) for 3% of the simulation period.

9.23 Diatoms concentration

It was known that diatoms have low light saturation values and tend to grow better in winter, as the winter water temperature was within its maximum growth rates. The following graph shows the diatom concentration for the 20-year period and it was noted that each of the peaks seen corresponds to a winter season.

Figure 162 shows the cyclic peaks of diatoms concentrations as well as the good agreement between models for the present day.

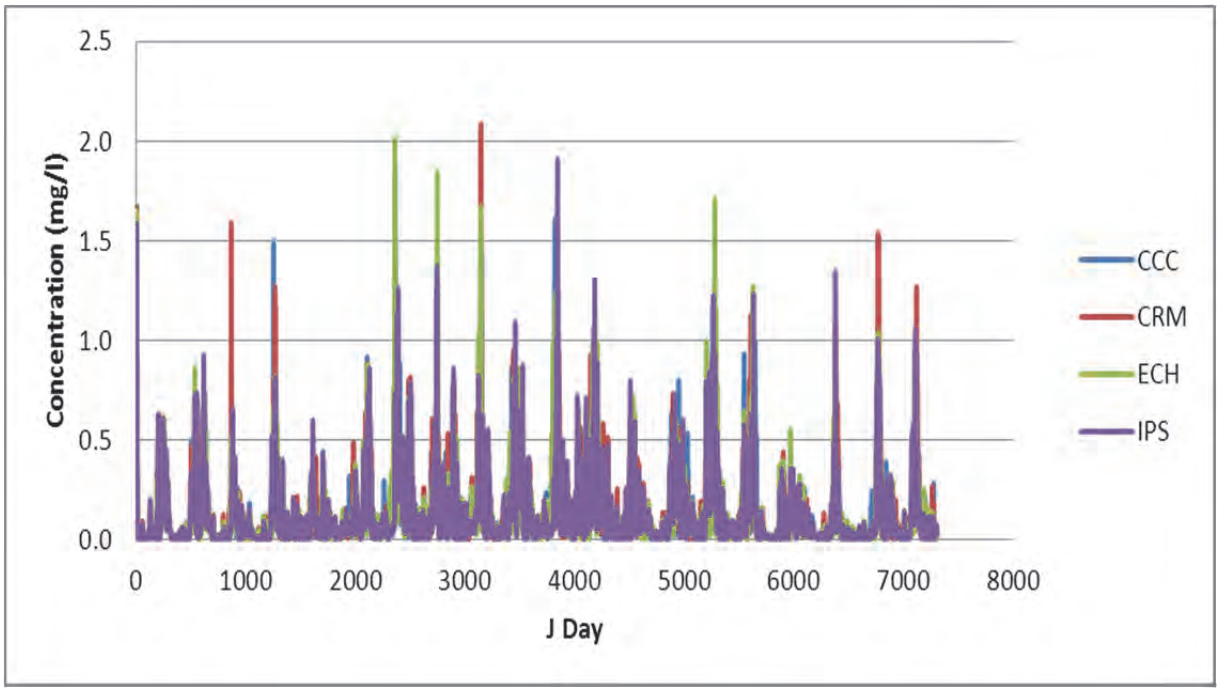

Figure 162: The present day surface diatom concentration of Voëlvlei Dam (mg/l)

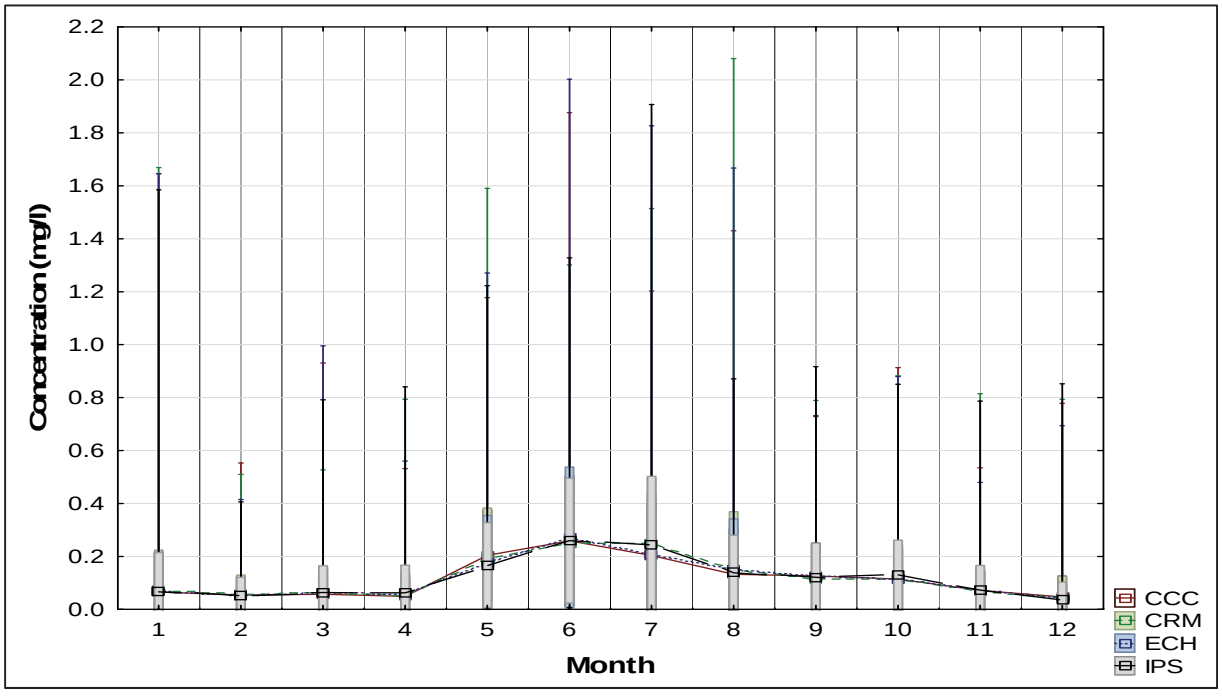

Figure 163: The present day monthly surface diatom concentration of Voëlvlei Dam (mg/l)

Table 59: The present day mean monthly surface diatom concentration of Voëlvlei Dam (mg/l)

	Jan	Feb	Mar	Apr	May	June	July	Aug	Sep	Oct	Nov	Dec
CCC	0.066	0.054	0.057	0.050	0.204	0.259	0.204	0.133	0.126	0.114	0.071	0.047
CRM	0.071	0.055	0.062	0.051	0.191	0.250	0.248	0.152	0.113	0.117	0.069	0.043
ECH	0.069	0.052	0.062	0.058	0.179	0.272	0.210	0.149	0.123	0.114	0.072	0.039
IPS	0.066	0.054	0.064	0.062	0.167	0.259	0.243	0.138	0.121	0.129	0.073	0.038

From Figure 163 and Table 59 it was seen that there was a much greater mean concentration of diatoms during the winter months as opposed to summer months. This would seem counterintuitive, as only during summer was the water temperature high enough to promote maximum growth. This difference could solely be attributed to the diatoms lower light saturation inhibiting plant growth in the high solar radiation summer months. The temperature growth multipliers for diatoms predict that their growth should be limited in winter as the water temperature was below the levels for maximum algal growth. It was noted that there was good agreement within climate models.

9.24 Green algae concentration

The type of green algae chosen for this study exhibits similar light saturation characteristics as the diatoms but has a higher temperature growth rate multiplier. Thus, it was expected to grow throughout the entire year as shown in Figure 164.

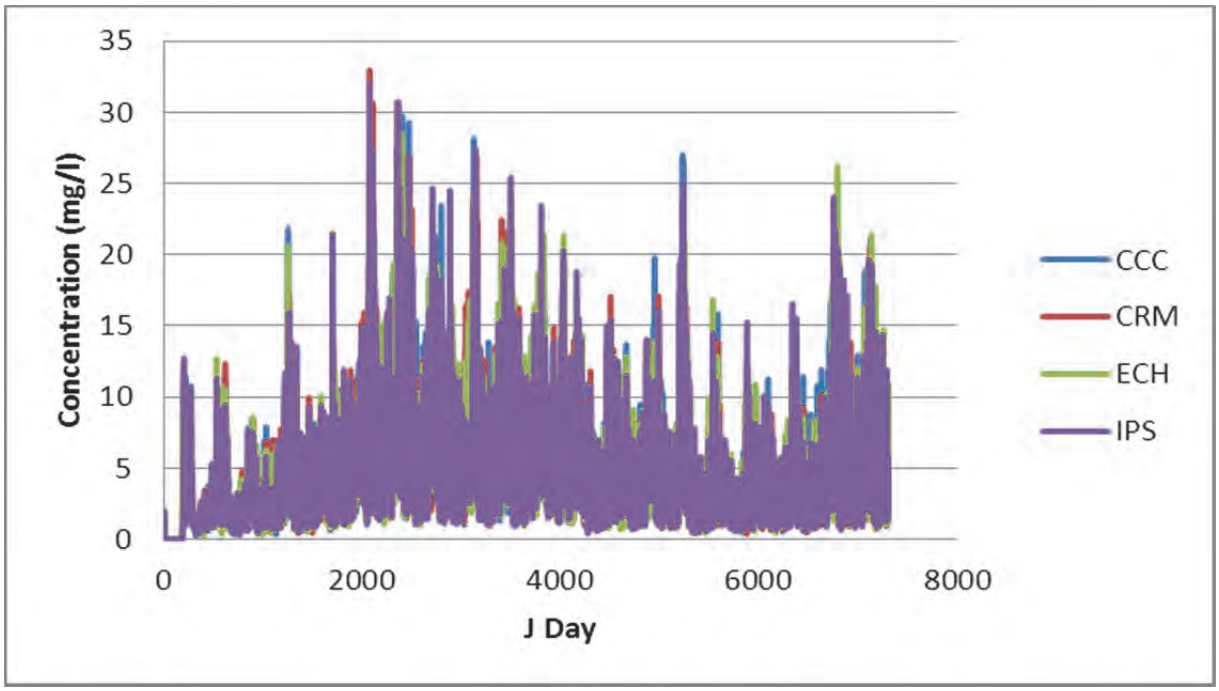

Figure 164: The present day surface green algae concentration of Voëlvlei dam (mg/l)

It was clear that green algae are the dominant species in Voëlvlei dam as they have the greatest concentration and compared well to the total algae concentrations.

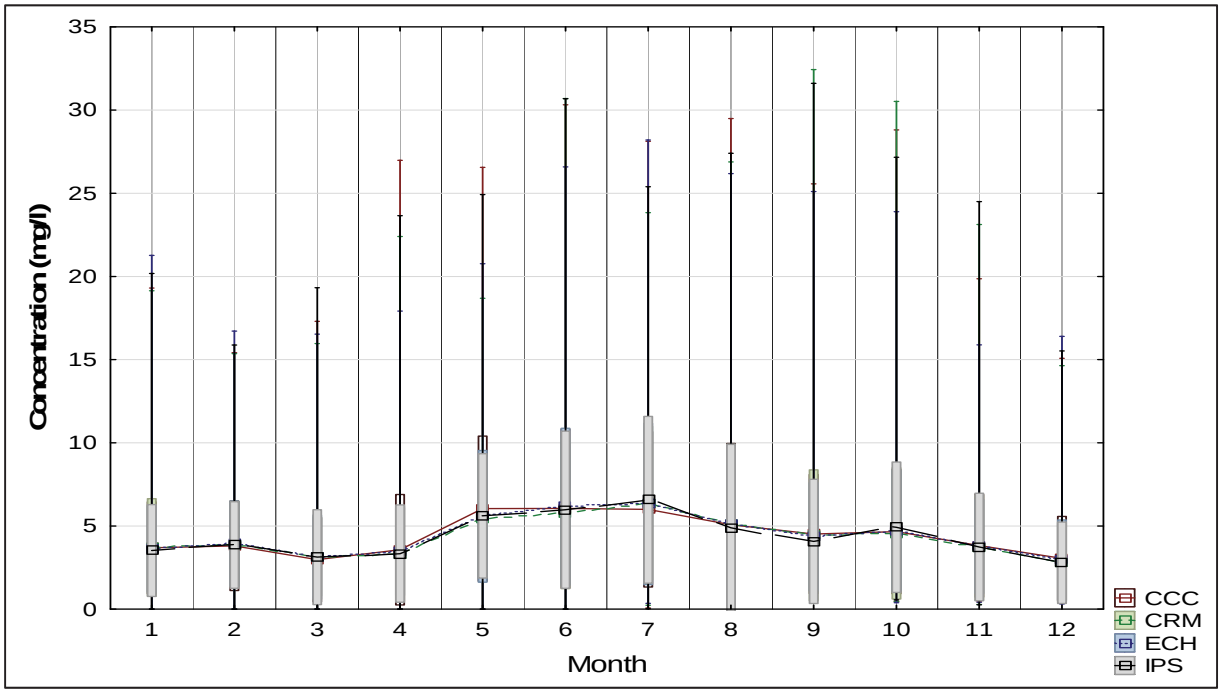

Figure 165: The present day monthly surface green algae concentration of Voëlvlei Dam (mg/l)

When comparing Figure 165 to Figure 162 it was seen that the mean monthly green algae concentration was greater than that of the diatom concentration but the months of greatest growth was seen to be winter for both species.

Table 60: The present day mean monthly surface green algae concentration of Voëlvlei Dam (mg/l)

	Jan	Feb	Mar	Apr	May	June	July	Aug	Sep	Oct	Nov	Dec
CCC	3.689	3.810	2.981	3.576	6.046	6.055	6.001	5.077	4.521	4.668	3.824	3.052
CRM	3.713	3.920	3.177	3.280	5.494	5.766	6.374	5.095	4.439	4.556	3.695	2.806
ECH	3.620	3.951	3.135	3.508	5.577	6.158	6.329	5.100	4.355	4.725	3.772	2.944
IPS	3.528	3.857	3.128	3.340	5.615	5.980	6.577	4.899	4.076	4.924	3.740	2.793

Table 60 compares the concentration of green algae in Voëlvlei dam for the 20-year period. It was interesting to note that the winter period growth was greater than that of summer, which would seem counterintuitive, as the warmer water of summer should promote algal growth. This could be explained again because of a lower light saturation of the species thereby favouring winter growth.

9.25 Cyanobacteria concentration

The cyanobacteria modelled have high light saturation intensities relative to the diatoms and greens and were capable of utilising the extra light during summer for photosynthesis unlike the diatoms and greens. Thus, it was expected that maximum cyanobacteria concentrations should occur mainly in summer due to the additional light and warmer water. Figure 166 shows the cyanobacteria concentration for the 20-year simulation period.

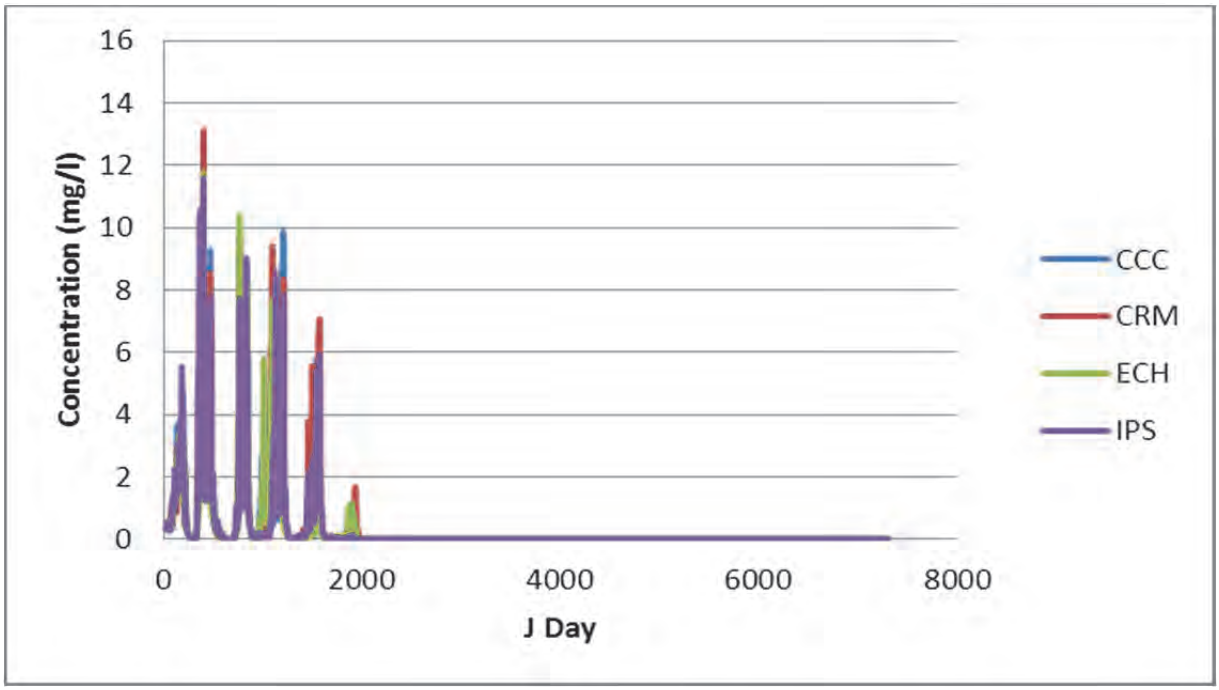

Figure 166: The present day surface cyanobacteria concentration of Voëlvlei Dam (mg/l)

From this figure, it was deduced that for the present day that all climate models predict seasonal cyanobacteria blooms and this was confirmed by the monthly statistical values shown Figure 167 and Table 61. Maximum mean values are during summer and autumn with a decrease during winter.

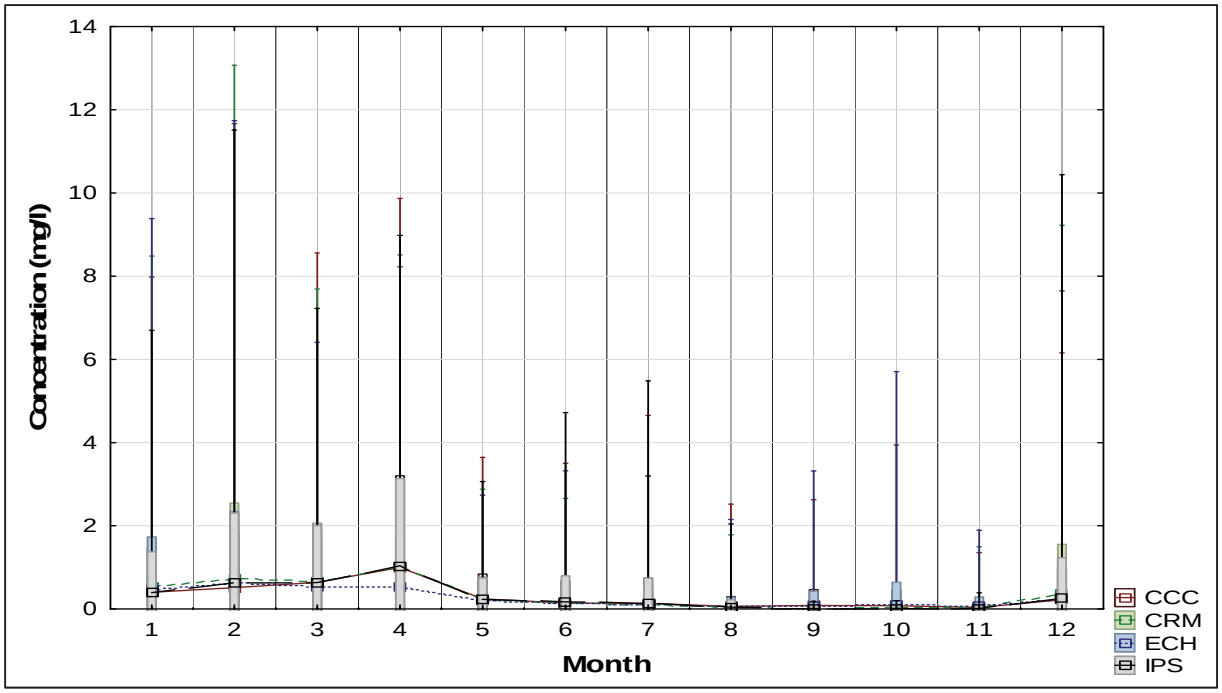

Figure 167: The present day monthly surface cyanobacteria concentration of Voëlvlei Dam (mg/l)

Table 61: The present day mean monthly surface cyanobacteria concentration of Voëlvlei Dam (mg/l)

	Jan	Feb	Mar	Apr	May	June	July	Aug	Sep	Oct	Nov	Dec
CCC	0.402	0.514	0.640	0.999	0.245	0.147	0.139	0.063	0.088	0.081	0.039	0.226
CRM	0.519	0.728	0.671	1.039	0.241	0.131	0.100	0.039	0.010	0.020	0.034	0.377
ECH	0.472	0.630	0.536	0.533	0.195	0.146	0.107	0.058	0.076	0.114	0.058	0.244
IPS	0.396	0.643	0.637	1.039	0.239	0.170	0.142	0.046	0.015	0.014	0.016	0.249

From the table it was seen that the mean summer to autumn cyanobacteria concentration was greater than that of winter as well as the summer maximum concentrations. This could be directly linked to the cooler waters during winter.

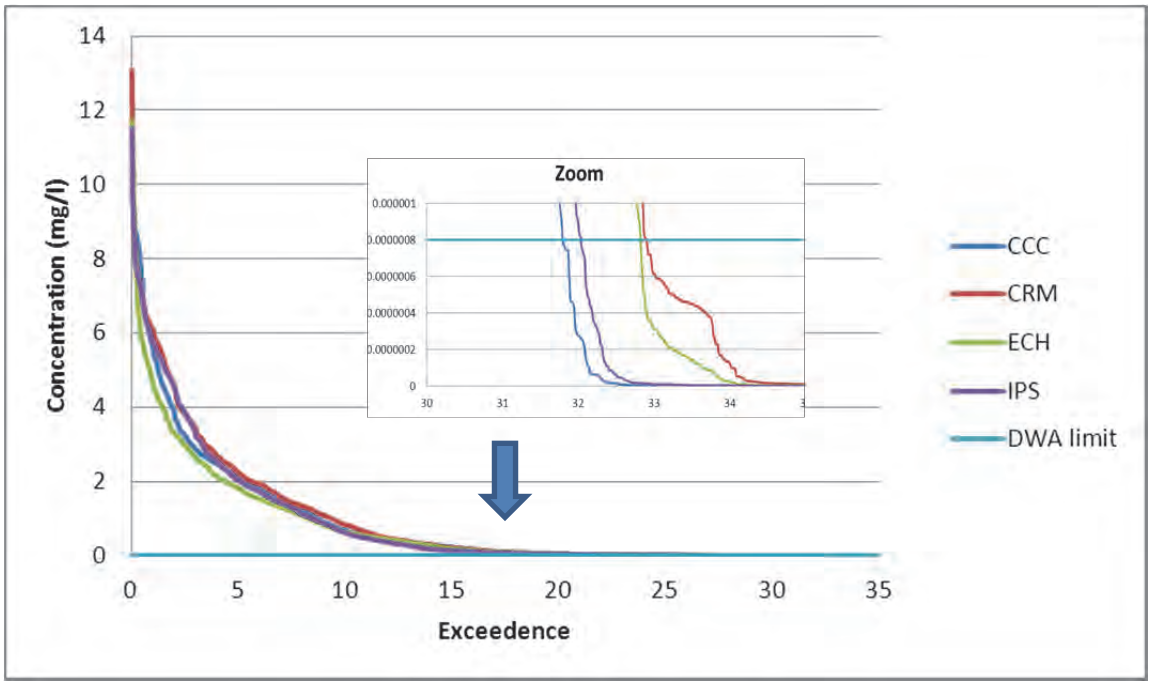

Figure 168: The present day surface cyanobacteria exceedance of Voëlvlei dam

From the exceedance plot, it was estimated that for the DWA limit of 0.8µg/l the surface cyanobacteria concentration in Voëlvlei dam exceeded this about 32 to 33% of the simulation time depending on the climate model.

The accuracy of the prediction of the present day algal growth was not confirmed but was believed to representative enough as the model had been calibrated and validated. The outcome of this study was to firstly establish baseline conditions and then show changes induced by climate change on the baseline conditions.

9.26 Zooplankton growth

To investigate the effect of predation on diatoms and green algae, zooplankton was also modelled to preferring diatoms and green algae over cyanobacteria and the resulting concentrations are shown in Figure 169. This figure resembles Figure 164 in shape and this was because green algae are present throughout the entire year and that zooplankton feed on them.

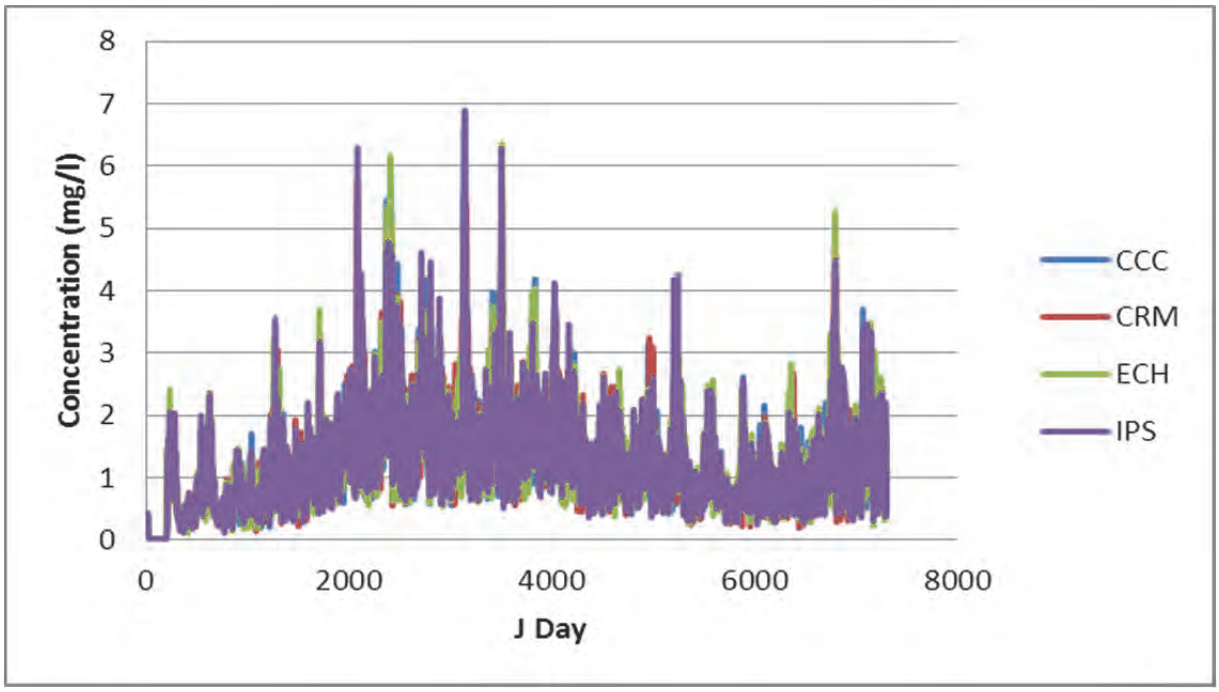

Figure 169: The present day surface zooplankton concentration of Voëlvlei dam (mg/l)

The following figure show the monthly averages of zooplankton concentration for the 20-year simulation period. It showed that zooplankton was present in Voëlvlei dam throughout the entire year but at show a greater concentration during the winter months. This was probably due to the greater concentration of its diet namely diatoms and green algae during these months.

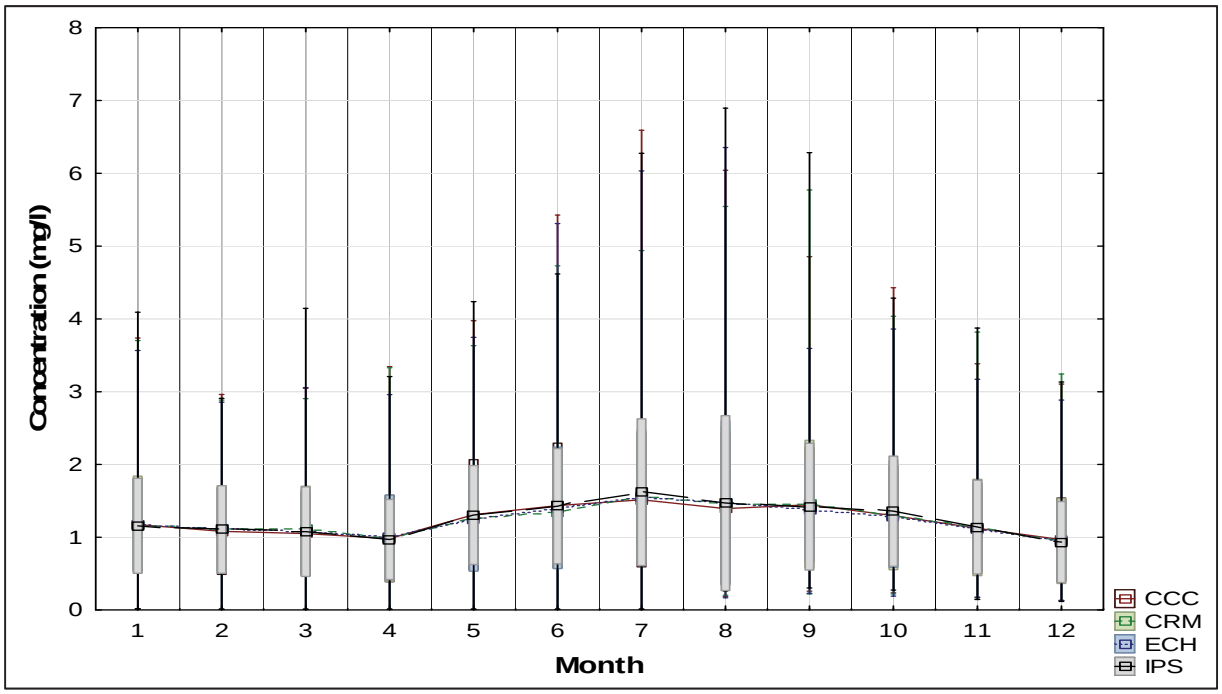

Figure 170: The present day monthly surface zooplankton concentration of Voëlvlei Dam (mg/l)

Table 62: The present day mean monthly surface zooplankton concentration of Voëlvlei Dam (mg/l)

	Jan	Feb	Mar	Apr	May	June	July	Aug	Sep	Oct	Nov	Dec
CCC	1.174	1.083	1.050	0.982	1.309	1.435	1.515	1.394	1.447	1.296	1.124	0.968
CRM	1.177	1.113	1.115	0.975	1.273	1.339	1.570	1.448	1.456	1.304	1.134	0.946
ECH	1.178	1.113	1.069	0.996	1.240	1.404	1.556	1.470	1.376	1.279	1.119	0.953
IPS	1.157	1.107	1.077	0.969	1.306	1.426	1.619	1.470	1.420	1.358	1.141	0.933

Figure 169 and Table 62 shows the monthly statistics of zooplankton for the four climate models. Winter has the greatest mean surface zooplankton concentration as well as maximum concentrations, this being an indication that greater predation of diatoms and greens occurred during the winter months even though the zooplankton temperature growth rate was more suited to the summer months.

9.27 Eutrophication level

The trophic level indicator chosen for this study was the TRIX level, but its shortcoming was that it did not include secchi depth, which was not measured as part of this modelling process. This index characterised the trophic levels in coastal marine areas and was adopted by the Italian national legislation and was applied here as way of representing the trophic level. It was the linearization of chlorophyll-*a* concentration (ChA in µg/ℓ), the dissolved oxygen concentration in percent (DO %), the total nitrogen (N_{min} = $N_{nitrate}$ + $N_{nitrite}$ + $N_{ammonia}$ in µg/ℓ) and the total phosphorous (TP µg/ℓ). This was represented mathematically as:

$$TRIX = \frac{(\log(ChA + aDO\% + N\min + TP) + 1.5)}{1.2}$$

From this the following states of water was classified (Table 62).

Table 63: TRIX trophic level categories

TRIX value	Trophic category
< 4	Low trophic level
4-5	Middle trophic level
5-6	High trophic level
6-8	Very high trophic level

From Pavluk *et al.*, 2008:3602

The output of the study for mean monthly surface trophic level was shown in Figure 171 for the present day. It was clear that Voëlvlei was at the low trophic level with peaks into the middle trophic level mostly during winter.

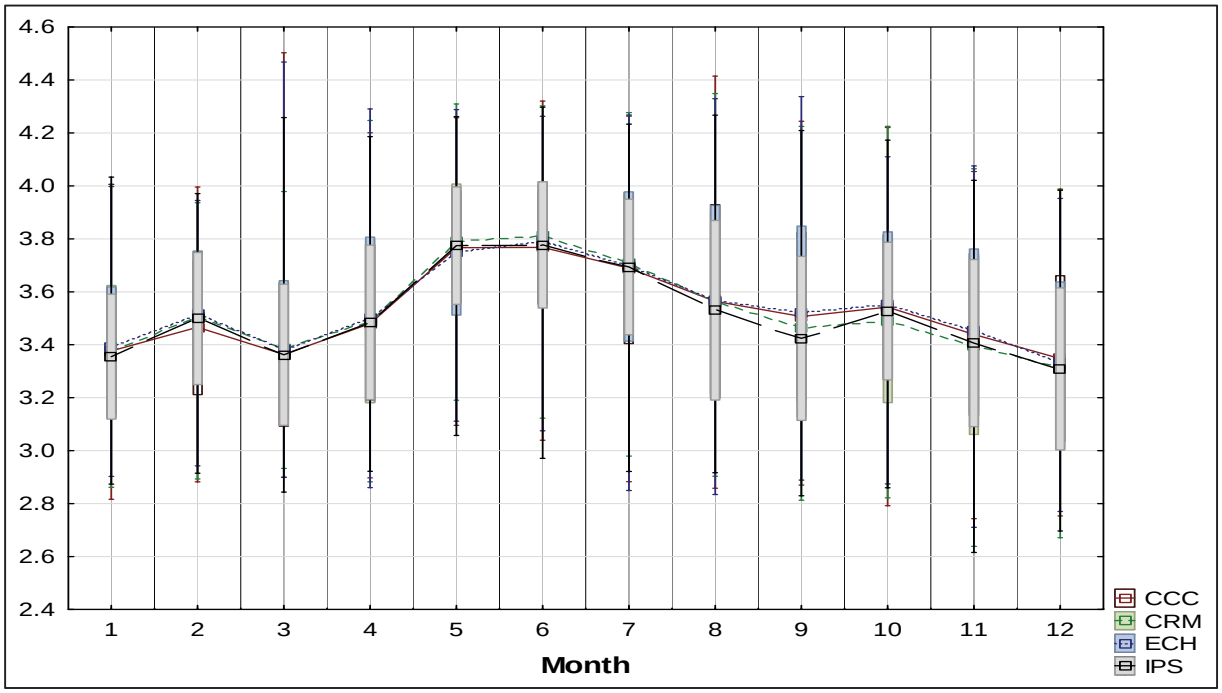

Figure 171: The present day monthly surface TRIX level of Voëlvlei Dam

Table 64 shows that the TRIX level of Voëlvlei dam peaks during winter for all four present day climate models. It was expected that with climate change that this levels should increase due to changes in total algal concentration

Table 64: Present day monthly mean surface TRIX level of Voëlvlei Dam

	Jan	Feb	Mar	Apr	May	Jun	Jul	Aug	Sep	Oct	Nov	Dec
CCC	3.4	3.5	3.4	3.5	3.8	3.8	3.7	3.6	3.5	3.5	3.4	3.3
CRM	3.4	3.5	3.4	3.5	3.8	3.8	3.7	3.6	3.5	3.5	3.4	3.3
ECH	3.4	3.5	3.4	3.5	3.7	3.8	3.7	3.6	3.5	3.6	3.5	3.3
IPS	3.4	3.5	3.4	3.5	3.8	3.8	3.7	3.5	3.4	3.5	3.4	3.3
Monthly mean	3.4	3.5	3.4	3.5	3.8	3.8	3.7	3.6	3.5	3.5	3.4	3.3

When examining the formulae for TRIX it was seen that every term increases during winter and thereby increasing the TRIX during winter. Thus, winter was considered the season of least water quality and greatest eutrophication for Voëlvlei dam.

9.28 Voëlvlei dam climate change scenarios

Now, once the preliminary present day climate had been established as the baseline, the effect of future climate change on the eutrophication of Voëlvlei dam was investigated. This effect was determined by rerunning the water quality model, CE-QUAL-W2 but with the climate changed meteorological input data (air temperature, dew point temperature, wind-speed and direction, cloud cover and solar radiation) from the four climate change models (CCC, CRM, ECH and IPS). Trends were noted from each of the runs and compared with the present day runs. For this study, 1/1/2046-31/12/2065 represented the intermediate future and 1/1/2081-31/12/2100 was the distant future. The CCC model only had present day and intermediate future data.

The inflow streams were not adjusted for increased temperature for the future runs but since the inflow was at segment 21 and the segment under study was segment 11, assuming that Voëlvlei was a well-mixed dam this was considered not a problem.

Air temperature

Once the mean monthly air temperature for the present day had been established, the effect of climate change on Voëlvlei dam was quantified. The water quality model (CE-QUAL-W2) was rerun with the same initial conditions and parameters but with the intermediate future and distant future meteorological inputs. The intermediate future and distant future for each of the four climate change models was shown in the following figure.

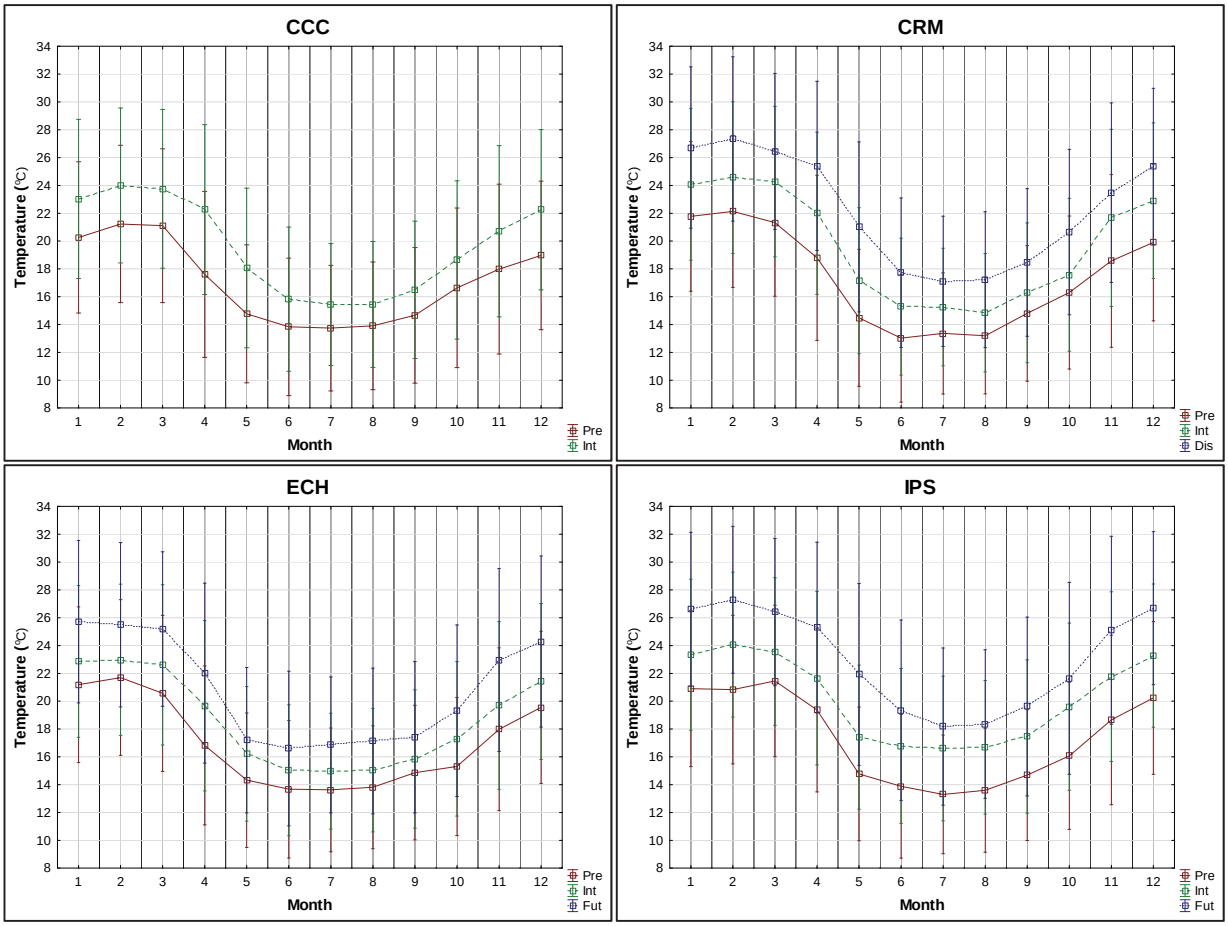

Figure 172: The projected climate change air temperature of Voëlvlei Dam (°C)

Figure 172 shows that the mean air temperature increased into the intermediate future and rose even higher into the distant future for all four climate models. This higher air temperature was expected to have a marked effect on the surface water temperature in the form of energy transfer at the surface interface, thereby increasing water temperature. The extent of this increase was investigated in conjunction with solar radiation, the other source of energy that influences water temperature.

Table 65: The mean monthly air temperature of Voëlvlei Dam (°C) under projected climate change

	Jan	Feb	Mar	Apr	May	Jun	Jul	Aug	Sep	Oct	Nov	Dec
CCC pre	20.3	21.2	21.1	17.6	14.8	13.8	13.7	13.9	14.7	16.6	18.0	19.0
Difference	2.7	2.8	2.7	4.7	3.3	2.0	1.7	1.5	1.8	2.0	2.7	3.3
CCC int	23.0	24.0	23.8	22.3	18.1	15.8	15.4	15.4	16.5	18.6	20.7	22.3
CRM pre	21.8	22.1	21.3	18.8	14.5	13.0	13.4	13.2	14.8	16.3	18.6	19.9
Difference	2.3	2.5	3.0	3.2	2.7	2.3	1.9	1.6	1.5	1.3	3.1	3.0
CRM int	24.1	24.6	24.3	22.0	17.2	15.3	15.3	14.8	16.3	17.6	21.7	22.9
CRM int	24.1	24.6	24.3	22.0	17.2	15.3	15.3	14.8	16.3	17.6	21.7	22.9
Difference	2.6	2.7	2.1	3.4	3.8	2.4	1.8	2.4	2.2	3.1	1.8	2.5
CRM fut	26.7	27.3	26.4	25.4	21.0	17.7	17.1	17.2	18.5	20.7	23.5	25.4
ECH pre	21.2	21.7	20.6	16.8	14.3	13.7	13.6	13.8	14.9	15.3	18.0	19.6
Difference	1.7	1.3	2.0	2.9	1.9	1.3	1.4	1.2	0.9	2.0	1.7	1.8
ECH int	22.9	23.0	22.6	19.7	16.2	15.0	15.0	15.0	15.8	17.3	19.7	21.4
ECH int	22.9	23.0	22.6	19.7	16.2	15.0	15.0	15.0	15.8	17.3	19.7	21.4
Difference	2.8	2.5	2.6	2.3	1.0	1.6	1.9	2.1	1.6	2.0	3.3	2.9
ECH fut	25.7	25.5	25.2	22.0	17.2	16.6	16.9	17.1	17.4	19.3	23.0	24.3
IPS pre	20.9	20.8	21.5	19.4	14.8	13.9	13.3	13.6	14.7	16.1	18.7	20.2
Difference	2.4	3.3	2.1	2.3	2.6	2.9	3.3	3.1	2.8	3.5	3.1	3.1
IPS int	23.3	24.1	23.6	21.7	17.4	16.8	16.6	16.7	17.5	19.6	21.8	23.3
IPS int	23.3	24.1	23.6	21.7	17.4	16.8	16.6	16.7	17.5	19.6	21.8	23.3
Difference	3.3	3.2	2.8	3.6	4.5	2.6	1.6	1.7	2.1	2.0	3.3	3.4
IPS fut	26.6	27.3	26.4	25.3	21.9	19.4	18.2	18.4	19.6	21.6	25.1	26.7

From the table and the figure, it was seen that the mean monthly temperature increases when going from present day to intermediate day and was maximum for the distant future scenario. The warmest months are shown are the orange to red colours and the cooler months are greener. It was clear from this that May to September was the cooler months and November to April was the warmer months.

It was interesting to note that the change in mean air temperature in progressing from the present day to the intermediate future was similar of that from intermediate future to distant future. This was a consequence of the accelerated anthropogenic loading as the time span from present day to intermediate future was much greater than that of intermediate future to distant future.

The climate models are ranked from the ‘coolest’ to the ‘hottest’ as ECH, CRM then IPS. This would imply that the ECH model produced the least change in temperature and thus a subsequent lower algal growth as compared to CRM and the IPS, which would have the maximum effect on algal growth.

The inter-variability between the climate models was now more evident and some discrepancies are noticed. The inter-variability was produced from the climate models themselves in assigning different assumptions of greenhouse gas loadings to the atmosphere.

Solar radiation

Wetzel in 2001 and others had established the diurnal link between solar radiation and surface water temperature from the aspect of an energy balance. Increased water temperature was the direct result of the diurnal shortwave solar radiation on a water-body. Figure 130 shows the present day solar radiation over Voëlvlei dam and it was seen that May, June, July and August has the lowest radiation values. Figure 173 shows the incident solar radiation over Voëlvlei dam for climate change for the four climate change models.

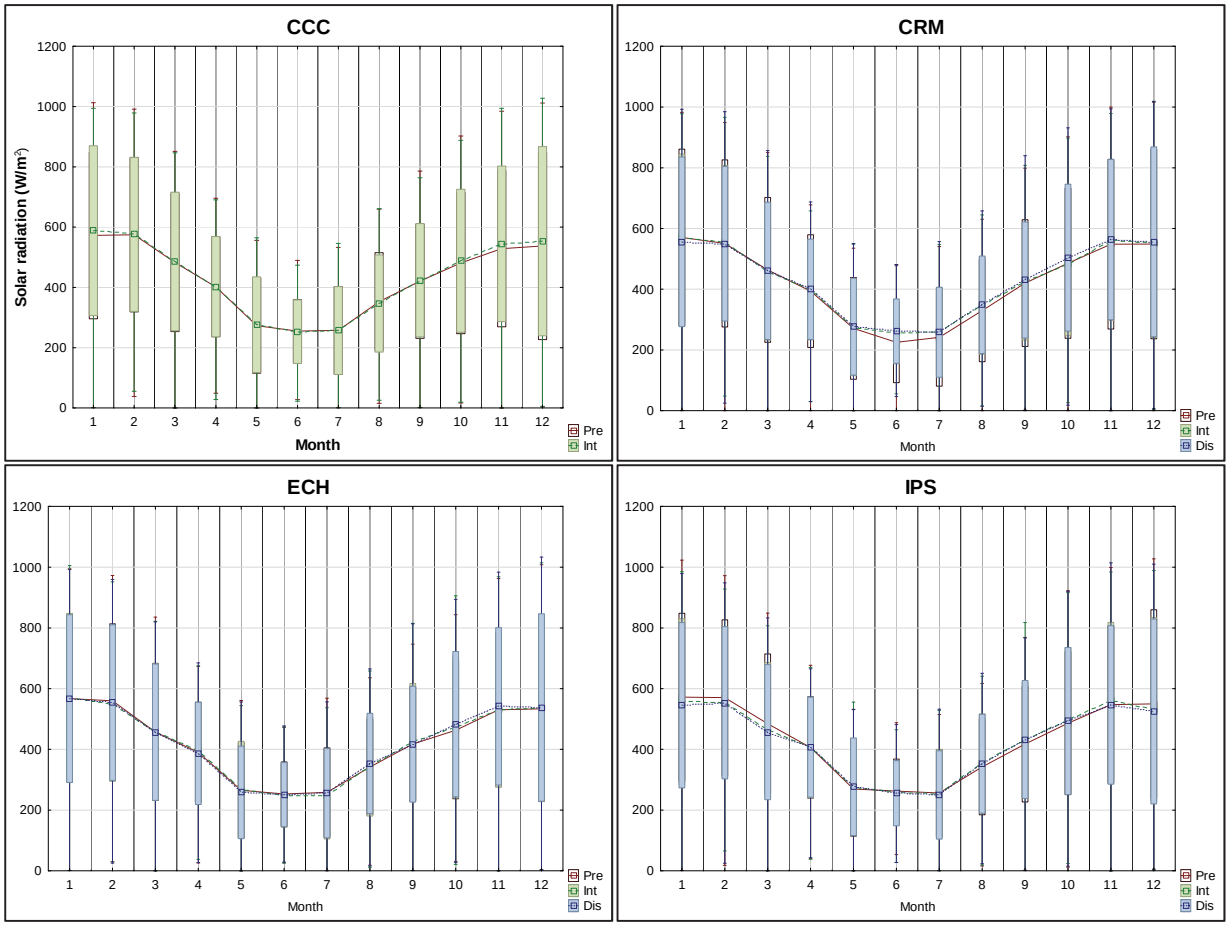

Figure 173: The projected monthly incident solar radiation of Voëlvlei dam (W/m^2)

This figure shows that for the intermediate future and distant future climates the change in incident solar radiation was negligible over that of the present day for all four climate change models. This would imply that the effect of solar radiation of the present time and the future was comparably the same and does not have a substantial change on the growth of algae in the future. The months with the greatest incident solar radiation was that of January and February for all climate models as well as into the distant future.

When comparing the driving effect of air temperatures and solar radiation on surface water temperatures for future events, air temperatures had the greatest effect, as solar radiation remained unchanged for future climate change events.

Surface water temperature changes

Long-term surface water temperature change had now been linked to air temperature increase due to climate change and the perceived changes due to diurnal fluxes are seen to be negligible within the four climate models used. Solar radiation influenced water temperature on a daily basis, but there was no nett climate change effect on solar radiation

and thus it did not contribute to a long-term increase in water temperature. Essentially the long-term increase in surface water temperature was a result of increased air temperature, due to the greenhouse effect.

Figure 174 and Table 66 show the mean surface water temperature increase due to climate change into the intermediate future and distant future. They show that surface water temperature increases progressive for each month of the simulation period for all the future scenarios of climate change. If all other factors that support algal growth were favourable during this time then this increase in water temperature would have a marked increase in total algal growth in Voëlvlei dam throughout the entire year. This premise was investigated further in the ensuing sections.

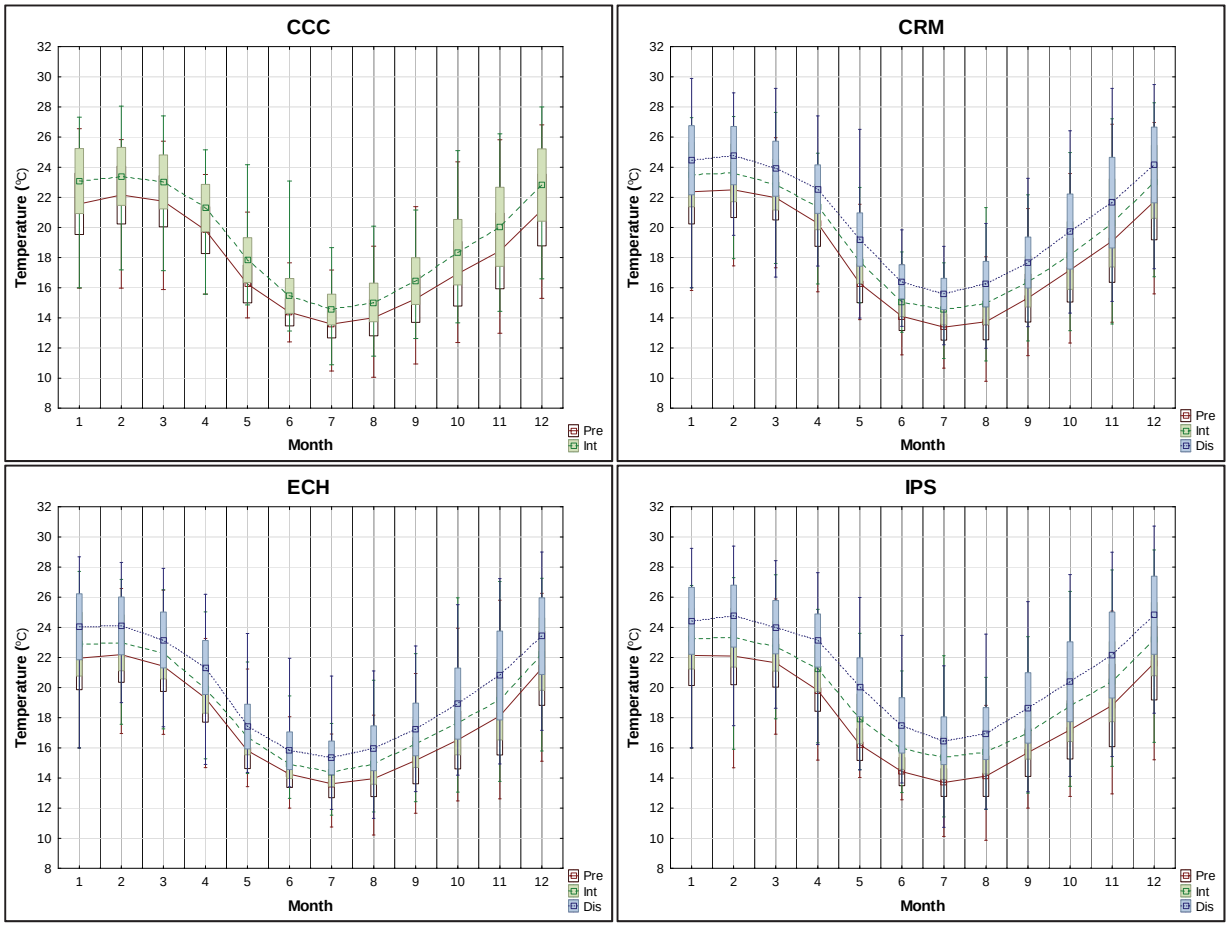

Figure 174: The projected climate change surface water temperature of Voëlvlei dam (^{o}C)

It was clear that the mean surface water temperature increased from present day to distant future, with the intermediate future mean water temperatures between them.

Table 66: The mean monthly surface water temperature of Voëlvlei Dam (°C) under projected climate change

	Jan	Feb	Mar	Apr	May	Jun	Jul	Aug	Sep	Oct	Nov	Dec
CCC pre	21.6	22.2	21.7	19.8	16.3	14.4	13.6	14.0	15.3	16.9	18.4	21.2
Difference	1.5	1.2	1.3	1.5	1.6	1.1	1.0	1.0	1.2	1.4	1.6	1.7
CCC int	23.1	23.4	23.0	21.3	17.8	15.5	14.6	15.0	16.4	18.4	20.0	22.8
CRM pre	22.4	22.5	22.0	20.3	16.3	14.1	13.4	13.7	15.3	17.2	19.1	21.7
Difference	1.1	1.1	0.9	1.1	1.5	1.0	1.2	1.2	1.1	1.0	1.2	1.3
CRM int	23.5	23.6	22.8	21.4	17.7	15.1	14.5	14.9	16.4	18.1	20.3	23.0
CRM int	23.5	23.6	22.8	21.4	17.7	15.1	14.5	14.9	16.4	18.1	20.3	23.0
Difference	0.9	1.2	1.1	1.2	1.5	1.3	1.0	1.3	1.3	1.6	1.4	1.1
CRM fut	24.5	24.8	23.9	22.6	19.2	16.4	15.6	16.2	17.7	19.7	21.7	24.2
ECH pre	22.0	22.2	21.4	19.3	15.8	14.3	13.6	14.0	15.2	16.5	18.1	21.3
Difference	0.9	0.8	0.8	0.6	0.9	0.7	0.7	1.0	1.1	1.2	1.1	0.9
ECH int	22.9	23.0	22.3	19.9	16.7	15.0	14.4	14.9	16.3	17.7	19.2	22.2
ECH int	22.9	23.0	22.3	19.9	16.7	15.0	14.4	14.9	16.3	17.7	19.2	22.2
Difference	1.2	1.1	0.9	1.4	0.7	0.9	1.0	1.1	0.9	1.3	1.6	1.2
ECH fut	24.0	24.1	23.2	21.3	17.4	15.8	15.3	16.0	17.2	18.9	20.8	23.4
IPS pre	22.1	22.1	21.7	19.8	16.2	14.4	13.7	14.1	15.7	17.2	18.8	21.6
Difference	1.1	1.2	1.1	1.5	1.7	1.5	1.6	1.6	1.3	1.5	1.6	1.6
IPS int	23.2	23.3	22.7	21.3	17.9	16.0	15.3	15.7	17.0	18.7	20.4	23.2
IPS int	23.2	23.3	22.7	21.3	17.9	16.0	15.3	15.7	17.0	18.7	20.4	23.2
Difference	1.2	1.4	1.3	1.9	2.1	1.5	1.1	1.2	1.6	1.7	1.8	1.6
IPS fut	24.4	24.7	24.0	23.1	20.0	17.5	16.5	17.0	18.7	20.4	22.2	24.8

The accelerated trend of surface water heating due to climate change from intermediate future to distant future was also evident. From the table it was seen that the pattern for mean surface water temperatures follows that of mean air temperatures for monthly trends and climate change events, thereby consolidating the premise that air temperature was the driver for surface water temperature.

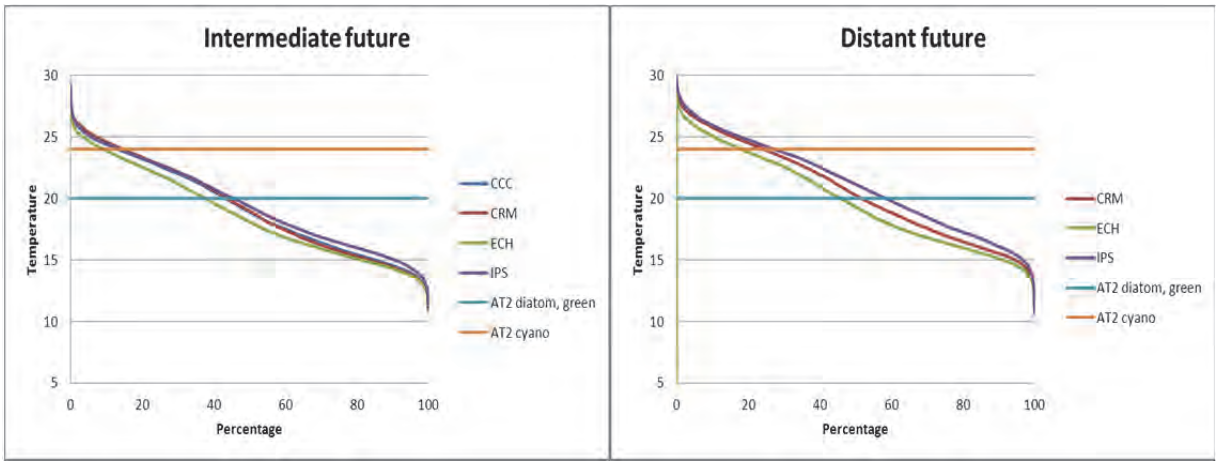

Figure 175: The projected future surface water temperature exceedance with respect to algal growth of Voelvlei Dam

To investigate the effect of a raised water temperature on the algae an exceedance plot was performed related to the algal growth rate multipliers. It was seen that the mean surface water temperature increased by about 2^{o}C in progressing from present day to distant future. This had a direct effect on the perceived favourable growth rates of all algae in Voëlvlei dam. For diatoms and greens, the favourable temperature was exceeded between 45-60% of the time, which was about double that of the present day, thereby implying twice as much blooms or greater concentrations for a future scenario than the present day. Similarly, for cyanobacteria the exceedance was 18-28%, which was 3 times greater than that of the present day.

It was noted that for the three distant future climate models, their surface water temperatures was more spread than for the present day and it was possible to rate their individual effect on the surface water temperature with ECH being the coolest and IPS the hottest with CRM the intermediate climate model.

Surface water elevations

It was expected that since the air temperature and surface water temperature increased, that the rate of evaporation from Voëlvlei would be greater than for the present day period. The result of fixing the inflow and withdrawals the same for the future simulations would be a decreased water level for the dam.

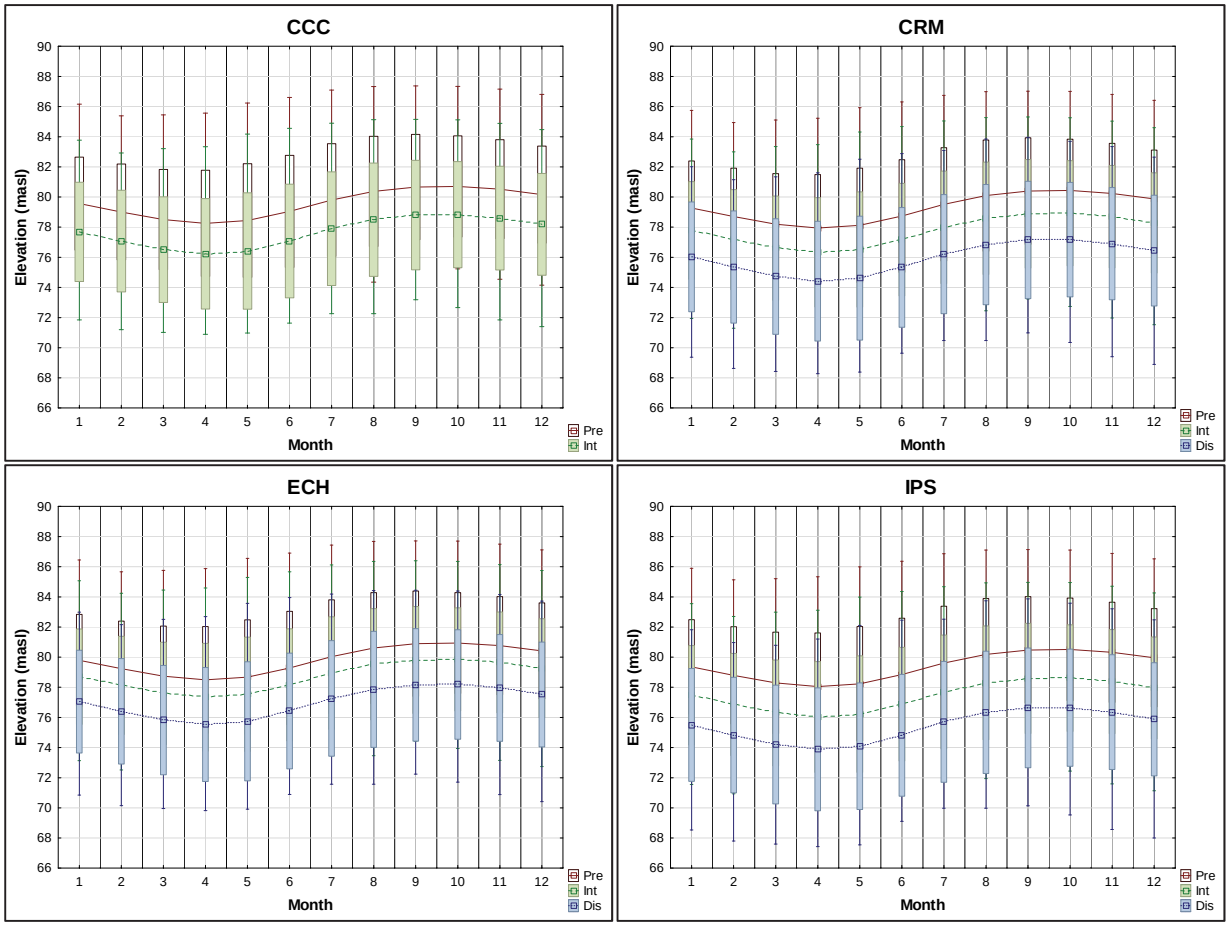

Figure 176: The projected climate change surface water elevations of Voëlvlei Dam (masl)

This phenomenon was shown in Figure 176 and Table 67 where green represents a minimum and red a maximum. The mean monthly surface water levels was decreasing in going from present day to intermediate future and finally distant future scenarios at the accelerated rate explained before.

It was clear from Table 67 that the mean monthly surface water levels decreased for future climate change scenarios due to increased air temperatures causing greater rates of evaporation. If the inflow concentration of constituents remained the same for climate change scenarios, which it did for this study, this phenomenon would concentrate all constituents in the dam as concentration was directly related to the volume of the dam, which was decreasing.

Table 67: The surface water elevations of Voëlvlei Dam (masl) under projected climate change

	Jan	Feb	Mar	Apr	May	Jun	Jul	Aug	Sep	Oct	Nov	Dec
CCC pre	79.6	79.0	78.5	78.3	78.4	79.1	79.8	80.4	80.7	80.7	80.5	80.2
Difference	-1.9	-1.9	-2.0	-2.0	-2.0	-2.0	-1.9	-1.9	-1.9	-1.9	-1.9	-2.0
CCC int	77.7	77.1	76.5	76.2	76.4	77.1	77.9	78.5	78.8	78.8	78.6	78.2
CRM pre	79.3	78.7	78.2	77.9	78.1	78.7	79.5	80.1	80.4	80.4	80.2	79.9
Difference	-1.5	-1.5	-1.6	-1.6	-1.6	-1.6	-1.5	-1.5	-1.5	-1.5	-1.5	-1.6
CRM int	77.8	77.2	76.6	76.3	76.5	77.2	78.0	78.6	78.9	78.9	78.7	78.3
CRM int	77.8	77.2	76.6	76.3	76.5	77.2	78.0	78.6	78.9	78.9	78.7	78.3
Difference	-1.8	-1.8	-1.9	-1.9	-1.9	-1.9	-1.8	-1.8	-1.7	-1.8	-1.8	-1.9
CRM fut	76.0	75.4	74.7	74.4	74.6	75.3	76.2	76.8	77.2	77.2	76.9	76.4
ECH pre	79.8	79.2	78.7	78.5	78.7	79.3	80.0	80.6	80.9	80.9	80.8	80.4
Difference	-1.1	-1.1	-1.1	-1.1	-1.1	-1.1	-1.1	-1.1	-1.1	-1.1	-1.1	-1.1
ECH int	78.7	78.1	77.6	77.3	77.5	78.2	79.0	79.5	79.8	79.9	79.7	79.3
ECH int	78.7	78.1	77.6	77.3	77.5	78.2	79.0	79.5	79.8	79.9	79.7	79.3
Difference	-1.7	-1.7	-1.8	-1.8	-1.8	-1.7	-1.7	-1.7	-1.7	-1.7	-1.7	-1.7
ECH fut	77.1	76.4	75.8	75.5	75.7	76.4	77.3	77.9	78.2	78.2	78.0	77.5
IPS pre	79.4	78.8	78.3	78.1	78.2	78.8	79.6	80.2	80.5	80.5	80.3	80.0
Difference	-1.9	-1.9	-2.0	-2.0	-2.0	-2.0	-1.9	-1.9	-1.9	-1.9	-1.9	-2.0
IPS int	77.5	76.9	76.3	76.0	76.2	76.9	77.7	78.3	78.6	78.6	78.4	78.0
IPS int	77.5	76.9	76.3	76.0	76.2	76.9	77.7	78.3	78.6	78.6	78.4	78.0
Difference	-2.0	-2.0	-2.1	-2.1	-2.1	-2.1	-2.0	-2.0	-2.0	-2.0	-2.0	-2.1
IPS fut	75.5	74.8	74.2	73.9	74.1	74.8	75.7	76.3	76.6	76.6	76.4	75.9

In conclusion, if the dam were to be operated at the current inflows and withdrawal rates for the future, it was see that the surface water levels decreased due to increased evaporation from the dam. This effective decrease was discussed in the following sections.

Ortho-Phosphorous concentration

The phosphorous concentration within the dam was influenced by various factors such as inflow and withdrawal as well as assimilation by the various algae as it was the limiting nutrient for algal growth. The future inflow concentration of phosphorous was kept the same as was for the present day scenario. The future in-dam surface concentration of phosphorous was shown for the four climate models in Figure 177.

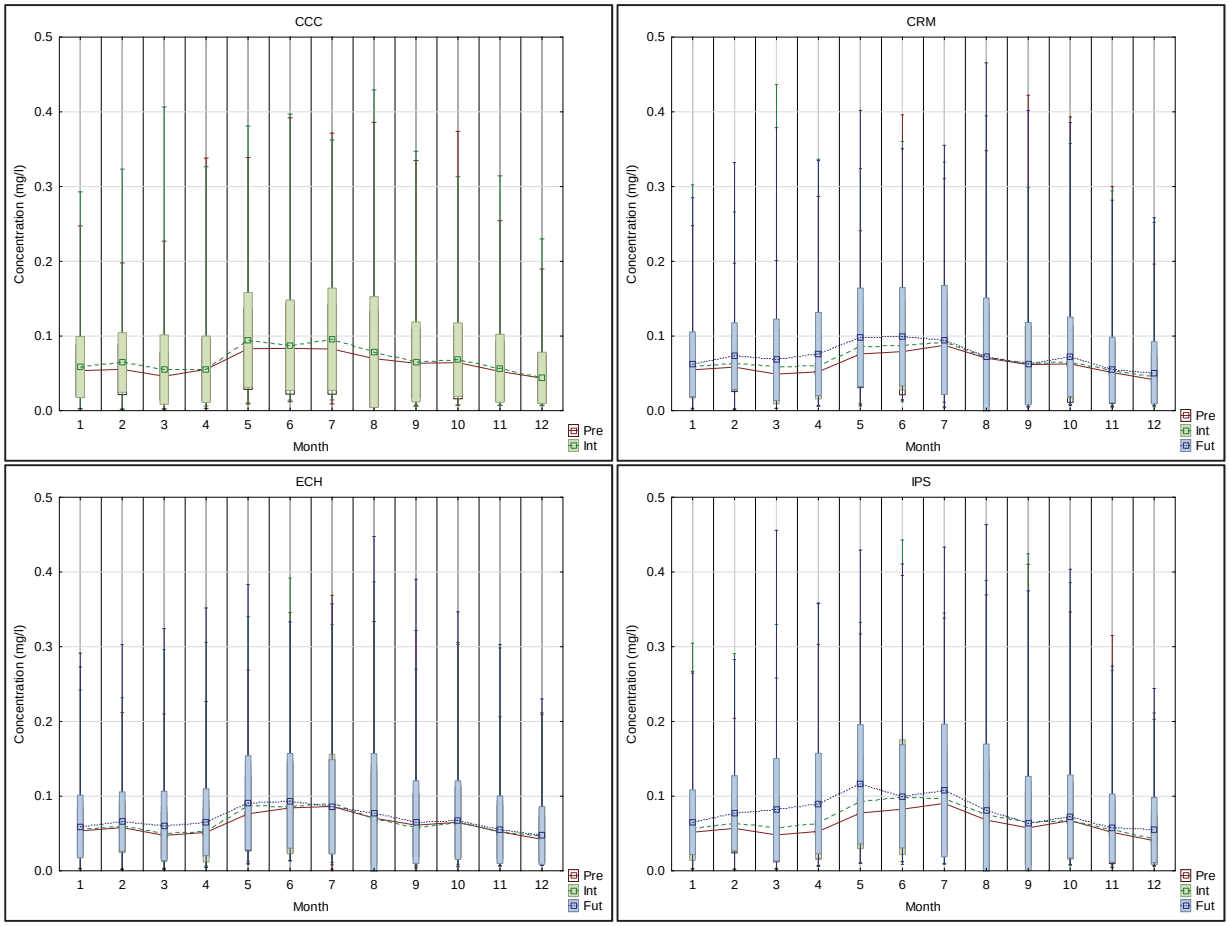

Figure 177: The projected climate change surface phosphate concentration of Voëlvlei Dam (mg/l)

From Figure 177 it was seen that the surface phosphate concentration increased for all model with climate change with inter-variability between climate models likened to that of water temperature. Since the inflow of phosphorous into the dam was kept the same for the future events the plausible reasons for the increase in surface concentration was amongst others:

- Increased upwelling of the phosphorous from the sediments due to wind action and lower surface water levels;
- Concentration of the phosphates in the dam due to evaporation of water.

Table 68: The surface phosphate concentration of Voëlvlei Dam (mg/l) under projected climate change

	Jan	Feb	Mar	Apr	May	Jun	Jul	Aug	Sep	Oct	Nov	Dec
CCC pre	0.054	0.055	0.046	0.055	0.083	0.083	0.083	0.070	0.063	0.064	0.053	0.044
Difference	0.004	0.010	0.009	0.000	0.012	0.005	0.013	0.008	0.002	0.004	0.004	0.000
CCC int	0.058	0.065	0.055	0.055	0.095	0.088	0.096	0.078	0.065	0.068	0.057	0.044
CRM pre	0.055	0.058	0.049	0.052	0.076	0.079	0.087	0.070	0.062	0.063	0.051	0.041
Difference	0.004	0.006	0.010	0.008	0.010	0.008	0.005	0.001	0.002	0.002	0.003	0.004
CRM int	0.059	0.064	0.059	0.060	0.086	0.087	0.092	0.071	0.064	0.065	0.054	0.045
CRM int	0.059	0.064	0.059	0.060	0.086	0.087	0.092	0.071	0.064	0.065	0.054	0.045
Difference	0.003	0.009	0.009	0.016	0.012	0.012	0.003	0.001	-0.001	0.007	0.001	0.006
CRM fut	0.062	0.073	0.068	0.076	0.098	0.099	0.095	0.072	0.063	0.072	0.055	0.051
ECH pre	0.053	0.058	0.047	0.052	0.076	0.084	0.086	0.071	0.061	0.065	0.052	0.042
Difference	0.003	0.002	0.003	0.001	0.011	0.002	0.004	-0.001	-0.003	0.000	0.001	0.004
ECH int	0.056	0.060	0.050	0.053	0.087	0.086	0.090	0.070	0.058	0.065	0.053	0.046
ECH int	0.056	0.060	0.050	0.053	0.087	0.086	0.090	0.070	0.058	0.065	0.053	0.046
Difference	0.003	0.006	0.010	0.012	0.004	0.008	-0.004	0.007	0.007	0.003	0.002	0.001
ECH fut	0.059	0.066	0.060	0.065	0.091	0.094	0.086	0.077	0.065	0.068	0.055	0.047
IPS pre	0.052	0.057	0.048	0.053	0.077	0.083	0.090	0.068	0.057	0.067	0.051	0.040
Difference	0.005	0.007	0.009	0.010	0.016	0.016	0.007	0.007	0.008	0.001	0.004	0.003
IPS int	0.057	0.064	0.057	0.063	0.093	0.099	0.097	0.075	0.065	0.068	0.055	0.043
IPS int	0.057	0.064	0.057	0.063	0.093	0.099	0.097	0.075	0.065	0.068	0.055	0.043
Difference	0.008	0.013	0.025	0.027	0.023	0.001	0.010	0.006	-0.002	0.005	0.002	0.012
IPS fut	0.065	0.077	0.082	0.090	0.116	0.100	0.107	0.081	0.063	0.073	0.057	0.055

From Table 68 it was seen that the mean monthly phosphorous concentration increased with climate change into the future. The order of increasing surface phosphorous concentration was ECH, CRM then IPS in terms of climate models. The only variable between these models was the air temperature difference that causes the lower surface water levels. Thus, the lower surface water levels have a concentrating effect on the surface phosphorous concentration. The increase in phosphorous was seen during summer as well as having the greatest increases during autumn.

It was concluded that the concentration of phosphorous in Voëlvlei was sufficiently great that it never poses a limitation for algal growth from the present day to distant future climate events. For this dam, a point source reduction of phosphorous for the inflows would greatly

reduce algal blooms in all climate change scenarios, based on the premise that phosphorous was the limiting nutrient for algal growth.

The sources of phosphorous that could contribute to an increase are increased algal respiration, increased anaerobic release from sediments as well as decay. Decreases are due to photosynthesis and system losses to withdrawal and adsorption/settling.

Ammonium concentration

For the future climate change events it was seen in Figure 178 and Table 69 that the surface concentration of ammonium was increased for all the climate models and that the mean monthly concentration was below the DWA limit of 1mg/l, although peaks beyond this did occur. ECH, CRM followed by the IPS was the order in which the surface concentration of ammonium mirrors that of air temperature.

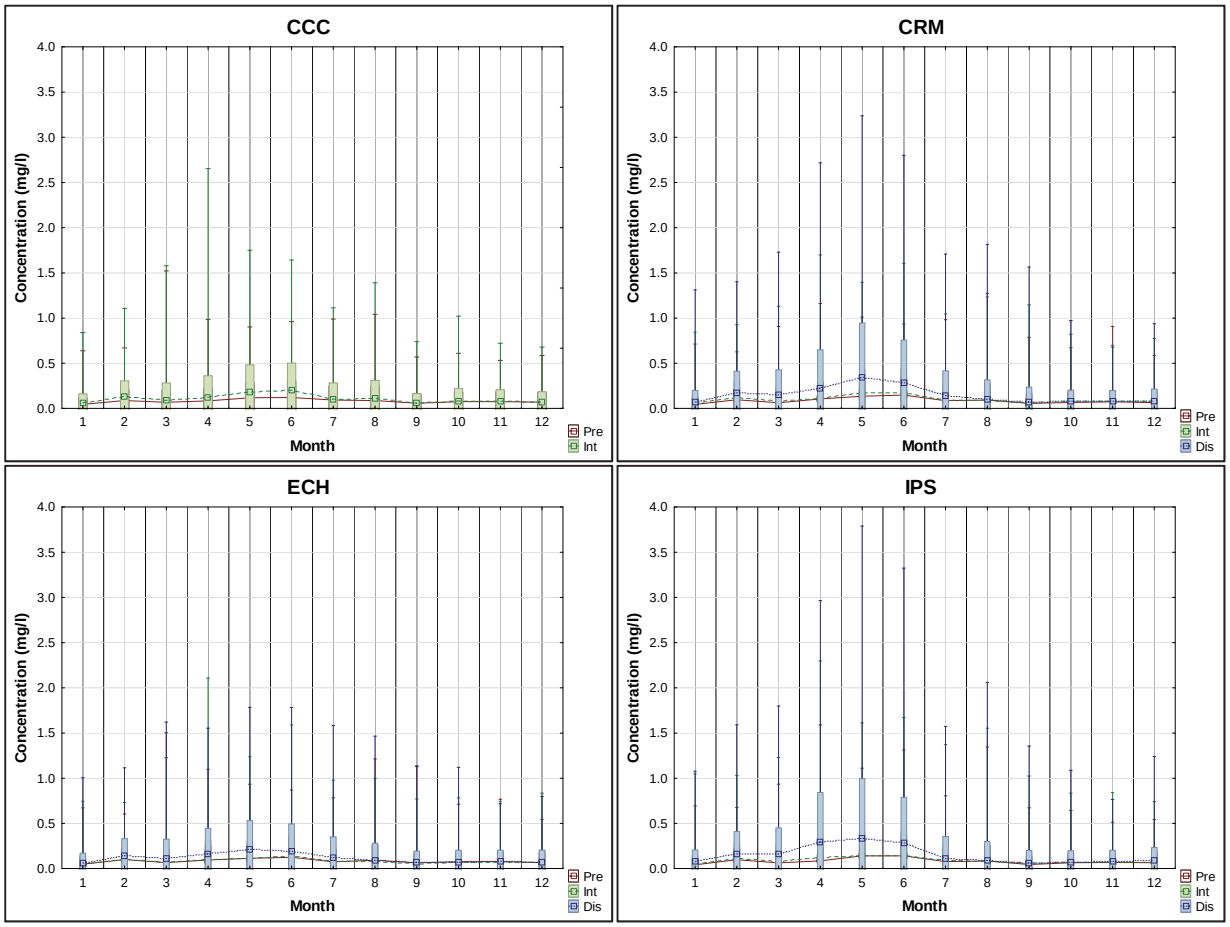

Figure 178: The projected climate change surface ammonium concentration of Voëlvlei Dam (mg/l)

Table 69: The mean monthly surface ammonium concentration of Voëlvlei Dam (mg/l) under projected climate change

	Jan	Feb	Mar	Apr	May	Jun	Jul	Aug	Sep	Oct	Nov	Dec
CCC pre	0.046	0.088	0.069	0.084	0.118	0.123	0.093	0.088	0.058	0.076	0.076	0.071
Difference	0.016	0.039	0.022	0.034	0.061	0.080	0.010	0.022	0.000	0.009	0.007	0.000
CCC int	0.062	0.127	0.091	0.118	0.179	0.203	0.103	0.110	0.058	0.085	0.083	0.071
CRM pre	0.046	0.096	0.063	0.105	0.136	0.149	0.086	0.093	0.056	0.068	0.073	0.065
Difference	0.013	0.030	0.021	0.004	0.038	0.028	0.004	-0.001	0.001	0.010	0.007	0.012
CRM int	0.059	0.126	0.084	0.109	0.174	0.177	0.090	0.092	0.057	0.078	0.080	0.077
CRM int	0.059	0.126	0.084	0.109	0.174	0.177	0.090	0.092	0.057	0.078	0.080	0.077
Difference	0.015	0.042	0.066	0.118	0.167	0.106	0.053	0.011	0.016	-0.001	-0.003	0.004
CRM fut	0.074	0.168	0.150	0.227	0.341	0.283	0.143	0.103	0.073	0.077	0.077	0.081
ECH pre	0.049	0.101	0.068	0.095	0.115	0.125	0.076	0.094	0.064	0.078	0.077	0.067
Difference	0.003	0.003	0.001	0.008	0.002	0.021	0.009	-0.011	-0.012	-0.005	-0.002	0.009
ECH int	0.052	0.104	0.069	0.103	0.117	0.146	0.085	0.083	0.052	0.073	0.075	0.076
ECH int	0.052	0.104	0.069	0.103	0.117	0.146	0.085	0.083	0.052	0.073	0.075	0.076
Difference	0.011	0.036	0.046	0.062	0.092	0.043	0.041	0.012	0.016	0.001	0.003	0.000
ECH fut	0.063	0.140	0.115	0.165	0.209	0.189	0.126	0.095	0.068	0.074	0.078	0.076
IPS pre	0.042	0.098	0.064	0.087	0.142	0.141	0.078	0.084	0.046	0.064	0.069	0.065
Difference	0.011	0.016	0.021	0.033	0.001	0.004	0.013	0.001	0.016	0.010	0.006	0.005
IPS int	0.053	0.114	0.085	0.120	0.143	0.145	0.091	0.085	0.062	0.074	0.075	0.070
IPS int	0.053	0.114	0.085	0.120	0.143	0.145	0.091	0.085	0.062	0.074	0.075	0.070
Difference	0.023	0.050	0.075	0.173	0.189	0.136	0.026	0.005	0.002	0.001	0.003	0.017
IPS fut	0.076	0.164	0.160	0.293	0.332	0.281	0.117	0.090	0.064	0.075	0.078	0.087

All models showed increases but the greatest increase occurred in going from intermediate future to distant future as shown by the table. An increase in ammonium was attributed to increased algal respiration, decay of dissolved organic material and anaerobic release from the sediments. System losses of ammonium were due to photosynthesis and nitrification to form the nitrate-nitrite complex ion.

Nitrate-nitrite concentration

The surface nitrate-nitrite concentration was shown in Figure 179 and Table 70. From this, it was seen that the future surface concentrations remain relatively unchanged when

compared to present day surface concentrations, with winter having the higher concentrations.

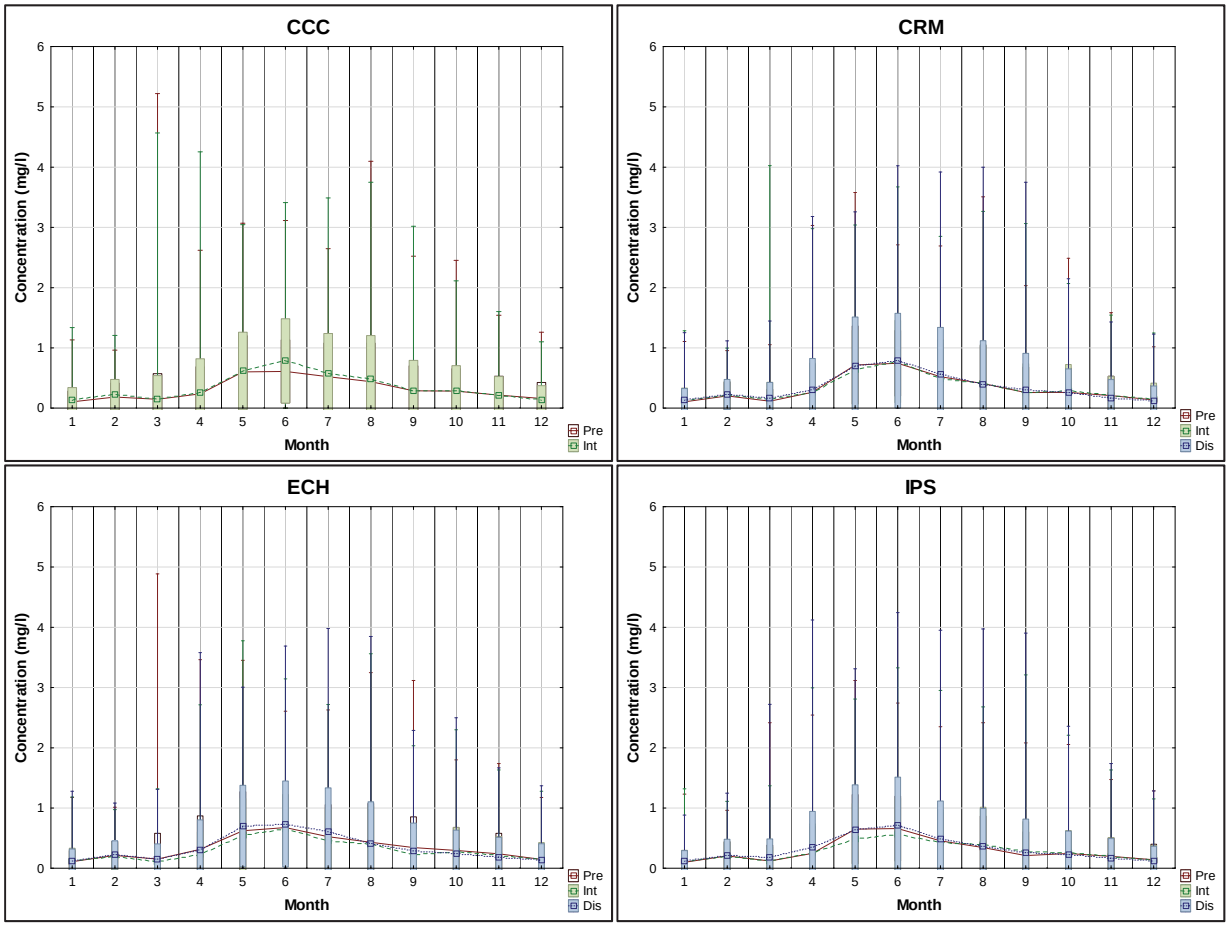

Figure 179: The projected climate change surface nitrate-nitrite concentration of Voëlvlei Dam (mg/l)

It was interesting to note that some months showed a decrease in concentrations whereas other months show an increase. The nitrate-nitrite complex was an intermediary and its losses are due to photosynthesis and de-nitrification to the water column. It was generated from ammonium via nitrification.

Table 70: The mean monthly surface nitrate-nitrite concentration of Voëlvlei Dam (mg/l) under projected climate change

	Jan	Feb	Mar	Apr	May	Jun	Jul	Aug	Sep	Oct	Nov	Dec
CCC pre	0.10	0.19	0.15	0.24	0.60	0.61	0.52	0.44	0.29	0.28	0.22	0.16
Difference	0.03	0.03	0.00	0.02	0.02	0.18	0.06	0.05	0.00	0.01	-0.01	-0.03
CCC int	0.13	0.22	0.15	0.26	0.62	0.79	0.58	0.49	0.29	0.29	0.21	0.13
CRM pre	0.11	0.20	0.12	0.26	0.72	0.75	0.52	0.41	0.26	0.26	0.21	0.14
Difference	0.02	0.01	0.03	0.00	-0.08	0.03	-0.03	0.00	0.00	0.03	0.00	0.01
CRM int	0.13	0.21	0.15	0.26	0.64	0.78	0.49	0.41	0.26	0.29	0.21	0.15
CRM int	0.13	0.21	0.15	0.26	0.64	0.78	0.49	0.41	0.26	0.29	0.21	0.15
Difference	0.00	0.02	0.02	0.05	0.07	0.01	0.08	-0.01	0.04	-0.04	-0.04	-0.02
CRM fut	0.13	0.23	0.17	0.31	0.71	0.79	0.57	0.40	0.30	0.25	0.17	0.13
ECH pre	0.11	0.21	0.15	0.31	0.62	0.68	0.52	0.43	0.35	0.30	0.24	0.15
Difference	0.01	-0.01	-0.04	-0.08	-0.07	-0.03	-0.06	-0.03	-0.12	-0.02	-0.03	0.00
ECH int	0.12	0.20	0.11	0.23	0.55	0.65	0.46	0.40	0.23	0.28	0.21	0.15
ECH int	0.12	0.20	0.11	0.23	0.55	0.65	0.46	0.40	0.23	0.28	0.21	0.15
Difference	0.00	0.02	0.05	0.08	0.15	0.09	0.14	0.02	0.06	-0.04	-0.02	-0.01
ECH fut	0.12	0.22	0.16	0.31	0.70	0.74	0.60	0.42	0.29	0.24	0.19	0.14
IPS pre	0.10	0.21	0.12	0.25	0.65	0.66	0.45	0.34	0.21	0.25	0.20	0.14
Difference	0.01	-0.01	0.01	0.01	-0.16	-0.09	-0.03	0.06	0.07	0.01	-0.01	-0.01
IPS int	0.11	0.20	0.13	0.26	0.49	0.57	0.42	0.40	0.28	0.26	0.19	0.13
IPS int	0.11	0.20	0.13	0.26	0.49	0.57	0.42	0.40	0.28	0.26	0.19	0.13
Difference	0.01	0.02	0.05	0.08	0.15	0.14	0.07	-0.04	-0.02	-0.03	-0.02	0.00
IPS fut	0.12	0.22	0.18	0.34	0.64	0.71	0.49	0.36	0.26	0.23	0.17	0.13

When examining Figure 180 it was seen that the exceedance of total surface N does not vary significantly with respect half-saturation constant for green algae. This would imply that total surface N concentration did not affect the growth of green algae from an increased limiting aspect, in the event of climate change.

The concentration of total surface N increased similarly to that of air temperature with the different climate models i.e. ECH, CRM then IPS.

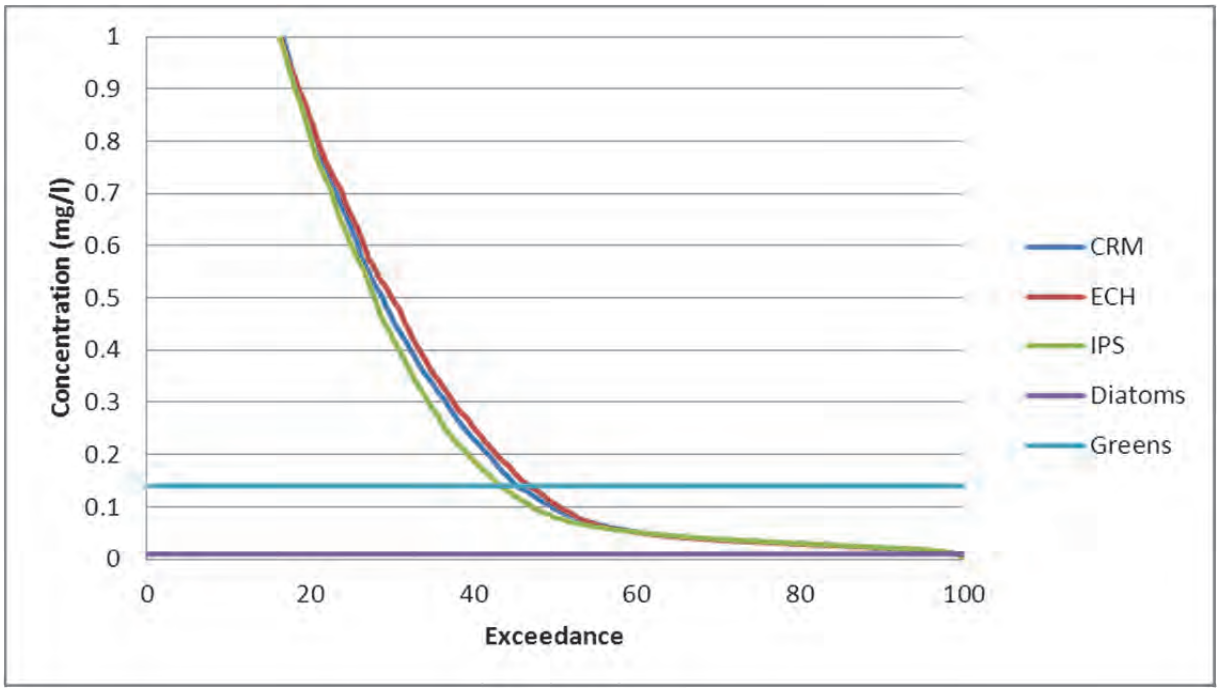

Figure 180: The projected distant future total surface N exceedance with respect to algal growth of Voëlvlei Dam

Dissolved silicon

It had been established that only diatoms are silicon limited for growth and when comparing Figure 181 and Table 71 to their present day counterparts, it was seen that the mean monthly surface dissolved silicon concentration increases for future events and winter had the greatest concentration. It was noted that the surface dissolved silicon concentration does not exceed the DWA limit of 150mg/l.

The inter-variability of the climate models was shown but was within reasonable limits of themselves, but it was noted that the greatest increases are seen when progressing from intermediate future to the distant future. This increase seemed to be directly related to the climate model as the least change was seen with the cooler models and the greatest with the hottest model, namely the IPS model.

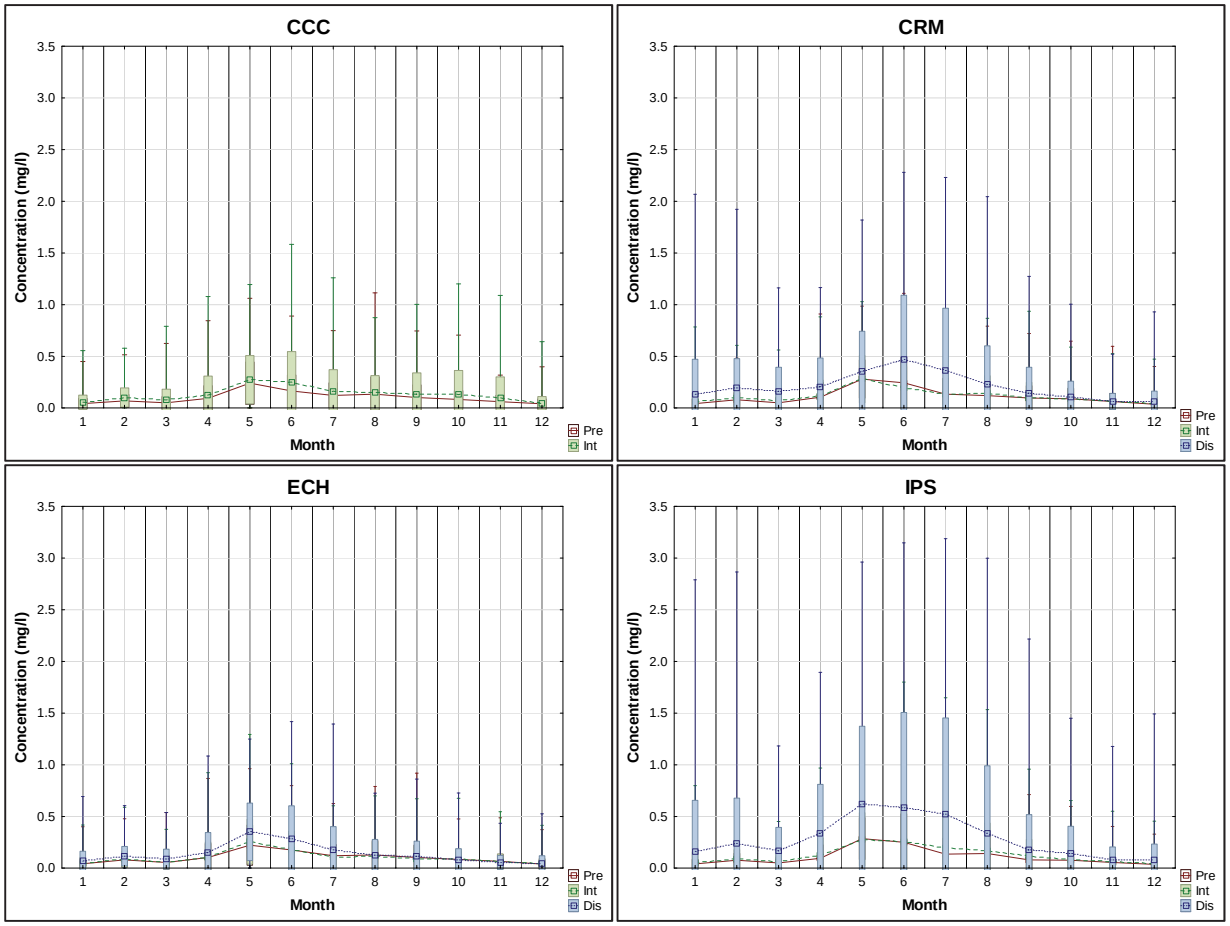

Figure 181: The projected climate change surface dissolved silicon concentration of Voëlvlei dam (mg/l)

The inter-variability was shown in the Table 71 and the dissolved silicon increased with climate change except for the ECH model, which was seen to be cooler.

Table 71: The mean monthly surface dissolved silicon concentration of Voëlvlei Dam (mg/l) under projected climate change

	Jan	Feb	Mar	Apr	May	Jun	Jul	Aug	Sep	Oct	Nov	Dec
CCC pre	0.043	0.069	0.050	0.093	0.241	0.165	0.122	0.134	0.102	0.084	0.062	0.041
Difference	0.013	0.033	0.029	0.028	0.033	0.087	0.041	0.013	0.033	0.046	0.039	0.004
CCC int	0.056	0.102	0.079	0.121	0.274	0.252	0.163	0.147	0.135	0.130	0.101	0.045
CRM pre	0.043	0.080	0.050	0.105	0.280	0.244	0.134	0.120	0.097	0.088	0.062	0.037
Difference	0.020	0.017	0.024	0.009	0.000	-0.047	-0.003	0.019	0.005	0.002	0.000	0.008
CRM int	0.063	0.097	0.074	0.114	0.280	0.197	0.131	0.139	0.102	0.090	0.062	0.045
CRM int	0.063	0.097	0.074	0.114	0.280	0.197	0.131	0.139	0.102	0.090	0.062	0.045
Difference	0.070	0.098	0.089	0.093	0.072	0.272	0.232	0.088	0.043	0.016	0.000	0.016
CRM fut	0.133	0.195	0.163	0.207	0.352	0.469	0.363	0.227	0.145	0.106	0.062	0.061
ECH pre	0.043	0.080	0.055	0.102	0.223	0.177	0.120	0.128	0.103	0.084	0.066	0.039
Difference	0.006	0.006	0.002	0.005	0.033	0.003	-0.011	-0.011	-0.012	0.002	-0.003	0.003
ECH int	0.049	0.086	0.057	0.107	0.256	0.180	0.109	0.117	0.091	0.086	0.063	0.042
ECH int	0.049	0.086	0.057	0.107	0.256	0.180	0.109	0.117	0.091	0.086	0.063	0.042
Difference	0.019	0.029	0.031	0.042	0.096	0.103	0.066	0.011	0.023	-0.003	-0.007	0.007
ECH fut	0.068	0.115	0.088	0.149	0.352	0.283	0.175	0.128	0.114	0.083	0.056	0.049
IPS pre	0.041	0.077	0.051	0.096	0.286	0.250	0.135	0.142	0.079	0.077	0.055	0.036
Difference	0.016	0.014	0.014	0.025	-0.008	0.011	0.059	0.030	0.033	0.005	0.010	0.008
IPS int	0.057	0.091	0.065	0.121	0.278	0.261	0.194	0.172	0.112	0.082	0.065	0.044
IPS int	0.057	0.091	0.065	0.121	0.278	0.261	0.194	0.172	0.112	0.082	0.065	0.044
Difference	0.106	0.148	0.100	0.217	0.347	0.325	0.327	0.169	0.063	0.058	0.011	0.035
IPS fut	0.163	0.239	0.165	0.338	0.625	0.586	0.521	0.341	0.175	0.140	0.076	0.079

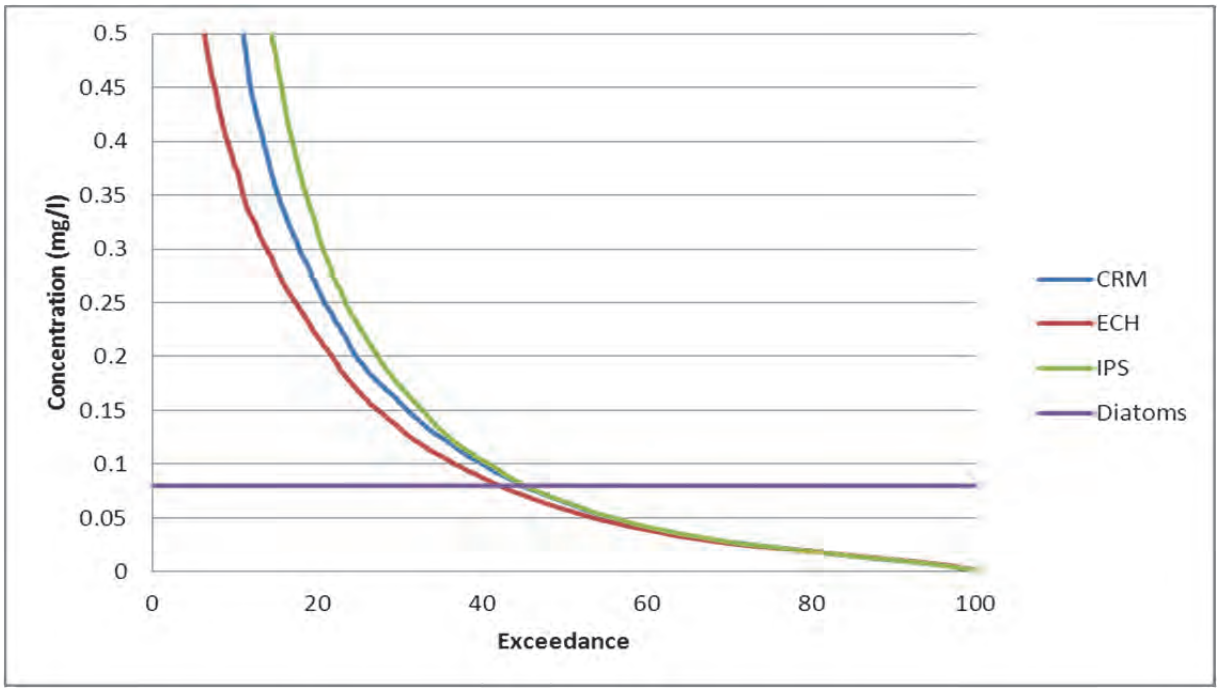

Figure 182: The projected distant future surface dissolved silicon concentration exceedance with respect to diatom growth of Voëlvlei Dam

From the exceedance plot for surface dissolved silicon with regards the half-saturation constant (0.08 mg/l) for diatoms it was seen that this had increased to 43-48% depending on the climate model. This would imply that the concentration of surface dissolved silicon was great enough to allow the maximum growth of diatoms 43 % of the simulation period.

Dissolved oxygen

It was expected from the dissolved oxygen concentration that for the surface water it would decrease due to the increased temperature causing greater dissociation of oxygen to the atmosphere. This phenomenon was shown in Figure 183 with climate change events the concentration of dissolved oxygen in the surface water levels decreased. The figure also shows that the dissolved oxygen concentration was greatest during winter, when the surface water was cooler and can hold more oxygen as showed by the mean surface dissolved oxygen concentrations in Table 72.

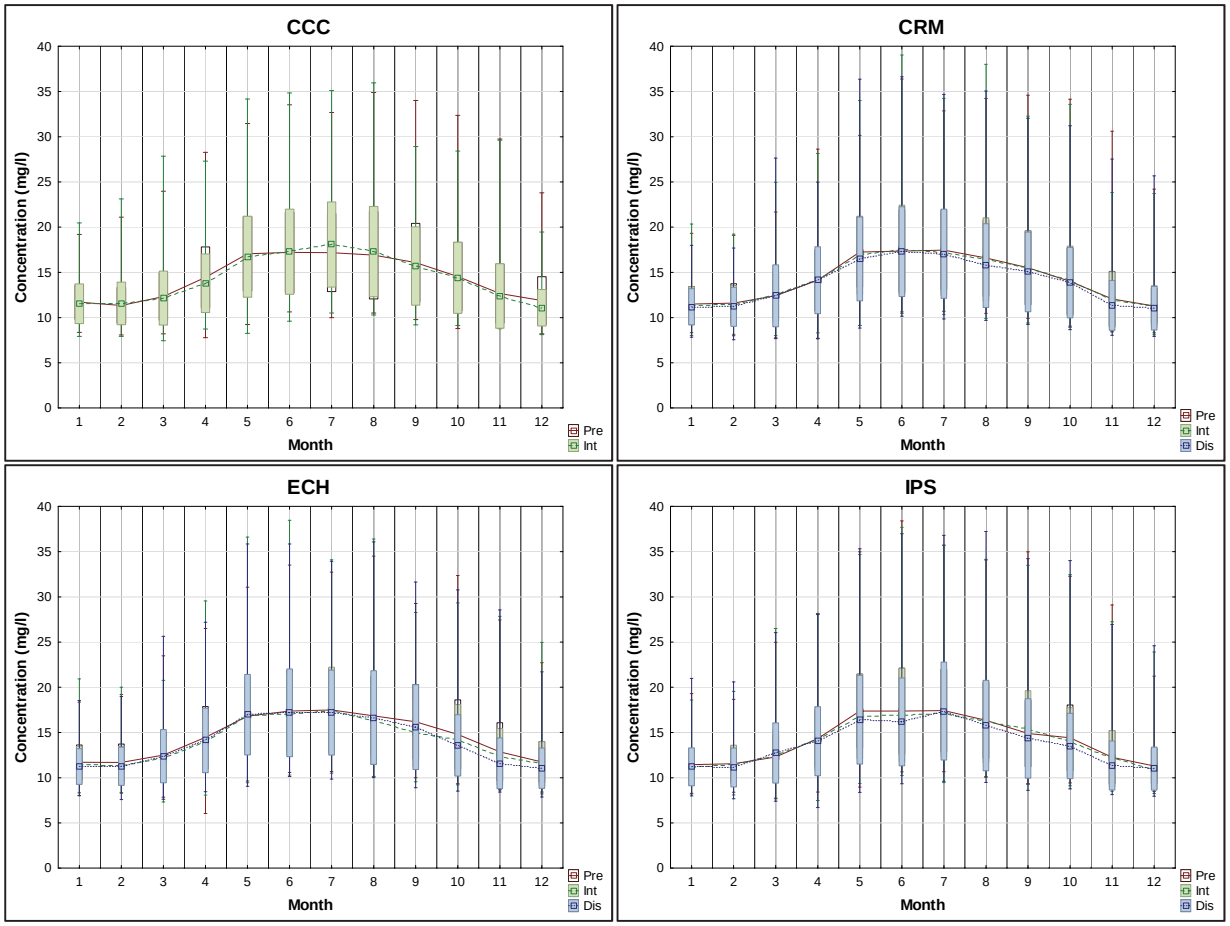

Figure 183: The projected climate change surface dissolved oxygen concentration of Voëlvlei Dam (mg/l)

It has been explained that these dissolved oxygen rates were deemed very high and super-saturated and thus considered unrealistic but that this study showed the difference due to climate change.

Table 72: The mean monthly surface dissolved oxygen concentration of Voëlvlei Dam (mg/l) under projected climate change

	Jan	Feb	Mar	Apr	May	Jun	Jul	Aug	Sep	Oct	Nov	Dec
CCC pre	11.71	11.34	12.32	14.45	17.05	17.21	17.18	16.90	16.08	14.53	12.66	11.89
Difference	-0.18	0.24	-0.16	-0.65	-0.31	0.08	0.90	0.40	-0.38	-0.12	-0.26	-0.80
CCC int	11.53	11.58	12.16	13.80	16.74	17.29	18.08	17.30	15.70	14.41	12.40	11.09
CRM pre	11.49	11.61	12.41	14.13	17.26	17.36	17.47	16.60	15.51	14.01	12.06	11.28
Difference	-0.17	-0.21	0.20	0.01	-0.36	0.13	-0.26	-0.17	-0.01	0.05	-0.08	-0.06
CRM int	11.32	11.40	12.61	14.14	16.90	17.49	17.21	16.43	15.50	14.06	11.98	11.22
CRM int	11.32	11.40	12.61	14.14	16.90	17.49	17.21	16.43	15.50	14.06	11.98	11.22
Difference	-0.13	-0.20	-0.20	-0.01	-0.42	-0.20	-0.14	-0.67	-0.45	-0.19	-0.64	-0.17
CRM fut	11.19	11.20	12.41	14.13	16.48	17.29	17.07	15.76	15.05	13.87	11.34	11.05
ECH pre	11.70	11.68	12.50	14.47	16.80	17.37	17.50	16.83	16.18	14.78	12.86	11.74
Difference	-0.25	-0.29	-0.38	-0.45	0.07	-0.37	-0.04	-0.53	-1.20	-0.58	-0.55	-0.22
ECH int	11.45	11.39	12.12	14.02	16.87	17.00	17.46	16.30	14.98	14.20	12.31	11.52
ECH int	11.45	11.39	12.12	14.02	16.87	17.00	17.46	16.30	14.98	14.20	12.31	11.52
Difference	-0.21	-0.11	0.26	0.11	0.11	0.18	-0.25	0.36	0.62	-0.62	-0.71	-0.46
ECH fut	11.24	11.28	12.38	14.13	16.98	17.18	17.21	16.66	15.60	13.58	11.60	11.06
IPS pre	11.44	11.55	12.30	14.33	17.37	17.37	17.43	16.34	14.90	14.42	12.26	11.30
Difference	-0.30	-0.10	0.11	-0.02	-0.58	-0.41	-0.26	-0.16	0.51	-0.49	-0.15	-0.36
IPS int	11.14	11.45	12.41	14.31	16.79	16.96	17.17	16.18	15.41	13.93	12.11	10.94
IPS int	11.14	11.45	12.41	14.31	16.79	16.96	17.17	16.18	15.41	13.93	12.11	10.94
Difference	0.07	-0.31	0.32	-0.27	-0.37	-0.79	0.20	-0.41	-1.07	-0.41	-0.75	0.06
IPS fut	11.21	11.14	12.73	14.04	16.42	16.17	17.37	15.77	14.34	13.52	11.36	11.00

From Table 72 it was seen that dissolve oxygen concentrations for the surface decreased with all climate models especially during summer. The distant future showed the greatest changes due to climate. The inter-variability between the models was not much and all showed a decrease with increased water temperature.

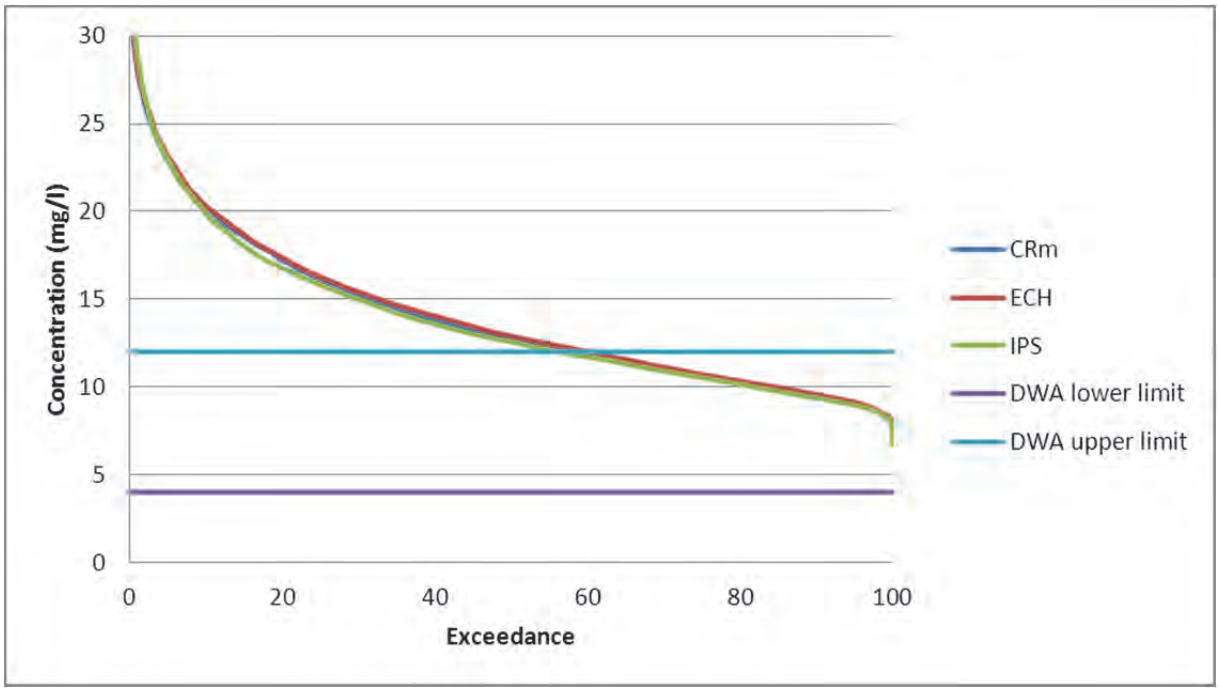

Figure 184: Distant future surface dissolved oxygen DWA limit exceedance plot

From the plot in Figure 184 it was seen that the surface dissolved oxygen exceedance has decreased from 65% in the present day to 58% in the distant future. This means that approximately an additional 7% of the simulation period that the surface dissolved oxygen was outside the TWQR limits set by DWA in the distant future as compared to the present day.

Total algae concentration

It was seen that with climate change the increased air temperatures would lead to increased surface water temperatures. To establish a link to this increased water temperature and algal blooms the total algae was plotted in Figure 185 for Voëlvlei dam.

From Figure 185 it was seen that with climate change the mean monthly total algal concentration was greater than for the present day. This was attributed directly to the increased air temperature driving the growth of the algae.

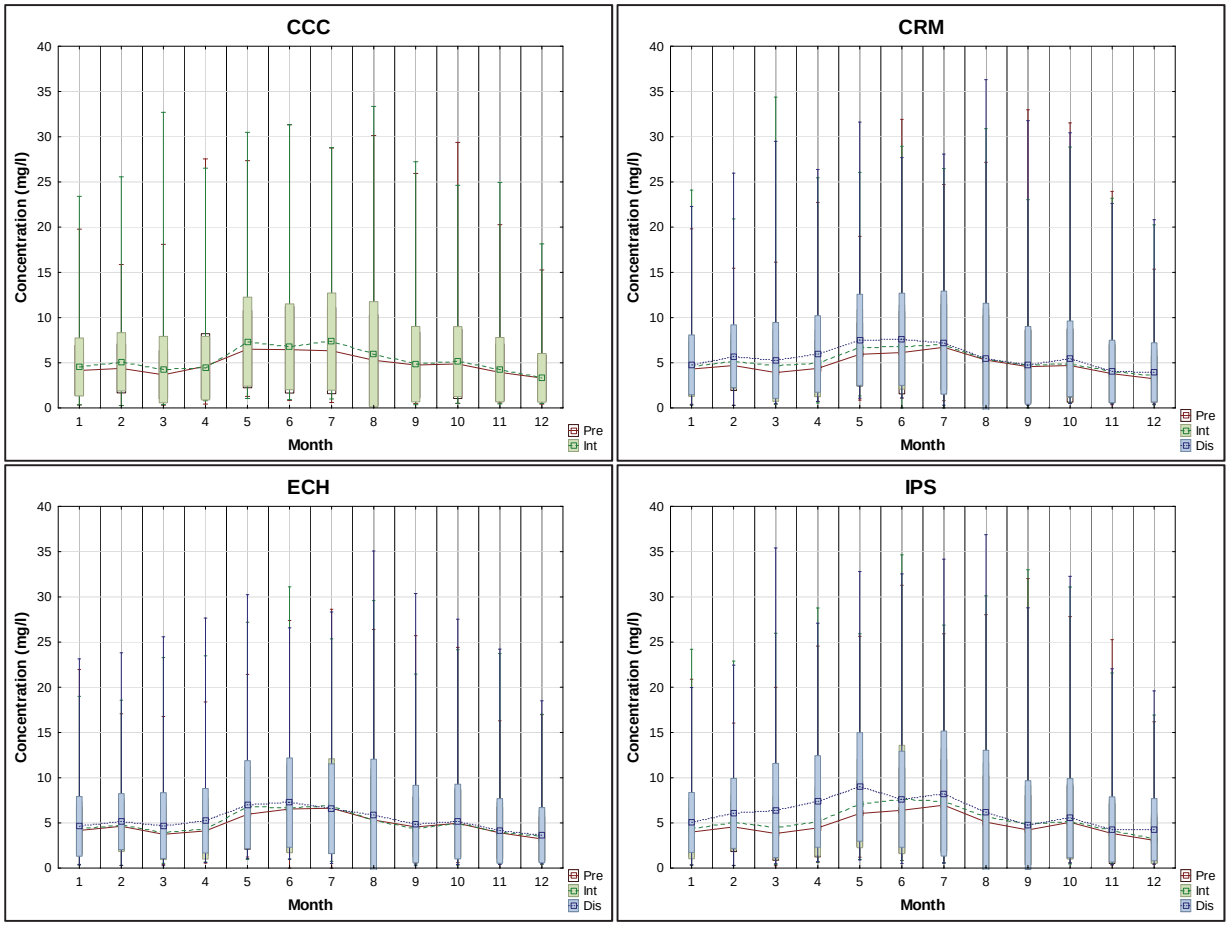

Figure 185: The projected climate change surface total algae concentration of Voëlvlei Dam (mg/l)

It was seen that the mean monthly surface total algae concentration was greatest for winter and that for a climate change scenario the concentration was increasing in going from present day to intermediate future to distant future. Most of the increased concentration occurs late summer to autumn with the mean winter concentrations remaining relatively unchanged. This could imply a seasonal shift or algal succession.

Table 73: The mean monthly surface total algae concentration of Voëlvlei Dam (mg/l) under projected climate change

	Jan	Feb	Mar	Apr	May	Jun	Jul	Aug	Sep	Oct	Nov	Dec
CCC pre	4.16	4.38	3.68	4.64	6.51	6.45	6.34	5.28	4.74	4.87	3.94	3.33
Difference	0.38	0.73	0.57	-0.22	0.83	0.31	1.01	0.65	0.11	0.27	0.30	0.01
CCC int	4.54	5.11	4.25	4.42	7.34	6.76	7.35	5.93	4.85	5.14	4.24	3.34
CRM pre	4.31	4.71	3.91	4.37	5.94	6.14	6.71	5.30	4.57	4.70	3.80	3.23
Difference	0.25	0.44	0.77	0.57	0.74	0.61	0.32	0.10	0.16	0.20	0.21	0.27
CRM int	4.56	5.15	4.68	4.94	6.68	6.75	7.03	5.40	4.73	4.90	4.01	3.50
CRM int	4.56	5.15	4.68	4.94	6.68	6.75	7.03	5.40	4.73	4.90	4.01	3.50
Difference	0.22	0.58	0.59	1.03	0.86	0.85	0.20	0.07	-0.02	0.55	0.04	0.44
CRM fut	4.78	5.73	5.27	5.97	7.54	7.60	7.23	5.47	4.71	5.45	4.05	3.94
ECH pre	4.17	4.64	3.74	4.11	5.96	6.55	6.62	5.31	4.56	4.96	3.91	3.23
Difference	0.22	0.14	0.24	0.25	0.82	0.11	0.32	-0.02	-0.22	0.03	0.06	0.33
ECH int	4.39	4.78	3.98	4.36	6.78	6.66	6.94	5.29	4.34	4.99	3.97	3.56
ECH int	4.39	4.78	3.98	4.36	6.78	6.66	6.94	5.29	4.34	4.99	3.97	3.56
Difference	0.23	0.37	0.73	0.89	0.25	0.59	-0.38	0.58	0.54	0.15	0.14	0.09
ECH fut	4.62	5.15	4.71	5.25	7.03	7.25	6.56	5.87	4.88	5.14	4.11	3.65
IPS pre	4.00	4.56	3.83	4.44	6.04	6.40	6.95	5.10	4.22	5.08	3.83	3.08
Difference	0.39	0.52	0.68	0.74	1.11	1.20	0.49	0.61	0.66	0.09	0.31	0.19
IPS int	4.39	5.08	4.51	5.18	7.15	7.60	7.44	5.71	4.88	5.17	4.14	3.27
IPS int	4.39	5.08	4.51	5.18	7.15	7.60	7.44	5.71	4.88	5.17	4.14	3.27
Difference	0.67	0.97	1.87	2.20	1.83	0.03	0.81	0.45	-0.11	0.36	0.15	0.99
IPS fut	5.06	6.05	6.38	7.38	8.98	7.63	8.25	6.16	4.77	5.53	4.29	4.26

Table 73 shows the percentage mean monthly increase in total algae concentration in going from the present day to the distant future. It was clear that all the climate models predicted a mean monthly increase with the maximum increases occurring during autumn to early winter. On average, the annual increase was 15.5% increase in total algal concentration. The ECH model predicted the lowest percentage increase as it was the climate model with the lowest increase in air temperature. The IPS model predicted the greatest increase in diatom concentration and it was the hottest of all the climate models. This confirms that the air temperature was the driver for surface algal growth when all other conditions were equal for algal growth such as nutrients and light.

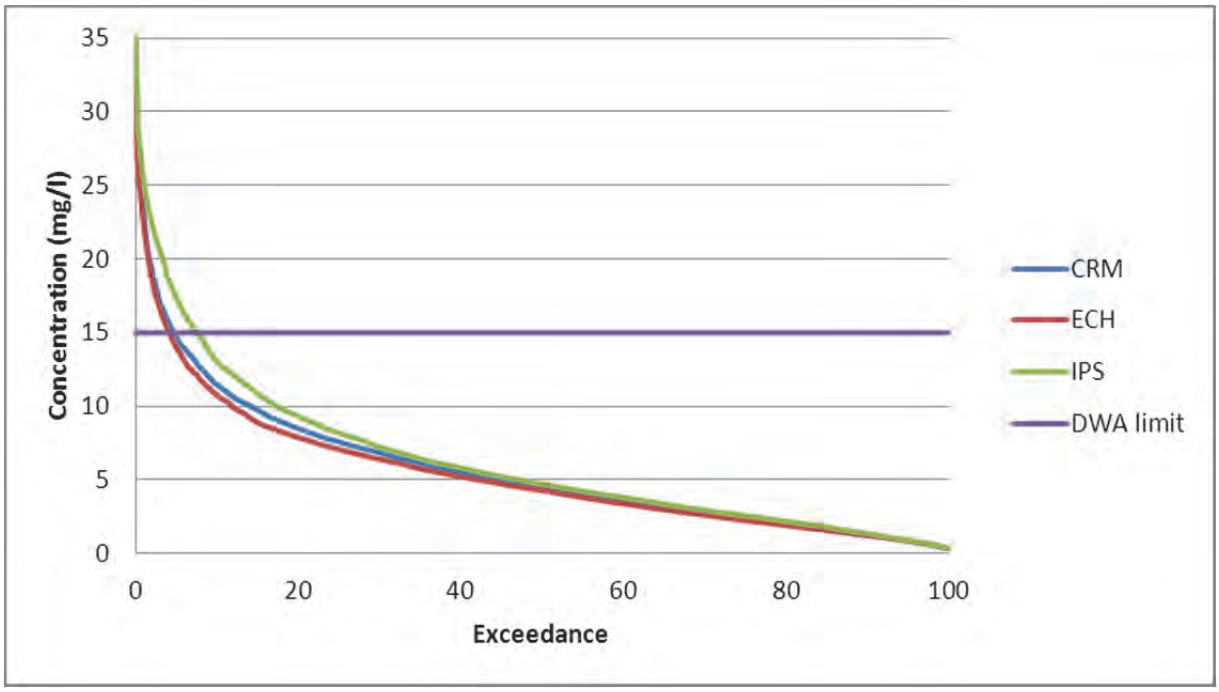

Figure 186: The projected distant future surface total algae DWA exceedance plot of Voëlvlei Dam

Figure 186 show that the surface total algae would exceed the DWA limit of 15mg/l of total algae for the distant future by 3% to 5% for CRM and ECH climate model and 8% for the IPS climate model.

An investigation into which species of algae (diatom, green or cyanobacteria) dominated in Voëlvlei dam follows.

Diatom concentration

The mean annual increase in algal growth in going from the present day to the distant future was predicted at 15.5% increase in algal concentration, what was required was to see which of the three species of algae, namely diatoms, green or cyanobacteria was responsible for the majority of this increase. It was clear from Figure 187: The projected climate change surface diatom concentration of Voëlvlei Dam (mg/l)

that the surface concentration of diatoms that it does increase especially in autumn to winter as expected due to increased air temperature, with the greatest concentrations during winter for all climate change models.

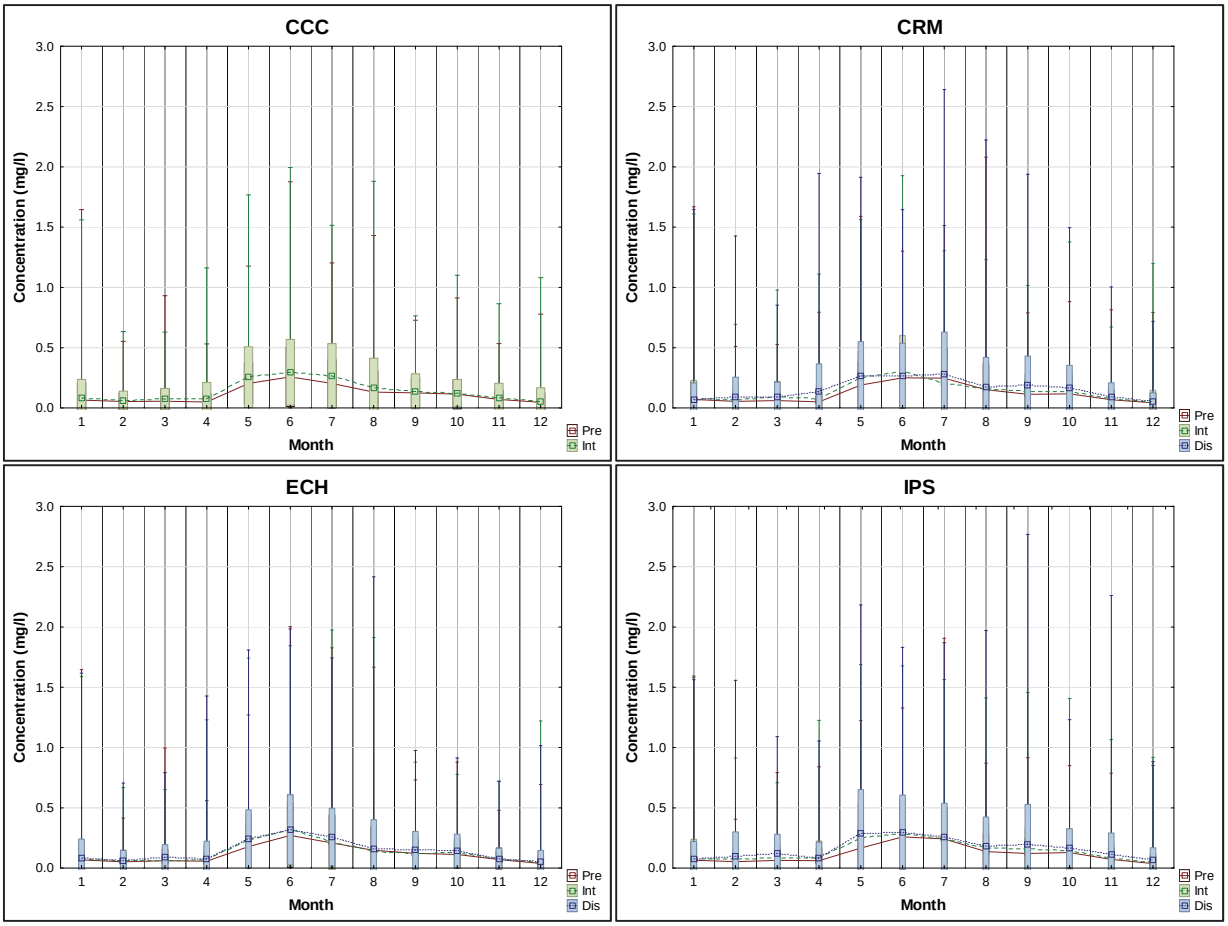

Figure 187: The projected climate change surface diatom concentration of Voëlvlei Dam (mg/l)

From Table 74 it was seen that the monthly mean surface diatom concentration increased between 18.9% and 30% depending on the climate model used. The average annual mean surface diatom concentration increased by 24.6% in progressing from the present day to distant future. The months that showed the greatest increase were autumn and spring. This could be likened to a seasonal shift for diatoms and they show increasing concentrations earlier during the year. This could mean a seasonal shift in the blooms of surface diatoms to autumn as well as a lengthening of the season of diatom blooms until late spring. This was because of the increased air temperature.

Table 74: The mean monthly surface diatom concentration of Voëlvlei Dam (mg/l) under projected climate change

	Jan	Feb	Mar	Apr	May	Jun	Jul	Aug	Sep	Oct	Nov	Dec
CCC pre	0.066	0.054	0.057	0.050	0.204	0.259	0.204	0.133	0.126	0.115	0.072	0.047
Difference	0.016	0.009	0.017	0.031	0.051	0.037	0.062	0.032	0.012	0.010	0.016	0.009
CCC int	0.082	0.063	0.074	0.080	0.256	0.296	0.266	0.164	0.138	0.124	0.088	0.056
CRM pre	0.071	0.055	0.062	0.051	0.191	0.250	0.248	0.152	0.113	0.117	0.069	0.043
Difference	0.008	0.013	0.027	0.022	0.063	0.052	-0.042	0.008	0.024	0.021	0.006	0.005
CRM int	0.079	0.068	0.089	0.073	0.254	0.302	0.206	0.161	0.137	0.138	0.075	0.048
CRM int	0.079	0.068	0.089	0.073	0.254	0.302	0.206	0.161	0.137	0.138	0.075	0.048
Difference	-0.007	0.020	0.005	0.061	0.011	-0.035	0.073	0.012	0.051	0.028	0.014	0.004
CRM fut	0.072	0.088	0.093	0.134	0.266	0.267	0.279	0.173	0.188	0.165	0.089	0.052
ECH pre	0.069	0.052	0.062	0.058	0.179	0.272	0.210	0.149	0.123	0.114	0.072	0.039
Difference	0.004	0.011	0.000	0.010	0.054	0.044	0.008	-0.011	-0.003	0.015	0.006	0.010
ECH int	0.073	0.064	0.062	0.069	0.232	0.316	0.218	0.138	0.120	0.129	0.077	0.049
ECH int	0.073	0.064	0.062	0.069	0.232	0.316	0.218	0.138	0.120	0.129	0.077	0.049
Difference	0.010	0.001	0.026	0.011	0.010	0.002	0.039	0.022	0.029	0.012	-0.001	0.004
ECH fut	0.082	0.065	0.088	0.080	0.243	0.318	0.257	0.160	0.149	0.141	0.076	0.053
IPS pre	0.066	0.054	0.064	0.062	0.167	0.260	0.243	0.138	0.121	0.129	0.073	0.038
Difference	0.013	0.022	0.020	0.020	0.085	0.030	-0.001	0.033	0.037	0.018	0.015	0.005
IPS int	0.079	0.076	0.084	0.082	0.252	0.290	0.242	0.171	0.158	0.147	0.088	0.043
IPS int	0.079	0.076	0.084	0.082	0.252	0.290	0.242	0.171	0.158	0.147	0.088	0.043
Difference	-0.001	0.025	0.039	0.002	0.037	0.006	0.017	0.011	0.044	0.020	0.025	0.023
IPS fut	0.078	0.101	0.123	0.085	0.289	0.296	0.259	0.182	0.202	0.167	0.112	0.066

The ranking of the climate models was as that for air temperature, i.e. ECH, CRM then CCC and IPS for increasing concentrations of surface diatoms. The greatest increases occurred during autumn and spring. The surface growth of diatoms was significant as they were light limited and have low light saturation (61.2 W/m^2 for maximum photosynthetic rate) thus thereby limited to mainly to surface growth.

Green algae concentration

An investigation into the surface green algae concentration leads to Figure 188. It was seen that the surface green algae concentration also increased with progressive climate change

to the distant future. As with the diatoms, the green also showed a season shift of sorts because they share the same growth temperature rate multipliers as that of the diatoms.

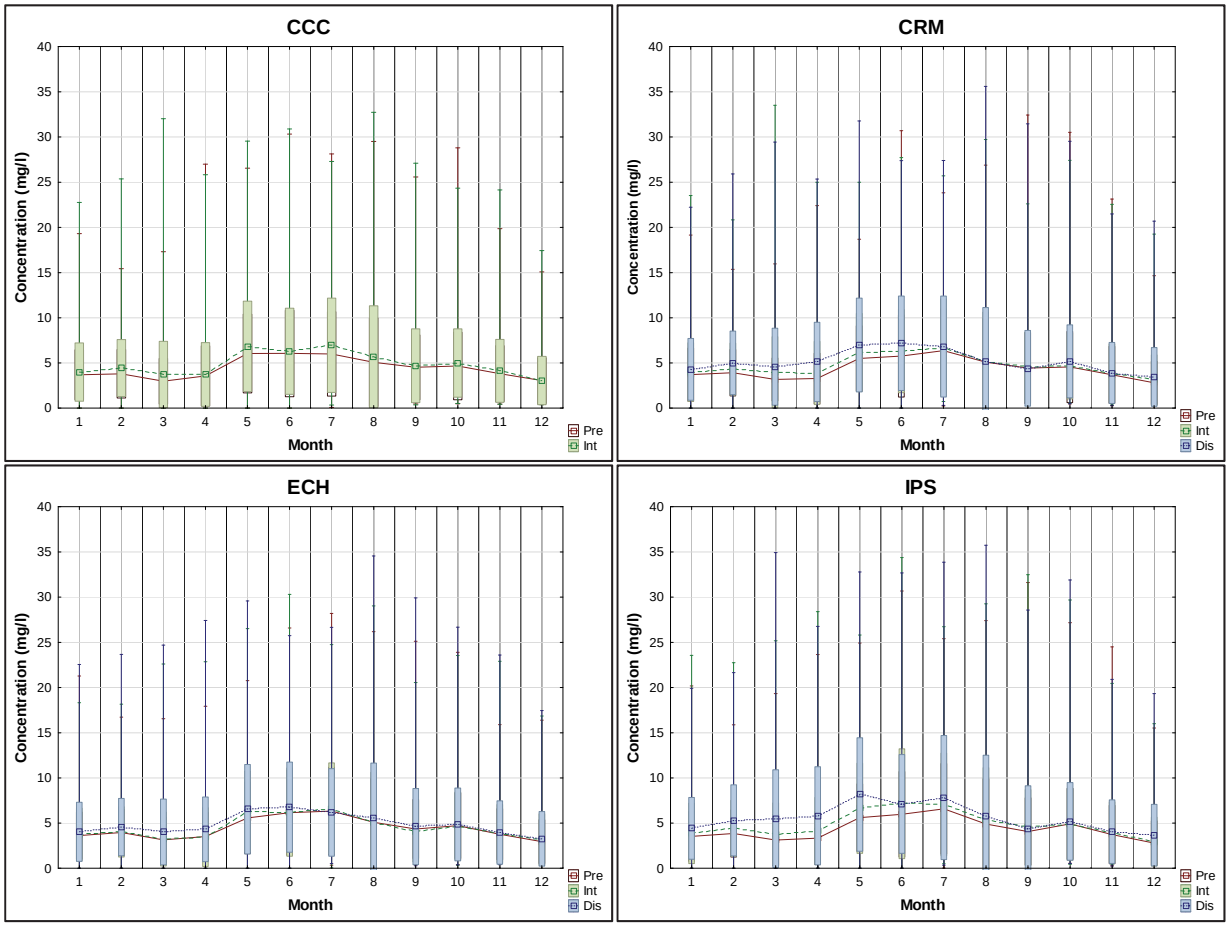

Figure 188: The projected climate change surface green algae concentration of Voëlvlei Dam (mg/l)

Each of the subsequent climate change scenarios from present day to intermediate future and distant future produced an increase in the surface concentration of green algae. Table 75 shows the mean monthly surface concentrations of green algae and winter had the greatest concentrations, whilst summer had the lowest. The compounding effect of climate change was once again shown whereby the increase from present day to intermediate future was similar to intermediate future to distant future, albeit the timespan being much shorter.

Table 75: The mean monthly surface green algae concentration of Voëlvlei Dam (mg/l) under projected climate change

	Jan	Feb	Mar	Apr	May	Jun	Jul	Aug	Sep	Oct	Nov	Dec
CCC pre	3.69	3.81	2.98	3.58	6.05	6.06	6.00	5.08	4.52	4.67	3.82	3.05
Difference	0.30	0.63	0.75	0.15	0.79	0.24	0.96	0.61	0.17	0.33	0.31	0.01
CCC int	3.99	4.44	3.73	3.73	6.84	6.30	6.96	5.69	4.69	5.00	4.13	3.06
CRM pre	3.71	3.92	3.18	3.28	5.49	5.77	6.37	5.09	4.44	4.56	3.70	2.81
Difference	0.29	0.41	0.79	0.62	0.67	0.53	0.35	0.05	0.10	0.10	0.17	0.28
CRM int	4.00	4.33	3.97	3.90	6.16	6.30	6.72	5.14	4.54	4.66	3.87	3.09
CRM int	4.00	4.33	3.97	3.90	6.16	6.30	6.72	5.14	4.54	4.66	3.87	3.09
Difference	0.29	0.69	0.62	1.22	0.82	0.88	0.11	0.00	-0.13	0.52	0.03	0.37
CRM fut	4.29	5.02	4.59	5.12	6.98	7.18	6.83	5.14	4.41	5.18	3.90	3.46
ECH pre	3.62	3.95	3.13	3.51	5.58	6.16	6.33	5.10	4.35	4.72	3.77	2.94
Difference	0.12	0.08	0.10	-0.06	0.71	0.06	0.29	-0.03	-0.26	-0.03	0.07	0.25
ECH int	3.74	4.03	3.23	3.45	6.29	6.22	6.62	5.07	4.09	4.69	3.84	3.19
ECH int	3.74	4.03	3.23	3.45	6.29	6.22	6.62	5.07	4.09	4.69	3.84	3.19
Difference	0.31	0.53	0.80	0.86	0.25	0.54	-0.44	0.54	0.52	0.17	0.12	0.07
ECH fut	4.05	4.56	4.03	4.31	6.54	6.76	6.18	5.61	4.61	4.86	3.96	3.26
IPS pre	3.53	3.86	3.13	3.34	5.61	5.98	6.58	4.90	4.08	4.92	3.74	2.79
Difference	0.33	0.57	0.67	0.79	1.04	1.17	0.49	0.47	0.44	-0.05	0.26	0.17
IPS int	3.86	4.43	3.80	4.13	6.65	7.15	7.07	5.37	4.52	4.87	4.00	2.96
IPS int	3.86	4.43	3.80	4.13	6.65	7.15	7.07	5.37	4.52	4.87	4.00	2.96
Difference	0.56	0.88	1.70	1.68	1.51	-0.03	0.76	0.37	-0.16	0.32	0.06	0.71
IPS fut	4.42	5.31	5.50	5.81	8.16	7.12	7.83	5.74	4.36	5.19	4.06	3.67

The greatest increases were in autumn and the least was in late winter and spring, which in effect signalled a seasonal shift. Thus, distant future climates produced excessive surface green algae from December until June and increased in the surface concentrations during winter and late summer.

Cyanobacteria concentration

The final group of algae examined for the effect of climate change on surface concentrations was cyanobacteria. The mean monthly surface concentrations are shown in Figure 189. This highlighted the inter-variability between climate models as it showed an increase in some months and a decrease in others for the various climate models. The greatest increases

occurred during spring, which represented a seasonal shift in cyanobacteria blooms with negligible to decreased concentrations during late summer and autumn. In this study, algal succession was not found rather increases in the overall growth of algae as well as a seasonal shift for diatoms and greens. The light saturation for cyanobacteria was 60 W/m^2 and similar to that of diatoms, thus similar surface growth patterns for the cyanobacteria was expected, but this did not materialise as the algal temperature growth multipliers varied. From Figure 190 it was seen that the DWA limit for surface cyanobacteria concentration was exceeded by 30 to 53% in the distant future, depending on the climate model. Both warmer climate models, namely CRM and IPS showed an increase in this exceedance whereas the cooler model ECH showed a decrease in exceedance.

Table 76 shows the mean monthly surface cyanobacteria concentration and the greatest occurs from December to May, corresponding to summer to autumn. The maximum surface concentration of cyanobacteria occurs during April, which was autumn.

The inter-variability between the climate models was at its maximum as 2 models show a decrease in cyanobacteria concentrations for the intermediate future, whist 2 show an increase in cyanobacteria concentrations.

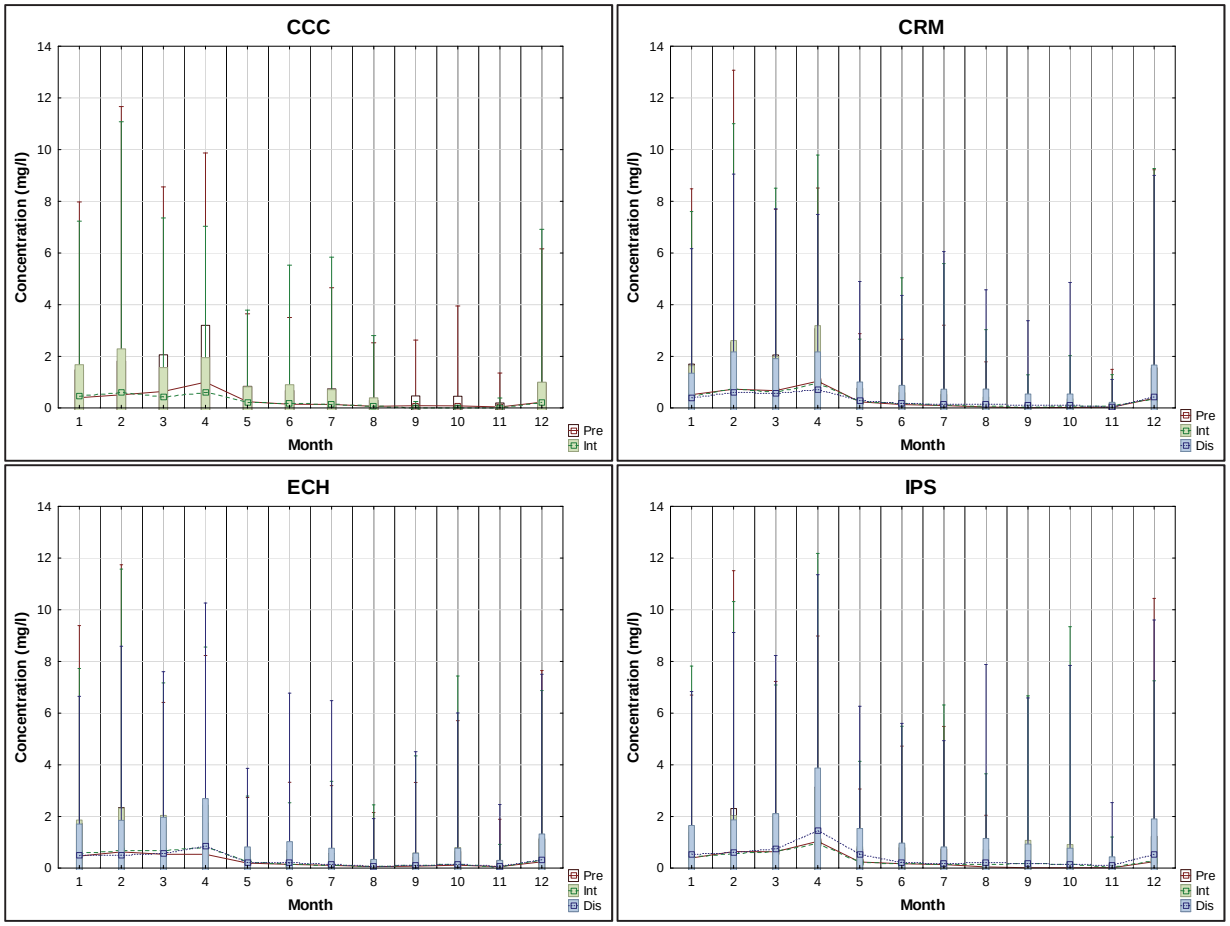

Figure 189: The projected climate change surface cyanobacteria concentration of Voëlvlei Dam (mg/l)

The greatest increases occurred during spring, which represented a seasonal shift in cyanobacteria blooms with negligible to decreased concentrations during late summer and autumn.

In this study, algal succession was not found rather increases in the overall algal growth as well as a seasonal shift for diatoms and greens.

The light saturation for cyanobacteria was 60 W/m^2 and similar to that of the diatoms, thus similar surface growth patterns for the cyanobacteria was expected, but this did not materialise as the algal temperature growth rate multipliers varied.

From Figure 190 it was seen that the DWA limit for surface cyanobacteria concentration was exceeded by 30% to 53% in the distant future, depending on the climate model. Both warmer climate models, namely CRM and IPS showed an increase in this exceedance whereas the cooler model ECH showed a decrease in exceedance.

Table 76: The mean monthly surface cyanobacteria concentration of Voëlvlei Dam (mg/l) under projected climate change

	Jan	Feb	Mar	Apr	May	Jun	Jul	Aug	Sep	Oct	Nov	Dec
CCC pre	0.402	0.514	0.640	0.999	0.245	0.147	0.139	0.063	0.088	0.081	0.039	0.226
Difference	0.055	0.081	-0.198	-0.400	-0.013	0.034	-0.011	0.003	-0.080	-0.076	-0.028	-0.007
CCC int	0.457	0.595	0.442	0.599	0.232	0.181	0.128	0.066	0.008	0.005	0.011	0.219
CRM pre	0.519	0.728	0.671	1.039	0.241	0.131	0.100	0.039	0.010	0.020	0.034	0.377
Difference	-0.045	0.012	-0.049	-0.076	-0.001	0.043	0.021	0.047	0.044	0.070	0.021	-0.018
CRM int	0.474	0.740	0.622	0.963	0.240	0.174	0.121	0.086	0.054	0.090	0.055	0.359
CRM int	0.474	0.740	0.622	0.963	0.240	0.174	0.121	0.086	0.054	0.090	0.055	0.359
Difference	-0.075	-0.135	-0.051	-0.268	0.046	0.010	0.013	0.061	0.050	0.003	-0.001	0.067
CRM fut	0.399	0.605	0.571	0.695	0.286	0.184	0.134	0.147	0.104	0.093	0.054	0.426
ECH pre	0.472	0.630	0.536	0.533	0.195	0.146	0.107	0.058	0.076	0.114	0.058	0.244
Difference	0.101	0.049	0.144	0.295	0.045	-0.009	-0.001	0.015	0.043	0.040	-0.006	0.075
ECH int	0.573	0.679	0.680	0.828	0.240	0.137	0.106	0.073	0.119	0.154	0.052	0.319
ECH int	0.573	0.679	0.680	0.828	0.240	0.137	0.106	0.073	0.119	0.154	0.052	0.319
Difference	-0.091	-0.167	-0.098	0.016	-0.015	0.062	0.028	0.007	-0.016	-0.019	0.013	0.007
ECH fut	0.482	0.512	0.582	0.844	0.225	0.199	0.134	0.080	0.103	0.135	0.065	0.326
IPS pre	0.396	0.643	0.637	1.039	0.239	0.170	0.142	0.046	0.015	0.014	0.016	0.249
Difference	0.049	-0.082	-0.009	-0.081	-0.007	0.015	-0.003	0.111	0.182	0.130	0.026	0.019
IPS int	0.445	0.561	0.628	0.958	0.232	0.185	0.139	0.157	0.197	0.144	0.042	0.268
IPS int	0.445	0.561	0.628	0.958	0.232	0.185	0.139	0.157	0.197	0.144	0.042	0.268
Difference	0.107	0.059	0.115	0.499	0.286	0.047	0.026	0.058	-0.011	0.012	0.070	0.250
IPS fut	0.552	0.620	0.743	1.457	0.518	0.232	0.165	0.215	0.186	0.156	0.112	0.518

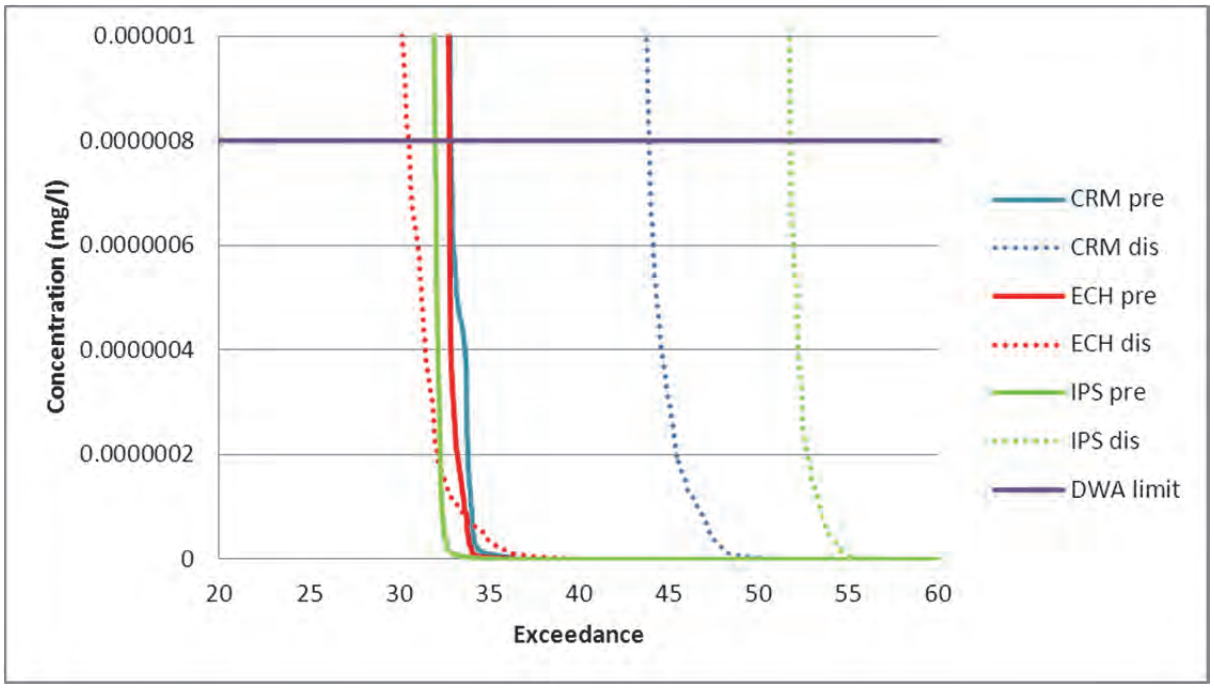

Figure 190: The projected distant future surface cyanobacteria exceedance plot of Voëlvlei Dam

The dominant algal group

It had now been established that with climate change the mean annual air temperature will increase by about 22% (Table 65) and this had a profound effect on the growth of algae in Voëlvlei dam, in particular, it increased the surface concentrations of all algal groups present. The mean annual surface total algae increased by 15.5% (Table 73) because of a 24.6% increase in mean annual surface diatom concentrations, 15.5% increase in the mean annual surface green algae concentration and a 27.6% increase in the mean surface cyanobacteria concentration. This was shown graphically in Figure 191.

Thus, the dominant surface algal group in Voëlvlei dam for the distant future was the green algal group, but the group with the greatest increase was the cyanobacteria at 27.7% mean annual increase in surface concentration.

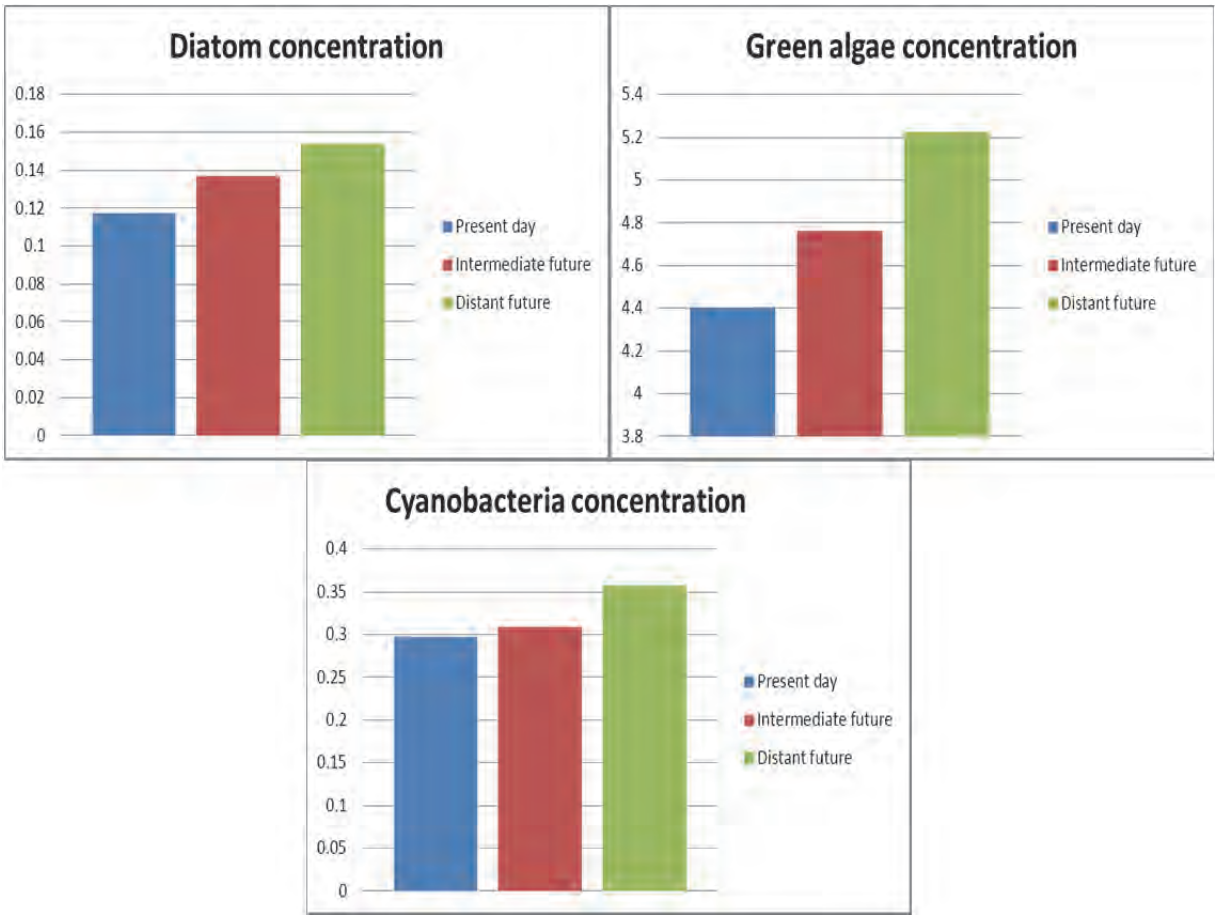

Figure 191: The projected climate change effect on surface algal concentrations of Voëlvlei dam (mg/l)

Zooplankton concentration

The zooplankton in Voëlvlei dam fed only on diatoms, green algae and other zooplankton present and since their surface concentration increased, it was expected that the surface concentrations of zooplankton should increase. For the purpose of this study, the predation of cyanobacteria by zooplankton was set to zero, i.e. zooplankton did not feed on cyanobacteria. The surface zooplankton concentration was shown in Figure 192 where all future climate models predicted a greater concentration of surface zooplankton with maximum concentrations in winter.

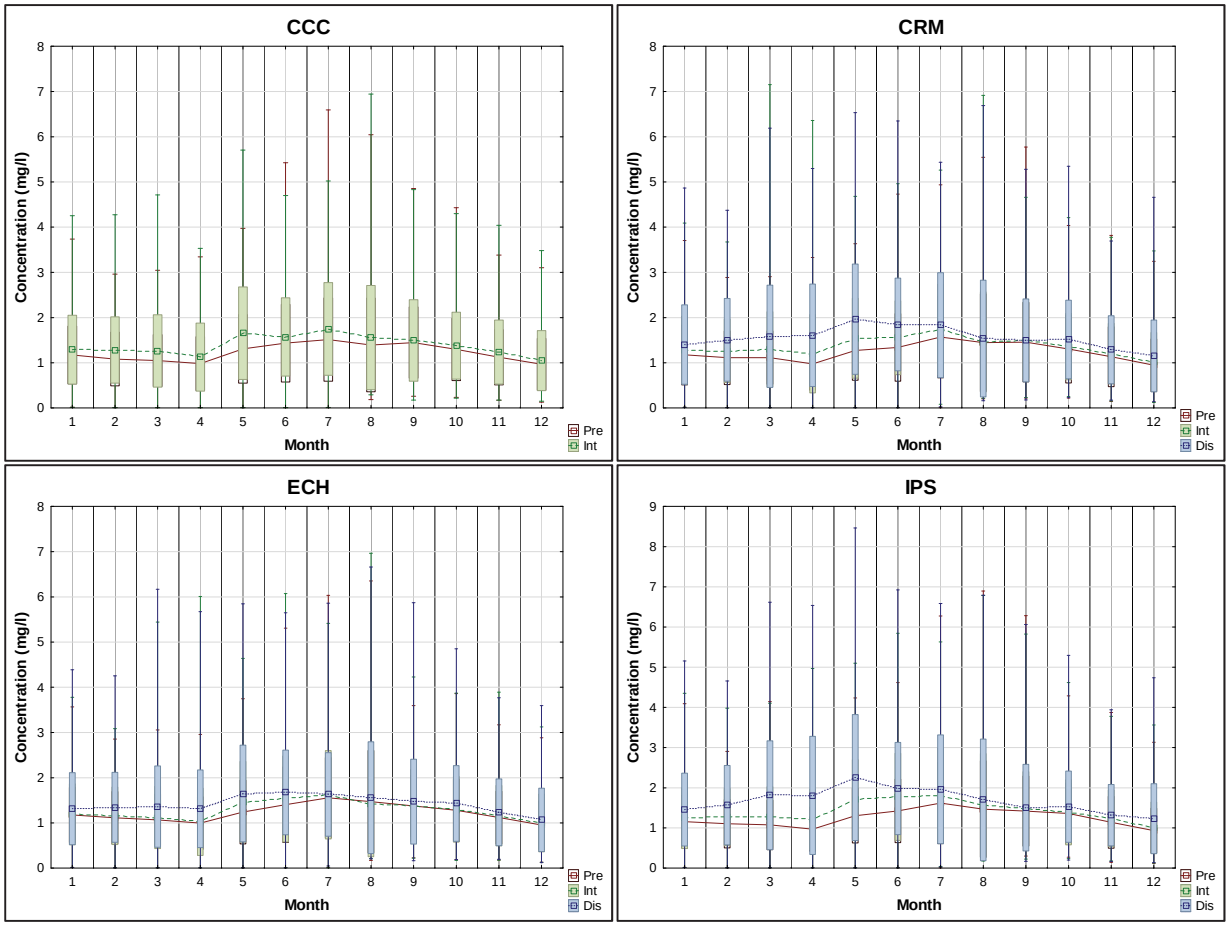

Figure 192: The projected climate change surface zooplankton concentration of Voëlvlei Dam (mg/l)

It was expected that the greater concentrations of zooplankton would emulate that of diatoms and green algae and this emulations was shown in Table 77.

Table 77: The mean monthly surface zooplankton concentration of Voëlvlei Dam (mg/l) under projected climate change

	Jan	Feb	Mar	Apr	May	Jun	Jul	Aug	Sep	Oct	Nov	Dec
CCC pre	1.174	1.083	1.050	0.982	1.309	1.435	1.515	1.394	1.447	1.296	1.124	0.968
Difference	0.116	0.200	0.213	0.144	0.345	0.136	0.233	0.164	0.047	0.082	0.114	0.079
CCC int	1.290	1.283	1.263	1.126	1.654	1.571	1.748	1.558	1.494	1.378	1.238	1.047
CRM pre	1.177	1.113	1.115	0.975	1.273	1.339	1.570	1.448	1.456	1.304	1.134	0.946
Difference	0.104	0.153	0.185	0.225	0.271	0.214	0.164	0.012	0.041	0.055	0.069	0.076
CRM int	1.281	1.266	1.300	1.200	1.544	1.553	1.734	1.460	1.497	1.359	1.203	1.022
CRM int	1.281	1.266	1.300	1.200	1.544	1.553	1.734	1.460	1.497	1.359	1.203	1.022
Difference	0.123	0.242	0.286	0.410	0.421	0.295	0.101	0.076	0.000	0.155	0.086	0.131
CRM fut	1.404	1.508	1.586	1.610	1.965	1.848	1.835	1.536	1.497	1.514	1.289	1.153
ECH pre	1.178	1.113	1.069	0.996	1.240	1.404	1.556	1.470	1.376	1.279	1.119	0.953
Difference	0.013	0.044	0.051	0.029	0.228	0.126	0.067	-0.042	0.012	0.025	0.042	0.048
ECH int	1.191	1.157	1.120	1.025	1.468	1.530	1.623	1.428	1.388	1.304	1.161	1.001
ECH int	1.191	1.157	1.120	1.025	1.468	1.530	1.623	1.428	1.388	1.304	1.161	1.001
Difference	0.123	0.188	0.241	0.288	0.184	0.144	0.008	0.131	0.082	0.126	0.075	0.066
ECH fut	1.314	1.345	1.361	1.313	1.652	1.674	1.631	1.559	1.470	1.430	1.236	1.067
IPS pre	1.157	1.107	1.077	0.969	1.306	1.426	1.619	1.470	1.420	1.358	1.141	0.933
Difference	0.088	0.164	0.191	0.240	0.400	0.349	0.190	0.096	0.053	0.030	0.094	0.072
IPS int	1.245	1.271	1.268	1.209	1.706	1.775	1.809	1.566	1.473	1.388	1.235	1.005
IPS int	1.245	1.271	1.268	1.209	1.706	1.775	1.809	1.566	1.473	1.388	1.235	1.005
Difference	0.212	0.297	0.546	0.601	0.549	0.206	0.152	0.134	0.032	0.142	0.083	0.224
IPS fut	1.457	1.568	1.814	1.810	2.255	1.981	1.961	1.700	1.505	1.530	1.318	1.229

Eutrophication level

The influence of climate change was seen to have implications for Voëlvlei dam in the form of increase algal blooms and this had a direct effect on the surface TRIX levels. From Figure 193 and Table 78 it was seen that for climate change, the mean monthly TRIX levels increased for all climate models and the overall shape resembled that of the surface phosphorous concentration.

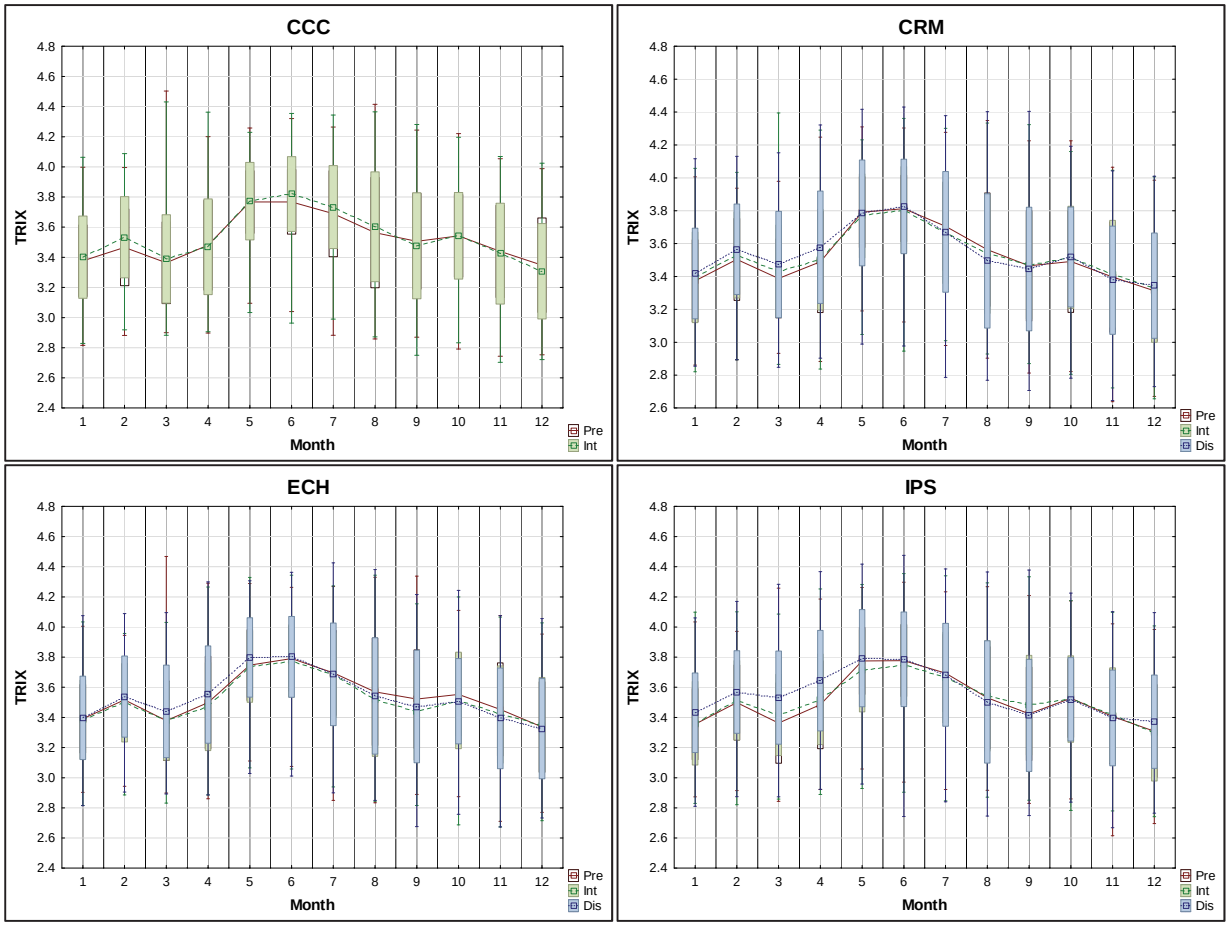

Figure 193: The projected climate change surface TRIX level of Voëlvlei dam

The inter-variability between climate models was apparent from these findings in that for differences for monthly TRIX levels for different climate model of the same time-period showed either an increase or decrease. TRIX levels showed increases mainly in late summer and autumn with decreases during winter and spring. In examining the equation that renders TRIX levels it was seen that:

$$TRIX = \frac{(\log(ChA + aDO\% + N\min + TP) + 1.5)}{1.2}$$

All the constituents increase for climate change effects except for the total nitrogen, which was negligible over that of the present day. It may be argued that the TRIX levels were significant as:

- The formulae was usually applied to marine waters and was adopted here as a guide
- It was applied here only to the surface water
- The formulae was of the logarithmic type which increases exponentially and any increase was significant
- The constituents were weighted equally

- It did not take water transparency into account

Even with its shortcomings, the TRIX levels provided a first estimate at the increase in trophic levels.

Table 78: The mean monthly surface TRIX level of Voëlvlei Dam under projected climate change

	Jan	Feb	Mar	Apr	May	Jun	Jul	Aug	Sep	Oct	Nov	Dec
CCC pre	3.38	3.47	3.36	3.48	3.77	3.77	3.69	3.56	3.51	3.54	3.44	3.35
Difference	0.02	0.07	0.03	-0.01	0.01	0.05	0.04	0.04	-0.03	0.00	-0.01	-0.04
CCC int	3.40	3.53	3.39	3.47	3.77	3.82	3.73	3.60	3.48	3.54	3.42	3.31
CRM pre	3.37	3.50	3.39	3.49	3.79	3.81	3.71	3.56	3.46	3.49	3.40	3.31
Difference	0.02	0.03	0.04	0.01	-0.02	-0.01	-0.04	-0.02	0.00	0.02	0.02	0.02
CRM int	3.40	3.53	3.43	3.50	3.77	3.81	3.67	3.54	3.47	3.52	3.42	3.33
CRM int	3.40	3.53	3.43	3.50	3.77	3.81	3.67	3.54	3.47	3.52	3.42	3.33
Difference	0.02	0.03	0.04	0.08	0.02	0.02	0.01	-0.04	-0.02	0.00	-0.04	0.01
CRM fut	3.42	3.57	3.47	3.58	3.79	3.83	3.67	3.49	3.45	3.52	3.38	3.34
ECH pre	3.39	3.52	3.38	3.50	3.75	3.79	3.70	3.57	3.52	3.55	3.45	3.34
Difference	-0.01	-0.02	0.00	-0.03	-0.01	-0.02	-0.02	-0.05	-0.08	-0.04	-0.03	0.01
ECH int	3.39	3.50	3.38	3.47	3.74	3.78	3.68	3.52	3.44	3.51	3.42	3.35
ECH int	3.39	3.50	3.38	3.47	3.74	3.78	3.68	3.52	3.44	3.51	3.42	3.35
Difference	0.01	0.04	0.06	0.08	0.06	0.03	0.01	0.02	0.03	-0.01	-0.02	-0.02
ECH fut	3.40	3.54	3.44	3.55	3.80	3.80	3.69	3.54	3.47	3.51	3.39	3.33
IPS pre	3.36	3.50	3.36	3.48	3.77	3.78	3.69	3.53	3.42	3.53	3.41	3.31
Difference	0.01	0.01	0.05	0.04	-0.06	-0.03	-0.03	0.01	0.06	-0.01	0.01	-0.01
IPS int	3.36	3.51	3.42	3.52	3.71	3.75	3.66	3.54	3.48	3.52	3.41	3.30
IPS int	3.36	3.51	3.42	3.52	3.71	3.75	3.66	3.54	3.48	3.52	3.41	3.30
Difference	0.07	0.06	0.12	0.12	0.08	0.04	0.02	-0.04	-0.07	0.00	-0.02	0.07
IPS fut	3.43	3.57	3.53	3.64	3.79	3.79	3.68	3.50	3.41	3.52	3.40	3.37

Limitations of this Study

All water quality studies have inherent limitations especially where algal growth was to be simulated as algae adapts and modifies its growth to its environment and conditions. Some species are known to be motile which was virtually impossible to model accurately. This studies limitation was subdivided into:

- Model and data limitations
- Data limitations

CE-QUAL-W2 model limitations

The model had successfully been applied to Voëlvlei in the past and the limitations were specifically on the model and not its application to Voëlvlei. From the aspect of hydrodynamics and transport, the models governing equations are laterally and layer averaged. Lateral averaging assumes lateral variations in velocities, temperatures, and constituents are negligible. This assumption may be inappropriate for large water-bodies exhibiting significant lateral variations in water quality. Eddy coefficients are used to model turbulence. Currently, the user must decide among several vertical turbulence schemes the one that was most appropriate for the type of water-body being simulated. The equations are written in the conservative form using the Boussinesq and hydrostatic approximations. Since vertical momentum was not included, the model may give inaccurate results where there was significant vertical acceleration (Cole, 2008)

Water quality interactions are, by necessity, simplified descriptions of an aquatic ecosystem that was extremely complex. This was especially so for modelling algae as they adapt to varying environmental conditions such as low light and nutrient sparse zones. Some species are capable of independent movement throughout the water column, something not modelled by CE-QUAL-W2. This could explain difference between measured and modelled values.

The model includes a user-specified sediment oxygen demand that was not coupled to the water column. SOD only varies according to temperature. The first order model was tied to the water column settling of organic matter. The model does not have a sediment compartment that models kinetics in the sediment and at the sediment-water interface, i.e., a complete sediment diagenesis model. This places a limitation on long-term predictive capabilities of the water quality portion of the model (Cole, 2008). It was hope that this limitation if carried forward by each of the modelling periods studies and that what was presented was still the different in state of water quality in proceeding from the present day to the distant future. Future releases of CE-QUAL-W2 will include additional capabilities that will remedy this limitation (Cole, 2008) and version 3.7 has just been released (2012).

Climate data limitations

The availability of input data was not a limitation of the model itself. However, it was most often the limiting factor in the application or misapplication of the model. The GCMs employed in this study was of such coarse resolution (about 300km) that they cannot be used directly for the meteorological data. The GCMs are firstly downscaled statistically to regional level (RCMs). The advantage of this technique was that it was easily applied. One disadvantage of the statistical method of downscaling was that it relies on the availability of sufficient high-resolution data over long periods so that statistical relationships may be established. It was not possible to be sure how valid the statistical relations are for a climate-changed situation (Houghton, 2007; Quintana-Seguí *et al.*, 2010).

In the absence of another type of downscaling such as dynamic downscaling, it was not possible to determine the accuracy of the downscaled data or compare it.

Wind-speed and direction was not supplied by CSAG (UCT) and was thus a limitation. CE-QUAL-W2 requires wind-speed and direction as part of its meteorological data input to predict water quality. In the absence of this, wind-speed and direction was replicated from past data. For 1971 the recorded wind-speed and direction from 1 January 1971 to 31 December 1971 was repeated for the 20 years of all the simulation periods including the intermediate and future events, in the absence of any downscaled data.

Inflow and withdrawal limitations

The daily averaged inflow to the Dam was obtained from the DWAF's Hydrological Information System (HIS) database. Outflows from Voëlvlei Dam consist of abstractions of raw water to supply the Voëlvlei (G1H070M01) and Swartland (G1H068M01) WTW. Water was also released via an outlet canal (G1H065A01) to the Berg River for run-of-river irrigation (DWAF, 1999). An additional outflow to the ICS pipeline was also operational but flow data for this gauging station (G1H069M01) was only available up to 1982. This pipeline was excluded from the simulation as it was deemed to have too little effect on the water quality.

Inflow water quality data was not as readily available as flow data, and was at best measured only on a weekly basis. Although a reasonably good water quality record exists at gauging station G1H029Q01, it was not used. This was because the volume of water diverted from the Twenty-Four Rivers River was substantially greater than that diverted from

the Leeu River and it was therefore assumed that the water quality of the Twenty-Four Rivers River would more representative of the water quality entering the Dam at G1H067Q01. Similarly, gauging station G1H008Q01 was representative of the water quality at G1H066Q01. This choice could be vindicated by the fact that measured and modelled values were not vastly different but overshoots and undershoots were noted.

Since no inflow and outflow data was available for the predicted future scenarios it was proposed to use the current DWA HIS databases' flow-data from 1 January 1971 until 31 December 1990's (present scenario) for each of the subsequent intermediate and future simulations. This would assume that demand and allocation of the water resource does not change for the simulation periods.

Algal growth rates

For the study it was imperative that the growth of the 3 groups of algae namely diatoms, greens and cyanobacteria be modelled as accurately as possible so as to show the changes with climate change. The more important parameters were discussed in the parameterisation section and summarised in Table 44. To predict the growth of algae these parameters have to be as accurate as possible for the species of algae present in the water-body under study. Finding some of these parameters proved difficult and futile in some instances and default values were used.

The choice of algal growth constant also affected the DO concentrations to such an extent that the dam became super-saturated at the surface for extended periods, which was not common in reality. This also consolidated the fact that the choice of growth constant was extremely important and in-situ measurements should be collected for future studies.

General limitations

For each run, the initial conditions were the same as the present day initial conditions. This allowed for a direct comparison of present day to intermediate future and distant future. In essence, for each simulation period it was the same original dam being subjected to climate change. What was absent was climate date from 1971 to 2100 so that the dam may be modelled for the entire period. This mean that when the time of simulation approaches 2045 the model has already run for over 50 years and the in-situ conditions are that of 2045. Currently the intermediate future and distant future initial conditions are that of the present day.

9.29 Discussion of results for Voëlvlei dam

The object of this study was to find any links between predicted climate changes on eutrophication of surface waters. It was postulated that with climate change from the present day to intermediate future and into the distant future that the air temperature would increase by between 2 and 4.5^{o}C for southern Africa and this increase would heat the surface waters sufficiently to amplify the growth of algae within such waters. It was also postulated that the three groups of algae (namely diatoms, green and cyanobacteria) that are present, would experience varying rates of growth because of the increased water temperature with a preference for warmer conditions. This would be due to the temperature growth multipliers, which stipulate algal growth for different water temperatures. It was possible that seasonal shifts of the bloom season would become apparent with climate change. It was postulated that cyanobacteria would be the algal group that benefits the most from the increased water temperature and all other factors remaining constant, thereby allowing for the unabated growth of cyanobacteria and a greater frequency of harmful algal blooms.

Water temperature, pH, available light, turbidity, suspended solids (TSS), dissolved solids (TDS), nitrogen, phosphorous, salinity and trace elements influence water quality and algal growth. Water quality and algal growth was dependent on several variables for its lifecycle, such as conducive environmental conditions and nutrients, which for the purpose of this study may be categorised as:

- Water temperature and solar radiation;
- The quantity of dissolved oxygen in the water-body;
- Availability of nitrogen within the water-body;
- Availability of phosphorous within the water-body; and

The present day study was conducted by utilising the water quality model CE-QUAL-W2 and establishing baseline water quality conditions for all the relevant factors that affect algal growth in the dam. The air temperature over the dam site was the classical southern hemisphere climate with summer being roughly December to February and winter May to July. The inflow and withdrawal quantity and quality as well as wind-speed and direction was constrained to be the same for the duration of each the simulation periods, namely present day, intermediate future and distant future thereby allowing for more controlled comparison as only the effect of increased temperature on the dam was investigated.

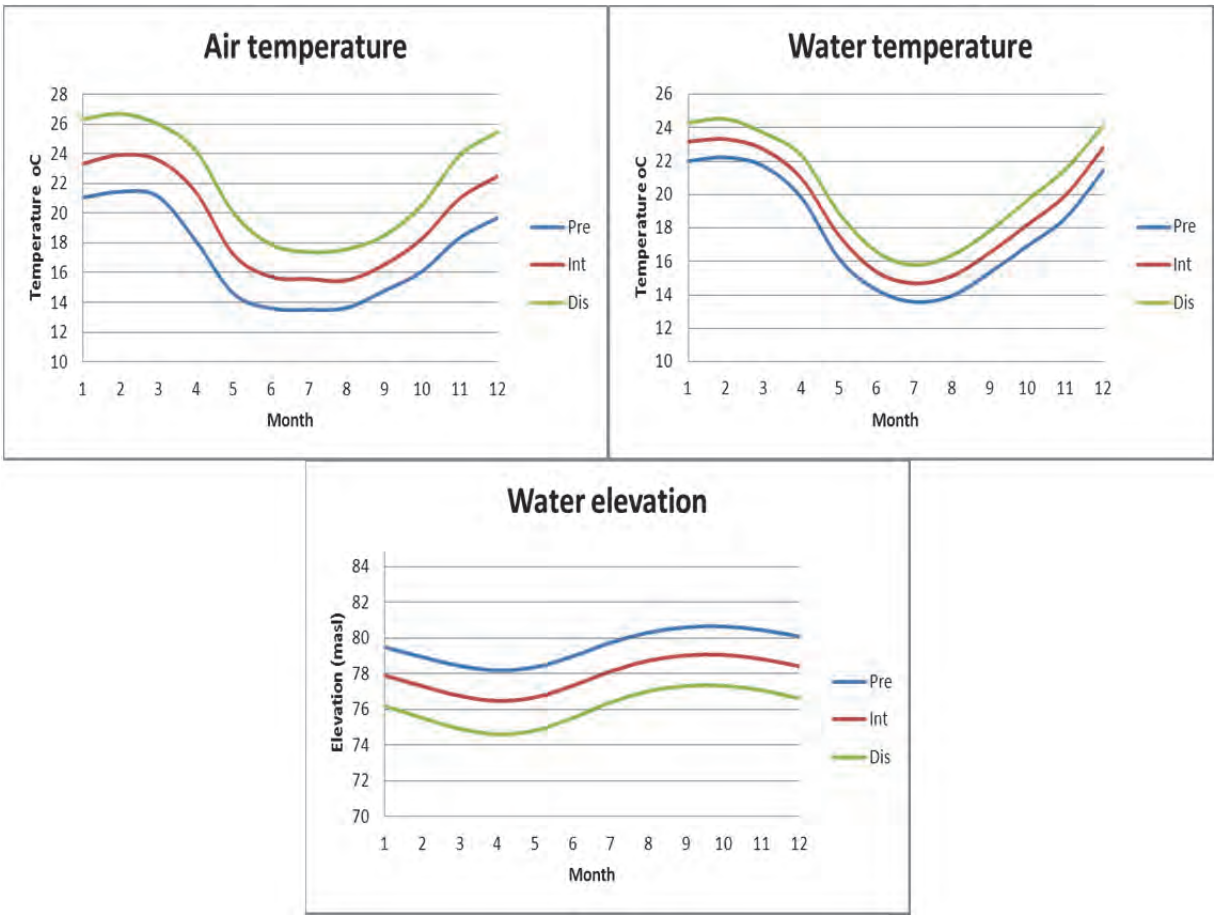

Figure 194: The projected effect of air temperature on Voëlvlei dam

From Figure 194 all of the future climate models showed varying ranges of monthly air temperature increases, which drive an increase in surface water temperatures, which then affected the algal growth. It was noted that the greatest increase in air temperature occurred during winter and due to the heat transfer to the surface waters. It was thought that this would enhance algal growth especially the diatom growth in winter as well as start a shift towards earlier annual algal blooms. The inter-variability between climate models was small and they all predicted similar air temperatures for each of the time scenarios. The climate models were also ranked in order of coolest to hottest that being ECH, CRM, CCC and then IPS. This was a consequence of the anthropogenic assumptions used to generate the GCM. It was concluded that air temperature was the major driver for surface water temperatures and solar radiation was the diurnal driver.

Climate change thus affected the surface waters by heating the water and subsequently increased the evaporation rate of the water. This heating should have the effect of enhancing algal growth as well as lowering the surface water level if the dam was to be operated at the present day levels. This heated water evaporated more in the distant future than the intermediate future a result of the increased water temperature. This poses a

secondary problem for the Western Cape Province as it was a semi-arid area of the country and the effect of climate change was that its dam waters would evaporate faster in the future than at the current rate. For Voëlvlei dam, this was not as import as other dams in the area as it was an off-channel dam. The dam's capacity was pumped as operations dictate and does not rely on rainfall in its catchment.

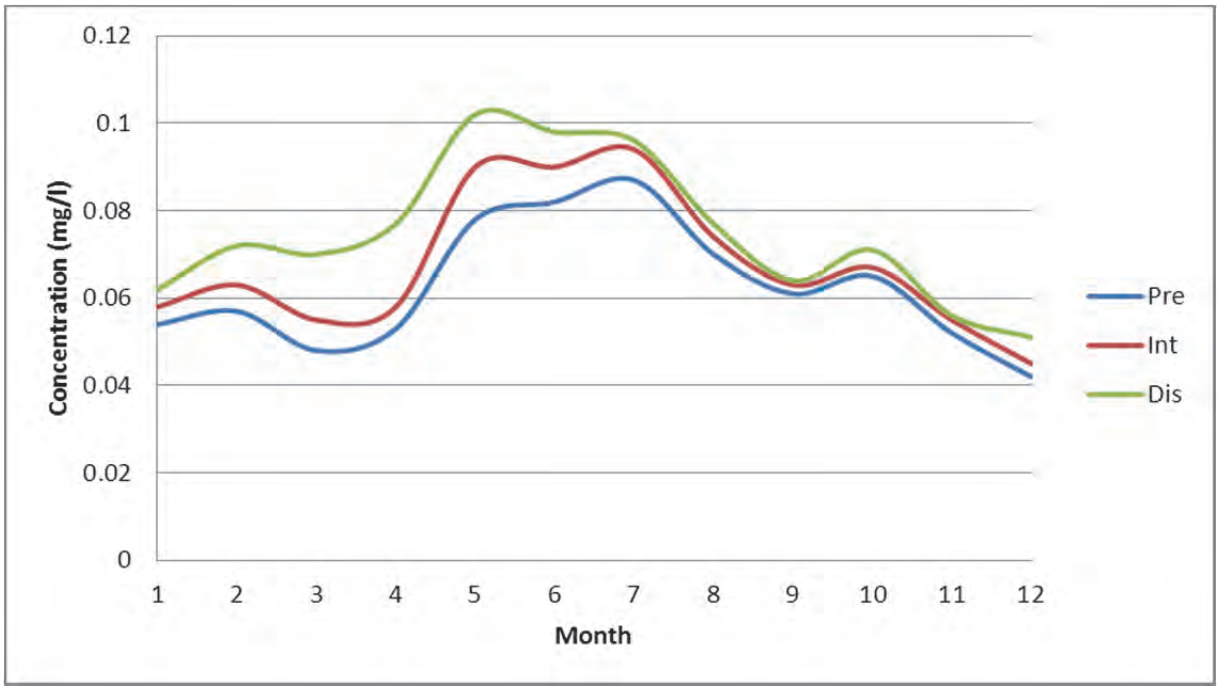

Figure 195: The projected mean monthly surface phosphorous concentration of Voëlvlei Dam (mg/l)

Once climate change has heated the surface waters of the dam and lowered its surface level a concentration increase for the constituents in the dam resulted. Figure 195 shows the surface phosphates increased in all months but especially in autumn. When comparing this to Figure 139 it was seen that the increase was not due to increased concentrations in the inflow. Together with the warmer water and a greater supply of nutrients the total algal growth was increased annually but especially during autumn, signalling a seasonal shift toward an earlier annual increased concentration of total algae as well as compounding the annual load in the dam.

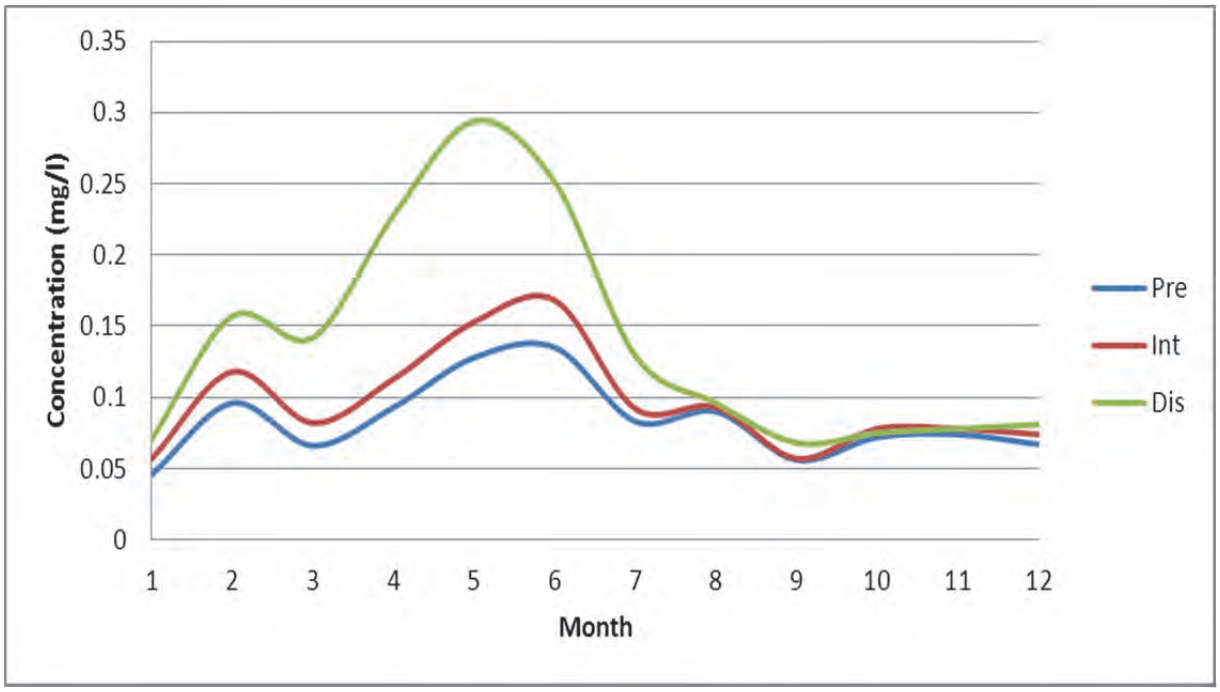

Figure 196: The projected mean monthly surface ammonium concentration of Voëlvlei Dam (mg/l)

The surface ammonium was used by the algae during photosynthesis so it was expected that for an increase in algal concentrations that the ammonium concentrations should decrease. It was found from Figure 196 that although the algal concentration increased, the concentration of surface ammonium also increased because of the concentrating effect of decreasing the surface water level. Annually the increase occurred mainly during autumn and winter with small changes and decreases during spring and summer. This increase along with the increase in phosphorous during late summer and autumn along with higher water temperatures will increase the algal growth at the surface during these months.

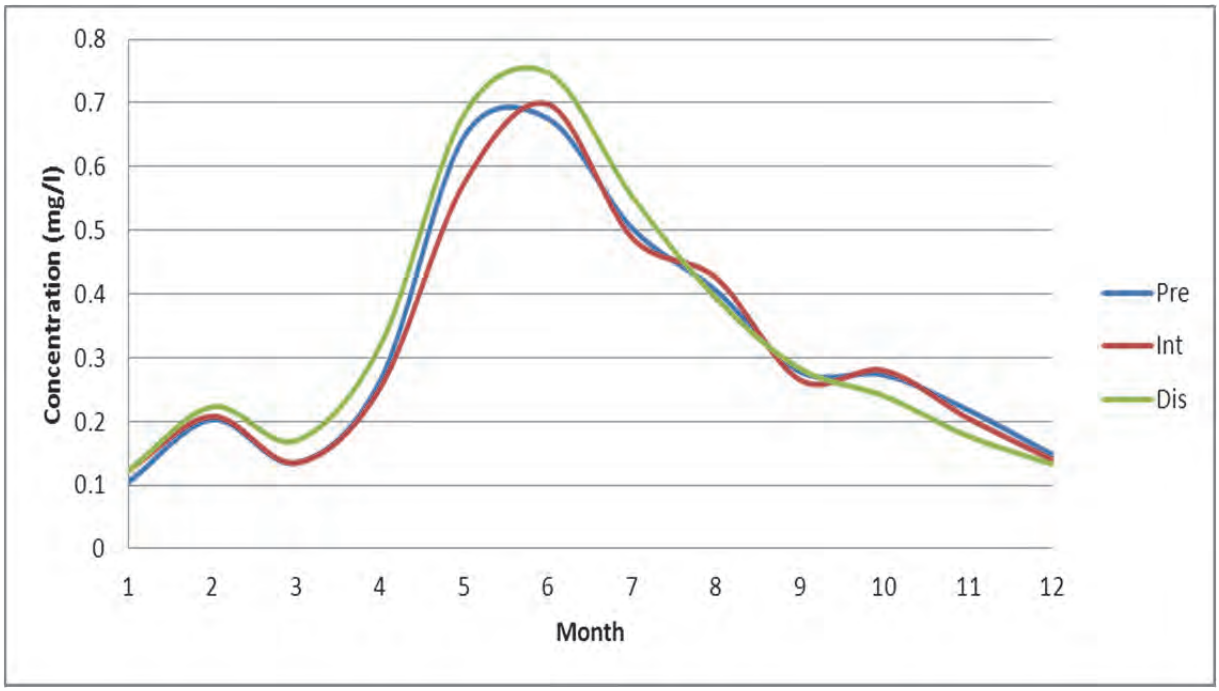

Figure 197: The projected mean monthly surface nitrate-nitrite concentration of Voëlvlei Dam (mg/l)

Nitrate-nitrites are an intermediate product as well as a source of nitrogen during photosynthesis. From Figure 197 the effect of climate change on nitrate-nitrites was very slight as its main source was from the nitrification of ammonium. It was expected that for an increase in temperature and ammonium that the nitrification reaction would respond in an Arrhenius manner and produce more nitrate-nitrite but this was not so. It could be that the rate of generation of nitrate-nitrites was similar to its assimilation by algae.

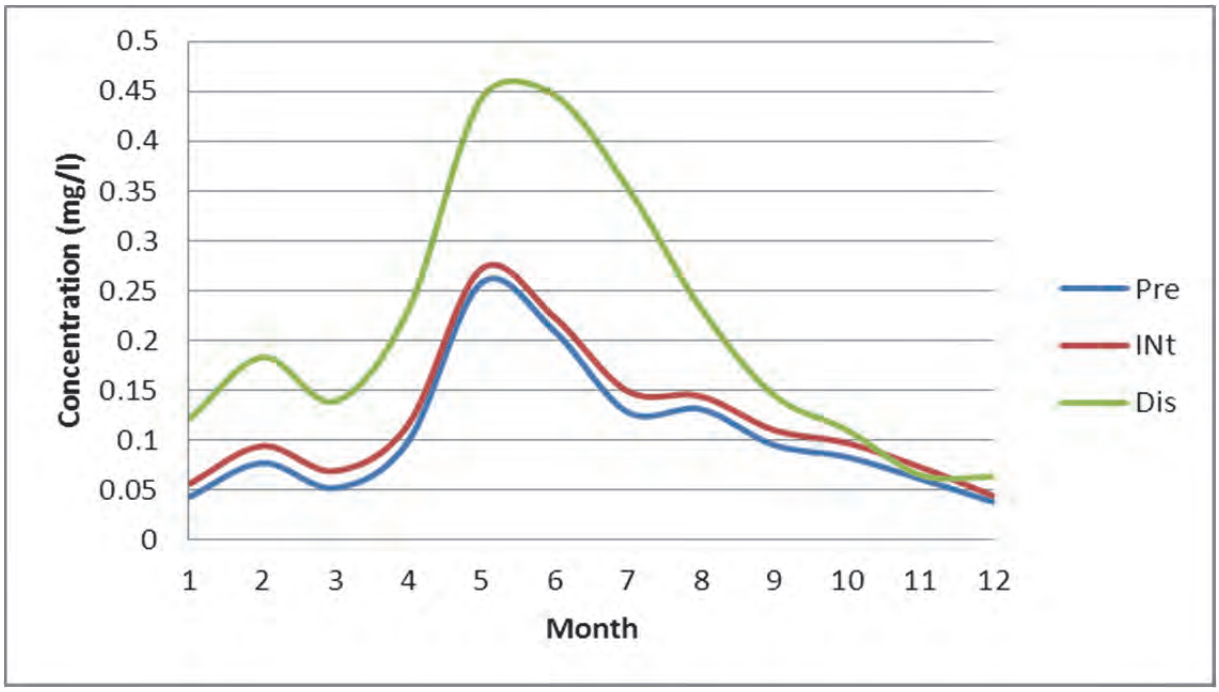

Figure 198: The projected mean monthly surface dissolved silicon concentration of Voëlvlei Dam (mg/l)

Dissolved silicon was exclusively used by diatoms during photosynthesis. From Figure 198 the concentrating effect of evaporation was noted especially in autumn and winter for the intermediate and distant future. This would allow for diatom growth throughout the year and an earlier seasonal shift with diatoms was noted. Thus, the effect of warmer water due to climate change favours the growth of diatoms throughout the year in the distant future, with the greatest increases during autumn, signalling a seasonal shift to an earlier bloom of diatoms.

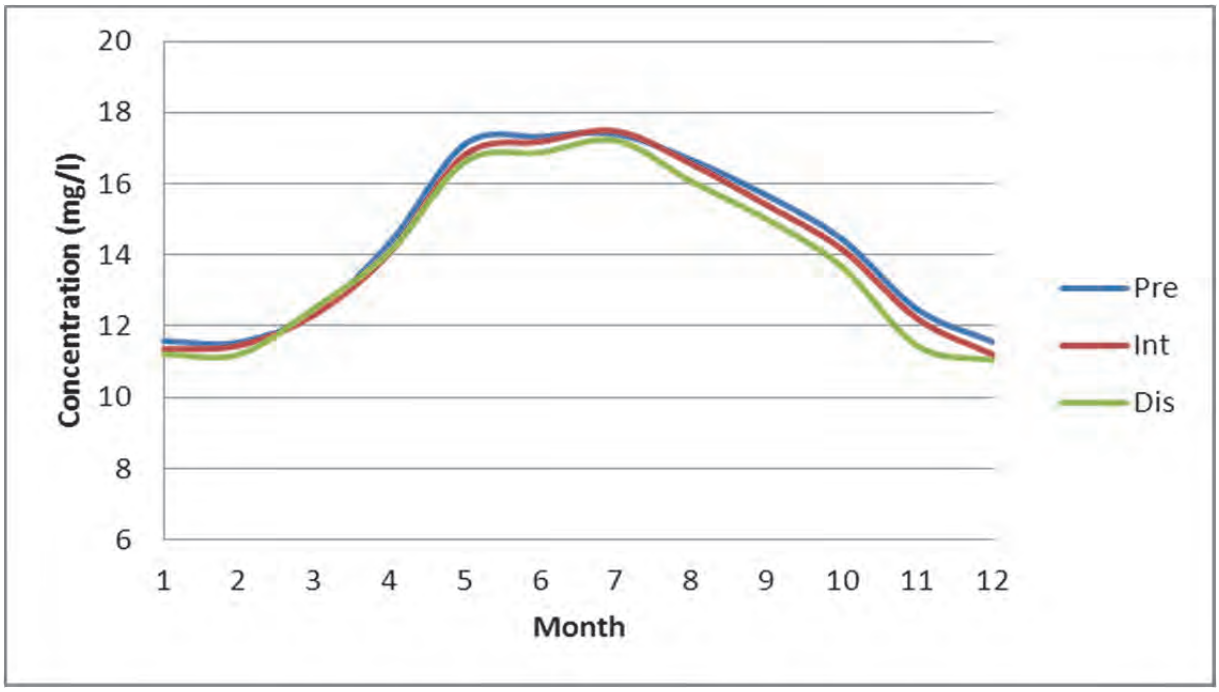

Figure 199: The projected mean monthly surface dissolved oxygen concentration of Voëlvlei dam (mg/l)

The modelling of dissolved oxygen proved daunting, as the results were supersaturated dissolved oxygen concentrations. The only sources of dissolved oxygen were that from the atmosphere and as a product of photosynthesis, with photosynthesis rates being driven by the algal groups. From Figure 199 it was seen that the concentration of DO did not vary much with climate change as would be expected due to the warmer waters. This was attributed to the greater photosynthetic rates of the algae producing more oxygen. The results shown are critiqued as being too high and have been ascribed to the algal growth rates. The selection of accurate algal growth rates was imperative for the quantification of algae in the dam and these are linked to the model output of dissolved oxygen. Varying the algal growth rates had the desired effect of lowering the DO concentrations but then the algal growth was adversely affected. This was not investigated further and it was not known if this was a problem in the water quality model or not.

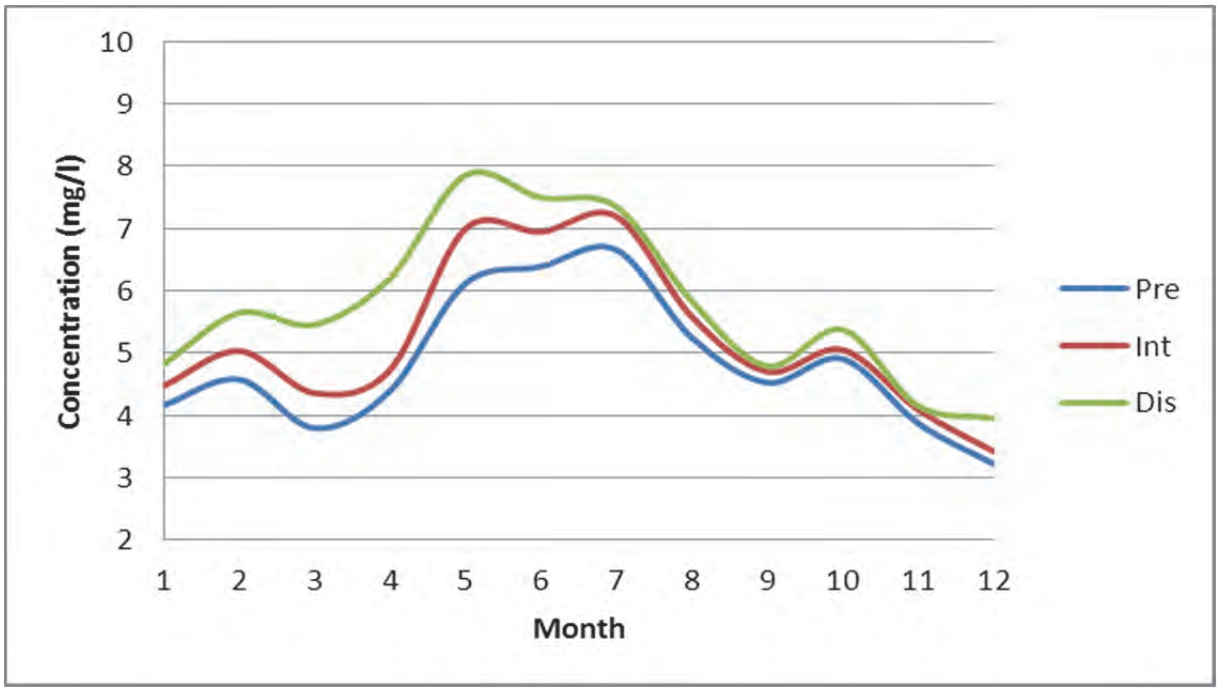

Figure 200: The projected mean monthly surface total algae concentration of Voëlvlei Dam (mg/l)

Upon examining, the total surface algal growth it was seen that for climate change the concentration of total algae increased at the surface with a prominent shift earlier in the year for the distant future. This was a lengthening of the bloom season for total algae and it would persist for longer periods annually.

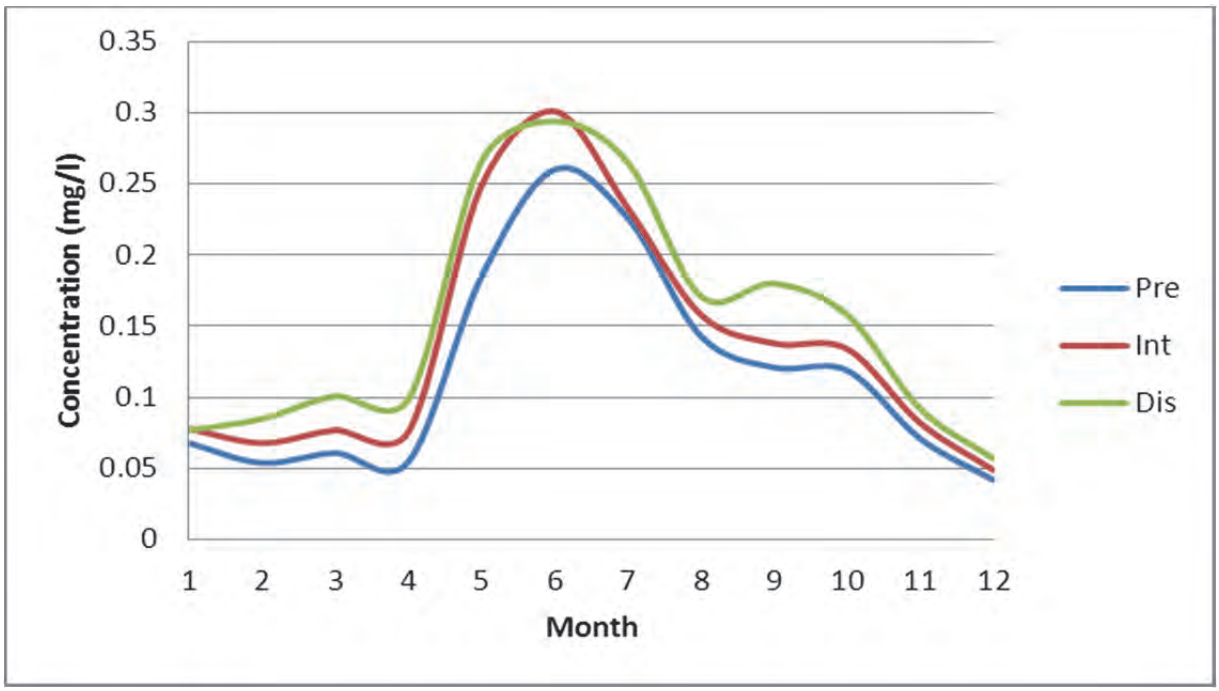

Figure 201: The projected mean monthly surface diatom concentration of Voëlvlei Dam (mg/l)

It was established that the total algae increased especially in the first half of the year and Figure 201 show that diatoms concentrations would peak in winter with climate change but will also increase during the rest of the year. Diatoms are present in the dam for the entire year but are not responsible for the increased total algal due to its low concentrations.

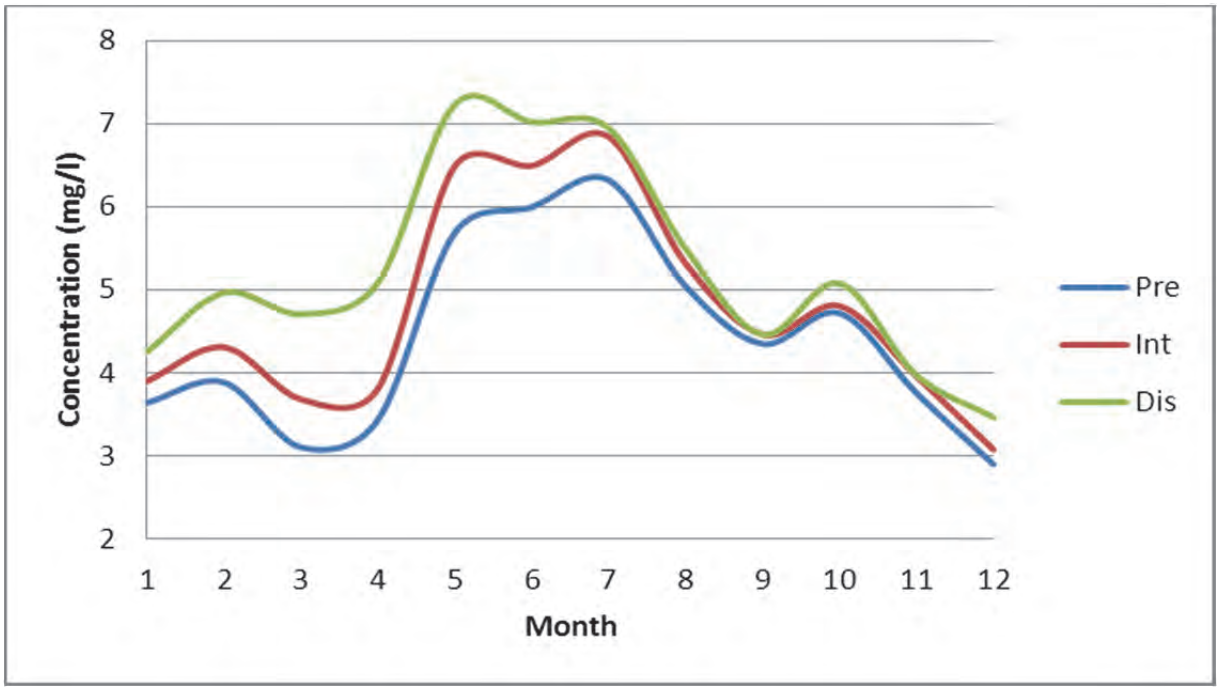

Figure 202: The projected mean monthly surface green algae concentration of Voëlvlei Dam (mg/l)

The green algae are the dominant group in the dam and are present in the highest concentrations when compared to diatoms and cyanobacteria as seen in Figure 202. The increase in its nutrients throughout the year as well as the increased water temperature allowed for an unabated growth for the entire year with seasonal extensions earlier in the year during autumn, with climate change. The green algae showed a lengthening of its bloom period with increases in summer and autumn. The accelerated growth with climate change was clearly visible here as the increases during late summer and autumn are greater in the distant future than in the intermediate future.

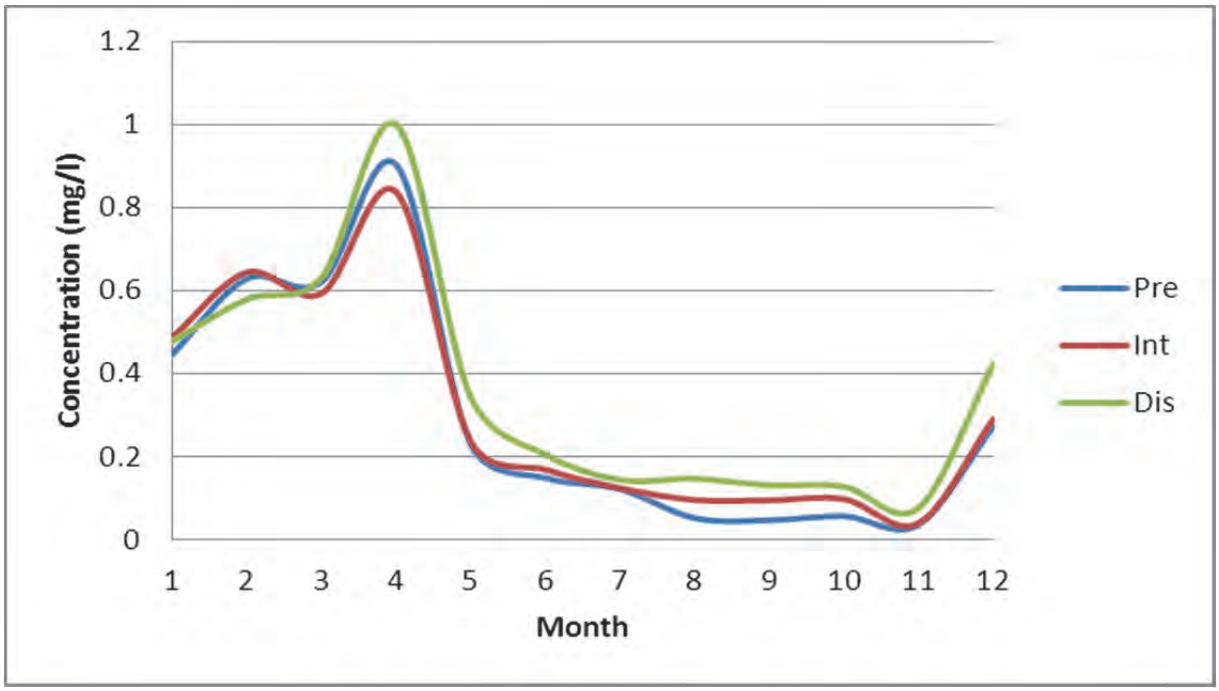

Figure 203: The projected mean monthly surface cyanobacteria concentration of Voëlvlei Dam (mg/l)

Cyanobacteria were present at the surface for the entire year at significant concentrations but with intermediate and future climate change their concentrations did not change significantly for the chosen algal groups. It was expected to see larger growths and succession but this was not the outcome of the study. The current months of cyanobacteria blooms (January to May) will remain relatively unchanged but increases in incident of cyanobacteria blooms should occur during the current 'low' season for blooms (Autumn-August to November). It was therefore plausible the since Voëlvlei had a HAB of *Anabaena* during December 2000 to May 2001 (Downing, 2004) that for the distant future it would still have this season bloom as these months remain relatively unchanged but with climate change that blooms could also occur during spring. This would serve to lengthen the bloom season throughout the year. The result was inconclusive as the inter-variability between the climate models was the greatest for cyanobacteria, with 2 models showing an increase in surface cyanobacteria concentration and 2 a decrease in cyanobacteria concentration for intermediate and future time-period.

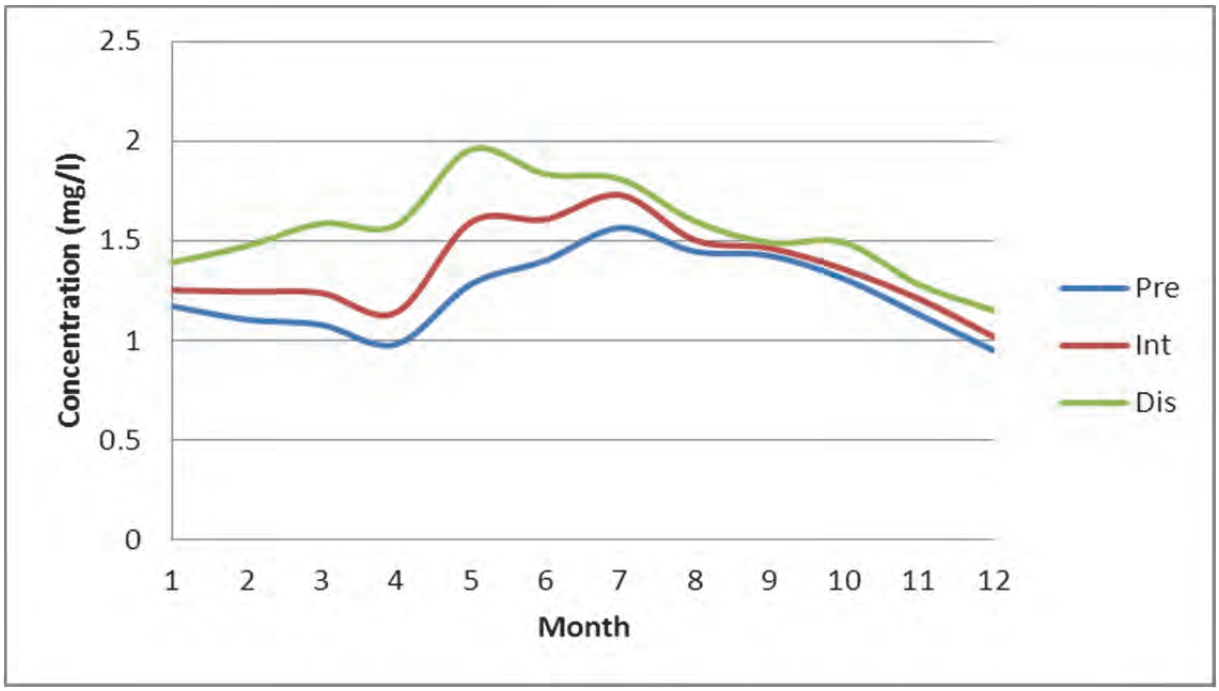

Figure 204: The projected mean monthly surface zooplankton concentration of Voëlvlei Dam (mg/l)

Along with the increase in total surface algae, it was seen that surface zooplankton concentration increased mimicking that of the green and diatoms on which it predates. The zooplankton grazed on diatoms and green algae as their surface concentration increases for future climate the concentration of zooplankton follows it.

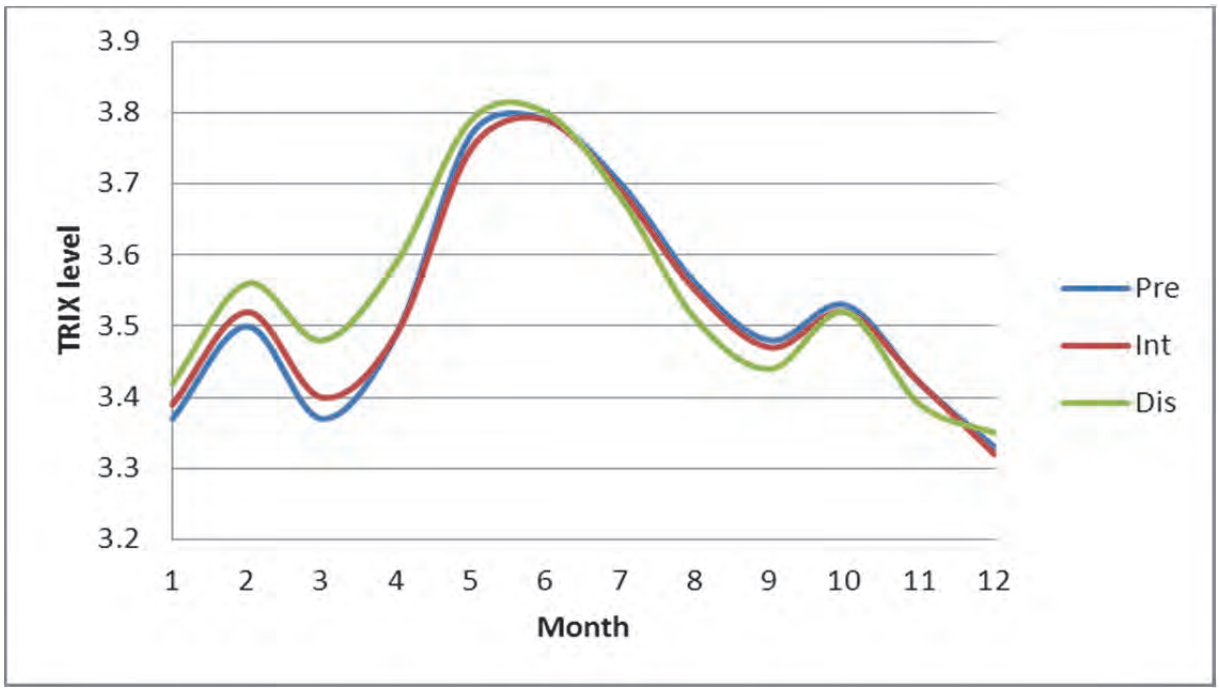

Figure 205: The projected mean monthly surface TRIX level of Voëlvlei Dam

The influence of climate change was seen to have implications for Voëlvlei dam in the form of increased algal blooms and this had a direct effect on the surface eutrophication level especially for the distant future. For the distant future, a seasonal shift was observed and this was due to the decrease in DO and nitrate-nitrites in the latter half of the year at the surface. It was seen for climate change the mean monthly TRIX levels increased for all climate models with maximum in winter. With climate change, this level shifted its peak earlier in the year once again confirming a seasonal shift for worsening water quality.

The following table (Table 79) summarise the water quality of Voëlvlei dam for the projected climate change events.

Table 79: Summary of water quality of Voëlvlei Dam under projected climate change

	Jan	Feb	Mar	Apr	May	Jun	Jul	Aug	Sep	Oct	Nov	Dec
Air temperature (°C)												
Present day	21.05	21.45	21.13	18.15	14.60	13.60	13.50	13.63	14.78	16.08	18.33	19.68
Difference	2.28	2.48	2.45	3.28	2.63	2.13	2.08	1.85	1.75	2.20	2.65	2.80
Intermediate	23.33	23.93	23.58	21.43	17.23	15.73	15.58	15.48	16.53	18.28	20.98	22.48
Difference	3.01	2.78	2.43	2.81	2.81	2.18	1.83	2.09	1.98	2.26	2.89	2.99
Future	26.33	26.70	26.00	24.23	20.03	17.90	17.40	17.57	18.50	20.53	23.87	25.47
Difference	3.01	2.78	2.43	2.81	2.81	2.18	1.83	2.09	1.98	2.26	2.89	2.99
Overall change	5.28	5.25	4.88	6.08	5.43	4.30	3.90	3.94	3.73	4.46	5.54	5.79
Water temperature (°C)												
Present day	22.01	22.23	21.70	19.81	16.15	14.29	13.58	13.96	15.36	16.96	18.62	21.45
Difference	1.17	1.09	1.02	1.16	1.40	1.08	1.12	1.19	1.19	1.28	1.36	1.37
Intermediate	23.18	23.32	22.71	20.96	17.54	15.37	14.70	15.15	16.55	18.23	19.98	22.82
Difference	1.13	1.21	0.98	1.37	1.34	1.20	1.10	1.25	1.31	1.46	1.56	1.30
Future	24.31	24.53	23.69	22.33	18.88	16.57	15.80	16.39	17.85	19.69	21.54	24.12
Difference	1.13	1.21	0.98	1.37	1.34	1.20	1.10	1.25	1.31	1.46	1.56	1.30
Overall change	2.30	2.30	2.00	2.53	2.73	2.28	2.22	2.43	2.49	2.73	2.92	2.68
Total algae (mg/l)												
Present day	4.160	4.573	3.790	4.390	6.113	6.385	6.655	5.248	4.523	4.903	3.870	3.218
Difference	0.310	0.458	0.565	0.335	0.875	0.558	0.535	0.335	0.178	0.148	0.220	0.200
Intermediate	4.470	5.030	4.355	4.725	6.988	6.943	7.190	5.583	4.700	5.050	4.090	3.418
Difference	0.350	0.613	1.098	1.475	0.863	0.551	0.157	0.251	0.087	0.323	0.060	0.533
Future	4.820	5.643	5.453	6.200	7.850	7.493	7.347	5.833	4.787	5.373	4.150	3.950
Difference	0.350	0.613	1.098	1.475	0.863	0.551	0.157	0.251	0.087	0.323	0.060	0.533
Overall change	0.660	1.071	1.663	1.810	1.738	1.108	0.692	0.586	0.264	0.471	0.280	0.732
TRIX												
Present day	3.37	3.50	3.37	3.49	3.77	3.79	3.70	3.56	3.48	3.53	3.42	3.33
Difference	0.01	0.02	0.03	0.00	-0.02	0.00	-0.01	-0.01	-0.01	-0.01	-0.01	-0.01
Intermediate	3.39	3.52	3.40	3.49	3.75	3.79	3.69	3.55	3.47	3.52	3.42	3.32
Difference	0.03	0.04	0.08	0.10	0.05	0.02	-0.01	-0.04	-0.02	-0.01	-0.03	0.03

	Jan	Feb	Mar	Apr	May	Jun	Jul	Aug	Sep	Oct	Nov	Dec
Future	3.42	3.56	3.48	3.59	3.79	3.80	3.68	3.51	3.44	3.52	3.39	3.35
Difference	0.03	0.04	0.08	0.10	0.05	0.02	-0.01	-0.04	-0.02	-0.01	-0.03	0.03
Overall change	0.04	0.06	0.11	0.10	0.02	0.02	-0.02	-0.04	-0.04	-0.01	-0.03	0.02

9.30 **Conclusions**

Study limitations

Similar limitations as expressed for the BRD modelling exercise in terms of climate change data (statistical downscaling, meteorological data, etc.) are noted for this part of the modelling exercise.

An additional outflow to the ICS pipeline was operational but flow data for this gauging station (G1H069M01) was only available up to 1982. This pipeline was excluded from the simulation as it was deemed to have too little effect on the water quality when the calibration and validation was done.

Inflow water quality data was not as readily available as flow data, and was at best measured only on a weekly basis. No inflow and outflow data was available for the predicted future scenarios, and it was proposed to use the current DWA HIS databases flow-data from 1 January 1971 until 31 December 1990 (present scenario) for each of the subsequent intermediate and future simulations. This would assume that demand and allocation of the water resource did not change for the simulation periods.

In order to predict the growth of algae parameters had to be as accurate as possible. Finding some of these parameters proved difficult and futile in some instances and default values were used. The choice of algal growth constant also affected the DO concentrations to such an extent that the dam became super-saturated at the surface for extended periods, which was not common in reality. This also consolidated the fact that the choice of growth constant was extremely important and *in situ* measurements should be collected for future studies.

For each run, the initial conditions were the same as the present day initial conditions. This allowed for a direct comparison of present day to intermediate future and distant future. For each simulation period, the original dam was consistently subjected to climate change. Climate change data was not available from 1971 to 2100 to allow the dam to be modelled for the entire period. This meant that when the time of simulation approached 2045 the

model has already run for over 50 years and the in-situ conditions are that of 2045. Currently the intermediate future and distant future initial conditions are that of the present day.

Water quality modelling

The variability between the four climate models was minor, and they projected similar air temperatures for each of the time scenarios studied. The climate models were also ranked in order of coolest to hottest, being ECH, CRM, CCC and then IPS. It was noted that the greatest increase in air temperature occurred during winter.

It was concluded that air temperature was the major driver for surface water temperatures and solar radiation was the diurnal driver. Climate change affected the surface waters by heating the water and subsequently increased the evaporation rate of the water. This heated water evaporated more in the distant future than the intermediate future a result of the increased water temperature.

Once climate change has heated the surface waters of the dam, the water level dropped due to increased evaporation, an increase in the concentration of water quality constituents in the dam resulted.

The concentration of surface ammonium increased because of the concentrating effect of decreasing the surface water level. Annually this increase occurred mainly during autumn and winter with small changes and decreases during spring and summer.

The effect of climate change on nitrate-nitrites was very slight as its main source was from the nitrification of ammonium. It was expected that for an increase in temperature and ammonium that the nitrification reaction would respond in an Arrhenius manner and produce more nitrate-nitrite but this was not so. It could be that the rate of generation of nitrate-nitrites was similar to its assimilation by algae.

It was seen that the concentration of DO did not vary much with climate change as would be expected due to the warmer waters. This was attributed to the greater photosynthetic rates of the algae producing more oxygen. Varying the algal growth rates had the desired effect of lowering the DO concentrations but then the algal growth was adversely affected.

The present day mean total algal growth was greater for the winter months than for summer. Upon examination of the total surface algal growth it was seen that for climate change the

concentration of total algae increased at the surface with a prominent shift earlier in the year for the distant future. This was a lengthening of the bloom season for total algae and it would persist for longer periods annually.

For both intermediate future and distant future, the mean total algal growth was greater for the winter months than for summer. There was a much greater mean concentration of diatoms during the winter months as opposed to summer months. The study suggested that there would be an annual presence of diatoms in the dam that increased with climate change but diatoms are not entirely responsible for the increased total algal due to its low concentrations. The green algae showed a lengthening in the duration of its bloom period with increases in summer and autumn. It was clear that green algae are the dominant species in Voëlvlei dam as they have the greatest concentration and compares well to that total algae concentrations.

The present day showed seasonal cyanobacteria blooms with maximum mean values during summer and autumn with decreases during winter. Cyanobacteria were present at the surface for the entire year at significant concentrations, but with intermediate and future climate change their concentrations did not change significantly.

Zooplankton was present in Voëlvlei dam throughout the entire year but at show a greater concentration during the winter months due to the greater concentration of diatoms and green algae during these months. Winter had the poorest water quality for the present day. Zooplankton was present in Voëlvlei dam throughout the entire year but at show a greater concentration during the winter months due to the greater concentration of diatoms and green algae during these months. Zooplankton grazes on diatoms and green algae, and as their surface concentration increased for future climate, the concentration of zooplankton followed it. It was observed that for climate change the mean monthly water quality levels worsen for all climate models with the worst water quality levels in winter. With climate change, the months of worst water quality would shift to earlier in the year and confirmed a seasonal shift for worsening water quality.
Climate change favoured the growth of diatoms throughout the year in the distant future, with the greatest increases during autumn, signalling a seasonal shift to an earlier bloom of diatoms. Diatoms were present in the dam for the entire year but were not responsible for the increased total algal due to its low concentrations.

The green algae are the dominant group in the dam and are present in the highest concentrations when compared to diatoms and cyanobacteria. The increase in its nutrients

throughout the year as well as the increased water temperature allowed for an unabated growth for the entire year with seasonal extensions earlier in the year during autumn, with climate change. The green algae showed a lengthening of its bloom period with increases in summer and autumn. The accelerated growth with climate change was clearly visible as the increases during late summer and autumn are greater in the distant future than in the intermediate future.

Cyanobacteria were present at the surface for the entire year at significant concentrations but with intermediate and future climate change their concentrations did not change significantly for the chosen algal groups. The result for cyanobacteria was inconclusive as the variability between the climate models was the greatest for cyanobacteria, with two models showing an increase in surface cyanobacteria concentration and two models showing a decrease in cyanobacteria concentration for intermediate and future time-period.

It was expected to see larger growths and succession but this was not the outcome of the study.

Along with the increase in total surface algae, it was seen that surface zooplankton concentration increased, mimicking that of the green and diatoms on which it predates. The zooplankton grazed on diatoms and green algae as their surface concentration increases for future climate the concentration of zooplankton follows it.

The influence of climate change was seen to have implications for Voëlvlei dam in the form of increased algal blooms and this had a direct effect on the surface eutrophication level especially for the distant future. For the distant future a seasonal shift was observed and this was due to the decrease in DO and nitrate-nitrites in the latter half of the year at the surface.

For the distant future, a seasonal shift was observed in the water quality level and this was due to the decrease in DO and nitrate-nitrites in the latter half of the year at the surface. It was noted that under climate change the mean monthly TRIX levels increased for all climate models with maximum in winter. With climate change, this level shifted its peak earlier in the year.

It was clear that phosphorous had an annual cycle with maximum concentrations reached during winter and the concentration was sufficiently high not to limit algal growth. The dam is eutrophic and nitrogen limits algal growth for the entire year except during winter when it switches to phosphorous limited algal growth at the surface. The limiting nutrient,

phosphorous was seasonal. If algal blooms are to be controlled, it would be imperative to abate the inflow of phosphorous into Voëlvlei dam. This would be achieved by lowering the inflow concentrations via legislation and applying new technologies or some form of cleaner production to the WWTP upstream to the dam.

Results from the study also showed that the dam was supersaturated with dissolved oxygen for a greater part of the year, which needs further investigation. The calibration of DO was not possible as there were no measured values to compare with. Calibration would involve assessing the aeration rate at the surface as well as the effect of the algal growth rates on the observed DO concentrations. A sensitivity analysis should show which parameters affect the DO concentrations and subsequent changes to rectify this may be implemented.

In essence, with future climates and current operating variables, water quality and trophic status in Voëlvlei dam would worsen through algal growth due to having sufficiently high concentrations of phosphates, and measures have to be implemented to prevent this.

Recommendations

This study concentrated on the water quality of the surface waters of Voëlvlei dam. The study produces vast amounts of data and the limitation of presenting the only the surface waters only was vindicated for this dam as it was almost entirely mixed for the simulation time. The model used was CE-QUAL-W2, which is a 2 dimensional laterally averaged model which returns an adequate solution. A more representative model would produce a true 3 dimensional solution but this would only be possible with using a 3 dimensional model and greater accuracy for inflow and withdrawals.

It was shown that surface water quality would worsen for future climate change events with the decrease in DO and a lengthening of the total algal season. A similar recommendation is made in terms of reduction of phosphorous at the source for management of eutrophication levels. Monitoring and measuring of all the channels into and out of Voëlvlei dam is also recommended, as for BRD, as well as *in situ* measurement. Notes made regarding meteorological and sedimentation data for BRD also apply to future studies at Voëlvlei Dam.

10 IMPACT ASSESSMENT

It is evident from both of the modelling exercises that stringent control over nutrient release to South Africa's water courses and impoundments is vital for the management of eutrophication. Furthermore, investigation of climate change projections indicates that with higher temperatures and varying evaporation, climate change is likely to exacerbate the effects of eutrophication.

For the purpose of this report, the impacts were viewed from a sustainability perspective, and were therefore grouped into environmental, economic and social impacts. This classification is however not absolute, as many of the issues affect one another and are not mutually exclusive, for example effects on ecosystem services which have a direct social and potentially economic benefit. These interactions will also be discussed.

The following sections outline these impacts.

10.1 Environmental impacts

The environmental impacts of climate change on eutrophication are extensive and are difficult to thoroughly capture due to their complexities and knock-on effects. However it should also be noted that many of these impacts already exist, and climate change is only likely to accelerate and or exacerbate the current problems in South Africa's water courses.

Climate change effects on water temperature, suspended loads, nutrients and dissolved oxygen

The modelling exercises outlined above have indicated that with an increase in temperature under climate change, as well as the associated changes in evaporation and other physical variables, there are likely to be increases in suspended loads and nutrient release through deepened thermocline depths and increases in circulation. These effects (with reference to Komatsu *et al.*, 2007) are simplified in Figure 206.

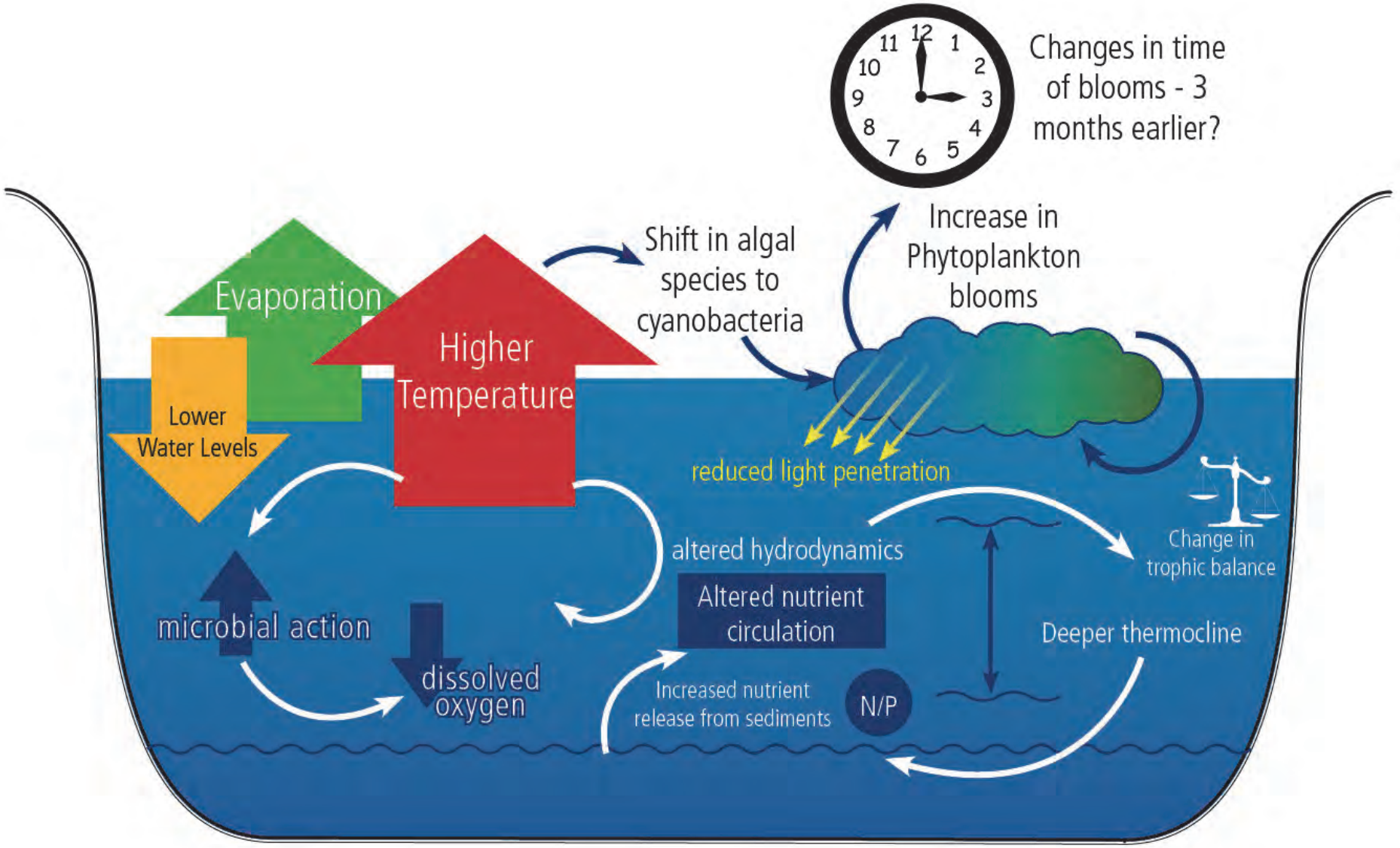

Figure 206: Simplified diagram of the interactions between climate change, nutrient release and algal prevalence

The changes include, amongst others:

- Increased microbial action due to warmer temperatures and associated reduction in DO;
- Increase in the rate of decomposition of organic material under higher temperatures;
- Decreased DO due to warmer water temperature which reduces its solubility and reduces the suitability of habitat for oxygen-breathing vertebrates and invertebrates;
- Increase in BOD resulting in anoxia and biomass reduction. The aquatic organisms would release their nutrients during decay compounding the situation (Meisner *et al.*, 1987);
- Reduced water volumes due to higher evaporation should this occur, and consequent concentration of nutrients in the water body, encouraging algal growth which is not likely to be nutrient limited;
- Potential longer retention times and decreased flushing resulting in increased eutrophication and salinity (Jørgensen, 2008);
- Altered hydrodynamics in the water body due to changes in water temperature, leading to deepening thermoclines, release of nutrients from sediments and increased circulation of these, increasing the movement of solutes and encouraging algal growth;
- Change in the trophic balance of the water body;
- Alteration in terms of the species of algae, with increase in concentrations of temperature-tolerant cyanobacteria, which can cause toxicity-associated health problems in cases of ingestion and treatment;
- Increased levels of algal growth, which reduces light penetration to lower strata of the water body, thus reducing the suitability of habitat for various plant and animal species (which may in fact counteract the warming effects);
- Seasonal shifts in algal blooms to potentially occur earlier in the year and to last for longer periods, leading to requirements for longer, more intensive and expensive domestic treatment methods.

This list is by no means complete, but it can be seen that the existing problems of eutrophication in various parts of South Africa are likely to be exacerbated under climate change.

It should also be noted that anthropogenic causes of thermal pollution also exist, which can further affect the warmth of a water body, and should be reduced into the future if possible to further reduce the conduciveness of a water course to algal growth. These include:

- heated industrial and wastewater effluent discharges;
- returning heated cooling waters from power stations; and
- inter-basin water transfer (Dallas and Day, 2004; Snaddon and Davies, 1999).

Eutrophication is due to excess nutrients, in particular nitrogen and phosphorous in the water. The removal of these nutrients increases the cost and need to treat the water (discussed under Section 10.3). The removal of algal toxin and algal decomposition products is also necessary, which also increases the cost of water treatment (Pretty *et al.*, 2003). Cyanobacteria cause a distinct taste and odour, as well as causing a discolouring of the water, which requires activated carbon in the treatment facility (Dennison and Lyne, 1997).

As mentioned earlier in this report, water quality is also reduced by the presence of algal blooms which occur because of the increase in nutrients in the water. Algae cause lower concentrations of dissolved oxygen in rivers, which leads to a loss of biodiversity and resilience in the aquatic ecosystem (Dennison and Lyne, 1997). Aesthetically, water quality is reduced by the unsightly presence of the algae, and by the unpleasant odour that is a characteristic of deoxygenated water (Dennison and Lyne, 1997).

Climate change effects on algal blooms

As mentioned elsewhere in this report, temperature increases and associated changes are likely to cause an increase in algal blooms. However, these changes are also likely to influence the species of algae which are prevalent. Some impacts of increased algal blooms may be direct, including possible effects of cyanobacterial toxins on fish, invertebrates and other aquatic fauna. Other impacts may be indirect, such as a reduction in submerged plants on account of an increase in plankton biomass, or changes in fish community structure if summer cold water refuges are lost due to hypolimnetic anoxia (Havens, 2008).

Cyanobacterial (*Microcystis*) algal blooms occur in waters with temperatures above 20°C, so an increase in water temperature is likely to lead to an increase in these species (Oberholster *et al*., 2009). The growth of cyanobacteria species that has previously been hampered due to low temperature and nutrient concentrations may form mixed algal blooms

with existing species, which could potentially lead to the simultaneous occurrence of both neuro and hepatic biotoxins in one algal bloom. As higher water temperatures are likely to promote evaporation from the water surface and change concentrations of organic and inorganic compounds, the likelihood of mixed algal blooms will increase. This change will be more important for marine and estuarine waters as the evaporation would increase the salinity as well as being problematic for freshwater purification managers, but should also be noted for fresh water courses and dams. The South African winters, with air temperatures of 7 to 8°C, usually provide a barrier to the growth of cyanobacterial species, but if the winter temperatures are increased due to climate change, there would potentially be a two fold increase in cyanobacteria growth, as the period in which it would die off would be severely diminished (Oberholster *et al*., 2009).

Havens (2008) furthermore explains that when cyanobacteria become dominant in rivers, the particle size, nutrient stoichiometry and some other properties of the organic material in water are altered. Organic export increases to the sediment layers within the water body, which can lead to sediment anoxia, altering the makeup of the invertebrate community. The anoxic conditions can in turn reduce the extent to which iron binds to phosphate (Havens, 2008) at the sediment/water interface, leading to the release of more phosphate. Anoxic sediment also tends to release ammonia (this process is known as internal nutrient loading (Boström *et al*., 1988, Ahlgren *et al*., 1994). Entrainment of nutrients from the hypolimnion to the epilimnion can support summer blooms of cyanobacteria which may produce problematic taste and odour compounds.

Increased eutrophication effects under climate change on fish and other vertebrates

Increased eutrophication leads to a number of primary and secondary effects on ecosystems and in turn on the communities of vertebrates and invertebrates which live within these ecosystems, for example, the food webs and reproductive cycles within these ecosystems. Some of these effects are discussed below.

As described in this report, increased temperature with climate change is likely to cause increased eutrophication, which increases the consumption of oxygen within the river. Oxygen depletion during algal blooms can have biological impacts, the most visible being fish kills. Algal blooms could also lead to wider fluctuations in DO as a result of photosynthesis and respiration at night. In temperate and boreal regions, where piscivores (salmonids) require a cold water refuge during summer, eutrophication may eliminate those fish if the hypolimnion becomes anoxic in lakes and reservoirs (Colby *et al*., 1972). This

could further be impacted if climate change alters the temperature of these traditional “cold water” areas significantly, i.e. refuges could be lost under climate change.

Breitburg *et al*. (1997) reported that the effects of low oxygen (potentially related to higher temperatures and/or increased biological activity and heightened use of oxygen through respiration) on trophic interactions vary among species. Low (but non-lethal) concentrations of oxygen (hypoxia) reportedly greatly increased predation on fish larvae by jellyfish in the 1997 study, but decreased predation by other species (Breitburg *et al*., 1997). Changes in predator-prey interactions indicate variation among species in terms of their physiological tolerance to low oxygen and the effects of this on escape behaviour of prey, as well as on swimming and feeding behaviours of predators. These effects can potentially affect the food chain and associated energy flow in water bodies. This indicates that the effects of climate change on dissolved oxygen, and the resultant effects of specific species, is uncertain and it is difficult to predict such effects.

O’Brien *et al*. (2011) conducted an assessment of the threats to the yellowfish *(Labeobarbus* spp.) and the ecosystem services they provide in the Vaal River system. The risks to yellowfish were found to be:

- chemical pollution;
- flow alterations; and
- alterations in habitat (O’Brien *et al.*, 2011).

All of the above factors can be affected by climate change.

Chemical pollution can be altered and aggravated through a change in water temperature and reduction in water volumes with increased evaporation, should this occur under climate change projections. Furthermore the resilience of the water body to chemical pollution can be affected through reduced dilution. The effects of increased extreme rainfall event frequency could assist with flushing of chemicals, but the associated disruptions to the water body due to heavy rain are unlikely to render this a positive feature of the climate change impact.

Flow patterns, as explained elsewhere in this report is likely to be affected by climate change through differing rainfall regimes, evaporation and the frequency of occurrence of extreme rainfall. These changes are likely to affect the movements and behaviour of various species and the species with which they interact. Habitats are likely in turn to be affected due to alterations in plant communities under climate change, as well as release of sediments and nutrients. Food chains are likely to change, which may favour certain species over others.

Specifically with regard to algal blooms, these can directly impact fish and other aquatic vertebrates through the toxins that certain algae release. This can indirectly impact aquatic life by changing fish community structures, the habitat of aquatic species, leading to changes in the behaviour of certain fish species and threats to their spawning grounds (Havens, 2008).

Amphibians that are exposed to high nutrient environments of eutrophication are at risk due to altered feeding and swimming activity, and decreasing growth of and development of larvae reactions. Nutrients increase the density of planorbid snails and the intensity of parasite infection, resulting in malformations in amphibians affecting species diversity within the water body (Peltzer *et al.*, 2008).

Increased eutrophication effects under climate change on invertebrates

In addition to the ecosystem and food web effects mentioned in preceding sections of this report, cyanobacterial toxins can impact on the tissue development of invertebrates and lead to an accumulation of toxins within this tissue (Havens, 2008). The cyanobacterial toxins also affect aquatic snails by impacting their growth, their potential to reproduce and their general survival (Havens, 2008).

In addition, there have been observations of adverse impacts of high concentrations of ammonia during algal senescence. For example, during collapse of a dense *Anabaena circinalis* bloom in Lake Okeechobee, Florida, the combination of low oxygen concentrations and ammonia was considered the cause of mortality for snails and other macro-invertebrates (Jones, 1987).

10.2 Social impacts

Effects on recreation and visual appeal

Recreational activities, which are of great importance in areas such as the Vaal River, can be severely affected by the increase of eutrophication under climate change, and in fact these are already under threat in certain parts of the Vaal area. Effects such as bad odour and discolouring of the water (aesthetics) lead to reduced appeal in terms of recreational activities in the river (Dennison and Lyne, 1997).

The social impacts of these changes are difficult to quantify, although there is likely to be a reduction in quality of life through the decrease in recreational activities, and the knock-on financial benefits that these activities bring into the local area (Brand *et al.*, 2009). Increased algal blooms lead to physical interference with recreational activities and the use of the river, as well as a general degrading of the beauty of the area (Dennison and Lyne, 1997).

Effects on community livelihoods

It is important to note that traditional communities have established practices based on existing ecosystems which are now affected by climate change and eutrophication threats. A decline in numbers of yellowfish in the Vaal River, for example, where local communities harvest yellowfish for food, could have considerable knock-on effects as regional ecotourism endeavours are underpinned by this species (which acts as a flagship species). The loss or reduction in numbers of this species could lead to the loss of a major protein source in local communities, as well as the loss of the community engagements that comes with the conservation and ownership of local lands and resources. Communities furthermore benefit directly from improvements in the health of the river when yellowfish are successfully used as ecological indicators (O'Brien *et al*., 2011).

Climate change/eutrophication effects on human health

Algal blooms and cyanobacteria in particular, can result in many human health-related impacts. The potential impacts of climate change could increase the frequency of toxic algal blooms, and this is likely to increase the likelihood of human-related health impacts and potentially toxic algal-related fatalities for communities that drink water directly from the river.

Cyanobacteria Toxin Poisonings (CTPs) occur in lakes, ponds, rivers and reservoirs throughout the world. The main organisms include *Anabaena*, *Aphanizomenon*, *Cylindrospermopsis*, *Lyngbya*, *Microcystis*, *Nostoc*, and *Oscillatoria* (*Planktothrix*). Toxins

which are derived from cyanobacteria (cyanotoxins) include cytotoxins and biotoxins. Biotoxins are responsible for acute lethal, acute, chronic and sub-chronic poisonings of wild/domestic animals and humans. These include several neurotoxins, including ana-toxin-a, anatoxin-a(s) and saxitoxins, plus the hepatotoxins; microcystins, nodularins and cylindrospermopsins (Carmichael, 2001). Cyanobacteria can cause skin irritation when contact with the skin is made. It also leads to gastro-enteritis if ingested (Dennison and Lyne, 1997). One of the characteristics of cyanobacteria is that is produces “low-molecular-weight cyanotoxins” (Oberholster *et al.,* 2009). Neurotoxins have been shown to cause damage in the nervous system while the hepatotoxins cause a breakdown in the liver cells (Oberholster *et al.*, 2009).

Some of these toxins produced by cyanobacteria blooms can result in the loss of livestock and other mammals that ingest the raw river water (Dennison and Lyne, 1997). Livestock health can indirectly affect the human health of the local communities.

Water treatment is further complicated by the formation of trihalomethanes (THMs) after chlorination during the treatment process, which can lead to further health complications. Information in this section was sourced from an Environmental Health Sheet on THMs (New Hampshire Department of Environmental Services, 2006). THMs are a group of organic chemicals that occur in drinking water as a result of chlorine treatment for disinfectant purposes. They are also known as "disinfection by-products" (DBPs). THMs are formed when chlorine reacts with naturally occurring organic material found in water such as decaying vegetation. Typically, the following four THMs are found as a result of chlorination:

- trichloromethane (chloroform);
- bromodichloromethane (BDCM);
- dibromochloromethane (DBCM); and
- tribromomethane (bromoform).

Untreated or raw water rarely contains THMs in significant concentrations, but environmental release of THMs is largely to air during water chlorination. Swimming in chlorinated pools will also contribute to the total exposure from the same exposure paths. One study observed that a greater percentage of chloroform passed through the skin when bathing water temperatures were increased. Chloroform does not concentrate in plants; therefore, the contribution from food to total chloroform exposure is small.

Chronic oral exposure of humans to chloroform at high doses results in adverse effects on the central nervous system, liver, kidneys and heart. In studies of human populations using chlorinated drinking water in which chloroform is the main THM, small increases in the incidence of rectal, colon and bladder cancer have been consistently observed, with evidence strongest for bladder cancer. However, because other possible carcinogens were found in this water, it is impossible to identify chloroform as the sole carcinogenic agent. Studies have suggested an increased risk of early-term miscarriage from high concentrations of THMs in tap water, particularly BDCM. The American Environmental Protection Agency has established a Maximum Contaminant Level (MCL) for total THMs in public drinking water systems, with the MCL for total THMs being 80 parts per billion (ppb = micrograms per litre (µg/l).

Although chloroform is considered to be a likely human carcinogen, evidence indicates that it causes cancer only if exposure exceeds the threshold level needed to cause cell toxicity. This threshold has been calculated to be greater than the exposure level at which the most sensitive fatty cyst formation in the liver (non-cancerous), may occur. Therefore, exposure at or below the state drinking water standard for chloroform (70 ppb) is not anticipated to result in adverse non-cancer health effects or cancer. The state drinking water standard developed for BDCM is 0.6 ppb, for DBCM is 60 ppb and for bromoform is 5 ppb.

10.3 **Economic impacts**

The implications of increased eutrophication under climate change are likely to be varied and numerous. A recent project was undertaken by Graham *et al.* (2012) towards the development of a generic model to assess the costs associated with eutrophication. The findings of this report are not duplicated here, but are briefly summarised in the graphic below (Figure 207). Certain economic factors are explored in more detail.

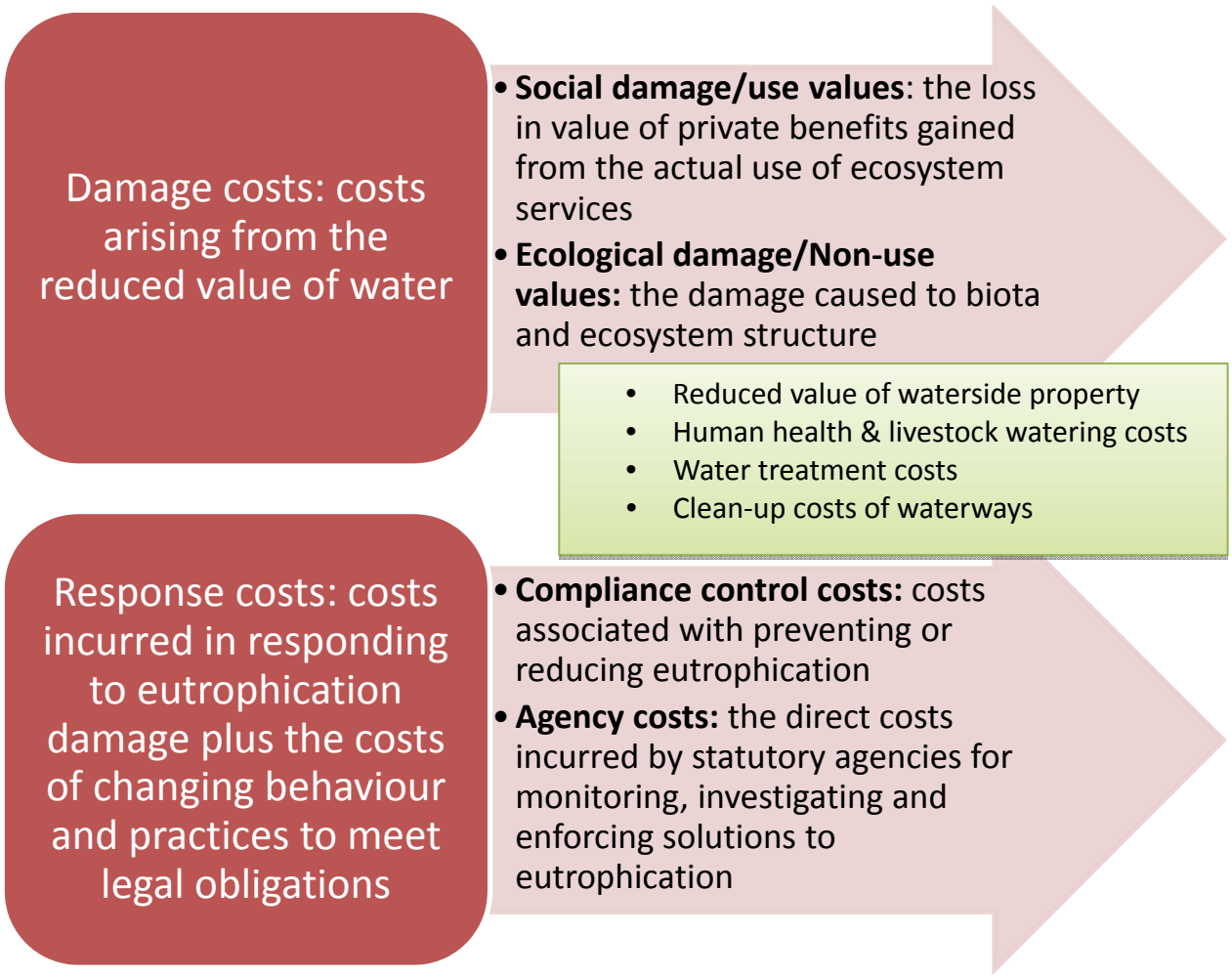

Figure 207: Summary of the costs of eutrophication (after Graham *et al*., 2012 and Pretty *et al*., 2002)

Increased health costs from health damages from algal blooms as mentioned in the previous section both from recreational use and ingestion should also be noted (Dennison and Lyne, 1997)

Water treatment implications

Discussions with the Midvaal Water Company (Marina Kruger *pers. Comm.*) indicated that high levels of eutrophication are already problematic for their treatment process. The following points were raised:

- Specific types of alga cause severe filter blockage, with filamentous types forming “mats” on the surface of the sand, and slime builds up in the filter sand and reduces the filtration capacity;

- Algal build up leads to reduced filter operating cycles (e.g. reduced from the normal 24 hours between back wash cycles to as low as 6 hours between back wash cycles);
- More back washing results in extra operating costs, including labour, wash water requirements, electricity, the volume of wastewater produced that has to be handled, and maintenance issues;
- The method of back washing has had to be changed to a more vigorous simultaneous air-and-water scenario, and the weir heights in the filters had to increase to prevent excessive media/filter sand losses. This implies additional capital cost and future maintenance costs;
- The Company invested R 45 million in 2011 to increase filtration capacity; and
- At times of high algal concentrations in the raw water almost 30% more chemicals are required to improve the colour and/or taste and odour as a result of the algae.

This section documents a specific exercise carried out by the team to investigate the potential cost implications at water treatment plants resulting from the increased algal concentration in feed water. End of pipe treatment options can prove extremely costly and upstream migratory measures need to be considered. We have included recommendations for further upstream migratory measures.

A high level investigation was carried out to understand the potential cost implications to drinking water suppliers as a result of increased algal concentrations in feed sources.

Case Study

The Midvaal Water Company treatment plant was selected as a case study for this evaluation.

Chlorophyll concentrations

Chlorophyll concentrations from January 2004 to January 2012 were obtained from the water treatment plant. The data is presented in Table 80 and illustrated in Figure 208.

Table 80: Statistical analysis of the chlorophyll concentrations in the inlet of the Midvaal Water Treatment Plant

Description	Concentration (µg/ℓ)
50 percentile	82
75 percentile	131
95 percentile	211

It can be noticed that the concentrations fluctuate considerably with lower concentrations noted over the winter months, which coincides with the dry season in this area.

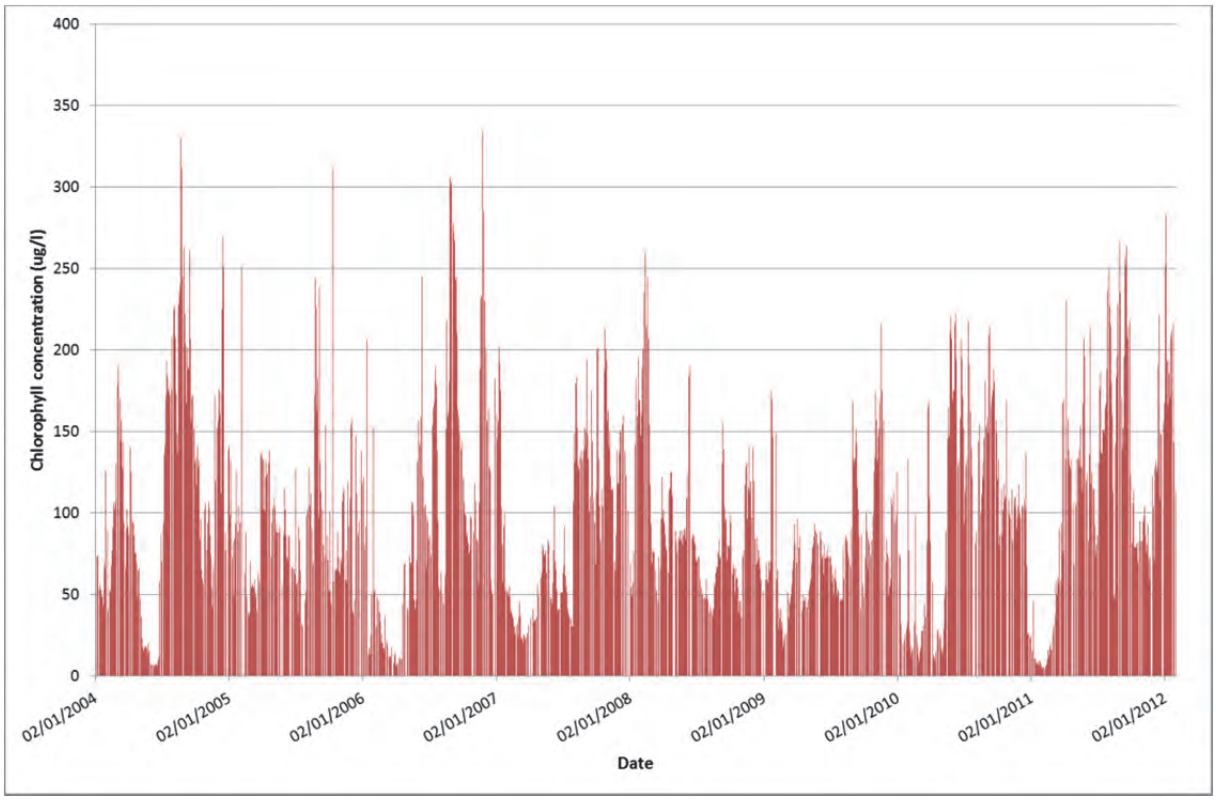

Figure 208: Chlorophyll concentrations (µg/ℓ) at the inlet of the Midvaal water treatment plant

Treatment process

The Midvaal water treatment process is presented in Figure 209.

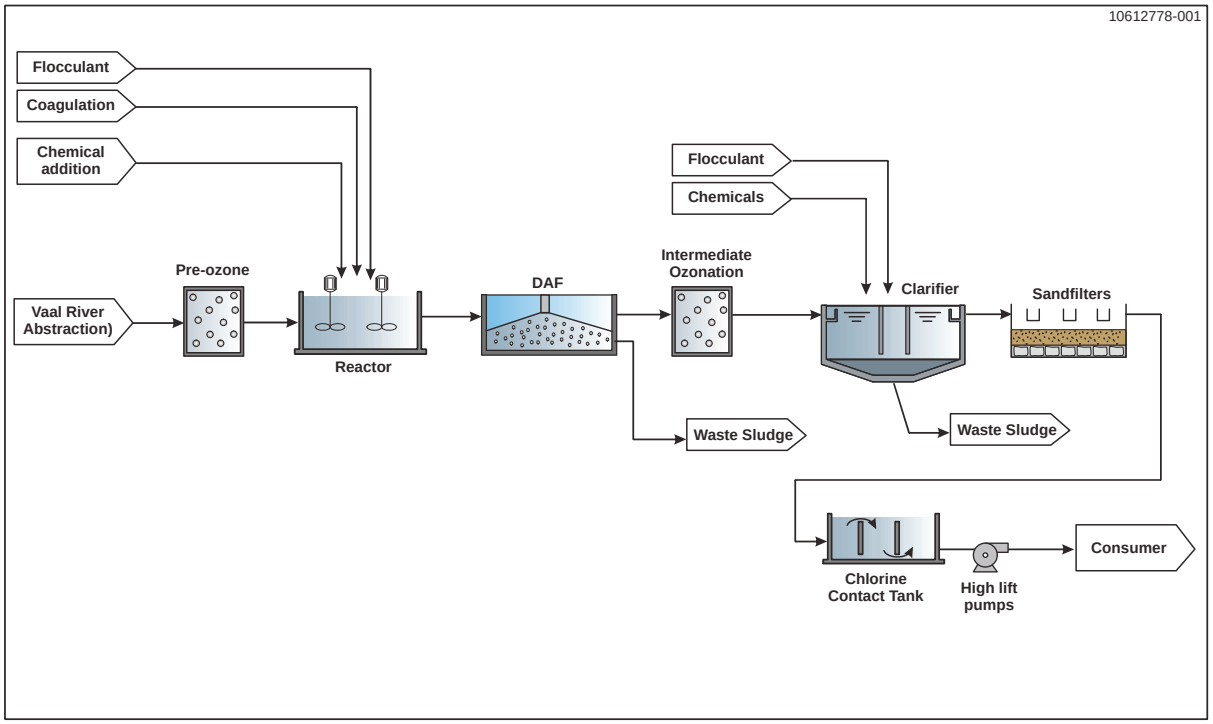

Figure 209: Current water treatment process at Midvaal Water Company

Pre-ozonation

The pre-ozonation step was added for the purpose of algal removal. The process has been designed such that the unit is not used for low algal concentrations in the water. Doses of between 1-1.5 mg/ℓ of ozone are used here. The algae is immobilised in this step and can then be easily removed in the flotation process. A maximum dosage of 1.5 mg/ℓ is maintained in order to prevent cell lysis, the breaking down of the cell wall, which will lead to increased odour and taste concerns in the treated water.

Dissolved Air Flotation (DAF)

The DAF step removes a large proportion of the algal biomass. With high algal concentrations however, only 60 to 70 % of the algae is removed in this stage.

Intermediate ozonation

The purpose of the intermediate ozonation step is for manganese and iron removal from the water and to aid flocculation. The ozone dosage at this stage can however be increased up to a concentration of 2.5 mg/ℓ without the risk of cell lysis in order to reduce algae which was carried over from the DAF units.

Chemical addition

Flocculants are added for the purpose of sediment removal. An increase of chlorophyll concentrations from 82 µg/ℓ to 130 µg/ℓ results in a 30% increase in chemical costs. When concentrations exceed 130 µg/ℓ, chlorine, which kills the algal cells, is added at this intermediate step in order to reduce algal concentrations reporting to the filters. Live algal cells photosynthesise, producing air, making them less dense than water. In this case the algae will float to the surface and be carried over in the clarifier. The dead cells are more likely to form clumps and are then removed in the sedimentation step.

Sedimentation

The purpose of the sedimentation step is the remove the flocs which have formed as the result of the ozonation and chemical addition steps. Immobilised algal cells will be removed with the flocs.

Filtration

The filtration step will remove suspended particles and solids carried over from the sedimentation step. High algal concentrations at this stage have led to increased clogging of the filters. The filtration system was recently upgraded at a capital cost of R 45 million in order to increase the plants filtration capacity. During periods of high algal concentrations (approximately 130 µg/l), the time between backwash cycles is reduced to 6 hours. Under normal operating conditions, the filters are operated with backwashes every 24 hours.

Disinfection

The disinfection step is required in order to destroy pathogens and bacteria in the water, ensuring that the water is suitable for consumption.

Algal concentrations projected under climate change

The projected concentrations as result of climate change were based on four general circulation models, viz. CCC, CRM, ECH and IPS. The results obtained for the Midvaal abstraction point are presented in Table 81.

Table 81: Recorded and projected long-term phytoplankton concentrations (µg/ℓ) based on general circulation models at the Midvaal extraction point

		CCC	CRM	ECH	IPS
Base case (2005)	118				
Present (modelled)		119	114	117	120
Intermediate (2046-2065)		127	124	128	128
Distant (2081-2100)		-	138	139	143

The present modelled values were used to calculate the percentage increase for the intermediate and distant projected concentrations. Refer to Table 82.

Table 82: The recorded and projected percentage increase in phytoplankton concentrations for the intermediate and distant projections at the Midvaal extraction point

	CCC	CRM	ECH	IPS
Intermediate (2046-2065)	7%	8%	10%	7%
Distant (2081-2100)	-	21%	19%	19%

Results were compared to the projected values for a point 2 km away from a wastewater treatment plant discharge point and presented in Table 83 and Table 84. One can expect up to a 40% increase in phytoplankton concentrations at sample points closer to the point source discharge.

Table 83: Recorded and projected long-term phytoplankton concentrations (µg/ℓ) based on general circulation models at a point 2 km away from the nutrient source

		CCC	CRM	ECH	IPS
Base case (2005)	200				
Present (modelled)		200	187	195	204
Intermediate (2046-2065)		226	216	230	228
Distant (2081-2100)		-	262	265	278

Table 84: The projected percentage increase in phytoplankton concentrations for the intermediate and distant projections at a point 2 km away from the nutrient source

	CCC	CRM	ECH	IPS
Intermediate (2046-2065)	13%	15%	18%	12%
Distant (2081-2100)	-	40%	36%	36%

Implications for the Midvaal treatment process

The Midvaal operations are currently treating water with an average chlorophyll concentration of 82 µg/ℓ, and 75th percentile concentration of 132 µg/ℓ and a maximum recorded concentration of 334 µg/ℓ. Complaints on odour and taste have been received when high chlorophyll concentrations were noted in the feed water.

Results indicate that the Midvaal treatment plant has sufficient capacity to treat the concentrations projected for the intermediate and long-term climate change projections. The operational costs will however increase, as additional chemicals will be required and more frequent backwashes will be needed as a result of increasing algal concentrations.

In the long-term, Granular Activated Carbon (GAC) may be required to remove the odour and improve the taste of the water. This will result in capital expenditure, additional operational costs and annual carbon replacement costs.

Costs for additional treatment equipment

Ozone generation

Ozone is an unstable gas that needs to be produced on site. Ozonation systems typically consist of four units, viz. ozone generator, feed gas preparation unit, contacting tank and off-gas destruction unit. The capital cost for such a system is approximately R 6 000 000 for a 10 Mℓ/day treatment plant.

Ozonation has been proven to be effective in the removal of organics in water. The equipment is however specialised and would require skilled operators. Care would need to be taken to maintain the ozone doses below 1.5 mg/ℓ in order to reduce the risk of cell lysis.

Granular activated carbon

Granular activated carbon (GAC) filters are effective at removing taste and odour from treated water streams. A GAC filter will consist of a feed pump, a filter tank, filled with GAC medium, a sump and a backwash system. The capital cost for GAC filters would be in the region of R 5 500 000 for a 10 Mℓ/day treatment plant.

Depending on the organics load on the system, the filter media would require replacement every 1 to 5 years.

Recommendations for resource economic assessment (section still in progress)

This report indicates that climate change has the potential to increase the eutrophication on the Vaal River. In turn, eutrophication dramatically reduces the condition of aquatic systems, and consequently, the functionality of the river ecosystems. Well-functioning rivers have the ability to deliver a wide range of ecosystem services (Mander, 2001). These services are often unrecognised and undervalued (Mander, 2001). For example, an analysis by (Brand, 2008), shows that yellowfish angling is worth some USD 16.7 million per year, with 5 000 anglers spending significantly on equipment (USD 1.8 million), travel (USD 5.2 million) and accommodation (USD 9.4 million). However, these economic benefits are at risk, with the lack of effective management (O'Brien, 2013). This may be further exacerbated eutrophication induced by climate change.

However, this is only a single one of the Vaal River ecosystem services' values, with several other important values not considered, such as:

- The savings made on water treatment costs by municipalities due to the river ecology assimilating pollutants;
- The savings made by farmers in accessing quality irrigation water due to the river ecology assimilating pollutants; and
- The increased property values for home owners, and the associated elevated rates for municipalities.

It would be insightful to determine these additional values in order to move towards a more comprehensive understanding of economic values associated with riverine ecosystem services. However, while the values estimated for the yellowfish angling industry have been known for some years (Brand, 2008), poor management and over use of the river continues (O'Brien, 2013). So while generating further knowledge on the value of the river may be useful, more work is necessary to develop an understanding of the implications of changes in values due to elevated eutrophication.

Consequently, we recommend that in addition to developing a broader perspective of potential value declines from changes in ecosystem services supply, we develop a better understanding of the economic implications of these changes for municipalities and local economies. For example, if property values decline, what is the expected decline in associated rates revenue to municipalities, and what are the implications of reduced revenue for municipal budgets and service costs. These implications may go some way to

understanding the incentives driving Vaal River management, or the lack there-of. Without placing ecosystem services values in context, there is a danger that the research outcomes are perceived as interesting curiosities, and are not considered in relation to current municipal investment priorities. By developing an understanding of the economic implications of changes in ecosystem services induced by elevated eutrophication, it will be possible to identify what incentives there are for local government and land owners to invest in management of the river.

We recommend that the following research questions are investigated:

- The changes to property values along the Vaal River, and their economic implications for land owners and municipalities;
- The economic implications of changes to recreation expenditures associated with the Vaal River, for land owners, tourism enterprises and municipalities;
- The changes to water treatment coasts, and their economic implications for water boards, municipalities and urban water consumers;
- The changes to irrigation water quality, and their economic implications for water boards, municipalities and farmers;
- The changes to recreation water quality, and their economic implications for households, enterprises and health services;
- The costs of improving Vaal River ecosystem services, and associated aquatic river ecology, to meet legal and/or best practice standards; and
- A comparison of the costs and benefits of Vaal River management to determine where the above losses to society (induced by eutrophication) are at least balanced with the management costs. Costs of the additional management necessary to buffer against possible climate change effects could also be assessed. This would be a purely economic optimisation process, notwithstanding the moral and legal issues associated with pollution, human health and wellbeing.

10.4 Cumulative or feedback impacts

This report has largely concentrated on the effect climate change is likely to have on eutrophication. Moss *et al.* (2011) have however explored the feedback impact that eutrophication may have on climate change, showing the need for a more intensive effort to control nutrients and improve water quality as eutrophication increases. While climate change is likely to lead to an increase in the water temperature and alter the hydrological patterns which lead to lower level rivers with warmer environments for algal blooms to survive, the input of nutrients through agricultural activities and waste products further increases the growth and abundance of algae. The increase of eutrophication leads to the decrease of piscivorous fish, and so nutrients remain in the water system, adding effect to the eutrophication (Moss *et al*., 2011). Eutrophication may indeed ***promote*** climate change in turn through the increase in production of methane from deoxygenated waters and nitrous oxide from denitrification. Both of these greenhouse gases have a higher global warming potential than carbon dioxide (Moss *et al.,* 2011). This concept is well illustrated in the figure below.

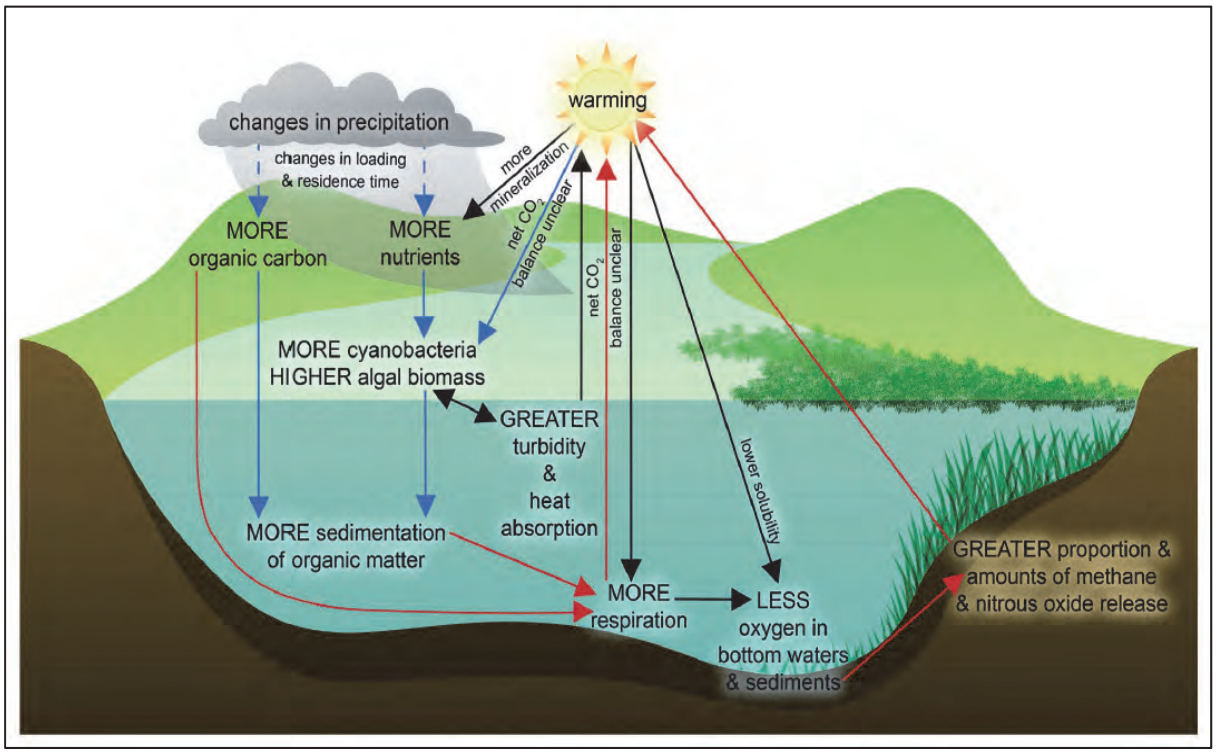

Figure 210: Current indications of feedback effects of eutrophication on climate change. Blue arrows indicate carbon sequestration routes; red arrows indicate carbon emission routes, black arrows indicate other climate effects (Moss *et al.*, 2011)

11 ADAPTIVE MANAGEMENT MEASURES AND RECOMMENDATIONS

Nutrient over-enrichment (or eutrophication) of freshwater and coastal ecosystems is a rapidly growing environmental crisis worldwide (WRI, 2009). Increased input of nutrients, especially phosphorous, leads to an increased incidence of nuisance blooms of blue-green algae, leading to an increase of water turbidity, a building of organic and nutrient-rich sediments, loss of oxygen from the bottom waters of the lake which, in turn, accelerates nutrient recycling processes, and changes in the lake's food web structure. Secondary nutrient limitation of silica or nitrogen that results when phosphorus levels are elevated also leads to changes in the phytoplankton community and to the development of nuisance species of algae (Mendiondo, 2008).

During the past 40 years, eutrophication has become an increasing threat to the usability of South African freshwater resources. Despite legislation moderating the discharge of phosphorus from some wastewater treatment works since the 1980s, eutrophication of freshwater resources is now widespread. Two important consequences are blooms of cyanobacteria, carrying the threat of cyanotoxin contamination, and excessive growth of macrophytes, which clog water-supply structures and reduce the recreational value of aquatic resources (Van Ginkel, 2011).

Common stresses affecting lakes and reservoirs include eutrophication from nutrient and organic matter loadings at local scales which provoke accumulated effects at long-term and global scales. Siltation from inadequate erosion control in agricultural, construction, logging, or mining activities is coupled with eutrophication; moreover, introduction of exotic species, acidification from atmospheric sources, acid mine drainage, and global warming can aggravate trophic states.

Chemical stresses (including nutrients) are categorized according to source as (1) point sources, i.e. municipal wastewater, which generally are the easiest to identify and control; (2) non-point or diffuse sources such as urban and agricultural runoff from a lake's watershed; and (3) long-range atmospheric transport of contaminants, which is the most difficult to measure and control. These local stresses become cumbersome, because in the last century the intercepted continental runoff grew up 15 times as urban centre intensified (Mendiondo, 2008).

Although increases in nutrient levels enhance fish production, the loss of habitat, e.g., by sediment buildup, deoxygenation, undesirable proliferation of macrophytes, and food web

simplification cause a shift from fish diversity to less desirable species, especially in more extreme cases of eutrophication. Stocking of exotics and overfishing exacerbate this problem.

From a human use perspective these changes create numerous problems, i.e. fouling of boats and structures by algal growths, loss of aesthetic appeal, accessibility problems for swimmers and boaters because of macrophytes, economic damage to resort and property owners, and increased costs and technical difficulties of treating water for drinking purposes because of taste and odour problems and increased potential for trihalomethane production (Mendiondo, 2008).

Drinking water is a necessity that needs to be made available to consumers at an affordable price. Similarly, the in-stream water quality needs to be maintained for the preservation of ecosystem services.

Rising algal concentrations could negatively influence the price of drinking water. Whilst end of pipe treatment is possible, the costs associated with the available treatment options is likely to be passed on to the consumers. Improved treatment at source is necessary in order to reduce the impact on downstream users.

11.1 **Management approaches**

Eutrophication is a serious problem in a number of catchment areas in South Africa which appears to have escalated over time. The root of the problem is nutrient enrichment in freshwater resources and therefore the most important management approach involves minimising the influx of nutrients into freshwater systems. However, this approach is being supplemented with several other methods that are currently being evaluated or have been assessed in the recent past (Van Ginkel, 2011).

Given the diversity of pathways, sources, and drivers of nutrient pollution, policies to address eutrophication cannot be limited to traditional command-and-control approaches such as regulatory standards, nor can they be focused exclusively on a single sector such as municipal wastewater. Policymakers should look more broadly at agricultural, energy, land use, and public health policies and design these policies to mitigate nutrient pollution.

Eutrophication-management options include reduction of phosphorus in detergents, biomanipulation of the food web, accurate prediction of cyanobacterial growth cycles, and

mechanical disturbance of the epilimnion. The implementation of adaptive management to deal with eutrophication would ensure the testing and application of the most appropriate methodology to each eutrophic water body. Continued monitoring and reporting of trophic status are essential to establish whether interventions are having any effect.

Various initiatives are under way for managing eutrophication in South Africa. The nation's research advisors will need to develop strategies to implement the most effective methods. One way to formalise the process is through adaptive eutrophication management (Figure 211). *Adaptive management* is a characteristic of restoration programs to assess and survey measures in progressive ways in companion to natural reaction of system to changes in time and in space. Herewith the 6 steps that should be followed for successful adaptive eutrophication management (Van Ginkel, 2011):

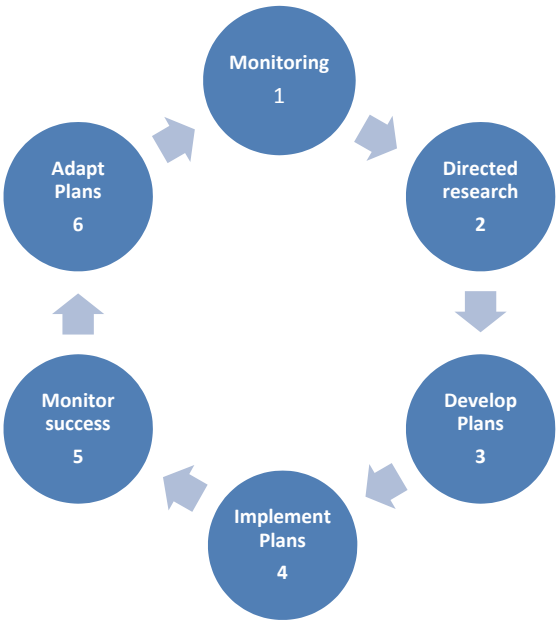

Figure 211: The 6 steps in the adaptive eutrophication management system (Van Ginkel, 2011)

Step 1: Monitoring

Monitoring is the first step in combating the problem. If monitoring does not happen, the extent of the problem, or sites in need of management, will not be known. Monitoring the extent of eutrophication in the country should lead to directed research to discover or investigate the most appropriate methods to implement at each impacted site.

Step 2: Directed research

Directed research determines the most effective management options for each specific site. This may be done by investigating all potential management options on small or large scale,

leading to a better understanding of the problem. Directed research encourages the development of new monitoring methodology, management, and predictive capabilities, nutrient-limiting approaches and in-lake management options. Preferably, research or investigation of each management option should take place at different localities, to enable prioritisation according to efficiency and financial implications. In this way, management options can be considered in isolation and decisions can be based on scientifically sound research. This process will provide managers with several options to select from, when developing the management plans for a specific site.

Step 3: Develop plans

Next, the selected eutrophication-management plans need to be developed with a view to implementation. An adequate budget is essential for this purpose.

Step 4: Implement plans

Next, the eutrophication-management plans need to be implemented. Budgeting for sufficient funds is the sole responsibility of the national, regional and local institutions.

Step 5: Monitor successes

The functioning of implemented plans needs to be monitored and reported on in order to determine their effectiveness. When successes and failures are monitored and documented well, decisions to adapt management plans should fall in place.

Step 6: Adapt plans

The management plans need to be adapted, if necessary. Adaptation aligned to the outcome of implementation monitoring should ensure that the necessary funding is available for implementing the adapted implementation plans.

The responsibility to manage eutrophication in South Africa lies with the national, regional and local management institutions. In addition to the measures outlined in Steps 2, 3, 5 and 6, research institutions at national, regional and local levels should apply their knowledge in order to assist and improve eutrophication management in South Africa.

By following these 6 steps, South African water-resource managers can select the appropriate eutrophication-management strategy for each impacted site. This pre-empts crisis control. Sustainable management plans can be implemented to ensure safe water and accessible recreational sites to all end users.

Many control methods have been suggested and tested internationally.

Nutrient minimisation

- Nutrient inactivation;
- Flow augmentation or flushing;
- Hypolimnetic aeration;
- Destratification;
- Selective removal of hypolimnetic water;
- Laminar epilimnion disturbance;
- Water-level drawdown;
- Covering bottom sediment;
- Dredging;
- Harvesting;
- Biomanipulation; and
- Chemical control.

Research on the effectiveness and applicability of these different methods in South Africa is critically important. The results will assist in selecting eutrophication-control measures suitable for South African climatic and economic conditions, in order to reach the ultimate goal of combating eutrophication sustainably in South African inland waters.

It is furthermore vital that in-stream habitat (river bank and riparian) is effectively conserved to ensure that ecosystem services are protected along the river, and that ecosystem health is therefore preserved. Wetlands protection is a key action towards this end, including the rehabilitation of wetlands which are currently in a poor state and are unable to perform their services in terms of flood attenuation and water purification effectively, as well as potentially the establishment of artificial wetlands to assist with the provision of these services.

Catchment management is vital to the preservation of good quality water resources in any location. This includes effective land use practices including responsible grazing, burning and livestock regimes (prevention of access to river banks to reduce erosion of these,

subsequent erosion and water quality pollution), as well as control of invasive plant species and maintenance of wetlands and other green corridors.

Key to the maintenance of healthy flow regimes is also the improved management of water volumes, including the efficient and prudent storage, as well as responsible distribution to and use of water.

The food industry, agriculture and waste water treatment plants are often the cause of point source discharges. Stricter regulations are being applied to industry and wastewater treatment plants. Assistance is required at smaller treatment plants in order to ensure that adequate nutrient removal is taking place.

The most cost effective method recommended by the Stellenbosch project team for reducing eutrophication into a warmer future climate would be to reduce the inflow of nutrients into a water body, particularly that of phosphorous. Source reduction at facilities that discharge phosphorous into the catchment is required, however this is extremely difficult to enforce and monitor and governance issues must be addressed and established effectively for this to be successful.

Management of the practices causing non-point source (NPS) pollution of water resources in South Africa is vital for the mitigation of long-term negative effects. As part of WRC project K5/1516 (Lorentz *et al*., 2010), the ACRU-NPS model was modified to include crop yield associated with water and nitrogen stress, and output from the model was used to simulate the effects of control structures in the catchment. Models such as this one can be used to restrict land use practices which might impact the water resources, and can aid in the identification of sources which impact water quality in downstream river networks.

The following conclusions were documented following the completion of this modelling exercise with regard to non-point source pollution from agricultural sources:

- Farming with vegetables, whether tilled or not tilled, can lower the quality of the water resources through the enhancement of sediment yields and increasing loads of both nitrogen and phosphorous in rivers;
- Limiting the current addition of nutrients to crops are not likely to enhance the river water quality significantly;
- Over-fertilization of crops could lower the quality of water resources significantly;

- Significant reductions in nitrogen, phosphorous and sediments can occur in wetlands with large storage;
- Farm dams generally reduce the downstream movement of sediments and nutrients. However, extreme events mix the reservoir sediments and solutes and result in larger outflow loads than inflow loads on these occasions;
- Buffer strips surrounding cultivated fields can enhance the quality of the water resources of the catchment; and
- Phosphorous may even migrate in the subsurface to compound nutrient discharge to water courses.

Modelling techniques can estimate the quality of water resources in catchments where formal farming are practiced (Lorentz *et al*., 2010). Scenario modelling can be indicative of formal farm management practices that will improve the quality of water resources.

New technologies

Biomimetic solutions

Biomimicry is a study of nature and mimicking nature to manage our everyday challenges. The current WRC study K5/2096, in looking to nature for solutions on water treatment problems faced in South Africa. The examples identified for algal management are summarised in this section.

Available Biomimetic solutions

Biohaven floating island

Figure 212: Photograph of a Biohaven floating island

The biohaven floating island mimics natural floating islands in order to create a concentrated wetland effect (The Bright Water Company, 2010). The floating island consists of a polymer island, made up of layered recycled material with pre-cut pockets. Plants are inserted in the pockets and the layers and porous structure enables the roots of the plant to reach the water. In wetland systems, 80% of the biological action is performed by aggregates of microorganisms attached to submerged surfaces. The porous texture on the island enables microbes to attach and multiply. The roots provide additional surface area for the microbes to attach. Floating islands have been shown to successfully reduce nutrient concentrations in water.

Algal turf scrubbers

Figure 213: Algal turf scrubber application (left); Natural algal growth (right)

The algal turf scrubber mimics natural surfaces that algae will preferentially grow on. The algae feed on the nutrients in the water, reducing the downstream impact of the nutrients, and can easily be harvested to produce biofuels (Ask Nature, 2012).

Potential biomimetic interventions

Salps

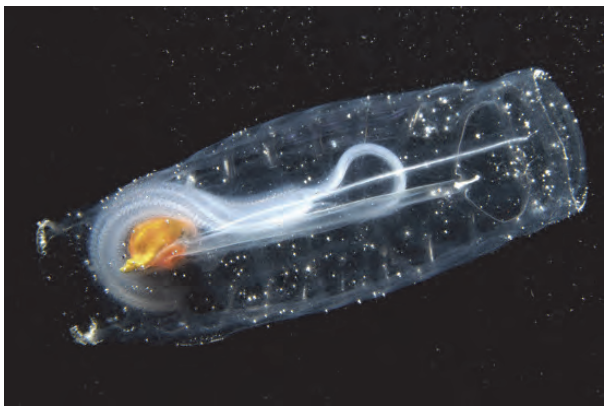

Figure 214: Photograph of a salp

Salps (Salpidae) are free swimming marine creatures with gelatinous bodies. They have an inner mucus net which traps algae which it feeds on as it moves by jet propulsion (Joel Greenberg, 2010).

Salps draw water in the siphon at one end and force it out the siphon at the other end, providing movement by jet propulsion and food from the water. The water drawn in is also used for feeding, because while inside the body it is strained through a baglike net of mucus, which traps any tiny algae present (Shuker, 2001).

If sufficient knowledge can be gained on the bag-like mucous structure used by the salp to trap algae, one can reproduce a similar structure to produce a filter which can be used upstream of a water treatment process and reduce the need for chemical interventions at the water treatment plant.

Clams

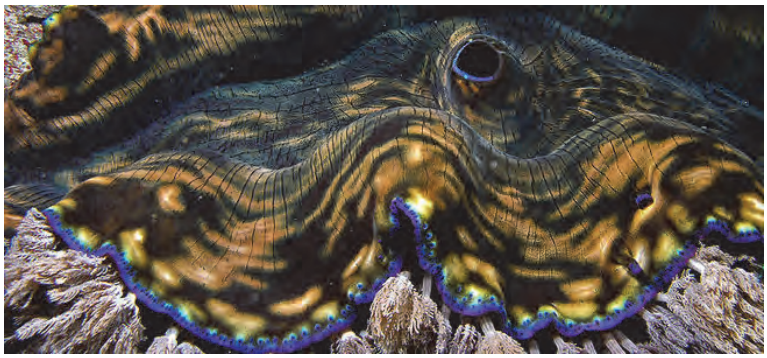

Figure 215: Photograph of a clam

Giant Clams are able to determine algal concentrations within their habitat (Ask Nature, 2010). When algal concentrations are high, the clam produces digestive juices which digest the algae. Studying the composition on the digestive juice can lead to an alternate chemical treatment process for algae.

Anthropogenic thermal pollution

Thermal pollution from anthropogenic sources should be reduced so far as possible. Holding ponds could be provided to allow water to cool for a specified length of time before release.

Additional actions

Additional *in situ* remediation actions can also be implemented, including the release of water from the upstream dams in “pulses” into a eutrophied river to disrupt the algae settling

process and flush existing algal blooms. Harvesting of algae for alternative uses is also an affective adaptation measure which accepts that algal biomass is likely to increase with climate change, e.g. nutritional supplements, compost, pigments. Specific treatment areas could also be set up within rivers/dams for prevention of cyanobacterial blooms.

The figure below illustrates the key actions undertaken by the Harties Metse-a-me programme at the Hartbeespoort Dam in North-West province to combat an extensive eutrophication problem. Many of these actions have been successful.

Figure 216: Summary of the Harties Metsi a me eutrophication control programme (Department of Water Affairs and Rand Water, 2012)

An unconventional technique of controlling algal growth is through the use of solar powered machines which mix dam water to prevent the establishment of algal colonies.

11.2 Governance and capacity building

Compliance and enforcement of in-stream water quality and effluent guidelines is vital for the control of eutrophication into a warmer climate (Integrated Water Resource Management). The lack of resources in South Africa in terms of extension officers and water quality professionals is an important point to be addressed. It is recommended that a communication and implementation plan for the capacitation of governmental staff is devised

such that existing resources can be more effectively deployed, and perhaps more importantly to establish public-private partnerships and forums which could assist in monitoring and enforcement of water quality and effluent guidelines, and taking action against non-compliance. An education campaign should accompany this exercise to inform the various stakeholders involved of the causes of and remediation actions towards the management of eutrophication.

In terms of policy interventions, in order to reverse eutrophication trends and mitigate nutrient losses to aquatic ecosystems, policymakers should (WRI, 2009):

1. *Implement research and monitoring programs* to characterize the effects of eutrophication, collect water quality data, and inform adaptive management strategies. Information is a key element in the development of robust strategies to reduce eutrophication.
2. *Raise awareness of eutrophication.* Eutrophication and its effects are not well understood by the public or policymakers. Public awareness campaigns, school environmental education programs, and targeted outreach and technical assistance are all important components of raising the profile of eutrophication within communities and building a foundation and support for effective actions to reduce nutrient losses and eutrophication.
3. *Implement regulations to mitigate nutrient losses*, such as standards, technology requirements, or pollution caps for various sectors. Environmental regulations can take two general forms: standards and emissions/effluent caps or limits. While standards specify certain technologies, practices, or processes that must be implemented, regulatory caps set a level of acceptable pollution.
4. *Create fiscal and economic incentives to encourage nutrient reducing actions* using taxes and fees, subsidies, or environmental markets. Economic and fiscal incentives for reducing eutrophication include ecotaxes, incentive payments/subsidies, ecolabeling, and environmental markets.
5. *Preserve and restore natural ecosystems* that capture and cycle nutrients. Preserving and restoring riparian vegetation, wetlands, and open areas can mitigate nutrient pollution by creating and maintaining natural nutrient sinks.
6. *Establish strong, engaged, and coordinated institutions* to address eutrophication. Effective institutions to implement and enforce policies are important to the success of any eutrophication strategy, especially where multiple jurisdictions are involved. Without

strong institutional authority, adequate funding, and properly trained personnel, the effectiveness of regulations, policies and actions to reduce eutrophication is limited.

7. *Capitalize on environmental synergies* when designing comprehensive policies to address eutrophication. Many policies and activities associated with reducing nutrient pollution have synergies with other environmental problems such as climate change, smog, and acid rain. Policies selected and implemented should seek to maximize environmental benefits. For example, policies aimed at reducing combustion of fossil fuels through energy conservation, energy efficiency, and promotion of alternative energy have multiple environmental and public health benefits (Moomaw 2002).

12 CONCLUSIONS AND OBSERVATIONS

A summary of the modelling results obtained from the modelling exercises is shown in the table below.

Table 85: Summary of modelling results

	Case Study	Berg River Dam		Voëlvlei Dam		Vaal River	
	Model Used	CE-QUAL				QUAL2K	
	Climate change projection dates	2046-2065	2081-2100	2046-2065	2081-2100	2046-2065	2081-2100
Parameter modelled	*Phytoplankton*					↑	↑↑
	Diatoms	↓≠	↓≠	↑≠	↑≠		
	Green algae	-		↑≠	↑≠		
	Blue-Green algae	-		No strong trend, ≠			
	Total algae	No trend, ≠		↑≠	↑↑≠		
	Zooplankton	↓	↓	↑	↑↑		
	Water temperature	↑	↑	↑	↑	↑	↑↑
	Flow (river)/Level (dam)	↓	↓↓	↓	↓	↓	↓
	Dissolved oxygen	↓	↓	↓	↓	↓	↓↓
	Orthophosphate	Unchanged		↑	↑		
	Ammonium	↓	↓	↑≠	↑↑≠		
	Nitrate/nitrite	No trend		No trend, ≠			
	Dissolved silicon	↓	↓	↑≠	↑↑≠		

↑	increase (↓↓ - approximately double magnitude of the increase into the distant future)
↓	decrease (↓↓ - approximately double the magnitude of the decrease into the distant future)
-	Species does not establish
≠	Seasonal shift
	Not modelled

The results are consistent between the two water quality models for the common parameters modelled (water temperature – increase, volume of water – decrease, dissolved oxygen – decrease). The results vary between the various species of algae, but in general an increasing trend in algal concentration is seen.

The variability between the four climate models used in this project is recognised, and the importance of using an ensemble of validated climate change models is therefore highlighted. All of the models however projected an *increase in air temperatures* for each of the time projections studied, and based on both of the modelling exercise concluded that air temperature is the major driver for surface water temperature, which is the parameter driving algal growth most strongly.

Climate change causes heating of water within dams and rivers, and consequently increases the evaporation rate of the water. This heated water evaporates to a greater degree into the distant future when compared with the intermediate future a result of the increased water temperature. With an increase in temperature of surface waters, the water volume is lowered due to increased evaporation, should this occur, and a consequent increase in the concentration of water quality constituent results.

Climate change can also affect the seasonal behaviour of various parameters, such as phosphate concentration. One of the modelling exercises indicated that a peak in concentration could be experienced a month earlier in the future projections when compared with present day concentrations. This could result in an increase in algal bloom season. Dissolved oxygen concentration was shown to be highest during winter and spring, when the surface water was cooler and could hold more oxygen, but decreases into the warmer temperature projections. Seasonal shifts of total algal concentrations in the dams modelled were evident due to the decrease in DO and nitrite-nitrates in the latter half of the year at the surface. Accelerated growth of algae under climate change is clearly visible as the increases during late summer and autumn are greater into the distant future than into the intermediate future.

Water quality data for the modelling exercise was found to be limited and inconsistent. It appears that monitoring data from the Department of Water Affairs is highly variable, particularly with regard to parameters important for the assessment of eutrophication potential, such as temperature and chlorophyll-a. It appears that monitoring was consistent for a large number of points up until recent years, but the thoroughness and geographic range of monitoring has reduced.

Both Midvaal Water Company and Sedibeng Water have good monitoring programs along the Vaal River, and in particular include the monitoring of water temperature and chlorophyll-a, which can be used for eutrophication modelling. These comprehensive monitoring programmes can add significant value to water resource management going forward. However, monitoring and measuring of the channels into and out of the country's major dams and rivers should be implemented to allow for more accurate modelling exercises. This would include both flow and water quality constituents. The parameters that govern algal growth should furthermore be measured in a laboratory or *in situ.* This would also provide a quantitative analysis on the sensitivity of certain parameters as well as their effect on dissolved oxygen concentrations. Sedimentation data should be measured and incorporated

and the simulation rerun to investigate this effect on the eutrophication rate and subsequent water quality.

A method for reducing eutrophication into a warmer future climate would be to reduce the inflow of nutrients into a water body, particularly that of phosphorous. Source reduction at facilities that discharge phosphorous into the catchment is required, however this is extremely difficult to enforce and monitor and governance issues must be addressed and established effectively for this to be successful.

Key concepts in the control of eutrophication, particularly in the face of climate change, include:

- ***Collaboration and integration*** (Government departments (DWA, provincial bodies), private companies, communities);
- Dam/river and upstream ***catchment management***;
- ***Capacity building and education***;
- ***Resourcing and compliance enforcement***;
- The concept of treating the ***cause and not the symptom***; and
- ***Job creation and community involvement*** (sustainability of a public works programme for example, with associated knock-on economic effects into communities).

Compliance and enforcement of in-stream water quality and effluent guidelines is vital for the control of eutrophication into a warmer climate (Integrated Water Resource Management). The lack of resources in South Africa in terms of extension officers and water quality professionals is an important point to be addressed. It is recommended that a communication and implementation plan for the capacitation of governmental staff is devised such that existing resources can be more effectively deployed, and perhaps more importantly to establish public-private partnerships and forums which could assist in monitoring and enforcement of water quality and effluent guidelines, and taking action against non-compliance. An education campaign should accompany this exercise to inform the various stakeholders involved of the causes of and remediation actions towards the management of eutrophication.

Within the past 50 years, eutrophication—the over enrichment of water by nutrients such as nitrogen and phosphorus—has emerged as one of the leading causes of water quality impairment (WRI, 2008). Shallow lakes are important components of the biosphere, but they are also highly vulnerable to damage from human activities in their catchments, such as nutrient pollution. They may also be particularly vulnerable to current warming trends. Jeppesen *et al*. (2009) stated that during the next 25 years, the effects of the increasing human population and the economic development in a gradually warmer climate are the key environmental threats on small lakes and ponds.

The growth of the human population in the first decade of the twenty-first century is estimated at 100 million people per year. Considering the per capita production of 4 g of phosphorous, 15 g of nitrogen and 100 g carbon, as biological oxygen demand we can get an insight into the eutrophication problems that humanity has to face on a global scale. Human waste and wastewater from the human, agricultural and industrial activities will continue as permanent inputs into lakes, rivers, reservoirs, wetlands, coastal waters shallow lakes and coastal lagoons (Mendiondo, 2008).

13 LIST OF REFERENCES

Ahl T (1980) Eutrophication in relation to the load of pollution. *Progressive Water Technology* 12:49-61

Ahlgren I, Sörensson F, Waara T, Vrede K (1994) Nitrogen budgets in relation to microbial transformations in lakes. Ambio. 23(6):367-377.

Ask Nature (2010) Digestive solution removes excess algae. Retrieved January 2013, from Ask Nature: www.asknature.org/strategy/89f6ad5e72f55e6883480a777fa483

Ask Nature (2012) Algal turf scrubber. Retrieved January 2013, from Ask Nature: http://www.asknature.org/product/e37ad98658974d79f8b34b1da2574b49

Australian Bureau of Meteorology (2003) Climate research, Climate activities in Australia, Chapter 5, Australian Government Bureau of Meteorology, Melbourne.

Barenbrug AWT (1974) Psychrometry and Psychrometric Charts, 3rd Edition, Cape Town, SA: Cape and Transvaal Printers Ltd.

Bergant K, Bogataj LK, Trdan S (2006) Uncertainties in modelling of climate change impact in future: An example of onion thrips (*Thrips Tabaci* Lindeman) in Slovenia. *Ecological Modelling* 194: 244-255.

Bondar-Kunze E, Preiner S, Schiemer F, Weigelhofer G, Hein T (2009) Effect of enhanced water exchange on ecosystem functions in backwaters of an urban floodplain. Aquatic Sciences – Research across Boundaries. 71:4, 437-447

Bowie G, Mills WB, Porcella DB, Campbell CL, Pagenkopf JR, Rupp GL, Johnson KM, Chan PWH, Gherini SA (1985) Rates, Constants, and Kinetics Formulations in Surface Water Quality Modelling (Second Edition) Tetra Tech Incorporated. Lafayette, California, USA and Charles E Chamberlin, Humboldt State University, Arcata, California, USA.

Boström B, Andersen JA, Fleischer S, Jansson M (1988) Exchange of phosphorous across the sediment-water interface. *Hydrobiol*. 179:229-244.

Brand M (2008) Characterisation of the social and economic value of the use and associated conservation of the yellowfishes in the Vaal River. Water Research Commission.

Brand M, Maina J, Mander M, O'Brien G (2009) Characterisation of the social and economic value of the use and associated conservation of the Yellowfishes in the Vaal River. Report to the Water Research Commission Report KV 226/09, Pretoria.

Breitburg DL, Loher T, Pacey CA, Gerstein A (1997) Varying effects of low dissolved oxygen on trophic interactions in an estuarine food web. *Ecological Monographs* 67 (4), 1997, pp 489-507.

Brock TD (1981) Calculating solar radiation for ecological studies. *Ecological modelling* 14 (1981) pp 1-19. Elsevier Scientific Publishing Company, 1981.

Brown LC, Barnwell TO (1987) The Enhanced Stream Water Quality Models QUAL2E and QUAL2E-UNCAS, EPA/600/3-87-007, US Environmental Protection Agency, Athens, GA, 189 pp.

Carmichael, WW (2001) Health Effects of Toxin-Producing Cyanobacteria: "The CyanoHABs" *Human and Ecological Risk Assessment* 7, 5: 1395-1407

Carter TR, Perry ML, Harasawa H, Nishioka S (1994) IPCC Technical Guidelines for Assessing Climate Change Impacts and Adaptations, Department of Geography, University College London, United Kingdom, 1-72

Carter TR, Alfsen K, Barrow E, Bass B, Dai X, Desanker P, Gaffin SR, Giorgi F, Hulme M, Lal M, Mata LJ, Mearns LO, Mitchell JFB, Morita T, Moss R, Murdiyarso D, Pabon-Caicedo JD, Palutikof J, Parry ML, Rosenzweig C, Seguin B, Scholes RJ, Whetton PH (2007) General Guidelines on the use of Scenario Data for Climate Impact and Adaptation Assessment, Version 2. Task Group on Data and Scenario Support for Impact and Climate Assessment (TGICA) Intergovernmental Panel on Climate Change

Cerco CF, Cole TM (1994) Three-dimensional eutrophication model of Chesapeake Bay. Volume 1, U.S. Army Engineer Waterways Experiment Station, Vicksburg, Mississippi, 1994-05

Chan TU, Hamilton DP, Robson BJ, Hodges BR, Dallimore, C (2002) Impacts of Hydrological Changes on Phytoplankton Succession in the Swan River, Western Australia. *Estuaries and Coasts* 25(6B) 1406-1415

Chapra SC, Pelletier GJ, Tao H (2007) QUAL2K: A Modelling Framework for Simulating River and Stream Water Quality, Version 2.07: Documentation and User's Manual. Civil and Environmental Engineering Dept., Tufts University, Medford, MA.

Chapra SC (2008) Surface water-quality modelling, Illinois, Waveland Press Inc.

Chapra SC, Pelletier GJ and Tao H (2011) QUAL2K: A modelling framework for simulating river and stream water quality, Version 2.12: Documentation and User's Manual. Civil and Environmental Engineering Dept., Tufts University, Medford, MA, Steven.Chapra@tufts.edu

Chen M, Dickinson RE, Zeng X, Hahmann AN (1996) Comparison of precipitation observed over the continental United States to that simulated by a climate model. *Journal of Climate* 9, 2233-2249.

Christensen JH, Hewitson B, Busuioc A, Chen A, Gao X, Held I, Jones R, Kolli RK, Kwon W-T, Laprise R, Magaña Rueda V, Mearns L, Menéndez CG, Räisänen J, Rinke A, Sarr A and Whetton P (2007) *Regional Climate Projections*. In: Climate Change 2007: The Physical Science Basis. Contribution of Working Group I to the Fourth Assessment Report of the Intergovernmental Panel on Climate Change [Solomon S, Qin D, Manning M, Chen Z, Marquis M, Averyt KB, Tignor M and Miller HL (eds.)]. Cambridge University Press, Cambridge, United Kingdom and New York, NY, USA

City of Cape Town, CMC Administration. 2002. *Voëlvlei Augmentation Scheme Phase 1*. Prepared by Ninham Shand (Pty) Ltd as part of the CMA Bulk Water Supply Study.

Codd GA, Metcalf JS, Beattie KA (1999) Retention of *Microcystis aeruginoa* and *microcystin* by salad lettuce after spray irrigation with water containing cyanobacteria. *Toxicon* 37:1181-1185

Codd GA (2000) Cyanobacterial toxins, the perception of water quality and the prioritisation of eutrophication control. *Ecological Engineering* March, 16:51-60

Colby PJ, GR, Spangler D, Hurley, McCombie AM (1972) Effects of eutrophication on salmonid communities in oligotrophic lakes. *Journal of the Fisheries Research Board of Canada* 29: 975-83

Cole TM, Wells SA (2008) CE-QUAL-W2: A two-dimensional, laterally averaged, Hydrodynamic and Water Quality Model, Version 3.6, Department of Civil and Environmental Engineering, Portland State University, Portland, OR.

Correll DL (1998) The role of phosphorous in eutrophication of receiving waters: A review, March-April, *Journal of Environmental Quality*, 27:261-266

Correll DL (1999) Phosphorous: a rate limiting nutrient in surface waters, *Poultry Science*, 78(5):674-682

Dai A, Trenberth K, Qian T (2004) A Global Dataset of Palmer Drought Severity Index for 1870-2002: Relationship with Soil Moisture and Effects of Surface Warming, *Journal of Hydrometeorology*, December, 5:1117-1130

Dallas HF, Day JA (2004) The effect of water quality variables on aquatic ecosystems: a review, Water Research Commission Report no TT 224/04, February, viii+222pp

DeNicola DM (1996) Periphyton response to temperature at different ecological levels, *Algal Ecology*, 149-181 pp

De Nobel WT, Huisman J, Snoep JL and Mur LR (1997) Competition for phosphorous between nitrogen-fixing cyanobacteria Anabaena and Aphanizomenon. *FEMS Microbiology Ecology* 24: 259-267

De Senerpont Domis LN, Mooij WM, Huisman J (2007) Climate induced shifts in an experimental phytoplankton community: a mechanistic approach. *Hydrobiologia* 584: 403-413.

Dennison DB, Lyne MC (1997) Analysis and prediction of water treatment costs at the DV Harris Plant in the Umgeni catchment area. *Agrekon*, 36(1):24-42

Department of Water Affairs and Forestry (1996) South African Water Quality Guidelines (1st edition). Volume 8: Field Guide

Department of Water Affairs and Forestry (1996) South African Water Quality Guidelines (2nd edition). Volume 2: Recreational Water Use

Department of Water Affairs and Forestry (2002) Memorandum of Agreement between Department of Water Affairs and Forestry and the City of Cape Town for Water Supplied out of the Western Cape Water System Including the Berg Water Project.

Department of Water Affairs and Forestry (2009). Integrated Water Quality Management Plan for the Vaal River System: Task 2: Water Quality Status Assessment of the Vaal River System. Directorate National Water Resource Planning. Report No. P RSA C000/00/2305/1, South Africa.

Department of Water Affairs (2011) Directorate Water Resource Planning Systems: Water Quality Planning. Resource Directed Management of Water Quality. Planning Level Review of Water Quality in South Africa. Sub-series No. WQP 2.0. Pretoria, South Africa.

Department of Water Affairs and Rand Water (2012) Hartbeespoort Dam Integrated Biological Remediation Programme: Harties Metsi a me (My Water).

Directorate National Water Resource Planning, Department of Water Affairs, South Africa (2009) Integrated Water Quality Management Plan for the Vaal River System: Task 4: Integration of the Resource Water Quality Objectives. Report No. P RSA C000/00/2305/3.

Downing TG, Van Ginkel CE (2004) Cyanobacterial monitoring 1990-2000: Evaluation of SA data, Water Research Commission Report no 1288/1/04, March, ix+44pp

Du Plessis S, Kruskopf MM, Venter A, Conradie KR (2007) The role of nutrient utilisation and photosynthetic capacity in micro-algal bloom formation and the production of cyanotoxins, Water Research Commission Report no 1401/2/07, October, xiii+72pp

DUFLOW (2000) DUFLOW for Windows V3.3: DUFLOW Modelling Studio: User's Guide, Reference Guide DUFLOW, and Reference Guide RAM. Utrecht, The Netherlands, EDS/STOWA

El Herry S, Fathalli A, Rejeb AJ, Bouaïcha N (2008) Seasonal occurrence and toxicity of *Microcystis* spp. and *Oscillatoria tenuis* in the Lebna Dam, Tunisia. *Water Research*, 42:1263-1273

Fujihara Y, Tanaka K, Watanabe T, Nagano T, Kojiri T (2008) Assessing the impacts of climate change on the water resources of the Seyhan River Basin in Turkey: Use of dynamical downscaled data for hydrological simulations. *Journal of Hydrology* 353:33-48

Genkai-Kato M, Carpenter SR (2005) Eutrophication due to phosphorous recycling in relation to lake morphology, temperature and macrophytes. *Ecology*, January, 85(1):210-219.

Global Carbon Project (2010) Carbon budget and trends 2009. Available at http://www.globalcarbonproject.org/carbonbudget/09/hl-compact.htm

Golder Associates (2009) QUAL2K Model for the Vaal River. Golder Associates Report No: 8487-8451-2, Prepared for the Department of Water Affairs and Forestry, Johannesburg, 2009.

Goldman JC, Carpenter EJ (1974) A kinetic approach to the effect of temperature on algal growth. *Limnology and Oceanography*, 19(5): 756-766

Goldman JC, Porcella DB, Middlebrooks EJ, Toerien DF (1972) The effect of Carbon on algal growth- Its relation to eutrophication. *Water Research* June, 6(6): 637-679

Graham M, Blignaut J, de Villiers L, Mostert D, Sibande X, Gebremedhin S, Harding W, Rossouw N, Freese S, Ferrer S, Browne M (2012) Development of a generic model to assess the costs associated with eutrophication. Water Research Commission Report No 1568/1/12, Water Research Commission, Pretoria, RSA.

Hansen J, Sato M, Ruedy R, Kharecha P, Lacis A, Miller R, Nazarenko L, Lo K, Schmidt GA, Russell G, Aleinov I, Bauer S, Baum E, Cairns B, Canuto V, Chandler M, Cheng Y, Cohen A, Del Genio A, Faluvegi G, Fleming E, Friend A, Hall T, Jackman C, Jonas J, Kelley M, Kiang NY, Koch D, Labow G, Lerner J, Menon S, Novakov T, Oinas V, Perlwitz Ja, Perlwitz Ju, Rind D, Romanou A, Schmunk R, Shindell D, Stone P, Sun S, Streets D, Tausnev N, Thresher D, Unger N, Yao M, Zhang S (2007) Climate simulations for 1880-2003 with GISS model E. *Climate Dynamics* 29:661-696

Harding W (2006) A research strategy for the detection and management of Algal Toxins in water sources, Report to the Water Research Commission, Water Research Commission Report TT 277/06 June 2006, xv + 42 pp. Pretoria

Harremoës, P (1998) The challenge of managing water and material balances in relation to eutrophication. *Water, Science and technology* 37(3):3-17

Hauer FR, Hill WR (2007) Methods in stream ecology. 2nd edition, Elsevier press

Havens KE (2008) Cyanobacterial harmful algal blooms, In: Hudnell HK (ed.) Advances in experimental medicine and biology. Springer, 619(chpt 33): 733-748

Heath, R, Kamish W, Hughes C, Russell C and Coleman T (2011) Investigation of Effects of Climate Change on Eutrophication and Related Water Quality and Secondary Impacts on the Aquatic Ecosystem K5/2028/1 – Deliverable 2: Case Study Selection Report. Water Research Commission [draft]. Pretoria, 2011

Heisler J, Gilbert PM, Burkholder JM, Anderson DM, Cochlan W, Dennison WC, Dortch Q, Gobler CJ, Heil CA, Humphries E, Lewitus A, Magnien R, Marshall HG, Sellner K, Stockwell DA, Stoecker DK, Suddleson M (2008) Eutrophication and harmful algal blooms: A scientific consensus, August. *Harmful Algae* 8:3-13

Hewitson BC, Crane RG (2006) Consensus between GCM climate change projections with empirical downscaling: precipitation downscaling over South Africa. *Int J Climatol* 26:1315-1337

Hewitson B, Reason C, Tennant W, Tadross M, Jack C, MacKellar N, Lennard C, Hansingo K, Walawege R, Mdoka M (2004) Dynamic modelling of present and future climate systems, Water Research Commission Report no k5/1154, vii+92pp

Hewitson BC, Tadross M, Jack C (2005) Climate Change Scenarios: Conceptual Foundations, Large Scale Forcing, Uncertainty and the Climate Context. In: Schulze RE (ed) Climate Change and Water Resources in Southern Africa: Studies on Scenarios, Impacts, Vulnerabilities and Adaptation. Water Research Commission, Pretoria, RSA. Water Research Commission Report 1430/1/05. Chapter 2, 21-38.

Hodges BR, Dallimore C (2006) Estuary Lake and Coastal Ocean Model: ELCOM V2.2 Science, User's Manual, Centre for Water Research, Perth, 54 pp.

Holm NP, Armstrong DE (1981) Role of nutrient limitation and competition in controlling the populations of *Asterionella Formosa* and *Microcystis aeruginosa* in semicontinuous culture. *Limnol. Oceanogr.* 26(4): 622-634.

Horne AJ, Goldman CR (1983) Limnology, 2nd edition, McGraw-Hill inc, New York, Chapter 22, 499-520

Houghton J (2007) Global Warming: The complete briefing, 3rd edition, Cambridge University Press, Cambridge.

Hughes C, Kamish W, Heath R, Schulze RE (2011) Investigation of Effects of Climate Change on Eutrophication and Related Water Quality and Secondary Impacts on the Aquatic Ecosystem K5/2028/1 – Deliverable 3: Climate Change Scenario Selection Report. Water Research Commission [draft]. Pretoria, 2011

Incropera FP, Thomas JF (1977) A model for solar radiation conversion to algae in a shallow pond, Solar Energy, 20:157-165 pp

IPCC (2006) Integrated Pollution Prevention and Control Reference Document on Best Available Techniques for the Waste Treatment Industries

IPCC (2007) Climate Change 2007: Impacts, Adaptation and Vulnerability. Contribution of Working Group II to the Fourth Assessment Report of the Intergovernmental Panel on Climate Change. Parry ML, Canziani OF, Palutikof JP, van der Linden PJ, Hanson CE (Eds.), Cambridge University Press, Cambridge, UK, 976pp.

IPCC (2007) Summary for Policymakers. In: Climate Change 2007: The Physical Science Basis. Contribution of Working Group I to the Fourth Assessment Report of the Intergovernmental Panel on Climate Change [Solomon, S., D. Qin, M. Manning, Z. Chen, M. Marquis, K.B. Averyt, M. Tignor and H.L. Miller (eds.)]. Cambridge University Press, Cambridge, United Kingdom and New York, NY, USA.

IPCC (2011) Fourth assessment report. Available from http:/www.ipcc.ch/index.htm, January 2011.

Jeong S, Yeon K, Hur Y, Oh K (2010) Salinity intrusion characteristics analysis using EFDC model in downstream of Geum River. *Journal of Environmental Science* (China) 22(60): pp 934-939

Jeppesen E, Kronvang B, Meerhoff M, Sondergaard M, Hansen KM, Andersen HE, Lauridsen TL, Liboriussen L, Beklioglu M, Ozen A, Olesen JE (2009) Climate change effects on runoff, catchment phosphorus loading and lake ecological state, and potential adaptations. *J. Environ. Qual.* 38:1930-1941

Jiang T, Chen YD, Xu C, Chen Xia, Chen Xi, Singh VP (2007) Comparison of hydrological impacts of climate change simulated by six hydrological models in the Dongjian Basin, South China. *Journal of Hydrology* 336:316-333.

Joel Greenberg LL (2010) Salps Catch the Ocean's Tiniest Organisms. Retrieved 07 05, 2012, from Woods Hole Oceanographic Institute: http://www.whoi.edu/oceanus/viewArticle.do?id=79766

Jones BI (1987) Lake Okeechobee eutrophication research and management. *Aquatics* 9: 21-26

Jørgensen SE (2008) Ecosystems: Freshwater Lakes, 1686-1689

Kamish W, Rossouw JN, Petersen AM (2007) Development of strategies to address nuisance algal growth problems in Voëlvlei dam, report for the Department of Water Affairs and Forestry by Ninham Shand, report number 6950/4382

Kay AL, Reynard NS, Jones RG (2006) RCM rainfall for UK flood frequency estimation. I. Method and Validation. *Journal of Hydrology* 318: 151-162

Kgatuke MM (2006) The internal variability of the regional climate model RegCM3 over southern Africa for the University of Pretoria. Unpublished Masters dissertation. Pretoria: University of Pretoria.

Kernan M, Battarbee RW, Binney HA (Eds) (2007) Climate Change and Aquatic Ecosystems in the UK: science policy and management. Proceedings of a meeting held at the Environmental Change Research Centre, University College London, 16 May 2007

Khan MS, Coulibaly P, Dibike Y (2006) Uncertainty analysis of statistical downscaling methods. *Journal of Hydrology* March, 319(1-4): 357-382

Kim J, Jung H-S, Mechoso CR, Kang H-S (2008) Validation of a mutidecadal RCM hindcast over East Asia. *Global and Planetary Change* 61:225-241

Knoesen D, Schulze R, Pringle C, Summerton M, Dickens C, Kunz R (2009) Water for the Future: Impacts of climate change on water resources in the Orange-Senqu River basin. Report to NeWater, a project funded under the Sixth Research Framework of the European Union. Institute of Natural Resources, Pietermaritzburg, South Africa

Komatsu E, Fukushima T, Harasawa H (2007) A modelling approach to forecast the effect of long-term climate change on lake water quality. *Ecological Modelling* 209: 351-366

Kuo J, Lung W, Yang C, Liu W, Yang M, Tang T (2006) Eutrophication modelling of reservoirs in Taiwan. *Environmental Modelling and Software* 21: 829-844

Landman WA, Kgatuke M, Mbedzi M, Beraki A, Bartman A, Du Piesanie A (2006) Skill comparison of some dynamical and empirical downscaling methods for Southern Africa from a seasonal climate modelling perspective. Water Research Commission Report no 1334/1/06, pp86

Laprise R (2008) Regional climate modelling. *Journal of Computational Physics* 227:3641-3666

Lau L, Young RA, McKeon G, Syktus J, Duncalfe F, Graham N, McGregor J (1999) Downscaling global information for regional benefit: coupling spatial models at varying space and time scales. *Environmental Modelling & Software* 14:519:529

Lawrence MG (2005) The Relationship between Relative Humidity and the Dewpoint Temperature in Moist Air: A Simple Conversion and Applications. *Bull. Amer. Meteor. Soc*., 86, 225-233.

Lee GF, Jones RA (1991) Effects of eutrophication on fisheries. *Reviews in Aquatic Sciences* 5: 287-305

Limno-Tech (2002) Descriptive inventory of models with prospective relevance to ecological impacts of water withdrawals, Prepared for The Great Lakes Commission

Lin CK, Schelske CL (1979) Effects of nutrient enrichment, light intensity, and temperature on growth of phytoplankton from Lake Huron. EPA-600/3-79-049.

Linvill DE (1990) Calculating chilling hours and chill units from daily maximum and minimum temperature observations, *HortScience*, Vol. 25(1), January 1990 pp 14-16

Litchman E (2000) Growth rates of phytoplankton under fluctuating light. *Freshwater biology* 44:223-235

Lorentz SA, Kollongei J, Snyman N, Berry SR, Jackson W, Ngaleka K, Pretorius JJ, Clark D, Thornton-Dibb S, le Roux JJ, Germishuyse T, Görgens A (2010) Development of an integrated modelling approach to prediction of agricultural non-point source (NPS) Pollution from field to catchment scales for selected agricultural NPS pollutants: Catchment scale sediment and nutrient prediction (WRC Report number K5/1516).

Ludwig A, Matlock Ma, Haggard BE, Matlock Mo, Cummings E (2008) Identification and evaluation of nutrient limitation on periphyton growth in headwater streams in the Pawnee Nation, Oklahoma. *Ecological Engineering* 32:178-186

Luo L, Hamilton D and Han B (2010) Estimation of total cloud cover from solar radiation observations at Lake Rotorua, New Zealand. *Solar Energy* 84 (2010) pp 501-506

Mander M (2001) Incorporating economic considerations into the quantification, allocation and management of the environmental reserve for rivers: synthesis report. Pretoria: Water Research Commission.

May W (2007) The simulation of the variability and extremes of daily precipitation over Europe by the HIRHAM regional climate model. *Global and Planetary Change* 57: 59-82

Meisner JD, Goodier JL, Regier HA, Shuter BJ, Christie WJ (1987) An assessment of the effects of climate warming on great lakes basin fishes. *Journal Great Lakes Res*., 13(3): 340-352

Mendiondo EM (2008) Global Review of Lake and Reservoir Eutrophication and associated management challenges. International Lake Environment Committee (ILEC). Paper at URL: http://wldb.ilec.or.jp/ILBMTrainingMaterials/resources/eutrophication_challenges.pdf

Merel S, Clement M, Thomas O (2010) State of the art on cyanotoxins and their behaviour towards chlorine. *Toxicon* 55(4), April: 677-691

MET4 and MET4A Calculation of Dew Point (undated) Paroscientific, Inc. 4500 148th Ave. N.E. Redmond, WA 98052. 2007-09-13. http://www.paroscientific.com/dewpoint.htm.

Moomaw W (2002) Energy, Industry and Nitrogen: Strategies for Decreasing Reactive Nitrogen Emissions. *Ambio* 31(2): 184-189

Mortimer CH (1956) The oxygen content of air-saturated fresh waters, and aids in calculating percentage saturation. Intern. Assoc. *Theoret. Appl. Commun*. No 6.

Moss B, Kosten S, Meerhoff M, Battarbee RW, Jeppesen E, Mazzeo N, Havens K, Lacerot G, Liu Z, De Meester L, Paerl H, Scheffer M (2011) Allied attack: Climate change and eutrophication. *Inland Waters* (2011) 1, pp 101-105

Moss RH (ed) (2007) Improving information for managing an uncertain future climate. *Global Environmental Change* 17:4-7

Nakićenović N, Alcamo J, Davis G, de Vries B, Fenhann J, Gaffin S, Gregory K, Grübler A, Jung TY, Kram T, La Rovere EL, Michaelis L, Mori S, Morita T, Pepper W, Pitcher H, Price L, Raihi K, Roehrl A, Rogner H-H, Sankovski A, Schlesinger M, Shukla P, Smith S, Swart R, van Rooijen S, Victor N, Dadi Z (2000) Emissions Scenarios. A Special Report of Working Group III of the Intergovernmental Panel on Climate Change. Nakicenovic N and Swart R (Eds) Cambridge University Press, UK and New York, NY, USA. pp 599.

New Hampshire Department of Environmental Services (2006) Environmental Fact Sheet ARD-EHP-13: Trihalomethanes: Health Information Summary. Available at http://des.nh.gov/organization/commissioner/pip/factsheets/ard/documents/ard-ehp-13.pdf

Nielsen EJ (2005) Algal succession and nutrient dynamics in Elephant Butte reservoir, Unpublished masters dissertation, Brigham Young University

Nitsche NC (2000) Assessment of a hydrodynamic water quality model, DUFLOW, for a winter rainfall river, MSc Engineering thesis, University of Stellenbosch

O'Brien G, Smit N, Wepener V (2011) Regional Scale Risk Assessment of threats to the yellowfish (*Labeobarbus* spp.) and the ecosystem services they provide in the in the Vaal River, South Africa's hardest working river.

Oberholster PJ, Ashton PJ (2008) An overview of the current status of water quality and eutrophication in South African rivers and reservoirs, State of the Nation report, Parliamentary grant deliverable, March, 1-15

Oberholster PJ, Botha A-M, Myburgh JG (2009) Linking climate change and progressive eutrophication to incidents of clustered animal mortalities in different geographical; regions of South Africa. *African Journal of Biotechnology* November, 8(21): 5825-5832

Osborn TJ, Hulme M (1997) Development of a relationship between station and grid-box rainday frequencies for climate model evaluation. *Journal of Climate* 10, 1885-1908

Owuor K, Onkonkwo J, Van Ginkel C, Scott W (2007) Environmental factors affecting the persistence of toxic phytoplankton in the Hartbeespoort dam, Water Research Commission Report no 1401/3/07, October, xi + 77 pp

Pannell DJ, Ewing MA (2006) Managing secondary dryland salinity: Options and challenges. *Agricultural Water Management* February, 80(1-3): 41-56

Paerl H, Huisman J (2008) Blooms like it hot. *Science* 320: 57-58.

Park SS, Lee YS (2002) A water quality modelling study of the Nakdong River, Korea. *Ecol. Model.* 152, 65-75

Pavluk T, bij de Vaate A (2008) Ecological Indicators: Trophic Index and Efficiency, pp 3602-3608

Peltzer PM, Lajmanovicha RC, Sánchez-Hernandez JC, Cabagnab MC, Attademoa AM, Bassób A (2008) Effects of agricultural pond eutrophication on survival and health status of *Scinax nasicus* tadpoles. *Ecotoxicology and Environmental Safety* 70 (1): 185-197

Perry RH, Green D (1985) Perry's Chemical Engineers' Handbook, 6th edition, McGraw-Hill

Pretty JN, Mason CF, Nedwell DB, Hine RE, Leaf S, Dils R (2003) Environmental Costs of Freshwater Eutrophication in England and Wales. *Environmental Science and Technology* American Chemical Society, 37(2):201-208

Prinsloo JF, Pieterse AJH (1994) Preliminary observations on the effect of increased concentration of total dissolved salts on growth and photosynthetic effects of different algal species. *Water SA* July, 20(3): 219-222

Quintana-Seguí P, Ribes A, Martin E, Habets F, Boé J (2010) Comparison of three downscaling methods in simulating the impact of climate change on the hydrology of the Mediterranean basins. *Journal of Hydrology* 383: 111-124.

Rand Water (2012) Suitability of Water in the Vaal Barrage Reservoir for Recreational Use [Available Online: http://www.reservoir.co.za/catchments/vaal%20barrage/barrage%20reservoir %20forum/barrage%20recreation%202012/barrage_recreation_02mar2012.pdf, accessed March 2012].

Reicosky DC, Winkelman LJ, Baker JM, Baker DG (1989) Accuracy of hourly air temperatures calculated from daily minima and maxima. *Agricultural and Forest Meteorology* 46: 193-209

Reynolds CS (1984) The Ecology of Freshwater Phytoplankton (Cambridge Studies in Ecology) Cambridge University Press, Cambridge, United Kingdom.

River Health Programme (2003) State-of-Rivers Report: Free State Region River Systems. Department of Water Affairs and Forestry, Pretoria

Robarts RD, Zohary T (1987) Temperature effects on photosynthetic capacity, respiration, and growth rates of bloom-forming cyanobacteria. *NZJ Mar. Freshwater Res*. 21: 391-399.

Rosenzweig C, Casassa G, Karoly DJ, Imeson A, Liu C, Menzel A, Rawlins S, Root TL, Seguin B, Tryjanowski P (2007) Assessment of Observed Changes and Responses in Natural and Managed Systems. In Parry ML, Canziani OF, Palutikof JP, van der Linden PJ, Hanson CE (eds.), Climate Change 2007: Impacts, Adaptation and Vulnerability,

Contribution of Working Group II to the Fourth Assessment Report of the Intergovernmental Panel on Climate Change. Cambridge, UK: Cambridge University Press.

Rossouw JN (2000) The extension of management oriented models for eutrophication control, Water Research Commission Report No 266/1/01 xiii+69pp

Rossouw JN, Harding WH, Fatoki OS (2008) A guide to catchment-scale eutrophication assessments for rivers, reservoirs and lacustrine wetlands, Water Research Commission Report TT 352/08, April, xv+158 pp

Rossouw JN (2012) Water Research Commission stakeholders meeting at Civil Engineering Stellenbosch University, Stellenbosch (Water Research Commission Project No K5/2028/1 – *pers. Comm*.)

Scheffer M, Hosper SH, Meijer ML, Moss B, Jeppesen E (1993) Alternative equilibria in shallow lakes. *Trends in Ecology and Evolution* 8: 275-279

Schulze RE (1995) Hydrology and Agrohydrology. Water Research Commission, Pretoria, RSA, Water Research Commission Report TT69/95.

Schulze RE (1997) South African Atlas of Agrohydrology and -Climatology. Water Research Commission, Pretoria, RSA. Water Research Commission Report TT82/96. pp 273.

Schulze RE, Maharaj M (2004) Development of a Database of Gridded Daily Temperatures for Southern Africa. Water Research Commission, Pretoria, RSA, Water Research Commission Report 1156/2/04.

Schulze RE (2004) Modelling as a Tool in Integrated Water Resources Management: Conceptual Issues and Case Study Applications. Water Research Commission, Pretoria, RSA. Water Research Commission Report 749/1/04. pp 258. (ISBN 1-77005-143 -0).
Schulze RE, Smithers JC (2004) The ACRU Modelling System as of 2002: Background, Concepts, Structure, Output, Typical Applications and Operations. In: Schulze, R.E. (ed) Modelling as a Tool in Integrated Water Resources Management: Conceptual Issues and Case Study Applications. Water Research Commission, Pretoria, RSA, Water Research Commission Report 749/1/02. Chapter 3, 47-83.

Schulze RE (2005a) Hydrological Modelling: Concepts and Practice. UNESCO-IHE, Delft, the Netherlands. pp134.

Schulze RE (2005b) Climate Change and Water Resources in Southern Africa: Studies on Scenarios, Impacts, Vulnerabilities and Adaptation. Water Research Commission, Pretoria, RSA, Water Research Commission Report 1430/1/05. pp 470

Schulze RE (2006) Climate change and water resources in Southern Africa, Water Research Commission Report No 1430/1/05, liv+compact disc

Schulze RE (2007a) Climate Change and the Agriculture Sector in South Africa: An Assessment of Findings in the New Millennium. University of KwaZulu-Natal, Pietermaritzburg, RSA, School of Bioresources Engineering and Environmental Hydrology, ACRUcons Report, 55. pp 71.

Schulze RE (2007b) Some foci of integrated water resources management in the 'South' which are oft forgotten by the 'North'. *Water Resources Management* 21, 269-294.

Schulze RE (2007c) South African Atlas of Climatology and Agrohydrology. Funded by the Water Research Commission (Report 1489/1/06) and titled 'Development of interactive updated and updateable, extended Atlas of South African Agroclimatology and Agrohydrology'.

Schulze RE (Ed) (2008) South African Atlas of Climatology and Agrohydrology. Water Research Commission, Pretoria, RSA. pp535 (On interactive DVD).

Schulze RE, Hewitson BC, Barichievy KR, Tadross MA, Kunz RP, Horan MJC, Lumsden TG (2010) Methodological approaches to assessing eco-hydrological responses to climate change in South Africa. Water Research Commission, Pretoria, RSA. Water Research Commission Report No. 1562/1/10.

Sellner KG, Lacouture RV, Parrish CR (1988) Effects of increasing salinity on a cyanobacteria bloom in the Potomac River estuary. *Journal of Plankton Research* 10(1):49-61.

Shuker K (2001) The Hidden Powers of Animals: Uncovering the Secrets of Nature. London: Marshall Editions Ltd.

Snaddon CD, Davies BR (1999) An assessment of the ecological effects of inter-basin water transfer schemes (IBTs) in dryland environments, WRC report no 665/1/00, xxviii + 113 pp

Solomon S, Qin D, Manning M, Alley RB, Berntsen T, Bindoff NL, Chen Z, Chidthaisong A, Gregory JM, Hegerl GC, Heimann M, Hewitson B, Hoskins BJ, Joos F, Jouzel J, Kattsov V, Lohmann U, Matsuno T, Molina M, Nicholls N, Overpeck J, Raga G, Ramaswamy V, Ren J, Rusticucci M, Somerville R, Stocker TF, Whetton P, Wood RA and Wratt D (2007) Technical Summary. In: Climate Change 2007: The Physical Science Basis. Contribution of Working Group I to the Fourth Assessment Report of the Intergovernmental Panel on Climate Change [Solomon S, Qin D, Manning M, Chen Z, Marquis M, Averyt KB, Tignor M, Miller HL (eds.)]. Cambridge University Press, Cambridge, United Kingdom and New York, NY, USA.

Southern Waters (1999) Voëlvlei Augmentation Scheme (VAS): Impact of Berg River transfer on in-lake phosphorous concentrations and the trophic state of the Voëlvlei impoundment. Prepared for Gibb Africa by W.R Harding.

Talling JF (1955) The relative growth rates of three plankton diatoms in relation to underwater radiation and temperature. *Ann. Bot. N.S*. 19:329-341

Tamiya HT, Sasa T, Nikei T, Ishibashi S (1965) Effects of variation of daylength, day and night temperatures, and intensity of daylight on the growth of Chlorella. *J. of General and Applied Microbiology* 4:298-307

Tempelhoff E (2012) Woede oor 'groen mat'. Beeld [Available online: http://www.beeld.com/Suid-Afrika/Nuus/Woede-oor-groen-mat-20120223, accessed March 2012]

The Bright Water Company (2010) Floating Island. Retrieved April 2011, from Floating Island International: http://www.floatingislandinternational.com

Thomann RV, Di Toro DM, Winfield RP, O'Connor DJ (1975) Mathematical Modelling of Phytoplankton in Lake Ontario, Part 1 – Model Development and Verification. U.S. Environmental Protection Agency, Office of Research and Development, ERL-Corvallis, Large Lakes Research Station, Grosse Ile, Michigan. EPA/660/3-75/005, 177 pp.

Trenberth KE, Jones PD, Ambenje P, Bojariu R, Easterling D, Klein Tank A, Parker D, Rahimzadeh F, Renwick JA, Rusticucci M, Soden B, Zhai P (2007) Observations: Surface and Atmospheric Climate Change. In: Climate Change 2007: The Physical Science Basis. Contribution of Working Group I to the Fourth Assessment Report of the Intergovernmental Panel on Climate Change Cambridge University Press, Cambridge, United Kingdom and New York, NY, USA.

Tsujimura S, Okubo T (2003) Development of Anabaena blooms in small reservoirs with dense sediment akinete population, with special reference to temperature and irradiance. *Journal of plankton research* 25(9):1059-1067

Tyson, P. D., Preston-Whyte, R. A., 2000, The weather and climate of Southern Africa. Oxford: Oxford University Press.

Van Ginkel C (2002) Trophic status assessment, Executive summary, www.DWA.gov.za/iwqs/eutrophication/NEMP/default.htm, June, i-xvii

Van Ginkel CE (2004) A National Survey of the Incidence of Cyanobacterial Blooms and toxin production in major impoundments. Internal Report No. N/0000/00/DEQ/0503. Resource Quality Services, Department of Water Affairs and Forestry. Pretoria, South Africa, 54 pp.

Van Ginkel CE (2011) Eutrophication: Present reality and future challenges for South Africa. *Water SA* 37(5): 693-701. WRC 40-Year Celebration Special Edition 2011.

Van Nguyen V, Wood EF (1979) On the morphology of summer algae dynamics in non-stratified lakes. *Ecological modelling* 6(1979): 117-131pp

Vézie C, Rapala J, Seitsonem J, Sivonen K (2002) Effect of Nitrogen and Phosphorous on Growth of Toxic and Nontoxic Microcystis Strains and on Intracellular Microcystin Concentrations. *Microbial Ecology* June, 43(4):443-454

Vuren MJ and Grobbelaar JU (1982) Selection of algal species for use in open outdoor mass cultures. *Water SA* 8(2):86-91

Walmsley RD (2000) Perspectives on eutrophication of surface waters: policy/research needs in South Africa, Water Research Commission Report no KV129/00, v+60 pp

Wang S, Chen W and Cihlar J (2002) New calculation methods of diurnal distribution of solar radiation and its interception by canopy over complex terrain. *Ecological Modelling* 00 (2002) pp 1-14

Waichler SC and Wigmosta MS (2002) Development of hourly meteorological values from daily data and significance to hydrological modelling at H.J. Andrews experimental forest, Journal of Hydrometeorology, 4 (2003) pp 251-263

Walmsley RD (2000) Perspectives on eutrophication of surface waters: policy/research needs in South Africa, Water Research Commission Report no KV129/00, v+60 pp

Wetzel RG (2001) Limnology, Lake and river ecosystems, 3rd edition, London, Academic press.

Wilby RL, Charles SP, Zorita E, Timbal B, Whetton P, Mearns LO (2004) Guidelines for use of climate scenarios developed from statistical downscaling methods: supporting material of the Intergovernmental Panel on Climate Change. Task Group on Data and Scenario Support for Impacts and Climate Analysis, Rotherham.

World Health Organization (2003) Guidelines for safe recreational water environments, Volume 1, Coastal and fresh waters, http://www.who.int/water_sanitation_health/dwq/en/ , ISBN 92 4 154580 1

Wotton RS (1995) Temperature and lake-outlet communities, Journal of Thermal Biology, 20(1/2):121-125 pp

WRI, Water Resources Institute (2008) WRI Policy Note No. 1: Eutrophication and hypoxia in coastal areas: a global assessment of the state of knowledge. Washington DC, USA, www.wri.org.

WRI, Water Resources Institute (2009) WRI Policy Note No. 3: Eutrophication: Policies, Actions, and Strategies to Address Nutrient Pollution. Washington DC, USA, www.wri.org.

Appendix A

List of stakeholders

Name	Surname	Organisation	
Hanief	Ally	University of Stellenbosch	Project Team
Marna	Butler	Midvaal Water Company (Microbiologist)	Stakeholder
Trevor	Coleman	Golder Associates	Project Team
Carlo	de Waard	AngloGold Ashanti	Stakeholder
Willem	Grobler	DWA: Free State (Water Regulation)	Stakeholder
Ralph	Heath	Golder Associates	Project Team
Catherine	Hughes	Golder Associates	Project Team
Shalene	Janse van Rensburg	Midvaal Water Company, Scientific Services	Stakeholder
Jackie	Jay	DWA: WQP	Stakeholder
Wageed	Kamish	University of Stellenbosch	Project Team
Lisa	Coop	University of Cape Town	Reference Group
Marina	Krüger	Midvaal Water Company	Stakeholder
Neo	Leburu	DWA: Free State	Stakeholder
M	Ludick	Sedibeng Water	Stakeholder
Joël	Malan	AngloGold Ashanti	Stakeholder
Dumisani	Mchunu	DWA: Free State	Stakeholder
Chris	Moseki	Water Research Commission	Reference Group
Kevin	Murray	Water Research Commission	Reference Group
Jan	Pietersen	Midvaal Water Company, Scientific Services	Stakeholder
Jan	Roos	Water Quality Consultants	Reference Group
Nico	Rossouw	Aurecon	Reference Group
Roland	Schulze	University of KwaZulu-Natal	Reference Group
Nadine	Slabbert	DWA	Reference Group
Jurgo	van Wyk	DWA: WRP: WQP	Stakeholder
Bertrand	Van Zyl	DWA: Western Cape	Stakeholder
Günther	Wiegenhagen	AngloGold Ashanti	Stakeholder